Japan Geoscience Union Meeting 2014
(28 April - 02 May 2014 at Pacifico YOKOHAMA, Kanagawa, Japan)

PPS01-01 Room:418 Time:April 30 14:15-14:35

The Solar Power Sail for Round Trip Exploration to Jupiter Trojans and Deep Space Cruising Observation

YANO, Hajime[1*] ; NAKAMURA, Ryosuke[2] ; MATSUURA, Shuji[1] ; SEKINE, Yasuhito[3] ; TOYODA, Michisato[4] ; AOKI, Jun[4] ; YOSHIDA, Fumi[5] ; TAKATO, Naruhisa[5] ; KINOSHITA, Daisuke[6] ; YONETOKU, Daisuke[7] ; YOSHIKAWA, Makoto[1] ; MORI, Osamu[1] ; SOLAR SYSTEM SMALL BODY EXPLORATION WGT, .[1] ; SOLAR POWER SAIL WG, .[1]

[1]JAXA/ISAS, [2]AIST, [3]The University of Tokyo, [4]Osaka University, [5]NAOJ, [6]Taiwan Central University, [7]Kanazawa University

Since 2002, the Solar Power Sail WG has been studying a mission design of Japan's first outer planet region exploration, by demonstrating the solar power sail technology, and it is bound to Jupiter Trojan asteroids, which may hold fundamental clues of the Solar System formation and revolution discussed by two competing hypotheses between the classic model and the planetary migration model. The former suggests that Trojan asteroids are mainly survivors of building blocks of the Jupiter system, while the latter claims that they must be intruders from outer regions after the planetary migration of gas planets settled.

After Jupiter flyby, the spacecraft will reach to a candidate Trojan asteroid, hopefully being larger than a few 10's of km in size. Both global remote observation and deployment of an autonomous lander will be conducted. On the surface of the Trojan asteroid, sampling will be attempted for in-situ TOF mass spectrometry and passing the sample container to the mothership for a possible sample return option.

Also during the cruising operation, "dust free" astronomical platform beyond the cocoon of the zodiacal light formed by the main asteroid belt for the benefit of infrared astronomy searching for the first generation light of the Universe, let alone continuous observation of the zodiacal light structure of the Solar System. Extremely long baseline with the observation from the Earth, gamma-ray burst observation can identify their sources.

This presentation discusses major scientific objectives of an exploration mission to Jupiter Trojans for the first time in the history, its mission design and spacecraft system using solar power sail, a hybrid propulsion system of electric propulsion and photon sail, which inherited from the IKAROS deep space solar sail spacecraft, together with major engineering challenges, in-situ observation instruments and operational options including landing and sample return from the surface of a Trojan asteroid.

Keywords: Solar Power Sail, Jupiter Trojans, Deep Space Exploration, Deep Space Astronomy, Zodiacal Light, Sample Return

Japan Geoscience Union Meeting 2014
(28 April - 02 May 2014 at Pacifico YOKOHAMA, Kanagawa, Japan)

PPS01-02 Room:418 Time:April 30 14:35-14:55

EUROPA CLIPPER MISSION CONCEPT OVERVIEW

PAPPALARDO, Robert[1] ; GOLDSTEIN, Barry[1] ; MAGNER, Thomas[2] ; PROCKTER, Louise[2] ; SENSKE, David[1] ; PACZKOWSKI, Brian[1] ; COOKE, Brian[1] ; VANCE, Steven[1*] ; PATTERSON, G. wesley[2]

[1]Jet Propulsion Laboratory, California Institute of Technology, Pasadena, CA 91109, [2]The Johns Hopkins University, Applied Physics Laboratory, Laurel, MD, 20723

A NASA-appointed Science Definition Team (SDT) recently considered options for a future strategic mission to Europa, with the stated science goal: Explore Europa to investigate its habitability. The team worked closely with a technical team from the Jet Propulsion Laboratory (JPL) and the Applied Physics Laboratory (APL). Together, the group considered several mission options, which were fully technically developed, then costed and reviewed by technical review boards and planetary science community groups. Study results strongly favored an architecture consisting of a spacecraft in Jupiter orbit, making many close flybys of Europa, and concentrating on remote sensing to explore the moon. The resulting nominal mission design is innovative for its use of gravitational perturbations of the spacecraft trajectory to permit flybys at a wide variety of latitudes and longitudes. The design enables globally distributed regional coverage of the moon's surface, nominally with 45 close flybys at altitudes from 25 to 100 km. We will present the science and reconnaissance goals and objectives, a mission design overview, and the notional spacecraft for this concept, which has become known as the Europa Clipper. The Europa Clipper concept provides a cost-efficient means to explore Europa and investigate its habitability, through understanding the satellite's ice and ocean, composition, and geology. The set of investigations derived from these science objectives traces to a notional payload for science, consisting of: Ice Penetrating Radar (for sounding of ice-water interfaces within and beneath the ice shell), Topographical Imager (for stereo imaging of the surface), ShortWave Infrared Spectrometer (for surface composition), Neutral Mass Spectrometer (for atmospheric composition), Magnetometer and Langmuir Probes (for inferring the satellite's induction field to characterize an ocean), and Gravity Science (to confirm an ocean). Among the many science investigations addressed, Europa Clipper could potentially characterize plumes linked to Europa's internal lakes or ocean. The mission would also include the capability to perform reconnaissance for a future lander, with the Reconnaissance goal: *Characterize safe and scientifically compelling sites for a future lander mission to Europa*. To accomplish these reconnaissance objectives and the investigations that flow from them, principally to address issues of landing site safety, two additional instruments would be included in the notional payload: a Reconnaissance Camera (for high-resolution imaging) and a Thermal Imager (to characterize the surface through its thermal properties). These instruments, in tandem with the notional payload for science, could assess the science value of potential landing sites. This notional payload serves as a proof-of-concept for the Europa Clipper during its formulation stage. The actual payload would be chosen through a NASA Announcement of Opportunity. If NASA were to proceed with the mission, it could be possible to launch early in the coming decade, on an Atlas V or the Space Launch System (SLS).

Keywords: Europa, Icy Worlds, Astrobiology, Europa Clipper, Missions, Planetary Science

Japan Geoscience Union Meeting 2014
(28 April - 02 May 2014 at Pacifico YOKOHAMA, Kanagawa, Japan)

PPS01-03 Room:418 Time:April 30 14:55-15:10

Investigation of the Galilean Moons with the Ganymede Laser Altimeter (GALA)

HUSSMANN, Hauke[1*] ; LINGENAUBER, Kay[1] ; MICHAELIS, Harald[1] ; KOBAYASHI, Masanori[2] ; THOMAS, Nicolas[3] ; LARA, Luisa M.[4] ; ARAKI, Hiroshi[5] ; BEHNKE, Thomas[1] ; GWINNER, Klaus[1] ; KIMURA, Jun[6] ; NAMIKI, Nori[2] ; NODA, Hirotomo[5] ; OBERST, Juergen[1] ; ROATSCH, Thomas[1] ; RODRIGO, Rafael[4] ; SASAKI, Sho[7] ; SEIFERLIN, Karsten[3] ; SPOHN, Tilman[1] ; BARNOUIN, Olivier[8] ; BREUER, Doris[1] ; CASOTTO, Stefano[9] ; CASTRO, Jose[4] ; CHOBLET, Gael[10] ; CHRISTENSEN, Ulrich[11] ; FERRAZ-MELLO, Sylvio[12] ; GIESE, Bernd[1] ; KALLENBACH, Reinald[11] ; KURITA, Kei[13] ; LAINEY, Valery[14] ; LICHOPOJ, Alexander[1] ; LOETZKE, Horst-georg[1] ; LUPOVKA, Valery[15] ; MOORE, William B.[16] ; RODRIGUEZ, Adrian[6] ; SANTOVITO, Maria rosaria[17] ; SCHREIBER, Ulrich[18] ; SCHROEDTER, Rolf[1] ; SOHL, Frank[1] ; DEL TOGNO, Simone[1] ; VERMEERSEN, Bert[19] ; WIECZOREK, Mark[20] ; YSEBOODT, Marie[21]

[1]DLR Institute of Planetary Research, Berlin, Germany, [2]Chiba Institute of Technology, Planetary Exploration Research Center, Chiba, Japan, [3]Physics Institute, University of Bern, Switzerland, [4]CSIC, Instituto de Astrofisica de Andalucia, Granada, Spain, [5]National Astronomical Observatory of Japan, Mizusawa, Japan, [6]Earth-Life Science Institute, Tokyo Institute of Technology, Japan, [7]Osaka University, Toyonaka Japan, [8]Space Dept., The Johns Hopkins University Applied Physics Laboratory, Laurel, MD, USA, [9]University of Padua, Dept. of Physics and Astronomy and Center for Space Studies, Padova, Italy, [10]Laboratoire de Planetologie et Geodynamique de Nantes, France, [11]Max Planck Institute for Solar System Research, Katlenburg-Lindau, Germany, [12]Institute of Astronomy, Geophysics and Atmospheric Science, Sao Paulo, Brasil, [13]University of Tokyo, Earthquake Research Institute, Tokyo, [14]IMCCE-Observatoire de Paris, France, [15]Moscow State University of Geodesy and Cartography, (MIIGAiK), Russia, [16]Hampton University, National Institute of Aerospace, USA, [17]CO.RI.S.T.A. Consortium of Research on Advanced Remote Sensing Systems, Napoli, Italy, [18]Technische Universitat Munchen, Fundamentalstation Wettzell, Germany, [19]Astrodynamics & Space Missions, Faculty of Aerospace Engineering, TU Delft, Netherlands, [20]Institut de Physique du Globe de Paris, France, [21]Royal Observatory of Belgium , Brussels, Belgium

The icy moons of Jupiter ? Europa, Ganymede, and Callisto ? are believed to contain global subsurface water oceans underneath their icy crusts. The possibility is intriguing that these large liquid water oceans represent ”habitable” environments. Investigation of the latter is a major objective of ESA’s Jupiter Icy Moons Explorer (JUICE) mission. The Ganymede Laser Altimeter (GALA) is one of the instruments focusing on aspects related to the presence and characterization of subsurface water oceans by measuring Ganymede’s tidal deformation. GALA will further contribute (a) to the exploration of the surface morphology and physical properties of Ganymede, Europa and Callisto, (b) to determination of their interior structures from a combination of shape, topography and gravitational field data, and (c) to understanding the satellites formation and evolution especially with respect to subsurface water oceans. GALA will investigate the surface and topography of Ganymede in particular. Topography data is needed to account for the effects of topographic heights on the gravity field and to account for near surface mass distribution anomalies above the reference figure; to support geological studies, e.g. to identify and characterize tectonic and cryo-volcanic regions on the icy moons and to identify periodic variations of Ganymede’s shape due to tides.

Investigations by GALA will furthermore contribute to determine the orientation and rotational state of Ganymede and to study surface characteristics (roughness, slopes, and albedo) on Ganymede, Europa, and Callisto.

The instrument can be operated from ranges smaller than about 1000 to 1300 km (depending on the different albedo values and surface slopes of Europa, Ganymede and Callisto) during flybys and orbital pericenter passages. The main phases for acquiring data at Ganymede are the final circular orbit phases, where continuous operations are possible from altitudes around 500 km and 200 km, respectively.

Here, we will give an overview on the GALA experiment focusing on its scientific goals and performance.

Keywords: Laser altimetry, Satellites of Jupiter, Ganymede, Tides

Japan Geoscience Union Meeting 2014
(28 April - 02 May 2014 at Pacifico YOKOHAMA, Kanagawa, Japan)

PPS01-04 Room:418 Time:April 30 15:10-15:25

Longevity of an internal ocean in Ganymede

KIMURA, Jun[1*] ; VANCE, Steven[2] ; HUSSMANN, Hauke[3] ; KURITA, Kei[4]

[1]Earth-Life Science Institute, Tokyo Institute of Technology, [2]Jet Propulsion Laboratory, [3]DLR Institute of Planetary Research, [4]Earthquakle Research Institute, The University of Tokyo

The outer solar system may provide a potential habitat of extra-terrestrial life. Most moons orbiting planets in the outer Solar System, at orbits beyond the snow line, such as Jupiter or Saturn, are covered with water ice and are referred to as ”icy moons”. Galileo’s detection of induced magnetic fields combined with imaged surface characteristics and thermal equilibrium modeling of the moons, support that the Jovian icy moons Europa and Ganymede, and possibly Callisto, may harbor liquid water oceans underneath the icy crusts. The presence of internal oceans in the icy moons means that a deep habitat different from Earth’s biosphere may exist, located beyond the ”habitable zone” of the Sun. Evidence for oceans is not definitive, however, and awaits confirmation measurements. Also, the depth and composition of the oceans remain unclear, as do their variability through time.

Here we focus on Ganymede, the largest moon in the Solar System and the primary target of a new mission to the Jupiter system, the Jupiter Icy Moons Explorer (JUICE), which is planned by the European Space Agency (ESA). The bulk density of Ganymede, 1.936 g/cc, indicates a composition of approximately equal amounts of rocky material and water. Previous measurements of Ganymede’s gravitational field and intrinsic magnetic field by the Galileo orbiter suggest that its interior is completely differentiated into three layers, a convecting metallic core at the center, a rocky mantle surrounding the core, and an outermost water-ice shell. The water-ice layer in total has a thickness of 800-1000 km. A layer of melted, salty water that lies beneath the icy crust would be the best way to explain the signal of magnetic induction.

To investigate the lifetime of an ocean (thickness change through time) assumed to be initially in an entirely liquid state, we performed numerical simulations for the internal thermal evolution using a spherically symmetric model for the convective and conductive heat transfer with radial dependence of viscosity, heat source distribution, and other material properties. Here we take into account the energy due to decay of long-lived radioactive elements and also evaluate the effect of tidal heating. If the ocean were composed of pure water, a primordial ocean would have disappeared (completely solidified) within 1 Gyr even if tidal heating for the current orbital state were included. Consistent with previous predictions , this result indicates that significant tidal heating in the past, or strong antifreeze components (e.g., salts or ammonia),

are needed if the presence of the internal ocean in Ganymede would be confirmed from future JUICE observations. We numerically investigate their effect on the lifetime of the ocean.

Keywords: satellite, evolution, ocean, habitability, ice, Ganymede

Japan Geoscience Union Meeting 2014
(28 April - 02 May 2014 at Pacifico YOKOHAMA, Kanagawa, Japan)

PPS01-05 Room:418 Time:April 30 15:25-15:40

Impact basin relaxation on Pluto: Implications for the presence of a subsurface ocean

KAMATA, Shunichi[1*] ; NIMMO, Francis[2]

[1]Hokkaido University, [2]UC Santa Cruz

Large-scale topographies, such as impact basins, on solid planetary bodies deform in geologically long timescales. The degree of deformation depends mainly on the viscosity, and the viscosity is strongly controlled by temperature. Consequently, viscous relaxation of large impact basins has been studied to investigate the thermal evolution of terrestrial planets as well as that of icy satellites of giant planets [e.g., 1-4].

Pluto, an icy dwarf planet, is likely to possess large impact basins. In this study, we investigate long-term viscoelastic deformation of impact basins on Pluto which can be compared with forthcoming observational data from New Horizons, the first Pluto explorer.

Although little is known for Pluto, its interior is likely differentiated into a rocky core and an outer H_2O layer [e.g., 5]. The presence of a subsurface ocean, however, is highly uncertain. If the outer (solid) H_2O layer is convective, the radiogenic heat from the rocky core is efficiently transferred to the surface, and temperature of the H_2O layer can be lower than its melting temperature. On the other hand, if the outer H_2O layer is conductive, the heat from the core can melt the H_2O layer. The main controlling factor whether the H_2O layer is convective or conductive is the reference viscosity: the ice viscosity at its melting temperature [6]. In this study, we calculate viscoelastic deformation of impact basins assuming different viscosity profiles and examine the effect of the presence of a subsurface ocean on basin relaxation.

For the initial study, we use two time-independent viscosity profiles; one profile assumes a stiff top shell overlying a thick subsurface ocean, and the other assumes a completely solidified interior. The same viscosity profile in the shell is assumed.

Our results indicate that the instantaneous elastic response largely differ between the viscosity models. However, long-term relaxation does not differ much because it is controlled by the viscosity profile in the shell, which is identical in our calculations. Nevertheless, long-term relaxation strongly depends on the reference viscosity, the main controlling factor whether the shell is convective. Consequently, relaxation state of impact basins can be used to infer the reference viscosity as well as the presence of a subsurface ocean. This result would be applicable to icy satellites of Jupiter and Saturn.

Our next step is to use time-dependent viscosity profiles. To do so, we have modified our relaxation code to take into account the temporal change in the shell thickness. The results will be discussed.

[1] Kamata et al. JGR 118, 398-415, 2013. [2] Mohit and Phillips, GRL, 34, L21204, 2007. [3] Robuchon et al. Icarus 207, 959-971, 2010. [4] Solomon et al. JGR 87, 7763-7771, 1982. [5] McKinnon et al. in Pluto and Charon, pp. 295-343, 1997. [6] Robuchon and Nimmo, Icarus 214, 426-439, 2011.

Keywords: Impact basin, Relaxation, Pluto, Viscoelasticity

Japan Geoscience Union Meeting 2014
(28 April - 02 May 2014 at Pacifico YOKOHAMA, Kanagawa, Japan)

PPS01-06 Room:418 Time:April 30 15:40-15:55

Sub-millimeter observations of icy bodies toward understanding of planetary formation and cosmochemistry

SEKINE, Yasuhito[1*] ; KASAI, Yasuko[2] ; SAGAWA, Hideo[2] ; KURODA, Takeshi[3] ; KODAMA, Kenya[1] ; HORI, Yasunori[4] ; IKOMA, Masahiro[1] ; KURAMOTO, Kiyoshi[5] ; YURIMOTO, Hisayoshi[5]

[1]University of Tokyo, [2]NICT, [3]Tohoku University, [4]NAOJ, [5]Hokkaido University

The present-day composition of regular icy satellites consists of combinations of initial conditions and subsequent evolution. These icy satellites are considered to have been formed in a circumplanetary disk associated with giant planet formation. Thus, icy satellites that are not geologically active, such as Callisto, would serve as solar system fossils, which may preserve the information of the protoplanetary disk and planetary formation. On the other hand, geologically active satellites, such as Europa and Enceladus, would provide particular geological processes and consequent products of geochemical reaction. Sub-millimeter observations are capable of providing unique isotopic and chemical compositions of gas molecules in atmospheres and plumes of the icy satellites. In this paper, we discuss key observational targets and their importance for planetary formation theory and geo/cosmochemistry, especially focusing on sub-millimeter observations of Galilean satellites by the Jupiter Icy moons Explorer mission, JUICE.

Keywords: sub-millimeter observation, icy satellite, planetary formation, cosmochemistry

Japan Geoscience Union Meeting 2014
(28 April - 02 May 2014 at Pacifico YOKOHAMA, Kanagawa, Japan)

PPS01-07 Room:418 Time:April 30 16:15-16:30

Proto-atmospheres on giant icy satellites forming within gaseous circum-planetary disks

MIKAMI, Takashi[1*] ; KURAMOTO, Kiyoshi[1]

[1]Department of Cosmosciences, Graduate School of Science, Hokkaido University

In spite of the great similarity in size and mean density, the giant icy satellites Ganymede, Callisto, and Titan have very different surface environments. In particular, only Titan holds a thick atmosphere dominated by N_2. Recent data of the Cassini spacecraft indicated that atmospheric N_2 is probably originated from other nitrogen-bearing species like NH_3. However, it still remains an open question when and how N_2 was generated. This is partly because the physical states of giant icy satellites have been poorly understood.

According to a widely-accepted theory of regular satellites formation, the giant icy satellites were formed in subnebulae with low temperature and low pressure taking a long accretion time. Some models assert that their surfaces were kept too cold to induce significant differentiation during accretion. However, these satellites may capture a significant amount of subnebula gas, which possibly forms proto-atmospheres along with gases volatilized from icy components. Such a hybrid-type proto-atmosphere may have significant blanketing effect.

Here, we numerically analyze the structure and effect of a hybrid-type proto-atmosphere. Our model atmosphere is hydrostatically connected with subnebula at the satellite Hill radius. It contains H_2 and He as nebula gas components, H_2O and NH3 as volatilized ice components. The radiative-convective equilibrium structure is solved as a function of surface temperature. The subnebula conditions are given by Canup and Ward (2002), the temperatures are 150 K at Ganymede, 120 K at Callisto, and 50 K at Titan, and the corresponding subnebula pressures are varied over 0.1-10 Pa.

For all the boundary conditions, the proto-atmosphere is opaque due to water vapor, so that the outgoing thermal radiation (OTR) flux at top of the atmosphere is smaller than that of black body radiation without atmosphere when the surface temperature is higher than 273 K. When the surface temperature is lower, the OTR fluxes from the proto-atmospheres of Ganymede and Callisto are close to black-body radiation because these atmospheres have low surface pressure and are optically thin due to large scale height under high background temperature. On the other hand, the proto-atmosphere of Titan has another type of solution with the OTR fluxes significant lower than blackbody radiation under low surface temperature. This is due to the formation of optically thick atmosphere tightly bounded by gravity because of low background temperature.

These results imply that a warm proto-atmosphere near 200 K could be kept on Titan for a long time after the end of accretion. Our stability analysis suggests that the proto-atmospheres of Ganymede and Callisto were lost associated with the dissipation of the Jovian subnebula, but that of Titan survived after the dissipation of the Saturnian subnebula.

In the case, NH_3 vapor pressure would be kept high under the irradiation of the solar UV for a long time. The present atmospheric N_2 of Titan may be generated by photochemical reaction of NH_3 vapor in such a warm proto-atmosphere.

Keywords: Giant icy satellites, Atmosphere, Circum-planetary disks

Japan Geoscience Union Meeting 2014
(28 April - 02 May 2014 at Pacifico YOKOHAMA, Kanagawa, Japan)

PPS01-08 Room:418 Time:April 30 16:30-16:45

The difference of cloud formation process between Jupiter and Saturn.

TAKAHASHI, Yasuto[1*] ; HASHIMOTO, George[2] ; ISHIWATARI, Masaki[1] ; TAKAHASHI, Yoshiyuki[3] ; ONISHI, Masanori[3] ; KURAMOTO, Kiyoshi[1]

[1]Hokkaido Univ, [2]Okayama Univ, [3]Kobe Univ

Gas giant planets have hydrogen-rich, thick atmospheres, and their styles of cloud activities are thought to be closely related to the profile of radiative cooling rate in troposphere. For example, Recent studies indicate that it basically controls the intermittency of cumulonimbus clouds. In spite of its significance, however, no systematic estimate has been made for the radiative cooling profiles of gas giant planets.

Recently, we have developed a 1D radiative-convective equilibrium model for such hydrogen-rich atmospheres. The model atmosphere continues to a lower boundary where the optical depth from the top of atmosphere is sufficiently large and the thermal structure follows convective equilibrium. The atmospheric composition and potential temperature of each planet are given from observational constraints. The mixing ratios of H2O, CH4, NH3, H2S, PH3 and NH4SH follow their saturation vapor pressure in the altitudes where their condensation occurs. Collision induced absorption of H2-H2 and H2-He, and line absorption of H2O, CH4, NH3, H2S, PH3 are included while the extinction by condensates is neglected. Under these settings, our model can calculate a reasonable atmospheric vertical structure by the iteration of radiative transfer calculation and convective adjustment.

For the case of Jupiter, the peak of radiative cooling rate is 1.6e-7 K/sec at 0.7 bar level. Also, our model predicts the radiative-convective boundary i.e., tropopause to be located around 0.3-0.4 bar level, where is slightly higher than the uppermost NH3 condensation layer ˜0.5 bar. For the case of Saturn, the peak of radiative cooling rate is 3.5e-8 K/sec at 0.53 bar, and the separation of tropopause and NH3 cloud layer is larger than that of Jupiter. This implies that the Saturnian NH3 cloud formation is essentially confined in the troposphere, whereas the Jovian one is also affected by the stratospheric processes.

Figure description : Radiative heating rate profile (solid lines, bottom x axis, K/sec) and Volume mixing ratio of NH3 profile (dashed lines, top x axis, mole fraction). Y axis is pressure (bar). Shaded area represents between NH3 condensation level and tropopause level. Red means Jovian model, and blue means Saturnian model. Note that these results are calculated with the polytropic temperature profiles for preliminary calculation, not thermal equilibrium profiles.

Keywords: Jupiter, Saturn, Cloud, Radiative transfer, Convection

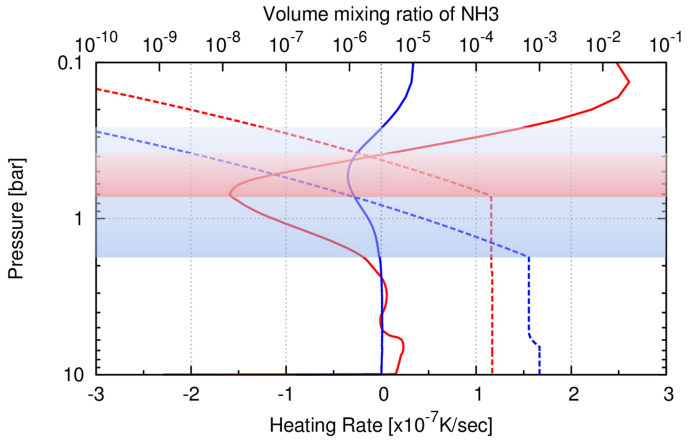

Japan Geoscience Union Meeting 2014
(28 April - 02 May 2014 at Pacifico YOKOHAMA, Kanagawa, Japan)

PPS01-09 Room:418 Time:April 30 16:45-17:00

Near-infrared detections of surprisingly bright Ganymede and Callisto in the Jovian shadow

TSUMURA, Kohji[1*] ; ARIMATSU, Ko[2] ; EGAMI, Eiichi[3] ; HAYANO, Yutakla[4] ; HONDA, Chikatoshi[5] ; KIMURA, Jun[6] ; KURAMOTO, Kiyoshi[7] ; MATSUURA, Shuji[1] ; MINOWA, Yosuke[4] ; NAKAJIMA, Kensuke[8] ; NAKAMOTO, Taishi[9] ; SHIRAHATA, Mai[1] ; SURACE, Jason[10] ; TAKAHASHI, Yasuto[7] ; WADA, Takehiko[1]

[1]Institute of Space and Astronautical Science, Japan Aerospace Exploration Agency, [2]University of Tokyo, [3]Arizona University, [4]Subaru Observatory, Natinal Astronomical Observatory of Japan, [5]The University of Aizu, [6]Earth-Life Science Institute, Tokyo Institute of Technology, [7]Hokkaido University, [8]Kyushu University, [9]Tokyo Institute of Technology, [10]California Institute of Technology

The Galilean satellites (Io, Europa, Ganymede, and Callisto) are expected to be dark when eclipsed by the Jovian shadow. However, we have discovered that Ganymede and Callisto are still surprisingly bright at 1.5 μm even when not directly lit by sunlight, based on observations from the Hubble Space Telescope and the Subaru Telescope. Their eclipsed luminosity was one-millionth of their uneclipsed brightness (i.e. $\sim$50 μJy for Ganymede and $\sim$30 μJy for Callisto in eclipse), which is low enough that this phenomenon has been undiscovered until now. In contrast, Europa in eclipse was not detected ($<$5.5 μJy), a potential clue to the origin of the source of luminosity. Likewise, Ganymede was observed at 3.6 μm by the Spitzer Space Telescope but it was not detected either ($<$3.6 μJy), suggesting a significant wavelength dependence. Why are they luminous even when in the Jovian shadow? These facts may be consistent with sunlight scattered by dust in the Jovian upper atmosphere, and if this is the case, observations of Ganymede and Callisto while eclipsed by the Jovian shadow provide us with a new method to investigate Jupiter's atmospheric composition.

Keywords: Galilean satellite eclipse, Ganymede, Callisto, Europa, Jovian upper atmosphere

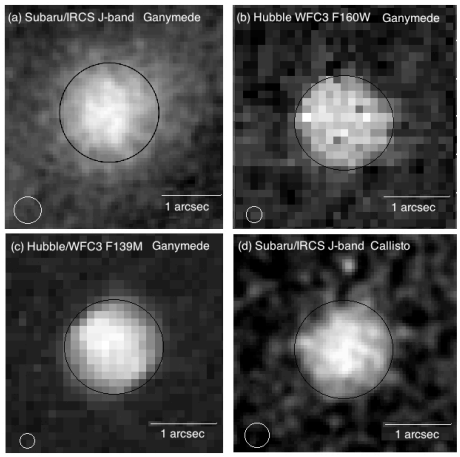

Japan Geoscience Union Meeting 2014
(28 April - 02 May 2014 at Pacifico YOKOHAMA, Kanagawa, Japan)

PPS01-10 Room:418 Time:April 30 17:00-17:15

Simulated radiative forcing by molecules in Jupiter's stratosphere

KURODA, Takeshi[1*] ; MEDVEDEV, Alexander[2] ; HARTOGH, Paul[2]

[1]Tohoku Univ., [2]MPS

We present the radiative heating and cooling rates by molecules for Jupiter's upper troposphere and stratosphere (10^3 to 10^{-3} hPa) with a newly developed parameterization which is suitable for general circulation models. The scheme is a band model based on the correlated *k*-distribution approach, which accounts for the heating due to absorption of solar radiation by CH_4, and cooling in the infrared by C_2H_6, C_2H_2, CH_4 and collision-induced transitions of H_2-H_2 and H_2-He.

The band model achieved the accuracy of within 10% in comparison with the line-by-line calculations. We show the sensitivity of the heating/cooling rates due to variations of the mixing ratios of hydrocarbon molecules calculated with this scheme, in addition to the calculated radiative-convective equilibrium temperature which is in agreement with observations in the equatorial region. Our results suggest that the radiative forcing in the upper stratosphere is much stronger than it was thought before [Conrath et al., 1990]. In particular, the characteristic radiative relaxation time decreases exponentially with height from 10^8 s near the tropopause to 10^5 s in the upper stratosphere.

Keywords: Jupiter, atmospheric radiation, gas giants, JUICE

Japan Geoscience Union Meeting 2014
(28 April - 02 May 2014 at Pacifico YOKOHAMA, Kanagawa, Japan)

PPS01-11 Room:418 Time:April 30 17:15-17:35

EXCEED EUV spectral images of Jupiter and Venus

YOSHIKAWA, Ichiro[1*] ; YOSHIOKA, Kazuo[2] ; MURAKAMI, Go[2] ; TSUCHIYA, Fuminori[3]

[1]University of Tokyo, [2]ISAS, [3]Tohoku University

An earth-orbiting Extreme Ultraviolet (EUV) spectroscopy is the first mission of the Small scientific satellite Platform for Rapid Investigation and Test -A (Sprint-A) conducted by ISAS/JAXA. A single science instrument (EXCEED) is boarded on Sprint-A. We have started to observe the solar planets in the EUV spectral range, and will extend to the identification of extrasolar planet atmosphere.

I will show the first light of the EXCEED and the next.

Keywords: Planetary Airglows, Sprint-A, EUV, plasma, visualization

Japan Geoscience Union Meeting 2014
(28 April - 02 May 2014 at Pacifico YOKOHAMA, Kanagawa, Japan)

PPS01-12 Room:418 Time:April 30 17:35-17:50

Occurrence characteristics of Saturn's short-term radio burst

MARUNO, Daichi[1] ; KASABA, Yasumasa[1*] ; KIMURA, Tomoki[2] ; MORIOKA, Akira[1] ; CECCONI, Baptiste[3]

[1]Tohoku Univ., [2]ISAS/JAXA, [3]Obs. Paris

Saturn kilometric radiation (SKR) is emitted from auroral electrons and suggested to be correlated with Saturn's auroral processes. We extracted northern SKR (N-SKR) and southern SKR (S-SKR) burst events, by newly defined selection criteria, with radio data observed by the Cassini Radio and Plasma Wave Science (RPWS) instrument in the period from day 250 of 2005 to day 200 of 2006. The data was separated into northern and southern components according to its circular polarization degree. As a result, 16 N-SKR burst events and 36 S-SKR burst events were identified in this period. Based on statistical studies of these events, we obtained the following results: (1) We derived typical frequency profiles of N- and S-SKR during SKR bursts to compare the intensity of N- and S-SKR bursts. The profiles show that the S-SKR burst was more intense than the N-SKR by 7 dB in the main frequency range. From the recent studies, the north-south asymmetry could be explained by the difference in solar illumination due to the tilted the magnetic and rotational axis. (2) By comparing onset timings of N- and S-SKR bursts, we found that 67 % of S-SKR burst events were accompanied by N-SKR bursts or burst-like enhancements. (3) To elucidate what determines the timing of SKR burst onsets, we compared the onset timing of N- and S-SKR bursts with each SKR phase of the periodic modulations. The result showed that the timing of SKR burst onsets generally depends on both the N- and S-SKR modulation phases. This suggests the existence of the internal control of SKR burst onsets. It is, however, noted that some SKR bursts occurred out of phases with SKR modulation phases. That indicates the timing of SKR bursts can also be determined by the external process, i.e., solar wind compressions. (4) We investigated the time evolutions of SKR intensities in the main frequency range and the low frequency range before and after SKR bursts. By comparing them with AKR intensity evolutions at AKR breakup, we found that they had two similarities: the enhancement of lower-altitude source regions prior to onsets and the formation of the distinct higher source regions. On the other hand, their timescales are quite different. In addition, this study pointed out that the two-step evolution scenario could not be directly applied to Saturn's case.

In conclusion, our study demonstrated the north-south asymmetry, the conjugacy and the dependence on the SKR periodic modulations of SKR bursts. These results would be helpful for understanding the auroral process at Saturn's magnetotail reconnections by elucidating the relationship between SKR bursts and reconnections. We consider the third result is particularly important because this suggests that both northern and southern periodicities would affect magnetotail reconnections.

Keywords: Saturn, SKR, aurora, Cassini

Japan Geoscience Union Meeting 2014
(28 April - 02 May 2014 at Pacifico YOKOHAMA, Kanagawa, Japan)

PPS01-P01 Room:Poster Time:April 30 18:15-19:30

Submillimeter-Wave Instrument (SWI) for JUICE: Current Status of the Instrumental Development

SAGAWA, Hideo[1*] ; KASAI, Yasuko[1] ; KIKUCHI, Kenichi[1] ; NISHIBORI, Toshiyuki[2] ; MANABE, Takeshi[3] ; OCHIAI, Satoshi[1] ; KURODA, Takeshi[4] ; SEKINE, Yasuhito[5] ; HARTOGH, Paul[6]

[1]National Institute of Information and Communications Technology (NICT), [2]Japan Aerospace Exploration Agency, [3]Osaka Prefecture University, [4]Tohoku University, [5]University of Tokyo, [6]Max Planck Institute for Solar System Research

The Submillimetre-Wave Instrument (SWI) is a passive submillimeter-wave heterodyne instrument proposed as one of the scientific payload instruments for the Jupiter Icy Moons Explorer (JUICE) mission. It measures the thermal emission from atmosphere of Jupiter and its moons at the frequency region of 500 - 600 GHz (with keeping 1200 GHz range as an optional concept). Thermal emission from the surface of moons will also be measured. JUICE/SWI provides unique observational data for characterization of the Jovian stratosphere such as thermal structure, dynamics, and distribution of minor species; and for exploration of tenuous-atmosphere and surface environment of the Jovian moons. By detecting hydrogen and oxygen isotopes in the water vapor of Jovian moons' atmosphere, SWI can also contribute to understanding the origin and distribution of water in our solar system.

This paper presents the current status of the development of SWI instrument, including the updates on the science targets and their feasibility studies. The SWI instrument is being developed through international cooperation. The Japanese team contributes to the development of the submillimeter reflector (mirror). The submillimeter reflector is one of the key components of SWI, and it determines the spatial resolution of observations. Currently a 30-cm aperture diameter reflector is considered, providing a spatial resolution of 2 mrad (FWHM) at 600 GHz. In order to fulfill the stringent requirement of weight reduction, we evaluated the material of the reflector and optimized its rib structure. The side lobe suppression is also an important factor to improve the quality of observations.

Keywords: Jupiter, Icy moon, JUICE, Submillimeter wave, Heterodyne

Japan Geoscience Union Meeting 2014
(28 April - 02 May 2014 at Pacifico YOKOHAMA, Kanagawa, Japan)

PPS01-P02 Room:Poster Time:April 30 18:15-19:30

Development of JUICE/Ganymede Laser Altimeter (GALA)

NAMIKI, Noriyuki[1] ; KIMURA, Jun[2*] ; KOBAYASHI, Masanori[1] ; HUSSMANN, Hauke[3] ; LINGENAUBER, Kay[3] ; TEAM, Gala-japan[4]

[1]PERC/Chitech, [2]Earth-Life Science Institute, Tokyo institute of Technology, [3]DLR Institute of Planetary Research, [4]JUICE Japan Group

The overarching theme for JUICE is: The emergence of habitable worlds around gas giants, and the focus is to characterise the conditions that may have led to the emergence of habitable environments among the Jovian icy satellites, with special emphasis on the three oceanbearing worlds, Ganymede, Europa, and Callisto. JUICE will be launched in 2022, and will arrive at Jupiter in 2030. After several fly-bys to Europa and Callisto, JUICE will be inserted into an orbit around Ganymede in 2032 and will continue scientific observations for eight months until the end of nominal mission in 2033. Ganymede Laser Altimeter, GALA, measures distance between the spacecraft and the surface of the satellite from time of flight of a laser pulse. Together with positions of the spacecraft and mass center of the satellite, surface topography of the satellite is calculated from measured distances. The GALA data are particularly important for finding of internal ocean.

1) if the ocean exists beneath icy crust, tidal deformation of the satellite is so large that temporal variation of the topography as great as a few tens meter shall be detected.

2) small eccentricity of orbit of Ganymede causes libration that will be observed as lateral shifts of footprint of laser beam at the surface.

3) improved determination of spacecraft orbits by cross over analysis results in precise estimate of low degree harmonics of gravity field. Thus accurate Love number will be calculated to infer internal density structure of the satellite.

Global topographic data derived by GALA are also important for the study of tectonic history at the surface, elastic and viscous structure of ice crust, and thermal evolution of interior of the icy satellite. For example, linear structures such as ridges and grabens reveal extension stresses due to past variation of thermal states. As well, flat surface and thin crust may indicate partial melting of the crust and consequent internal lake. These observations on various geologic activities lead to understanding of transport of heat and materials from interior to the surface. Further, a comparison of styles of tectonics of ice crust and that of silicate lithosphere will likely shed a new light on the theory of plate tectonics of the Earth.

GALA is developed by international collaboration of scientists and engineers in Germany, Switzerland, and Japan. Its conceptual design is based on the laser altimeter on board of Mercury orbiter, BepiColombo, and consists of transceiver unit (TRU) with laser optics and appropriate electronics, electronic unit (ELU) with digital range finder module, digital processing module and power converter module, and laser electronic unit (LEU) with laser control electronics. Japanese team provides receiver telescope, backend optics, detector, and analogue electronics of TRU. The transmission optics of TRU and entire LEU are developed at DLR in Germany, and ELU is developed at Bern University in Switzerland. Assembly and integration are conducted at DLR under a supervision of the principal investigator of GALA. We therefore need to pay special caution on interfaces between analogue electronics and range finder, low-temperature environment, and radiation environment that Japanese space scientists have never experienced before.

Keywords: Jupiter, Ganymede, Laser Altimeter, Exploration, Spacecraft, Habitability

Japan Geoscience Union Meeting 2014
(28 April - 02 May 2014 at Pacifico YOKOHAMA, Kanagawa, Japan)

PPS01-P03 Room:Poster Time:April 30 18:15-19:30

Accretion of Solid Materials onto Circumplanetary Disks from Protoplanetary Disks

TANIGAWA, Takayuki[1*] ; MARUTA, Akito[2] ; MACHIDA, Masahiro[2]

[1]ILTS, Hokkaido University, [2]Kyushu University

We investigate accretion of solid materials onto circumplanetary disks from heliocentric orbits rotating in protoplanetary disks, which is a key process for the formation of regular satellite systems. In the late stage of gas-capturing phase of giant planet formation, the accreting gas from protoplanetary disks forms circumplanetary disks. Since the accretion flow toward the circumplanetary disks affects the particle motion through gas drag force, we use hydrodynamic simulation data for the gas drag term to calculate the motion of solid materials. We consider wide range of size for the solid particles (10^{-2}-10^{6}m), and find that the accretion efficiency of the solid particles peaks around 10m-sized particles because energy dissipation of drag with circumplanetary disk gas in this size regime is most effective. The efficiency for particles larger than 10m size becomes lower because gas drag becomes less effective. For particles smaller than 10m, the efficiency is lower because the particles are strongly coupled with the back-ground gas flow, which prevent particles from accretion. We also find that the distance from the planet where the particles are captured by the circumplanetary disks is in a narrow range and well described as a function of the particle size.

Keywords: satellite formation, circumplanetary disks

Japan Geoscience Union Meeting 2014
(28 April - 02 May 2014 at Pacifico YOKOHAMA, Kanagawa, Japan)

PPS02-01 Room:418 Time:April 28 09:00-09:25

Hydrogen Isotope Ratio and Thickness of Martian Ground Ice: Implication from Multi-Water-Reservoir Model

KUROKAWA, Hiroyuki[1*] ; USUI, Tomohiro[2] ; DEMURA, Hirohide[3] ; SATO, Masahiko[4]

[1]Nagoya University, [2]Tokyo Institute of Technology, [3]University of Aizu, [4]Kyushu University

Martian surface ice is currently observed only as polar layered deposits (PLDs), whereas Mars Odyssey Gamma Ray Spectrometer (Boynton et al., 2002; Boynton et al., 2007) and Mars Express radar sounder observations (Mouginot et al., 2012) propose the presence of much larger amount of ground ice in the mid- to high-latitudes. The total volume of PLDs is 20-30 m in Global Equivalent Depth (Zuber et al., 1998; Plaut et al., 2007). Ground-ice region is expected to spread over a few tenths of percent of the total Martian surface, yet the thickness (i.e. volume) is poorly constrained (Mouginot et al., 2012).

The thickness of the ground ice is related to the evolution history of the Martian water reservoirs. After ancient oceans became extinct (˜4Ga), the oceanic water would become ”surface ice”, which currently occur as PLDs, and ”ground ice” which would extend from high latitude to mid- or low-latitude. Atmospheric escape of hydrogen and oxygen through the Martian history causes decrease of the amount of the ice. The signature of the evolution history is recorded by hydrogen isotope ratio (D/H). Martin atmosphere and soil have D/H ratio of ˜6 (relative to SMOW) (Owen et al., 1988; Webster et al., 2013), which is higher than the Martian primitive D/H ratio of ˜1.3 (Usui et al., 2012).

We constrain the hydrogen isotope ratio of surface ice and ground ice, and estimate the thickness of ground ice, using a multi-water-reservoir box model (see figure shown below). The model solves the evolution of water inventories and D/H ratio of atmosphere, surface ice, and ground ice during the ice age. Atmospheric escape and sublimation are considered as D/H fractionation processes. We adapt our model to the Matian ice age (4Ga to present). The initial D/H ratio is that of ancient ocean, which is informed by D/H data of the Martian meteorite ALH84001 formed at ˜4.1Ga (Lapen et al., 2010): D/H = 2.2-4.0 (relative to SMOW) (Boctor et al., 2003,Greenwood et al., 2008).

First, we show the results from two water-reservoir box model (ice and atmosphere). The ratio of atmospheric D/H and ice D/H is in a quasi-equilibrium state of the fractionation caused by atmospheric escape and sublimation. The ratio of the present Mars is mainly determined by the fractionation caused by sublimation.

Second, we show the results from four water-reservoir box model (surface ice, ground ice, high-latitude atmosphere, and mid- to high-latitude atmosphere). Assuming the atmospheric condition of the present Mars, the mixing of two atmospheric reservoir is inefficient in D/H exchange between surface ice and ground ice, which results in the independent growth of D/H ratio of the surface ice and the ground ice. To fractionate the D/H ratio of the surface ice and the ground ice into ˜6, the thickness of active ground ice which can exchange water with atmosphere is constrained. Thin active ice causes high deuterium concentration. The required thickness is a few hundred meters, which is distinctly large value compared to the thickness that HDO diffusion works (˜10 m in 1 Gyrs). Nature of this active ground ice might be partially melted ice suggested by recent observations of recurring slope lineae (McEwen et al., 2014), hydrated clathrates in underground cryosphere, or breathing porous permafrosts.

Keywords: ground ice, hydrogen isotope ratio, atmospheric escape

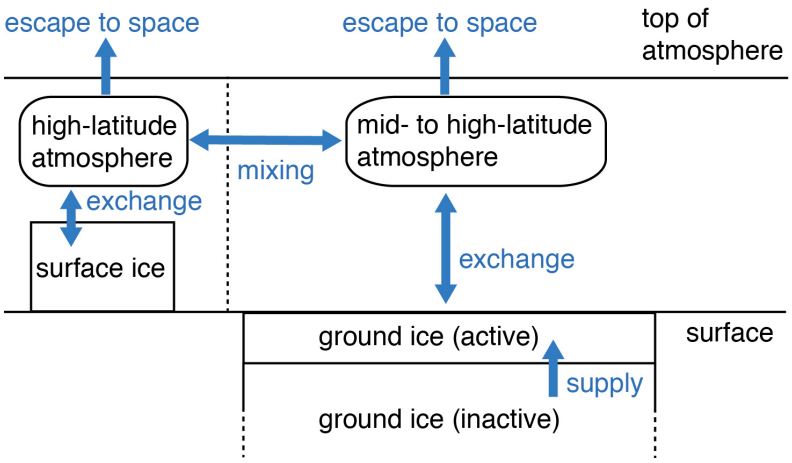

Japan Geoscience Union Meeting 2014
(28 April - 02 May 2014 at Pacifico YOKOHAMA, Kanagawa, Japan)

PPS02-02 Room:418 Time:April 28 09:25-09:50

New evidence for plate tectonism on Mars: Accreted Terrains

DOHM, James[1*] ; MARUYAMA, Shigenori[1]

[1]Earth-Life Science Institute, Tokyo Institute of Technology

Reported evidence for plate tectonism has included spatial association among magnetic anomalies, large (thousands of kilometers long) structures, and highly degraded promontories interpreted to be andesitic domes, thrust faults, folds, structurally-controlled basins, large mountain ranges, and topographic and crustal-thickness-model signatures of structural control (including plate movement) within and along the margin of the northern plains. Significant evidence for an ancient phase of plate tectonism on Mars, newly identified, is accretionary complexes, informed through Earth analogs exquisitely detailed here in Japan. This finding represents a new frontier in the geologic investigation of Mars, bringing greater attention to pre-Tharsis (˜>4.0 Ga) terrains, which record Earth-like conditions. Pre-Tharsis, Earth-like conditions include an active dynamo and plate tectonism, as well as Habitable-Trinity conditions?an ocean, relatively thick atmosphere, and primordial crustal materials enriched in phosphorous, iron, among other elements important to life, all of which interact due to hydrological cycling driven by the Sun. Accreted terrains, which mark major crustal shortening through subduction of oceanic crustal materials and associated accumulation of andesites and granites, could comprise rock records on Mars dating back more than 4.2 Ga. Considering planetary evolution of Mars, largely informed through our understanding of the evolution of Earth, the accretionary complexes are likely to record environmental conditions during a time range of several hundred million years, which includes possible fossil life if initiated and evolved during the extremely ancient (>4.0 Ga) Habitable-Trinity conditions. A prime example of an extremely ancient accretionary complex is located to the west of Claritas rise, southwest margin of the Tharsis superplume. At the meeting we will present evidence of a Martian accretionary complex and discuss the implications of such a significant finding, including highlighting the next phase of geologic investigation of the evolution of Mars and its bearing on Astrobiology.

Keywords: Plate tectonics, accretional complex, OPS

Japan Geoscience Union Meeting 2014
(28 April - 02 May 2014 at Pacifico YOKOHAMA, Kanagawa, Japan)

PPS02-03 Room:418 Time:April 28 09:50-10:15

Environmental monitoring camera system for the Martian aerosols and water vapor for the Japanese Mars rover, MELOS

MANAGO, Naohiro[1*] ; NOGUCHI, Katsuyuki[2] ; OGOHARA, Kazunori[3] ; SUZUKI, Makoto[4] ; HASHIMOTO, George[5]

[1]Chiba University, [2]Nara Women's University, [3]University of Shiga Prefecture, [4]Japan Aerospace Exploration Agency, [5]Okayama University

We propose the environmental monitoring camera system of aerosols and water vapor in the Martian atmosphere for the Japanese Mars rover, MELOS. The meteorology and the climate of Mars are strongly controlled by the aerosols, which consists of dust and clouds in the Martian atmosphere, and the better understanding of the basic parameters such as optical depth, radius distribution and composition of the aerosols enables us to describe the effect on the Martian meteorology and climate quantitatively. The water vapor also affects the Martian meteorology and climate through the infrared radiation and the generation of clouds. The MELOS aims at the search for life, and it needs the basic knowledge of the meteorology and climate at the landing site for detailed discussion. Therefore we should conduct the measurements of aerosols and water vapor at the MELOS landing site simultaneously.

To satisfy the requirement of monitoring the aerosols and water vapor in the MELOS rover mission, we propose a three-CMOS-camera system, which consists of a direct sunlight camera, a scattering light camera and a high-resolution color camera. The direct sunlight camera has four wavelength band (340 or 450nm and 550nm for aerosols and 870 and 940nm for water vapor). The scattering light camera also has the same wavelength band, but it is directed at the neighborhood of the sun and at several points along the great circle including the sun and is utilized for aerosol measurements. The arrangement proposed here basically follows the previous Mars missions, e.g., Viking lander, Mars Pathfinder and Mars Exploration Rover. The high-resolution color camera obtains pseudo color pictures around the rover and is intended to support the navigation for the life search experiment.

Keywords: MELOS rover mission, Martian atmosphere

Japan Geoscience Union Meeting 2014
(28 April - 02 May 2014 at Pacifico YOKOHAMA, Kanagawa, Japan)

PPS02-04 Room:418 Time:April 28 10:15-10:30

Examination of Mission Scenario and Spacecraft System to Study Martian Atmospheric Escape

MATSUOKA, Ayako[1*] ; SEKI, Kanako[2] ; TERADA, Naoki[3] ; YOKOTA, Shoichiro[1] ; YAMAZAKI, Atsushi[1] ; KAWAKATSU, Yasuhiro[1] ; ABE, Takumi[1] ; FUTAANA, Yoshifumi[4] ; HIRAHARA, Masafumi[2] ; IMAMURA, Takeshi[1] ; ISHISAKA, Keigo[5] ; KUMAMOTO, Atsushi[3] ; KURIHARA, Junichi[6] ; NAKAGAWA, Hiromu[3] ; OGURA, Satoshi[1] ; SAKANOI, Takeshi[7] ; TAGUCHI, Makoto[8] ; YAGITANI, Satoshi[9]

[1]ISAS/JAXA, [2]STEL, Nagoya Univ., [3]Dept. Geophys., Grad. Sch. Sci., Tohoku Univ., [4]IRF, Sweden, [5]Toyama Pref. Univ., [6]Planet. Plasma Atmos. Res. Cent., Tohoku Univ., [7]Cosmosciences, Hokkaido Univ., [8]Rikkyo Univ., [9]Kanazawa Univ.

The atmospheric escape from Mars is considered to be closely associated with the evolution of the Martian atmosphere as well as the existence of the water on Mars. We are now investigating a project to study the global feature and the physical process of the atmospheric escape from Mars. It is expected to consist of at least two orbiters; one of the orbiters is aimed to make in-situ observation of plasma and thin atmosphere at about 100 km altitude, and the other is for the atmospheric imaging and solar-wind monitor. We are planning to make simultaneous observation of the atmospheric escape by the interaction with the solar wind by both of in-situ measurement orbiter and remote-sensing one. Now we are examining the quantitative measurement targets to fully understand the Martian atmospheric escape. At the same time, the sorts and performance of scientific instruments on these orbiters are examined. And furthermore, the preliminary spacecraft design, orbit design and mission plan to achieve the scientific goal are investigated.

Japan Geoscience Union Meeting 2014
(28 April - 02 May 2014 at Pacifico YOKOHAMA, Kanagawa, Japan)

PPS02-05 Room:418 Time:April 28 10:30-10:45

Development of a dust imager for Mars landing mission

SATOH, Takehiko[1*] ; OGOHARA, Kazunori[2] ; HASHIMOTO, George[3] ; MIURA, Kazuhiko[4] ; MANO, Takaaki[5]

[1]Japan Aerospace Exploration Agency, [2]University of Shiga Prefecture, [3]Okayama University, [4]Tokyo University of Science, [5]National Institute for Materials Science

We report progress in developing a dust imager for future Mars landing missions. As Martian dust is a key element of its environment and a potential hazard for human exploration, it is essential to know what is Martian dust and how it works. However, little is known about the Martian dust due primarily to lack of measurements. Direct imaging would greatly increase our knowledge about the Martian dust (previously, an Atomic-Force Microscope onboard Phoenix acquired just one image).

The dust imager under development is not a microscope but a ”bare” imaging sensor of which pixels are fine pitched. After exposing the sensor to the air with dust for a while, we illuminate the sensor with a parallel beam so that shadows of particles on the sensor are directly imaged. In this way, the imager does not need a focusing mechanism and is expected to be very light-weighted and robust. Although the status is still the laboratory-experiment level, this small tool would greatly contribute to the Mars science and exploration.

Keywords: Mars, dust, imager, landing, mission

Japan Geoscience Union Meeting 2014
(28 April - 02 May 2014 at Pacifico YOKOHAMA, Kanagawa, Japan)

PPS02-06 Room:418 Time:April 28 11:00-11:25

Life Detection Microscope: Search for Microbes on the Mars Surface with a Fluorescent Microscope

YAMAGISHI, Akihiko[1*] ; SATOH, Takehiko[2] ; ENYA, Keigo[2] ; MIYAKAWA, Atsuo[1] ; SASAKI, Satoshi[3] ; YOSHIMURA, Yoshitaka[4] ; HONDA, Hajime[5] ; DEMURA, Hirohide[6] ; IMAI, Eiichi[5] ; USUI, Tomohiro[7] ; FUJITA, Kazuhisa[8] ; ISHIGAMI, Genya[9] ; OZAWA, Takashi[8] ; OHNO, Sohsuke[10] ; SASAKI, Sho[11] ; MIYAMOTO, Hideaki[12]

[1]Tokyo University of Pharmacy and Life Sciences, [2]ISAS/JAXA, [3]Tokyo University of Technology, [4]Tamagawa University, [5]Nagaoka Univ. Tech., [6]The University of Aizu, [7]Tokyo Institute of Technology, [8]JAXA, [9]Keio University, [10]Chiba Institute of Technology, [11]Osaka University, [12]The University of Tokyo

Past trial of direct detection of life on Mars by 1970's Viking mission reported a negative conclu-sion, whereas numbers of circumstances provided by recent Mars exploration missions in the last dec-ade indicate that there are good reasons to perform another life detection program.

Here we propose Life Detection Microscope that has much higher sensitivity than the instrument onboard Viking. Indeed Life Detection Microscope (LDM) that we propose here could detect less than 104 cells in 1 gram clay. Our life detecting instru-ment has the sensitivity that is three orders of mag-nitude higher than the one onboard Viking that issued the negative conclusion. LDM is capable of identifying what we think to be the most fundamen-tal features that a cell should possess to constitute life.

Our Investigation Goals are:

1: High-resolution characterization of regolith and dust particles.

2: Search for any type of organic compounds in Mars surface samples. The compounds include cells, other biological materials, and abiotic polycyclic aromatic hydrocarbon (PAH).

3: Identify cell-like structure in which organic compounds are enveloped by membrane, which may represent Martian life.

Keywords: Mars, Life search, Fluorescence microscope, Microbe, Organic compounds

Japan Geoscience Union Meeting 2014
(28 April - 02 May 2014 at Pacifico YOKOHAMA, Kanagawa, Japan)

PPS02-07 Room:418 Time:April 28 11:25-11:40

Landing-site candidates for the Life Detection Microscope instrument

MIYAMOTO, Hideaki[1*] ; USUI, Tomohiro[2] ; KOMATSU, Goro[3] ; DOHM, James[2] ; NIIHARA, Takafumi[4] ; OGUMA, Midori[1] ; SATOH, Takehiko[5] ; YAMAGISHI, Akihiko[6]

[1]University of Tokyo, [2]TiTech, [3]IRSPS, [4]National Institute of Polar Research, [5]ISAS, [6]Tokyo University of Pharmacy and Life Science

Mars explorations of past decades indicate that ancient Mars had environment somehow similar to that of Earth. Existence of large bodies of water, chemical building blocks of life, a wide range of oxidation states, and a magnetic field indicate that Mars would have been habitable. Recent studies of microbes in extreme environments show that some terrestrial microbes have possibilities for surviving and proliferating under the current martian environment, if these are placed in some specific conditions such as with sufficient shield from UV light (attained only at more than several centimeters below the surface) and with the existence of gradients of free energy. Such environmental conditions likely exist at some specific locations even the present Mars. For this reason, we are developing a new instrument called LDM (Life Detection Microscope), which is designed to detect less than 10^4 cells in 1 gram clay, orders of magnitude higher than previous attempts performed by Viking landers. To maximize the chances of the detection of organisms, the landing sites should be carefully selected in terms of the possibility of the existence of near-surface water, as well as recent geological activities and release of volatiles. Traces of possible liquid water flow have been reported at a number of locations including those recognized as the recurring slope lineae, seasonal flows on slopes of several craters, and anastomosing slope streaks. These are proposed to be the result of small and continuous seeps of subsurface brine water, which could persist for a longer period providing a habitable environment. In this talk, we examine the morphologic characteristics of these features and discuss their origins in the line of geological contexts for selecting appropriate landing sites for the LDM instrument.

Keywords: Mars, extraterrestrial life, life detection microscope, landing site, water

Japan Geoscience Union Meeting 2014
(28 April - 02 May 2014 at Pacifico YOKOHAMA, Kanagawa, Japan)

PPS02-P01 Room:Poster Time:April 28 18:15-19:30

Interannual analyses of the meridional distributions of Martian dust and clouds obtained by MRO-MCS

NOGUCHI, Katsuyuki[1*] ; IMAE, Kaori[1] ; KAWANISHI, Mai[1]

[1]Nara Women's University

We investigated the interannual variability of the meridional distributions of dust and clouds in the Martian atmosphere by using Mars Reconnaissance Orbiter Mars Climate Sounder (MRO-MCS) measurements. As the previous analyses did not consider measurement errors to depict the zonal averages, we took a criterion of 10% for the measurement error. Results show that Mars Year (MY) 29, which is regarded as a standard year in the previous analyses, had an enhancement of dust in the high altitudes (above 10 Pa) in the tropical region, and such an enhancement was not found in other MYs (28, 30 and 31). On the other hand, the distribution of ice clouds in MY 29 roughly agreed with other MYs' distribution.

Japan Geoscience Union Meeting 2014
(28 April - 02 May 2014 at Pacifico YOKOHAMA, Kanagawa, Japan)

PPS02-P02 Room:Poster Time:April 28 18:15-19:30

Implementing Martian dust lifting scheme into DCPAM, and a diagnosis experiment of surface dust flux

OGIHARA, Hirotaka[1*] ; TAKAHASHI, Yoshiyuki O.[2] ; ISHIWATARI, Masaki[1] ; ODAKA, Masatsugu[1] ; HAYASHI, Yoshiyuki[3]

[1]Department of Cosmosciences, Graduate school of Science, Hokkaido University, [2]Graduate School of Science, Kobe University, [3]Department of Earth and Planetary Sciences, Graduate School of Science, Kobe University

The Martian dust cycle influences thermal states of its atmosphere, hence it plays an important role for determining states of the Martian atmosphere(Gierasch and Goody, 1968). Dust processes to be considered are dust lifting, turbulent mixing, advection, and gravitational sedimentation. Parameterizations of lifting by model resolved wind stress and by model unresolved vortices such as dust devils are considered. The Martian dust cycle has been simulated with general circulation models implemented above dust process schemes by some research groups. For example, Kahre et al.(2006) roughly simulated a seasonal variation of dust loading. The seasonal variation of dust loading has a peak in during northern autumn and winter. In contrast, DCPAM (Takahashi et al., 2012), which is a general circulation model developed by our group, has not been implemented above dust process schemes. Aims of this study are to implement dust process schemes into DCPAM, and to perform numerical experiments on the dust cycle with it. In the future, we will consider about interannual variability of the Martian dust distribution, which still has not been reproduced. In this work, we implement dust lifting scheme by model resolved wind stress into DCPAM. Addtionally, we perform an experiment with dust lifting to investigate behavior of this dust lifting scheme. And, we compare our model's results with thoses of Kahre et al.(2006).

The model utilized is DCPAM which is developed by GFD Dennou Club. DCPAM adopted three dimensions primitive equations. A radiative scheme by Takahashi et al.(2003, 2006) is used. This include the radiative effects of gaseous CO_2 and suspended dust. And, used suspended dust distribution is spatially and temporally fixed. A turbulent process is estimated by used vertical diffusivity based on Mellor and Yamada(1974). A surface process is estimated based on Louis et al.(1982). Each parameter are selected as Martian values. We use a surface distribution of thermal inertia, albedo and topography observed by Mars Grobal Surveyor. A horizontal discretization is the spectral method, and the trauncation wavenumber is 21. A vertical discretization is the finite difference method, and the number of layor is 32. We integrate 3 Mars year, and use the last 1 Mars year for analysis.

First, we implement a dust lifting scheme called by KMH scheme(Kahre et al., 2006) into DCPAM. Then, we perform a diagnosis experiment of surface dust flux with this. This result is similar to result by Kahre et al.(2006) as follows. In regions around latitude 50N degree and 30S degree, strongly dust lifting occurs during northern autumn and winter. At latitude 50N degree, it appears that eastward waves, which have zonal wavenumber 1 and period 6 Mars days, contribute to dust lifting. it is to be considered the baroclinic wave(Briggs et al., 1979). At latitude 30S degree, it appears that westward waves, which have zonal wavenumber 1 and period 1 Mars days, contribute to dust lifting. It is to be considered the diurnal thermal tidal wave(Joshi et al., 1979), and dust lifting tends to occur at 16 o'clock local time. These results qualitatively are consistent with these of Kahre et al. (2006), but are not quantitatively consistent with these of Kahre et al.(2006). For example, our model's surface dust flux is greater by a degree of magnitude then these of Kahre et al.(2006) in the northen polar cap. The reason is probably that the number of vertical levels and the method for estimating turbulent mixing are diffrent from those of Kahre et al.(2006). In this work, we implemented dust lifting scheme by model resolved wind into DCPAM. We are now implementing dust lifting scheme by dust devils into DCPAM. Then, we are going to implement advective scheme and gravitational sedimentation scheme into DCPAM in turn, and perform numerical experiments for their implementation test.

Keywords: Dust, Mars, General Circulation Model

Japan Geoscience Union Meeting 2014
(28 April - 02 May 2014 at Pacifico YOKOHAMA, Kanagawa, Japan)

PPS02-P03 Room:Poster Time:April 28 18:15-19:30

Assessment of Mars surface environment for MELOS1 lander using Planetary General circulation model DCPAM

ODAKA, Masatsugu[1*] ; SUGIYAMA, Ko-ichiro[2] ; TAKAHASHI, Yoshiyuki O.[3] ; NISHIZAWA, Seiya[4] ; HAYASHI, Yoshiyuki[5] ; HASHIMOTO, George[6]

[1]Department of Cosmosciences, Hokkaido University, [2]Institute of Space and Astronautical Science, Japan Aerospace Exploration Agency, [3]Center for Planetary Science, [4]RIKEN Advanced Institute for Computational Science, [5]Department of Earth and Planetary Sciences, Graduate School of Science, Kobe University, [6]Department of Earth Sciences, Okayama University

1. Introduction

The Mars exploration program MELOS1, which is to mainly challenge life and surface environment exploration, is now planning by space engineering and planetary science community in Japan. To support designing the landing module and observation instruments and ensure safety experiments during entry, decent and landing phase, plausible range of meteorological conditions at MELOS1 landing site is required.

We try to assess the Mars surface environment from planetary to atmospheric boundary layer scale by using simulation results obtained by General Circulation Model (GCM), Regional Meteorological model, and Large Eddy Simulation (LES) model (LES). For mesoscale assessment, CReSS which is developed by HyArc Nagoya University will be used. For boundary layer scale, SCALE-LES which is developed by RIKEN AICS will be used as LES model. Both numerical model are now tuned to Mars and preliminary experiments are performed (Sugiyama et al. 2013; Nishizawa et al. 2013). For planetary scale assessment, we use a planetary atmospheric general circulation model DCPAM which is developed by GFD Dennou Club (Takahashi et al. 2012). In this study, we compare simulation results of DCPAM to observation results of Viking and Mars Path Finder (MPF) and investigate proper method for assessment of Mars surface environment by using DCPAM data. By using this method, we show some assessment results at proposed landing sites of MELOS1.

2. Data

DCPAM is a spectral GCM including physical processes appropriate for Martian atmosphere. The topography, surface albedo and thermal inertia in the model is based on observation results obtained by Mars Global Surveyor (MGS). The horizontal truncation wave number is 31, which corresponding horizontal resolution is about 200 km. The number of vertical layer is 16 and the height of lowest level is about 3 m. The seasonal variation of atmospheric dust distribution is given which is based on typical case of MGS observation. Numerical integration is performed for 7 Mars years with isothermal no motion initial condition. The data of last two years are used for analysis. The proposed landing sites are Newton Crater, Nili Fossae, and Isidis Planitia. The period of analysis is 90 sols from Ls = 331, 324, 14, and 135 which are corresponding to four mission window. In each period, diurnal variations every 15 sols are investigated.

3. Methods of analysis and results

In comparing the DCPAM results to observation results of Viking and MPF, the atmospheric temperature and wind velocity at observed altitude are estimated assuming the boundary layer similarity theory in neutral case is valid near the model surface. The surface pressure at actual altitude is estimated assuming hydrostatic balance with constant scale height which is calculated by the using model temperature. The comparison between estimated values from DCPAM results and observations show that the observed diurnal variation of atmospheric temperature is well reproduced by using 2nd level (about 12.5 m height) temperature of DCPAM, and seasonal variation of surface pressure is almost represented by using the scale hight corresponding to 10th level (about 1.35 km height) model temperature and subtracting offset value (60 Pa).

Based on above results, analysis of the DCPAM data at the three proposed landing site during four mission periods are performed. At Newton Crater, which is the first proposed site, during 90 sols from Ls = 331, the diurnal mean atmospheric temperature ranges from 190 to 220 K. The amplitude of diurnal change of atmospheric temperature is about 50 - 70 K. The air temperature is almost constant during this period and its value is about 140 K. The maximum values of direct and diffuse solar radiative flux are 480 Wm^{-2} and 40 Wm^{-2}, respectively. We will also estimate the extent of variation of meteorological variables, such as temperature and pressure, at the proposed landing sites by analyzing DCPAM data with different dust distribution.

PPS02-P03 Room:Poster Time:April 28 18:15-19:30

Keywords: Exploration of Mars, General Circulation Model, Surface environment of Mars

Japan Geoscience Union Meeting 2014
(28 April - 02 May 2014 at Pacifico YOKOHAMA, Kanagawa, Japan)

PPS02-P04 Room:Poster Time:April 28 18:15-19:30

Estimation of Martian atmospheric composition change caused by CO2 condensation and its application to radio occultation

IKEDA, Sayaka[1*] ; NOGUCHI, Katsuyuki[1] ; KURODA, Takeshi[2] ; PAETZOLD, Martin[3]

[1]Nara Women's University, [2]Tohoku University, [3]University of Cologne

We estimated the Martian atmospheric composition change caused by CO_2 condensation using the Ar measurements obtained by Gamma Ray Spectrometer (GRS) onboard the 2001 Mars Odyssey. We applied this estimation of the composition change to the rederivation of the radio occultation (RO) measurements of Mars Global Surveyor (MGS) obtained at polar latitudes of the winter hemisphere, because the MGS RO standard product which is available to the public did not consider the atmospheric composition change by CO_2 condensation. Using the rederived MGS RO measurements, we investigated the occurrence of CO_2 supersaturation in the Martian polar winter atmosphere and found that there were more supersaturation in the rederived data than in the original data.

Keywords: Mars, CO2, supersaturation, condensation, radio occultation

Japan Geoscience Union Meeting 2014
(28 April - 02 May 2014 at Pacifico YOKOHAMA, Kanagawa, Japan)

PPS02-P05 Room:Poster Time:April 28 18:15-19:30

Equation of state of $(Fe,Ni)_3S$ phase - Implications for Mars internal structure

AKAGI, Shunsuke[1] ; SAKAI, Takeshi[1*] ; HIRAO, Naohisa[2]

[1]Geodynamics Research Center, Ehime University, [2]Japan Synchrotron Radiation Research Institute

The existence of lower mantle ($MgSiO_3$-perovskite layer) has an important role on Mars thermal evolution. The layer thickness of Mars lower mantle depends on the depth of the core-mantle boundary (CMB). The depth of CMB is related to the Mars core density. Although the structure model of Mars core was discussed based on the equation of state of pure iron and FeS (e.g., Urakawa et al., 2004), Fe_3S phase and also the effect of nickel on the density should be considered.

We newly established the equation of state (EoS) of $(Fe_{0.89},Ni_{0.11})_3S$ up to about 40 GPa by high pressure experiment using diamond anvil cell. Considering EoSs of γ-Fe (Tsujino et al., 2013), γ-FeNi (Tsujino, 2012), Fe_3S (Seagle et al., 2006), and $(Fe_{0.89},Ni_{0.11})_3S$, the effects of nickel and sulfur on the density was determined. Then, we determined the Mars core density corresponding to the composition model based on SNC meteorites. Our new model shows relatively thin lower mantle compare to previous one. Moreover, if Mars core contains 16 wt.%S and 7 wt.%Ni (Sanloup et al., 1999) and if Mars has an entirely liquid core (Fei and Bertka, 2005), there is a possibility of disappearance of Mars lower mantle.

Keywords: Mars core, equation of state, Mars lower mantle

Japan Geoscience Union Meeting 2014
(28 April - 02 May 2014 at Pacifico YOKOHAMA, Kanagawa, Japan)

PPS03-01 Room:424 Time:April 29 09:00-09:15

About drift, oscillations and steps of the center of mass of the Moon

BARKIN, Yury[1*] ; HANADA, Hideo[2]

[1]Sternberg Astronomical Institute, Moscow, Russia, [2]National Astronomical Observatory of Japan, Mizusawa, Japan

We have previously predicted and studied a step (abrupt) shift of the center of mass of the Earth in 1997 - 1998 years relatively to the mantle (Zotov, Barkin, Lubushin, 2009). In accordance with the basic provisions of the geodynamic model of excitation of planets and satellites shells (Barkin, 2002) we expected and we expect similar displacements of the centers of mass for other bodies in the solar system (for Mercury, Moon, Sun, Titan, Mars, etc.). Moreover, according to our hypothesis these abrupt geodynamic phenomena for solar system bodies are synchronous (Barkin, 2000) and, in particular, it should appear in 1997-1998. On the Earth, the similar jumps in 1997-1998 were observed in almost all planetary processes (Barkin, 2009). In the case of the Moon similar jump of center of mass obtains a confirmation in the data of laser observations and accounts for a specified period of time 1997-1998.

The jump (step) in the center of mass of the Moon in 1997 on data of laser ranging of reflectors on the lunar surface. On the basis of current laser measurements of distances to reflectors mounted on the Moon the preliminary estimates of the parameters of drift, oscillations and jump of the center of mass of the Moon were obtained. Their dynamic interpretation on the base of a geodynamic model of forced relative oscillations of the shells of planets and satellites has been done (Barkin, 2002). In the paper of G.A. Krasinskii (2003) from the analysis of lunar laser range measurements (or rather their residual differences compared with the theoretical celestial-mechanical design values of ranges) an abrupt (step) changes (in 1997 - 1998) in the coordinates of reflectors on the very substantial distances of about 15 -25 cm in selenographic coordinate system of the epoch have been discovered. Since jumps of coordinates for all four observed reflectors were quite close, it is natural to assume that the jump occurred in the position of the center of mass of the Moon by about 25-35 cm relatively to the lunar crust (in direction toward the Earth). Extremely important here is the fact that the jumps occurred in 1997-1998, as it was predicted by the theory of the unified geodynamic synchronous rhythms in variations of the activity of natural processes on the bodies of the solar system (Barkin, 2000). For the mean values of displacements of reflectors the following values were obtained (in meters): -0.15 +/- 0.04 m (offset along x coordnate - from the Earth), 0.23 +/- 0.07 m (offset on y - east), - 0.23 +/- 0.07 m (offset along z - to the north). Thus in 1997, the center of mass of the Moon abruptly shifted to a geographical point on the lunar surface with coordinates 40.0o N, 32.1o W approximately on distance in 0.36 +/- 0.11 m. According to the Krasinskii work (2003) we have identified trends in the changes of distances to reflectors and their abrupt changes before 1997 and after 1998, with rates of about 0.036 ns / year (before the jump) and at a rate of 0.128 ns / year (after the jump). If we consider only the drift relatively to the axis x, then estimates the drift velocities decrease: 0.98 cm / year - until 1997 and 1.47 cm / year - since 1998. It is expected to perform a spectral analysis of the residual differences of distances in order to identify their cyclic variations (with lunar months periods and with multiple periods).

Keywords: center of mass of the Moon, jumps and trends of center of mass of the Moon, LLR data

Japan Geoscience Union Meeting 2014
(28 April - 02 May 2014 at Pacifico YOKOHAMA, Kanagawa, Japan)

PPS03-02 Room:424 Time:April 29 09:15-09:30

Interpretation of unexplained secular changes of the lunar orbit

BARKIN, Yury[1*]

[1]Sternberg Astronomical Institute, Moscow, Russia

Unexplained secular effects in the orbital motion of the Moon are consequences of the observed phenomenon of remove of the center of mass of the Moon relatively to its mantle and crust toward the back-side. An explanation of anomalous part of secular variation in the longitude of the Moon and in the eccentricity of the lunar orbit has been obtained.

Unexplained secular variation of the eccentricity of the lunar orbit. In the works of James Williams and his colleagues showed that the observed rate of secular change of the eccentricity of the orbit of the Moon in 2.3x10 (-11) 1/year can not be explained within the framework of the classical model of the tides. Earth tides give only a fraction of the value specified in 1.3x10 (-11) 1/year and lunar tides result even effect with the opposite sign and give part of the acceleration in -0.6x10 (-11) 1/year. Remains unexplained an anomalous part of the secular change in the eccentricity (1.6 +/- 0.4) x10 (-11) 1/year. This value corresponds to abnormal changes in the distances to the perigee and apogee at 6 mm / year. ”Abnormal speed distances to the perigee and apogee of the lunar orbit is up to 6 mm / year and its cause is unknown” (Williams J.,2006).

Tidal acceleration and evolution of the Moon’s orbit. Laser ranging method proved to be very sensitive to the tidal acceleration of the Moon. Tides on the Earth dominate in the transfer of angular momentum, and energy in the orbital motion, in particular in the removal of the Moon from the Earth. Tidal effects on the Moon are separable from the effects of Earth tides in laser range measurements to the Moon (Chapront et al., 2002; Williams et al., 2009). Full tidal acceleration in the mean orbital longitude (due to the tides of the Earth and the Moon) is estimated at -25.85” 1/cy2, corresponding to the removal of the Moon from the Earth at a speed of 3.81 cm / year (Williams et al., 2009). The rate of secular variation of the eccentricity of the lunar orbit e = (9 +/- 3) x10 (-12) 1/year also detected on the basis of long laser observations over a period of 38.7 years (March 16, 1970 - November 22, 2008) (Williams, Boggs, 2009). The basis of dynamical studies makes a precision lunar ephemeris DE421, taking into account all of Newtonian and Einsteinian effects. The authors believe that the study of the evolution of the lunar orbit is an important and surprisingly difficult task. Lunar laser ranging provides the numerical values for the two sources of dissipation on the Earth and the Moon.

Possible secular drift of the center of mass of the Moon relative to its crust and mantle toward the back side and an explanation of the anomalies of the orbital motion. In this report we give some first estimations of the possible rate of the secular drift of the Moon center of mass with respect to its crust and mantle in the 10 - 15 mm / year toward the back-side of the satellite. This secular drift of the center of mass of the Moon should be considered by the studying of the orbital motion of the Moon on laser-based observations. Namely, to add to the value obtained by laser observations. The result will be an estimate of the secular increasing of semi-major axis is the center of mass of the Moon. It should be expected that this will obtain the interpretation and explanation of the unexplained part of the secular acceleration of the Moon orbit and the anomalous part of the secular variation of the eccentricity of the lunar orbit, identified according to the perennial laser observations of the Moon. An anomalous part of the orbital acceleration (unexplained) of the Moon is 0.7” / cy2, and the anomalous part of the secular variation of the eccentricity is characterized by rate in 1.23x10 (-11) 1/year (Williams et al., 2011). Found offset - drift of the center of mass of the Moon (12 - 15 mm / year) is explained by the mechanism of excitation and the relative displacements of the shells of the Moon (solid core, liquid core, mantle) (Barkin, 2002).

Keywords: anomalous secular variation of the eccentricity of the lunar, tidal and non-tidal acceleration of the Moon, the center of mass of the Moon drift

Japan Geoscience Union Meeting 2014
(28 April - 02 May 2014 at Pacifico YOKOHAMA, Kanagawa, Japan)

PPS03-03 Room:424 Time:April 29 09:30-09:45

Deep interior structure of the Moon inferred from Apollo seismic data and the latest selenodetic data

MATSUMOTO, Koji[1*] ; YAMADA, Ryuhei[1] ; KIKUCHI, Fuyuhiko[1] ; KAMATA, Shunichi[2] ; IWATA, Takahiro[3] ; ISHIHARA, Yoshiaki[3] ; HANADA, Hideo[1] ; SASAKI, Sho[4]

[1]RISE Project Office, NAOJ, [2]University of California Santa Cruz, [3]JAXA, [4]Osaka University

Internal structure and composition of the Moon provide important clue and constraints on theories for how the Moon formed and evolved. The Apollo seismic network has contributed to the internal structure modeling. Efforts have been made to detect the lunar core from the noisy Apollo data (e.g., [1], [2]), but there is scant information about the structure below the deepest moonquakes at about 1000 km depth. On the other hand, there have been geodetic studies to infer the deep structure of the Moon. For example, LLR (Lunar Laser Ranging) data analyses detected a displacement of the lunar pole of rotation, indicating that dissipation is acting on the rotation arising from a fluid core [3]. Bayesian inversion using geodetic data weakly suggests a fluid core and partial melt in the lower mantle region [4]. Further improvements in determining the second-degree gravity coefficients and the Love numbers will help us to better constrain the lunar internal structure.

Recent analyses of GRAIL data have achieved the improved k_2 accuracy; JPL solution is 0.02405 ± 0.00018 [5], and GSFC solution is 0.02427 ± 0.00026 [6]. The two solutions are consistent with each other within their error bounds, and the accuracy of k_2 is now about 1 %. By introducing the improved gravity coefficients and k_2 from GRAIL mission, the updated LLR data analysis has also resulted in a better h_2 determination. Such accurately-determined Love numbers will contribute to constrain the structure of the lunar deep interior, such as the radius of the possible liquid core. It is difficult, however, to tightly constrain the internal structure from the geodetic data only because there are trade-offs among the structures of crust, mantle, and core. The combination of the Apollo seismic data and the geodetic data therefore afford the key to better determination of the lunar interior structure. We included geodetic data of the mass, the mean moment of inertia, the Love numbers h_2 and k_2, and 262 P and S travel time data in the analysis.

Markov Chain Monte Carlo (MCMC) method is used to infer the model parameters. When we used a five-layer model consisting of crust, upper-mantle, mid-mantle, lower-mantle, and core, the core radius is estimated to be 483 ± 22 km, and the core density values tend to be sampled around the assumed lower limit of 3600 kg/m^3. However, the inferred core radius is significantly larger than the magnetic constraint from SELENE data [7] which predicts the upper bound of the core radius to be 400 km. This discrepancy might be attributed to a possible low velocity layer above the core-mantle boundary which was not included in the five-layer model. We will discuss the results when such a low velocity layer is taken into account.

[1] Weber et al. (2011), Science, 331, 309-312, doi:10.1126/science.1199375
[2] Garcia et al. (2011), PEPI, doi:10.1016/j.pepi.2011.06.015
[3] Williams et al. (2001), JGR, 106, E11, 27,933-27,968
[4] Khan and Mosegaard (2005), GRL, 32, L22203, doi:10.1029/2005GL023985
[5] Konopliv et al (2013), JGR, 118, doi:10.1002/jgre.20097
[6] Taken from the PDS label of GRAIL Derived Data Products
[7] Simizu et al. (2013), Icarus, 222, doi:10.1016/j.icarus.2012.10.029

Keywords: Moon, internal structure, gravity field, tidal Love number, GRAIL

Japan Geoscience Union Meeting 2014
(28 April - 02 May 2014 at Pacifico YOKOHAMA, Kanagawa, Japan)

PPS03-04 Room:424 Time:April 29 09:45-10:00

Observations of lunar rotation on the Moon: possibility and problems.

HANADA, Hideo[1*] ; TSURUTA, Seiitsu[1] ; ASARI, Kazuyoshi[1] ; CHIBA, Kouta[2] ; INABA, Kenta[2] ; FUNAZAKI, Ken-ichi[2] ; SATOH, Atsushi[2] ; TANIGUCHI, Hideo[2] ; KATO, Hiromasa[2] ; KIKUCHI, Mamoru[2] ; ARAKI, Hiroshi[1] ; NODA, Hirotomo[1] ; KASHIMA, Shingo[1]

[1]RISE Project, National Astronomical Observatory, [2]Faculty of Engineering, Iwate University

The lunar rotation is one of the essential and basic target of selenodetic observations for investigation of the interior of the Moon as well as those of gravity fields, and high accuracy of the observations have a potential to detect signals related to the structure of lunar deep interior including the core. We have developed a small telescope like a PZT (Photographic Zenith Tube) for observations of Lunar rotation with the target accuracy of 1 milli-seconds of arc (1 mas)[1]. Theoretical investigation shows that observations by the telescope in the polar area of the Moon will open great possibilities for determining the libration in inclination ρ and node Iσ with the accuracy much better than before, although the determination of the libration in longitude will not be very well. It also showed that the determination error in the libration angles will not exceed $\sqrt{2}\varepsilon$, where ε is the positioning error of stars and is regarded as 1 milli-seconds of arc [2].

There are several technical problems to be solved in the development of the telescope. Effect of large temperature change is one of the most serious problem for such a precise observation, and we can loosen thermal condition by about ten times by introducing a diffraction lens compared with the case not introducing it. It is possible, on the other hand, that the vibrations of the mercury surface caused by the ground vibrations lead to fluctuations of star positions on CCD as large as 1 second of arc judging from laboratory experiments. The amplitude of the fluctuations depend on the amplitude of the ground vibrations and the depth of mercury pool. We can reduce the effect of the vibrations by making the mercury pool shallow down to the minimum depth. In the case of the mercury pool of 64mm diameter, the depth of 0.5mm is the best according to our experience [3]. It is important to keep the proper period of the mercury pool away from the period of ground vibrations in order to avoid the resonance. It is also effective to lengthen the integration time, and it can improve the reliability of the mean value of the center of a star image by statistical procedure.

We have already made a bread board model (BBM) and we will observe the deflection of the vertical on the ground by using the BBM for the time being in order to evaluate the characteristics of the total system of the telescope.

References

[1] Hanada, H. et al., Development of a digital zenith telescope for advanced astrometry, Science China, 55, 723?732, 2012.
[2] Petrova, N. and H. Hanada, Computer simulation of observations of stars from the Moon using the polar Zenith Telescope of the Japanese Project ILOM, Solar Sys. Res., 47, 504-517, 2013.
[3] Tsuruta, S. et al., Stellar imaging experiment using a mercury pool as a ground test of the telescope for In-situ Lunar Orientation Measurements(ILOM), Proc. 14th Space Science Symposium, 2014.

Keywords: rotation, moon, telescope, PZT, librations

Japan Geoscience Union Meeting 2014
(28 April - 02 May 2014 at Pacifico YOKOHAMA, Kanagawa, Japan)

PPS03-05 Room:424 Time:April 29 10:00-10:15

THE EARTH ORIENTATION PARAMETERS AND THE VARIATION OF THE SECOND ZONAL HARMONIC OF THE GEOPOTENTIAL

BARKIN, Mikhail[1*] ; FILIPPOVA, Alexandra[1] ; NOVIKOVA, Daria[1] ; PEREPELKIN, Vadim[1]

[1]Moscow Aviation Institute, Moscow, Russia

The study of the time variations of the geopotential as a result of the rotary-oscillatory processes of the Earth motion is of a significant natural-sciences and practical interest. Oscillations of the Earth ′ s inertia tensor components depend on many factors, among them the mechanical and physical parameters of the planet, the motions of tide-forming bodies, and the observed large-scale phenomena in nature. Time-dependent variations of these and other factors (regular and irregular oscillations, stochastic fluctuations, secular variations) affect the Earth rotary-oscillatory processes and the rotational parameters of the planet. The dynamic processes of the Earth orientation parameters (EOP) in turn have an effect on its figure and lead to the fluctuations of the gravitation field. Observed variations of the EOP, the variations of the Earth ′ s gravitational field and oscillations in the large-scale geophysical events appear to be in a considerable correlation.

An amplitude-frequency analysis of the rotary-oscillatory Earth motion under the action of gravitational-tidal perturbing torques from the Sun and the Moon is carried out using the classical mechanics' methods. The simulation results of the oscillatory process in the motion of the Earth pole and the variations of the second zonal harmonic of the geopotential are studied. Based on the dynamic Euler-Liouville equations expressions for amplitude and phase of the Earth pole oscillations are obtained. A comparison of the spectral power densities of the time series between the Earth pole coordinates and the variations of the gepotential is carried out. A functional dependence of the aforementioned component of the geopotential from the amplitude and phase of the Earth ′ s pole oscillatory process is shown.

Keywords: the rotary-oscillatory processes, secular variations, stochastic fluctuations, geopotential

Japan Geoscience Union Meeting 2014
(28 April - 02 May 2014 at Pacifico YOKOHAMA, Kanagawa, Japan)

PPS03-P01 Room:Poster Time:April 29 18:15-19:30

The free and forced librations of the Moon with liquid shell and solid core

BARKIN, Yury[1*] ; HANADA, Hideo[2] ; MATSUMOTO, Koji[2] ; BARKIN, Mikhail[3]

[1]Sternberg Astronomical Institute, Moscow, Russia, [2]National Astronomical Observatory of Japan, Mizusawa, Japan, [3]Moscow Aviation Institute, Moscow, Russia

In report we present our results of the study of lunar physical libration of the Moon on the base of its two and three layers models. On the base of analytical solution for two layers model (the Moon with liquid core) and empirical theory of the Moon ′ s rotation (Rambaux, Williams, 2011), we have identified period, amplitude, and the initial phase of the forth mode of free libration of the Moon, caused by liquid ellipsoidal core. Preliminary results of studies of three-layers model of physical librations of the Moon have been obtained on the base of some simplified approach for the problem of rotation of the Moon with liquid and rigid cores. The plans for future studies of the Moon rotation are discussed.

The modern view of internal structure of the Moon planet takes into account a complex two- or three-layer model. In our work the analytical theory of lunar physical libration based on its two-layer model consisting of a non- spherical solid mantle and of the ellipsoidal liquid core has been developed. The Moon moves on high-accurate perturbed orbit in the gravitational field of the Earth and other celestial bodies. On the base of two layers model of the Moon we have fulfilled systematic studies of the Moon physical librations. And in first we have presented a solution of the problem in components of vector of angular velocity of the Moon. An analytical presentation of LOD of the Moon with high accuracy in form of trigonometric series has here the progressive value. In first we have determined the fourth mode of free libration of the Moon caused by the influence of the liquid core oscillations of pole axis of rotation of the Moon (its mantle), with a long period in 205.7 yr, with an amplitude of 0 ″ 0395 and the initial phase of -134 ^{0} (for the initial epoch 2000.0). This oscillation reflects the so-called phenomenon of free oscillation of the liquid core. The estimates for the dynamic (meridional) oblatenesses of the ellipsoidal liquid core of the Moon: 0.000442 and 0.000283 have been obtained. These fundamental parameters of geodynamics of the Moon could be determined only on the base of data of observations. Earlier the attempts to determine the period of free core nutation undertaken. Our results were obtained by comparing of the developed analytical theory of lunar physical libration with empirical theory libration of the Moon, constructed on the basis of laser observations in last about 40 years (Rambaux, Williams, 2011).

Preliminary results of studies of three-layers model of physical librations of the Moon have been obtained on the base of some simplified approach for the problem of rotation of the Moon with liquid and rigid cores. We have analyzed the Cassini ′ s motion of the decoupled solid core and its librations in longitude to compare with the Moon motions. On the base of Getino, Ferrandiz et al. approach we give estimations of the periods of free librations of this system. We have constructed differential equations of rotational motion of three layers Moon from positions of the Hamiltonian formalism with application of Andoyer ′ s and Poincare ′ s variables. Now we construct analytical theory of rotation of the Moon system consisting from the non-spherical mantle, ellipsoidal liquid core and solid core.

Keywords: Moon rotation, free libration, liquid core, solid core

Japan Geoscience Union Meeting 2014
(28 April - 02 May 2014 at Pacifico YOKOHAMA, Kanagawa, Japan)

PPS03-P02 Room:Poster Time:April 29 18:15-19:30

Viscosity structure dependence of large-scale polar wander rate of the Earth: A potential impact of a low-viscosity zone

HARADA, Yuji[1*] ; XIAO, Long[1]

[1]China University of Geosciences

In this study, we make an attempt to quantitatively evaluate an effect of presence of a low-viscosity layer inside the mantle of the Earth on the timescale of its polar wander. In particular, we perform model calculation of the viscoelastic Love number which characterizes the mechanical response of the interior of the Earth, and then investigate how the timescales and strengths of some relaxation modes in the Love number depend on the viscosity structure. I compare the structure dependence of these relaxation modes with that of the polar wander speed. For the sake of convenience of this numerical calculation, we simplify the multilayered structure of the Earth and assume its incompressibility to compute the relaxation modes.

In this calculation, we apply the quasi-fluid approximation which makes it possible to integrate the polar motion equation as a non-linear one. Its reason is because the linear approximation is not allowed for the large-scale polar wander as dealt with in here. Following the applicable condition of the quasi-fluid approximation, we consider load history which timescale is slower than the characteristic one of the viscoelastic deformation of the asthenosphere.

As a result of the calculation mentioned above, we find that the timescale of the polar wander depends almost only on the longest relaxation mode. It is a remarkable point here that, in fact, the ratio of the strength of this relaxation mode governing the polar wander to the total viscoelastic Love number is not so large. In other words, this fact means that the other modes which amplitudes of tidal deformation are more dominant have almost no effect with respect to the timescale of the polar wander. Apparently, this might seem to be a peculiar result.

The reason for this dependence is because the timescale only of the above-mentioned longest mode is much longer by a few orders of magnitude compared to those of the other modes. A mode with a longer time constant of viscous relaxation has an effect which stabilizes rotation axis in a longer term even if its strength is smaller. Oppositely, a mode with a shorter time constant contributes less to the long-term rotational stability because of its faster relaxation even if its strength is larger.

In the light of this result, we can tell that the structure dependence of the true polar wander rate also basically reflects just that of the relaxation time of this longest mode. Actually, even assuming the internal structure without the low-viscosity layer inside the mantle, we still find the influence of this mode to be prominent. Once we take the existence of the low-viscosity layer into account, lower its viscosity is, shorter the timescale of the longest mode is. It can be less than forty percent at shortest. However, if this viscosity becomes lower than a certain value, the timescale of this mode is asymptotic to a constant value. Such a trend results from that this layer behaves as a fluid rather than a viscoelastic body in a sufficiently long timescale due to its too low viscosity.

Here we conclude from the calculation result shown above that the presence of the low-viscosity layer inside the Earth generally shortens the timescale of the large-scale polar wander, and also that this impact mainly stems from the variation in the timescale of the longest relaxation mode. Indeed, the preexisting works have already discussed the dependence of the timescale of the large-scale polar wander on the internal structure of the Earth as well. However, they have not examined the impact of the low-viscosity layer therein, considering a more simplified viscosity structure. Also, they have not clearly stated that the major controlling factor on the true polar wander speed. On the contrary, this work estimates the timescale of the polar wander with explicitly including the impact of this layer, and shows the non-negligible effect of the heterogeneous viscosity structure on the large-scale polar wander.

Keywords: true polar wander, the Earth, mantle, low-viscosity layer, relaxation mode, time constant

Japan Geoscience Union Meeting 2014
(28 April - 02 May 2014 at Pacifico YOKOHAMA, Kanagawa, Japan)

PPS03-P03 Room:Poster Time:April 29 18:15-19:30

Effects of global geodynamics in a series of astrometry observations of latitude at Poltava

KHALYAVINA, Lydmila[1] ; BARKIN, Yury[2*]

[1]Gravimetry Observatory, Poltava, Ukraine, [2]Sternberg Astronomical Institute, Moscow, Russia

Diverse geodynamic phenomena observed in the modern era, received a convincing explanation in the framework of the northern drift of Earth's core. Model proposed and developed by Yuri Barkin relative to the set of ancient geodynamic processes: the secular drift of the Earth's pole, non-tidal acceleration of the Earth's rotation, secular change of gravity, the evolution of the earth's figure, plate tectonics, the formation of specific geological structures, etc.

The North drift of the core generates mass redistribution of the Earth and leads to changes in the gravitational field. Since astrometry instruments have as a reference axis direction of the local plumb line, then this process should be displayed in the slow position changes no polar zenith Observatory. It is shown that for locations in the northern hemisphere, the north drift of the core causes the displacement of local plumb in a southerly direction. Is the picture of long-term changes in the direction of gravity (NST) in the meridian of Poltava for the period 1962 - 2013 based on long-term observations of latitude prismatic astrolabe taking into account: 1) high-precision catalogs (HIPPARCOS, ARIHIP, Tycho-2), 2) improved model of the pole C01 IERS; 3) the theory of the precession-nutation IAU2000; 4) plate tectonics (NUVEL1A-NNR). The resulting long-period changes in NST can be represented as the sum of three components: a linear trend with velocity ~-0.0003 ″ /yr, the nonlinear part of the trend, consisting of two branches (descending - in 1962 to 1996. And rising - in 1998 and 2010.), which can be regarded as a fragment of a wave with period T~50 years and amplitude A~0.02 ″ ; quasi cyclic part with 11 - year period, close to the main period of index of solar activity period and amplitude <0.01 ″ .

The linear part of the translational displacement means the plumb line to the south of Poltava, which is consistent with the above Barkin ′ s model. The observed velocity of motion of zenith corresponds to moving the center of mass of the Earth in a northerly direction at the velocity in 1.4 cm/yr. Found that the nonlinear part of the trend and the 11-year cyclicity in the shifts of plummet quite clearly reproduce the form of low-frequency polar latitude variations at Poltava derived from model C01 (EOP IERS). Actually observed amplitude of long-period oscillations of latitude caused by pole motion, in 2 times higher than the calculated amplitude. The non-linear part of the trend is the projection on the Poltava meridian of the Markowitz wave.

It is shown that both low-frequency cycles are negatively correlated with the corresponding components of the index of solar activity. The most probable mechanism of solar activity influence on the motion of the pole is the North Atlantic Oscillation. An increase in the amplitude of low-frequency polar displacements of Poltava zenith in astrometric observations requires a special study. One from possible explanations - the influence of the features of the geological structure in the vicinity of Poltava, which is located in the center of the so-called rift Poltava site.

Keywords: plate tectonics, secular change of gravity, Markowitz wave

Japan Geoscience Union Meeting 2014
(28 April - 02 May 2014 at Pacifico YOKOHAMA, Kanagawa, Japan)

PPS03-P04 Room:Poster Time:April 29 18:15-19:30

Minerals detection on Mars from Mars Reconnaissance Orbiter (MRO) CRISM data

JIN, Shuanggen[1] ; BARKIN, Yury[2*]

[1]Shanghai Astronomical Observatory, Chinese Academy of Science, [2]Sternberg Astronomical Institute, Moscow State Uniersity

Martian mineral detection and mapping can provide important information and constraints on Martian aqueous history, which can be used to assess the potential habitability of Mars. Degrees of addressing the key question for Martian aqueous alteration are dictated by the depth and extent of grasping the Martian hydrous mineral. Therefore, it is important to know detailed minerals and chemical induction of the existence of water on the Martian surface at past or present. In-situ observations of the Martian rovers, such as Spirit, Opportunity and Curiosity have provided the mineralogical analysis of Martian surface, but restricting in a limited areas. Compact Reconnaissance Imaging Spectrometer for Mars (CRISM) aboard the Mars Reconnaissance Orbiter (MRO) with enhanced spectral resolution can provide more information at spatial and time scale. In this paper, CRISM near-infrared spectral data are used to identify mineral classes and distribution at Martian Gale region, including kaolinite, chlorites, smectite, jarosite, northupite and salts. The detection of northupite that is indicative of evaporation in Gale region suggests that the Gale region has experienced the climate change from moist condition with mineral dissolution to dryer climate with water evaporation.

Keywords: Martian minerals, Mars Reconnaissance Orbiter, CRISM

Japan Geoscience Union Meeting 2014
(28 April - 02 May 2014 at Pacifico YOKOHAMA, Kanagawa, Japan)

PPS21-01 Room:416 Time:April 29 09:00-09:15

The solidification of a magma ocean of Vesta

KAWABATA, Yusuke[1*] ; NAGAHARA, Hiroko[1]

[1]Earth and Planetary Science, The University of Tokyo

Asteroid 4 Vesta is the only preserved intact example of a large, differentiated protoplanet. Observations of surface spectra of Vesta provide convincing evidence for a differentiated interior. Vesta is considered as the parent body of HED meteorites.

Whether growing mineral grains remain suspended in the magma ocean or settled out is crucial for the primary interior structure of a planet.

The purpose of this study is to understand the role of grain size of crystals on solidification of a magma ocean under a turbulent flow. We select asteroid 4 Vesta as a subject of this study due to the presence of HED chondrites as a reference. In this study, we consider the solidification before the rheological transition occurs.

We assume that the interior structure of Vesta had already differentiated to form a core. We use the bulk silicate Vesta composition proposed by Righter and Drake (1998), which is a mixture of L and CV chondrites with the ratio of 7 to 3 adjusted for core separation. We calculate liquidus, solidus and solid fractions using the MELTs program (Ghiorso and Sack 1995; Asimow and Ghiorso 1998).In vigorously convective systems such as magma oceans, the temperature distribution is nearly adiabatic and isentropic (Solomatov, 2000).

The heat flux can be calculated with the help of the blackbody radiation. This heat flux must match the heat flux transported to the surface by convection. Convection changes to a regime sometimes called hard turbulence at very high Rayleigh number such as those in the magma ocean, of which heat flux is shown by Siggia (1994).

To describe the rate at which particles settle out of a turbulently convective fluid, we use the model by Martin & Nokes (1989).The particle number is calculated by

$dN/dt=N(-g\triangle\rho a^2)/(18\rho\nu h)$

where N is the particle number, g is the acceleration due to gravity, a is the diameter of the particle, $\triangle\rho$ is the density difference between the crystal and the magma, ν is the kinematic viscosity, and h is the depth of the fluid layer (Martin & Nokes, 1989).

The adiabat, liquidus and solidus of the magma ocean of Vesta are very steep, that is, they have negligibly small dependence on pressure.

Thermodynamic calculations with the MELTs program showed that olivine is the first liquidus phase at ˜1900K, followed by orthopyroxene and spinel. At the very late stage, clinopyroxene appears consuming orthopyroxene if chemical equilibrium is maintained.

The fluid dynamic evaluation shows that a very small fraction of crystals are separated from the magma ocean until the rheological transition which varied from 100um to 1cm in the current work. The thickness increases with time, which is shown in Figure.

Evaluation of fluid dynamic regime shows that the magma ocean on Vesta was at the hard turbulence regime, suggesting near equilibrium crystallization until the rheological transition takes place at the crystal fraction of 60% at 1649K.

The role of grain size on fluid dynamics is very small, but the amount of crystals settled down to the bottom of the magma ocean has small dependence on the grain size. If the crystal size is 1cm, 1km thickness bottom layer is formed.

The fluid dynamic regime changes into soft turbulence in 100 years in the order in the magma ocean of Vesta.

The summary of our conclusion is as follows.

(1)The pressure effect in the interior of Vesta is negligibly small.
(2)The solidification of a magma ocean of Vesta before the rheological transition follows batch solidification.
(3)The size of crystallizing grains has a minor effect on the evolution of magma ocean until the rheological transition.
(4)The mantle would be harzburgite if the interstitial melt was effectively extracted at the later soft turbulence stage.

Fig. The thickness of the bottom layer consisting of settled crystals from the main body of a magma ocean.

PPS21-01 Room:416 Time:April 29 09:00-09:15

Keywords: Vesta, magma ocean

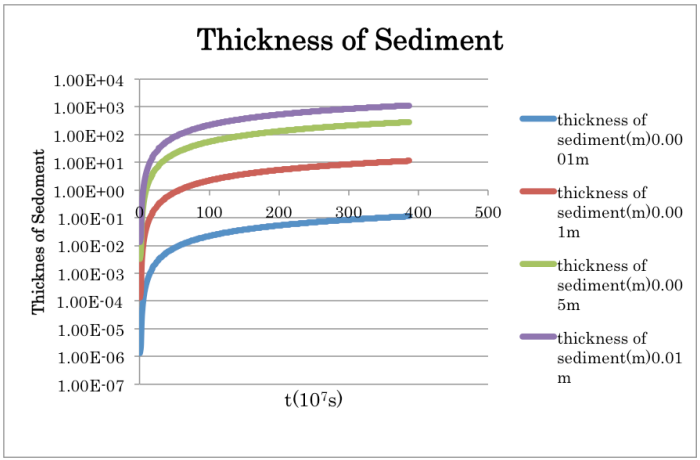

Japan Geoscience Union Meeting 2014
(28 April - 02 May 2014 at Pacifico YOKOHAMA, Kanagawa, Japan)

PPS21-02 Room:416 Time:April 29 09:15-09:30

Thermal evolution simulation of Vesta including convection and melt migration

NOGAMI, Tatsuhiko[1*] ; SIRONO, Sin-iti[2]

[1]Division of Earth and Planetary Sciences, Graduate School of Science, Nagoya University, [2]Division of Earth and Planetary Sciences, Graduate School of Science, Nagoya University

Vesta has been regarded as the parent body of the HED meteorites. From the observation of DAWN spacecraft, the uppermost layer of Vesta is composed of howardite and its thickness ranges from 50km to 80km (Jutzi et al. 2013). It is known that the ratio of the number of eucrites to diogenites is around two. Based on these facts, rapidly cooled magma layer on Vesta should be more than 10km in thickness.

In this work, I studied the evolution of internal thermal evolution of Vesta due to heating of decay of 26Al. I calculated the temperature distribution by solving numerically heat conduction equation. According to Formisano et al.(2013), if Vesta completed its formation within 1.4Ma from the injections of 26Al into the solar nebula, the degree of silicate melting inside Vesta exceeds 50 vol%. But in that work, convection and melt migration were not taken into account. These two mechanisms contribute to cool down Vesta. It is expected that the formation of Vesta should be completed earlier if these effects are taken into account. On the other hand, it is known that it takes about a few million years for Vesta-size planet to complete its formation according to the standard model of planetary formation.

As a convection model, I adopted the model of Kaula (1979). It was assumed that generated melt migrates to the surface instantaneously, and the migrating melt to the surface was accounted as the rapidly cooled magma. There are two parameters in this study, including a (the percentage of melt migration) and t0 (formation time of Vesta), and perform simulation taking into account the convection and melt migration.

As a result, convection and melt migration substantially change the evolution of internal thermal structure, and total volume of magma considerably depends on a and t0. The magma volume increases as a increases. On the other hand, the magma volume decreases as t0 increases.

When t0=0, corresponding to no decay of 26Al at the beginning, and if $a>0.3$, the erupting magma layer of 10km in thickness is formed. When a=1, corresponding to total melt migration, the magma layer of 10km is formed if $t0<0.9$Ma. According to these results, Vesta should be completed its formation within 0.9Ma after CAI formation, and more than 30% of generated melt should migrate the surface. But total generated melt migration is not reasonable . If $a<1$, Vesta has to be formed earlier than a=1.

Therefore, it is suggested that the formation time of Vesta should be earlier than the estimate by Formisano et al.(2013), and rapid formation mechanism of 100km sized objects is needed.

Japan Geoscience Union Meeting 2014
(28 April - 02 May 2014 at Pacifico YOKOHAMA, Kanagawa, Japan)

PPS21-03 Room:416 Time:April 29 09:30-09:45

Thermal conductivity measurements of sintered glass beads and application to planetesimal thermal evolution

TSUDA, Shoko[1] ; SAKATANI, Naoya[2*] ; OGAWA, Kazunori[3] ; TANAKA, Satoshi[3] ; ARAKAWA, Masahiko[4] ; HONDA, Rie[5]

[1]University of Tokyo, [2]The Graduate University for Advanced Studies, [3]Institute of Space and Astronautical Science, [4]Kobe University, [5]Kochi University

In the planetary formation process, dusts in the early solar nebula would have formed into planetesimals. Planets and asteroids have been formed by collisions of planetesimals. To constrain planetesimal ' s formation process and internal structure is an important issue. Especially, thermal evolution of planetesimal is key phenomenon for this purpose, and thermal conductivity of the planetesimal constituents is an essential parameter for understanding the thermal evolution.

As planetesimals are treated as dust aggregates, they would experience sintering when their temperature increases as a result of thermal evolution. The sintering makes neighbor particles bonded. The thermal conductivity of powered materials before sintering has been researched recently. However, thermal conductivity of sintered dust has not been measured under vacuum. Once dusts undergo the sintering, contact faces, so-called neck, are formed between dusts. The sintering causes growth of the neck and decrease of the porosity. It is thought that these changes make thermal conductivity higher than not-sintered dusts.

Based on our previous measurements of the thermal conductivity of glass beads, a positive correlation between thermal conductivity and compressional stress (thus, the inter-particle contact area) was observed with sample porosity remaining constant. Therefore, the thermal conductivity should be expressed as a function of not only porosity but also contact area between the particles.

This study aims at investigating thermal conductivity of the sintered materials under vacuum condition, in order to estimate effect of the sintering on thermal evolution of planetesimals. Especially, we focus on the dependence of neck size on the thermal conductivity.

We used three sizes of glass beads (250, 500, and 1000 μm) as analogous samples of dusts. For respective glass beads, we made three sintered samples with different degrees of sintering, or different neck size, in order to investigate the neck size dependence of the thermal conductivity. To measure the neck size, the sintered particles were separated and the neck crack size was observed using optical microscope. The thermal conductivity was measured by line heat source method under vacuum.

As a result of these experiments, we confirmed that the neck sizes of the nine samples had different ratio of neck size to beads radius, whose average values were ranged from 0.075 to 0.30. The thermal conductivity was ranged from 0.036 to 0.25 W/mK. These values were more than 10 times higher than that of not-sintered glass beads. Combining the results of neck size and thermal conductivity measurements, it was found that the thermal conductivity is proportionally related to the neck size ratio independent of the particle size. In these experiments, the porosity was constant about 40%. Therefore, when we calculate thermal evolution of planetesimals under sintering, the thermal conductivity should be estimated from the neck size at least until the neck size ratio grows up to 0.3 (initial stage of sintering).

Finally, we calculated the thermal evolution of the planetesimal using the relation of the thermal conductivity and the neck ratio we found in this experiment. Hypothesized planetesimals have radius between 100 m and 1000 m, formation age between 1 Myr and 3 Myr after CAI formation, and dust diameter of 1 and 1000 μm. As a result of the calculation, it was found that the sintering and resulting increase of the thermal conductivity make internal peak temperature more than 1000 K lower than the case when the sintering effect is not included in the calculation. In addition, internal temperature structure and neck size (or material strength) distribution in the planetesimals vary widely depending on the size and formation age of the planetesimals and particle size of dust.

Japan Geoscience Union Meeting 2014
(28 April - 02 May 2014 at Pacifico YOKOHAMA, Kanagawa, Japan)

PPS21-04 Room:416 Time:April 29 09:45-10:00

The effect of melt on frictional behavior and the implication for deep moonquake

AZUMA, Shintaro[1*] ; KATAYAMA, Ikuo[1]

[1]Department of Earth and Planetary Systems Science, Hiroshima University

Apollo program (Passive Seismic Experiment) investigated a number of seismic events in moon (e.g., Nakamura 2003). These seismic events (moonquakes) are classified to four categories; thermal moonquake, shallow moonquake, impact moonquake and deep moonquake (Latham et al., 1969). In kinds of moonquake, deep moonquake is especially interesting because the occurrence depth of deep moonquake (700?1200 km) is obviously in plastic deformation region where frictional behavior and fracture does not occur. Analysis of PSE (Passive Seismic Experiment) data and modelling in previous studies suggest that the partial melt layer underlies near the occurrence depth of deep moonquake (Weber et al., 2011). Therefore partial melt possibly is one of important factor on the deep moonquake. Here we show the results of frictional experiments using a borneol?diphenylamine which can be adjusted in melt fraction and dihedral angle (Takei 2000). When dihedral angle is 30o, frictional coefficient becomes small with decrease of melt fraction. Although frictional coefficient is significantly decreased when dihedral angle is 0o, frictional coefficient does not depend on melt fraction. When dihedral angle of partial melt is 0o, frictional behavior is fully dominated by partial melt. Partial melt is considered to have the three effects on the shear strength. First, our frictional experiments found that partial melt decrease frictional coefficient. Second, partial melt behave as the pore pressure. Third, partial melt extracts the water from the surrounded rocks, and induces the shear localization (the stress concentration). Considering these effects of partial melt on frictional behavior, partial melt might be one of important factors on deep moonquake.

Keywords: melt, deep moonquake, moon, frictional behevior

Japan Geoscience Union Meeting 2014
(28 April - 02 May 2014 at Pacifico YOKOHAMA, Kanagawa, Japan)

PPS21-05 Room:416 Time:April 29 10:00-10:15

Velocity scaling of granular convection and its application to timescale of regolith migration

YAMADA, Tomoya[1*] ; KATSURAGI, Hiroaki[1]

[1]Graduate School of Environmental Studies, Nagoya University

On the basis of accurate surface observation of asteroid Itokawa, it has been thought that regolith migration and sorting could occur [1]. Besides, Nagao et al. revealed that cosmic-ray exposure age of Itokawa's surface grains is less than 8 Myr [2]. As a possible explanation for such active and young surface of Itokawa, regolith convection caused by impact-induced seismic shaking has been considered [1]. Indeed, granular convection can be readily observed in the laboratory experiment of vertically vibrated granular matter (e.g. [3]). However, the quantitative feasibility of granular convection under the microgravity environment has not been studied well so far. Although the direct control of gravity is quite difficult, we instead employ the scaling approach to figure out the gravity dependence of granular convective velocity. Specifically, we measure the granular convective velocity under various experimental conditions. Then, using the systematically obtained data, we find a scaling relation among the convective velocity, gravitational acceleration, and other control parameters such as vibration frequency, grain size, and so on. We also estimate the timescale of regolith migration due to the granular convection by using the obtained scaling.

The grains used in this experiment are glass beads of diameter d = 0.4, 0.8, or 2 mm (AS-ONE corp. BZ04, BZ08, BZ2). The experimental setup consists of a cylinder made by plexiglass of its height 150 mm and inner radius R = 16.5, 37.5, or 75 mm. The cylindrical cell is filled by glass beads to make a granular bed of the height H = 20, 50, 80, or 110 mm. The system is mounted on an electromechanical vibrator (EMIC 513-B/A) and shaken vertically. The vibration frequency f is varied from 100 to 300 Hz and the maximum dimensionless acceleration is varied from 2 to 6. Motions of glass beads on the sidewall of the container are captured by a high-speed camera (Photoron SA-5) with a macro lens. PIV (Particle imaging velocimetry) method is used to compute the vertical component of the convective velocity, v_z. The maximum value of the velocity is nondimensionalized as $v_{zmax}/(gd)^{1/2}$, where g is the gravitational acceleration. Using the obtained experimental data, we scale $v_{zmax}/(gd)^{1/2}$ by the shaking parameter S [4] and the dimensionless system size L. S represents the energy balance between vibration and gravity, $S=(2\pi Af)^2/gd$, where A is shaking amplitude. L is the scaled system size defined by $L=(RH)^{1/2}/d$.

As a result of systematic dimensional analysis, we obtain a scaling form, $v_{zmax}/(gd)^{1/2} \sim S^{0.47}L^{0.82}$. From this scaling form, we find that the granular convective velocity v_{zmax} depends on the gravitational acceleration g as $v_{zmax} \propto g^{0.97}$ when the maximum dimensionless acceleration is fixed. This means that the granular convective velocity is almost proportional to the gravitational acceleration. We also find that the timescale of regolith migration due to the granular convection is almost independent of its roll size, by assuming that L is the dimensionless convective roll size. In the presentation, we are going to discuss the consistency between the regolith migration timescale and cosmic-ray exposure age of Itokawa's surface grains.

[1]H. Miyamoto *et al.*, Science **316**, 1011 (2007)
[2]K. Nagao *et al.*, Science **333**, 1128-1131 (2011)
[3]A. Garcimartín *et al.*, Physical Review E **65**, 031303 (2002).
[4]P. Eshuis *et al.*, Physics of Fluids **19**, 123301-1 (2007)

Keywords: granular convection, scaling analysis, gravitational acceleration, regolith migration, Itokawa

Japan Geoscience Union Meeting 2014
(28 April - 02 May 2014 at Pacifico YOKOHAMA, Kanagawa, Japan)

PPS21-06 Room:416 Time:April 29 10:15-10:30

Experimental study on impact-induced seismic wave propagating in granular materials

MATSUMOTO, Eri[1] ; YASUI, Minami[2*] ; ARAKAWA, Masahiko[1]

[1]Graduate school of Science, Kobe University, [2]Organization of Advanced Science and Technology, Kobe University

Introduction:

A seismic wave survey is a direct method to investigate the sub-surface structures of solid bodies, so we measured and analyzed these seismic waves propagated through these interiors. Earthquake and Moonquake are the only two phenomena that have been observed to explore these interiors until now, while the future surveys on the other bodies, (solid planets and/or asteroids) are now planned. To complete the seismic wave survey during the mission period, the artificial method that activates the seismic wave is necessary and the one candidate for the artificial one is a projectile collision on the target body. However, to utilize the artificial seismic wave generated on the target body, the relationship between the impact energy and the amplitude and the decay process of the seismic wave should be examined. If these relationships are clarified, we can estimate the required sensitivity of seismometers installed on the target body and the distance from the seismic origin measurable for the seismometer. Furthermore, if we can estimate the impact energy from the observed seismic wave, it is expected to estimate the impact flux of impactors collided on the target body. In this study, we carried out impact experiments in the laboratory, observed the seismic waves by accelerometers, and examined the effects of projectile properties on the amplitude and the decay process of the seismic wave.

Experimental methods:

We did impact experiments by using the one-stage gas gun at Kobe University. The projectile was a polycarbonate cylinder with the diameter of 10 mm and the height of 10 mm, and a stainless and an alumina ball with the diameter of 3 mm. The stainless and the alumina balls was accelerated with the sabot made by polyethylene. The impact velocity was $\sim$100 m/s. The target was prepared by putting 200 μm glass beads into the container with the diameter of 300 mm and the height of 100 mm, up to 80 mm depth. Three accelerometers (response frequency $<$10 kHz) were set on the target surface at different distances from the impact point. The observed seismic waves were recorded as voltage on the data logger (A/D conversion efficiency 100 kHz).

Experimental results:

We calculated the propagation velocity of seismic wave by using the traveling time from the impact point to the site of accelerometer and the impact velocity, and obtained 105 $\pm$ 15 m/s. Additionally, the relationship between the maximum acceleration, g_{max}, and the normalized distance, x/R (x: distance from impact point, R: crater radius), was determined as g_{max} =268$(x/R)^{-2.8}$. From these results, it is found that the seismic wave attenuates with similar waveform on the same target, irrespective of projectile type. The duration keeping the maximum acceleration was estimated to be $\sim$0.3 ms, and this value was almost consistent with the penetration time of projectile estimated by using the model proposed by Niimi *et al.* (2011). McGarr *et al.* (1969) studied the energy conversion efficiency from impact energy to seismic momentum and obtained the ratio of the impulse of projectile during the penetration, I, to the kinetic energy of projectile, E_k. As a result of this study, the I/E_k was obtained to be $1.6 \times 10^{-2} \pm 1.0 \times 10^{-2}$. On the other hand, McGarr *et al.* (1969), which the lexan projectile collided on the sand target with the impact velocity of 2-8 km/s, was obtained to be $6 \times 10^{-6} \pm 4 \times 10^{-6}$. This difference might be caused by the dependence of impact velocity on the energy conversion efficiency.

Keywords: impact-induced seismic wave, granular materials, decay process, planetary exploration, crater formation, accelerator

Japan Geoscience Union Meeting 2014
(28 April - 02 May 2014 at Pacifico YOKOHAMA, Kanagawa, Japan)

PPS21-07 Room:416 Time:April 29 10:30-10:45

Velocity measurements of impact jetting during oblique impacts

KUROSAWA, Kosuke[1*] ; NAGAOKA, Yoichi[1] ; HASEGAWA, Sunao[2] ; SUGITA, Seiji[3] ; MATSUI, Takafumi[1]

[1]PERC, Chitech, [2]ISAS, JAXA, [3]Dept. of Complexity Sci. & Eng., The Univ. of Tokyo

Impact jetting is a widely-known phenomenon in both hypervelocity impact experiments and hydrocode calculations. There are two important features in impact jetting, which are (1) extremely high velocity greater than the impact velocity and (2) the high degree of shock heating. Jetting has been considered as a mechanism for the origin of chondrules, tektites and impact glasses, Pluto, and the Moon. Jetting during a symmetric collision between two thin plates has been well studied. However, the understanding of jetting for spherical impactors is essential for planetary applications and it has not been obtained. One of the reasons for this is the lack of the experimental data of hypervelocity jetting of obliquely-impacted spherical projectiles. Although the temperature of jetted vapor has been investigated under a wide range of experimental conditions, only 3 data points, including unpublished data, have been reported as the jet velocity, which is one of the important anchors for developing a jetting model.

In this study, we conducted a series of oblique impact experiments using spherical projectiles and 3 different targets and investigated the jet velocity as a function of impact velocity and target materials. The frame rate of a high-speed imaging was 100 ns/frame to resolve the jetting initiation during projectile penetration. We found that the velocity ratio of the jet velocity to the impact velocity increases as the shock impedance of target increases at a given impact velocity and decreases with as impact velocity increases.

We obtained the first systematic data set for the jet velocity of spherical projectiles during oblique impacts. Using the data set, we constructed a physical model to explain the observed jet velocities. We found that (1) a classical phenomenological model constructed by Ang (1990) predicts well observed jet velocities if we use the vertical component of impact velocity instead of impact velocity in his model and that (2) observed jet velocities can be obtained by the sum of the horizontal component, the deformation velocity of the shocked projectile, and the particle velocity after isentropic release. The latter model may provide a physical basis of the jet formation

Both the standard and our physical model predict the jet velocity during oblique impacts reaches 2.5 times than the impact velocity. Although the mass of jetted materials must be small for energy conservation, the aerodynamic interaction between such hypervelocity jet and an ambient atmosphere may be significant because the heating rate of aerodynamic ablation is proportional to the cube of the velocity. In the case for an oblique impact on Titan, the jet velocity may reach 30 km/s in the case of typical cometary impacts and may generate strong EUV radiation from produced high-temperature plasma in the N2CH4 atmosphere via aerodynamic interaction near the surface of Titan. Active chemical reactions of C-bearing species may be driven by the produced EUV. The available energy source near the current Titan surface is only cosmic rays. Thus, hypervelocity jetting may be a new energy source for atmospheric chemistry on Titan.

Keywords: Hypervelocity impacts, Oblique impacts, High-speed video camera, Ultrafast imaging observation, Impact jetting, Titan

Japan Geoscience Union Meeting 2014
(28 April - 02 May 2014 at Pacifico YOKOHAMA, Kanagawa, Japan)

PPS21-08 Room:416 Time:April 29 11:00-11:15

The stability of amino acids in early ocean by meteorite impacts: Implication for chemical evolution of biomolecules

UMEDA, Yuhei[1*] ; SEKINE, Toshimori[1] ; FURUKAWA, Yoshihiro[2] ; KAKEGAWA, Takeshi[2] ; KOBAYASHI, Takamichi[3]

[1]Graduate School of Science, Hiroshima University, [2]Graduate School of Science, Tohoku University, [3]National Institute for Materials Science

Prebiotic oceans may have contained abundant amino acids, and were subject to meteorite impacts, especially during the late heavy bombardment. It has been unknown how meteorite impacts affected such dissolved amino acids in the early oceans. Experiments in the present study were performed using aqueous solutions containing olivine or hematite powders and ^{13}C-labeled glycine and alanine. In particular, the reaction products from ^{13}C-labeled amino acids are expected to compose ^{13}C, distinguishing if they are contaminants or not. Two powders of olivine and hematite help to keep the oxygen fugacity low and high during experiments, respectively in order to investigate the effect of oxygen fugacity on chemical reaction of amino acids. The run product of selected amino acids and amines in samples were analyzed with liquid chromatography-mass spectrometry (LC/MS). Some experiments were carried out in the presence of ammonia and/or benzene. The results revealed that amino acids survived partially or reacted out in early ocean through meteorite impacts. It was found that glycine changes into alanine and large amounts of methylamine and ethylamine are formed. Amine formation from alanine was increased considerably in the presence of Fe_2O_3 rather than olivine under similar impact conditions. XRD for the recovered hematite powders indicated the presence of a small amount of magnetite, suggesting that the oxygen fugacity was kept high enough to be close to the Fe_2O_3-Fe_3O_4 buffer. The formation of n-butylamine, detected as the largest number of carbon species in the recovered samples from the solutions with ammonia and benzene, suggests that chemical reactions to form new biomolecules can proceed through marine impacts. These results suggest that amino acids in early oceans can proceed further by impact-induced reactions, implying that impact energy plays a role in the prebiotic formation of various biomolecules, although the reactions depend upon the chemical environments as well.

Japan Geoscience Union Meeting 2014
(28 April - 02 May 2014 at Pacifico YOKOHAMA, Kanagawa, Japan)

PPS21-09 Room:416 Time:April 29 11:15-11:30

Organic aerosol experiments for CH_4/CO_2 atmospheres using a hydrogen/helium UV lamp

HONG, Peng[1*] ; SEKINE, Yasuhito[1] ; SUGITA, Seiji[1]

[1]Complexity Sci. & Eng., Univ. of Tokyo

Organic aerosols are photochemically produced in CH_4-rich reducing atmospheres, but their production mechanisms are not well constrained. Organic aerosol layers are believed to influence the surface temperature of early Earth, through its anti-greenhouse (Pavlov et al., 2001) and/or indirect greenhouse effects (Wolf and Toon, 2010), however, because of the uncertainty of the aerosol production mechanism, there are large uncertainties inherent in previous estimates of the aerosol production rate and optical depth of aerosol layers (Trainer et al., 2006). In order to put a constraint to the production mechanism and obtain aerosol production rate applicable to CH_4/CO_2 atmospheres, we conducted laboratory experiments to form organic aerosol analogues using a hydrogen/helium lamp that simulates solar far UV (FUV) with wavelengths longer than 110 nm. We measured the aerosol production rate as functions of UV flux and of CH_4/CO_2 ratio in the reactant gas. The aerosol production rates were determined by ellipsometrically measuring the growth rates of thin organic films deposited on a substrate. The UV fluxes from the hydrogen/helium lamp were measured by N_2O/CO_2 actinometry. Our experimental results show that the aerosol production rate is not a second-order function but a linear function of UV flux. This leads to a lower estimate for aerosol production rate due to FUV irradiation, when extrapolating the production rate in Titan's atmosphere to early Earth and exoplanets. We also found that the aerosol production exhibits a steep decrease when the CH_4/CO_2 ratio becomes less than unity. In order to interpret the dependence of aerosol production rate on the CH_4/CO_2 ratio, we also performed one-box photochemical calculations, including 791 reactions and 134 species up to C_8 hydrocarbons. The one-box photochemical model was validated against some basic carbon species (CH_4, C_2H_2, C_2H_4, C_2H_6, CO, CO_2), in which the abundances of those species calculated with the model and observed with a quadruple mass spectrometer (QMS) show a good agreement. We found that the observed production rate is in a good agreement with polymerization reaction rates involving aromatic hydrocarbons (i.e., benzene), suggesting benzene is the key parent molecule controlling the aerosol production. On the other hand, polymerization reactions involving polyynes do not account for the experimental data, suggesting that they are not the limiting molecules. This implies that aerosol production rate in an early Earth atmosphere due to solar FUV would become significantly lower than a previous estimate which includes polymerizations of polyynes as formation reactions of aerosols (Pavlov et al., 2001), resulting in an optically thinner aerosol layer by a factor of 100. Thus the optical depth of organic aerosol layers produced by solar FUV in an early Earth atmosphere would not have had efficient anti-greenhouse effect or indirect greenhouse effect, which makes other greenhouse effect important for the Archean climate, such as greenhouse effect of ethane. We will also discuss the possibility of aerosol formation through nitrile reactions driven by high-energy particle irradiation, which could be more efficient than the aerosol production due to solar FUV.

Keywords: organic aerosol, photochemistry, laboratory experiment, reducing atmosphere

Japan Geoscience Union Meeting 2014
(28 April - 02 May 2014 at Pacifico YOKOHAMA, Kanagawa, Japan)

PPS21-10 Room:416 Time:April 29 11:30-11:45

Proto-atmosphere on giant icy satellites forming within gaseous circum-planetary disks

MIKAMI, Takashi[1*] ; KURAMOTO, Kiyoshi[1]

[1]Department of Cosmosciences, Graduate School of Science, Hokkaido University

In spite of the great similarity in size and mean density, the giant icy satellites Ganymede, Callisto, and Titan have very different surface environments. In particular, only Titan holds a thick atmosphere dominated by N_2. Recent data of the Cassini spacecraft indicated that atmospheric N_2 is probably originated from other nitrogen-bearing species like NH_3. However, it still remains an open question when and how N_2 was generated. This is partly because the physical states of giant icy satellites have been poorly understood.

According to a widely-accepted theory of regular satellites formation, the giant icy satellites were formed in subnebulae with low temperature and low pressure taking a long accretion time. Some models assert that their surfaces were kept too cold to induce significant differentiation during accretion. However, these satellites may capture a significant amount of subnebula gas, which possibly forms proto-atmospheres along with gases volatilized from icy components. Such a hybrid-type proto-atmosphere may have significant blanketing effect.

Here, we numerically analyze the structure and effect of a hybrid-type proto-atmosphere. Our model atmosphere is hydrostatically connected with subnebula at the satellite Hill radius. It contains H_2 and He as nebula gas components, H_2O and NH_3 as volatilized ice components. The radiative-convective equilibrium structure is solved as a function of surface temperature. The subnebula conditions are given by Canup and Ward (2002), the temperatures are 150 K at Ganymede, 120 K at Callisto, and 50 K at Titan, and the corresponding subnebula pressures are varied over 0.1-10 Pa.

For all the boundary conditions, the proto-atmosphere is opaque due to water vapor, so that the outgoing thermal radiation (OTR) flux at top of the atmosphere is smaller than that of black body radiation without atmosphere when the surface temperature is higher than 273 K. When the surface temperature is lower, the OTR fluxes from the proto-atmospheres of Ganymede and Callisto are close to black-body radiation because these atmospheres have low surface pressure and are optically thin due to large scale height under high background temperature. On the other hand, the proto-atmosphere of Titan has another type of solution with the OTR fluxes significant lower than blackbody radiation under low surface temperature. This is due to the formation of optically thick atmosphere tightly bounded by gravity because of low background temperature.

These results imply that a warm proto-atmosphere near 200 K could be kept on Titan for a long time after the end of accretion. Our stability analysis suggests that the proto-atmospheres of Ganymede and Callisto were lost associated with the dissipation of the Jovian subnebula, but that of Titan survived after the dissipation of the Saturnian subnebula.

In the case, NH_3 vapor pressure would be kept high under the irradiation of the solar UV for a long time. The present atmospheric N_2 of Titan may be generated by photochemical reaction of NH_3 vapor in such a warm proto-atmosphere.

Keywords: Giant icy satellite, Atmosphere, Circum-planetary disk

Japan Geoscience Union Meeting 2014
(28 April - 02 May 2014 at Pacifico YOKOHAMA, Kanagawa, Japan)

PPS21-11 Room:416 Time:April 29 11:45-12:00

Atmospheric formation and thermal evolution of a proto-Mars growing in the solar nebula

SAITO, Hiroaki[1*] ; KURAMOTO, Kiyoshi[1]

[1]Cosmo Sci., Hokkaido Univ

It is widely accepted that Mars is a survivor of proto-planets formed by oligarchic growth i.e., the runaway accretion of planetesimals. Numerous planetesimals impacts onto the growing proto-Mars likely cause shock-melting, resulting into the early core formation as constrained by the chronology of Martian meteorites. Such impacts should also induce the degassing of H_2O and other molecular species from accreting materials, which contributes to atmosphere formation. Since the oligarchic growth proceeds within the solar nebula, a growing Mars probably acquired a proto-atmosphere consisting of the mixture of nebula gas component and degassed component. Such a hybrid-type proto-atmosphere may play important role in thermal balance and volatile partitioning between the planetary surface and interior. However, the structure and behavior of such atmosphere has been poorly investigated so far.

In this study, we build a one-dimensional radiative-convective (RT) equilibrium model for a hybrid-type proto-atmosphere assuming a compositional double layer structure. Here the upper layer is dominated by H_2-He continuing from the solar nebula and the lower one is dominated by degassed components enriched in H_2O. Radiative transfer is modeled, taking into account the absorptions by H_2, He and H_2O. RT equilibrium structures are obtained as a function of thermal luminosity that would be balanced with accretional heating rate and the amount of degassed component. The degassed component consists of H_2O and H_2 with molar ratio 1:5 in equilibrium with metal and silicate. The accretion time is taken 10^6-10^7 years.

For the pure H_2-He atmosphere, the surface temperature is kept lower than 700 K. Supply of degassed component increases the surface temperature that can exceed 1500 K given the mass of degassed component more than 1% of the Mars mass. If planetesimals contain enough proportions of H_2O and other heavy volatiles, growing Mars would have global magma ocean sustained by the blanketing effect of proto-atmosphere. This would promote core formation and transport of dissolved volatiles.

Japan Geoscience Union Meeting 2014
(28 April - 02 May 2014 at Pacifico YOKOHAMA, Kanagawa, Japan)

PPS21-12 Room:416 Time:April 29 12:00-12:15

Line-by-line calculations of radiation properties for exoplanets with steam atmosphere

ONISHI, Masanori[1*] ; HASHIMOTO, George[2] ; KURAMOTO, Kiyoshi[3] ; TAKAHASHI, Yoshiyuki O.[1] ; TAKAHASHI, Yasuto[3] ; ISHIWATARI, Masaki[3] ; HAYASHI, Yoshi-yuki[1]

[1]Department of Earth and Planetary Sciences, Kobe University, [2]Department of Earth Sciecnes, Okayama University, [3]Department of Cosmosciences, Graduate School of Science, Hokkaido University

For a hot water rich atmosphere, there is an upper limit on the thermal emission that is unrelated to surface temperature (Simpson, 1927, Nakajima et al., 1992). The radiation limit is deeply related to evolution of planetary atmosphere. Hamano et al., 2013 showed that terrestrial planets can be divided into two distinct types on the basis of their evolutionary history during solidification from the initially hot molten state depending on whether incoming flux from a host star is larger or less than the radiation limit. On the other hand, the first direct image of an exoplanet has finally occurred in 2004 (Chauvin et al., 2004), it is expected to observe radiation spectrum from terrestrial planets near future. If we can observe the spectrum, we have potential to clarify the atmospheric and surface environment and history of the planets. In order to estimate the planetary environment from the observation, numerical simulation of radiative transfer is needed. The most reliable calculation method of the radiation is line-by-line treatment. Goldblatt et al., 2013 calculates the radiative transfer of a pure water atmosphere by line-by-line treatment. Goldblatt et al., 2013 investigates only one case of surface water amount, one current ocean mass case. In this study, we calculate the radiative transfer in steam atmosphere by line-by-line treatment in several surface water amount cases.

Absorption cross section of water vapor was calculated from HITEMP2010 (Rothman et al., 2010) and MT_CKD continuum model (Mlawer et al., 2012). We used a 1D convective model in pure water atmosphere. The surface temperature was varied from 250 to 2000 K. The total water amount of water was varied from 0.01 to 5 current Earth ocean mass (270 bar). For rapid calculation, we prepared absorption cross section table and calculated required absorption cross section by cubic spline interpolation. A two-stream approximation (Toon et al., 1989) was used to calculate radiative transfer by line-by-line treatment with resolution of 0.01 cm^{-1} wavelength.

A radiation limit of our study is 282 W m^{-2}. The value is good agreement with that of Goldblatt et al., 2013. When the total water amount is lesser, increasing of outgoing thermal flux over radiation limit occurs in lower surface temperature conditions. In 0.01 current ocean mass condition, increasing of flux occurs in lower than 1000 K. In this case, most of flux radiate from 10 micron and 4 micron window region. Results of optical depth calculation indicate that we can't detect NIR and IR radiation from the surface of planets with surface temperature higher than 1500 K, even if the planet has 0.01 water amount.

Keywords: steam atmosphere, radiative property, radiation limit

Japan Geoscience Union Meeting 2014
(28 April - 02 May 2014 at Pacifico YOKOHAMA, Kanagawa, Japan)

PPS21-13 Room:416 Time:April 29 12:15-12:30

Dependence of the runaway threshold on water distributions on the surface of Earth-like planets

NITTA, Akira[1*] ; ABE, Yutaka[1] ; O'ISHI, Ryouta[2] ; ABE-OUCHI, Ayako[2]

[1]Department of Earth and Planetary Science, Graduate School of Science, University of Tokyo, [2]Atmosphere and Ocean Research Institute, University of Tokyo

Liquid water is one of the most important material not only for its large effect on planetary climate but also as a controlling factor of the habitability [e.g. Kasting et al., 1993]. Water planets, which are planets with liquid water on their surface, can be divided in 3 types: 'ocean planets', 'partial-ocean planets', and 'land planets'. Ocean planets have enough water to cover their surface entirely. Partial-ocean planets, which are like the Earth, have an interconnected ocean and lands. Land planets have little water in scattered lakes around both Poles [Abe et al., 2013, Hawaii, Kona]. The type of the water planet is determined by the balance between the surface water transport, which depends on the amount of water and topography, and the atmospheric water transport, which depends on the global circulation.

Surface water on each water planet is unstable and entirely vaporized when the planet receives insolation above a certain critical value. It is because of the positive feedback of the greenhouse effect of water vapor. This phenomenon is called the runaway greenhouse. In the following, the critical insolation is called 'runaway threshold' [e.g. Abe and Kasting 1988; Nakajima et al, 1992; Kopparapu et al., 2011].

Abe et al. [2011] discussed the difference of the runaway threshold between Earth-sized ocean planets and land planets using a 3-D model for the first time. They found that the surface water of land planet is significantly stable than that of ocean planet against the large insolation. While an ocean planet gets unstable and the runaway greenhouse occurs when the insolation reaches about 130% of that on the present Earth, a land planet remains stable until the insolation reaches 170%. However, a land planet that they represented is only one of the various situations of land planets, and they didn't mention the effect of variety of surface water distributions on the planetary climate.

Takao [2013] showed the dependence of the runaway threshold on latitudinal surface water distribution using the combination of meridional energy balance model (EBM) and the vertical radiative-convective equilibrium model. He suggested that runaway threshold of the Earth-sized water planet varies with the degree of latitudinal localization of surface water. Nevertheless, his 1-D EBM was so simple that he could neither discuss about the effects of longitudinal distribution of surface water, nor include dynamical global circulation.

In this study, we perform numerical experiments to clarify the effects of the surface water distribution on runaway threshold of Earth-sized planets with a 3-D model, GCM.

We use CCSR/NIES AGCM 5.4g [Numaguchi, 1999], which includes dynamical atmospheric circulation, radiative transfer, formation of clouds, and so on. While this model is adapted to the present Earth, it cannot calculate the change of surface water distribution determined by the water amount and topography. Therefore, we assumed the surface water distribution, which is determined as a result of the balance between the surface and atmospheric water transport in reality, and used it as the boundary condition. Then, we raised the insolation gradually until the surface water got unstable for each surface distribution, and evaluated the runaway threshold.

We found that the degree of localization of surface water significantly affects the runaway threshold, and it varies from 180% (extremely localized land planet) to 130% (ocean planet) continuously. Even if no surface water is given low latitudes area initially, because the Hadley circulation transports water to such area, when the initial surface water area reaches adequately low latitudes, the runaway threshold is almost the same as that of ocean planets, that is, 130%. We also investigated the dependence on the longitudinal water distribution. As a result, even if the total area of surface water is the same, there are about 10% of differences in the runaway threshold depending on its distribution.

Keywords: runaway greenhouse, GCM, Earth-like planet

Japan Geoscience Union Meeting 2014
(28 April - 02 May 2014 at Pacifico YOKOHAMA, Kanagawa, Japan)

PPS21-14 Room:416 Time:April 29 14:15-14:30

Dead zones by electric heating in protoplanetary disks

MORI, Shoji[1*] ; OKUZUMI, Satoshi[1]

[1]Tokyo Institute of Technology

Turbulence driven by magnetorotational instability (MRI) is a viable mechanism of angular momentum transport in accretion disks. In protoplanetary disks, however, there is a region where the ionization degree is too low for MRI to be active (e.g., Gammie 1996; Sano et al. 2000). Whether turbulence is present or not strongly affects the growth of dust particles to planetesimals. Therefore, a good knowledge of the size of dead zones is essential to understanding planet formation.

In this study, we focus on the heating of electrons by turbulent electric fields and its effect on the ionization state of protoplanetary disks. Previous studies have assumed that electrons in the disks have the same temperature as the neutral gas. However, this is not necessarily the case in MRI-driven turbulence, in which turbulent electric fields can significantly heat up electrons (Inutsuka & Sano 2005). Heated electrons efficiently adsorb onto dust grains, and therefore electron heating leads to a reduction of the ionization degree (Okuzumi & Inutsuka, in prep.). This could effectively increase the dead zone size by reducing the saturation level of MRI turbulence outside the conventional dead zone.

The aim of this study is to show where in protoplanetary disks the effect mentioned above becomes important. We calculate the ionization degree of disks assuming that MRI operates outside the dead zone. For a minimum-mass solar nebula with the dust grain radius of 0.1um and dust-to-gas mass ratio of 0.01, we find that the effect becomes significant in a region extending from the outer edge of the dead zone (at ˜20 AU from the central star) out to 70 AU. Furthermore, our analytic estimate suggests that the saturation level of turbulence in this region is significantly low.

Keywords: protoplanetary disk, ionization degree, dust grains, MHD turbulence, electric heating

Japan Geoscience Union Meeting 2014
(28 April - 02 May 2014 at Pacifico YOKOHAMA, Kanagawa, Japan)

PPS21-15 Room:416 Time:April 29 14:30-14:45

Collisional disruption of sintered dust aggregates

SIRONO, Sin-iti[1*] ; UENO, Haruta[1]

[1]Graduate School of Environmental Sciences, Nagoya University

Planets are formed in a protoplanetary nebula consisting of gas and dust grains. The first step of planetary formation is coagulation of dust grains, leading to the formation of dust aggregates. Further growth of the dust aggregates is promoted by mutual collisions between them. The motion of dust aggregates gradually decouples from that of the gas as aggregates grow. Dust aggregates drift inward due to gas drag. If the inward drift is faster than aggregate growth, solid components in a protoplanetary nebula disappears and planets cannot be formed. To prevent infalling, many mechanisms have been proposed (Kretke & Lin 2007, Lyla et al.2009, Sandor et al.2011). Fast collisional growth during the infalling of icy dust aggregates (Okuzumi et al. 2012) is another possibility. These studies are based on the assumption that the motion of aggregates decouples from gas. The infalling velocity is on the order of 1m/s when substantial decoupling is attained. Aggregates should grow to the sizes corresponding to the infalling velocity. Is it possible?

Experimentally, collisional breakup velocity of micron-sized SiO2 dust aggregates is on the order of 1m/s(Blum 2010). Breakup velocity for H_2O ice aggregates is also on the same order(Shimaki & Arakawa 2012). However, it is difficult to produce highly porous dust aggregates experimentally due to the Earth's gravity. I conducted two-dimensional numerical simulation of sintered dust aggregates in this study. It has been pointed out that sintering of H_2O ice proceeds in wide region of a protoplanetary nebula (Sirono 2013). As sintering proceeds, a neck between adjacent grains grows and mechanical interactions between grains greatly change. The effects of sintering are taken into account by changing breaking forces of a contact. The interactions between non-sintered contacts (Dominik & Tielens 1997) are adopted for newly formed contacts.

If sinterng proceeds sufficiently such that a neck is disappeared, catastrophic disruption was observed at low collision velocities (˜10cm/s). This is because a contact is broken by rolling of a grain. On the other hand, catastrophic disruption at low collision velocities was not realized for less-sintered aggregates. This is due to immediate reconnection between grains with a non-sintered mode. These results depends on the tensile strength of H_2O ice. The breakup velocity increases as the strength increases. From the results obtained in this study, the evolution of icy dust aggregates is various, depending on the location in a protoplanetary nebula.

Keywords: dust aggregate, protoplanetary nebula, collisional disruption, sintering

Japan Geoscience Union Meeting 2014
(28 April - 02 May 2014 at Pacifico YOKOHAMA, Kanagawa, Japan)

PPS21-16 Room:416 Time:April 29 14:45-15:00

Planetesimal size and protoplanetary disk turbulence

KOBAYASHI, Hiroshi[1*] ; TANAKA, Hidekazu[2] ; OKUZUMI, Satoshi[3]

[1]Nagoya University, [2]Institute of Low Temperature Science, Hokkaido University, [3]Tokyo Institute of Technology

When the random velocities of bodies are greater than their surface escape velocities, the runaway growth of bodies occurs, which produces a single large bodies surrounded by leftover bodies in each annual of a protoplanetary disk. The slope of the size distribution of bodies becomes steeper through runaway growth. The slope of runaway growth is seen in the size distribution of 100km sized or larger bodies in the main belt. Since the random velocities rises by turbulent stirring in the disk, the planetesimal size above which runaway growth occurs is determined by the strength of turbulence. We discuss turbulence strength in the solar nebula.

Keywords: Planetesimal, Protoplanetary disk, Asteroids, The size distribution of bodies, Planet formation

Japan Geoscience Union Meeting 2014
(28 April - 02 May 2014 at Pacifico YOKOHAMA, Kanagawa, Japan)

PPS21-17 Room:416 Time:April 29 15:00-15:15

The formation of gas planets from cores in type I migration

MAESHIMA, Naohiko[1*] ; WATANABE, Sei-ichiro[1]

[1]Division of Earth and Planetary Sciences, Graduate School of Science, Nagoya University

Many gas planets have been discovered. The formation of the gas planets requires that solid planets, which correspond to cores of gas planets, must achieve the critical core mass M_{crit} before the disk gas have entirely diffused. The cores moves radialy by torques caused by interaction with disk gas (type I migration). It was long thought that the cores fall into the star with very short timescale before achieveing M_{crit} by strong negative torque (Ward 1997, Tanaka et al. 2002). Recent study have showed that the region where positive torque operates is formed on the disk by corotation torque if we consider the non-isothermal process of the gas (Baruteau & Masset 2008,Paardekooper & Papaloizou 2008). As a result, equilibrium radii, where torque is zero, are created. The cores may accrete gas without falling into the star if they are trapped by equilibrium radius because the timescale of radial migration slows down to that of disk evolution. However, positive torque only operates for cores in limited mass range ($M_{p,min}<M_p<M_{p,max}$). If it takes long time for achieving $M_{p,min}$, the cores moves inward largely by negative torque. In this study, we examine how the orbit and mass of cores evolve depending on the disk model, and find the condition the disk must have for the gas planet formation.

The distribution of the gas surface density evolves by viscous diffusion and photoevaporation. The temperature distribution is determined by viscous heating and stellar irradiation. In the disk, an equilibrium radius is formed on the region where the main heating source shifts from the viscous heating to stellar irradiation. In this study, we investigate the possibility of the formation of gas planets at the equilibrium raidus. Cores grow by accreting planetesimals in their gravitational radius, and capture the disk gas if they achieve M_{crit}.

We find that the condition of gas planet formation is determined as follows. In diks evolving fast (α parameter of viscosity = 0.005), cores born in the middle region ($\sim$ 10AU) is captured by the equilibrium radius and capture the disk gas by achieving M_{crit} if core growth stars at the time when disk mass is still large (initial mass accretion rate $\sim 10^{-7} M\odot yr^{-1}$) and the ingredient of the cores is abundant (ratio of the solid material to gas is large $>$0.03). On the other hand, in the disks evolving slowly (α = 0.001), gas planets can be formed even if core growth stars at the stage when disk mass has been decreased (initial mass accretion rate $\sim 10^{-8} M\odot yr^{-1}$). In this case, the dependence on the ratio of the solid to gas is very weak.

Keywords: type I migration

Japan Geoscience Union Meeting 2014
(28 April - 02 May 2014 at Pacifico YOKOHAMA, Kanagawa, Japan)

PPS21-18 Room:416 Time:April 29 15:15-15:30

Protoplanet Spin by Planetesimal Accretion

SHIBATA, Takashi[1*] ; KOKUBO, Eiichiro[2]

[1]University of Tokyo, [2]National Astronomical Observatory of Japan

In the standard scenario of planet formation, protoplanets or planetary embryos are formed through runaway and oligarchic growth of planetesimals. We investigate the spin parameters of protoplanets using N-body simulations. By N-body simulations we can calculate consistently the orbital, accretionary, and spin evolution of planetesimals. The spin of protoplanets are important for terrestrial planet formation since it affects the accretion condition of protoplanets and determines the spin of terrestrial planets. For the standard model of a planetesimal disk, a Mars-sized protoplanet forms in 0.5 million years around 1 AU. We find that the spin angular velocity of planetesimals decreases as their mass increases. Planetesimals obtain their spin angular momentum on the early stage of accretion where their mass ratio is not so large. Once a runaway-growing planetesimal (protoplanet) becomes large enough, it mainly accretes smaller planetesimals whose collisional angular momentum tends to cancel out since they collide from random directions. Thus the protoplanet increases its mass but not the spin angular momentum, which leads to smaller angler velocity for larger protoplanets. When a protoplanet reaches the isolation mass, its typical spin angular velocity is as high as 10% of the critical angular velocity for rotational instability under the assumption of perfect accretion in collisions. We find that the obliquity of planetesimals is well expressed by an isotropic distribution. During the protoplanet growth, the scale height of the planetesimal system is much larger than the size of planetesimals. Thus, collisions are three-dimensional and isotropic, which leads to the isotropic obliquity distribution. We show the dependence of the spin parameters on the initial planetesimal system parameters. The spin angular velocity increases with the bulk density of planetesimals. The dependence of the spin angular velocity on the planetesimal mass becomes weaker as the initial mass of planetesimals increases. However, these system parameters do not affect the obliquity distribution.

Japan Geoscience Union Meeting 2014
(28 April - 02 May 2014 at Pacifico YOKOHAMA, Kanagawa, Japan)

PPS21-19 Room:416 Time:April 29 15:30-15:45

Gravitational accretion of particles onto moonlets embedded in Saturn's rings

YASUI, Yuki[1*] ; OHTSUKI, Keiji[1] ; DAISAKA, Hiroshi[2]

[1]Department of Earth and Planetary Sciences, Kobe University, [2]Graduate School of Commerce and Management, Hitotsubashi University

Collision and gravitational accretion of particles is an important issue related to the origin of ring-satellite systems of giant planets in the solar system. The Hill radii of Pan, Daphnis, Atlas, and Prometheus are found to be within 15 % of the observed long axes of these satellites given by the best-fit model ellipsoids. Also, the densities of these satellites (0.4 - 0.6 g cmˆ-3) are very low compared to the density of water ice and all approximately equal to the critical density at that distance, which is defined as the density of a body that entirely fills its Hill sphere. From these results, the small satellites within the orbit of Pandora are thought to be formed by accretion of small porous ring particles onto large dense cores, and further accretion seems to have been suppressed when the density of the satellite reaches the critical density at that distance. Local N-body simulations also demonstrated that a Hill sphere-filling body is produced by accretion of small porous particles onto a large dense core. However, it has not been studied how the degree of particle accretion onto moonlets in the inner parts of Saturn's rings depends on the distance from Saturn.

The shapes of these small ringmoons would also provide clues to the dynamical evolution of Saturn's rings. The fact that the shapes of these ringmoons approximately match those of their associated Hill sphere suggests that the moonlet cores were surrounded by a number of particles when they were formed. On the other hand, Pan and Atlas have the characteristic shapes with equatorial ridges, and are thought to be formed by two stages. First, their precursors whose shapes are similar to their Hill sphere without equatorial ridges were formed when the rings were thick. Then, equatorial ridges were formed through particle accretion onto the equatorial planes of the above formed objects after the rings became sufficiently thin and also before ring particles diffused. However, effects of dynamical properties of the rings on the shaping of moonlets formed by particle accretion have not been examined in detail.

Propeller-shaped structures have also been found in Cassini images of Saturn's rings. These propeller-shaped features are explained by gravitational interaction between ring particles and unseen embedded moonlets. From these observations, the sizes and orbital distributions of these unseen embedded moonlets are obtained, and such information provide us with clues to the evolution of the ring-satellite system. The propeller-shaped structures are mainly observed in the A ring. Recently, observations of similar structures have also been reported for the Cassini Division, and the B and C rings. Although some of these moonlets either may be collisional shards resulting from the breakup of a bigger icy progenitor ring body or may have formed by accretion of small low-density ring particles onto larger dense fragments, the origin of these moonlets is not clear.

Using local N-body simulation, we examine gravitational accretion of ring particles onto moonlets in Saturn's rings. We find that gravitational accretion of ring particles onto moonlets is unlikely to occur at radial locations interior to the outer edge of the C ring, unless the density of the moonlets is much larger than that of water ice or non-gravitational cohesive forces play a major role. Detailed analysis of accretion process of individual particles onto moonlets shows that particle accretion onto high-latitude regions of the moonlet surface occurs even if the rings' vertical thickness is much smaller than the moonlet's radius. The degree of particle accretion in outer rings is found to depend significantly on rings' vertical thickness and optical depth. Our results suggest that large boulders recently inferred from observations of transparent holes in the C ring are likely to be collisional shards, while propeller moonlets in the A ring would be gravitational aggregates formed by particle accretion.

Keywords: gravitational accretion, moonlet, Saturn's rings

Japan Geoscience Union Meeting 2014
(28 April - 02 May 2014 at Pacifico YOKOHAMA, Kanagawa, Japan)

PPS21-20 Room:416 Time:April 29 16:15-16:30

Mass-Loss Evolution of Super-Earths: Constraints on Their Compositions and Origins

KUROKAWA, Hiroyuki[1*] ; KALTENEGGER, Lisa[2] ; NAKAMOTO, Taishi[3]

[1]Nagoya University, [2]Max Planck Institute for Astronomy, [3]Tokyo Institute of Technology

Recent progress of he search for exoplanets, for example the transit observations with Kepler space telescope, has pushed toward small planets. Especially, ”Super-Earths”, that are planets having sizes from Earth to Neptune, are revealed as quite common: ˜30% of solar-type stars have super-Earths (Howard et al., 2012). Therefore, an understanding of their compositions, which is related to their origins, is important for planet formation and evolution.

We can speculate the compositions of super-Earths both whose masses and radii are known by using theoretical mass-radius relations for different compositions. Some fraction of super-Earths have low density, which suggests the presence of H/He envelopes formed by protoplanetary-disk gas capture. There exist. on the other hand. high-density super-Earths possibly having rocky- or water-rich compositions. The origin of this dichotomy is one problem that we address in this study, which possibly arises from the difference of the amount of captured disk gas due to different masses and disk temperature in their formation stages, or from XUV (X-ray and EUV)-driven atmospheric escape in later evolution stages (e.g., Lopez et al., 2012). Another problem that we address in this study is ”the degeneracy of composition”: The compositions of super-Earths can be fitted by various ratios of H/He envelope, rock, and water. Their atmospheric compositions have been speculated by measuring their transmission spectra, but recent observations using Hubble Space Telescope suggested that cloudy atmospheres of super-Earths (Kreidberg et al., 2014; Knutson et al., 2014). If clouds are common in atmospheres of Super-Earths, direct measurements of their compositions are difficult because clouds obscure any features of atmospheric species.

In this study, we show constraints on these problems of compositions and origins of super-Earths by calculating their mass-loss evolution due to XUV-driven atmospheric escape considering the differences of host-stellar types. The ratio of XUV luminosity and bolometric luminosity differs among stellar types, which enables us to distinguish formation origin and mass-loss origin of the dichotomy of super-Earths with or without H/He envelopes. Also, the degeneracy of compositions can be solved by considering stability criteria to lose H/He envelopes.

We calculated the critical orbital radii to lose H/He envelopes for different stellar types, that corresponds to different equilibrium temperature depending on stellar types. The obtained critical separations are consistent with the distribution of the observed super-Earths with or without H/He envelopes, suggesting that the observed dichotomy has a mass-loss origin.In this case, we expect that super-Earths having moderate density and orbiting inside the critical separation are water-rich super-Earths without H/He envelope.

We also evaluated uncertainty caused by mass-loss model and XUV luminosity and discuss the validity of our results.

Keywords: exoplanet, atmospheric escape, composition, super-Earth

Japan Geoscience Union Meeting 2014
(28 April - 02 May 2014 at Pacifico YOKOHAMA, Kanagawa, Japan)

PPS21-21 Room:416 Time:April 29 16:30-16:45

Exoplanet exploration for brown dwarfs with infrared astrometry

YAMAGUCHI, Masaki[1*] ; YANO, Taihei[1] ; GOUDA, Naoteru[1]

[1]National Astronomical Observatory of Japan

The astrometry is one of the oldest method for the exoplanet exploration. However, only one exoplanet has been found with the method. This is because the planet mass is sufficiently smaller than the mass of the central star, so that it is hard to observe the fluctuation of the central star by the planet. Therefore, we investigate the orbital period and mass of planets which we can discover by the future astrometric satellites for brown dwarfs with the mass less than a tenth of the solar mass.

So far five planetary systems have been found, whose mass ratios are larger than a tenth. For example, for the system whose distance, orbital period and mass ratio are 10 pc, 1 year and a tenth, respectively, the apparent semi-major axis reaches 3 milli-arcsecond, which can be well detected with the future astrometric satellites such as Small-JASMINE and Gaia. With these satellite, we can discover even super-Earth for the above system.

We further investigate where in the period-mass plane we can explore the planet for individual brown dwarf with Small-JASMINE and Gaia. As a result, we find that we can explore a wide region where period and mass are within 5 years and larger than 3 earth mass. In addition, we can explore the region around 0.1 day and 10 jovian mass, where planets have never found for any central star, and where we can explore only with Small-JASMINE for most target brown dwarfs.

Keywords: astrometry, brown dwarf, exoplanet exploration, infrared, Small-JASMINE, Gaia

Japan Geoscience Union Meeting 2014
(28 April - 02 May 2014 at Pacifico YOKOHAMA, Kanagawa, Japan)

PPS21-22 Room:416 Time:April 29 16:45-17:00

Experimental study on organic aerosol formation in super-Earths' atmosphere: Implications for transit observations

KOBAYASHI, Jumpei[1*] ; SEKINE, Yasuhito[2] ; HONG, Peng[2]

[1]Dept. Earth & Planet. Sci., Univ. Tokyo, [2]Dept. Complexity Sci. & Engr., Univ. Tokyo

A super-Earth is an extrasolar planet with a mass greater than Earth and below Neptune. Although there is no super-Earth in our solar system, astronomical observations demonstrate that it is one of the major categories of planets beyond the solar system. Recent transit observations of super-Earths, including GJ 1214b, indicate that their atmospheres contain opaque clouds or haze at high altitudes. One candidate for the opaque materials is metallic or salt dusts, such as KCl and ZnS, which would condense in the upper atmospheres of super-Earths. Another candidate is organic haze, such as those observed in the atmosphere of Saturn's moon Titan, which would be composed of high-molecular-weight hydrocarbon aerosols produced through photochemical reactions involving CH_4. Given the proposed formation mechanisms of nearby super-Earths, e.g., planetary migration, they would have a wide variety in chemical composition of atmosphere. However, previous laboratory experiments have mainly focused on organic aerosol formation in Titan's and early Earth's atmospheres. Thus, both the formation rate and optical property of organic haze for various atmospheric compositions have been poorly constrained by laboratory experiments.

In this study, we investigate the formation rate and optical property of organic aerosols formed by laboratory experiments simulating super-Earths' atmospheres with a wide variety in chemical composition. We used initial gas mixtures of H_2 and CH_4 or CO_2 and CH_4, and varied the H_2/CH_4 or CO_2/CH_4 ratios. The experiments were conducted at a total pressure of 1 Torr in a flow system. Cold plasma irradiation was used to initiate aerosol formation. We measured the aerosol formation rate, chemical compositions of intermediate gas molecules, and optical property of aerosol using a spectroscopic ellipsometer, a quadrupole mass spectrometer, and a UV/VIS spectrometer, respectively.

Our experimental results show that the aerosol formation rate decreases with increasing the H_2/CH_4 ratio, suggesting that recycling of high-molecular-weight hydrocarbons to CH_4 occurs through reactions with H and H_2 under H_2-rich conditions. We also show that organic aerosols are produced less efficiently at higher CO_2/CH_4 ratios. The results of gas analyses also show that formation of high-molecular-weight hydrocarbons are inhibited at higher CO_2/CH_4 ratios. These results indicate that oxygen-bearing molecules and radicals formed by CO_2 dissociation oxidizes hydrocarbons produced from CH_4, which results in a lower aerosol formation rate at higher CO_2/CH_4 ratios. Optical constant of the aerosols formed under the conditions simulating super-Earths' atmospheres is significantly lower than those of Titan aerosol analogs.

Based on the experimental results, we discuss the chemical composition and formation process of transiting super-Earths, such as GJ 1214b, by comparing the observed transmittance spectra with the model spectrum. We suggest that organic aerosol production in a H_2-rich or CO_2-rich atmosphere is inefficient so that organic haze would not be capable of explaining the observed transit spectra of super-Earths, even if they contains gaseous CH_4 in the atmospheres.

Keywords: exoplanet, super-Earth, organic aerosol, haze, atmospheric composition

Japan Geoscience Union Meeting 2014
(28 April - 02 May 2014 at Pacifico YOKOHAMA, Kanagawa, Japan)

PPS21-23 Room:416 Time:April 29 17:00-17:15

Transmission spectrum models of low-mass exoplanet atmospheres with haze: Application to GJ 3470b

KAWASHIMA, Yui[1*] ; IKOMA, Masahiro[1] ; FUKUI, Akihiko[2] ; NARITA, Norio[2]

[1]The University of Tokyo, [2]National Astronomical Observatory of Japan

Since the first exoplanet was discovered in 1995, detection of more than 1000 exoplanets has been reported. Recently, transit observations of an exoplanet have been done at multiple wavelengths. From a decline in apparent stellar brightness due to a planetary transit, we can measure the plantary radius. In addition, observed dependence of the planetary radius on wavelength (which is often called the transimission spectrum) provides the information of absorption and scattering by molecules and small particles such as haze and clouds in the planetary atmosphere. Thus, the composition of the planetary atmosphere can be constrained by comparison between the observational and theoretical transmission spectra. The constraint on atmospheric composition gives an important clue to the origin of the planet.

Our observational group has recently observed transits of two low-mass exoplanets, GJ 3470b and GJ 1214b, at multiple wavelengths. For both planets, the observed transit radii in the optical wavelength region are greater than those in the near-infrared region, inferring the existence of haze in the atmosphere. While the observed transmission spectrum was already analysed theoretically in detail as for GJ 1214b, there are few researches discussing the theoretical spectrum models incorporating the effect of haze systematically for GJ 3470b. In this study, we have modeled theoretical transmission spectra of low-mass exoplanets orbiting close to their host stars. Then, applying the calculated spectrum models to GJ 3470b and GJ 1214b, we discuss the property of the atmospheres of both planets.

In calculating theoretical spectrum models, we have taken into account the vertical distribution of molecular abundances from the chemical equilibrium calculations, in addition to absorption and scattering of the incident radiation from the host star by molecules and haze particles in the planetary atmosphere. We explore the dependences of the atmosphere's metallicity, C/O ratio and water vapor abundances on the transmission spectrum. We also probe the dependences of haze's height, particle sizes and number density. In comparing the observed and theoretical transmission spectra, we have performed the chi-squared analysis to quantify the validity of each atmospheric model.

Keywords: exoplanets, transits, transmission spectrum models, atmospheric composition, haze

Japan Geoscience Union Meeting 2014
(28 April - 02 May 2014 at Pacifico YOKOHAMA, Kanagawa, Japan)

PPS21-24 Room:416 Time:April 29 17:15-17:30

The SEEDS Exoplanet and Circumstellar Diks Survey

KUZUHARA, Masayuki[1*] ; TAMURA, Motohide[2] ; KUDO, Tomoyuki[3] ; HASHIMOTO, Jun[4] ; KUSAKABE, Nobuhiko[5] ; MATSUO, Taro[6] ; MCELWAIN, Michael[7] ; JANSON, Markus[8] ; TAKAHASI, Yasuhiro[2]

[1]Department of Earth and Planetary Sciences, Tokyo Institute of Technology, [2]Department of Astronomy, The University of Tokyo, [3]Subaru Telescope, [4]H. L. Dodge Department of Physics and Astronomy, University of Oklahoma, [5]National Astronomical Observatory of Japan, [6]Department of Astronomy, Kyoto University, [7]NASA Goddard Space Flight Center, [8]Astrophysics Research Centre, Queen's University Belfas

About 1,000 extrasolar planets (or exoplanets) have been discovered by now. Furthermore, Kepler survey has reported the presences of more than 3,000 exoplanet candidates (Huber et al. 2013). Thus, the planetary systems are common in our Galaxy, but it has known that those exoplanets have a variety of properties. Meanwhile, studies for circumstellar disks, which are the birth-places of planets, have also progressed. In particular, the radio telescope ALMA, whose operations have recently started, have provided intriguing data for the structure properties of protoplanetary disks (e.g., van der Marel et al. 2013; Casassus 2013). ALMA should provide a deep insight to the studies of circumstellar disks.

Direct imaging observations enable the discovery and study of exoplanets orbiting their host stars at wide orbital separations comparable to a few tens of AU, but the detections of those are impractical with indirect techniques such as radial velocity or transit method. Direct imaging is also useful to characterize circumstellar disks. The high-resolution observations of scattered light from protoplanetary disks or debris-disks have provided many important clues to reveal the physical disk-planet connections. We have progressed the SEEDS project, which aims at detecting and characterizing giant exoplanets and circumstellar disks with the Subaru 8-m ground-based telescope, state-or-the-art adaptive optics AO188, and a high-sensitivity infrared camera HiCIAO that we have newly developed. The total SEEDS sample will reach 500 targets, and this target sample adequately covers stellar ages ranging from 1 to 1000 Myr for solar-type stars. Also, intermediate-mass or low-mass stars are included in our SEEDS sample. The survey is currently in its fifth year, and to date, it has identified intriguing structures, such as gaps or spirals, in more than 10 transitional or debris disks (e.g., Hashimoto et al. 2012; Grady et al. 2013). Furthermore, SEEDS has discovered a massive giant planet candidate orbiting the B-type star Kappa Andromedae (Carson et al. 2013) and a Jovian planet in orbit with a size of about 44 AU (GJ 504b) around the G0-type Sun-like star GJ 504. GJ 504b has an estimated mass of about 4 Jupiter masses and effective temperature of 500 K. Among such the wide-orbit exoplanets directly imaged so far, GJ 504b represents the lowest-mass Jovian planet, and the inferred effective temperature is the coldest. The follow-up observations for GJ 504b have revealed the presences of methane in its atmosphere (Janson et al. 2013), allowing us to report the first methane detection in an atmospheres of directly imaged exoplanet. Thus, SEEDS has successfully identified and studied the exoplanets with the previously unknown properties. After the end of SEEDS survey, the comprehensive and statistical analysis of entire survey sample will be carried out. This analysis leads to improve our understanding about exoplanets and circumstellar disks. In addition, it should become a promising clue that connects to future exoplanet/disk studies, such as a survey of extrasolar Earths.

Here, we report the latest achievements of SEEDS project, such as the detection of GJ 504b. Moreover, its whole survey status and progress are also reported, as well as the future plan of SEEDS project.

Keywords: extrasolar planet, debris disk, protoplanetary disk, giant planet, direct imaging observation

Japan Geoscience Union Meeting 2014
(28 April - 02 May 2014 at Pacifico YOKOHAMA, Kanagawa, Japan)

PPS21-P01 Room:Poster Time:April 29 18:15-19:30

Sonic Boom Analysis of Meteorite at Hypersonic Speeds in Earth Atmosphere

YAMASHITA, Rei[1*] ; SUZUKI, Kojiro[1]

[1]Graduate School of Frontier Sciences, The University of Tokyo

The sonic boom followed by the passage of shock waves may cause serious damage on the ground, when a meteorite falls at hypersonic speeds as experienced at the Chelyabinsk meteorite event in February 2013. Therefore, it is important to evaluate the sonic boom generated by the meteorite. In this study, the prediction method of the sonic boom developed in the aeronautical engineering is applied to the case of the meteorite. The nature of the sonic boom propagation in the earth atmosphere is evaluated by the whole-domain simulation technique, which is based on the computational fluid dynamics in the domain bounded by the flying object and the ground (R. Yamashita and K. Suzuki, APISAT2013, No. 02-05-3). The flowfield around the sphere with 20 m diameter is numerically obtained by solving the three dimensional Navier-Stokes equations with the gravity term. The earth ' s atmospheric model is based on the international standard atmosphere (ISO 2533:1975). The flight Mach number is 10 (about 3 km/s), the flight altitude is 10 km and the flight condition is the steady level flight. The computational grid is constructed by rotating the two dimensional grid about the body axis and the number of the grid points is about 5.5 million. After the numerical calculation is conducted by using the initial grid, the calculation is performed again with the adaptive grid reconstructed to align the bow shock wave to avoid the artificial smearing of the shock wave. For computational efficiency, the domain is divided into several sectors from the body to the ground. The shape of the meteorite is approximated as a sphere and the axi-symmetric flowfield is assumed in the sector near the body. The numerical fluxes are evaluated by SHUS scheme (E. Shima and T. Jounouchi, NAL SP, pp.7-12, 1997) with the third order accuracy by MUSCL interpolation technique. The time integration is conducted by MFGS (E. Shima, proceedings of 29th Fluid Dynamic Conference, pp.325-328, 1997) method. The gravity term is added to the governing equations as a source term.

The flowfield around the sphere is composed of the bow shock wave in front of the body and the trailing shock wave in the wake. Both the waves propagating downward are merged into a single wave at 8 km altitude. In such case, the sonic boom sounds only once, while the sonic boom generated by a supersonic airplane creates explosive sounds twice without merging of the shock waves. It is reported that Chelyabinsk meteorite has been broken into three big pieces and the sonic boom sounds three times at the ground (NHK COSMIC FRONT, June 2013). Hence, the number of the pieces is equal to that of the sound of explosion. This fact seems consistent with the present simulation result. The pressure rise across the shock wave decreases with the distance from the body because of the geometric spreading. In the actual earth's atmosphere, however, the rate of decrease becomes smaller near the ground, because the atmospheric pressure and temperature increase toward the ground. Assuming the pressure augmentation factor of 1.9 at the reflection of the shock wave at the ground, the peak pressure rise is estimated at about 1.5 kPa, which is 63 times as large as the maximum allowable pressure rise (24 Pa) determined in the environmental regulation for the supersonic airplane. In the case of the Chelyabinsk meteorite, the pressure rise is estimated at 3.2±0.6 kPa (Nature 12741) from the observation of the damage of the glass windows there. Although the numerical condition is not the same as the actual flight condition of the meteorite, the pressure rise due to the passage of a meteorite at hypersonic speeds is expected to be in the order of 1 kPa or higher.

As mentioned above, the prediction method developed in the aeronautical engineering has a great potential to predict the flight condition, say, the size, altitude and Mach number, from the magnitude of the sonic boom measured on the ground by conducting the parametrical study.

Keywords: Sonic Boom, Meteorite, Hypersonic Flow, CFD, Shock Wave

Japan Geoscience Union Meeting 2014
(28 April - 02 May 2014 at Pacifico YOKOHAMA, Kanagawa, Japan)

PPS21-P02 Room:Poster Time:April 29 18:15-19:30

The brightness and the color temperature of the Chelyabinsk bolide

YANAGISAWA, Masahisa[1*]

[1]Univ. Electro-Communications

The bolide explosion on Feb. 15, 2013 over Chelyabinsk, Russia was the next most violent to the probable bolide explosion in Tunguska, Siberia in 1908. It was recorded by many dashboard movie cameras in a wide area around the city, and the movies are released on the Internet. We analyzed one of them and obtained the lightcurves of the bolide for three colors (see the figure for the temporal variations of the brightness). More than 95% of the radiant energy in the visible wavelengths was released in its flare-up for about 2 seconds. The luminosity ratios among the R (red), G (green), and B (blue) color bands are consistent with the 3500 K black-body radiation during the flare, while the pre-flare bolide was greenish-blue in color and the ratios do not agree to the black-body spectra. The maximum luminosity was 1.0 x 10^{15} W. The impact energy is estimated to be 1.9 x 10^{15} J or 450 kton in TNT equivalent (1 kton = 4.185 x 10^{12} J), based on an empirical formula for the radiant efficiency of bolides. The lightcurves and the impact energy almost agree to the results reported thus far.

Figure caption: Temporal variations of the source luminosities of the bolide in logarithmic scales. The thick (red), dotted (green), and thin (blue) lines correspond to the RGB color bands. The calculated intensities are negative in the periods without plot. The vertical scale on the right side shows the luminosity integrated over the wavelengths assuming 3500 K black body radiation. Seconds of 3:20 on Feb. 15, 2013 (UT) are shown in abscissa.

Keywords: bolide, meteoroid impact, small solar system objects, Chelyabinsk, Space guard, meteorites

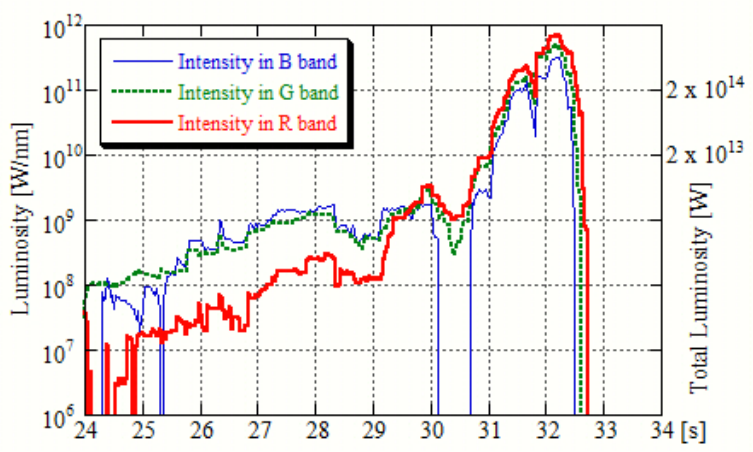

Japan Geoscience Union Meeting 2014
(28 April - 02 May 2014 at Pacifico YOKOHAMA, Kanagawa, Japan)

PPS21-P03 Room:Poster Time:April 29 18:15-19:30

Statistical distribution of the solar system dusts by meteor head echo observations with the large-aperture radar

ABE, Shinsuke[1*] ; KERO, Johan[2] ; NAKAMURA, Takuji[3] ; FUJIWARA, Yasunori[4] ; WATANABE, Jun-ichi[5]

[1]Department of Aerospace Engineering, College of Science and Technology, Nihon University, [2]Swedish Institute of Space Physics (IRF), [3]National Institute of Polar Research (NIPR), [4]Nippon Meteor Society, [5]National Astronomical Observatory of Japan

A meteor head echoes is caused by radio waves scattered from the intense region of the plasma surrounding and co-moving with a meteoroid during atmospheric entry at about 70-130 km altitude. Meteor head echo observations were carried out using the high-power large-aperture (HPLA) Kyoto university Shigaraki middle and upper atmosphere (MU) radar in Japan (34.85deg N, 136.10deg E). Since 2009 the atmospheric trajectories and interplanetary orbital elements have been derived by the MU radar meteor head echoes (e.g.; Kero et al. (2012); Kero et al. (2011)). Approximately 120,000 orbital elements of meteors with excellent accuracy were obtained until January 2014. Typical error for velocity and semi-major axis are 0.3 km/s and 0.1 AU, respectively. Such a huge number of meteoroid orbits with the precise orbital accuracy has not been observed before. Here we report some results obtained by the statistical analysis of the database, such as orbital distributions and associations of comets and asteroids.

Keywords: meteors, dusts, meteoroids, comets, asteroids, MU radar

Japan Geoscience Union Meeting 2014
(28 April - 02 May 2014 at Pacifico YOKOHAMA, Kanagawa, Japan)

PPS21-P04 Room:Poster Time:April 29 18:15-19:30

Laboratory experiment simulating Martian surface observation with submillimeter-wave polarimetric radiometry

ARIMURA, Taketo[1*] ; OCHIAI, Satoshi[2] ; KIKUCHI, Kenichi[2] ; KITA, Kazuyuki[3] ; KASAI, Yasuko[2]

[1]Graduate School of Science and Engineering, Ibaraki University, [2]National Institute of Information and Communications Technology, [3]Faculty of Science, Ibaraki University

Energies and materials exchange between the ground and atmosphere on Mars play important roles in the Martian general circulation. It is necessary to observe the spatial and temporal variability of the Martian surface from orbiter. However, it has been quite difficult to continually monitor the Mars surface in optical observation due to opaqueness of the Martian dust. Millimeter/submillimeter radiometers enable to observe the Martian surface through dust, though such measurement has never been conducted in planetary exploration. We assess the effectiveness of this observation method by laboratory experiment.

By observing millimeter/submillimeter emission from the Martian surface in several emission angles and two polarizations, we can derive physical temperatures, permittivity and roughness of the surface from brightness temperatures. In order to estimate each property from polarized brightness temperatures, we need to know relationship between emissivity or/and reflectivity in millimeter/submillimeter wave region and the parameters of surface.

We developed an experiment system to examine millimeter/submillimeter scattering and emission characteristics of the simulated Martian surface in a chamber. Measurement samples in the chamber are coolable at Martian surface temperature. The chamber is designed to measure emission of samples using a receiver and reflection of samples using a transmitter and a receiver. We can also obtain arbitrary-polarized emission with arbitrary incident angle by controlling mirrors in our system.

To discuss relationship between emission and surface parameters on the Martian surface, it is necessary to know influences of permittivity and surface roughness on the reflectivity. Therefore, we measured reflectance of Acrylic plate and Alumina grain at millimeter/submillimeter waves region. We discuss effects of permittivity and roughness on measured reflectivity of measurement samples in known polarization and incident angle. Moreover, we retrieve the permittivity and the roughness of sample from measured reflectivity. Using this measurement results, we expect a step closer to explanation of relationship between emission and surface parameters in the Martian surface at millimeter/submillimeter waves region.

Keywords: Mars, surface observation, submillimeter-wave

Japan Geoscience Union Meeting 2014
(28 April - 02 May 2014 at Pacifico YOKOHAMA, Kanagawa, Japan)

PPS21-P05 Room:Poster Time:April 29 18:15-19:30

Scientific importance and possibility of HCN detection in Enceladus plumes by ALMA

KODAMA, Kenya[1*] ; SEKINE, Yasuhito[1] ; IINO, Takahiro[2] ; SAIGO, Kazuya[6] ; KASAI, Yasuko[3] ; SAGAWA, Hideo[4] ; MAEZAWA, Hiroyuki[5]

[1]Dept. Complexity Sci. and Engr. Univ. of Tokyo, [2]Solar-Terrestrial Environment Laboratory,Graduate school of science,Nagoya University, [3]Senior Researcher Global Environment Division National Institute of Information and Communications, [4]National Institute of Information and Communications Technology, [5]Department of Physical Science Osaka Prefecture University, [6]National Astronomical Observatory of Japan

Saturn's icy moon, Enceladus, exhibits ongoing geological activities, including eruption of water-rich plumes from warm fractures near the south-pole region. These geological activities together with the findings of Na-rich salts in the plumes suggest the presence of an interior liquid ocean beneath the icy crust. This demonstrates that Enceladus' plumes provide a unique opportunity to investigate the chemical composition of oceanic water, possible geochemical reactions, and habitability of the icy moon. However, due to limitations of in-situ measurements of the plumes by the Cassini spacecraft, it is not able to identify or quantify some key molecules, which could probe physical and chemical conditions of the ocean.

Here we discuss scientific importance and possibility of detection of HCN in the plumes by large ground-based, sub-millimeter telescope, ALMA. Because HCN is one of the fundamental materials contained in icy planetasimals in the outer solar system, and because it readily hydrolyzes in warm water($>$50 ℃), a lack of HCN suggests that Enceladus' interior would have experienced relatively high temperatures, i.e., a presence of hydrothermal activity. On the other hand, if HCN were presence in the plumes, this in turn means that Enceladus would have been cold throughout its history. Given the results of thermal evolution model, the latter case suggests late formation of the Saturnian system($>$5Myr) after CAI formation, which would result in a depletion of short-lived radiogenic heat source in Enceladus.

To evaluate the possibility to detect HCN in the plumes by ALMA, we first estimate a special distribution of H_2O gas density based on results from Cassini's observations and plume eruption modeling. Then, we calculate radiactive temperatures of HCN in the field of view of ALMA as a function of HCN concentration. Finally, the upper limit of HCN as a function of observation time will be obtained. For instance, if HCN were not detected within 4-6 hours of observation time, an upper limit of the HCN concentration in the plumes becomes 0.2% relative to water, which is comparable to a typical concentration of HCN in comets. Thus, the ALMA telescope is capable of detecting HCN in Enceladus' plumes within a reasonable observation time, if it were present in an amount comparable to that of comets. In either case whether HCN were presence or not, we would be able to constrain geochemical reactions and thermal history of Enceladus as well as the timing of formation of Saturnian system.

Japan Geoscience Union Meeting 2014
(28 April - 02 May 2014 at Pacifico YOKOHAMA, Kanagawa, Japan)

PPS21-P06 Room:Poster Time:April 29 18:15-19:30

Development of SPH: Toward Understanding of Disk-planet Interaction Near the Disk Inner Edge

FUJII, Yuri[1*] ; IWASAKI, Kazunari[1] ; TSUKAMOTO, Yusuke[1] ; INUTSUKA, Shu-ichiro[1]

[1]Nagoya University

Recent observations of exoplanets reveal the existence of close-in planets. These planets are thought to form in outer disks and migrate inward because of the disk-planet interaction. If there are disk inner cavities, planets can stop migrating and stay in close-in orbit. Disk evolution is highly affected by these planets. Thus, the understanding of the interaction between disks and close-in planets is crucial. In this study, we develop a numerical scheme to investigate the interaction between disks and planets. Although the grid-based schemes are widely used in this context, there are difficulties in calculating with a disk inner cavity or eccentric planets. These difficulties can be removed by smoothed particle hydrodynamics (SPH) with high accuracy. In this presentation, we will talk about the development of code and the performance evaluation.

Keywords: exoplanet, protoplanetary disk, smoothed particle hydrodynamics

Japan Geoscience Union Meeting 2014
(28 April - 02 May 2014 at Pacifico YOKOHAMA, Kanagawa, Japan)

PPS21-P07 Room:Poster Time:April 29 18:15-19:30

Evolution of a protoplanetary disk and chemical composition of planetesimals

NAGAHARA, Hiroko[1*] ; OZAWA, Kazuhito[1]

[1]Dept. Earth Planet. Sci., The Univ. Tokyo

We investigate physico-chemical evolution of the proto-solar disk at the early stage by developing a new model that combines physics and chemistry with special interest to temporal and spatial evolution of the disk. Then, we discuss how the composition of planetesimals varies depending on the time and space for their formation including refractory or volatile rich ones.

The basic of the model is a radial advection-diffusion equation, which includes drift and dispersion by turbulence with stochastic diffusion term calculated by the Monte Carlo method and which shows the diffusivity by the viscosity of the disk. The difference from conventional disk models is that the present method stands on the Lagrangean differentiation, and it is able to trace the movement of individ- ual particles.

A considerable amount of materials in the inner regions are transported outward at the early stage (t <10^5 yrs), which is because the surface density is much larger in the inner region at the early stage of the disk evolution. Although the outward flux is large at the early stage, there comes a larger amount of materials from the outer region even within ~10^5 yrs. The mixing ratio of materials from the inner regions to outer regions is almost unity within several AU all through the disk evolution, suggesting that thermally processed materials and unprocessed materials were mixed in the inner region of the disk. It is important that the relative abundance of materials from outer regions becomes larger with time, which implies that planetesimals formed within several AU at the early stage of the disk evolution consists partly of materials initially located at the inner regions and partly from outer regions, but those formed at the later stage contain more abundant law materials transported from the outer regions.

The mixing ratio of materials from the inner and outer regions is almost unity at the early stage but the fraction of materials from the outer regions increases with time. Combining the information about the maximum temperature that the particles experienced, we can constrain that early differentiated planetesimals such as the parent body of angrites and planetesimals with refractory-rich compositions such as CV chondrites were formed at the inner region of the disk in ~10^5 yrs. On the other hand, planetesimals for other carbonaceous chondrites or ordinary chondrites that are depleted in sulfur were formed later, possibly at ~10^6 yrs.

Keywords: protoplanetary dsik, chemical evolution, dust movement

Japan Geoscience Union Meeting 2014
(28 April - 02 May 2014 at Pacifico YOKOHAMA, Kanagawa, Japan)

PPS21-P08 Room:Poster Time:April 29 18:15-19:30

Simulating global dust coagulation with grain charging

OKUZUMI, Satoshi[1*] ; TANAKA, Hidekazu[2]

[1]Graduate School of Science and Engineering, Tokyo Institute of Technology, [2]Institute of Low Temperature Science, Hokkaido University

Growth of dust particles by collisions is the initial step of planet formation. Conventionally, the theory of dust coagulation in protoplanetary disks assumed electrically neutral dust particles, but in reality dust in the disks is likely to be charged given that the disks are ionized by cosmic rays and stellar X-rays. In our previous work (Okuzumi 2009; Okuzumi et al. 2011a,b), we extensively studied the role of grain charging in protoplanetary dust growth, and concluded that dust growth stalls at its early stage because of the excessively large (negative) charges carried by small dust aggregates. We also predicted that this ”charge barrier” could be overcome (albeit on a very long timescale) if dust in the disks is globally transported by radial drift and turbulent diffusion.

The purpose of the present work is to demonstrate the breakthrough of the charge barrier in a global setup. In order to do this, we have developed a new simulation code for global dust coagulation including the effect of grain charging. The new code is based on a previous code for planetesimal formation (Brauer et al. 2008; Okuzumi et al. 2012) but now calculates charging and Coulomb repulsion of dust particles at each location in a disk consistently with the particle size distribution at the same location. To verify the code, we perform some test simulations and compare them with the prediction from our previous theory.

Keywords: dust, charging, planet formation, protoplanetary disk

Japan Geoscience Union Meeting 2014
(28 April - 02 May 2014 at Pacifico YOKOHAMA, Kanagawa, Japan)

PPS21-P09 Room:Poster Time:April 29 18:15-19:30

N-body simulations of Rubble pile Collisions in Tidal fields

HYODO, Ryuki[1*] ; OHTSUKI, Keiji[1]

[1]Kobe University, Graduate School of Science

We examine collisional disruption of gravitational aggregates in the tidal environment by using local N-body simulations. We find that outcomes of such collision largely depend on impact velocity, direction of impact, and radial distance from the planet. In the case of a strong tidal field corresponding to Saturn's F ring, collisions in the azimuthal direction is much more destructive than those in the radial direction. Numerical results of collisions sensitively depend on impact velocity, and complete disruption of aggregates can occur even in impacts with velocity much lower than their escape velocity. In such low-velocity collisions, deformation of colliding aggregates plays an essential role in determining collision outcomes, because the physical size of the aggregate is comparable to its Hill radius. On the other hand, the dependence of collision outcomes on impact velocity becomes similar to the case in free space when the distance from the planet is sufficiently large. We submitted the results to the Astrophysical Journal.

Keywords: rings, satellites, aggregates

Japan Geoscience Union Meeting 2014
(28 April - 02 May 2014 at Pacifico YOKOHAMA, Kanagawa, Japan)

PPS21-P10 Room:Poster Time:April 29 18:15-19:30

An improved fragmentation model on outcome of planetesimal collisions

FUJITA, Tomoaki[1] ; GENDA, Hidenori[2*] ; KOBAYASHI, Hiroshi[3] ; TANAKA, Hidekazu[4] ; ABE, Yutaka[1]

[1]Department of Earth and Planetary Science, University of Tokyo, [2]Earth-Life Sicence Institute, Tokyo Institute of Technology, [3]Department of Physics, Nagoya University, [4]Institute of Low Temperature Science, Hokkaido University

Collisions between planetesimals or a planetesimal and a protoplanet are thought to occur frequently in the stage of planet formation, and these planetary bodies grow up through these collisions. However, if destructive collisions between them occur frequently, these bodies break up into fragments rather than promote the growth of them. Therefore, in order to understand the process of the growth for planetesimals and protoplanets, it is important to know the impact conditions under which a collision is destructive. The critical specific impact energy for catastrophic disruption $Q_D{}^*$, where the largest remnant has half the target mass, has been well investigated under various conditions so far (Holsapple et al., 2002; Benz & Asphaug, 1999; Leinhardt & Stewart, 2009). Such catastrophic impacts have been regarded as important process for planet formation. The values of $Q_D{}^*$ which has been referred and used most frequently were calculated by Benz and Asphaug (1999). Although they performed many impact simulations to determine $Q_D{}^*$, the resolution of their numerical simulation were quite low and they did not check the resolution convergence of $Q_D{}^*$. In addition, recent studies (Kobayashi & Tanaka, 2010; Kobayashi et al., 2010) have suggested that non-disruptive small-scaled impacts were also important to the growth of protoplanets, because these small-scaled impacts are much more frequent than disruptive impacts.

In order to discuss more correctly the growth of planets, a correct value of $Q_D{}^*$ and the relation between ejecta mass and impact energy for small-scaled impacts should be required. In this thesis, I investigate the resolution dependence of $Q_D{}^*$ and obtain a correct value of $Q_D{}^*$ for planetesimal collisions by numerical impact simulations with sufficient resolution. I also investigate small-scaled impacts, and formulate the relation between the ejecta mass and impact energy.

Using the smoothed particle hydrodynamics method (SPH) with self-gravity and without strength, I systematically perform the hydrodynamic simulations of collisions between rocky planetesimals. I consider collisions of 10 km and 100 km rocky targets and various sized impactors under various conditions such as impact velocity, impact angle and resolution.

I found that the value of $Q_D{}^*$ depended on resolution. This is because distribution ratio of initial impact energy to kinetic and internal energy of a target differs depending on resolution due to shear flows which appears during propagation of shock wave and rarefaction wave and ejection process. This energy distribution ratio, probably also $Q_D{}^*$, converges in using 7.5×10^7 particles. The resolution in Benz & Asphaug (1999), where they performed impact simulations with 5×10^4 particles, was insufficient. The $Q_D{}^*$ obtained by higher-resolution simulations is about a half order of magnitude smaller than that of Benz and Asphaug (1999). This means collisions between planetesimals or a planetesimal and a protoplanet are more destructive than previously thought. I applied improved $Q_D{}^*$ to the growth of protoplanets using analytical method proposed by Kobayashi et al. (2010). As a result, the mass of the finally formed protoplanet is a half smaller than the case for previous $Q_D{}^*$. In addition, I derived the formulation of scaling law representing the relation between ejecta mass and impact energy from small-scaled impacts to destructive impacts. I found that this relation can be scaled by target size, impact energy normalized by $Q_D{}^*$, and impact velocity, but it depend on impact angle. With $Q_D{}^*$ and the scaling law obtained in this study, the final grown mass of a protoplanet is 0.058 M_{earth} at 1AU and 0.17M_{earth} at 5 AU, where M_{earth} represents the Earth mass.

Japan Geoscience Union Meeting 2014
(28 April - 02 May 2014 at Pacifico YOKOHAMA, Kanagawa, Japan)

PPS21-P11 Room:Poster Time:April 29 18:15-19:30

Numerical modeling of impact phenomena using iSALE shock physics code

KUROSAWA, Kosuke[1*] ; SENSHU, Hiroki[1] ; WADA, Koji[1] ; MIKAMI, Takashi[2] ; HIRATA, Naru[3] ; KAMATA, Shunichi[2] ; ISHIHARA, Yoshiaki[4] ; GENDA, Hidenori[5] ; NAKAMURA, Akiko[6] ; TAKATA, Toshiko[7]

[1]PERC, Chitech, [2]Dept. of CosmoSciences, Hokkaido Univ., [3]Dept. of Computer Sci. & Eng., The University of Aizu, [4]ISAS, JAXA, [5]ELSI, Titech, [6]Dept. of Earth and Planetary Sciences, Kobe University, [7]Division of Science Education, Miyagi University of Education

iSALE (impact-SALE) is a shock physics code based on the SALE hydrocode (Simplified Arbitrary Lagrangian Eulerian), which is an open code for planetary scientist. iSALE contains a number of option to model impact phenomena of geological materials. The calculation results can be easily visualized and analyzed using included software. A number of ANEOS tables and strength models of geological materials, including water ice, silicate rocks, and iron are also included. We have formed a user community called " iSALE users group in Japan " to introduce iSALE to the Japanese society for planetary science and to share information on the usage of iSALE. The URL of our wiki page and the mailing list are as follows.

The URL of the wiki page of iSALE users group in Japan
https://www.wakusei.jp/~impact/wiki/iSALE/

Mailing list
isale-users-jp@perc.it-chiba.ac.jp

In the presentation, we show the results of a number of test calculations using iSALE.

We gratefully acknowledge the developers of iSALE, including Gareth Collins, Kai W$\bar{u}$
nnemann, Boris Ivanov, Jay Melosh and Dirk Elbeshausen.

Keywords: Hypervelocity impacts, Shock physics code, Hydrocode calculation, Equations of state, strength model, iSALE

Japan Geoscience Union Meeting 2014
(28 April - 02 May 2014 at Pacifico YOKOHAMA, Kanagawa, Japan)

PPS21-P12 Room:Poster Time:April 29 18:15-19:30

Study on fundamental characteristics of penetration dynamics into icy target

NAMBA, Kazuya[1*] ; SUZUKI, Kojiro[2]

[1]Grad. Sch. Eng., The University of Tokyo, [2]GSFS, The University of Tokyo

A penetrator, which penetrates the surface of a planet, a satellite and so on to investigate the interior by high-speed hard landing, is expected to play an important role in the solar system exploration of the future. Comparing to soft lander, penetrator has advantages of consuming less fuels, enabling us to launch multiple probes at a time because of its low mass, and so on. However, probe must survive hard impact in collision, thus no penetrator missions have been successfully achieved so far. The icy object, such as 24 Themis and Europa, is expected to contain organics which serve as the precursor of life in their subsurface. Therefore, the cryo-penetrator, which penetrates the icy object and investigate specimens of subsurface which have not been contaminated by cosmic rays, should have a high importance. For a penetrator into regolith, a fully-developed flyable penetrator has been successfully developed for the Lunar-A mission, though the mission itself has been cancelled. For icy target, however, the number of studies from the engineering viewpoint is quite limited, for example, the conceptual study on CRAF mission to a comet nucleus (Adams et al., NASA CR-177393, 1986). In this study, we investigated the fundamental properties of the penetration dynamics of the cryo-penetrator, by conducting penetration experiments into the target made from H_2O ice.

Penetration experiments were conducted by using a ballistic range in our laboratory. The projectile is accelerated by the compressed air, launched horizontally and crashed into a target body. Impact speed is set from 100 m/s to 300 m/s. Two types of projectile, a needle-like one (iron, size: ϕ2.45x15mm, mass: 1.71g) and a blunt cone-like one (brass, ϕ8.4x15mm, 2.33g) are used. Three types of target, pure H_2O ice (size: 270x175x130mm, mass: 5.5kg, density: 0.90g/cm^3, porosity: 3%), low purity H_2O ice (150x120x100mm, 1.5kg, 0.75g/cm^3, 19%) and an oil clay (155x120x70mm, 2.2kg, 1.7g/cm^3) are used. A high-speed camera (frame rate: 2200-8800fps, exposure time: 15μs) is used to observe a sequence of events: the free-flight of the projectile, impact, crater formation, penetration, and so on.

We found that the penetration into H_2O ice produces ejecta of icy fragments, which erupt conically immediately after collision, and then produces the jet-like ejecta in the almost perpendicular direction to the surface that continues more than 100 msec. On the other hand, the penetration into clay target produces ejecta outward-conically for duration of a few msec. Moreover, we found that the penetrator tends to be pushed back from the target by the ejecta, since the ice around the projectile has been almost broken into pieces erupting as the ejecta and the penetrator cannot be fixed inside the target without receiving the gripping force from the ice. We also found that eruption was continued even after the projectile has completely bounced from the target. This phenomena is frequently observed when the projectile with a less slender body. In the case of a slender penetrator, however, it is hardly subject to bounce-back. Consequently, a slender shape seems more suitable to the penetrator for icy target. The shape of crater consists of the pit region on the center, the spall region which is a shallow depression on the periphery of the pit, and cracks spread a wide range of target. It is qualitatively consistent with previous researches using bullet shape (e.g. Kato et al., Icarus 113(2) 423-441, 1995., Arakawa, Low Temperature Science 66 113-121, 2008). The pressure at a point of impact is estimated by using the one-dimensional planar impact approximation (Wada, JSIAM 16(4) 19-31, 2006): the result shows that it is beyond the Hugoniot elastic limit (HEL), thus the H_2O ice is expected to behave like fluid in the vicinity of the impact point.

This work is supported by Grant-in-Aid for Scientific Research (B) No. 25289301 of Japan Society for the Promotion of Science.

Keywords: icy object, penetrator, crater, ballistic range

Japan Geoscience Union Meeting 2014
(28 April - 02 May 2014 at Pacifico YOKOHAMA, Kanagawa, Japan)

PPS21-P13 Room:Poster Time:April 29 18:15-19:30

Experimental study of compaction process of powder bed by centrifuge experiment

OMURA, Tomomi[1*] ; KIUCHI, Masato[1] ; GUETTLER, Carsten[2] ; NAKAMURA, Akiko[1]

[1]Graduate School of Science, Kobe University, [2]Max-Planck-Institute for Solar System Research

Dust aggregates in protoplanetary disk are compacted by dust-dust collisions, ram pressure of the disk gas and self-gravity (Kataoka et al., 2013). At reaccumulation phase of asteroids, porosity of rubble pile and regolith would be determined by collisional pressure and self-gravity.

Relationship of porosity of powder layer and particle's radius is given by (Yu et al., 2003; Kiuchi and Nakamura, 2014)

$p=p_0+(1-p_0)\exp\{-mR_F^{-n}\}$ (1)

where R_F is the ratio between the magnitudes of the van der Waals force between two particles and gravity force on particles, therefore a function of particle radius. p_0, m, and n are constants. p_0 should be understood as the porosity without any interparticle force.

It is not clear if Eq.1 can be applied for powder layer under different gravity from 1 G. Eq.1 was originally derived for particles at surface, and we don't know to what extent this equation is able to be applied for the interior of planetary bodies, i.e., it has not examined for the porosity evolution of bodies due to the accumulation of new grains and blocks onto the surface. If Eq.1 is applicable to such case, porosity given by Eq.1 should be consistent with the result of the case in which R_F is reduced by increasing the gravity. In this study we perform experiments, under different gravitational accelerations, and we compare the results with Eq.1.

We use silica sand, 60 wt% of grains have sizes ranging from 7.5 μm and 80 μm and fly ash, 60 wt% of grains have sizes ranging from 1 μm and 8 μm. They were sieved into a cylindrical container of diameter 5.8 cm and depth 3 cm. After that, the top part of the bed over the height of the container was leveled off. Porosity of each granular bed is approximately 60 % and 70 %. The experiments were performed at elevated acceleration on a centrifuge to provide 1-18 G and observed with a video camera. In contrast with unidirectional compressive compaction using a piston, centrifugal compaction is capable of applying uniform compressive force at any place of the container without causing any local disturbance (Mizuno et al., 1991). After the materials were compressed, bed height was measured with a laser displacement meter and the difference between the initial bed height and the average bed height after acceleration was calculated.

As a result, it is shown that Eq.1 is consistent with experimental result within 6 % (silica sand) and 5% (fly ash) in porosity when assuming the grain diameter=24 μm and 4.5 μm, respectively. This diameter corresponds to the median of cumulative weight distribution of the grains. Also, the diameter of the small silica sand grains sticked with large grains is close to 24 μm.

Keywords: planetesimal, asteroid, porosity, high gravity, powder and granular material

Japan Geoscience Union Meeting 2014
(28 April - 02 May 2014 at Pacifico YOKOHAMA, Kanagawa, Japan)

PPS21-P14 Room:Poster Time:April 29 18:15-19:30

High velocity impact cratering experiments on ice-sand mixture simulating the surface of icy satellites

TAKANO, Shota[1*] ; ARAKAWA, Masahiko[1] ; YASUI, Minami[2]

[1]Graduate School of Science, Kobe University, [2]Organization of Advanced Science and Technology, Kobe University

It is well known that ice-rock mixtures could be a main component of icy satellites, the surface crust of asteroid Ceres. Ceres' icy crust could be impacted by various asteroids with different components and physical properties will affect the crater morphology. Therefore, we would obtain various information from the investigation of the observed craters such as material properties of impacted asteroids and the internal structures of the icy crust and so on. To conduct these investigation, the laboratory experiments would be necessary to derive such information from the observed crater. Then, we should carry out the cratering experiments on ice, ice-rock mixtures and the layered target.

Impact experiments on ice has been conducted systematically under various conditions. However, the cratering experiments on ice-rock mixture were limited in the impact velocity range and the rock contents. It is necessary to experiment at the velocity higher than 4km/s to apply to craters on Ceres, but it is not done now. Therefore, we made cratering experiments on ice?rock mixtures at the impact velocity higher than 1km/s using the several types of the projectile, and compared them with the pure ice to clarify the effects of rock inclusion on the crater morphology and crater scaling law.

We installed and used a new two-stage light gas gun at Kobe University in 2013. We prepared ice-rock mixture targets simulating Ceres crust which consisted of water ice and quartz sand having a particle size of about 500μm, and the quartz content was regulated to be 81$\pm$2wt%. The ice-sand mixture was made in a cylindrical metal container with the height of 5$\sim$10cm and the diameter of 15cm. The water-sand mixture was frozen in a freezer with the temperature from -23 ℃ to -15 ℃. Used spherical projectiles were made of aluminum (2.7g/cm3), titanium (5g/cm3), and zirconium (5.7g/cm3), respectively. We lunched projectiles at 1.6$\sim$5.1km/s with nylon sabots to use various types of projectiles. To prevent targets from melting, the vacuum chamber was evacuated for insulation. The chamber pressure during the experiments was from 200 to 230Pa. A crater formation process was taken by an image-converter camera every 5μs, and 18 successive images were obtained for each shot. From these images, we examined the characteristics of impact eject such as the growth rate, and the shape, and it was compared with that of pure ice. We measured the crater shapes by a caliper.

We found that the spallation was difficult to occur on the ice-rock mixture targets compared to pure ice targets. So, the depth-diameter ratio of the crater for ice-rock mixtures, these dependencies on the velocities, and the projectile densities was different from that of pure ice targets. We found that the crater diameter on the ice-rock mixture is about a half of that on pure ice at the same impact energy. Hiraoka et al. (2004) made the cratering experiments on ice-rock mixture with the rock contents from 0 to 50 wt% at the constant impact energy. We compared their results with our results obtained for 80 wt% and found that our result is almost consistent with their results of 50 wt% content. This means that the crater size stop decreasing at 50 wt%, then it becomes almost constant until 80 wt%. We speculate that the crater size might drastically change to be small between 80 to 100 wt% corresponding to rock itself. It might be possible that the crater size could be controlled by the ice strength from 0 to 80wt% and by the rock strength at the range of content near 100 wt%. The crater scaling law proposed by Housen and Holsapple (2012) was applied, and the scaled crater radius π_R and the scaled strengthπ_Y were investigated in our results. Our results were compared with that of pure ice and the ice-rock mixture's dynamic tensile strength was supposed to be 100MPa if the ice-rock mixture was scaled by the same parameter as that of pure ice.

Keywords: icy satellites, ice-sand mixture, impact crater, high velocity impact experiments

Japan Geoscience Union Meeting 2014
(28 April - 02 May 2014 at Pacifico YOKOHAMA, Kanagawa, Japan)

PPS21-P15 Room:Poster Time:April 29 18:15-19:30

Experimental study on the decay process of impact-induced stress propagating through granular materials

MATSUE, Kazuma[1*] ; ARAKAWA, Masahiko[1] ; YASUI, Minami[2]

[1]Graduate School of Science, Kobe University, [2]Organization of Advanced Science and Technology, Kobe University

Introduction: Impact process is one of the most important physical processes in the solar nebula. In order to understand the impact histories related to planetary formation process, it is important to study the impact cratering process and the scaling law. Impact cratering experiments have been performed on granular material, and the crater size is found to be different depending on the target material. So, it is necessary to study how physical properties affect the cratering process, especially for excavation stage. Excavation flow is a main process that controls the crater size, so we should examine the effects of material properties. However, it is difficult to observe the flow inside the target, so we used the in-material sensor to measure the pressure. The pressure distribution in the granular target would show the flow and we can compare the crater size and the pressure distribution to clarify the effect of target materials on the crater formation process.

Experimental method: We prepared a target container with a pressure sensor to measure the stress generated by impact. It is made of aluminum with the size of 10cm×10cm×10cm, and we changed the depth of the granular target from 1 to 10cm. The pressure sensor (20kPa, ≤2kHz)was attached on the bottom of the container just below the impact point, and impact experiments were conducted by a free-fall or by a one-stage vertical He-gas gun in Kobe University. We studied the effects of projectile size and impact velocity on the crater size and the stress wave. We used glass beads and quartz sand with the diameter of 100 and 500μm as granular target, and glass balls (ϕ=7.75, 10, 15mm) in free-fall, nylon and alumina (ϕ= 3mm) in vertical gun experiments as projectile. Impact velocity is 2-5.5m/s in free-fall and 60-70m/s in vertical gun experiments. We observed crater size and pressure wave in each experiment.

Results: We found that the size of the impact crater strongly depends on the granular materials, that is, the crater formed on the quartz sand was systematically smaller than that formed on the glass beads. Then, we found that the pressure wave increased suddenly and decreased with a relaxation time depending on target materials. The relaxation time is small for quartz sand and long for glass beads, and the relaxation time of 100μm quartz sand was not measured because of normal mode oscillation of the pressure sensor: it means that the time is less than 0.5ms.

Although the normal mode oscillation of the sensor was observed in the high velocity impact and the shallow depth impact in the case of gas gun experiments, we analyzed the peak of measure pressure waves (P_{max}) and obtained the relaxation time (τ) by fitting them with the following function: $P(t)$-$P(\infty)$=$A\exp(-t/\tau)$, where t is time after the impact. As a result, τ is obtained to be 1ms for glass beads target irrespective of the bead size, and 0.1ms for 500μm quartz sand. The relationship between the pressure and the propagation distance was described by $P(r)=P_0(r/L)^{-b}$, where L is a projectile radius, r is distance, P_0 is an initial impact pressure, and b is a decay constant. The decay constant was found to change with the impact velocity and the target materials: it was derived to be 0.79,0.94 in a low velocity range, 1.61,1.71 in a high velocity range for glass beads, quartz sand.

We found that the relationship between the crater size and P_{max} at 4cm depth was different in each granular material. The crater size of the glass beads target was larger than that of the quartz sand at the same P_{max} . Then, we introduce a new parameter expressed by τ times P_{max}, so called impulse, I. We renewed the relationship using I instead of P_{max} and found that all data set were merged on one line. This means that I could be a suitable parameter to describe the material dependence of the cratering efficiency. We would like to clarify what material properties determine the τ and how it changed with the physical condition in the future.

Keywords: Excavation flow, Granular material, Cratering process

Japan Geoscience Union Meeting 2014
(28 April - 02 May 2014 at Pacifico YOKOHAMA, Kanagawa, Japan)

PPS21-P16 Room:Poster Time:April 29 18:15-19:30

Effects of impact angles on the impact strength of icy and rocky planetesimals for the collision among equal size bodies

KOMOTO, Yasunari[1] ; ARAKAWA, Masahiko[1] ; YASUI, Minami[2*]

[1]Graduate School of Science, Kobe University, [2]Organization of Advanced Science and Technology, Kobe University

Introduction: There are a lot of impact experiments to simulate planetesimals collisions, and most of them had a large mass difference between a projectile and a target. The impact strength is well known that they are described by the energy density: the ratio of the projectile kinetic energy to the mass of the target and the projectile. So, when the projectile is rather smaller than the target (this is an usual situation in the lab. experiments), the very high speed more than 1 km/s is necessary to disrupt the target. This is an analogy of the present asteroid collisions, but it might be far from the simulation expected in planetesimals collisions. Because we speculate the collisions among the similar size small bodies in the solar nebula, and the relative collisional velocity among them could be several 10 m/s. Therefore, it should be important that the planetesimals were disrupted or not at the impact speed around several 10m/s for the collisions among similar size small bodies, then we must conduct the collisional experiments to derive the impact strength of planetesimals in the similar size collisions. In this study, we carried out the impact experiments using the equal size ball made of ice, gypsum, and gypsum-glass beads mixture. These samples simulate icy planetesimals, planetesimlas for chondrite parent bodies. We also conducted not only head-on collision but also oblique collision and studied the effects of impact angles on the impact disruption.

Experimental methods: We prepared three types of ball sample with the size of 25 mm and 30 mm made of ice, gypsum-glass beads mixture, and gypsum. They were made by putting each solution in a round mold to form spherical sample. The impact experiments were made by using three types of accelerators: they are a spring gun for low velocity collision, a vertical gas gun for ice and a horizontal gas gun for gypsum, and the achieved velocity is from 4 to 160m/s. The oblique impact was also conducted by shifting the impact point from the geometrical center of the target. The impact angle was changed from 0 deg. (normal impact) to 80 deg. (nearly passing away impact). Impact experiments were observed by a high-speed camera and all of the impact fragments were collected to measure the weight and establish the size distribution. We looked for the recovered fragments to identify the same fragment found in the video image, and tried to construct the velocity-mass distribution of the impact fragments.

Results: We used the reduce mass to calculate the impact energy in the center-of-mass system, so the energy density Q_g was defined by the ratio of the kinetic energy of two bodies in the center-of-mass system to the mass of the two equal balls. The impact strength was obtained for the similar size collisions by using this Q_g. As a result, the impact strength ${Q_g}^*$ of ice and gypsum was derived to be almost similar to that obtained for the impact experiments with the mass difference more than 10. However, the ${Q_g}^*$ of glass beads-gypsum mixture was derived to be rather smaller than that obtained in the previous experiments. In the oblique impacts, the mass of the maximum impact fragment was found to decrease with the increase of the impact angle. So, we modify the energy density by using the velocity component normal to the impact surface which effectively work for the disruption, then this modified energy density enabled us to fit all of the data on one line for each target. Finally, we estimated the re-accumulation condition of planetesimals according to the velocity distribution of the impact fragments that obtained in this study. As a result, it is speculated that icy planetesimals could re-accumulate for the bodies larger than 20 km in the diameter, and this threshold size for the planetesimals of ordinary chondrite parent bodies is 5.2km and that for the planetesimals of carbonaceous chondtite parent bodies is 6.7km.

Keywords: Planetesimals, Oblique impact, Impact strength, Energy partition, Re-accretion

Japan Geoscience Union Meeting 2014
(28 April - 02 May 2014 at Pacifico YOKOHAMA, Kanagawa, Japan)

PPS21-P17 Room:Poster Time:April 29 18:15-19:30

Dynamic compaction experiments of porous materials: Implications for impact compaction of pre-planetesimals

YASUI, Minami[1*] ; YOKOTA, Mizuki[2] ; SAKAMOTO, Kana[2] ; ARAKAWA, Masahiko[3]

[1]Organization of Advanced Science and Technology, Kobe University, [2]Faculty of Science, Kobe University, [3]Graduate School of Science, Kobe University

Introduction: Two theories are proposed for the growth mechanism of bodies with the diameter from cm to several hundreds meters (pre-planetesimals). One is that planetesimals could form by a gravitational instability in the dust layer of a protoplanetary disk. The other is that planetesimals could form by a repeating impact coagulation of dust aggregates. In this study, we focus on the latter theory. There are some problems that planetesimals could not grow because of rebound and catastrophic disruption among pre-planetesimals caused by the increase of average density. Sakamoto (2013) did free-fall impact experiments of porous snow simulating icy pre-planetesimals by using the stainless cylinder to examine the compaction conditions, and clarified the relationship between the impact stress and the final density profile and the size of compaction area. However, the impact velocities in her study were 0.7 to 3.5 m/s, relatively lower compared to the average impact speed of pre-planetesimals. In this study, we conducted impact experiments of porous materials at $>$5 m/s to examine the compaction mechanism, impact stress, and density profile.

Experimental methods: The target was high porous snow with the initial porosities of 70 and 80% and perlite particles with the density of 85 kg/m^3 simulating the icy and rocky pre-planetesimals. We did impact experiments of snow in the cold room (-10 ℃) at ILTS, Hokkaido University, and perlite at Kobe University, by using the one-stage vertical and horizontal light gas guns. The vertical gun was used for only snow targets. The target was prepared by packing ice grains or perlite particles into the acrylic tube, up to 120 mm depth, and the blue ice grains or the red perlite particles were put into the target every 20 mm from the bottom due to measure the density changing with depth. The piston was set on the target surface in the acrylic tube, and accelerated by the projectile to compress the target. The projectiles were an elastic ball with the diameter of 25 mm for horizontal gun and same ball installed on the cylindrical sabot with the diameter of 30 mm for vertical gun. The pistons were a polycarbonate, an aluminum, and a polyacetal cylinders with the diameter of 30 mm and the height of 10-30 mm to examine the effects of piston type. The impact velocities were 2-118 m/s. The impact compaction of the target was observed by a high-speed digital camera. The shutter speed was set to be 20 to 100 μs, and the frame rate was set to be 6000 to 10000 fps.

Results: First, we measured the impact stress from the motion of piston, σ_p, and compared σ_p with the strength calculated by Kinoshita method, Y. As a result, the σ_p was almost same with the Y for both perlite and snow targets.

Next, we measured the final density of target, ρ_f, and obtained the relationship between the ρ_f and the kinetic energy or the momentum of projectile. As a result, we found that the ρ_f for perlite was determined by the kinetic energy while that for snow was determined by the momentum. Furthermore, we proposed the model of ρ_f for perlite and snow by assuming these compaction mechanisms: the perlite compressed due to the fracture of perlite particles while the snow compressed due to the decrease of area among ice grains. We compared these models with our experimental results and found that they were almost consistent with each other.

Finally, we examined the relationship between the σ_p and the final density of top layer in the target, ρ_{f1}. As a result, we obtained as ρ_{f1}=3.0${\sigma_p}^{0.8}$ for perlite and ρ_{f1}=127${\sigma_p}^{0.3}$ for snow in kPa. The data for snow at σ_p $>$100 kPa was scattered because the compaction mechanism was changed at σ_p $>$100 kPa.

Keywords: pre-planetesimal, dynamic compaction, impact experiment, final density, Kinoshita strength, compression viscosity

Japan Geoscience Union Meeting 2014
(28 April - 02 May 2014 at Pacifico YOKOHAMA, Kanagawa, Japan)

PPS21-P18 Room:Poster Time:April 29 18:15-19:30

Effect of particle size distribution on thermal conductivity of powdered materials

SAKATANI, Naoya[1*] ; OGAWA, Kazunori[2] ; HONDA, Rie[3] ; ARAKAWA, Masahiko[4] ; TANAKA, Satoshi[2]

[1]The Graduate University for Advanced Studies, [2]Institute of Space and Astronautical Science, [3]Kochi University, [4]Kobe University

Understanding about heat transport mechanism of powdered materials, such as lunar surface regolith, is important issue in order to estimate planetary thermal evolution and present thermal state. Thermal conductivity of powdered materials depends on various parameters (particle size and its distribution, temperature, compressional stress, etc.). Depending on these parameters, thermal conductivity can vary by one order of magnitude. Due to insufficiency of the experimental studies, heat transfer mechanism is not understood enough, and it is difficult to constrain in-situ thermal conductivity on planetary surface.

Our purpose is to understand the heat transfer mechanism of powdered materials under vacuum conditions by means of systematic survey of parameter dependences of the thermal conductivity. This will enable us to model the thermal conductivity, which can apply the estimation of thermal conductivity structure on planetary surface. Most of previous studies focus on the powdered samples with uniform particle size. However, actual planetary regolith has wide range of particle size from sub-μm to mm. Moreover, parent bodies of chondritic meteorites would be composed of mixture of meteoritic matrix and chondrule. In this presentation, we will report the effect of particle size distribution on the thermal conductivity under vacuum.

Glass beads mixtures of 100 μm and 200 μm in diameters were used. Prepared samples had volume mixing ratio of 1:0, 2:1, 1:1, 1:2, and 0:1. Porosity of each sample was 0.38, 0.35, 0.32, 0.35, and 0.38, respectively. The thermal conductivity of these samples was measured by line heat source method.

As a result, 100 and 200 μm glass beads of uniform sizes had 0.0023 and 0.0035 W/mK, respectively. This difference in the conductivity would be caused by the difference of radiative heat transfer. On the other hand, mixing samples had thermal conductivity of 0.0039, 0.0029, and 0.0039 W/mK for mixing ratio of 2:1, 1:1, and 1:2, respectively. These conductivities related well to porosity. There were no linear relation between thermal conductivity and mixing ratio. We found M-shaped correlation between them.

The measured thermal conductivity can be represented by the sum of solid conductivity, which is conductive contribution through contact area between the particles, and radiative conductivity, which is radiative contribution through the pore between the particle surfaces. Our results will be explained by the variation of these conductivities with particle size distribution. Therefore, it is necessary to separate the measured values into solid and radiative conductivities for explanation of our experimental results. This can be accomplished by investigation of temperature dependence of the conductivity. In this presentation, we will report dependence of solid and radiative conductivities on the particle size distribution.

Japan Geoscience Union Meeting 2014
(28 April - 02 May 2014 at Pacifico YOKOHAMA, Kanagawa, Japan)

PPS21-P19 Room:Poster Time:April 29 18:15-19:30

Measurement experiments of thermal conductivity and sound velocity in sintered glass beads

TSUDA, Shoko[1] ; OGAWA, Kazunori[1*] ; SAKATANI, Naoya[2] ; ARAKAWA, Masahiko[3] ; YASUI, Minami[3]

[1]The University of Tokyo, [2]The Graduate University for Advanced Studies, [3]Kobe University

The thermal conductivity and sound velocity of sintered particle materials (glass beads) were experimentally measured, and a correlation between them was investigated. Particles have often played important roles in the solar system history. Especially dust particles condensed in the early solar nebula formed planetesimals, and they remained as the main structure material of the bodies. The particles were then gradually sintered as temperature increased by disintegrations of radioactive isotopes. Finally, a part of planetesimals might be completely sintered and began to melt. Currently the sintered materials may also exist on the lunar and asteroid subsurface for example. Mechanical and thermal properties of such sintered materials are essential information for investigating the history of these bodies.

In the thermal issues, particles are known as a strong thermal insulator in vacuum. Although the thermal conductivity of sintered materials has never been measured, it is considered to be a value between the unsintered and a continuous rock, depending on degree of the sintering process. Concerning the sound velocity, characteristic feature depending on the sintering degree is expected to be similar to the thermal conductivity, because basically the phonon conduction is a common mechanism for both the thermal and sound phenomena in electrical insulation materials.

In this presentation, we report results of the first experiments of the thermal conductivity and sound velocity measurements in sintered particle materials. For measurement samples, 9 different blocks of sintered soda-lime glass beads were prepared: three bead diameters of 180-255, 355-500, and 710-1000 μm, and three degrees of sintering that have nearly the same porosity 40%. The cross section of sintering contact sites (neck) was evaluated for each sample. The thermal conductivity was measured by the line heat source method by a line heater and temperature sensors given in the sample in advance. The sound velocity was directly measured by a transmitter and receiver put at both ends of the block samples.

As results of the experiments, both the thermal conductivity and the sound velocity had an apparent correlation with each other, and with degree of sintering. They appeared almost in proportion to the neck diameter, which feature obviously indicates that the neck or contact size controls the bulk thermal and sound conductions, in weakly-sintered particle systems at least. These results can be directly applied to estimation of thermal and mechanical property of the ancient planetesimals. These results also suggest that the thermal conductivity of sintered materials, and also of unsintered particles probably, can be evaluated by measurements of the sound velocity.

Keywords: Particle material, Regolith, Thermal Conductivity, Sound velocity, Glass beads

Japan Geoscience Union Meeting 2014
(28 April - 02 May 2014 at Pacifico YOKOHAMA, Kanagawa, Japan)

PPS21-P20 Room:Poster Time:April 29 18:15-19:30

Experiment to know the power to pull mutually between things that are axisymmetric for the Saturn's-like magnetic axis

MASE, Hirofumi[1*]

[1]none

The magnetic axis of magnetic field in the Saturn is corresponding to the rotation axis(1). And, Saturn's rings revolve on the equatorial plane of the Saturn(2). I want to think that the reason why beautiful rings exist miraculously is related to these miraculous features. The power to pull against each other between things that are axisymmetric for the magnetic axis is generated on the plane that passes center of the axial dipole field and intersects vertically for the magnetic axis. Because the material that composes the ring is tied to the material on the 180-degree other side by the surcharge-gravitation, Saturn's rings are generated and maintained. I am making the experiment that proves the truth of this hypothesis. I introduce the result of it.

∗∗∗∗Composition of experiment (Please refer to the drawing)∗∗

"A","C":the one(34L∗25W∗25H) that natural whetstone(sandstone) was cut

"B":the one(40L∗40W∗40-80H) that 4-8 pieces of permanent magnet(anisotropic ferrite,40L∗40W∗10H,B=79mT,F=2.746kgf)s were piled up

Device box:I used "two step box" on the market and remodeled it. The front side of the left cell of this box is glazed. The front side of the right cell of this box is opening. Plywood in which "B" is set is put on the medium plate of this box to close the hole in the plate. The left cell is airtight exclusive of the top of the vinyl chloride pipe. "A" is hung from the ceiling by two strings(1,700L) and can swing freely in the left cell. The space of "B" and "A" in geostationary point is about 20mm. "C" is hung from the top board in the right cell by the string. The edge of another string is bonded on the right side of "C". (State:"C1")"C" can be separated from "B" by pulling this string from the right side of this box. (State:"C2")"C" can approach "B" by loosening this string.

∗∗∗∗Condition of experiment∗∗I experimented on the following three kinds of by changing the composition and direction of "B". Condition 1:pile 8 pieces vertically(magnetic axis is perpendicular) Condition 2:pile 4 pieces vertically(axis, perpendicular) Condition 3:pile 4 pieces horizontally(axis, horizontal right and left)

∗∗∗∗Procedure of one experiment∗∗1.I wait as much as possible until the swing of "A" stops(now"C1"). 2.I begin taking a picture of the animation of "A" with the video camera(now"C1"). 3.After 2 minutes pass, I change State from "C1" into "C2"(now"C2"). 4.After 4 minutes pass, from "C2" into "C1"(now"C1"). 5.After 6 minutes pass, from "C1" into "C2"(now"C2"). 6.After 8 minutes pass, I end taking a picture.

∗∗∗∗Result of experiment∗∗"A" swung faintly when taking a picture was begun. 1.In case of Condition 1 and 2, the swing was controlled at time zone in State "C2" of the first times, and was amplified at time zone in State "C2" of the second times. 2.In case of Condition 3, I could not confirm special change of "A" during all time.

∗∗∗∗Consideration∗∗I seem I can conclude that static electricity and magnetism don't influence the result by the comparison between Condition 2 and 3. There is a possibility that the power that I had expected was detected.

Reference literature

(1)Hori/"The School of the Universe (13th)"/NAOJ
http://th.nao.ac.jp/MEMBER/hori/pdf/HORI_2013Mar26_part1.pdf P23
(2)Hiratsuka City Museum http://www.hirahaku.jp/hakubutsukan_archive/tenmon/00000050/59.html

PPS21-P20 Room:Poster Time:April 29 18:15-19:30

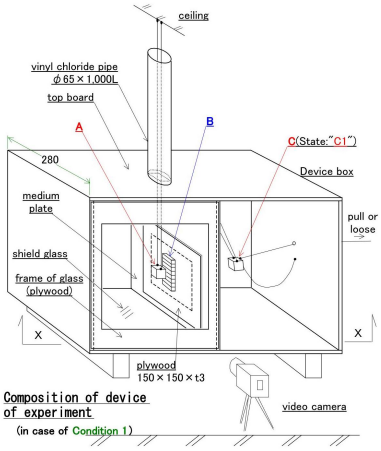

Composition of device of experiment
(in case of Condition 1)

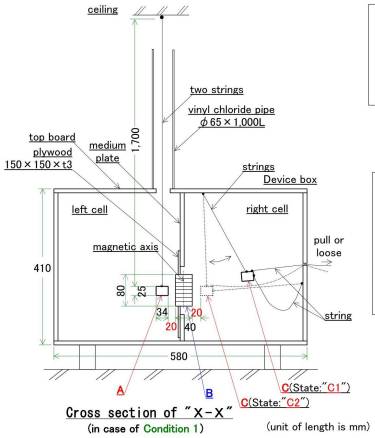

Cross section of "X-X"
(in case of Condition 1)
(unit of length is mm)

A, C : natural whetstone(sandstone)
34L × 25W × 25H

B : permanent magnet(anisotropic ferrite,40L × 40W × 10H, B=79mT,F=2.746kgf) piled up 4～8 pieces
40L × 40W × 40～80H

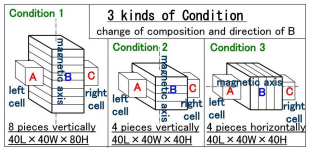

Japan Geoscience Union Meeting 2014
(28 April - 02 May 2014 at Pacifico YOKOHAMA, Kanagawa, Japan)

PPS22-01 Room:415 Time:May 1 09:00-09:15

Compositional and textural inhomogeneity of Chelyabinsk meteorites

ARAI, Tomoko[1*] ; ABE, Shinsuke[2] ; OHTSUKA, Katsuhito[3] ; HIROI, Takahiro[4] ; KOMATSU, Mutsumi[5] ; FAGAN, Tim[5]

[1]Chiba Inst. of Technology, Planetary Exploration Research Center, [2]Nihon University, [3]Tokyo Meteor Network, [4]Brown University, [5]Waseda University

Meteorites are important sources of information on composition and age of the solar system materials. However, collected meteorites are likely biased and unrepresentative of the near-Earth meteoroid population. Mineralogy and reflectance spectra of meteorites are used to link specific classes of meteorites and asteroids, but are not definitive enough. Meteorites of which fall were witnessed are rare and substantial case when meteorites and their parent bodies are directly linked, and both orbital and material data of the near-Earth bodies are known. The fireball was eye-witnessed near Chelyabinsk city of Russia in 15 February 2013, and associated meteorites of total mass of 4-6 ton, were subsequently recovered. Survey of physical and chemical nature of small bodies with an Earth-crossing orbit is crucial in understanding the origin and evolution of the near-Earth materials and in planetary defense. While near-Earth objects (NEO) >1 km dia. have been largely identified by NEO survey programs, most NEOs <?100 m dia. remain unknown. Thus, it is important to study the Chelyabinsk-sized objects. We present mineralogy and reflectance spectra of several chips of Chelyabinsk meteorites, which indicate chemical and spectral inhomogeneity, suggesting the complex history of the parent body.

Keywords: Chelyabinsk meteorites, Meteoroid impacts, Inhomogeneity

Japan Geoscience Union Meeting 2014
(28 April - 02 May 2014 at Pacifico YOKOHAMA, Kanagawa, Japan)

PPS22-02 Room:415 Time:May 1 09:15-09:30

Classification and petrologic features of chondrites of petrologic type 7

KIMURA, Makoto[1*] ; YAMAGUCHI, Akira[2] ; FRIEDRICH, Jon[3]

[1]Ibaraki University / National Institute of Polar Research, [2]National Institute of Polar Research, [3]Fordham University / American Museum of Natural History

Chondrites are classified into petrologic types 1-6, which distinguish the degrees of aqueous alteration (types 1-2), and thermal metamorphism (types 4-6). In addition, a petrographic type 7 has also been proposed to indicate an even higher degree of thermal metamorphism [1]. Such chondrites contain only relict chondrules, and plagioclase is commonly coarse-grained. Low-Ca pyroxene contains >1% CaO. However, most of these chondrites may actually be melt rocks or melt breccias [2], and the occurrence of a type 7 is controversial problem. However, LEW 88663 seems to be a genuine type 7 chondrite [3], not a melt rock.

Here we report the preliminary results of our petrographic study on ordinary chondrites classified as type 7, to explore their thermal history, classification, and genetic relationships to melt breccia and others.

Many chondrites are classified as type 7 in NIPR and other collections (77 chondrites at present). However, the detailed petrography has been rarely reported for these chondrites. Here we studied 4 H7, 4 L7, and 4 LL7 in NIPR collections. We also examined Uden (LL7).

All of the chondrites studied here show a well recrystallized texture. Triple junctions among olivine and pyroxene is commonly observed. However, Y-790124 and -790446 include many chondrules, indicative of type 6. A-880844 and -880993 contain clasts of various petrologic types, and are genomict breccias (H5-6 and LL4-6, respectively). Although Y-790144 does not seemto contain any chondrules, it is shock-darkened chondrite, and has lost its original texture.

Y-74160 has been extensively studied [e.g., 4]. This chondrite, Y-791067, and Uden consist of clasts among fine-grained matrix. The clasts comprise coarse-grained olivine, low-Ca pyroxene, and plagioclase. Olivine is typically included as chadacryst in pyroxene. The matrix is also highly recrystallized. Friedrich et al. [5] suggested that Y-74160 and Uden were subjected to Fe-FeS mobilization. These chondrites experienced partial melting, recrystallization, and brecciation, and may be classified as recrystallized breccias.

On the other hand, five chondrites, Y-75008, -790120, and -790960 (H7s), Y-82088 (L7), and Y-82067 (LL7), contain no or only a few relic chondrule in each section. They show highly recrystallized texture, and are not subjected to brecciation and melting. Y-82067 has composition identical to equilibrated LL chondrites [5]. These five chondrites are temporarily classified as type 7, if type 7 chondrite is defined to have experienced only a high degree of thermal metamorphism.

We are now examining modal mineral abundances and conducting mineral analyses, which will shed light on the classification criteria for type 7 chondrites.

References: [1] Dodd et al. (1975) GCA, 39, 1585-1594. [2] Huss et al. (2006) in Meteorites and the Early Solar System II. [3] Mittlefehldt and Lindstrom (2001) MAPS, 36, 439-457. [4] Takeda et al. (1984) EPSL, 71, 329-339. [5] Friedrich et al. (2014) submitted to GCA.

Keywords: ordinary chondrite, type 7, thermal metamorphism

Japan Geoscience Union Meeting 2014
(28 April - 02 May 2014 at Pacifico YOKOHAMA, Kanagawa, Japan)

PPS22-03 Room:415 Time:May 1 09:30-09:45

Origin of eclogitic clasts in a CR2 chondrite: Evidence of frequent collisions and disruptions of large planetesimals?

HIYAGON, Hajime[1*] ; SUGIURA, Naoji[1] ; KITA, Noriko T.[2] ; KIMURA, Makoto[3] ; MORISHITA, Yuichi[4] ; TAKEHANA, Yoshie[1]

[1]Graduate School of Science, The University of Tokyo, [2]Department of Geoscience, University of Wisconsin -Madison, USA, [3]Faculty of Science, Ibaraki University, [4]Department of Geosciences, Shizuoka University

Achondritic clasts found in the Northwest Africa 801 (NWA801) CR2 chondrite have significant importance in planetary science (Sugiura et al., 2008; Kimura et al., 2010, 2013): (i) it provides strong evidence that achondrites formed earlier than chondrites, (ii) the clasts contain eclogitic high mineral assemblages (garnet and omphacite), suggesting formation at a high pressure (˜3 GPa and ˜1000 C; Kimura et al., 2013), and (iii) the clasts contain two lithologies, graphite-bearing (GBL) and graphite-free (GFL), and the presence of graphite in GBL implies some relations to ureilite.

We performed ion microprobe studies of oxygen isotopes and rare earth element (REE) abundances for selected minerals in the clasts (Hiyagon et al., 2014). Based on the newly obtained data and diffusion calculations, we discuss possible origin of the clasts, esp., whether they formed under a static high pressure in a large planetesimal or formed under a shock high pressure.

Key observations are as follows. (1) Olivine (ol) grains in the clasts (˜20 micrometers in size) are chemically homogeneous with Mg# 66-68. (2) Most of orthopyroxene (opx) grains (˜20 micrometers in size) are homogeneous with Mg# 70-75, but a few large opx grains (50-80 micrometers in size) have Mg-rich cores with Mg# 78-87. (3) Various geothermobarometers (7 equations for mineral pairs of opx-cpx, garnet-cpx, garnet-opx and garnet-olivine) consistently give a high P-T condition of 940-1080 C and 2.8-4.2 GPa. (4) All the oxygen isotopic data of ol and opx fall on a correlation line with a slope of ˜0.6. Data for GFL (ol) are homogeneous with delta18O ˜+5 permil, located close to the CCAM line and the ureilite field, but data for GBL (ol +opx) are variable with delta18O from +2.4 to +4.3 permil. (5) Major host minerals of REEs are chlorapatite (both LREEs and HREEs) and garnet (for HREEs). The estimated bulk REE patterns for GBL and GFL are almost flat (unfractionated) with ˜1.2 x CI and ˜1.8 x CI, respectively.

We consider that the presence/absence of graphite in the two lithologies may be due to absence/presence of smelting reactions, FeO (in silicates) + C (graphite) = Fe (metal) + CO (gas). This means that GBL might form at a deeper portion and GFL might form at a shallower portion, respectively, of a planetesimal.

We consider two different models: a shock high-P model and a static high-P model. Based on careful diffusion calculations, we argue that (1) almost homogeneous Fe/Mg ratios in ol and opx (with some Mg-rich cores) can be explained by heating at 1000 C for 120-800 years, (2) oxygen isotopic variations in GBL must have established before homogenization of Fe/Mg ratios in olivine, (3) consistency of different geothermobarometers requires equilibration of different elements among different mineral pairs, strongly suggesting a static high-P model, (4) in a static high-P model, ˜3 GPa corresponds to the pressure at the center of a large planetesimal with a radius of ˜1500 km, almost the size of the Moon, (5) consistency of different geothermobarometers also suggests a rapid cooling after heating several hundreds of years at ˜1000 C at ˜3 GPa, suggesting possibe disruption of the parent body.

In conclusion, the present results suggest frequent collisions and disruptions of a large planetesimals at a certain stage of the solar system evolution.

References: Kimura M. et al. (2010) (abstract) Meteoritics and Planetary Science 45, A105; Kimura M. et al. (2013) American Mineralogist, 98, 387-393; Sugiura N. et al. (2008) (abstract) Meteoritics and Planetary Science 43, A149. Hiyagon H. et al. (2014) in preparation.

Keywords: eclogite, CR chondrite, oxygen isotopes, rare earth elements, collisions of planetesimals, diffusion

Japan Geoscience Union Meeting 2014
(28 April - 02 May 2014 at Pacifico YOKOHAMA, Kanagawa, Japan)

PPS22-04 Room:415 Time:May 1 09:45-10:00

Estimation of the size of the angrite parent body

SUZUKI, Hiroko[1*] ; OZAWA, Kazuhito[1] ; NAGAHARA, Hiroko[1] ; MIKOUCHI, Takashi[1]

[1]Department of Earth and Planetary Science, University of Tokyo

Angrites has very old crystallization age yielding 4557 - 4564Ma (Brennecka and Wadhwa, 2012; Kleine et al., 2012) and are igneous rocks come from differentiated planetesimal or protoplanet (e.g. Prinz and Weisberg 1995; Baker et al., 2005; Weiss et al., 2008). Angrites preserve information on such differentiated planets, and are one of the best targets for studying processed operated in the early stages of planetary evolution of the solar system. However, the angrite parent body has not been found, and we have scarce knowledge on its planet size, which is one of the most important information in planetary science. The radius of angrite parent body is believed to be larger than 100 ? 200km because of the operation of dynamo, which requires prolonged high temperature of the planet interior due to heat production of ^{26}Al decay to achieve its core formation (Weiss et al., 2008; Elkins-Tanton et al., 2011). The upper limit of radius is not constrained at all, although 2440km is proposed based on ambiguous evidence for Mercury as the angrite parent body (Papike et al., 2003; Kuehner et al., 2006). The radius of the angrite parent body, particularly its upper limit, needs to be further constrained. In this study, we try to constrain the upper limit of the planet size from the presence of spherical voids as large as 25mm in D'Orbigny angrite.

D'Orbigny has many spherical voids suggesting that they formed in 100% molten magma before crystallization. The vesicles are deformed while ascending in the melt depending on several physical parameters such as, melt viscosity and the size of vesicles. There are two dimensionless numbers that determine the shape, Reynolds number and Eotvos (or Bond) number. Reynolds number is a ratio of inertia force and viscous force and Eotvos number is a ratio of buoyancy force and surface tension. These two numbers depends on gravity of the parental body, and the gravity depends on the radius of the parental body. Therefore, spherical shape of the largest void enables us to estimate the upper limit of the radius of the angrite parent body. The boundary conditions for spherical and nonspherical regimes have been determined by Bhaga and Weber (1981) based on fluid dynamic experiments and by Hua and Lou (2007) based on numerical simulations.

Spherical voids in D'Orbigny are armored by fine-grained olivine and plagioclase crystals, where are the first liquidus phases, suggesting that the spherical shape was frozen by heterogeneous nucleation and growth of these phases on the bubble wall. In order to know relationship between Reynolds and Eotvos numbers for D'Orbigny, accurate estimation of density and viscosity is very important, which are strongly dependent on temperature of shape freezing. The temperature was estimated by MELTS (Ghiorso and Sack, 1995) as metastable olivine liquidus for the D'Obigny bulk composition to be ˜1100 ℃, from which the density and viscosity of D'Obigny magma are estimated to be ˜3000 kg/m^3 and ˜1.0 Pa s, respectively. Surface tension of the melt is 0.35N/m according to Walker and Mullins (1981), which is corrected by 50% occupation of olivine and plagioclase on the bubble-melt interface. We assume the average density of the parent body as 4000kg/m^3 for the planet having core, such as asteroid 4 Vesta (Zuber et al., 2011). By using these parameters, we estimated the upper limit of radius to be 700±100 km, which is clearly much smaller than that of Mercury.

Keywords: angite, planetesimal, parent body radius, parent body internal structure, D'Orbigny, protoplanet

Japan Geoscience Union Meeting 2014
(28 April - 02 May 2014 at Pacifico YOKOHAMA, Kanagawa, Japan)

PPS22-05 Room:415 Time:May 1 10:00-10:15

Crystallization experiment of alpha-Fe, gamma-Fe and iron compounds found in the Almahata Sitta and Antarctic ureilites

AOYAGI, Yuya[1*] ; MIKOUCHI, Takashi[1] ; SUGIYAMA, Kazumasa[2] ; YOKOYAMA, Yoshihiko[2] ; GOODRICH, Cyrena A.[3] ; ZOLENSKY, Michael E.[4]

[1]Dept. of Earth & Planet. Sci., Univ. of Tokyo, [2]Inst. for Materials Research, Tohoku Univ., [3]Planet. Sci. Inst., [4]NASA-JSC

Ureilites are ultramafic achondrites whose origin and petrogenesis are still controversial. The cooling rate of ureilites estimated from silicates is approximately a few degrees per hour, and it was considered to reflect catastrophic disruption of the ureilite parent body. Ureilites were broken into meter-sized fragments and then formed daughter body(ies) by re-accumulation.

Fe-Ni metal is one of the major components of all types of ureilites. Almahata Sitta, having fallen on the earth in October 2008, was classified as a polymict ureilite and ureilitic fragments from the Almahata Sitta contain abundant Fe-Ni metal. In previous studies, some grain boundary metals in Almahata Sitta ureilites show unique textures, not found in main group ureilites. These textures show characteristic assemblages with various combinations of α-iron (bcc), γ-iron (fcc), cohenite ($[Fe,Ni]_3C$) and schreibersite ($[Fe,Ni]_3P$).

Those metal textures resemble the product by steelmaking process in the earth, for example martensite (α-iron and γ-iron). Generally, these textures require rapid cooling equivalent to quenching by water ($>$100 ℃/s). However, the cooling rate estimated from silicates (ca. several ℃/h) is much slower than that in producing the martensite. Thus, these metal textures may record the event separated from the event that recorded in the silicates, that is, disruption of parent body. Therefore, studying these complicated metal textures will contribute to a better understanding of the formation and origin of metal in ureilites with the information about their thermal histories.

Those metal textures were only found in Almahata Sitta fragment #44, in previous studies, but we found similar assemblages composed of iron metal and its compounds in other fragments of Almahata Sitta and Antarctic ureilites. Forms and abundances are variable depending on samples, but it is suggested that those mineral assemblages in Fe-Ni metal are commonly found in ureilites.

To estimate the cooling rate which can form these iron and iron compounds textures, we performed cooling experiments by the electric furnace to heat and quench metal whose compositions correspond to metals showing complex metal phase assemblages in Almahata Sitta ureilite. The results suggest that those metal textures can be achieved in the cooling rate faster than the lowest limit between 10 ℃/s and 0.83 ℃/s, whose chemical composition is $Fe_{79.2}Ni_{3.4}P_{2.5}Si_{2.7}C_{12.2}$. At lower cooling rate (0.83 or 0.04 ℃/s) and 10 ℃/s of other starting material ($Fe_{86.4}Ni_{2.8}P_{0.7}Si_{4.1}C_{6.0}$), interstitial schreibersite among rounded iron was detected and neither cohenite nor γ-iron has been formed. In the carbon-free composition ($Fe_{91.2}Ni_{3.9}P_{0.5}Si_{4.4}$), similar textures were not generated at all cooling rates. This cooling rate, forming metal textures, is much faster than that estimated from silicates, and thus it is concluded that the event recorded by the silicates and the event formed the metal textures were truly separated.

Before disruption of ureilite parent body, primary metals probably melted and mixed with surrounding materials (graphite, phosphide and other iron compounds) to various extents at high temperature. The iron phase was considered to be uniformly γ-iron. Then, the ureilite parent body was destroyed and silicate minerals obtained cooling rate by quenching. Later, daughter body(ies) formed by accumulation of meter-size fragments. If daughter body(ies) was either shocked while still hot or heated by shock and then disrupted into smaller fragments (cm-size), the formation of iron textures may be achieved by super rapid cooling exceeding 1 ℃/s. The metal grains without γ-iron would experience relatively slow cooling due to larger fragment size. Consequently, it is considered that the complex coexistences of iron and iron compounds found in ureilites have recorded temperature change and fragmentation process due to the impacts on the parent body and daughter body(ies).

Japan Geoscience Union Meeting 2014
(28 April - 02 May 2014 at Pacifico YOKOHAMA, Kanagawa, Japan)

PPS22-06 Room:415 Time:May 1 10:15-10:45

Early impact events on differentiated protoplanets: Evidence from basaltic achondrites

YAMAGUCHI, Akira[1*]

[1]National Institute of Polar Research

Impact events are a ubiquitous geological process on planetesimals and protoplanets, evidenced by the presence of shock and brecciated textures in asteroidal meteorites. However, evidence for early impact events were obliterated by overprints of later thermal events such as volcanism and thermal metamorphism. We investigated early impact events in these meteorites on the basis of mineralogical and geochemical data.

At present, there are ˜5 eucrites which were derived from distinct protoplanets. An anomalous eucrite, Ibitira, is a strongly recrystallized rock. Low-Ca pyroxene shows homogeneous compositions, indicating that these rocks experienced prolonged thermal metamorphism (˜900-1000 C), as did most basaltic eucrites. The presence of unequilibrated pyroxenes related to oxide grains can be explained by short reheating event (and partial melting) and rapid cooling. Normal eucrites, EET 90020 and Y 86763, and a cumulate eucrite Moore County seem to have experienced a similar history. Most likely explanation for this thermal history is that they were excavated by impact from hot interior.

Anomalous cumulate eucrites Dho 700 and EET 92023 are medium-grained granular rocks similar to cumulate eucrites. Anomalous basaltic eucrite, NWA 011 shows a recrystallized texture. These rocks are crystalline (unbrecciated) but contain significant amounts of impactor materials. Dho 700 and EET 92023 contain taenite which is not common in pristine eucrites. The high abundances of siderophile elements are explained by addition of ˜1% iron meteorites. Thus, these rocks experienced impact event before or during crystallization and thermal metamorphism.

All anomalous eucrites studied here show crystalline textures, but have evidence for impact melting or brecciation before thermal events. These meteorites record early collisional history possibly during the stage of runaway growth.

Japan Geoscience Union Meeting 2014
(28 April - 02 May 2014 at Pacifico YOKOHAMA, Kanagawa, Japan)

PPS22-07 Room:415 Time:May 1 11:00-11:15

Shock features in a Martian meteorite, Tissint

MIYAHARA, Masaaki[1*] ; OHTANI, Eiji[2] ; EL GORESY, Ahmed[3] ; GILLET, Philippe[4]

[1]DEPSS, Graduate School of Science, Hiroshima Univ., [2]Institute of Mineralogy, Petrology and Economic Geology, Graduate School of Science, Tohoku Uni., [3]BGI, [4]EPFL

Tissint is the fifth fall Martian meteorite collected in Morocco on 2011 [1]. The nomination of a fall Martian meteorite is since 1962. Tissint will bring new clues for Martian evolution because it is less contaminated with terrestrial materials. Tissint is a member of shergottite. Many shergottites experienced a heavy shock event on Mars [e.g., Ref. 2]. We expected that Tissint should be also heavily shocked. A high-pressure polymorph is one of clear evidences for such a dynamic event. Accordingly, we described shock features, especially a high-pressure polymorph by FEG-SEM, EMPA, Raman spectroscopy and FIB-TEM techniques to clarify shock history recorded in Tissint.

We prepared several petrographic thin sections of Tissint for this study. EMPA analysis show that Tissint studied here consists mainly of olivine (Fa_{18-66}), pigeonite or augite ($En_{43-62}Fs_{23-37}Wo_{10-34}$) and labradoritic feldspar ($An_{62-66}Ab_{34-37}Or_{0-1}$). There are many melt-pockets, which is suggestive of a heavy shock event. FEG-SEM and FIB-TEM observations show that olivine grains entrained in the melt-pockets dissociated into silicate-perovskite (now almost amorphous or poorly-crystallized) and magnesiowustite, which is found in a Martian meteorite DaG 735 for the first time [3]. Silicate-perovskite and magnesiowustite show equigranular texture and less than ˜100 nm in dimension. We also identified ringwoodite lamella in some olivine grains adjacent to the melt-pockets. TEM images show that ringwoodite has a dimension of less than ˜500 nm. Raman spectroscopy analysis indicates that most feldspar now transforms into maskelynite. Jadeite-like crystals appear in some feldspar grain adjacent to the melt-pockets.

Considering the dissociation reaction of olivine into silicate-perovskite and magnesiowustite, shock pressure condition recorded in Tissint is beyond ˜23 GPa based on phase diagram deduced from static synthetic experiments [4]. Phase transformation from olivine to ringwoodite also occurs besides the olivine dissociation reaction. Phase transformation from olivine to ringwoodite occurs instead of olivine dissociation reaction with decreasing temperature but under same pressure condition [5], which is due to thermal gradient in the olivine grains adjacent to the melt-pockets although pressure condition should be almost homogeneous. The nucleation and grain growth of a high-pressure polymorph is kinetically controlled. Baziotis et al. (2013)[6] propose that Tissint experienced the largest impact event among known Martian meteorites because ringwoodite appear to be a huge single crystal based on their SEM observations. However, our TEM images clearly depict that ringwoodite is a fine-grained grain assemblage, suggesting that it is unlikely that Tissint experienced the largest impact event.

References

[1] Chennaoui Aoudjehane H. et al. Tissint Martian Meteorite: A fresh look at the interior, surface, and atmosphere of Mars. Science 338, 785-788 (2012).

[2] El Goresy A. et al. Shock-induced deformation of Shergottites: Shock-pressures and perturbations of magmatic ages on Mars. Geochim.Cosmochim.Acta 101, 233-262 (2013).

[3] Miyahara M. et al. Natural dissociation of olivine to (Mg,Fe)SiO_3 perovskite and magnesiowustite in a shocked Martian meteorite. Proc.Nat.Acad.Sci.U.S.A. 108, 5999-6003 (2011).

[4] Presnall D.C. Phase diagrams of Earth-Forming Minerals. 248-268, in Mineral Physics & Crystallography, A Handbook of Physical Costants, T. J. Ahrens ed., AGU, Washington D. C (1995).

[5] Akaogi M. et al. Low-temperature heat capacities, entropies and enthalpies of Mg_2SiO_4 polymorphs, and a?b?c and post-spinel phase relations at high pressure. Phys.Chem.Minerals 34, 169-183 (2007).

[6] Baziotis I.P. et al. The Tissint Martian meteorite as evidence for the largest impact excavation. Nat.Commun., doi: 10.1038/ncomms2414 (2013).

Keywords: Tissint, Martian meteorite, Shock, High-pressure polymorph

Japan Geoscience Union Meeting 2014
(28 April - 02 May 2014 at Pacifico YOKOHAMA, Kanagawa, Japan)

PPS22-08 Room:415 Time:May 1 11:15-11:30

Estimation of bulk major element composition for Centimeter-Sized Impact Melt Clasts in Lunar Rocks using EPMA

NIIHARA, Takafumi[1*] ; KRING, David A.[2]

[1]NIPR / LPI / SSERVI, [2]LPI / SSERVI

Most of lunar surface rocks are brecciated and mixed with various types of rock fragments and impact melt clasts during multiple impact events. We are testing the Late Stage Heavy Bombardment on the Moon surface [1-3] using Apollo 16 centimeter-sized impact melt clasts in ancient regolith breccias. Bulk composition is a key to understand original (pre-impact) lithologies where the clasts come from [4, 5]. Large-sized impact melt rocks (>5 cm) have been classified into 4 major group (Group 1 to 4) according to Sm and Sc compositions [6]. We compiled major element compositions of the previously classified impact melt rocks [6] and found that we can classify major impact melt groups even when we use major element compositions. However, our samples, centimeter-sized impact melt clasts, are highly restricted on their masses and makes us difficult to obtain bulk composition using conventional techniques (e.g. INAA and XRF). Defocused beam analyses (DBA) with EPMA is used to estimate the bulk compositions for limited mass samples using petrological sections, however, nobody tested accuracy of DBA techniques using certified geochemical standard.

We use a thin section of BCR-2 (fine-grained basalt supplied from USGS) and tested accuracy of DBA method using an EPMA (CAMECA SX-100) at NASA Johnson Space Center. We measured 12 elements (Na, Mg, Si, Al, P, K, Ca, Ti, Fe, Mn, Cr, and Ni) at >250 points with 20 micrometer beam diameter. We corrected density effect following the Warren (1997) method [7]. Averaged SiO_2 and FeO have larger difference from USGS values (+4.4 wt.% for SiO_2, -4.68 Wt.% for FeO) relative to other elements (up to +/- 2.4 wt.%). Although there are major changes in SiO_2 and FeO values after correct the density effect (difference from USGS values are up to -4.1 Wt.% for SiO_2 and up to +4.6 Wt.% for FeO), we suggest the DBA compositions can useable for the fine-grained materials to estimate the bulk major element composition for Apollo 16 impact melt clasts.

We estimated the bulk composition by averaged DBA method for two impact melt clasts in an Apollo 16 ancient regolith breccia 61135 which have optically different 5 regions (Clast1 R1, R2, and R3; and Clast 2 R1 and R2) to reveal the original lithology of the impact melt clasts. Five regions from the two impact melt clasts can be divided into three chemical groups of high-K, low-K and intermediate compositions. Clast 1 R3 has high K (K_2O=0.72 wt.%) and P (P_2O_5=0.35 wt.%), and low Al (Al_2O_3=20.7 wt.%) and Ca (CaO=12.0 wt.%). On the other hand, Clast 1 R1 and R2 have low K (K_2O=0.31-0.27 wt.%) and P (P_2O_5=0.08-0.07 wt.%) with high Al (Al_2O_3=26.1-25.2 wt.%) and Ca (CaO=14.5-14.0 wt.%). Clast 2, in both dark and bright regions, has an intermediate composition between high-K and low-K melts (e.g. K_2O=˜0.46, P_2O_5=˜0.16 wt.%, Al_2O_3=˜22.9 wt.%, CaO=˜12.8 wt.%). The bulk Mg# of the 5 regions are similar (Mg#=80-78).

If the melts in the two clasts are related, there are two possible origins: (1) A single impact event hit a complex lithological target and incompletely mixed the melts, to produce high-K, intermediate-K, and low-K melt fractions. (2) An impact produced either a high- or low-K melt. A second impact produced a melt at the other end of the K spectrum. The melts in Clast 1 represent those two end member melts. If the second impact melt digested older fragments of the first impact melt, then that may have produced the intermediate compositions of Clast 2. Alternatively, the melts are not related and require three or more impact events.

Reference: [1] Papanastassiou D.A. and Wasserburg G.J. 1971. EPSL 11. 37-62. [2] Turner G. et al., 1973. Proc. LPSC 4, 1889-1914. [3] Tera F. et al., 1974. EPSL 22, 1-21. [4] Niihara, T. and Kring, D. A., 2012. LPSC. #1229. [5] Niihara, T. et al., 2013. LPSC. #2083. [6] Korotev, R.L. 1994. GCA 58, 3931-3969. [7] Warren, P.H., 1997. LPSC28, #1406.

Keywords: EPMA, Bulk composition, Apollo 16, Impact melt clast

Japan Geoscience Union Meeting 2014
(28 April - 02 May 2014 at Pacifico YOKOHAMA, Kanagawa, Japan)

PPS22-09 Room:415 Time:May 1 11:30-11:45

Formation processes of silica polymorphs in lunar meteorites

KAYAMA, Masahiro[1*] ; TOMIOKA, Naotaka[2] ; SEKINE, Toshimori[1] ; GöTZE, Jens[3] ; NISHIDO, Hirotsugu[5] ; OHTANI, Eiji[4] ; MIYAHARA, Masaaki[1] ; OZAWA, Shin[4]

[1]Department of Earth and Planetary Systems Science, Graduate School of Science, Hiroshima University, [2]Institute for Study of the Earth's Interior, Okayama University, [3]Department of Mineralogy, TU Bergakademie Freiberg, [4]Department of Earth and Planetary Materials Science, Graduate School of Science, Tohoku University, [5]Depertment of Biosphere-Geosphere Science, Okayama University of Science

Asteroid and meteorite collisions lead to formation of impact craters and thick regoliths on the Moon and also contribute to revolution of the Earth, e.g. Giant impact, the late heavy bombardments and the origin of life. Although lunar meteorites and Apollo samples have experienced such impact events during the ejection from the lunar surface or formation of immense basin, they were believed to contain few high-pressure mineral because of the volatilization during collision in the high vacuum (Papike 1998; Lucey et al., 2006). Recently, Ohtani et al. (2011) and Miyahara et al. (2013) discovered high-pressure silica polymorphs (coesite, stishovite and seifertite) in lunar meteorites, Asuka-881757 and NWA4734. Their existences provide constraints on the shock condition and give us valuable information on impact history on the Moon and the Earth.

The shock condition of meteorites has been estimated based on the pressure-temperature phase diagram obtained from high-pressure experiments using shock gun, multi-anvil press and diamond anvil cell (DAC) for various types of minerals including in silica polymorphs. There have been many investigations of the high-pressure experiments for quartz and amorphous silica glass, but not for the other polymorphs, regardless of dominant occurrence of cristobalite and tridymite in lunar meteorites. Since the transition pressure to high-pressure phase depends on a type of starting material (Kubo et al. 2012; Bläβ, 2013), it is necessary for understanding the detailed impact history of the Moon to conduct the high-pressure experiments for various types of silica polymorphs.

In this study, silica polymorphs in various types of lunar meteorites (anorthositic breccia, basalt, and gabbro and basalt clast-dominated breccia) were described using Raman spectroscopy, Scanning and Transmission Electron Microscope and X-ray diffraction analysis and the obtained results were compared with the data of high-pressure experiments for various types of silica polymorphs to clarify the phase transition process, interpret the formation process on the Moon and constrain shock pressure and temperature that the lunar meteorites have experienced.

Keywords: Lunar meteorite, Silica polymorph, High-pressure mineral, Collision, Shock experiment, Static compression experiment

Japan Geoscience Union Meeting 2014
(28 April - 02 May 2014 at Pacifico YOKOHAMA, Kanagawa, Japan)

PPS22-10 Room:415 Time:May 1 11:45-12:00

Discovery of stishovite in an Apollo 15 sample and impact record on the Moon

KANEKO, Shohei[1] ; OHTANI, Eiji[1*] ; MIYAHARA, Masaaki[2] ; OZAWA, Shin[1] ; ARAI, Tomoko[3]

[1]Tohoku University, [2]Hiroshima University, [3]Chiba Institute of Technology

Thick regolith layers and many craters on the Moon indicate that the Moon has been heavily bombarded after the lunar formation. Short time intervals of high-pressure and high-temperature occurred on the lunar surface during the collision of asteroids on the Moon, and the constituent minerals of the Moon and asteroids transformed into high-pressure polymorphs during the high-pressure and high-temperature conditions. Although many brecciated lunar rocks have been recovered by the Apollo missions, any high-pressure polymorph has not been observed in Apollo samples so far. Silica is one of constituent minerals of terrestrial planets and asteroid. We investigated a lunar regolith collected by the Apollo 15 mission with a special interest on silica, because high-pressure polymorphs of silica are recently reported from shocked lunar meteorites (Ohtani et al., 2011; Miyahara et al., 2013). Here, we show stark evidence for stishovite from a sample collected by the Apollo 15 mission. X-ray diffraction analysis and transmission electron microscopic observations clearly confirmed the existence of a high-pressure polymorph of silica, stishovite, in the Apollo sample, which suggests that the lunar legolith preserves records of early shock events. Considering radio-isotope ages, lithologies, and shock features, stishovite was formed by an impact event in the near side Moon ca. 3.8-4.1 Ga ago.

Keywords: Stishvite, Apollo mission, Impact, High pressure and temperature, Lunar sample

Japan Geoscience Union Meeting 2014
(28 April - 02 May 2014 at Pacifico YOKOHAMA, Kanagawa, Japan)

PPS22-11 Room:415 Time:May 1 12:00-12:30

Experimental constrains on shock conditions of meteorites based on non-equilibrium behaviors of silica and plagioclase

KUBO, Tomoaki[1*] ; KONO, Mari[1] ; KATO, Takumi[1]

[1]Dept. Earth Plant. Sci., Kyushu Univ.

Recent studies on shocked meteorites have revealed non-equilibrium behaviors of silica and plagioclase at high pressures. We focus on the following three points observed in meteorites to deduce the P-T-t shock conditions from high-pressure kinetic experiments. 1) The formation of seifertite as a high-pressure polymorph of silica, 2) The occurrence of jadeite from plagioclase that does not contain stishovite, 3) The formation of lingunite as a high-pressure polymorph of albite-rich plagioclase.

Seifertite is a polymorph of silica with alpha-PbO2 type structure that was found in shocked Martian and lunar meteorites (e.g., Sharp et al., Science1999; Miyahara et al., PNAS2013). Although this phase is thermodynamically stable at more than 90 GPa corresponding to the base of the lower mantle (Murakami et al., GRL2003), it has also been known that it metastably appears from cristobalite at around more than 40 GPa and room temperature (Dubrovinsky et al., CPL2001). We have carried out high-pressure and high-temperature in-situ XRD experiments of cristobalite using a Kawai-type multi-anvil (KMA) apparatus, and determined the formation kinetics of metastable seifertite and the following stable phase of stishovite. Because the activation energy for the seifertite formation is very low (˜10 kJ/mol), which is consistent with the recently proposed formation mechanism (Blab, PCM2013), it can metastably appear at low T conditions beyond the negative PT boundary from ˜10 GPa and 400C to ˜30 GPa and room T. We found the clear difference in the formation kinetics between seifertite and stishovite, which enables to estimate the P-T-t shock conditions from the coexistence of these phases in various ratios in meteorites.

The occurrence of jadeite from plagioclase that does not contain stishovite has been often reported in shocked meteorites (e.g., Kimura et al., MAPS2000). In-situ XRD study using KMA apparatus have revealed that jadeite forms first from (amorphous) plagioclase, whereas the nucleation of other minerals such as stishovite or garnet is significantly delayed (Kubo et al., NGEO2010). The missing stishovite problem can be explained owing to the differences in crystallization kinetics of high-pressure phases from plagioclase. The hybrid shock indicator combining these non-equilibrium behaviors of silica and plagioclase mentioned above consistently and strongly constrains the P-T-t shock conditions of Martian meteorites.

The formation of lingunite (albite-rich hollandite) in shocked meteorites (e.g., Gillet et al., Science2000; Tomioka et al., GRL2000) has remained unsolved. This phase appears in lase-heated diamond anvil cell (LHDAC) experiments as a minor phase at around ˜20-24 GPa and ˜1000C (Liu, PEPI1978) and ˜2000C (Tutti, PEPI07). However, KMA experiments indicate that the maximum solubility of NaAlSi3O8 component in hollandite structure is limited to ?50 mol% (Yagi et al., 1994, Liu, 2006). This clear contradiction may be due to the non-equilibrium origin. It has been suggested that the rapid T quenching in LHDAC experiments is important for the survival of lingunite metastably to the ambient condition. Our previous in-situ XRD study using KMA apparatus have indicated that lingunite is not formed at least ˜1200C at these pressure conditions (Kubo et al., NGEO2010). We are also preliminarily conducting some LHDAC experiments, however we have not observed lingunite at least ˜1400C. Further studies on the formation process of lingunite are needed to solve this problem, which may lead to construct another P-T-t shock indicator.

Japan Geoscience Union Meeting 2014
(28 April - 02 May 2014 at Pacifico YOKOHAMA, Kanagawa, Japan)

PPS22-P01 Room:Poster Time:May 1 18:15-19:30

Laboratory impact experiments of rock projectiles onto simulated asteroid regolith: Impactor fragmentation and capture

NAGAOKA, Hiroki[1] ; NAKAMURA, Akiko[1*] ; SUZUKI, Ayako[2] ; HASEGAWA, Sunao[2]

[1]Graduate School of Science, Kobe University, [2]Institute of Space and Astronautical Science

We conducted laboratory impact experiments of rock projectiles onto target consist of silica sand used as simulated regolith surface. We investigate the relationship between degree of projectile fragmentation and impact velocity and particle size of silica sand.

Laboratory impact experiments have been performed to study the degree of target fragmentation, however, much less attention has been paid to the fate of the impactors. Experiments with impact velocity lower than 1 km/s were conducted using a powder gun and a gas gun at Kobe University, while experiments with higher impact velocity up to 5 km/s were conducted using a two-stage light-gas gun at Institute of Space and Astronautical Science. We collected the projectile fragments in the sand and weighed the mass of the largest fragments.

Destruction of rock projectiles is found to occur when the peak pressure is about equal to the dynamic tensile strength of the rock in the low velocity impact experiments (Nagaoka et al., 2014, MAPS). The largest fragment mass fractions in the high velocity impact experiments are higher than the expected from the result of low velocity impact experiments. The discrepancy is larger for the target with smaller silica sand particles. The larger fragments consist of multiple fragments and silica sand particles which were consolidated into larger particles by compression and the heating due to compaction of silica sand.

Keywords: meteorites, impact process, asteroids

Japan Geoscience Union Meeting 2014
(28 April - 02 May 2014 at Pacifico YOKOHAMA, Kanagawa, Japan)

PPS22-P02 Room:Poster Time:May 1 18:15-19:30

Secondary Ion Mass Spectrometry (SHRIMP) U-Pb dating of Chelyabinsk meteorite

KAMIOKA, Moe[1*] ; TERADA, Kentaro[1] ; HIDAKA, Hiroshi[2] ; KIMURA, Kosuke[2] ; SKUBLOV, Sergey[3]

[1]Osaka University, Department of Earth and Space Science, [2]Guraduate school of Science, Hiroshima University, [3]Institute of Precambrian Geology and Geochronology,

On Feburuary 15,2013, a meteorite fell into the area of Chelyabinsk in Russia .The petrographic and chemical analysis of the Chelyabinsk meteorite unambiguously classifies it as an LL5 ordinary chondrite (Galimov et al.2013). The reported Sm-Nd age of 3.7 Ga and Rb-Sr age of 0.29 Ga suggest that the Chelyabinsk meteorites could have suffered from the secondary event possibly due to shock metamorphism.For further understanding of the thermal history of Chelyabinsk meteorite, we carried out an in-situ U-Pb dating of phosphates of which closure temperatures is high (~600 ℃), using Hiroshima-SHRIMP.(Sensitive High-Resolution Ion MicroProbe).

Keywords: Chelyabinsk meteorite, SHRIMP, phosphate, U-Pb dating

Japan Geoscience Union Meeting 2014
(28 April - 02 May 2014 at Pacifico YOKOHAMA, Kanagawa, Japan)

PPS22-P03 Room:Poster Time:May 1 18:15-19:30

Crystallization and subsolidus processes of the NWA 6704 ungrouped achondrite

TAKAGI, Yasunari[1] ; NOGUCHI, Takaaki[1*] ; KIMURA, Makoto[1] ; YAMAGUCHI, Akira[2]

[1]Ibaraki University, [2]National Institute of Polar Research

Introduction: NWA 6704 is an unique ungrouped achondrite. It consists of low-Ca pyroxene, less abundant olivine and plagioclase, minor chromite and merrilite, and trace awaruite, heazlewoodite, and pentlandite (1, 2). Although its bulk oxygen isotopic ratio is within the ranges of the acapulucoite-lodranite and CR chondrites, its petrography and mineralogy are evidently different from both of them (1). The U-Pb dating of this meteorite gives a $^{207}Pb/^{206}Pb$ date of 4563.75 +/- 0.41 Ma (3). To deduce its formation processes is important to understand formation of its parent body that may have predated the formation of chondrite parent bodies.

Methods: Polished thin sections were investigated by optical microscopes, electron microprobe analyzer (EPMA), field-emission scanning electron microscope (FE-SEM), Raman spectroscopy, and electron backscattered diffraction (EBSD).

Results: The most abundant mineral in NWA 6704 is orthopyroxene containing blobs of augite. Both Raman spectroscopy and EBSD data indicate that this pyroxene is orthopyroxene. The texture of the blob-bearing orthopyroxene is very similar to Kintokisan-type orthopyroxene (inverted pigeonite) (4). We call it early formed (ef-) pigeonite. There are another less abundant low-Ca pyroxenes: augite blob-free orthopyroxene, and pigeonite containing sub-micrometer-size augite exsolution lamellae. Here we call them primary orthopyroxene and later formed (lf-) pigeonite. Lf-pigeonite occurs as coherent overgrowth of the primary orthopyroxene and discrete grains in the interstices of large ef-pigeonite. Lf-pigeonite also occur as inclusions in olivine. Based on the EBSD data, modal abundances of ef-pigeonite, olivine, lf-pigeonite, primary orthopyroxene, feldspar, chromite, awaruite are 67.2, 16.8, 3.4, 0.6, 10.9, 0.4, and 0.4 vol.%, respectively. Crystallization sequence estimated based on the petrography is following: primary orthopyroxene =>awaruite =>ef-pigeonite =>chromite =>lf-pigeonite =>olivine =>augite (quite rare crystallized from melt) =>heazlewoodite =>pentlandite =>merrilite =>feldspar. Early formed pigeonite (blob-bearing orthopyroxene) shows a LPO of the [010] axis. Lf-pigeonite contains complex exsolution lamellae of augite. The thickest lamellae have ˜0.2 micrometer in width and 1-2 micrometer wavelength. Finest lamellae have <0.1 micrometer thick and ˜0.2 micrometer wavelength.

Discussion: Because [010] lattice preferred orientation of pyroxene in terrestrial rocks has been interpreted as settling of tabular pyroxene crystals in a stagnant magma chamber (5), ef-pigeonite could have settled in a stagnant magma chamber. Presence of Fe^{3+} in chromite and high NiO concentration in olivine (0.89 wt.% on average) suggest that this meteorite crystallized under an oxidized condition. About 1100 ^{o}C equilibrium temperature was estimated by using two pyroxene geothermometry and ˜950 ^{o}C by using olivine-spinel geothermometry. These high temperatures suggest that the meteorite cooled rapidly in this range of temperature. Multiple exsolution lamellae with thickness and wavelength similar to this meteorite were observed in Zagami martian meteorite. Its cooling rate between 1100 ^{o}C to 950 ^{o}C was estimated to be ˜0.02 ^{o}C/hr (6). This meteorite could be cooled as slow as Zagami did. Further studies are needed to clarify if a monotonous cooling can accomplish both high equilibrium temperatures estimated by geothermometers and sub-micrometer-size exsolution lamellae in lf-pigeonite. NWA 6704 has petrography similar to that of NWA 6693. However, there is a stark difference between these two meteorites. Blob-bearing orthopyroxene is the most abundant pyroxene in the former. On the other hand, low-Ca pigeonite is the most abundant in the latter. Therefore, it is possible that NWA 6704 is not mere a pair of NWA 6693.

References: (1) Irvine et al. (2011), (2) Warren et al. (2012), (3) Iizuka et al. (2013), (4) Ishii and Takeda (1974), (5) Jackson (1961), (6) Brearley (1991).

Keywords: NWA 6704, achondrite

Japan Geoscience Union Meeting 2014
(28 April - 02 May 2014 at Pacifico YOKOHAMA, Kanagawa, Japan)

PPS22-P04 Room:Poster Time:May 1 18:15-19:30

Petrologic type from plagioclase size distribution

KAWASAKI, Takehiro[1] ; KIMURA, Makoto[1*] ; NOGUCHI, Takaaki[1]

[1]Faculty of Science, Ibaraki University

Ordinary chondrites are classified into petrologic types 3-6, reflecting thermal metamorphism. One of the criteria to classify types 5 and 6 is the size distribution of plagioclase. The size, 50 microns, has been commonly used to classify types 5 and 6. However, no any statistic study for plagioclase size has been conducted. Here we measured the size distribution, and discuss the classification of types 5 and 6. We studied 26 thin sections of types 5 and 6 from the H, L, and LL chondrite groups. Our study indicates that plagioclase of 50 microns are commonly encountered both in types 5 and 6. However, plagioclase of 80-100 microns is more abundant in type 6 than type 5. We also noticed that the size distribution of plagioclase in H6 is similar to that in type H5. The different criteria to classify H from L and LL are necessary.

Keywords: ordinary chondrite, petrologic type, plagioclase, thermal metamorphism

Japan Geoscience Union Meeting 2014
(28 April - 02 May 2014 at Pacifico YOKOHAMA, Kanagawa, Japan)

PPS22-P05 Room:Poster Time:May 1 18:15-19:30

Systematic isotopic studies of REE, Sr and Ba in eucrites

SERA, Kohei[1*] ; HIDAKA, Hiroshi[1] ; YONEDA, Shigekazu[2]

[1]Department of Earth and Planetary Systems Science, Hiroshima University, [2]National Museum of Nature and Sci.

The eucrites is meteorites that probably originate from the crust of asteroid 4-Vesta. Cosmochemical and chronological information of eucrites puts important constraints of on the evolutional history of the eucrite parent body (EPB). In this study, systematic istopic isotopic studies of Sr, Ba, Ce, Nd, Sm and Gd were performed on eight eucrites for better understanding of differentiation on the EPB. ^{138}Ce, ^{142}Nd, and ^{143}Nd include radiogenic components, and their isotopic variations correlate with La/Ce and Sm/Nd elemental ratios, respectively. The results were consistent with the isochron from previous studies (Makishima and Masuda, 1991; Boyet and Carlson, 2005; Andreasen and Sharma, 2007). The Rb-Sr chronometer consisting of ^{87}Sr/^{86}Sr and Rb/Sr for these eucrites is now in progress. Sm and Gd isotopic compositions of the eucrites showed the isotopic shifts caused by neutron caputure reactions due to cosmic rays irradiation. These isotopic shifts correspond to the neutron fluences ranging from 0.28 to 4.05 $\times$ 10^{15} n cm^{-2}, but these are almost consistent with their cosmic-ray exposure ages, suggesting no strong evidence of initial cosmic-ray irradiation on the surface of EPB. Most previous Ba isotopic studies of meteorites focused on the variation of r- and s-process nucleosynthetic components due to additional inputs in the early solar system. ^{135}Ba and ^{137}Ba isotopes are sensitive to s- and r-process variations, and often have deficits and/or excesses in chemical separates in carbonaceous chondrites due to the existence of presolar grains. In case of eucrites, there are no isotopic variations of all Ba isotopes, but some samples showed the slight excess of radiogenic ^{135}Ba probably from ^{135}Cs decay. Systematic isotopic data obtained in this study provide a hint to understand the evolution processes of differentiated meteorites. We are now applying this technique for the analyses of cumulate eucrites and diogenites.

Keywords: eucrite, REE, chronology, isotope

Japan Geoscience Union Meeting 2014
(28 April - 02 May 2014 at Pacifico YOKOHAMA, Kanagawa, Japan)

PPS22-P06 Room:Poster Time:May 1 18:15-19:30

Preliminary experiments on the formation process of lingunite in shocked meteorites

KONO, Mari[1*] ; KUBO, Tomoaki[1] ; KATO, Takumi[1] ; KONDO, Tadashi[2]

[1]Kyushu Univ., [2]Osaka Univ.

Albite-rich hollandite (lingunite) has been frequently found in shocked meteorites with other high-pressure minerals (Gillet et al., 2000; Tomioka et al., 2000). According to the laser-heated diamond anvil cell (LHDAC) experiments by Liu (1978), following the decomposition of albite ($NaAlSi_3O_8$) into jadeite ($NaAlSi_2O_6$) plus quartz (SiO_2) at 2-3 GPa, these phases recombine to form lingunite in the range of pressure between 21 and 24 GPa at about 1000 ℃, and then it decomposes again into calcium ferrite-type NaAlSiO4 plus stishovite at pressures above 24 GPa. Similarly, Tutti (2007) observed $NaAlSi_3O_8$ lingunite at 21-23 GPa and 2000 ℃ using LHDAC. In contrast to these LHDAC studies, high-pressure experiments using multi-anvil type (MA) apparatus revealed that the maximum solubility of $NaAlSi_3O_8$ component in hollandite structure is limited to ˜50 mol% at 14-25 GPa and 800-2400 ℃ (Yagi et al., 1994, Liu, 2006). This contradiction has not been solved yet, which makes it difficult to understand the shock conditions for the presence of lingunite in shocked meteorites. Tutti (2007) suggested that the stability of lingunite might be sensitive to temperature and could transform back when quenching rate is slow like MA experiments. However, the formation conditions of lingunite has not been well constrained even by LHDAC experiments.

To investigate the formation process of lingunite, we preliminarily carried out LHDAC experiments using a powder of natural albite as a starting material. The samples were compressed at room temperature, and then heated by the double-sided laser heating method using a Nd:YAG laser. The emission spectra were measured on both side of the heated sample, and used to estimate temperature. Heating duration at the maximum temperature was several minutes. Recovered samples were analyzed by X-ray diffraction method at BL-ARNE7 and BL-ARNE1 of photon factory, KEK. The results obtained suggest that jadeite and stishovite are present at 22 GPa and 1230 ℃. The assemblage changed into calcium ferrite-type structure and stishovite at 25 GPa and 1400 ℃. Hydrous aluminum silicate (phase egg) was also present in both samples probably due to the effect of absorbed water in the powdered stating material. We measured X-ray diffraction patterns at several points in the sample, which showed changes of the ratio of the constituent minerals due to the presence of pressure and temperature gradients, however we did not observe lingunite in any measured points. Although experimental conditions are still rather limited, our preliminary results suggest that the formation condition of lingunite is more than 1400 ℃ at these pressure ranges.

Keywords: lingunite, high pressure, LHDAC, shocked meteorite

Japan Geoscience Union Meeting 2014
(28 April - 02 May 2014 at Pacifico YOKOHAMA, Kanagawa, Japan)

PPS23-01 Room:413 Time:May 2 09:00-09:15

Surface roughness effect on KAGUYA LRS surface echo observation and its calibration

KOBAYASHI, Takao[1*] ; LEE, Seung ryeol[1]

[1]Korea Institute of Geoscience and Mineral Resources

KAGUYA Lunar Radar Sounder (LRS) was an HF (5MHz) radar whose primary mission was to explore subsurface of the Moon. Its footprint covered whole surface of the Moon in its operation period. All the data was processed by applying Synthetic Aperture Radar (SAR) algorithm so that the signal-to-noise ratio of target echoes as well as the spatial resolution was improved.

The data was further processed to extract nadir surface echoes so that the surface property of the Moon was studied in a spectral range of the HF band. The physical property that can be known directly from the data was the apparent reflectivity of the lunar surface in the frequency range of the HF band: The data contains scattering effect of surface roughness due to the surface terrain. We need to separate this scattering effect from the data so that we can make quantitative evaluation of the surface reflectivity. In order to meet this requirement, we carried out simulation of KAGUYA LRS observation to evaluate the surface scattering effect due to the lunar surface terrain.

The simulation was based on Kirchhoff approximation method. The Lunar Imager/SpectroMeter (LISM) Digital Elevation Model (DEM) data was utilized to simulate actual lunar surface terrain. Flat surface observation was simulated as the reference case before the simulation of actual LRS observation was carried out. We assumed that the dielectric constant of the lunar surface material was 4.0.

Our simulation revealed that even a mare surface where the surface is often regarded to be flat certainly behaved as a rough surface which gave a rise to decrease of the nadir echo intensities for a few decibels in comparison to the flat surface reflection. This effect gives a significant influence on estimation of regolith thickness in maria. Newly estimated regolith thickness was approximately a meter smaller than previously estimated value: it turned out to be 6 - 7 m in Mare Imbrium.

Keywords: KAGUYA, LRS, HF radar, surface echo, scattering

Japan Geoscience Union Meeting 2014
(28 April - 02 May 2014 at Pacifico YOKOHAMA, Kanagawa, Japan)

PPS23-02 Room:413 Time:May 2 09:15-09:30

Determination of the dielectric constant of the lunar surface based on the radar echo intensity observed by the Kaguya

KUMAMOTO, Atsushi[1*] ; ISHIYAMA, Ken[1] ; KOBAYASHI, Takao[2] ; OSHIGAMI, Shoko[3] ; HARUYAMA, Junichi[4]

[1]Tohoku Univ., [2]KIGAM, [3]NAOJ, [4]JAXA

In the planetary radar observation, echo power and delay time depend on the effective dielectric constant, or equivalent dielectric constant including the voids in the planetary uppermost media. As for the Moon, because there is almost no material whose dielectric constant is far from the basalt rocks, the effective dielectric constant of the lunar uppermost media is considered to depend mainly on their porosity. So if we can determine the effective dielectric constant of the lunar uppermost media, we can derive their bulk density, or density including the voids based on the empirical relation between the dielectric constant and bulk density of the Apollo samples [Carrier et al., 1991].

If we are going to use echo power for determination of the permittivity, we should note that the radar echo intensity depends not only on the dielectric constant but also on the roughness of the surface. Therefore, we have determined the permittivity of the lunar surface with considering the surface roughness. In the analysis, the dielectric constant is determined by using the radar echo intensity obtained by Kaguya Lunar Radar Sounder (LRS) [Ono et al, 2000; 2008; 2010], and the surface roughness parameters derived from Digital Terrain Model (DTM) based on Kaguya Terrain Camera (TC) observation [Haruyama et al., 2008]. The global distributions of the echo powers in a frequency range of 4-6 MHz were derived from the Kaguya/LRS dataset. We have used the intensity of off-nadir echoes in an incident angle from 5 to 15 degree. The reason why nadir echoes are not used in the analysis is because the echo intensity changes drastically in small incident angle range due to the poor range resolution from the spacecraft to the off-nadir reflection point. The echoes arrived after the arrival of the nadir surface echo were identified as off-nadir echoes in this study. In addition, we have also derived the global distribution of the surface roughness parameters. The RMS height of the surface can be obtained by <(z(x+L)-z(x))ˆ2>, where z(x) is height of the surface derived from the Kaguya TC/DTM, L is baseline length, and <>denotes the average. If we assume the self-affine surface model, the roughness parameters H and s can be obtained by the least square fitting of the RMS heights to s LˆH. The off-nadir surface echo power can be calculated based on the radar equation. Assuming Kirchhoff Approximation (KA), the backscattering coefficient in the radar equation can be obtained from the roughness parameters H and s, and assumed dielectric constant [cf. Bruzzone et al., 2011]. Using the backscattering coefficient, we can calculate the expected off-nadir surface echo powers. By performing the comparison between calculated and observed echo powers, we can determine most plausible dielectric constant. In the calculation of the echo powers, the transmitting loss of LRS have to be determined, which are however difficult to measure in the ground tests. So we estimated the transmitting loss to be 5.8 dB by assuming that the average dielectric constant is to be 5.3, which are derived from bulk density of 2.55 g/cm3 in the highlands reported based on GRAIL observations[Wieczorek et al., 2013].

The obtained Hurst exponent H is less than 0.5 in the maria, and about 0.9 in the highland. The parameter s is about 1 in the maria, and about 0.3 in the highland. By applying the analysis method mentioned above, we could obtain the observed and calculated surface echo powers in the regions where H˜0.5, and H˜0.9. Based on them, we could estimate the average dielectric constant in the maria (H?0.5) to be 7, and that in the highland (H?0.9) to be 4. The bulk densities are therefore estimated to be 3.0g/cm3 in the maria (H˜5), and 2.1g/cm3 in the highland. It suggests that there are more voids in the highland than in the maria due to longer exposure to the meteorite impacts.

Keywords: Kaguya (SELENE), Lunar Radar Sounder (LRS), Terrain Camera (TC), Surface roughness, Bulk density, Dielectric constant

Japan Geoscience Union Meeting 2014
(28 April - 02 May 2014 at Pacifico YOKOHAMA, Kanagawa, Japan)

PPS23-03 Room:413 Time:May 2 09:30-09:45

Tectonic evolution of Sinus Iridum and northwestern Imbrium regions

DAKE, Yuko[1*] ; YAMAJI, Atsushi[1] ; SATO, Katsushi[1] ; HARUYAMA, Junichi[2] ; MOROTA, Tomokatsu[3] ; OHTAKE, Makiko[2] ; MATSUNAGA, Tsuneo[4]

[1]Graduate School of Science, Kyoto University, [2]Japan Aerospace Exploration Agency / Institute of Space and Astronautical Science, [3]Graduate School of Environmental Studies, Nagoya University, [4]National Institute for Environmental Studies

Tectonic features, including mare ridges and lobate scarps, visualize the permanent strains of the lunar crust, and show ancient stress field in the shallow part of the crust, which can further places constraint on global thermal history [1], orbital evolution [2] or basin-scale mascon loading [3, 4]. Their formation ages are clues to understand the origin of tectonic movements. The subsidence of mare basalts began to affect the lithosphere as soon as they were deposited, but global tectonics can affect it long after their deposition. Some of the lobate scarps were recently estimated to be younger than 0.1 Ga [5]. It was pointed out there are some mare ridges even on the youngest mare basalts. These young tectonic structures suggest their origins other than the mascon loading. However, the amount of contraction induced by mascon loading have not yet been elucidated. The formation age of each mare ridge is not well understood. In this study, we estimated the ages of mare ridges in northwestern Imbrium and Sinus Iridum regions.

By means of optical data taken by the cameras onboard SELENE, we estimated the depositional ages of mare units and constrained the formation ages of ridges. Mare basalt lavas were so inviscid that the lava field initially made level surfaces. Therefore, the ages of deformed and dammed mare units by tectonic structures help us to determine the upper and lower bound of formation ages of the structures. We defined geological units by spectral features. The absolute ages of the units were estimated by crater-size frequency distribution measurements, applicable to craters with diameters ranging from 0.25 to 1 km, where the production and chronology functions of Neukum and Ivanov [6, 7].

The prominent mare ridges in the study area are ENE-WSW trending ridge system, hereafter Ridge System A, and NE-SW trending ridge system, Ridge System B. They are located at just to the south of Promontorium Laplace. They are parts of the concentric ridge system of Mare Imbrium, suggesting that the ridges are results of mascon loading. The eastern part of Ridge System A branches into three relatively small ridges. There is a unit boundary runs along the southern foot of Ridge System A. Relatively Ti-poor basalt [8] makes up the ridge, and relatively Ti-rich one [8] lies on the plain at the foot of the ridge. This indicates that the unit was dammed by the ridge. Therefore, the upper and lower limits of ridge formation are determined by the ages of the deformed and dammed basalt units. As a result, we estimated the ages of nine units and constrained the ages of tectonic structures as follows. Western part of Ridge System A and northern part of Ridge System B were formed between 3.0 to 2.1 Ga and 3.3 to 2.1 Ga, respectively. However, Ridge System A partially reactivated and become higher after 2.1 Ga. The middle part of Ridge System B also partially reactivated after 2.1 Ga. The southern part of Ridge System B deforms the youngest basalt indicating it was formed after 2.1 Ga.

Most of mare ridges in the study area can not be explained by mascon loading, because the major subsidence by mare basalt was occurred before 3.0 Ga in Mare Imbrium. Accordingly, this area was tectonically active after the deposition of mare basalts.

We also report other young tectonic features, such as lobate scarps and arcuate rilles in the study area.

References: [1] Prichard M.E. and Stevenson D.J., in Origin of the Earth and Moon, Canup R.M. and Righter K., Eds. (Arizona Univ. Press, 2000), 179-196. [2] Melosh H. (1980) Icarus, 43, 334-337. [3] Solomon S.C. and Head J.W. (1979) JGR, 84,148-227. [4] Freed A.M. et al. (2001) JGR, 106, 20603-30620. [5] Watters T.R. et al. (2010) Science, 329, 936-940. [6] Neukum G. (1983) Meteoritenbombardment und Datierung planetarer oberflachen, Habil. Thesis, Univ. Munich. [7] Neukum G. et al. (2001) Space Sci. Rev. 96, 55-86. [8] Lucey P.G. et al. (1998) JGR, 103, E2, 3679.

Keywords: Mare ridges, Deformation ages, Crater ages, Mascon tectonics

Japan Geoscience Union Meeting 2014
(28 April - 02 May 2014 at Pacifico YOKOHAMA, Kanagawa, Japan)

PPS23-04 Room:413 Time:May 2 09:45-10:00

Evaluation of the horizontal shortening in the shallow part of the lunar crust

YAMAJI, Atsushi[1*] ; DAKE, Yuko[1] ; SATO, Katsushi[1] ; HARUYAMA, Junichi[3] ; MOROTA, Tomokatsu[2] ; OHTAKE, Makiko[3] ; MATSUNAGA, Tsuneo[4]

[1]Divisin of Earth and Planetary Scieces, Kyoto University, [2]Graduate School of Environmental Studies, [3]Institute of Space and Astronautical Science, JAXA, [4]Center for Environmental Measurement and Analysis, National Institute for Environmental Studies

The topography of tectonic features in northwestern Imbrium and Sinus Iridum were studied in detail using SELENE-LISM data to estimate the horizontal shortening achieved by the formation of the features. As a result, it was found that the shortening by the formation of mare ridges was smaller than previous estimations by two orders of magnitudes except for a ridge, along which shortening was as large as ~500 m at maximum.

Keywords: tectonics, wrinkle ridge, graben, restoration

Japan Geoscience Union Meeting 2014
(28 April - 02 May 2014 at Pacifico YOKOHAMA, Kanagawa, Japan)

PPS23-05 Room:413 Time:May 2 10:00-10:15

Volcanic activity of lunar maria: Verification of super hot plume event at 2.0 Ga ago

KATO, Shinsuke[1*] ; MOROTA, Tomokatsu[1] ; WATANABE, Sei-ichiro[1] ; YAMAGUCHI, Yasushi[1] ; OTAKE, Hisashi[2] ; OHTAKE, Makiko[2]

[1]Nagoya University Graduate School of Environmental Studies, [2]Japan Aerospace Exploration Agency

Because the Moon is an endmember of terrestrial planetary bodies, to understand the thermal evolution of the Moon is necessary for understanding that of terrestrial planetary bodies. However, the process of magma ocean solidification and the thermal and structural evolution of the lunar mantle are still unknown.

Lunar mare basalts provide insights into compositions and thermal history of lunar mantle. Using image data from orbital satellites, a considerable number of maria have been dated by various techniques such as crater degradation measurement, crater size?frequency measurement, and stratigraphic relationship. Mare basalt ages indicate that eruptive activity has a second peak at the end of lunar volcanism (∼2 Ga), and the latest eruptions were limited in the Oceanus Procellarum and Mare Imbrium regions.

Using multiband images data obtained by SELENE/Kaguya, we have reinvestigated the relationship between titanium contents and eruption ages of mare basalts. Although the systematic relationship is not observed globally, an obvious increase in mean titanium content occurred at 2.3 Ga in the Oceanus Procellarum and Mare Imbrium regions, suggesting that the magma source changed at that time (hereafter, we call the volcanism before 2.3 Ga as Phase 1 volcanism, the volcanism after 2.3 Ga as Phase 2 volcanism.) The high-titanium basaltic eruption, which occurred at the late stage of mare volcanism, can be correlated with the second peak of volcanic activity at ∼2 Ga. The latest volcanic activity can be explained by the occurrence of a super hot plume originated from the core-mantle boundary.

To verify the super hot plume hypothesis, we calculate the difference between topography and selenoid in the mare region. We found a plateau structure around the center of the PKT region, whose the diameter is 1,000 km from southwest to northeast and 1,200 km from northwest to southeast and the altitude is 700 m. This plateau structure may be formed with ascending of super hot plume. Then, Phase 2 basaltic lava flows formed. If the ascending of super hot plume occurred ∼2.0 Ga ago, most mare formation had finished at that time and some transitional structures may have been left. In this presentation, we will discuss the relationship between Phase 2 high-titanium volcanisms and the super hot plume.

Keywords: Moon, lunar mare, titanium content, the Procellarum KREEP Terrane, super hot plume, selenoid

Japan Geoscience Union Meeting 2014
(28 April - 02 May 2014 at Pacifico YOKOHAMA, Kanagawa, Japan)

PPS23-06 Room:413 Time:May 2 10:15-10:30

Numerical models of mantle evolution in the moon

OGAWA, Masaki[1*]

[1]Graduate School of Arts and Sciences, Univ. of Tokyo

Numerical models of magmatism in convecting mantle are presented to understand the lunar magmatism that was active for the first 1 Gyr but rapidly declined after that. In the model, the characteristic time of magmatism is on the order of several hundred million years, much longer than that of the model of magmatism on larger planets like Mars, because a positive feedback between magmatism and mantle convection does not work: Upwelling flow of mantle convection induces magma by decompression melting. The buoyancy of the magma enhances the upwelling flow itself, and hence makes magmatism vigorous in a large planet. This positive feedback, however, does not work in the moon because of its low Rayleigh number. The long characteristic time of magmatism in the model is consistent with observations. The suggested mild magmatism implies that the heat extraction by magmatism is inefficient in the moon. Since the convective heat extraction is also inefficient in the moon because of its low Rayleigh number, this inefficient heat extraction by magmatism suggests that the most important mechanism of mantle cooling in the moon is thermal diffusion. Indeed, the thickening of the lithosphere with time by thermal diffusion makes the activity of magmatism decline within the first 1 Gyr of its history regardless of the initial content of heat producing elements in the mantle and other parameters that controls magmatism and mantle convection in the models. It may be necessary to carry out further numerical studies that include the early chemical differentiation of the mantle by magma-ocean to understand the magmatism that remained active till 2 Ga locally in some areas of the moon.

Keywords: mantle evolution, mantle convection, magmatism, the moon

Japan Geoscience Union Meeting 2014
(28 April - 02 May 2014 at Pacifico YOKOHAMA, Kanagawa, Japan)

PPS23-07 Room:413 Time:May 2 10:30-10:45

Identification of secondary craters based on the Voronoi diagram of the lunar craters

KINOSHITA, Tatsuo[1] ; HONDA, Chikatoshi[1*] ; HIRATA, Naru[1] ; MOROTA, Tomokatsu[2]

[1]The University of Aizu, [2]Graduate School of Environmental Studies, Nagoya University

We developed an automatic method for detecting crater clusters with crater spatial distribution based on the Area Voronoi tessellation technique. In the method based on the hierarchical cluster analysis, the evaluation of crater strongly depends on the closest one crater (or one cluster). In the method based on Voronoi tessellation on the other hand, it depends on the adjacent all craters. Since, this approach does not misjudge the pair craters evaluated cluster by the method based on the hierarchical cluster analysis. When a small crater is close adjacent a large crater, a boundary line of Voronoi tessellation is in the rim of the crater. This is different from the line a person pulls by intuition. So, we select Area Voronoi tessellation. For estimate an area of Voronoi, we adopted the wave front method (Watanabe and Murashima, 2006). We applied the Area Voronoi tessellation to observed crater spatial distribution. If the area of Voronoi cell is small, the crater becomes the candidate of the crater cluster. As a result, for the evaluation of crater spatial distribution, we propose that the Area Voronoi diagram is suitable to identify candidates of secondary crater.

Keywords: secondary crater, Voronoi diagram

Japan Geoscience Union Meeting 2014
(28 April - 02 May 2014 at Pacifico YOKOHAMA, Kanagawa, Japan)

PPS23-08 Room:413 Time:May 2 11:00-11:15

Development of a web application for dynamic analysis of the Kaguya Spectral Profiler data

SUGIMOTO, Kohei[1] ; HAYASHI, Yohei[2] ; OGAWA, Yoshiko[1*] ; HIRATA, Naru[1] ; TERAZONO, Junya[1] ; DEMURA, Hirohide[1] ; MATSUNAGA, Tsuneo[3] ; YAMAMOTO, Satoru[3] ; YOKOTA, Yasuhiro[3] ; OHTAKE, Makiko[4] ; OTAKE, Hisashi[4]

[1]University of Aizu, [2]AIST, [3]NIES, [4]ISAS/JAXA

Kaguya is a Japanese lunar orbiter launched on September 14, 2007 and observed the moon for about 2 years. The Spectral Profiler (SP) on board Kaguya was a spectrometer which provided global data set of visible-near infrared continuous reflectance spectra of the Moon. GEKKO is a web-application used to visualize the data observed by SP. GEKKO displays the graph of SP spectra and tables of ancillary data with thumbnail images simultaneously taken by Kaguya imager/camera. The current version of GEKKO is very useful for viewing SP spectra, but does not include analysis functions.

The goal of this study is to develop a framework for implementing analysis functions of the SP data. For transferring the data from the client, the original GEKKO connects to the server using MapServer. However, in case of MapServer, the client-researchers can only analyze in a predetermined manner. Therefore, we prepared CGI scripts and incorporated them into GEKKO.

By using the new GEKKO system, the clients-researchers will be able to dynamically analyze the SP data. The clients can select, coordinate and add the functions according to their objectives. We prepared the basic functions commonly used for the spectral analysis, such as running average, normalization and also similarity measurement.

Japan Geoscience Union Meeting 2014
(28 April - 02 May 2014 at Pacifico YOKOHAMA, Kanagawa, Japan)

PPS23-09 Room:413 Time:May 2 11:15-11:30

Rock and mineral distribution of the lunar South Pole-Aitken basin

UEMOTO, Kisara[1*] ; OHTAKE, Makiko[2] ; HARUYAMA, Junichi[2] ; YAMAMOTO, Satoru[3] ; NAKAMURA, Ryosuke[4] ; MATSUNAGA, Tsuneo[3] ; IWATA, Takahiro[2]

[1]The University of Tokyo, [2]Japan Aerospace Exploration Agency, [3]National Institute for Environmental Studies, [4]National Institute of Advanced Industrial Science and Technology

South Pole-Aitken (SPA) basin is one of the largest basin (2500 km in diameter [1]) on the lunar farside. In pre-vious studies, it has been suggested that most of the crustal material was excavated and that the mantle materials have been exposed [e.g., 1]. Particularly, because this excavation was the biggest at the central area of the basin, mantle materials exposed. Mantle material of this area is melted by the basin impact and produced impact melt [e.g., 2], therefore we suggest that investigation within this impact melt area lead up to understand mantle material conpo-sition. However, because SPA is very old and large, we cannot identify the impact melt area. In our study, we pro-duce a new mineralogical map of SPA basin interior, based on data derived from SELENE Multiband Imager (MI). In particular, we investigated mineralogy within the central depression of SPA by iron and titanium concentration and altitude data derived from SELENE. Using these method, we identified the impact melt area of SPA.

We prodused a mineralogical map within the central depression of SPA. As a result, we classified into three mineral type layers on this map ; low-Ca pyroxene layer, high-Ca pyroxene layer and very high-Ca pyroxene layer. From correlations of these layers and occurrences, we created the column diagrams of respective areas. Then, we suggested origins of these mineral type layers : The high-Ca pyroxene layer is impact melt area of the basin. The low-Ca pyroxene layer and the very high-Ca pyroxene layer is the ejecta of SPA basin and mare erupted after SPA basin formation, respectively. In fact, the area of the high-Ca pyroxene layer is impact melt area of SPA. In the fu-ture work, we will analyze mineral and chemical compositions within this area.

References: [1] Spudis et al., 1994. [2] Pieters et al., 2000

Keywords: South Pole-Aitken, lunar, rock, mineral

Japan Geoscience Union Meeting 2014
(28 April - 02 May 2014 at Pacifico YOKOHAMA, Kanagawa, Japan)

PPS23-10 Room:413 Time:May 2 11:30-11:45

Global Distribution Trend of High-Ca Pyroxene on the Lunar Highland by Satellite Hyperspectral Remote Sensing

YAMAMOTO, Satoru[1*] ; NAKAMURA, Ryosuke[2] ; MATSUNAGA, Tsuneo[1] ; OGAWA, Yoshiko[3] ; ISHIHARA, Yoshiaki[4] ; MOROTA, Tomokatsu[5] ; HIRATA, Naru[3] ; OHTAKE, Makiko[4] ; HIROI, Takahiro[6] ; YOKOTA, Yasuhiro[1] ; HARUYAMA, Junichi[4]

[1]NIES, [2]AIST, [3]Univ. of Aizu, [4]JAXA, [5]Nagoya Univ., [6]Brown Univ.

The studies using the spectral data obtained by Spectral Profiler (SP) and Multiband Imager (MI) onboard the Japanese lunar explorer SELENE/Kaguya revealed the global distributions of the purest anorthosite (PAN), olivine-rich materials, orthopyroxene-rich, and spinel-rich materials over the entire Moon. However, the global distribution of high-Ca pyroxene (HCP)-rich sites has been unclear so far. In addition to mare region, which is dominated by HCP, it has been reported that several ray craters on highland regions show HCP-dominant spectra. Thus, the global distribution of HCP-rich sites, especially for the lunar highland regions, would provide important information for the structure and evolution of the lunar crust and mantle. Thus, using the global data set of the SP, we conducted the global survey to find HCP-rich sites on the Moon, especially for the lunar highland regions. Here, we report the global distribution trend of the HCP-rich sites based on this survey.

Keywords: Remote-sensing, Hyperspectral, Kaguya

Japan Geoscience Union Meeting 2014
(28 April - 02 May 2014 at Pacifico YOKOHAMA, Kanagawa, Japan)

PPS23-11 Room:413 Time:May 2 11:45-12:00

Solidification of the lunar magma ocean suggested by composition of the highland crust

OHTAKE, Makiko[1*] ; KOBAYASHI, Shingo[2] ; TAKEDA, Hiroshi[3] ; MOROTA, Tomokatsu[4] ; ISHIHARA, Yoshiaki[1] ; MATSUNAGA, Tsuneo[5] ; YOKOTA, Yasuhiro[5] ; HARUYAMA, Junichi[1] ; YAMAMOTO, Satoru[5] ; OGAWA, Yoshiko[6] ; KAROUJI, Yuzuru[1] ; SAIKI, Kazuto[7]

[1]Japan Aerospace Exploration Agency, [2]National Institute of Radiological Sciences, [3]Chiba Inst. of Technology, [4]Nagoya University, [5]National Institute for Environmental Studies, [6]The University of Aizu, [7]Osaka University

Introduction: Previously we reported that highland materials with higher Mg# (Mg/[Mg+Fe] in mole percent in mafic minerals) (up to 80) than those on the lunar nearside were found on the lunar farside [1]. The observed higher Mg# on the lunar farside indicates that the farside crust consists of rocks that crystallized from less-evolved magma than the nearside crust. One of the other key parameters for evaluating solidification of the lunar magma ocean is Th abundance. Th is an incompatible element and concentrates in the liquidus phase when magma cools, therefore highland material that solidified earlier must have lower Th abundance than the highland material that solidified later. Th abundance distribution and its dichotomic nature were found to be lower on the farside than on the nearside [2].

If the dichotomic distribution of lunar highland Mg# and the Th abundance were formed by lunar magma ocean solidification, as the solidification proceeds, Mg# will decrease while Th abundance will increase, giving the two parameters a negative correlation. This study investigated the correlation of the two observed parameters of the lunar highland to validate the magma ocean origin of Mg# and Th abundance distribution on the lunar surface. We also tried to estimate the chemical composition of the lunar magma ocean by combining two remote-sensing data sets.

Method: Using Kaguya gamma-ray data, we derived the relative Th abundance (count of the observed gamma-ray data) map of the Moon as gridded data. We then derived the Mg# map of the lunar highland so that it had the same grid as the Th abundance map. For comparison with the derived Mg# and Th abundance correlation trend, we calculated the Mg# of the lunar magma ocean starting with different bulk chemical compositions by using the MELTS program [3]. The calculated starting magmatic compositions were bulk silicate Earth and bulk lunar magma ocean.

Results: The derived Mg# and Th concentration ratio of the same location indicates a negative correlation of the two parameters. In addition to the negative correlation, another interesting feature is that there seems to be two separate trends with lower and higher Th concentration ratios. Comparison of the observed Mg# and Th concentration ratio trend with that of the model calculation suggests that the observed data of the lower Th concentration ratio group matches the bulk silicate Earth composition better than the lunar magma ocean.

Discussion: The negative correlation of observed Mg# and Th concentration ratio suggests that current values of these parameters on the lunar surface are likely due to cooling of the lunar magma ocean as each location crystallized at a different solidification stage though the origin of the two apparent sets of the observed trends is not clear. The fact that the observed data of the lower Th concentration ratio group matches the bulk silicate Earth model better may imply that the chemical composition of the lunar magma ocean needs to re-evaluated and that the Mg# of the actual bulk lunar magma ocean may be higher than previously estimated although we need to further evaluate the effect of calculation conditions. The possibly higher Mg# of the bulk lunar magma ocean agrees with the reported higher Mg# (up to 80) in the farside highland than previously estimated based on the nearside sampled FAN compositions.

[1] Ohtake, M. et al. (2012) Nature GeoSci. 5, 384-388. [2] Kobayashi, S. et al. (2012) Earth Planet. Sci. Lett. 337, 10?16. [3] Ghiorso and Sack (1995) Contrib. Mineral. Petrol. 119, 197?212.

Keywords: Moon, Kaguya, SELENE, Crust, Magma Ocean

Japan Geoscience Union Meeting 2014
(28 April - 02 May 2014 at Pacifico YOKOHAMA, Kanagawa, Japan)

PPS23-12 Room:413 Time:May 2 12:00-12:15

Plagioclase with High Ca Contents from the Central Farside Highland.

TAKEDA, Hiroshi[1*] ; NAGAOKA, Hiroshi[2] ; KAROUJI, Yuzuru[3] ; OHTAKE, Makiko[4] ; YAZAWA, Yuuki[5] ; YAMAGUCHI, Akira[6]

[1]Graduate School of Sciences, The University of Tokyo, [2]Waseda Univ., [3]JAXA/ISAS, [4]JAXA/ISAS, [5]Faculty of Engineering, Chiba Institute of Technology, [6]National Inst. of Polar Research

Some lunar meteorites contain clasts of nearly pure calcic plagioclase with high An values and low FeO (1). We proposed that these meteorites are derived from the lunar farside on the basis of estimated low concentrations of Th and FeO by the remote sensing data on the farside of the Moon (2). The Lunar Magma Ocean (LMO) model deduced from the Apollo samples is not able to explain such dichotmy of the Moon. Nyquist et al. (3) performed Sm-Nd and Ar-Ar studies of pristine ferroan anorthosites (FANs) of the returned Apollo samples and showed that a whole rock Sm-Nd isochron for selected FANs yields an isochron age of 4.47 Ga . Mineralogical studies of lunar meteorites of the Dhofar 489 group (2) and Yamato 86032 , all possibly from the farside highlands, showed some aspects of the farside crust. Nagaoka et al. (1) reported that many fragments in such meteorites contain clasts of nearly pure calcic plagioclase with high An values.

Mineralogy of magnesian anorthosite clasts in Dhofar 489, 309 and 307 (2) was used to deduce the ejection site of the Dhofar 489 group. Presence of fine-grained magnesian granulitic clast, and many crystalline clasts with rapid growth features were interpreted in terms of a large impact basin associated with small cratering. Among a few large basins of the farside, the Dirichlet-Jackson (DJ) basin has a few large craters on the floor, and the formation age by Morota et al. (4) is 4.25 Ga, which agrees with the Ar-Ar age (4.23 Ga) of Dhofar 489 (2). Based on the Th map made by KGRS, Kobayashi et al. (5) showed that the lowest Th regions in the lunar farside occurs near the equatorial region and noted that the regions well correspond to the high Mg number region (DJ) measured by SP, of the farside crust (6). These rocks with low Th may be crystallized from less-evolved magma than the nearside crust. Anorthosites composed of nearly pure anorthite (PAN) with low Th at many locations in the farside highlands and a map of the Mg numbers (6) also showed that the region around the DJ basin is consistent with the Mg numbers (70 to 76) of the magnesian anorthositic clast in Dhofar 489 (2). A large impact, which excavated a basin of the farside might have produced granulites in deep ejecta of a smaller impact.

We investigated a process of decomposition of Ca-rich plagioclase with fulvic acid, which is a complex natural organic acid produced in humified soils (7). The Ca ion released from plagioclase can be used to fix carbon dioxide as calcite as in oolites, and is useful for reducing carbon dioxide from the atmosphere on the Earth.

References: (1) Nagaoka H., Takeda H. et al. (2012) 75th Ann. Meet. Meteorit Soc. Abstr no. 5197. (2) Takeda et al. (2006) Earth Planet Sci Lett 247, 171-184. (3) Nyquist L. E. et al (2013) LPSC 45th no. 1125. (4) Morota T. et al. (2011) JGU Meeting, PPS024-10. (5) Kobayashi S. et al. (2012) EPSL, 337-338, 10-16. (6) Ohtake M. et al. (2012) Nature Geosci., 5, 384-388. (7) Yazawa Y. et al. (2012) Chapter. 5, in Moon, B. Viorel Ed., XXXVIII, 750 p, 105-138, Springer.

Keywords: plagioclase, lunar crust, farside highland, resource utilization

Japan Geoscience Union Meeting 2014
(28 April - 02 May 2014 at Pacifico YOKOHAMA, Kanagawa, Japan)

PPS23-13 Room:413 Time:May 2 12:15-12:30

Volatile accretion on the Moon - A clue for the emergence of a habitable Earth.

HASHIZUME, Ko[1*] ; HARUYAMA, Junichi[2]

[1]Osaka University, Graduate School of Science, [2]Japan Aerospace Exploration Agency / Institute of Space and Astronautical Science

I would like to introduce the recent advancement in deciphering the information on accretion of planetary volatile compounds to the moon using lunar regolith samples. I will also make a brief comment on the future lunar explorations, toward a better understanding of volatile accretion to the early Earth-Moon system that possibly lead to the emergence of the habitable Earth.

Keywords: Lunar Regolith, Volatile Compound, Isotope Composition, Accretion Rate

Japan Geoscience Union Meeting 2014
(28 April - 02 May 2014 at Pacifico YOKOHAMA, Kanagawa, Japan)

PPS23-14 Room:413 Time:May 2 12:30-12:45

Extraterrestrial solidified materials with multi-mixture on the Moon

MIURA, Yasunori[1*]

[1]In & Out Universities

The results of the present study are summarized as follows:

1) Study of the Moon provides largely valuable information on formation processes of primordial Earth and extraterrestrial celestial-bodies.

2) Identification of crystalline solids are almost similar between the Moon and Earth, though the Moon rocks might be formed by similar formation processes of terrestrial (Earth) rocks based on the crystalline parts. However, extraterrestrial solids are mixtures of multiple states shown as amorphous solids.

3) Formation of quasi-spherical Moon body formed mainly by impact-related melting process is found as heterogeneous and irregular distribution of lunar rocks with impact craters.

4) Fluid-bearing depositions irregularly distributed on the surface and interior of the Moon are largely based on storages on the interior formed by solidified mixtures of multiple states triggered by impact process on the Moon.

5) Different processes of solids between the Moon and Earth can be observed silica Si-O frameworks which can be obtained by the ion bombardment experiments. Crystalline rocks with hard silicate structures show higher ion-peaks of alkali ions (Na, K and Ca etc.), whereas solid-aggregates of the Moon rocks show higher ion-peaks of Si and Al ions which are easily destroyed by ion bombardment relatively.

6) Ion-peaks by the sputtering of Earth impact-breccias are clearly higher than those of the Moon breccias, which main differences are not rock textures but atomic bonding.

7) The air- and water-less Moon with solidified materials with multi-states is formed from nano-grains to macroscopic rocks by impact-related evolution process.

8) The primordial planet Earth with remained heterogeneous surface by impact-related process is considered to be different cyclic system of three states (air, liquid and solid) with macro-life activity which is formed by huge production from the interior triggered by huge collision process of the giant impact.

Keywords: the Moon, mixture, solidified material, material state, ilicate framework, ion bombarment run

Japan Geoscience Union Meeting 2014
(28 April - 02 May 2014 at Pacifico YOKOHAMA, Kanagawa, Japan)

PPS23-15 Room:413 Time:May 2 14:15-14:30

Re-examination of Excavation Cavity of the Impact Basins of the Moon based on GRAIL based Crustal Thickness Model

ISHIHARA, Yoshiaki[1*] ; NAKAMURA, Ryosuke[2]

[1]JAXA, [2]AIST

Large impact features, whose diameters are more than hundreds of kilometers, are called impact basins. Large impact basins can provide comparatively clear information of the cratering process and/or constrain the lunar thermal history. The internal or subsurface structures of basins can be assessed through an analysis of their associated gravitational and topographic signatures. The recently Kaguya/SELENE mission has improved the crustal thickness model not only for the nearside but also for the farside based on the first direct farside gravity and global topography mapping. Moreover most recent GRAIL mission vastry improved spatial resolution and overall accuracy of the lunar gravity models and lunar crustal thickness models. The GRAIL crustal thickness model gives us the opportunity to re-analyse excavation depth and diameter of basin forming impact processes anywhere on the Moon with improved accuracy. This study uses the GRAIL crustal thickness model, to reconstruct the excavation cavity geometry of large impact basins on the Moon.

Our method of reconstructing the excavation cavity of large impact basins is fairly simple. We assume that the thinned crust and uplifted Moho beneath features is a direct consequence of (1) the amount of crustal material excavated during the cratering process and (2) the subsequent rebound of the crater (basin) floor. We first construct azimuthally averaged profiles for the surface topography, mare thickness and subsurface structure of the Moho for each basin. Next, we restored the uplifted Moho and overlying crust to its pre-impact position. Estimating procedures of pre-impact position is almost the same as previous analysis. After removing mare fill, this process resulted in a roughly parabolic surface depression, that we interpret as being the first-order representation of the basin's excavation cavity.

One of the most important values of understanding the large impact basin is the depth-to-diameter ratio of the excavation cavity. We examine the depth versus the diameter of our reconstructed excavation cavities (excluding the Imbrium Basin and the South Pole-Aitken Basin). It seems that up to 400 km cavity diameter, the depth (hex) and diameter (Dex) are linearly related. Further more, the linear relationship (hex/Dex=0.079+/-0.006) is almost consistent with, though slightly smaller than, the value for craters orders of magnitude smaller in size (hex/Dex=0.1), suggesting that proportional scaling is valid for basin scale impact structures except the largest impact structures on the Moon. One of the reasons of smaller depth-to-diameter ratio are probably effects due to the post impact modifications. Impact basins which has excavation cavity diameter larger than 400 km show the different state. The average crustal thickness of GRAIL lunar crustal thickness model is 34 to 43 km. So excavation cavity diameter of 400 km is located the ragime boundary between the excavation/melting cavity within crust ragime and the excavation/melting cavity exeed the Moho interface ragime.

Keywords: Impact Basin, Excavation Cavity, Melting Cavity, Moon

Japan Geoscience Union Meeting 2014
(28 April - 02 May 2014 at Pacifico YOKOHAMA, Kanagawa, Japan)

PPS23-16 Room:413 Time:May 2 14:30-14:45

Lunar gravity anomaly recovery with the GRAIL level-1b and level-2 data

HASHIMOTO, Mina[1*] ; HEKI, Kosuke[1]

[1]Department of Natural History Sciences, Faculty of Science, Hokkaido University

First, we will talk about the lunar gravity anomaly recovery with the GRAIL level-1b data. Among several global lunar gravity field models available now, GRAIL offers the highest resolution. The Doppler tracking between Earth-based stations and lunar satellites can directly observe gravity field of the lunar nearside. SELENE could measure the farside, for the first time, by inter-satellite tracking using the high-altitude relay satellite. GRAIL employs the low-low inter-satellite tracking method, often called as ″ Tom and Jerry ″ . This is similar to GRACE, the twin satellites for the gravimetry of the earth. It observes the gravity field by ranging between the satellites using microwave. In this way, GRAIL got the global lunar gravity anomaly map. In our study, we use the GRAIL level-1b and level-2 data. Both data have become open to public at the PDS Geoscience Node at the Washington University, Saint Lewis. The level-1b data include satellite position data compiled as the GNV1b files, and inter-satellite ranging data (ranges, range rates, and range accelerations every five seconds) are compiled in the KBR1b files. In this study, we used these two data sets and estimated the mass distribution on the moon. We remodeled the moon ' s gravity anomaly program of the Lunar Prospector developed by Sugano and Heki (EPS 2004; GRL 2005). Using this program, we estimated the gravity anomaly of the specific parts of the lunar surface. We found the Level-1b data are able to recover them clearly. Then, we will introduce the next-stage study by using the GRAIL level-2 data set, and explain the scientific targets of our study. Recent study (Miljkovi?, K. et al., 2013) suggested that the size and depth of the crater depends on the mantle temperature as well as the size and speed of the projectile. We here study the gravity signatures of small to medium sized craters, and will find systematic difference between the lunar near and far sides.

Japan Geoscience Union Meeting 2014
(28 April - 02 May 2014 at Pacifico YOKOHAMA, Kanagawa, Japan)

PPS23-17 Room:413 Time:May 2 14:45-15:00

Consideration of the seismic moment distribution of deep moonquake and the lunar deep structure

YAMADA, Ryuhei[1*] ; NODA, Hirotomo[1] ; ARAKI, Hiroshi[1]

[1]National Astronomical Observatory of Japan / RISE Project

The Apollo seismic network consists of 4 seismic stations (Apollo12, 14, 15 and 16) have observed deep moonquakes which occur repeatedly from specific source regions at depth of 700-1200 km in the lunar deep region. The deep moonquake occurs periodically related with positions of the Earth, the Moon and the Sun; that is tidal forces (e.g., Lammlein, 1977, Bulow et al., 2007). The 106 deep moonquake sources are currently located (Nakamura, 2005), the activity and largeness of the deep event and maybe occurrence mechanism are different among the sources (Araki, 2001).

Yamada et al., (2013) have investigated seismic moment of each deep event occurred from active and well-located 15 deep sources from analysis of data obtained in Apollo 12 station. To derive the seismic moment, we have to correct for characteristics of the Apollo seismometers, elastic and attenuation parameters of the lunar interior where the seismic phase passes, geometrical spreading and radiation pattern of the fault at source region from amplitude of the seismic event (Goins et al., 1981). In Yamada et al., (2013), recent lunar interior model VPREMOON (Garcia et al., 2013) are used, and the results have shown that the values of seismic moments are different among active 15 sources and far deep sources occur the events which have larger seismic moment than near sources.

In this study, we have derived the seismic moments of identical deep events observed in Apollo 15 and 16 stations to verify the previous results derived from analysis of Apollo 12 data. This analysis indicates that the values of seismic moments derived from each station data are respectively different from even if the events are identical. We found a tendency which deep moonquakes occur from far sources indicates larger differences in seismic moments derived from each station data than near source events. This may mean that the recent lunar interior model applied in this study has some problems. Especially, seismic quality factor in the mantle mainly affects on amplitudes of the seismic events. Previous studies (e.g., Nakamura and Koyama, 1982) have described that values of seismic quality factor had large uncertainty in lunar deep region. We, therefore, derived appropriate seismic quality factor so as to minimize differences of the seismic moments derived from each station data. In this analysis, we considered effects of possible radiation patterns because these values also have large uncertainty and effect on derivation of the seismic moments. We will report and discuss our new seismic moment distribution of deep moonquakes and new values of seismic quality factor in this presentation.

Keywords: Deep Moonquake, Seismic Moment, Lunar Seismic Activity, Lunar Mantle, Lunar Seismic Quality Factor, Lunar Deep Structure

Japan Geoscience Union Meeting 2014
(28 April - 02 May 2014 at Pacifico YOKOHAMA, Kanagawa, Japan)

PPS23-18 Room:413 Time:May 2 15:00-15:15

Variation of the ionized lunar sodium and potassium exosphere

YOKOTA, Shoichiro[1*] ; SAITO, Yoshifumi[1] ; ASAMURA, Kazushi[1] ; NISHINO, Masaki n[2] ; TSUNAKAWA, Hideo[3]

[1]ISAS/JAXA, [2]STE Lab., [3]Tokyo Institute of Tech.

Lunar exosphere has been observed and studied on many occasions by ground-based telescopes since the discovery of surface-bounded alkali exosphere. The observed exospheric components were alkali atoms such as Na and K because the emission lines are much brighter than for other conceivable components. The structure, source, and the transport mechanisms of the lunar exosphere have been discussed based on these ground-based observations of the alkali atoms. As for the source mechanism of the thin lunar alkali exosphere, five processes were proposed as follows: thermal desorption, electron-stimulated desorption (ESD), photon-stimulated desorption (PSD), ion-induced desorption (sputtering), and vaporization by micrometeoroid impacts. Structure of the lunar exosphere gives us the key parameters to investigate the source mechanism. The observed Na exosphere distribution suggested that PSD and/or sputtering do not simply release the exospheric particles. Since PSD is capable of releasing alkali atoms only out of very shallow region in the lunar soils, PSD has relatively limited store of the exospheric particles in the lunar surface. If there was no replenishing process, PSD would deplete surface alkalis. We present latitude and longitude distributions of Na+ and K+ fluxes from the Moon derived from the Kaguya low-energy ion data. Although the latitude distribution agrees with the previous ground-based telescope observations, dawn-dusk asymmetry has been found in the longitude distribution. Our model of the lunar surface abundance and yield of Na and K demonstrates that the abundance decreases to around 50%, at dusk compared to that at dawn due to the emission of the exospheric particles. It is also implicated that the surface abundance of Na and K need to be supplied during the night in order to explain the observed lunar exosphere with the dawn-dusk asymmetry.

Keywords: Moon, Exosphere, Alkali atmosphere, Mass analyses

Japan Geoscience Union Meeting 2014
(28 April - 02 May 2014 at Pacifico YOKOHAMA, Kanagawa, Japan)

PPS23-19 Room:413 Time:May 2 15:15-15:30

Various appearances of whistler-mode waves observed near the Moon in the solar wind

TSUGAWA, Yasunori[1*] ; KATOH, Yuto[1] ; TERADA, Naoki[1] ; TSUNAKAWA, Hideo[2] ; TAKAHASHI, Futoshi[2] ; SHIBUYA, Hidetoshi[3] ; SHIMIZU, Hisayoshi[4] ; MATSUSHIMA, Masaki[2]

[1]Department of Geophysics, Tohoku University, [2]Department of Earth and Planetary Sciences, Tokyo Institute of Technology, [3]Department of Earth and Environmental Sciences, Kumamoto University, [4]Earthquake Research Institute, University of Tokyo

Narrowband whistler-mode waves whose frequencies close to 1 Hz have been observed near the Moon [Farrell et al., 1996; Nakagawa et al., 2003; Halekas et al., 2006; Tsugawa et al., 2011]. Broadband whistler-mode waves in the frequencies up to about 10 Hz with no preferred polarity have also been observed near the Moon [Halekas et al., 2008; Nakagawa et al., 2011, Tsugawa et al., 2012]. In addition, the lunar magnetometer (LMAG) aboard Kaguya detected right-hand polarized broadband waves, which is relatively weak and appears in the frequency range of several Hz. Since the angle between the wave vector and the sunward direction is large, the waves are not significantly Doppler shifted, indicating that they are whistler-mode waves. We also reveal the existence of harmonic waves whose fundamental waves appear in the frequencies near 1-2 Hz. The fundamental waves resemble the narrowband whistler-mode waves.

We construct criteria to select these waves and perform statistical analyses. Based on the statistical properties, we suggest possible scenarios of the generation and propagation of the four types of waves around the Moon. Whistler-mode waves in the frequency near the lower hybrid frequency generated through the reflection of ions by the Moon would be observed as (1) the narrowband waves in the spacecraft frame when the group velocity vector points to the sunward and is cancelled by the solar wind velocity, as (2) the broadband waves in the interaction region with various wave components, as (3) the right-hand polarized broadband waves when the wave vector points perpendicular to the sunward, and as (4) the harmonic waves in the same condition with NR with a large compressional component enough to be steepened.

Japan Geoscience Union Meeting 2014
(28 April - 02 May 2014 at Pacifico YOKOHAMA, Kanagawa, Japan)

PPS23-20 Room:413 Time:May 2 15:30-15:45

Detection experiment of Ar emission lines for K-Ar dating using Laser-Induced Breakdown Spectroscopy

OKUMURA, Yu[1*] ; SHIBASAKI, Kazuo[1] ; OISHI, Takahiro[1] ; CHO, Yuichiro[2] ; KAMEDA, Shingo[1] ; MIBE, Kenji[2] ; MIURA, Yayoi N.[2] ; SUGITA, Seiji[2]

[1]Rikkyo University, [2]The University of Tokyo

JAXA is currently planning the lunar lander SELENE-2 project, a follow-up mission of SELENE. This project involves the dispatch of a lunar rover to investigate the lunar surface and rocks. We propose Laser-Induced Breakdown Spectroscopy (LIBS) as an instrument for mounting rovers. The LIBS conducts in-situ analysis of elemental composition.

The LIBS instrument uses a high intensity laser pulse and induced plasma. The plasma emits energy in the form of photons. The spectroscopic analysis of the plasma enables the determination of the elemental composition.

K-Ar dating is a radiometric method used in geochronology. It is based on the measurement of the product of the radioactive decay of ^{40}K into ^{40}Ar with a half-life of 1.25 Gyr. K is found in many rocks. Therefore, we can determine the solidification age of rocks by measuring the ratio of ^{40}K to ^{40}Ar in the rock. In the existing K-Ar dating method, K is measured using LIBS and Ar is measured using quadrupole mass spectrometry (QMS); thus, the method needs two measuring instruments. Our method can be applied to measure both K and Ar using only LIBS. Therefore, the instrument weight will be reduced if our method is applied successfully. The Curiosity rover, a part of NASA's Mars Science Laboratory mission, used LIBS to obtain the spectra of rocks present on the surface of Mars. The Curiosity rover's LIBS instrument detected K in the rocks. However, Ar has not been detected using LIBS. We conducted experiments to detect the Ar emission lines using LIBS.

Commonly, the temperature of plasma induced using LIBS is approximately 1eV (11600K) in the atmosphere. When temperature of plasma was 1eV, we expected that it is possible to detect the Ar emission lines at the wavelengths of 104.8nm and 106.7nm in the vacuum ultraviolet spectral range because no emission lines of neutrals and singly-charged ions of major elements exist in the range. However, as a result, we found that the plasma temperature might be several tens of eV in vacuum. We found that relative intensity of multiply-charged ions (e.g. Si(Ⅳ), Fe(Ⅱ)) emission lines is much stronger than the Ar emission lines. Therefore, we decreased the temperature of plasma in vacuum by decreasing the pulse laser intensity and conducted experiments. In addition, we conducted experiments to investigate the Ar emission lines, which we might be able to detect when the plasma temperature is higher than 1eV, in the vacuum ultraviolet (VUV)-near infrared (NIR) range in vacuum.

Keywords: LIBS, elemental compositions, K-Ar dating, Planetary Explora, Moon

Japan Geoscience Union Meeting 2014
(28 April - 02 May 2014 at Pacifico YOKOHAMA, Kanagawa, Japan)

PPS23-21 Room:413 Time:May 2 15:45-16:00

Unprecedented Zipangu Underworld of the Moon Exploration (UZUME)

HARUYAMA, Junichi[1*] ; KAWANO, Isao[1] ; KUBOTA, Takashi[1] ; OTSUKI, Masatsugu[1] ; NISHIBORI, Toshiyuki[1] ; IWATA, Takahiro[1] ; ISHIHARA, Yoshiaki[1] ; YAMAMOTO, Yukio[1] ; NAGAMATSU, Aiko[1] ; HASENAKA, Toshiaki[3] ; SHIMIZU, Hisayoshi[4] ; MOROTA, Tomokatsu[5] ; MICHIKAMI, Tatsuhiro[6] ; SHIRAO, Motomaro[7] ; MIYAMOTO, Hideaki[4] ; KOBAYASHI, Kensei[2] ; YAMAMOTO, Satoru[8] ; YOKOTA, Yasuhiro[8] ; HASHIZUME, Ko[9] ; SAIKI, Kazuto[9] ; KOMATSU, Goro[10]

[1]Japan Aerospace Exploration Agency, [2]Yokohama National University, [3]Kumamoto University, [4]University of Tokyo, [5]Nagoya University, [6]Kinki University, [7]Planetary Geology Institute, [8]National Institute for Environmental Studies, [9]Osaka University, [10]Universita d'Annunzio

Japanese lunar explorer SELENE (Kaguya) discovered gigantic vertical holes of 100 m in diameters and depths in the Marius Hills, Mare Tranquillitatis, and Mare Ingenii of the Moon. These holes are possibly skylights of underground large caverns such as lava tubes, magma chambers, or faults. There are lots of scientific interests on the holes and associating caverns. In addition, these holes and underground structures are the best candidate locations for future lunar base. Similar holes have been also found on the Mars. The caverns connecting to the Martian holes may be the best place for Martian lives to emerge, evolve and survive because of their safer conditions than the Martian surface. We are now planning to establish a project working group to explore the lunar holes and caverns associating to the holes. We call the project as UZUME (Unprecedented Zipangu Underworld of the Moon Exploration).

Keywords: Moon, SELENE, hole, cavern

Japan Geoscience Union Meeting 2014
(28 April - 02 May 2014 at Pacifico YOKOHAMA, Kanagawa, Japan)

PPS23-P01 Room:Poster Time:May 2 16:30-17:30

Development of ILOM using DOE and situation of trial manufacturing of DOE

KASHIMA, Shingo[1*] ; ARAKI, Hiroshi[1] ; HANADA, Hideo[1] ; TSURUTA, Seiitsu[1] ; SUZUKI, Hirofumi[2] ; YASUDA, Susumu[3] ; UTSUNOMIYA, Shin[3]

[1]RISE Project Office, National Astronomical Observatory of Japan, [2]Mechanical Engg.,Chubu University, [3]Japan Aerospace Exploration Agency

We have a plan to install the photo-zenith telescope on the moon as part of a next SELENE project. The purpose is to explain the internal structure and the origin of the moon by measuring the small vibration and movement with very high accuracy. In this presentation, we show the development of ILOM using DOE that actualize the very high performance, i.e.,1 mas, in the severe thermal condition of the moon and show the situation of the trial manufacturing of DOE that is the key technology of this telescope.

Keywords: ILOM, DOE, SELENE

Japan Geoscience Union Meeting 2014
(28 April - 02 May 2014 at Pacifico YOKOHAMA, Kanagawa, Japan)

PPS23-P02 Room:Poster Time:May 2 16:30-17:30

Angle, deformation and DAO (Dihedral Angle Off-set) Analysys of the corner cube mirror for LL

KASHIMA, Shingo[1*] ; NODA, Hirotomo[1] ; ARAKI, Hiroshi[1] ; HANADA, Hideo[1] ; KUNIMORI, Hiroo[2] ; OTSUBO, Toshimichi[3]

[1]RISE Project Office, National Astronomical Observatory of Japan, [2]National Institute of Information and Communications Technology, [3]Social Sciences, Hitotsubashi University

We have a plan to install the corner cube mirror which has about 20cm aperture on the moon as part of a next SELENE project. The purpose is to explain the internal structure and the origin of the moon by measuring and analysing the distance between the moon and the earth with cm order accuracy. In order to actualize such a precise measurement, we have to manufacture the CCM with 0.1 sec angular precision and less the lambda/10 flatness for the mirror surface. In this presentation, we show the optical response analysis for deriving these degree of precision.

Keywords: LLR, CCM, SELENE

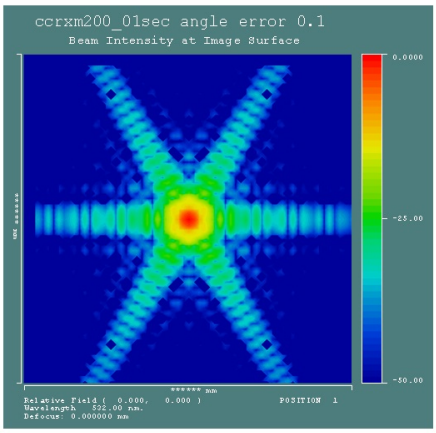

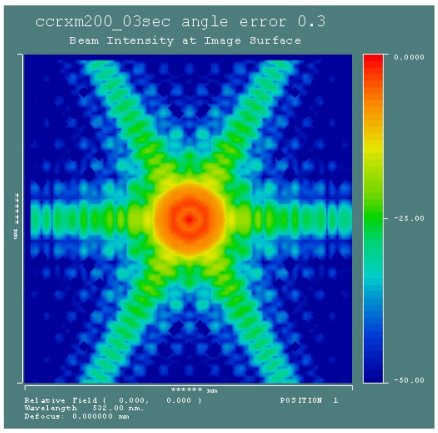

Japan Geoscience Union Meeting 2014
(28 April - 02 May 2014 at Pacifico YOKOHAMA, Kanagawa, Japan)

PPS23-P03 Room:Poster Time:May 2 16:30-17:30

Development of the Retroreflector on the Moon for the Future Lunar Laser Ranging

ARAKI, Hiroshi[1*] ; KASHIMA, Shingo[1] ; NODA, Hirotomo[1] ; KUNIMORI, Hiroo[2] ; CHIBA, Kouta[3] ; OTSUBO, Toshimichi[4] ; UTSUNOMIYA, Makoto[5] ; MATSUMOTO, Yoshiaki[6]

[1]National Astronomical Observatory of Japan, [2]National Institute of Communication and Technology, [3]Iwate University, [4]Hitotsubashi University, [5]Japan Aerospace Exploration Agency, [6]PLANET Co. Ltd.

Lunar Laser Ranging (LLR) data are important for the investigations of the lunar rotation, tide, and lunar deep interior structure. The range accuracy of LLR has been less than 2 cm for the last 20 years due to the progress of laser transmit/receive system on the ground stations and the atmospheric signal delay model, however, one order or more accurate ranging than 2cm is needed for better understanding of the lunar deep interior. We are developing 'single aperture and hollow' retroreflector (Corner Cube Mirror; CCM) to be aboard future lunar landing missions. The aperture of CCM is 20cm because the reflection efficiency of that size is found to be higher than that of Apollo 11 array CCP (Corner Cube Prism). For the CCM ultra low expansion glass-ceramic (ClearCeramRZ-EX, OHARA Inc.; hereafter CCZ-EX)' or 'single crystal Si' is selected for candidate material of CCM taking into account small |CTE|/K (Thermal expansion coefficient over thermal diffusivity) and large specific Young modulus. The optical performance of CCM deformed by lunar gravity or solar illumination in the holder model is presented for some cases.

Keywords: LLR, corner cube mirror, hollow, single crystal Si, deformation, optical performance

Japan Geoscience Union Meeting 2014
(28 April - 02 May 2014 at Pacifico YOKOHAMA, Kanagawa, Japan)

PPS23-P04 Room:Poster Time:May 2 16:30-17:30

Lunar Laser Ranging Trial at Koganei SLR station

NODA, Hirotomo[1*] ; KUNIMORI, Hiroo[2] ; ARAKI, Hiroshi[1]

[1]National Astronomical Observatory of Japan, [2]National Institute of Information and Communications Technology

Introduction: The Lunar Laser Ranging (LLR) is a technique to measure the distance between laser stations on the Earth and retroreflectors on the Moon, by detecting the time of flight of high-powered laser emitted from the ground station. Since the Earth-Moon distance contains information of lunar orbit, lunar solid tides, and lunar orientation and rotation, observation data of LLR have contributed to the lunar science, especially for the estimation of the inner structure of the Moon through orientation, rotation and tide. There are five refroreflectors on the Moon, Apollo 11, 14, 15 (U. S. A.), Lunokhod 1 and 2 (french-made, carried by former U. S. S. R.). The Apollo 15 has largest aperture among them, and almost 75 % of the total LLR data are from Apollo 15 site.

System Description: Since there is no Japanese station which can range the Moon so far, a precursor ranging experiment by using the Satellite Laser Ranging (SLR) facility in the NICT Koganei campus in Tokyo is ongoing. The SLR station has a 1.5 m Cassegrain telescope with Coude focus. Normally it is equipped with a laser with 20mJ, 20Hz repetition rate, and 35 picoseconds pulse width for satellite ranging. In addition to it, a wide-pulse width laser (3 nanoseconds, which corresponds to 45 cm in 2-way range) with energy of about 350 mJ per shot, repetition rate of 10Hz, wavelength of 532 nm is introduced to detect photons from the lunar retroreflectors for demonstration. As the pulse width is broad, the high accuracy ranging is not expected, therefore it is solely used for the confirmation of the optical link budget between the ground station and retroreflectors on the Moon. As the photon detector, we use a SPAD (Single Photon Avalanche Diode) and also an MCP (Micro Channel Plate) photo multiplier whose quantum efficiency is twice as much as that of the SPAD in use. For the pointing, a CCD imager is also available in the same detector box. They can be switched by reflecting mirrors. To suppress the background noise, a bandpass filter (0.3 nm FWHM, 50 % transparency) and spatial filter (pinhole) with diameter of 400 microns are installed and checked. For better link budget, the contamination of optical elements of the telescope and on the optical bench was checked. The alignment of the laser emission path with respect to the laser receiving path and laser beam divergence has been adjusted to maximize the efficiency of the laser emission.

Pointing: Because the retroreflectors are small and they are not visible from ground telescopes, we point the telescope to known small-sized craters (˜10 km in diameter) whose positions are known in selenographic coordinate and thus in topocentric coordinate at the observation site. Then the offset angles in azimuth and elevation direction from the predicted pointing direction are determined so that the center of the crater comes to the center of the CCD images which are coalligned with the SPAD and the MCP. This procedure confirms the pointing of the telescope.

Observations: Trials for the lunar return have been conducted since autumn 2013. As of the date of submission, the ranging to the Moon is not successful. Therefore we need to detect the return from the Apollo 15 site by using the nanosecond laser pulse for the first step. As the next step, we need to know the condition on which lunar ranging is successful in Koganei, for example, lunar phase, distance to the retroreflectors, libration angles, and atmospheric conditions.

Keywords: Lunar Laser Ranging, Satellite Laser Ranging, Moon, internal structure

Japan Geoscience Union Meeting 2014
(28 April - 02 May 2014 at Pacifico YOKOHAMA, Kanagawa, Japan)

PPS23-P05 Room:Poster Time:May 2 16:30-17:30

SELENE-2/Lunar ElectroMagnetic Sounder (LEMS): a test of inversion

MATSUSHIMA, Masaki[1*] ; SHIMIZU, Hisayoshi[2] ; TOH, Hiroaki[3] ; YOSHIMURA, Ryokei[4] ; TAKAHASHI, Futoshi[1] ; TSUNAKAWA, Hideo[1] ; SHIBUYA, Hidetoshi[5] ; MATSUOKA, Ayako[6] ; ODA, Hirokuni[7] ; OGAWA, Kazunori[6] ; TANAKA, Satoshi[6]

[1]Tokyo Institute of Technology, [2]ERI, University of Tokyo, [3]Kyoto University, [4]DPRI, Kyoto University, [5]Kumamoto University, [6]ISAS/JAXA, [7]AIST

Understanding of lunar origin and evolution can be advanced through investigation of the lunar interior structure. The present thermal state of the Moon can be clues to the Moon's thermal history. In the SELENE-2 mission, we propose a lunar electromagnetic sounder (LEMS) to estimate the electrical conductivity structure of the Moon, which can be used to deduce the thermal structure of the Moon.

Temporal variations in the magnetic field of lunar external origin induce eddy currents in the lunar interior depending on the electrical conductivity structure and frequencies of the temporal variations. The eddy currents, in turn, generate temporal variations in the magnetic field of lunar internal origin. Therefore electromagnetic response of the Moon is obtained from magnetic field measurements by magnetometers onboard a lunar orbiter and a lunar lander. The response function is then used to estimate the electrical conductivity structure by solving an inverse problem. Here we assume a one-dimensional structure for electrical conductivity distribution. We show some results for a test of inversion.

Japan Geoscience Union Meeting 2014
(28 April - 02 May 2014 at Pacifico YOKOHAMA, Kanagawa, Japan)

PPS23-P06 Room:Poster Time:May 2 16:30-17:30

Moonquake observation and lunar interior exploration by one penetrator station

YAMADA, Ryuhei[1*] ; ISHIHARA, Yoshiaki[2] ; KOBAYASHI, Naoki[2] ; MURAKAMI, Hideki[3] ; SHIRAISHI, Hiroaki[2] ; HAYAKAWA, Masahiko[2] ; TANAKA, Satoshi[2]

[1]National Astronomical Observatory of Japan / RISE Project, [2]Japan Aerospace Exploration Agency, [3]Kochi University

The penetrator developed through Japanese lunar explorer 'LUNAR-A' mission is system to deploy on-board sensors on the planetary surface by free-fall from an orbiter. The penetrator is smaller and lighter than typical soft-landers because it does not require complicated landing system and thermal control system, and it has an advantage to construct geophysical network on the planetary surface. However, on-board sensors require high shock durability to survive a penetrating impact. Through previous studies, we have already shown that seismometers for the penetrator can maintain the performance to detect moonquakes even after a shock over the impact to the lunar surface (Yamada et al., 2009) and the communication instrument on the penetrator properly operate for data transmission (Tanaka et al., 2010).

Although high shock durability of the penetrator was established, deployment of the penetrator has not been executed due to cancel of the LUNAR-A mission. We, therefore, have a plan to load the penetrator on a small satellite launched by the Epsilon Launch Vehicle. In the plan, we can carry only one penetrator due to strict weight limitation of the vehicle. For the reason, we currently study the expected scientific results obtained from the observation by one penetrator station.

The seismometers deployed through the NASA Apollo missions have detected some types of moonquakes; deep moonquake, shallow moonquake and meteoroid impacts. The seismometer for the penetrator has performance capable of observing these moonquakes, and verification of activities of these lunar seismic events through comparison with results from the Apollo mission will be one of important topics. Then, we can expect to obtain information about the lunar crustal thickness and structure if we can locate meteoroid impacts by their impact flashes from ground observation. In this presentation, we report that expected detection numbers of the lunar seismic events can be observed by the penetrator and the scientific results, and appropriate installation locations of the one penetrator to obtain good scientific results be described. Then, we also discuss the prospects for future network observation using the penetrator after the small satellite exploration.

Keywords: Penetrator, Moonquake Observation, Lunar Interior Exploration, Small Satellite Exploration, Meteoroid Impact Flash

Japan Geoscience Union Meeting 2014
(28 April - 02 May 2014 at Pacifico YOKOHAMA, Kanagawa, Japan)

PPS23-P07 Room:Poster Time:May 2 16:30-17:30

On the attenuation of reflected echoes of Lunar Radar Sounder onboard Kaguya

TOH, Hiroaki[1*] ; KUMAMOTO, Atsushi[2]

[1]Graduate School of Science, Kyoto University, [2]Graduate School of Science, Tohoku University

The successful Japanese Moon probe, KAGUYA, was equipped with a variety of state-of-the-art scientific instruments including the Lunar Radar Sounder (LRS; Ono et al., 2010). LRS is a frequency modulated continuous wave (FMCW) radar with carrier frequencies from 4 to 6 MHz, and succeeded in observing distribution of reflectors beneath almost all the Moon's surface (Ono et al., 2009). Pommerol et al. (2010) further pointed out that the presence of the reflectors in lunar maria is negatively correlated with abundance of TiO2 because of its high electrical conductivity.

Loss tangent is defined as a ratio of the conduction to displacement current within an electric medium and hence an indicator of high electrical conductivity. If loss tangent is small enough, the permittivity and the electrical conductivity of the Moon's surface can be determined at the same time by comparing the reflected echo of LRS with its source pulse. Namely, by estimating the complex ratio of the received signal to the transmitted pulse, the dielectric constant can be known from the phase difference while the electrical conductivity can be derived by the observed amplitude attenuation and the permittivity obtained from the phase difference.

However, determination of the complex ratios is not straightforward because the reflected echoes are the product of a pulse compression technique and thus needs deconvolution to restore the true amplitude and phase of the echoes. Preliminary analysis of the LRS waveform data collected at the end of the fast down-link (21.3 Gbpd) mode [Jun. - Sep. 2008] showed that quality of the data is sufficient enough to perform necessary deconvolution. This implies that LRS can also be used as a ground penetrating radar.

In this presentation, the principle and the method for estimating the permittivity and electrical conductivity are first described in addition to the data used. Interpretation of the derived complex ratios and its spatial distribution on the Moon's surface is finally discussed and summarized.

REFERENCES

Ono, T. et al., Lunar Radar Sounder Observations of Subsurface Layers Under the Nearside Maria of the Moon, Science, 323, 909-912 doi:10.1126/science.1165988, 2009.

Ono, T. et al., The Lunar Radar Sounder (LRS) onboard the KAGUYA (SELENE) spacecraft, Space Sci. Rev., 154, 145-192, doi:10.1007/s11214-010-9673-8, 2010.

Pommerol, A. et al., Detectability of subsurface interfaces in lunar maria by the LRS/SELENE sounding radar: Influence of mineralogical composition, Geophys. Res. Lett., 37, L03201, doi:10.1029/2009GL041681, 2010.

Keywords: Ground penetrating radar, Electrical conductivity, Permittivity, Source pulse, Reflected echo, Loss tangent

Japan Geoscience Union Meeting 2014
(28 April - 02 May 2014 at Pacifico YOKOHAMA, Kanagawa, Japan)

PPS23-P08 Room:Poster Time:May 2 16:30-17:30

The accmulation ages of subsurface layer in Mare Imbrium based on the SELENE observation data

ISHIYAMA, Ken[1*] ; KUMAMOTO, Atsushi[1] ; NAKAMURA, Norihiro[1]

[1]Graduate School of Science, Tohoku University

Lunar Radar Sounder (LRS) onboard SELENE succeeded in detecting the electromagnetic wave reflected at subsurface layer in low-titanium regions [Ono et al., 2009; Pommerol et al., 2010]. Multiband Imager (MI) and Terrain Camera (TC) onboard SELENE respectively investigated the lunar surface composition [e.g., Otake et al., 2012] and the eruption ages of lunar lava flows [e.g., Morota et al., 2011]. Besides, the studies combined the LRS, MI, and TC data revealed the subsurface structure around the impact crater [Oshigami et al., 2012], and suggests the brittle subsurface layer with a high-porosity [Ishiyama et al., 2013]. This study investigates the accumulated age of subsurface layer in lava flow units (Unit 12 and 8 [Bugiolacchi and Guest, 2008]) in the north Mare Imbrium. This investigation is significant for discussing lunar volcanic activity because we can estimate a eruption rate of lunar lava flow.

We identified three subsurface echoes under Unit 8 from the LRS data, and revealed that the margin of the deepest subsurface echo was consistent with the surface boundary between Unit 12 and Unit 8; Unit 8 is accumulated on Unit 12. These ages of the units were estimated to be 3.31±0.19 Ga [Bugiolacchi and Guest, 2008]. However, the previous study estimated these ages by using a lunar map data with a low spatial resolution (60 – 150 m/pixel). This low spatial resolution data causes a large error for estimating the age. Thus, this study used the lunar high-resolution ortho map data obtained from TC, which has 10 m/pixel. The age of Unit 12 was estimated to be ∼3.6 Ga, which was older than the age of Unit 8. This result is consistent with the order of the stratification identified from the LRS data.

In addition, we identified that Unit 8 can be divided into several units by using the plagioclase, FeO, and TiO2 Map data, produced from the MI data. We investigate the correspondence relationship between the subsurface echoes and the identified units, and then the history of lunar volcanic activity will be discussed in the presentation.

Japan Geoscience Union Meeting 2014
(28 April - 02 May 2014 at Pacifico YOKOHAMA, Kanagawa, Japan)

PPS23-P09 Room:Poster Time:May 2 16:30-17:30

Experimental evidence for the deep high-Ti basalt magma in the lunar mantle

IGARASHI, Mako[1*] ; SUZUKI, Akio[1] ; OHTANI, Eiji[1] ; ASAHARA, Yuki[1] ; SAKAMAKI, Tatsuya[1]

[1]Division of Earth and Planetary Materials Science, School of Science, Tohoku University

The existence of high seismic attenuation zone at the depths greater than about 800 km implies that the lower mantle of the Moon could be partially molten (Nakamura et al., 1973; 1974). There is a longstanding hypothesis that the last fraction of the lunar magma ocean crystallized into a layer of dense Ti-rich cumulates at the shallow depths (˜100 km) early in the lunar history. It has been suggested that the cumulates subsequently sank into the deep interior of the moon because of its gravitational instability (e.g., Ringwood and Kesson, 1976). It is necessary to investigate the melting relations of the high-Ti basalt that may be erupted from the depths at high pressure (>4 GPa).In this study, melting relations of Apollo 14 black glass (Delano, 1986), the most Ti-rich lunar ultramafic glasses, were experimentally determined at the pressure of 4 GPa and the temperature range from 1300 C to 1450 C.

The high-pressure and high-temperature experiments were performed by using 3000 ton Kawai-type multi-anvil apparatus of Tohoku University. The samples were packed into graphite capsules and the experimental temperatures were measured by using W-Re thermocouples. The compositions of run products were analyzed by using FE-SEM (Field Emission Scanning Electron Microscopy). Our experiments depicted that the liquidus and solidus temperatures were determined to be 1450 C and 1325 C respectively at 4 GPa.

The liquidus phase is garnet, and the first consuming phase is ilmenite. Estimated temperature profile of the Moon at depths of 700 km -1200 km are between 1100 C and 1400 C (e.g., Gagnepain-Beyneix et al., 2006). The densities of partial melts and total melt were calculated by using the partial molar volume of the oxide components at one atmosphere (Lange and Carmichael, 1987) and the Birch-Murnaghan equation of state (Sakamaki et al., 2010). The densities of the melts formed by partial and total melting of the Apollo 14 black glass were heavier than those of the lunar deep mantle. Crystal-liquid density crossover is inevitable at the depth around 800 km, the pressure corresponding to 4 GPa. Therefore, the high-Ti basalt magma can exist stably if the lunar temperature profile is close to the upper bound of the estimated lunar temperature profile, suggesting existence of the low-velocity and low attenuation anomalies caused by chemical heterogeneities in the lunar deep mantle.

Keywords: high pressure, lunar mantle, high-Ti basalt, mantle over turn

Japan Geoscience Union Meeting 2014
(28 April - 02 May 2014 at Pacifico YOKOHAMA, Kanagawa, Japan)

PPS23-P10 Room:Poster Time:May 2 16:30-17:30

History of heavenly bodies collision of the solar system inside of the past one billion years studing from a lunar crate

KATO, Mami[1*] ; MOROTA, Tomokatsu[1]

[1]Nagoya University Graduate School of Environmental Studies

The moon preserve the record of the bodies impact history of the past 4.0 Ga as a crater, it is important the information to solution impact and orbit evolution of the bodies of the solar system.

Standard lunar cratering chronologies have been based on combining Luna and Apollo sample radiometric ages and impact crater densities. However, the bombardment history cannot be resolved in the past 3.0Ga because of the absence of samples with radiometric age ranging from 3.0 to 1.0 Ga. On the other hand, from crater density of lunar rayed craters, radiometric ages of lunar glass spherules, and statistics of terrestrial craters it has been suggested the hypothesis that the production function has increased in recent.

In this study, we determine formation ages of rayed craters using SELENE image data. Based on the finding, we will discuss a temporal variation of the cratering rate in the past 1.0 Ga.

Keywords: Moon, crater, cratering chronology

Japan Geoscience Union Meeting 2014
(28 April - 02 May 2014 at Pacifico YOKOHAMA, Kanagawa, Japan)

PPS23-P11 Room:Poster Time:May 2 16:30-17:30

Formation process of linear gravity anomalies and thermal evolution of the Moon

SAWADA, Natsuki[1*] ; MOROTA, Tomokatsu[1] ; ISHIHARA, Yoshiaki[2] ; HIRAMATSU, Yoshihiro[3]

[1]Graduate School of the Enviromental studies, Nagoya University, [2]JAXA, [3]Graduate School of Natural Science and Technology, Kanazawa University

The investigation of the subsurface structure in the Moon through a gravity distribution is one of means to understand the early evolution history of the Moon. Andrew-Hanna et al. (2013) analyzed gravity data, obtained by GRAIL (The Gravity Recovery and Interior Laboratory) and identified linear gravity anomalies (LGAs). They suggested that the LGAs resulted from ancient intrusions formed by magmatism with globally expansion. We can expect that such intrusions leave other evidences on the surface. In this study, we analyze topography data and FeO concentration distribution to find some characters corresponding to the LGAs and magma intrusion, and, together with the thermal history of the Moon, discuss the formation process of the LGAs on the Moon.

In this study, we focus 20 of LGAs reported by Andrew-Hanna et al. (2013) that show clear gravity anomaly. We use the 1/1024-degree gridded lunar topographic data from LOLA and the 10pixel/degree lunar FeO concentration distribution map from Clementina.

For topography data analysis, we set a study area that ranges 300km in orthogonal direction from a LGA. We apply a filter to remove topographical perturbation due to small craters. On a vertical profile to a LGA, the average, the standard deviation, and the average gradient of relative altitude are calculated with a reference altitude on a LGA. We define a vicinity area as an area within 50km from a LGA and a surrounding area as an area farther than 100km from a LGA on a vertical profile. Based on topographical features of both a vicinity area and a surrounding area, we categorize the topographic feature of LGAs into three types: mountain type, valley type, and unclassified type.

For FeO concentration data analysis, we calculate the average and the standard deviation of FeO concentration in vicinity areas of a LGA from the FeO concentration map.

The topographical data analysis reveals that most of the LGAs regions are categorized as the valley type. This result suggests that the LGAs regions are distributed over trough regions formed by tensile stress in the early history of the Moon. The FeO concentration distribution analysis reveals that the average FeO concentration of the vicinity areas in highland is 6.72 ± 1.62 wt%. This value is higher than that in the highland (<6 wt%) of the Moon, suggesting that an ancient intrusion is possibly exposed by later crater gardening.

We propose a following hypothesis on the formation process of the linear structures as a cause of LGAs from these results and the thermal history of Head and Wilson (1992). The stress state in the early period of the Moon is tensile stress for thermal expansion process. After crack formation due to the tensile stress before 4.0 Ga, the linear structures are formed by magma intrusion. The linear structures are covered by magmatism that forms mare during 4.0-3.0Ga. Ridges are formed in mare during 3.8-3.0Ga because of the compressive stress with the cooling of the Moon or in the impact basin. The formation of the ridges occurs in association with cracks near the linear structures.

Keywords: magmatism intrusions event, expansion, ridge, FeO concentration, Lunar topography data

Japan Geoscience Union Meeting 2014
(28 April - 02 May 2014 at Pacifico YOKOHAMA, Kanagawa, Japan)

PPS23-P12 Room:Poster Time:May 2 16:30-17:30

Source of the lunar magnetic anomalies estimated with the prism model

YOKOYAMA, Takashi[1*] ; TAKAHASHI, Futoshi[1] ; TSUNAKAWA, Hideo[1]

[1]Department of Earth and Planetary Sciences, Tokyo Institute of Technology

Many magnetic anomalies have been observed on the Moon since the Apollo project, although the Moon has no global intrinsic magnetic field at present. The lunar magnetic anomalies are considered to be caused by remanent magnetization of the lunar crust. Several models of the lunar magnetic anomalies have been proposed (e.g. Hood et al., 2001, 2013; Richmond et al., 2008; Purucker et al., 2012; Nicholas et al., 2007; Hemingway and Garrick-Bethell, 2012; Wieczorek et al., 2012). However, the magnetized material and its magnetizing process have been still controversial. In the present study, we have analyzed several magnetic anomalies with the prism model, in which three dimensional position, size, horizontal direction and magnetization are parameterized. The observation data by Lunar Prospector and Kaguya at the low altitude were used in the analysis. We adapt a forward modeling approach, in which the source parameters are changed iteratively till the minimum RMS (Root-Mean-Squares) misfit between the model and data is achieved. The optimal number of the prisms for modeling is objectively determined using Akaike's Information Criterion.We will discuss possible source materials on the basis of the modeling results.

Keywords: moon, magnetic anomaly, prism source model, swirl

Japan Geoscience Union Meeting 2014
(28 April - 02 May 2014 at Pacifico YOKOHAMA, Kanagawa, Japan)

PPS23-P13 Room:Poster Time:May 2 16:30-17:30

Lunar Electromagnetic responses to the stepwise changes in the IMF

HIGA, Tetsuya[1*] ; YOSHIMURA, Ryokei[2] ; OSHIMAN, Naoto[2] ; SHIMIZU, Hisayoshi[3] ; MATSUSHIMA, Masaki[4] ; TAKAHASHI, Futoshi[4] ; SHIBUYA, Hidetoshi[5] ; TSUNAKAWA, Hideo[4]

[1]Graduate School of Science, Kyoto University, [2]Disaster Prevention Reseach Institute, [3]Earthquake Research Institute, University of Tokyo, [4]Department of Earth and Planetary Sciences, Tokyo Institute of Technology, [5]Department of Earth and Environmental Sciences, Kumamoto University

The electrical conductivity structure of the lunar interior provides us very important information for investigation of the lunar origin and evolution. We attempted to estimate on the lunar electrical conductivity from magnetic field measurements by LMAG on board KAGUYA (SELENE) during the period from 21 December 2007 to 31 October 2008, when KAGUYA was in the orbit of 100-km altitude.

Magnetic fields are induced in the moon by changes in the interplanetary magnetic field (IMF). In order to confirm whether the lunar electromagnetic induction signals are observed in KAGUYA data, we compared KAGUYA data and data of ACE and WIND satellites, which locate around the Lagrange point (Sun-Earth L1), when the stepwise changes are shown in each data. LMAG measured the sum of the inducing and the induced fields, while ACE and WIND measured only the inducing field. It was found that LMAG recorded the lunar electromagnetic responses to the stepwise changes in the IMF.

Dyal and Parkin (1971) gave the homogeneous moon model and estimated lunar conductivity. Their estimation was carried out using the data measured by Apollo 12 magnetometer fixed on the lunar surface. In this study, we applied their method to the data of the orbiting satellite, KAGUYA. The homogeneous moon model was able to explain the electromagnetic response against the stepwise changes in the IMF well, and the estimated homogeneous lunar conductivity was 1×10^{-4} - 4×10^{-4} S/m. On the other hand, we found that LMAG data also recorded the anomalous signals in the minor components, not predicted from the above model. In order to confirm whether such signals are unique to KAGUYA data, we scrutinized the data obtained by Apollo and Lunar Prospector. As a result, we concluded that such signals are common when the stepwise changes penetrate the moon.

In this presentation, we will report the new analysis results of KAGUYA, Apollo, and Lunar Prospector data, and discuss the anomalous signals in the minor component of the responses to the stepwise changes in the IMF.

Keywords: Moon, KAGUYA, SELENE, LMAG, induction, conductivity

Japan Geoscience Union Meeting 2014
(28 April - 02 May 2014 at Pacifico YOKOHAMA, Kanagawa, Japan)

PPS23-P14 Room:Poster Time:May 2 16:30-17:30

Plasma observations above strong lunar crustal fields in the solar-wind wake

NISHINO, Masaki n[1*] ; SAITO, Yoshifumi[2] ; TSUNAKAWA, Hideo[3] ; TAKAHASHI, Futoshi[3] ; YOKOTA, Shoichiro[2] ; MATSUSHIMA, Masaki[3] ; SHIBUYA, Hidetoshi[4] ; SHIMIZU, Hisayoshi[5] ; FUJIMOTO, Masaki[2]

[1]Nagoya University, [2]ISAS/JAXA, [3]Tokyo TECH, [4]Kumamoto University, [5]Earthquake Research Institute, The University of Tokyo

Plasma signature around crustal magnetic fields is one of the most important topics of the lunar plasma sciences. Although recent spacecraft measurements are revealing solar-wind interaction with the lunar crustal fields on the dayside, plasma signatures around crustal fields on the night side have not been fully studied yet. Here we show evidence of plasma trapping on the closed field lines of the lunar crustal fields in the solar-wind wake, using SELENE (KAGUYA) plasma and magnetic field data at 15 km altitude. In contrast to expectation on plasma cavity formation at the strong crustal fields, electron flux is enhanced above one of the strongest crustal fields, Crisium Antipode (CA), where the magnetic field along the spacecraft orbit is as strong as 80 nT. The enhanced electron fluxes above CA are characterized by bidirectional beams in the lower energy range (typically lower than 100 eV), which shows that these electrons are trapped on the closed field lines of the crustal magnetic fields, although a possibility of opened field configuration with cusps is not totally excluded. The observed electrons on the closed field lines may come from the lunar night side surface, while the mechanism of electron supply onto the closed field line remains to be solved.

Keywords: Lunar crustal field, Lunar plasma environment, Lunar wake, SELENE (KAGUYA)

Japan Geoscience Union Meeting 2014
(28 April - 02 May 2014 at Pacifico YOKOHAMA, Kanagawa, Japan)

PPS23-P15 Room:Poster Time:May 2 16:30-17:30

A long-term all-sky imager observation of lunar sodium tail

NISHINO, Masaki n[1*] ; SHIOKAWA, Kazuo[1] ; OTSUKA, Yuichi[1]

[1]Solar-Terrestrial Environment Laboratory, Nagoya University

The Moon possesses long tail of neutral sodium atoms that are emitted from the lunar surface and transported anti-sunward by the solar radiation pressure. Since the earth crosses the lunar sodium tail for a few days around the new moon, the resonant light emission from sodium atoms can be detected from the ground. Although it has been reported that bright emissions from sodium atoms of the tail is observed during the Leonids meteor shower, only few events without meteor shower have been investigated so far. Here we show a long-term (over 15 years) observation of the lunar sodium tail using all-sky imager at Shigaraki Observatory (35N, 136E), Japan. We have surveyed our database of all-sky sodium images at a wavelength of 589.3 nm to find that a bright spot emerges around the anti-lunar point for a few days around the new moon. Although the sodium spot is the brightest during the Leonids meteor shower, a weaker sodium spot is detected in the period without meteor shower as well. The sodium spot gradually moves eastward (roughly, 0.2 hours a day), which shows that the sodium tail is strongly affected by the earth's gravity. We will present the latest results of our data analysis to discuss signatures of the lunar sodium tail as well as the origin of the lunar sodium exosphere.

Keywords: Lunar sodium tail, Lunar exosphere, All-sky imager observation

Japan Geoscience Union Meeting 2014
(28 April - 02 May 2014 at Pacifico YOKOHAMA, Kanagawa, Japan)

PPS24-01 Room:415 Time:May 1 14:15-14:30

Crystal structure, morphology, and isotopic compositions of presolar alumina grains in unequibrated ordinary chondrites

TAKIGAWA, Aki[1*] ; STROUD, Rhonda M.[2] ; NITTLER, Larry, R.[3] ; VICENZI, Edward, P.[4]

[1]Department of Geology and Mineralogy, Kyoto University, [2]The U.S. Naval Research Laboratory, [3]Carnegie Institution of Washington, [4]Smithsonian Institution, [5]National Institute of Standards and Technology

Corundum, the thermodynamically stable phase of Al_2O_3, is predicted to be the most abundant refractory dust species condensed in envelopes around oxygen-rich asymptotic giant branch (AGB) stars. Many presolar Al_2O_3 grains, which are the survival circumstellar dust grains, have been identified from acid-residues of chondrites. The grain morphology and crystal structure of presolar grains may reflect condensation conditions in circumstellar envelopes of AGB stars and processing in the interstellar medium (ISM) and protosolar disk.

Using scanning electron microscopy (SEM) we obtained detailed secondary electron images, energy dispersive X-ray spectroscopy (EDS), electron backscattered diffraction (EBSD) patterns, and cathodoluminescence (CL) spectra of each Al_2O_3 grain prior to isotopic measurements. Focused ion beam (FIB) lift-out sections were made from the identified presolar grains and the interior structures were observed with a transmission electron microscope (TEM).

The Al_2O_3 grains were identified from acid residues of QUE97008 (LL3.05) by EDS and observed in detail by field emission (FE) SEM at the Carnegie Institution of Washington (CIW). Previously identified alumina grains from Semarkona (LL3.0), Roosevelt County 075 (H3.1), and Bishunpur (LL3.15) were also used in this study. CL spectra were obtained with a FE-SEM equipped with a Gatan Mono CL4 system at NIST. EBSD analysis was performed with an FEI Nova 600 FIB-SEM equipped with an HKL EBSD system at the Naval Research Laboratory (NRL). Isotope measurements were performed with the Cameca NanoSIMS 50L ion-microprobe at CIW. Oxygen isotopes of 163 grains were measured using ~100 nm Cs^+ beam rastered over each of the grains. An O^- beam was used to measure the Mg-Al isotopic compositions of the presolar and some solar Al_2O_3 grains. Ultra-thin sections of presolar grains QUE053, 060, and 067 were prepared with the NRL FIB-SEM. TEM studies were carried out at NRL with a JEOL 2200FS field-emission scanning transmission electron microscope (STEM).

Eight presolar grains from QUE97008 and one from RC 075 were newly found. Grain QUE060 is classified into Group 2 and has a subhedral shape with clear flat facets. The surface is smooth except for a face with a cavity. TEM diffraction patterns of the FIB section indicated that the grain consists of multiple corundum crystallites. Dark-field TEM image showed large (>100 nm) and small (<30 nm) scale orientation variation. The large-scale misorientation observed on the right side of the grain seems to relate to the cavity. Small-scale distortions occur uniformly within the grain. EDS spectra showed that the Mg/Al ratio of QUE060 is ~0.01, and the NanoSIMS measurement revealed this high Mg content to be essentially pure radiogenic ^{26}Mg, with inferred initial $^{26}Al/^{27}Al$~0.01, similar to other Group 2 grains.

QUE067 is a thin Group 4 grain with very irregular morphology. Its $^{27}Al/^{24}Mg$ ratio was three times lower than in QUE060, but its inferred $^{26}Al/^{27}Al$ ratio was similar. No EBSD patterns of crystals were obtained from the grain surface but TEM observation on the FIB section showed that the interior of QUE067 was corundum, not amorphous.

The subhedral shape and smooth surface of QUE060 suggest that this grain was likely single crystalline corundum when it condensed in a circumstellar envelope of a low-mass AGB star, and that the polycrystalline nature, voids and distorted crystal structure inside the grain are secondary features.

A possible process to form large-scale misorientation and the cavity is grain-grain collisions in a SN shock in the ISM. A high velocity collision creates a shockwave propagating inside the grain, finally forming a crater. Small-scaled distortions may have also formed by collisions with small particles in the ISM. Such collisions are less destructive than with larger grains, but their probability is high. Ion bombardment in the ISM may also contribute to the small-scale distortions.

Keywords: dust, early solar system, chondrite, presolar grain, transmission electron microscopy, evolved star

Japan Geoscience Union Meeting 2014
(28 April - 02 May 2014 at Pacifico YOKOHAMA, Kanagawa, Japan)

PPS24-02 Room:415 Time:May 1 14:30-14:45

3-D observation of GEMS by electron tomography

MATSUNO, Junya[1*] ; MIYAKE, Akira[1] ; TSUCHIYAMA, Akira[1] ; NAKAMURA-MESSENGER, Keiko[2] ; MESSENGER, Scott[2]

[1]Dep. of Geology and Mineralogy, Kyoto Univ., [2]NASA Johnson Space Center

Amorphous silicates in chondritic porous interplanetary dust particles (CP-IDPs) coming from comets are dominated by glass with embedded metal and sulfides (GEMS). GEMS grains are submicron-sized rounded objects (typically 100-500 nm in diameter) with nanometer-sized (10-50 nm) Fe-Ni metal and sulfide grains embedded in an amorphous silicate matrix. Several formation processes for GEMS grains have been proposed so far, but these models are still being debated [2-5].

Bradley et al. proposed that GEMS grains are interstellar silicate dust that survived various metamorphism or alteration processes in the protoplanetary disk and that they are amorphization products of crystalline silicates in the interstellar medium by sputter?deposition of cosmic ray irradiation, similar to space weathering [2,4]. This consideration is based on the observation of nano-sized crystals (~10 nm) called relict grains in GEMS grains and their shapes are pseudomorphs to the host GEMS grains.

On the other hand, Keller and Messenger proposed that most GEMS grains formed in the protoplanetary disk as condensates from high temperature gas [3,5]. This model is based on the fact that most GEMS grains have solar isotopic compositions and have extremely heterogeneous and non-solar elemental compositions. Keller & Messenger (2011) also reported that amorphous silicates in GEMS grains are surrounded by sulfide grains, which formed as sulfidization of metallic iron grains located on the GEMS surface.

The previous studies were performed with 2D observation by using transmission electron microscopy (TEM) or scanning TEM (STEM). In order to understand the structure of GEMS grains described above more clearly, we observed 3D structure of GEMS grains by electron tomography using a TEM/STEM (JEM-2100F, JEOL) at Kyoto University. Electron tomography gives not only 3D structures but also gives higher spatial resolution (~a few nm) than that in conventional 2D image, which is restricted by the sample thickness (~>50 nm). Three cluster IDPs (L2036AA5 cluster4, L2009O8 cluster13 and W7262A2) were used for the observations. IDP W7262A2 was collected without silicon oil, which is ordinary used to collect IDPs, so this sample has no possibility of contaminations caused by silicon oil or solvent to rinse it [6].

The samples were embedded in epoxy resin and sliced into ultrathin sections (50-300 nm) using an ultramicrotome. The sections were observed by BF-TEM (bright field-TEM) and HAADF-STEM (high angle annular dark field-scanning TEM) modes. Images were obtained by rotating the sample tilt angle over a range of $\pm$65 degree in 1 degree steps. The obtained images were reconstructed to slice images. Mineral phases in the slice images were estimated by comparing with a 2D elemental map obtained by an EDS (energy dispersive X-ray spectroscopy) system equipped in the TEM/STEM.

Careful examination of the slice images confirmed that iron grains are embedded in the amorphous silicate matrix of the GEMS grains, but sulfide grains were mainly present on the surface of the amorphous silicate. These results are consistent with the model that GEMS grains formed as condensates [3,5], although more data are needed to conclude the origin of GEMS grains. The present study is the first successful example adapting the electron tomography to the IDPs. This type of analysis will be important for planetary material sciences in the future.

[1] Bradley et al. (1999) Science, 285, 1716
[2] Bradley and Dai (2004) ApJ, 617, 650
[3] Keller and Messenger (2011) GCA, 75, 5336
[4] Bradley (2013) GCA, 107, 336
[5] Keller and Messenger (2013) GCA, 107, 341
[6] Messenger et al. (2012) 43rd LPSC, 2696 (abstr.)

Keywords: IDP, GEMS, TEM, tomography

Japan Geoscience Union Meeting 2014
(28 April - 02 May 2014 at Pacifico YOKOHAMA, Kanagawa, Japan)

PPS24-03 Room:415 Time:May 1 14:45-15:00

Condensation experiments of Si-rich gas into the chondrule melt for rapid low-Ca pyroxene formation using a new furnace

IMAE, Naoya[1*] ; ISOBE, Hiroshi[2]

[1]National Institute of Polar Research, [2]Kumamoto University

Introduction

Low-Ca pyroxenes (mainly enstatites) and the high-pressure polymorphs are the most major phases constituting rocks in the solar system. The formation mechanism of low-Ca pyroxenes in the solar nebula is problematic. It has been thermodynamically predicted that enstatite forms from forsterite by the reaction with Si-rich gas since enstatite and the preceding condensate Mg-silicate, forsterite, are in reaction relation (Grossman, 1972). However, the rate of the reaction is sluggish because of the solid diffusion-controlled in the enstatite layer, and the reaction is nearly treated as maximum fractional condensation (Imae et al., 1993). Also, the amount of enstatite condensed directly from the residual gas is very small. Tissandier et al. (2002) experimentally showed that pigeonite (CaO˜5-7 wt%) crystallized from chondrule melt by the interaction with Si-rich gas. In the present study, a new technique to simulate the solar nebula was developed and massive low-Ca pyroxenes (CaO˜1 wt%) were produced using the furnace.

Experiments

The total pressure was mainly controlled to be 100Pa under the hydrogen gas flow, using a butterfly valve indicated from the diaphragm-seal type pressure gauge. The maximum temperature for each run was 1200-1450^{o}C, in which pyroxene is in stable region and the cooling rate was mainly 100^{o}C/h. A tiny fragment of the Allende meteorite (˜30-50 mg for each run) was used as a starting material of the experiments. The staring material and silica powder were put avoiding the direct contact into the alumina cruicible with the 1 mm orifice. The experiments without silica powder were also carried out as reference experiments.

Result

Minor amount of low-Ca pyroxenes were found mainly with dominant olivines under the experiments without Si-rich gas source. While, a drastic change was observed from the experiments with Si-rich gas source: completely changed to low-Ca pyroxenes poikilitically enclosing rounded olivines were observed for the charges at 1450^{o}C, and low-Ca pyroxenes were observed mainly on the rim for the charges at 1350^{o}C and 1250^{o}C. The iron content increased on the decreasing temperatures.

Discussion

The collision frequency of the Si-rich gas on the melt of the Allende chondrite as a starting material is not so large to derive the crystallization of the massive low-Ca pyroxenes from the melt. Rather, the Si-rich gas helped the nucleation of low-Ca pyroxenes in the stability filed of low-Ca pyroxene. Massive crystallization of pyroxenes did not occur for the experiments without Si-rich gas source and here the forsterite continued to grow under metastable condition.

References

Grossman L. (1972) GCA 36, 597.
Imae N., et al. (1993) EPSL 118, 21.
Tissandier L., et al. (2002) MAPS 37, 1377.

Keywords: primordial solar nebula, condensation, low-Ca pyroxene, Si-rich gas, low-pressure experiments, chondrule

Japan Geoscience Union Meeting 2014
(28 April - 02 May 2014 at Pacifico YOKOHAMA, Kanagawa, Japan)

PPS24-04 Room:415 Time:May 1 15:00-15:15

Hydration of amorphous forsterite grains in protoplanetary disks

YAMAMOTO, Daiki[1*] ; KURODA, Minami[1] ; TACHIBANA, Shogo[2]

[1]Department of Natural History Sciences, Hokkaido University, [2]Department of Natural History Sciences, Hokkaido University

Hydrous silicate dust can be thermodynamically stable at low temperatures (~200K) in protoplanetary disks with the solar-system abundance of elements. Theoretical and experimental investigation (Fegley and Prinn, 1989; Imae et al., 1999) have shown that the hydration reaction between crystalline Mg-silicates and water vapor is too sluggish to occur during a lifetime of protoplanetary disks. However, infrared spectroscopic observation and investigation of extraterrestrial materials have shown that both crystalline and amorphous Mg-silicates may be present in protoplanetary disks and in the protosolar disk. Amorphous silicates are thermodynamically unstable, and thus could be hydrated more rapidly at higher temperatures than crystalline silicates (Nagahara and Ozawa, 2011). If hydration of amorphous silicates occurs within a disk lifetime, hydrated dust could be a source of water to terrestrial planets.

In this study, in order to investigate hydration of amorphous Mg-silicates, we conducted closed-system reaction experiments of amorphous forsterite and water vapor in sealed glass tubes at temperatures of 1023-423K and P_{H2O} of 0.05 -50 bar for 2-1344 hours. Run products were analyzed with FT-IR and XRD. We found that samples reacted at temperatures below 723K and P_{H2O} of 5-50 bar showed sharp 3μm absorption features, clearly suggesting the formation of hydrous phase(s). XRD analyses of some run products showed that the hydrous phase was serpentine. Because the stable temperature of hydrous phase(s) at P_{H2O} of 5-50 bar is~523K, the present results indicate that hydrous Mg-silicates can be formed metastably from amorphous forsterite at higher temperatures than the thermodynamic prediction. Moreover, hydration of amorphous forsterite occurred after 2-hour heating at 623K and P_{H2O} of 5 and 50 bar, implying that the activation energy for hydration of amorphous forsterite is much smaller than that for crystalline forsterite.

Hydration reaction seems to have little P_{H2O} dependence at P_{H2O} of 5-50 bar, indicating that hydration is controlled by a reaction between amorphous forsterite with saturated adsorbing water molecules. No hydration occurred, however, at 523K and P_{H2O} <1 bar, which could be due to less effective adsorption of water molecules at low-pressure conditions.

Keywords: protoplanetary disk, Mg-silicate, crystalline, amorphous, forsterite, hydrous mineral

Japan Geoscience Union Meeting 2014
(28 April - 02 May 2014 at Pacifico YOKOHAMA, Kanagawa, Japan)

PPS24-05 Room:415 Time:May 1 15:15-15:30

Sticking probability for homogeneous nucleation of iron dust

KIMURA, Yuki[1*] ; TANAKA, Kyoko[2] ; INATOMI, Yuko[3] ; TAKEUCHI, Shinsuke[3] ; TSUKAMOTO, Katsuo[1]

[1]Tohoku University, [2]Hokkaido University, [3]ISAS/JAXA

Nucleation theories have been used to understand the condensation sequence, number density and size of cosmic dust in a gas outflow of dying stars or a gas plume after shock wave heating in the primitive solar nebula. However, it has been well known that nucleation rates obtained by nucleation theories and by experiments have a large difference. We believe that the reason is uncertainties of the physical parameters of nanometer sized particles. Therefore, it is still not successful to explain the characters of cosmic dust by a nucleation theory. To determine the physical parameters of nanoparticles and evaluate nucleation theories, we constructed an in-situ observation system of temperature and concentration during homogeneous nucleation in vapor phase using interferometry for both of ground based and microgravity experiments.

Nanoparticles are formed from a supercooled vapor after evaporation by electrical heating in a controlled gas atmosphere. Using the new system in lab, we succeeded to determine surface free energy and sticking probability of manganese nanoparticle from timescale for gas cooling and condensation temperature based on nucleation theories [1]. In this laboratory experiment, convection of gas atmosphere caused by thermal heating generates heterogeneity of nucleation environment, such as temperature and concentration profiles around evaporation source. If same kinds of experiments are performed in microgravity, evaporated vapor defuses uniformly and the temperature profile becomes concentric around the evaporation source. As the result, nucleation will occur at concentric position. Then, we can obtain physical properties with relatively smaller error bars and then we may be able to evaluate nucleation theories more precisely. Therefore, we also performed a microgravity experiments using an aircraft and the sounding rocket S-520-28 launched on December 17^{th}, 2012.

We prepared specially designed Mach-Zehnder-type interferometers with an evaporation chamber and camera recording systems to fit the space and weight limitations of the rocket. Three systems, named DUST 1 to 3, with same configuration except evaporation source and gas pressure in the chamber were installed into the nosecone of the rocket. The evaporation source and gas atmosphere were tungsten and gas mixture of oxygen (4000 Pa) and argon (36000 Pa) for DUST 1, iron and argon (20000 Pa) for DUST 2, and iron and argon (40000 Pa) for DUST 3. The experiments were run sequentially and automatically started from 100 s after launch of the rocket. The evaporation source of iron was electrically heated under microgravity. Evaporated iron vapor was diffused, cooled and condensed in the gas atmosphere. The temperature and concentration at the nucleation site are determined from the movement of the fringe in the interferogram. Here, we will show the results of the homogeneous nucleation and determine the sticking probability of iron atoms into a nanoparticle based on nucleation theories. The results will be compared with that by ground based experiment.

[1] Y. Kimura, K. K. Tanaka, H. Miura, K. Tsukamoto, Direct observation of the homogeneous nucleation of manganese in the vapor phase and determination of surface free energy and sticking coefficient, *Crystal Growth & Design*, **12** (2012) 3278?3284.

Keywords: Nucleation, Sounding Rocket, Interferometer, In-situ Observation, Cosmic Dust

Japan Geoscience Union Meeting 2014
(28 April - 02 May 2014 at Pacifico YOKOHAMA, Kanagawa, Japan)

PPS24-06 Room:415 Time:May 1 15:30-15:45

Ion-induce nucleation experiment I: development of a new apparatus

WATANABE, Naoki[1*] ; HIDAKA, Hiroshi[1] ; NAKAI, Yoichi[2] ; KOJIMA, Takao[3]

[1]Institute of Low temperature Science, Hokkaido University, [2]Nishina Center, RIKEN, [3]Atomic Physics Laboratory, RIKEN

Mechanisms of grain nucleation have attracted researchers in various fields of science in connection with e.g. atmospheric aerosols and cosmic dust grains. Although there have been many theoretical and experimental works approaching this issue, the details of nucleation mechanism is still in debate. Most of works are performed assuming homogeneous nucleation in gas phase or heterogeneous nucleation on the bulk surfaces. The homogeneous nucleation often suffers from a ”critical size” of particle and requires high supersaturation condition to gain the efficient formation rate, while the nucleation on the bulk surface may not be relevant to the first stage of grain formation in realistic environments. It is know that ion-induce heterogeneous nucleation would play an important role in the particle formation because in this mechanism ion-neutral interaction overcome difficulties expected in neutral-gas-phase homogeneous nucleation. We recently developed a new experimental apparatus to investigate the elementary process of the ion-induced nucleation. We present the importance of ion-induced nucleation and advantages of the newly developed apparatus. Using this apparatus, we have been successful in obtaining an important physical parameter, free energy, of water cluster ions.

Keywords: cluster ion, ion-induced nucleation

Japan Geoscience Union Meeting 2014
(28 April - 02 May 2014 at Pacifico YOKOHAMA, Kanagawa, Japan)

PPS24-07 Room:415 Time:May 1 15:45-16:00

Mid-infrared Observation of sungrazing comet C/2012 S1 (ISON) with Subaru+COMCIS

OOTSUBO, Takafumi[1*] ; USUI, Fumihiko[2] ; TAKITA, Satoshi[3] ; WATANABE, Jun-ichi[4] ; KAWAKITA, Hideyo[5] ; FURUSHO, Reiko[6] ; HONDA, Mitsuhiko[7]

[1]Tohoku University, [2]University of Tokyo, [3]ISAS/JAXA, [4]NAOJ, [5]Kyoto Sangyo University, [6]Tsuru University, [7]Kanagawa University

Comets are the frozen reservoirs of the early solar nebula and are made of ice and dust. Dust grains in comets have been used to investigate the formation conditions of the solar system. A silicate feature is often observed in comet spectra in mid-infrared region, for example 11.3-micron, and may be used for probing early history of the solar system. In most cases the feature shows the existence of crystalline silicate together with amorphous silicate. Since the crystalline silicate grains are generally made through high-temperature annealing above 800K from amorphous ones, it is believed that the crystalline silicate grains produced at the inner part of the disk were transported to the outer cold regions where comet nuclei formed.

Comet C/2012 S1 (ISON) is a long-period Oort cloud comet, discovered in September 2012. In particular, comet ISON is a sungrazing comet, which is predicted to pass close by the Sun and Earth and becoming a bright object. Mid-infrared observations of this new comet and investigation of the 10-micron silicate feature help us to understand the formation of crystalline silicate grains in the early solar nebula.

We observed comet ISON in mid-infrared wavelength region using Cooled Mid-Infrared Camera and Spectrometer (COMICS) mounted on the Subaru Telescope on Mauna Kea, Hawaii. The observation of comet ISON was carried out on 2013 October 19th and 21st UT. Since the weather condition was not so good when we observed, we carried out N-band imaging observations (8.8 and 12.4 micron) and N-band low-resolution spectroscopy. The spectrum of C/ISON can be fit with 260–265 K blackbody spectrum when we use the 7.8–8.2 and 12.4–13.0 micron region as the continuum. The spectrum has only a weak silicate excess feature, which may be able to attribute to small amorphous olivine grains. We could not detect a clear crystalline silicate feature in the spectrum. We will compare the spectrum with other Oort cloud comets, such as comets C/2011 L4 (PanSTARRS) and C/2013 R1 (Lovejoy), and discuss the dust properties and the birthplace of the comet C/ISON.

Keywords: comet, dust, silicate, infrared

Japan Geoscience Union Meeting 2014
(28 April - 02 May 2014 at Pacifico YOKOHAMA, Kanagawa, Japan)

PPS24-08 Room:415 Time:May 1 16:15-16:30

Observation of surface structure of amorphous solid water by atomic force microscope at low temperatures

HIDAKA, Hiroshi[1*] ; SUGIMOTO, Yoshiaki[2] ; NAKATUBO, Syunichi[1] ; WATANABE, Naoki[1] ; KOUCHI, Akira[1]

[1]Inst. of Low Temp. Sci., Hokkaido Univ., [2]Grad. Sch. of Eng., Osaka Univ.

Amorphous solid water (ASW) is one of the important materials in space because it exists an abundant and effects to evolution of interstellar molecules. In molecular clouds, it is well known that chemical reactions on icy interstellar dust grains which consist of ASW mantle and mineral particle core are key processes in the formations of important organic molecules (ie. H_2CO, CH_3OH) and deuterium-enriched molecules. Although ASW surface play an important role as a field of chemical reactions, the surface structure of ASW has yet to be revealed.

Recently, we developed a low temperature atomic force microscope (AFM) for study of the surface structure of ASW. AFM is a powerful tool to study the surface structure of ASW because it can work even if the surface do not have a conductive property. In this presentation, we show AFM images of ASW surfaces which were formed at several conditions. ASW were formed on Si(111) 7×7 at 103-135 K with various deposition rate (0.08-0.8 nm/min) and various thickness(2.5-22 nm). From the observations of surface structure, we discuss the relation between the surface structure and the condition of ASW formation.

Keywords: amorphous ice, interstellar dust, molecular clouds, atomic force microscopy

Japan Geoscience Union Meeting 2014
(28 April - 02 May 2014 at Pacifico YOKOHAMA, Kanagawa, Japan)

PPS24-09 Room:415 Time:May 1 16:30-16:45

Experimental approach to the formation of organic molecules following vacuum-ultraviolet irradiation of interstellar ice

HAMA, Tetsuya[1*] ; TACHIBANA, Shogo[2] ; LAURETTE, Piani[2] ; ENDO, Yukiko[2] ; FUJITA, Kazuyuki[1] ; NAKATSUBO, Shunichi[1] ; FUKUSHI, Hiroki[1] ; MORI, Shoichi[1] ; CHIGAI, Takeshi[1] ; KOUCHI, Akira[1]

[1]Institute of Low Temperature Science, Hokkaido University, [2]Department of Natural History Scieces, Hokkaido University

Cosmic gases and dust grains ejected from dying stars gradually assemble under the influence of gravity to form interstellar clouds. Among these gases, heavy elements such as magnesium (Mg) and silicon (Si) are incorporated in dust. Lighter and chemically active elements (e.g., hydrogen, carbon, oxygen, and nitrogen; H, C, O, N, respectively) play important roles in the chemistry of interstellar clouds. After the temperature and photon field decrease when the density of dust particles increases in interstellar clouds, atoms (e.g., H, O, C, N) and molecules (e.g., CO) deposit onto the dust surfaces. Cold-surface reactions proceed on the grain surface, and an ice mantle, which is predominantly composed of H_2O combined with other molecules such as CO, CO_2, NH_3, CH_4, H_2CO, and CH_3OH, is formed.

The ice mantles are also subjected to substantial energetic processing by the prevailing ultraviolet radiation during the lifetime of a interstellar cloud. Followed by repeated processing when cycling between diffused clouds and dense clouds, new refractory organic molecules are formed in the ice mantles. The ice mantles undergo further photon radiations upon the formation of protoplanetary disks, and finally evolve to non-volatile complex organic residues by irradiation and thermal processing. However, the detail of the chemical evolution of the organic molecules has still been ambiguous. Although the previous laboratory studies using infrared spectroscopy can provide the presence of polar compounds such as amines, carboxylic acid or amides functions, it often suffers from the low sensitivity and the difficulty to obtain precise identifications of molecular species due to the overlapping of broad solid-state bands. Since dust grains and ice mantles are the precursors of planetary material, studying the photoprocesses is essential to understanding the origin of our solar system, and more powerful analytical techniques are required to unveil rich chemistry of the ices in interstellar clouds and protoplanetary disks.

Here, we are going to present a talk about a new apparatus which is now under construction to shed light on the chemical evolution of organic molecules in interstellar clouds and protoplanetary disks. The apparatus consists of three basic parts, i.e., a vacuum system, a copper-substrate equipped with a closed cycle helium refrigerator, and a vacuum ultraviolet source. Multi-component interstellar ice analogues are created on the cold (10 K) substrate by vapor deposition, and subjected to irradiation by the ultraviolet. The irradiated ice is subsequently heated up to 800 K. The gas composition desorbed from the ice during heating is analyzed by a high-resolution quadrupole mass spectrometer in the vacuum chamber. The survived organic residue from heating are studied using gas chromatography coupled to mass spectrometry (GC-MS) and high performance liquid chromatography coupled to mass spectrometry (HPLC-MS).

Keywords: interstellar cloud, protoplanetary disk, ice mantles, complex organic molecules

Japan Geoscience Union Meeting 2014
(28 April - 02 May 2014 at Pacifico YOKOHAMA, Kanagawa, Japan)

PPS24-10 Room:415 Time:May 1 16:45-17:00

Hydrogen addition reactions of C_2H_2 on cold grains; clue to the formation mechanism of cometary C_2H_6

KOBAYASHI, Hitomi[1*] ; WATANABE, Naoki[2] ; HIDAKA, Hiroshi[2] ; HAMA, Tetsuya[2] ; WATANABE, Yoji[1] ; KAWAKITA, Hideyo[1]

[1]Koyama Astronomical Observatory, Kyoto Sangyo Univeristy, [2]Institute of Low temperature Science, Hokkaido University

Volatiles incorporated into comets were formed in the pre-solar molecular cloud and probably chemically altered in the proto-planetary disk of the Sun. Although physico-chemical evolution from a molecular cloud to the disk is basically understood, detailed evolutional processes are still in debate; e.g., the fraction of the materials originated in the molecular cloud incorporated into the disk without physico-chemical alterations (some fraction of materials might sublimate via accretion shock) and physical conditions (temperature, densities of materials, etc.). To reveal those links, we focused on the molecules formed through grain surface reactions, which occurred under quite low temperature conditions like 10K. We discuss the origin of such molecules in comets (icy small body of the Solar system), which might preserve the information about chemical and physical conditions of proto-planetary disk. Cometary ethane (C_2H_6) and acetylene (C_2H_2) have been observed in multiple comets since 1996 and their abundances relative to H2O (the major component of cometary ices) is ~10^{-3} but with variations. This variation might be caused by the difference in the mixing ratios between the materials originated in the molecular cloud and the disk-processed materials. C_2H_6 has never been detected in the molecular cloud and the formation mechanism of C_2H_6 detected in comets is still in debate. One of the candidates of formation reactions of C_2H_6 is the hydrogen addition reaction of C_2H_2 on the cold grain surface (C_2H_2 ->C_2H_3 ->C_2H_4 ->C_2H_5 ->C_2H_6). In the previous experimental studies, those reactions were evaluated qualitatively and it was concluded that the reaction from C_2H_4 to C_2H_6 occurred more rapidly than the reactions from C_2H_2 to C_2H_4 and it would be a reason for the nondetection of C_2H_4. To investigate these reactions more quantitatively in realistic conditions for molecular clouds, we performed the laboratory measurements of hydrogen addition reactions of C_2H_2 and C_2H_4 on the amorphous solid water (ASW), respectively.

The experiments were conducted by using laboratory setup for surface reaction in interstellar environment (LASSIE) at the institute of low temperature science, Hokkaido University3. A cryogenic aluminum substrate is located in the center of the main chamber and surrounded by a large copper shroud connected to a liquid-nitrogen reservoir. Atomic hydrogen used for the reactions were produced by the dissociation of H2 molecules in microwave-induced plasma. The kinetic temperature of hydrogen atoms were ~120 K and the H-atom flux was ~10^{13} cm^{-2} s^{-1}. The samples of pure solid C_2H_2, C_2H_4, and those on ASW were produced on the substrate at 10, 15 and 20K. Infrared absorption spectra of the ices were measured by FTIR before and during the exposure of H-atom.

Our measurements show basically the same trend as shown in the previous studies. We will discuss the temperature and thickness dependence of the time constant for the sample ices in the poster.

Keywords: molecular formation, grain surface chemistry, Inter Stellar Medium

Japan Geoscience Union Meeting 2014
(28 April - 02 May 2014 at Pacifico YOKOHAMA, Kanagawa, Japan)

PPS24-11 Room:415 Time:May 1 17:00-17:15

High Resolution Spectroscopy of Laboratory-Produced Interstellar Molecule having Response to Visible Light

ARAKI, Mitsunori[1*] ; WAKO, Hiromichi[1] ; NIWAYAMA, Kei[1] ; TSUKIYAMA, Koichi[1]

[1]Tokyo University of Science

Diffuse interstellar bands (DIBs) still remain the longest standing unsolved problem in spectroscopy and astrochemistry, although several hundreds of DIBs have been already detected. It is expected that identifications of DIBs can give us crucial information for extraterrestrial organic molecule. One of the best approaches to identify carrier molecules of DIBs is a measurement of DIB candidate molecule produced in the laboratory to compare their absorption spectra with astronomically observed DIB spectra.

Radical in a gas phase is a potential DIB candidate molecule. The electronic transitions of polyaromatic hydrocarbon radicals result in optical absorption. However, because radicals are unstable, their electronic transitions are difficult to observe using a laboratory spectrometer system. To solve this difficulty, we have developed a glow-discharge cell using a hollow cathode in which radicals can be effectively produced as a high-density plasma. The radicals produced were measured by using the cavity ringdown (CRD) spectrometer and the discharge emission spectrometer.

The CRD spectrometer, which consists of a tunable pulse laser system, an optical cavity and a discharge device, is an apparatus to observe an high-resolution optical absorption spectrum. The electronic transition of thiophenoxy radical C_6H_5S was observed in the discharge emission of thiophenol C_6H_5SH. The frequency of the electronic transition of thiophenoxy radical was measured.

A optical discharge emission was examined by a HORIBA Jobin Yvon iHR320 monochromator. We detected the phenoxy radical C_6H_5O in the discharge of phenol C_6H_5OH. The band observed at 6107 A in the discharge was assigned to the electronic transition of phenoxy radical on the basis of the sample gas dependences and the reported low resolution spectra. The frequency of the electronic transition of phenoxy radical was measured.

Comparison studies of thiophenoxy and phenoxy radicals were made with known DIB spectra.

Keywords: Diffuse Interstellar Band, interstellar molecule, spectroscopy, cavity ringdown, molecular cloud, discharge

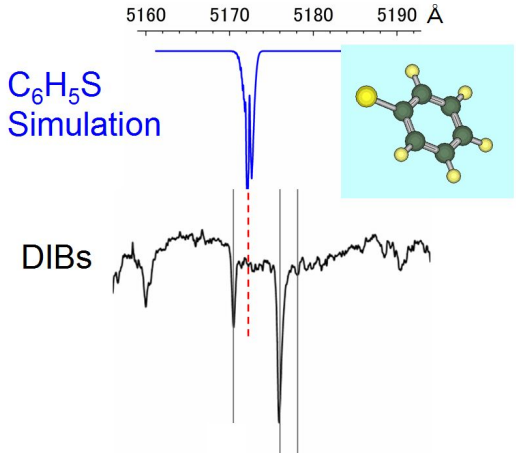

Japan Geoscience Union Meeting 2014
(28 April - 02 May 2014 at Pacifico YOKOHAMA, Kanagawa, Japan)

PPS24-12 Room:415 Time:May 1 17:15-17:30

Variation of organic compounds in the polar extract of Murchison meteorite

NARAOKA, Hiroshi[1*] ; YAMASHITA, Yohei[1] ; MITA, Hajime[2]

[1]Dept. Earth & Planet. Sci., Kyushu Univ., [2]Fukuoka Inst. Tech.

Various organic compounds have been found in carbonaceous chondrites, in which water-soluble bio-related organic compounds such as amino acids and carboxylic acids are fully studied mainly because of their great interests to origins of life in the universe and standards available for the analyses. The concentrations of these acids increase significantly after acid hydrolysis of the water extract. Even though a few studies attempted to identify the chemical structures of their precursors (Cooper and Cronin, 1995), the original structures remain largely unclear. The aqueous activity on the meteorite parent body also could proceed in a chemical oxidation (i.e. incorporation of oxygen by hydrous reaction), resulting in the alteration of original organic matter (Oba and Naraoka, 2009). The large abundance of carboxylic acids in the water extract may be attributable to such oxidation processes.

In contrast to the water extract, less polar methanol extract of chondrites has not been characterized well in spite of relatively high content of organic matter with the D- and 15N enrichment. Recently, ultrahigh-resolution mass spectral analysis on various solvent extracts of the Murchison meteorite (CM2) was performed by electrosplay ionization (ESI) using Fourier transform-ion cyclotron resonance/mass spectrometry (FT-ICR/MS) to reveal significant chemical diversity to tens of thousands of different mass peaks having CHO, CHOS, CHNO and CHNOS elemental compositions (Schmitt-Kopplin et al., 2010). With the assumption for molecular formulae calculation and no chromatographic separation, however, the detailed chemical structures of the compounds cannot be determined. In particular, the organic compounds with their elemental compositions of CH and CHN were not discussed. In this study, we performed high-performance liquid chromatography/high resolution mass spectrometry (HPLC/HRMS) analysis of organic compounds in polar solvent extracts of the Murchison meteorite.

Homologous series of alkylpyridines have been identified in the polar solvent extracts of the Murchison meteorite by liquid chromatography/high- resolution mass spectrometry. The wide range of saturated- and unsaturated-alkylated (C1 to C21) pyridines is more diverse relative to that previously found, which could be produced by aldehydes and NH3 through aldol condesation and Chichibabin-type synthesis on the meteorite parent body. This finding implies a high aldehyde activity under an alkaline condition with ammonia for the chemical evolution of organic matters in carbonaceous meteorites. In addition to the compound distribution of alkylpyridines, the occurrence of other compounds in the water extract will be also discussed with respect to their formation mechanisms in carbonaceous meteorites.

Keywords: polar organic compounds, carbonaceous meteorite, Murchison, high-resolution mass spectrometry

Japan Geoscience Union Meeting 2014
(28 April - 02 May 2014 at Pacifico YOKOHAMA, Kanagawa, Japan)

PPS24-13 Room:415 Time:May 1 17:30-17:45

Heating and evaporation of icy dust in transient heating events induced by nebular shocks

MIURA, Hitoshi[1*] ; YAMAMOTO, Tetsuo[2] ; NAKAMOTO, Taishi[3]

[1]Nagoya City University, [2]Kobe University, [3]Tokyo Institute of Technology

Icy dust plays an important role in chemical evolution from molecular clouds to protoplanetary disks. Simple organic molecules such as formaldehyde (H_2CO) and methanol (CH_3OH) can form in H_2O-CO ice by consecutive addition of hydrogen atoms to CO molecule (Watanabe & Kouchi 2002). Deuterium enrichment in these organic molecules was confirmed to occur by H-D substitution on icy dust surfaces (Nagaoka et al. 2005). More complex organic molecules such as amino acids were detected in the room-temperature residue of an interstellar ice analogue that was ultraviolet-irradiated in a high vacuum at 12 K (Munoz Caro et al. 2002). Sublimation of such icy dust will change the chemical composition of a gas phase in molecular clouds or protoplanetary disks. It is important to elucidate the thermal history of icy dust because it affects the chemical evolution of these organic molecules significantly.

In this paper, we investigated the transient heating event of icy dust induced by nebular shocks. In protostellar or protoplanetary disks, gas accretion from its parent molecular cloud or formation of planetary systems induces shock waves in various conditions. When icy dust passes through the shock front together with the ambient gas, the gas changes its velocity suddenly but the icy dust retains its velocity because of its large inertia. This results in a large relative velocity between them. The high-velocity collision of gas molecules to the icy dust surface raises the dust temperature and leads to its evaporation. Since the relative velocity is reduced by collisions with gas molecules, the heating event should cease within a short period of time. We calculated thermal history and evaporation experienced by icy dust during shock passage for various shock conditions systematically.

The physical model is as follows. We assume that the temperature and density of the post-shock gas are uniform. For simplicity, we consider a spherical icy dust composed of pure H_2O or CO. The icy dust temperature changes much faster than its velocity because of its small thermal inertia. It is shown that the evaporation fraction of individual icy dust defined by the ratio of the decrease in radius to the initial one depends only on the post-shock gas density (ρ_g) and the relative velocity between icy dust and gas just behind the shock front (v_0). We calculated the equations of motion and evaporative shrinkage of the icy dust to obtain the peak temperature and evaporation fraction experienced by the icy dust.

In general, icy dust experiences high temperature and significant evaporation for large v_0 and ρ_g. In addition, we obtained the results as follows: (i) Icy dust does not evaporate completely before it stops relative to the ambient gas even for quite large v_0 and ρ_g. This is due to a negative feedback between the evaporative shrinkage and the duration of heating. (ii) Icy dust hardly evaporates if v_0 is smaller than a certain value. For example, when $v_0 <\sim 3$ km/s for pure H_2O ice or $v_0 <\sim 1$ km/s for pure CO ice, the icy dust shrinks less than by 1% in radius for any gas density. (iii) Icy dust can experience an extremely high temperature at which it would evaporate completely if it were in equilibrium. This is a remarkable feature of the transient heating event that the short heating duration allows the icy dust to survive against superheating.

We elucidated the conditions of icy dust evaporation induced by nebular shocks for various shock conditions systematically. Our results would be useful to discuss the relation between the changes in chemical composition of molecular clouds or protostellar/protoplanetary disks and the evaporation of icy dust by shocks.

Keywords: icy dust, shock heating, evaporation, chemical evolution, protostellar disk, protoplanetary disk

Japan Geoscience Union Meeting 2014
(28 April - 02 May 2014 at Pacifico YOKOHAMA, Kanagawa, Japan)

PPS24-P01 Room:Poster Time:May 1 18:15-19:30

Importance of deuterium fractionation of ethanol by grain surface reactions: experiment of H-D tunneling substitution

OSAKA, Kazuya[1*] ; OBA, Yasuhiro[1] ; KOUCHI, Akira[1] ; WATANABE, Naoki[1]

[1]Inst Low Temp Sci, Hokkaido University

Since we have demonstrated the importance of tunneling grain surface reactions in deuterium fractionation of molecules, many works have targeted this process. To date, we have shown that the grain surface reactions play a crucial role in deuterium enrichments of water, formaldehyde, methanol, and methylamine. In this talk, we present the results of experiment on H-D substitution tunneling reactions of ethanol on cryogenic surfaces. Although C_2H_5OH was observed toward interstellar clouds, its deuterated species have not been detected. However, it was found that its homologous, CH_3OH can be highly deuterated by H-D substitution reactions on grain surfaces and thus it should be reasonable to focus on the potential importance of this process for ethanol. We demonstrated that deuterated methanol is efficiently produced by tunneling reaction of H atoms at very low temperatures relevant to grain surfaces in clouds. H-D reactions predominantly occur in CH_3-CH_2- groups but were hardly observed in an ?OH group which is consistent with the methanol case.

Keywords: deuterium enrichment, ethanol, grain surface reaction

Japan Geoscience Union Meeting 2014
(28 April - 02 May 2014 at Pacifico YOKOHAMA, Kanagawa, Japan)

PPS24-P02 Room:Poster Time:May 1 18:15-19:30

Ion-induce nucleation experiment II: free energy of the water-cluster ion

HIDAKA, Hiroshi[1*] ; NAKAI, Yoichi[2] ; KOJIMA M., Takao[3] ; WATANABE, Naoki[1]

[1]Inst. Low Temp. Sci., Hokkaido Univ., [2]RIKEN Nishina Center, [3]RIKEN Atomic Physics Laboratory

Ion-induce nucleation in gas phase is an important mechanism for grain formation in various circumstances. However, the number of works regarding this formation mechanism is very limited. To investigate the elementally processes of ion-nucleation mechanism, we recently developed a new apparatus (See, the presentation by N. Watanabe in this session). Using this apparatus, the cluster ion formation with an ion core mass-selected, which is the first stage of nucleation, can be observed quantitatively. In this presentation, we show the results of experiment on water-cluster ion formation in which free energies with the size of cluster have been determined. The experiment was performed at temperatures in range of 230-400 K with the supersaturation ratio of about 10^{-3}-10^{-2}.

Keywords: interstellar grain, cluster ion, nucleation

Japan Geoscience Union Meeting 2014
(28 April - 02 May 2014 at Pacifico YOKOHAMA, Kanagawa, Japan)

PPS24-P03 Room:Poster Time:May 1 18:15-19:30

Detection of levitation dust around the asteroid by Hayabusa-2 LIDAR

OSHIGAMI, Shoko[1*] ; SENSHU, Hiroki[2] ; WADA, Koji[2] ; KOBAYASHI, Masanori[2] ; NAMIKI, Noriyuki[2] ; MIZUNO, Takahide[3]

[1]National Astronomical Observatory of Japan, [2]Planetary Exploration Research Center, Chiba Institute of Technology, [3]Institute of Space and Astronautical Science, Japan Aerospace Exploration Agency

The micron-size particles are continuously produced at the surface of airless bodies like the Moon and asteroids by innumerable micro impacts and thermal stress related to large temperature difference between daytime and nighttime. Previous asteroid missions have revealed smooth appearance of topography on 951 Gaspra, 243 Ida, and 433 Eros suggesting that these asteroids are covered with particles smaller than resolution of camera images. Particularly, the exploration of Eros by NEAR Shoemaker has revealed as smooth surface as a liquid water at the base of craters whose diameter is between 20 and 300 m. This ”pond” is consistent with stagnant dusts of diameter smaller than 50 microns. Based on this observation, dust levitation hypothesis was proposed. According to this hypothesis, a photoelectric effect of solar UV positively charges both dust and the surface. Then a balance between electric repulsion and gravity causes 0.5-microns dusts to oscillate vertically over the surface of Eros long period of time. When a dust has a horizontal velocity, it transfers laterally until it reaches to a shadow of topography where electrostatic field is weaker than surroundings. Thus topographic depression such as a crater becomes a sink of levitating dusts.

LIDAR is one of four remote-sensing instruments onboard Hayabusa-2, and is used to measure altitudes of the spacecraft from a surface of the asteroid, 1999 JU3, for not only secure navigation but also scientific investigation of a C-type asteroid. Hayabusa-2 LIDAR has been improved from that onboard Hayabusa which explored and returned samples from asteroid 25143 Itokawa. A new function called dust count mode is implemented to Hayabusa-2 LIDAR to observe spatial distribution of dust number density in 8 levels with resolution of 20 m in bore sight direction. LIDAR can hardly observe lateral distribution of dusts, but distinguish a weak reflection of thin dust cloud from that of the surface. To plan an operation of the dust count mode observation is difficult because the number density of asteroid dust is not known at all. Instead, we evaluate the lower bound of number density that is geologically important for morphology of asteroid surface. For a given number density of dusts and under an assumption that a characteristic time of levitation is the rotation period of 1999 JU3, the rate of embayment of craters is calculated. If this rate of embayment is greater than that of crater production, we need to take into account a modification process for the study of crater morphology and crater counts of 1999 JU3. This lower bound is calculated to be 10^6 m^{-3} for a cloud of dusts whose radius is larger than a few microns. Then we set this value as a target of the dust count mode observation.

A detectability of dust count mode is dependent on sensitivity of Hayabusa-2 LIDAR and an altitude of the spacecraft. We calculate a reflection from dusts using Mie scattering model assuming that a diameter of dust particle is constant and is larger than the wavelength of laser, that is, 1064 nm. A characteristic distance between dusts is also assumed to be sufficiently larger than the wavelength so that interaction between dust particles is negligible. Using a lidar equation, we calculate a peak power of backscattering light from a dust cloud for various sets of the distance, the number density, and the dust radius. The peak power of reflection is generally stronger than noise level of the detector. The reflection from dust cloud is so weak that the targeted number density of 10^6 m^{-3} is hardly higher than the detection limit. Even at the lowest altitude, the reflection from a dust cloud of 10-microns radius for 10^6-m^{-3} number density is equivalent to the detection limit. If the dust radius is 5 microns, number density more than 10^7 m^{-3} is necessary to be detected. Therefore we plan to start the dust count operation from the HP and attempt to conduct as much operations as possible at low altitude.

Japan Geoscience Union Meeting 2014
(28 April - 02 May 2014 at Pacifico YOKOHAMA, Kanagawa, Japan)

PPS24-P04 Room:Poster Time:May 1 18:15-19:30

Condensation of forsterite under protoplanetary disk conditions

TACHIBANA, Shogo[1*] ; TAKIGAWA, Aki[2] ; MIYAKE, Akira[2] ; NAGAHARA, Hiroko[3] ; OZAWA, Kazuhito[3]

[1]Dept. Natural History Sci., Hokkaido Univ., [2]Dept. Geol. Mineral., Kyoto Univ., [3]Dept. Earth Planet. Sci., Univ. Tokyo

Meteoritic evidence indicates that dust condensation occurred in the early stage of solar system evolution. In this study, we succeeded in performing condensation experiments of forsterite under controlled protoplanetary-disk conditions, which will make significant contribution to understanding silicate formation and chemical fractionation in protoplanetary disks.

Condensation experiments were carried out in the system of Mg_2SiO_4-H_2-H_2O. A mixed gas of H_2 and H_2O was flowed into a continuously evacuated infrared vacuum furnace at a controlled rate to keep a pressure constant. Synthetic forsterite powder in an It crucible was heated as a gas source. A part of evaporated gases were condensed on a Pt mesh located at a cooler region in the chamber. The pressure and temperature conditions were close to those of protoplanetary disks. The total pressure of the system was 5.5 Pa, and the substrate temperature ranged from 1320 to 1160 K. The H_2O/H_2 ratio was set at 0.015, which was about 15 times larger than the solar ratio. The SiO/H_2 ratio was evaluated to be about 0.7-2 % of the solar ratio from the weight loss rate of the gas-source forsterite. Experimental duration ranged from 6 to 237 hours.

Sub-micron to micron-sized condensates covered with Pt substrates at 1160 and 1275 K, but no condensates were found at 1320 K. The typical size of condensates at 1160 K was less than 1 micron irrespective of experimental duration and no effective growth of each condensed grain was observed. Condensates at 1275 K for $>$40 hours partly had several micron-sized flat regions. EDS analyses showed that chemical compositions of condensates were consistent with the stoichiometry of forsterite, and their EBSD patterns were well fitted with the patterns from crystalline forsterite. Coincident EBSD patterns were obtained from the flat region of condensates at 1275 K, suggesting that the area was covered with a single crystal. TEM observation of condensates at 1160 K also found that the condensates were polycrystalline forsterite with a thickness of 30-150 nm, and infrared absorption spectra of condensates show clear 10-micron absorption features resembling those of crystalline forsterite. These evidence indicates that polycrystalline forsterite condensed at 1275 and 1160 K.

The mean free path of gas molecules under the present experimental conditions is less than 1 mm, and the evaporated forsteritic gas and the ambient H_2-H_2O gas are expected to be well mixed. Supersaturation ratios (S) for experiments at 1320, 1275, and 1160 K are thus estimated to be $<$1.2, $<$10, and $<$1000-2000. These supersaturation ratios correspond to the supercooling of $<$5, $<$60 and $<$170 K, respectively.

No condensates were found at 1320 K because the degree of supersaturation was too small for nucleation of forsterite or even the vapor was not saturated with forsterite ($S<1$). The condensates at the supercooling of $<$170 K (1160 K) imply that heterogeneous nucleation of new grains occurred successively on preexisting grains. On the other hand, with the supercooling of $<$60 K (1275 K), some grains seem to have grown up to several microns, and some seem to have newly nucleated on preexisting grains, suggesting that both nucleation and growth of each condensate occurred.

These differences would result in a structural difference in forsterite dust condensed in protoplanetary disks. Fluffy aggregates of sub-micron sized fine particle would form with a supersaturation of $>$1000, while aggregates of micron-sized grains would form with S of 10 that could be an analogue of amoeboid olivine aggregates in chondrites.

Keywords: forsterite, condensation, protoplanetay disk

Japan Geoscience Union Meeting 2014
(28 April - 02 May 2014 at Pacifico YOKOHAMA, Kanagawa, Japan)

PPS24-P05 Room:Poster Time:May 1 18:15-19:30

A New Experiment for Organic Molecule Formation by Catalytic Reactions on the Surface at Low Temperature and Pressure

KIMURA, Yuki[1*] ; TSUCHIYAMA, Akira[2] ; NAGAHARA, Hiroko[3]

[1]Tohoku University, [2]Division of Earth and Planetary Sciences, Graduate School of Sciece, Kyoto University, [3]Department of Earth and Planetary Science, Graduate School of Science, The University of Tokyo

Abundant H_2, CO and N_2 gases react to be more complex molecules mainly on the cooled surface of cosmic dust particles in the molecular cloud and/or primitive solar nebula [1]. The production of organic molecules and subsequent evolution to organic materials in the solar nebula may contribute to the primordial organic system of the Earth. Catalytic chemical reactions are possible production pathway of organic materials in the solar nebula after the formation of simple molecules on nanometer sized cosmic dust particles in the molecular clouds. Experimentally, organic molecules ranging from methane (CH_4), ethane (C_2H_6), benzene (C_6H_6) and toluene (C_7H_8), to more complex species such as acetone (C_3H_6O), methyl amine (CH_3NH_2), acetonitrile (CH_3CN) and N-methyl methylene imine (H_3CNCH_2) have been produced using such as the Fischer-Tropsch type (FTT) and Haber-Bosch type (HBT) reactions on analogs of naturally occurring grain surfaces [2]. Previous studies were performed at higher-temperature ($>$573 K) and pressure ($\sim$1 atm) than the expected conditions in the solar nebula [3-6]. However, since the actual environment is at lower temperature and pressure, it is not clear whether the previous experimental results can be extrapolated to the solar nebula. Our group seeks to elucidate the reaction rates of chemical reactions including isotopic fractionation at lower temperature (100-500 K) and pressure (10^{-3}-10^{0}) and their contribution to the primordial organic system of the Earth.

We are constructing a vacuum chamber based on a new concept to conduct the experiments mentioned above. The chamber with a differential pumping system has a temperature-controlled substrate, a Fourier transform infrared spectrometer (FT-IR), and two quadrupole mass spectrometers (Q-MSs). The substrate has an iron or silicate thin film for FTT and HBT reactions and the FT-IR measures the vibration modes of adsorbed and produced molecules on the surface and the Q-MSs detect volatile and nonvolatile molecules, respectively. As a result, reaction rates of molecules such as H_2, CO, N_2 and NH_3 on iron or silicate substrate will be obtained as a function of temperature and pressure.

[1] J. Llorca and I. Casanova, *Meteorit. Planet. Sci.* **35**, 841 (2000).
[2] H. G. G. M. Hill, and J. A. Nuth, *Astrobiology* **3**, 291 (2003).
[3] J. A. Nuth, N. M. Johnson, and S. Manning, *The Astrophysical Journal* **673**, L225 (2008).
[4] J. A. Nuth, N. M. Johnson, and S. Manning, *Organic matter in space, Proc.* **IAU Symp. 251**, edited by S. Kwok and S. Sandford, Cambridge Univ. Press, NY (2008), pp. 403-408.
[5] J. A. Nuth, Y. Kimura, C. Lucas, F. Ferguson, and N. M. Johnson, The *Astrophysical Journal Letters* **710**, 98 (2010).
[6] Y. Kimura, J. A. Nuth, N. M. Johnson, K. D. Farmer, K. P. Roberts, and S. R. Hussaini, *Nanoscience and Nanotechnology Letters* **3**, 4 (2011).

Keywords: Organic molecules, Catalytic reactions, Protoplanetary system

Japan Geoscience Union Meeting 2014
(28 April - 02 May 2014 at Pacifico YOKOHAMA, Kanagawa, Japan)

PPS24-P06 Room:Poster Time:May 1 18:15-19:30

Dust movement and chemical evolution of proto-solar disk

NAGAHARA, Hiroko[1*] ; NAKATA, Mamoru[1] ; OZAWA, Kazuhito[1]

[1]Hiroko Nagahara

Origin and evolution of the protoplanetary system have been developed mostly from the dynamic point of view, which includes two competing theories, and whichhas been improved by astrophysical observation of exoplanets and extrasolar planetary systems. On the other hand, examination of meteorites and samples by planetary explorations such as lunar samples, cometary particles, and regolith particles of the asteroid Itokawa enable us to gain insight into the evolution of the Solar System. Although those primitive materials give various information, they are not linked to the physical processes in the primary Solar System.

The purpose of this study is to demonstrate how chemical composition distribution evolves over time in the early stage of the proto-solar disk. In order to combine physical processes and chemistry, we have developed a new model consisting of chemical equilibrium calculation and particle tracking equations. At first, we calculate the chemical composition of starting particles at each position in the protoplanetary disk, to track their each motion in the evolving disk, and to analyze the bulk composition of particles that came from various positions in particular time and space. Then, the dynamic evolution of individual particles is calculated in one-dimensional steady-state disk model. In an early stage, particle located in the inner region of the disk have a composition rich in refractory components and those outside have unfractionated CI-like composition. Particles in average move inward by the angular momentum conservation, but a little fraction of them move outward by the turbulent diffusion. Therefore, mixing of refractory particles from inside and CI-like materials from outside takes place, and the mixing ratio vary with time and space.

Because of inward movement of many particles, the relative fraction of particles from outside increases with time for one particular region in the disk, that is, the bulk chemical composition of particles is getting more CI-like. Similarly, the bulk chemical composition of particles at particular place is getting more CI-like with time. Calculations with model parameters of higher temperature of the disk suggest that longer time is needed to replace refractory-rich compositions by a CI-like composition. It is because the radial distance between fractionated particles with refractory-rich composition and unfractionated CI-like materials is longer in a high temperature disk.

Comparing these results and the composition of CM, CO, CV chondrites, it is concluded that CV composition can be reproduced at the most inner region, CO in the next, and CM most outer region in the disk. The present work shows that the composition of carbonaceous chondrites were formed at the asteroid belt region at the early stage of disk evolution with the wide spread of high temperature region.

Keywords: protoplanetary disk, chemical evolution, dust movement, chemical equilibrium

Japan Geoscience Union Meeting 2014
(28 April - 02 May 2014 at Pacifico YOKOHAMA, Kanagawa, Japan)

PPS25-01 Room:213 Time:May 2 09:00-09:15

Age-cytometry : new approach for meteorite anatomy

HIRATA, Takafumi[1*] ; ITOH, Shoichi[1]

[1]School of Science, Kyoto University

The chronology for meteorite samples has played an important role to decode the early sequence of the solar system. Among the chronometers based on the radio-active decay of long-lived nuclides, because of the high time resolution of the resulting age data, the U-Pb chronometry has been widely used to define the timing of formation of refractory inclusions or to understand the formation sequence of the chondrite parental body. The high time resolution on the U-Pb chronometers was achieved by the small contribution of the analytical uncertainties in the isotope ratio measurements onto the resulting age data, and also because of the well-defined decay constants for ^{238}U, ^{235}U and ^{232}Th nuclides. Moreover, the U-Pb isotope systematics has further advantages of evaluating of system closure since the sample formation or crystallization of minerals, and therefore, reliability of the resulting age data can be rigorously tested. Using the U-Pb chronometer, the resulting time-resolution can become as small as 0.2 ? 1 Ma range for chondritic materials, but this could not be high enough to understand the planetary formation during the runaway growth or to understand the timing of the core formation. To overcome this, we are trying to measure in-situ 238U/235U ratio from individual minerals by means of combination of two ion collectors. Details of the instrumentation and operational conditions would be demonstrated in this talk.

Cytometry is the quantitative analysis of cells and cell systems. Cytometry measures optical properties of cells, and most often uses fluorescence to measure specific antigen molecules, intracellular ions and DNA/RNA using antibodies, indicator dyes, or nucleic acid-specific probes. Cells may be live or fixed, depending on the application, and individual cells can often be physically sorted. ? Advantage of the cytometry are the analysis speed, detection sensitivity, the ability to measure many parameters simultaneously, and the ability to sort individual cells, and therefore, mechanism or process of elemental metabolism could be precisely evaluated based on the extensive number of cells (e.g., Benfall et al., Science, 2011; Bodenmiller et al., Nature Biotechnology, 2012). This approach can also be applied to understand the solar system evolution based on the numerous number of age data. In recent ten years, we have demonstrated the unique study approach using the distribution pattern of sample ages based on the series of precise age data collected from large number of samples (i.e., age-cytometry) [e.g., Rino et al., PEPI, 2008; Iizuka et al., Geology, 2008; Iizuka et al., Iizuka et al., Chem. Geol., 2009; Iizuka et al., GCA, 2010]. With the high-time resolution age data obtained by present analytical technique using the LA-ICPMS, further precise and quantitative discussion could be made on the solar system evolution through the age-cytometry. The newly developed high-resolution and high-throughput age determination system using a laser ablation-ICP mass spectrometry has a potential to become a significant tool to promote an age-cytometry.

Keywords: meteorite anatomy, cytometry, solar system evolution, multiple collector mass spectrometry, laser ablation-ICPMS, ICP-mass spectrometry

Japan Geoscience Union Meeting 2014
(28 April - 02 May 2014 at Pacifico YOKOHAMA, Kanagawa, Japan)

PPS25-02 Room:213 Time:May 2 09:15-09:30

147Sm-143Nd and 146Sm-142Nd chronology of a basaltic eucrite, Juvinas

KAGAMI, Saya[1*] ; YOKOYAMA, Tetsuya[1]

[1]Dept. Earth and Planetary Sciences, Tokyo Tech

Eucrites are interpreted to have originated from the asteroid 4-Vesta which differentiated into crust and mantle. The chronology of eucrites is important to understand the formation and differentiation of planets/ planetesimals in the early Solar System. The combination of two chronometers, short-lived ^{146}Sm-^{142}Nd system ($T_{1/2}$=6.8×10^{7}yr) and long-lived ^{147}Sm-^{143}Nd ($T_{1/2}$=1.06×10^{11}yr), is useful to decode the thermal history of the eucrite parent body, because they have the same closure temperature [1]. To obtain precise Sm-Nd ages for eucrites and other achondrites, it is indispensable to develop highly precise Nd isotope analysis.

We investigated the ^{147}Sm-^{143}Nd and ^{146}Sm-^{142}Nd chronometers for a brecciated basaltic eucrite, Juvinas. We examined samples of whole rock powder (W.R.), 400 mesh grains, plagioclase (Pl), and pyroxene (Px). Plagioclase and pyroxene grains were obtained by handpicking. Samples were dissolved using a mixture of concentrated pure acid ($HClO_4$, HF, and HNO_3) and heating at 195 ℃. About ten percent of the solution was removed and spiked with ^{149}Sm-^{145}Nd in order to precisely measure Sm and Nd concentrations by ID-ICP-MS (Thermo X-series II at Tokyo Tech). We separated Nd from the rest of the solution via a four-step column chemistry. Nd isotope ratios in W.R., 400mesh, Pl, and Px were analyzed by TIMS (Thermo TRITON-plus at Tokyo Tech) with the dynamic multicollection method.

The ^{147}Sm-^{143}Nd mineral isochron diagram of Juvinas, yielded an age of 4610±410 Ma. In contrast, the ^{146}Sm-^{142}Nd systematic for Juvinas yielded an initial ^{146}Sm/^{144}Sm ratio of 0.0157±0.0074. This gives ?4618?_(-63)^(+38) Ma for the age of Juvinas when an initial solar system ratio of ^{146}Sm/^{144}Sm=0.0094 at 4568 Ma is assumed [1]. The self-consistency of the ^{147}Sm-^{144}Nd and ^{146}Sm-^{142}Nd ages for Juvinas supports early crust-mantle differentiation on the eucrite parent body as was proposed by previous chronological studies on basaltic eucrites (e.g., Pb-Pb, Al-Mg, Mn-Cr, and Hf-W; [2-5]).

It has been suggested that cumulate eucrites provide internal isochron ages younger than basaltic eucrites due to a longer history in the deep crust or late thermal disturbance during later meteorite bombardment event(s) [6]. Because of the limited Sm/Nd variation in the meteorite components analyzed, the Sm-Nd ages obtained in this study have uncertainties several times larger than those in previous studies [6]. The ^{147}Sm-^{143}Nd age and the initial ^{143}Nd/^{144}Nd ratio for Juvinas are consistent with those obtained by the mineral isochrons of three cumulate eucrites within analytical error (4546±8 Ma; [6]). However, our ^{146}Sm-^{142}Nd age is older than the proposed ^{147}Sm-^{143}Nd age for cumulate eucrites, indicating that the crystallization of basaltic eucrites predates the timing when the Sm-Nd systematics for cumulate eucrites reached a closure temperature. It should be noted that Juvinas is a brecciated basaltic eucrite which may not record a correct Sm-Nd age. Further investigation is required to obtain more precise Sm-Nd ages utilizing unbrecciated basaltic eucrite to reveal the thermal history on the eucrite parent body.

References: [1] N. Kinoshita et al., (2012) Science, 335, 1614 [2] S.J.G. Galer and G.W. Lugmair, (1996) MAPS, 31, A47. [3] M. Wadhwa et al., (2003) LPSC XXXIV, 2055. [4] G.W. Lugmair and A. Shukolyukov, (1998) GCA 62, 2863. [5] T. Kleine et al., (2004) GCA 68, 2935.
[6] M. Boyet et al., (2010) EPSL 291, 172.

Japan Geoscience Union Meeting 2014
(28 April - 02 May 2014 at Pacifico YOKOHAMA, Kanagawa, Japan)

PPS25-03 Room:213 Time:May 2 09:30-09:45

Al-Mg mineral isochron of a Type C CAI from Allende

KAWASAKI, Noriyuki[1*] ; KATO, Chizu[2] ; ITOH, Shoichi[3] ; ITO, Motoo[4] ; WAKAKI, Shigeyuki[4] ; YURIMOTO, Hisayoshi[1]

[1]Hokkaido University, [2]Washington University in St. Louis, [3]Kyoto University, [4]JAMSTEC

Ca-Al-rich inclusions (CAIs) show the record of ^{26}Al, which is a short-lived radionuclide with a half-life of 0.73 Myr (e.g., MacPherson et al., 1995), thus a relative chronometer with Al-Mg systematics is applicable for determining a precise time interval of individual CAI formation process. In this work, we report full petrologic and mineralogical studies of a Type C CAI from Allende, EK1-04-2, with more detailed analyses of O isotopic distributions and Al-Mg systematics than presented by Ito et al. (2000).

FE-SEM equipped with EDS and EBSD system (JEOL JSM-7000F; Oxford X-Max 150; Oxford HKL) was used for petrologic and mineralogical studies. O and Al-Mg isotopic compositions were measured by SIMS (Cameca ims-1270).

The EK1-04-2 is a CAI fragment with a size of ~2 mm across. The CAI mainly consists of spinel, anorthite, olivine and diopside. The CAI has mantle and core structure. In the core part, euhedral spinel crystals are enclosed by other mineral grains. Anorthite and olivine grains show euhedral or subhedral shape. Diopside grains show anhedral shape and include spinel and olivine grains. Thus, crystallization sequences of core minerals are spinel, anorthite, olivine and diopside. The mantle part has a same mineral assemblage as the core part, however, amount of spinel is lower than the core part, and anhedral spinel and anorthite grains are present, and the diopside is more Mg-rich and Ti-poor comparing with core diopside.

O isotopic compositions of the minerals are distributed along CCAM line (delta-^{18}O = -44 to +9 permil). Spinel is ^{16}O-rich (delta-^{18}O ~-43 permil), while anorthite is ^{16}O-poor (delta-^{18}O ~9 permil). Any differences of O isotopic compositions are not observed for these minerals among core and mantle parts while olivine and diopside show different O isotopic compositions between core and mantle parts. Olivine and diopside in the core have an intermediate O isotopic composition between spinel and anorthite (delta-^{18}O ~-15 permil). In contrast, the oxygen isotopic compositions of olivine and diopside in the mantle are not homogeneous and distributed to ^{16}O-poor direction compared with those in the core (delta-^{18}O = -13 to -4 permil). Olivine and diopside grains in the mantle are not in chemically equilibrium with those in the core. The O isotopic distributions among mineral grains indicate that the CAI experienced multiple and individual crystallization events: a crystallization of spinel, a crystallization of core olivine and diopside, and a crystallization of mantle olivine and diopside.

On the Al-Mg isochron diagram, spinel grains are plotted on a line of $^{26}Al/^{27}Al_0 = (3.52\pm0.15) \times 10^{-5}$, while olivine, diopside and anorthite grains of core are plotted on a line of $^{26}Al/^{27}Al_0 = (5\pm5) \times 10^{-7}$. The difference of the initial values corresponds to a relative age of ~4.6 Myr. In contrast, olivine and diopside grains in mantle are plotted below the line of olivine and diopside in core. The ^{16}O-poor and low delta-$^{26}Mg_0$ compositions of mantle olivine and diopside suggest mixing of Al-rich chondrule-like materials. The composition of the mantle diopside is consistent with this scenario.

The petrographic, oxygen isotopic and chronological studies indicate that the CAI experienced multiple heating events after a precursor CAI formation. After ~4.6 Myr later than the precursor CAI formation, the CAI partially melted at ~1600K. The melt exchanged oxygen isotopes with the surrounding ^{16}O-poor solar nebular gas. ^{16}O-poor olivine, diopside and anorthite grains recrystallized from the partial melt. Subsequently, Al-rich chondrule-like materials accreted on the CAI and experienced partial melting and recrystallization, again. Distinctive ^{16}O-poor composition of anorthite is a result of a thermal metamorphism at the Allende parent body.

Our study revealed that the CAI has retained in the protosolar nebula at least for 4.6 Myr and experienced multiple melting events.

Keywords: Al-Mg, CAI, SIMS, oxygen isotopes, solar nebula

Japan Geoscience Union Meeting 2014
(28 April - 02 May 2014 at Pacifico YOKOHAMA, Kanagawa, Japan)

PPS25-04 Room:213 Time:May 2 09:45-10:00

Water contents and hydrogen isotopic compositions of phosphate minerals from LL4-6 ordinary chondrites.

YANAI, Kaori[1] ; ITOH, Shoichi[2*] ; GREENWOOD, James[3] ; RUSSELL, Sara[4] ; YURIMOTO, Hisayoshi[1]

[1]Department of Natural History Sciences, Hokkaido University, [2]Department of Earth and Planetary Sciences, Kyoto University, [3]Department of Earth and environment Sciences, Wesleyan University, [4]Department of Earth Sciences, Natural History Museum, London

The origin of water on the earth is discussed by many researcher. The hydrogen isotopic compositions of earth ' s water were also studied to discuss the origin of water for Earth, Lunar and comet through the planetary scale in the solar system [Greenwood et al., 2011]. One of siginificant possible precursor of H20 in Earth ' s orbitary could be cometary ice but it is unclear. In preliminary results, we reported the hydrogen isotopic compositions of phosphate minerals (Merrilite and apatite) from Ensisheim LL6 ordinary chondrite (OC) on 2012 at JPGU and NIPR meeting in Japan. These D/H ratio are extremely duetrium-rich value (δD ˜15000permil). In addition, Deloule and Robert (1995) also reports that the hydrogen isotopic compositions of phyllosilicate from LL3.0 Semarkona OC is D-rich (˜4000permil) and suggest the origin of this D-rich isotopic compositions come from the interstellar space or in the outer regions of the solar nebula, like cometary ice. These results suggest that, as the Itokawa S-type asteroids with Earth ' s orbitary, the heavily hydrogen isotopic compositions of LL OCs resulted from cometary ice close to the earth. However, there is no sytematic study of hydrogen isotopic compositions of LL4-6 OCs because it is difficult to estimate the planetsimal hydrogen isotopic compositions of water due to very low water contents and contamination from adsorbed water. In this study, we applied the in-situ measurement technique of water content and hydrogen isotopic compositions of phosphate minerals from LL4-6 OCs by SIMS. All D/H ratio in the phosphate minerals are D-rich (δD ˜+2000 to +25000). The D/H ratio in the phosphate minerals from LL4 Soko-Banja and LL5 Tuxtuac could be resulting from degassing of H2 during Fe-water oxidation reaction but it is difficult to apply it for those of LL6 Ensisheim and Bandong LL6. These results suggest that the origin of D-rich hydrogen isotopic compositions of LL6 phosphate mineral is resulting from extra-planetary with cometary ice beause of extremely heavily hydrogen isotopic compositions.

Keywords: Hydrogen isotope, SIMS, phosphate, apatite

Japan Geoscience Union Meeting 2014
(28 April - 02 May 2014 at Pacifico YOKOHAMA, Kanagawa, Japan)

PPS25-05 Room:213 Time:May 2 10:00-10:15

Oxygen diffusion in perovskite with different Ca/Ti ratio

HASHIGUCHI, Minako[1*] ; SAKAGUCHI, Isao[1] ; HIROSE, Sakyo[2] ; OHASHI, Naoki[1]

[1]National Institute for Materials Science (NIMS), [2]Murata Manufacturing Co., Ltd.

<**Introduction**> Calcium-aluminum-rich inclusions (CAIs) in chondrites are believed to be the first solid formed in solar nebula and are composed of refractory minerals, such as spinel, mellilite, anorthite, and perovskite ($CaTiO_3$). Previous studies have been reported heterogeneous oxygen (O)-isotopic compositions among the CAI minerals [Clayton et al. (1973)]. The isotopic compositions are considered to be a marker of O-isotopic composition in the solar nebula [Yurimoto et al. (1998); Itoh and Yurimoto (2003); Park et al. (2012)]. Diffusion processes are important processes to affect the O-isotopic compositions of CAI minerals. To understand the effect, oxygen diffusivity of minerals should be investigated.

Perovskite crystals showed several order of larger oxygen diffusion coefficients than other CAI minerals [Gautason and Muehlenbachs (1993); Ryerson and McKeegan (1994); Sakaguchi and Haneda (1996)]. Thus, its O-isotopic compositions can provide us an important key to understand whether O-isotopic compositions of the CAI minerals have been modified or not. However, there still were a few reports on the oxygen diffusivity of perovskite, and the previously reported values are different by about one order of magnitude [Gautason and Muehlenbachs (1993); Sakaguchi and Haneda (1996)]. In this study, we focus on Ca/Ti ratio of perovskite and determined oxygen diffusion coefficients in perovskite with different Ca/Ti ratio experimentally.

<**Experimental**> Polycrystalline perovskite samples were prepared by a conventional sintering technique. High-purity reagent-grade powders of $CaCO_3$ and TiO_2 were used as the starting materials. These powders were mixed as Ca/Ti=0.098-1.002 by ball milling with PSZ balls. The powders were pressed as a sheet and were sintered at 1350 degC for 2 h in the atmosphere.. Then, perovskite samples with different Ca/Ti ratio were obtained. Because of a contamination of ZrO_2 from PSZ balls, Ca/Ti ratio of the samples may differ by 0.001-0.0015 from initial value.

The samples were polished and finished by a mechanical polishing using the several grade of diamond pastes. To remove damages by the polishing, the samples were annealed at 1200 degC for 1h in the atmosphere. The samples were annealed under $^{18}O_2$ gas at 750-1050 degC for several hours. Oxygen diffusion coefficients in the samples were determined using depth profiles of ^{18}O concentration of the samples obtained by secondary ion mass spectrometry (Cameca ims-4f).

<**Results and discussion**> Two contributions to the oxygen bulk diffusion mechanism are observed in depth profiles of ^{18}O concentration obtained from Ti-rich perovskite samples. One starts near surface (diffusion A) and the other starts from about a few 100 nm depth (diffusion B) of the sample. In Ca-rich perovskite samples, only a diffusion mechanism is observed.

We found that the oxygen bulk diffusion coefficients (D_b) in Ca-rich perovskite samples were larger than that of Ti-rich samples, in both diffusion A and B. The D_b value of 950 degC in a perovskite sample prepared by a powder with Ca/Ti=0.098 was $7x10^{-13}$ cm^2/s (diffusion A), $1x10^{-11}$ cm^2/s (diffusion B), whereas the value of a sample prepared by a powder with Ca/Ti=1.002 was $7x10^{-10}$ cm^2/s.

Previous reports showed ^{16}O-poor [Ito et al. (2004)] or ^{16}O-rich [Park et al. (2012)] perovskite in carbonaceous chondrites. It has been suggested that the former was changed from its original isotopic composition during thermal processes, the later was escaped the secondary processes. Larger oxygen diffusion coefficients of perovskite than that of other CAI minerals suggested that perovskite record the final thermal process, which the CAI experienced. Moreover, this study may suggest shorter timescale required for change of O-isotopic composition of perovskite than previously estimated and also indicates the importance of investigation on Ca/Ti ratio of perovskite to understand its oxygen diffusivity.

Keywords: Perovskite, Oxygen diffusion

Japan Geoscience Union Meeting 2014
(28 April - 02 May 2014 at Pacifico YOKOHAMA, Kanagawa, Japan)

PPS25-06 Room:213 Time:May 2 10:15-10:30

Newly identified hibonite-bearing FUN inclusions with low Al/Mg ratios

FUKUDA, Kohei[1*] ; HIYAGON, Hajime[1] ; SASAKI, Shogo[1] ; MIKOUCHI, Takashi[1] ; FUJIYA, Wataru[2] ; TAKAHATA, Naoto[3] ; SANO, Yuji[3] ; MORISHITA, Yuichi[4]

[1]Graduate School of Science, The Univ. of Tokyo, [2]Max Planck Institute for Chemistry, [3]AORI, The Univ. of Tokyo, [4]Graduate School of Science, Shizuoka Univ.

It has been recognized that a minor group of CAIs named FUN (*F*ractionation and *U*nknown *N*uclear effects) and some types of hibonite ($CaAl_{12}O_{19}$) inclusions show isotopic anomalies in ^{48}Ca, ^{50}Ti, and no or small excesses in ^{26}Mg from the decay of ^{26}Al. The existence of isotopic anomalies in Ca and Ti suggests that these inclusions formed at the earliest stage of the solar system evolution, when isotopic heterogeneity still existed. The lack of ^{26}Al may also be interpreted as their formation before the homogenization of ^{26}Al distribution in the early solar system. Hence, FUN inclusions and hibonite-bearing inclusions may have significant importance in studying the earliest stage of the solar system evolution.

In order to better understand the isotopic homogenization process(es) in the early solar system, I have conducted multiple isotopic analyses of three hibonite-bearing inclusions from the Murchison (CM2) meteorite using two ion microprobes (Cameca ims-1270 & NanoSIMS 50). I identified three new hibonite-bearing FUN inclusions (MC037, MC040, and MC003), which exhibit extremely large mass-dependent fractionation in Mg (up to ∼55 ‰/amu) but almost no excess in ^{26}Mg, and have resolvable isotopic anomalies in ^{48}Ca and ^{50}Ti. The results suggest that these inclusions formed during the isotopic homogenization process(es). The results of Mg isotopic compositions (extremely large isotopic fractionation) and elemental abundances (rather low Al/Mg ratios of 20-150) indicate that the precursors of these inclusions might have more Mg-rich (less refractory) compositions than the previously reported hibonite-bearing F(UN) inclusions (Al/Mg ratios from ∼500 up to ∼60000). In addition, their oxygen isotopic compositions are plotted on a mass-dependent fractionation line with Δ^{17}O values of ∼-23 ‰, similar to the value for the majority of typical CAIs. This suggests that oxygen isotopic compositions of their precursors are also ^{16}O-rich ($\delta^{17,18}$O ∼-50 ‰), identical to those of typical CAIs. Furthermore, the textual signatures suggests that a molten precursor of MC040 may have been quenched. Although the origin of FUN inclusions is still not known, the present results and previous works show that there are further variations in their precursor compositions, isotopic anomalies, and thermal processes.

Keywords: FUN inclusion, hibonite, ion microprobe, Mg isotopes, Ca and Ti isotopes, oxygen isotopes

Japan Geoscience Union Meeting 2014
(28 April - 02 May 2014 at Pacifico YOKOHAMA, Kanagawa, Japan)

PPS25-07 Room:213 Time:May 2 10:30-10:45

O-16-rich olivine in igneous rim from NWA 3118 (CV)

MATSUDA, Nozomi[1*] ; SAKAMOTO, Naoya[2] ; YURIMOTO, Hisayoshi[3]

[1]Natural History Sciences, Hokkaido University, [2]CRIS, Hokkaido University, [3]Natural History Sciences, Hokkaido University

Ca-Al-rich inclusions (CAIs) and chondrules in chondrites show mass independent oxygen isotopic fractionation. Normally, CAIs are enriched in O-16 whereas chondrules are depleted in O-16. However, olivine grains having O-16-rich composition were reported in chondrule rims from CR2 chondrites (Takeda et al., 2002; Nagashima et al., 2013). Existence of O-16-rich grains in the rims indicates that the chondrule rims preserve information about chondrule precursor components with oxygen isotope in the chondrule formation region. In addition, abundance and distribution of O-16-rich olivine in chondrule rims have not been studied for other chondrite groups. Therefore, we study petrology and oxygen isotopic mapping of an igneous chondrule rim from a CV3 chondrite in order to reveal the distribution of O-16-rich materials.

The sample used in this study is a polished thin section from NWA 3118 CV3 chondrite. The petrographic observation and chemical analysis were performed by FE-SEM-EDS (JEOL JSM-7000F + Oxford X-Max 150). Crystal orientation analysis was studied by EBSD (Oxford HKL). Isotope mapping technique for oxygen was applied by an isotope microscope (Cameca ims-1270 + SCAPS).

The chondrule studied here has 1.4 millimeters in diameter and Mg-rich (type I) porphyritic texture mainly composed of forsterite, low-Ca pyroxene and feldspathic mesostasis. The chondrule is surrounded by rim that shows an evidence of igneous process with the thickness of up to 400 micrometers. The rim is mostly composed of ferromagnesian olivine and also contains low-Ca pyroxene, high-Ca pyroxene, Fe-Ni metal and sulfide. The Fe-rich olivine grains often show Fe-Mg zoning, suggesting that diffusional Fe-Mg exchange has occurred during metamorphism on the parent body.

In this study, seven O-16-rich olivine grains with 10-30 micrometers in diameter were found in the igneous rim. O-16-enrichments are observed in core of the olivine crystals. The oxygen isotope heterogeneity and the chemical composition are not correlated. This result suggests that these O-16-rich parts are relict and overgrown by O-16-poor olivine crystallized from melt during rim formation.

The existence of O-16-rich olivine in the rim from CV chondrite indicates that both O-16-rich and O-16-poor materials exist in the chondrule formation region.

Keywords: chondrule rim, chondrule, oxygen isotopes, carbonaceous chondrite, SIMS

Japan Geoscience Union Meeting 2014
(28 April - 02 May 2014 at Pacifico YOKOHAMA, Kanagawa, Japan)

PPS25-08 Room:213 Time:May 2 11:00-11:15

Internal structure of chondrules and their possible origin

TAKAHASHI, Eiichi[1*] ; NAKAMOTO, Taishi[1]

[1]Earth & Planetary Sciences, Tokyo Institute of Technology

In order to clarify 3D shapes and internal structure of chondrules in Allende chondrite, we have separated 180 chondrules grains and investigated them with X-ray CT apparatus (Scan Xmate-D180RSS270) recently installed at the Museum of Natural History, Tohoku University (Tsuda et al., JPGU 2013). We also developed an optical device to measure 3D shape of chondrules or other spherical objects (Nishida et al. JPGU 2013). Our results revealed that chondrules shapes show wide distribution consisting of true spheres, prolate-spheres and oblate-spheres. Chondrules with porphyritic textures distribute in all shape categories. Chondrules with barred olivine texture (quenched from super-heated melt) show a distribution between true sphere and oblate-shape. Implication of the 3D shapes and internal texture of chondrules are consistent with the shock-wave heating model (e.g., Miura & Nakamoto, 2002, 2008).

Due to the density contrast, textures of Fe-FeS phase are most easily observed by X-ray tomography. By melting, coagulation and growth of Fe-FeS phase occur in chondrules. In some chondrules, coagulation resulted in mini-core formation (driven by surface energy minimization, see Fig.1). It is suggested that duration of heating episodes could be estimated by coagulation textures of Fe-FeS. If chondrules were formed by shock heating mechanism (e.g., Miura & Nakamoto, 2002, 2008), separation of molten silicate and coagulated Fe-FeS droplets would have taken place during acceleration and slow down of chondrules. Accordingly, significant chemical fractionation took place by dynamic processes during chondrules formation.

In X-ray CT images, many chondrules are surrounded by 50-200 micron thick rims. Coagulation and growth of Fe-FeS grains are observed in chondrules-rims as well as inside of chondrules indicating that temperature may have exceeded ˜1000C (eutectic point in the Fe-FeS) in the chondrule-rims. The common appearance of growth texture of Fe-FeS grains supports high-temperature origin of chondrule-rims rather than metasomatic origin. Clear textural distinction between chondrules and their ambient rims may correspond with presence or absence of melting in silicates. Most abundant element that volatilized below 1000C is sulfur. It is suggested that sulfur would have acted as a glue to coagulate dust particles onto molten droplets (chondrules) during shock heating episodes.

Keywords: meteorite, chondrule, texture, origin, X-ray CT

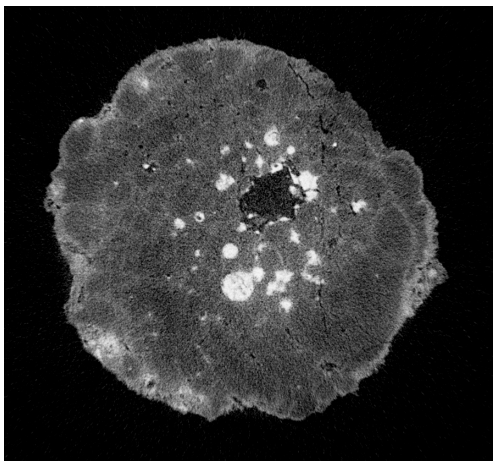

Japan Geoscience Union Meeting 2014
(28 April - 02 May 2014 at Pacifico YOKOHAMA, Kanagawa, Japan)

PPS25-09 Room:213 Time:May 2 11:15-11:30

Artificial cosmic spherules produced by heating and quenching experiments

GONDO, Takaaki[1*] ; ISOBE, Hiroshi[1]

[1]Grad. Sch. Sci. Tech., Kumamoto Univ.

Micrometeorites (MMs) are extraterrestrial fine particles derived from asteroids and comets and continuously falling to the Earth. Depending on their velocity, mass and entry angle, micrometeorites have undergone various degrees of heating during the atmospheric entry within a few seconds. This heating lead to significant textural, mineralogical and chemical modifications to MMs. The MMs larger them 70 micron meters in diameter show variously melted textures. In particular, completely melted micrometeorites are known as cosmic spherules. Cosmic spherules have experienced large degrees of melting of primary phases during atmospheric entry, and form molten droplets. In this study, we carried out rapid heating and quenching experiments on fine particles of three kinds of meteorites (CV, CM and H chondrite) to reproduce cosmic spherules by atmospheric entry.

The run products of meteorites as starting materials show quite analogous textures to cosmic spherules including porphyritic olivine and barred olivine. The most of molten particles show spherical shape due to surface tension of the silicate melt. The outside shape of the particles is various depending on melt fraction of the particle. We successfully reproduced artificial cosmic spherules with remarkably analogous textures to natural ones. We can compare textural variations of cosmic spherules to run products and possible precursors of cosmic spherules. Analogy of the run products to cosmic spherules can be applied from textural, mineralogical and chemical modifications during atmospheric entry to estimate abundance of the interplanetary fine particles in the vicinity of the Earth’s orbit.

Keywords: micrometeorite, carbonaceous chondrite, H chondrite, atmospheric heating, cosmic spherule

Japan Geoscience Union Meeting 2014
(28 April - 02 May 2014 at Pacifico YOKOHAMA, Kanagawa, Japan)

PPS25-10 Room:213 Time:May 2 11:30-11:45

Experimental reproduction of microtexutures of chondrules and CAIs by reducing-gas levitation technique

SETO, Yusuke[1*] ; ICHIMURA, Shun[1] ; MATSUNO, Junya[2] ; TAKAHASHI, Ryohei[2] ; TSUCHIYAMA, Akira[2] ; KOHARA, Shinji[3]

[1]Kobe Univ. Sci., [2]Kyoto Univ. Sci., [3]JASRI

Chondrules are the most abundant component in chondrites. They are mm-sized round (or irregularly) shaped particles mainly composed of silicates, which formed by the rapid cooling of droplets of molten or partially molten rock in space before they accreted. They show unique and diverse internal micro-textures (e.g., porphyritic olivine, barred olivine, radial pyroxene, etc.), even if they have same bulk compositions. These internal textures, therefore, should reflect not only stating material compositions, but also nebular conditions, such as gas species and their partial pressures, heating and cooling rate. CAIs are another major component in chondrites, which are also known to show the evidence of molten and quenching textures. The conditions of chondrule formation, however, remain poorly constrained, because the reproduction of the chondrule formation processes in a laboratory is experimentally difficult, especially in terms of container-less arrangement and reducing (low-fO_2) ambient. In the present study, we conducted gas-levitation and laser heating experiments in order to reproduce micro-textures of chondrules and CAIs, and constrain their formation conditions.

As stating materials, we used (i) natural olivine (Fo_{90}) from San Carlos, USA, (ii) matrices of Murchison CM meteorite, and (iii) mixed compounds of melilite ($Ca_2Al_2SiO_7$) + spinel ($MgAl_2O_4$) which are analogue to CAIs. The molten-quenched droplets of these samples were obtained using the gas-levitation and laser-heating experiments, which avoided both contamination of the molten samples and heterogeneous nucleation by crucible surfaces, at SPring-8 BL04B2. 1-2 mm-sized droplets were heated by a continuous-wave CO_2 laser, and were levitated in 96% Ar + 4% H_2 gas to achieve reducing ambient. The temperature during heating was monitored by a pyrometer. Surfaces and internal textures of the recovered samples were analyzed using SEM-EDX and -EBSD (JEOL, JSM-6480LAII and JSM-7100F).

(i) As a result of experiments using San Carlos olivine, olivine was re-crystallized under any condition. They show micro-porphyritic texture consisting of fine grained (1 to 5 μm) olivine, which are equal in composition to the starting material. Magnetite (Fe_3O_4) or hematite (Fe_2O_3) was completely absence, which suggests the low fO_2 (at least MFQ buffer) was maintained during the present experiments. (iii) The recovered sample of Murchison CM chondrite shows barred-olivine like texture. The platy (10 μm thickness) olivine crystals (Fa_{20-40}) are embedded in a FeO-SiO_2-rich glass. Idiomorphic fine (1 μm) magnetite are also observed in the glass. EBSD analyses revealed that most of the olivine plates are normal to b-axis, and the crystallographic orientations in a parallel platelet domain are identical. (iii) As a result of experiments using melilite and spinel compounds, dendritic spinel was always crystallized from surfaces to core irrespective of sample size and cooling rates, and they are embedded in Al-rich glass phase. The demonstrations of the present study show that reducing-gas levitation experiments is a powerful technique to simulate the molten-quenched texture of early solar materials.

Keywords: Chondrule formation, Molten-quenched texture, Crystal growth, Containerless heating, Barred olivine

Japan Geoscience Union Meeting 2014
(28 April - 02 May 2014 at Pacifico YOKOHAMA, Kanagawa, Japan)

PPS25-11 Room:213 Time:May 2 11:45-12:00

A unique lithology in the NWA 1232 CO3 chondrite containing clasts of different metamorphic grades

MATSUMOTO, Megumi[1*] ; TOMEOKA, Kazushige[2] ; SETO, Yusuke[2] ; YAMAMOTO, Yukiko[2] ; UMEHARA, Mariko[2] ; MIYAKE, Akira[3] ; HAMANE, Daisuke[4]

[1]CSREA, Kobe Univ., [2]Graduate School of Science, Kobe Univ., [3]Graduate School of Science, Kyoto Univ., [4]ISSP, Tokyo Univ.

Northwest Africa 1232 (NWA 1232) is a CO3 carbonaceous chondrite consisting of three lithologies (A, B, and C) that went through different thermal histories [1,2]. Kiriishi et al. [3] found that lithology A contains many small clasts (100-400 micron in diameter) scattering throughout the lithology. These small clasts typically consist of one chondrule surrounded by matrix and show little evidence of thermal metamorphism. Such unique lithology has not been known in other CO3 chondrites and potentially provides new insights into the formation of CO3 chondrites. Here we report the results of detailed mineralogical and petrological study of NWA 1232. The study was performed using SEM-EDS, TEM (STEM)-EDS, EPMA, and SR-XRD.

The thin section of NWA 1232 studied consists of lithologies A (738 mm^2), B (624 mm^2), and C (196 mm^2) that are separated by sharp boundaries. In lithology C, olivine phenocrysts in type I chondrules have relatively homogeneous compositions (Fa_{3-13}) and exhibit weak Fe-Mg zoning; these correspond to metamorphic grade 3.4. The matrix consists mainly of fine grained (100-500 nm in diameter) olivine that is relatively homogeneous in composition ($\sim Fa_{60}$). In lithology B, olivine phenocrysts are more Fe-rich (Fa_{19-42}) and exhibit distinct Fe-Mg zoning; these correspond to metamorphic grade 3.7. The matrix is mainly composed of relatively coarse-grained ($>$500 nm in diameter) olivine that is very homogeneous ($\sim Fa_{40}$).

In contrast, chondrules and matrix in lithology A exhibit considerable chemical and textural diversities. Olivine phenocrysts in chondrules vary widely in composition from Fa_1 to Fa_{43}. Most of Mg-rich olivine phenocrysts in Mg-rich chondrules show almost no Fe-Mg zoning; these are similar to those in CO 3.0 chondrites. Their surrounding matrix consists mainly of very fine-grained Mg-Si-Fe-rich amorphous material. On the other hand, most of Fe-rich phenocrysts in Fe-rich chondrules show distinct Fe-Mg zoning and their surrounding matrix consists mainly of coarse-grained ($>$500 nm in diameter) Fe-rich ($\sim Fa_{40}$) olivine; these are similar to those in highly metamorphosed CO 3.7 chondrite. There are also many other chondrules whose olivine phenocrysts have compositions intermediate between the Mg-rich and Fe-rich olivines described above. The matrix surrounding these chondrules mainly consist of fine-grained (100-500 nm in diameter) Fe-rich olivine similar to those mildly metamorphosed CO chondrites.

The chemical and textural heterogeneities observed in lithology A cannot be explained by thermal metamorphism of a single lithology. The results suggest that lithology A is composed of many clasts that underwent various degrees of thermal metamorphism in different locations of the parent body. The results further imply that CO chondrites had once experienced various degrees of thermal metamorphism in different locations in the parent body and subsequently went through extensive brecciation and mixing.

References: [1] Kiriishi and Tomeoka (2008), JMPS, 103, 161?165. [2] Umehara et al. (2009), JAMS Annual Meeting (abstract). [3] Kiriishi et al. (2009), JAMS Annual Meeting (abstract).

Keywords: CO chondrite, thermal metamorphism, brecciation, clast, TEM, SR-XRD

Japan Geoscience Union Meeting 2014
(28 April - 02 May 2014 at Pacifico YOKOHAMA, Kanagawa, Japan)

PPS25-12 Room:213 Time:May 2 12:00-12:15

Hydrothermal alteration experiments of the Allende meteorite

IIKUNI, Tsuneyuki[1*] ; TOMEOKA, Kazushige[1] ; SETO, Yusuke[1]

[1]Graduate school of Science, Kobe University

Among the processes that have affected early cosmic materials including carbonaceous chondrites, water perhaps played the most significant role in the chemical and mineralogical evolution of a range of small asteroidal bodies, by modifying the primary mineralogical characteristics of precursor materials. The obvious effect of aqueous alteration is the formation of secondary phases, such as serpentine and smectite. The diversity in alteration assemblages among various chondrites likely reflect the aqueous environment (e.g., temperature, dissolved ion, duration, water/rock ratio, fO_2, etc.) of the parent bodies. Although several hydrothermal experiments were made on olivine or pyroxene as starting materials[#1−#2], little is known about the actual behavior of chondrite toward aqueous fluid[#3]. Here we report hydrothermal alteration experiments of Allende meteorites.

We use Allende meteorites as starting materials. In order to observe micro-textures before and after alterations, we cut out block-shaped samples (2.5 mm×2.5 mm×6 mm) and never crushed. Hydrothermal alteration experiments were performed with PTFE double-vessels (1 ml and 25 ml) loaded into a steel autoclave. In order to maintain a reducing ambient, H_2 gas was generated in the outer vessel by reaction with HCl and magnesium,. All experiments were carried out at temperature of 200 deg.C, where the saturated vapor pressure reaches about 15 bar. As to reaction fluids, we use different pH solution (7, 8.5, 10, 14)[#4] with different water/rock (W/R) ratios (0.5, 2, 8 vol./vol.)[#5]. All run durations are 168 hours. Recovered products were analyzed by synchrotron X-ray diffraction (SR-XRD), scanning electron microscope (SEM) equipped with an energy-dispersive X-ray spectrometer (EDS).

As the results, except for condition of pH 7 and W/R 0.5, serpentine is observed in matrix, which formed at interstitial space of olivine grains of the matrix. As pH value increases, more abundance of matrix olivine are replaced by serpentine. Smectite is observed only under the condition of pH 14 and W/R 0.5. Calcite ($CaCO_3$) is formed on the sample surface under almost all conditions. Under pH 7 condition, anhydrite ($CaSO_4$) is also formed on the sample surface. The results of this study indicate that hydrated mineral formation easily proceeds compared with the previous studies where olivine or pyroxene were used as starting materials.

#1 Ohnishi and Tomeoka (2007) MPS, 42, 49-61. #2 Iishi and Han (2000) Neues Jahrbuch Fur Mineralogie-Monatshefte 2:49-59. #3 Jones and Brearley (2006) GCA, 70, 1040-1058. #4 Zolensky et al. (1989) Icarus, 78, 411-425. #5 Clayton and Mayede (1998) GCA, 63, 2089-2104.

Keywords: carbonaceous chondrite, hydrothermal experiments, hydrated minerals, Allende

Japan Geoscience Union Meeting 2014
(28 April - 02 May 2014 at Pacifico YOKOHAMA, Kanagawa, Japan)

PPS25-13 Room:213 Time:May 2 12:15-12:30

Electron Holography Reveals Nanometer Scale Magnetic Structure of Framboidal Magnetite and its Formation Process

KIMURA, Yuki[1*] ; SATO, Takeshi[2] ; NAKAMURA, Tomoki[1] ; NAKAMURA, Norihiro[1] ; NOZAWA, Jyun[3] ; TSUKAMOTO, Katsuo[1] ; YAMAMOTO, Kazuo[4]

[1]Tohoku University, [2]Hitachi High-Technologies Corporation, [3]Tohoku University, [4]Japan Fine Ceramics Center

Small solar system bodies were formed as agglomerates of dust and ices 4.6 billion years ago. Several million years after asteroid formation [1], the ice melted due to radioactive heating inside the larger asteroids [2] and/or highly energetic impacts [3]. Then, water plays several major roles in the chemistry of asteroids, both in mineralization and in the formation of organic compounds. Currently, bulk liquid water no longer exists in meteorites. We see only the signature of water in ancient asteroids as veins of hydrothermally deposited minerals [4] or water trapped in salt crystals [5] in meteorites. The Tagish Lake meteorite, which is a unique Type 2 carbonaceous chondrite, has a signature of aqueous process in the matrix that is abundant micrometer-sized polyhedral particles of magnetite [6]. The framboids are three-dimensionally ordered colloidal crystals of magnetite nanoparticles. The uniformity of the size distribution and the similar morphology of the magnetite nanoparticles in each of the colloidal crystals suggest that they were formed through homogeneous nucleation from a highly supersaturated isolated solution in a single nucleation event.

Here we show evidence of how magnetite nanoparticles assembled into periodic structures based on a nanometer scale paleomagnetic method using electron holography in an examination of the framboidal magnetite in the Tagish Lake carbonaceous chondrite [7]. An attractive force such as magnetism never contributes to the formation of colloidal crystals [8], but the repulsive force caused by the surface charge of the magnetite is able to work. To overcome the repulsive force, the density of magnetite nanoparticles in a solution must be sufficiently high in an isolated solution as a water droplet parches in microgravity. We used electron holography to visualize the magnetization of the meteoritic minerals for the first time and found that magnetite grains in the framboid have no external magnetic force, i.e., they have a flux-closure vortex structure, which allowed the formation and preservation of the colloidal crystals. We conclude that these framboids formed in tiny water droplets with pH of 7-12 containing ions such as Ca^{2+} and Mg^{2+} at levels of 10^{-14}-10^{-15} mol m^{-2}, just before exhaustion of water during thermal alteration in a hydrous asteroid.

[1] Fujiya, W., Sugiura, N., Hotta, H., Ichimura, K. & Sano, Y. Evidence for the late formation of haydrous asteroids from young meteoritic carbonates. *Nature Communications* **3**, 627 (2012).

[2] Endress, M., Zinner, E. & Bischoff, A. Early aqueous activity on primitive meteorite parent bodies. *Nature* **379**, 701-703 (1996).

[3] Rubin, A. F. Collisional facilitation of aqueous alteration of CM and CV carbonaceous chondrites. *Geochim. Cosmochim. Acta* **90**, 181-194 (2012).

[4] Tomeoka, K. Phyllosilicate veins in a CI meteorite: evidence for aqueous alteration on the parent body. *Nature* **345**, 138-140 (1990).

[5] Zolensky, M. E. *et al*. Asteroidal water within fluid inclusion-bearing halite in an H5 chondrite, Monahans (1998). *Science* **285**, 1377-1379 (1999).

[6] Nozawa, J. et al. Magnetite 3-D Colloidal Crystals Formed in the Early Solar System 4.6 Billion Years Ago, *Journal of the American C* **133**, 8782-8785(2011).

[7] Kimura, Y. et al. Vortex magnetic structure in framboidal magnetite reveals existence of water droplets in an ancient asteroid, *Nature Communications*, **4** (2013) 2649 doi: 10.1038/ncomms3649.

[8] Philipse, A. P. & Maas, D. Magnetic colloids from magnetotactic bacteria: chain formation and colloidal stability. *Langmuir* **18**, 9977-9984 (2002).

Keywords: Magnetite, Electron holography, Tagish Lake meteorite

Japan Geoscience Union Meeting 2014
(28 April - 02 May 2014 at Pacifico YOKOHAMA, Kanagawa, Japan)

PPS25-14 Room:213 Time:May 2 12:30-12:45

C-XANES analyses of carbonaceous solid inclusions from Monahans halite

KEBUKAWA, Yoko[1*] ; ZOLENSKY, Michael[2] ; KILCOYNE, David[3] ; RAHMAN, Zia[4] ; FRIES, Marc[2] ; CODY, George[5]

[1]Department of Natural History Sciences, Hokkaido University, [2]NASA Johnson Space Center, [3]Lawrence Berkeley National Laboratory, [4]Jacobs-Sverdrup, [5]Geophysical Laboratory, Carnegie Institution of Washington

Monahans meteorite (H5) contains fluid inclusion-bearing halite (NaCl) crystals [1]. Microthermometry and Raman spectroscopy showed that the fluid in the inclusions is an aqueous brine and they were trapped near 25^{o}C [1]. Their continued presence in the halite grains requires that their incorporation into the H chondrite asteroid was post metamorphism [2]. Abundant solid inclusions are also present in the halites. The solid inclusions include abundant and widely variable organics [2]. Analyses by Raman microprobe, SEM/EDX, synchrotron X-ray diffraction and TEM reveal that these grains include macromolecular carbon similar in structure to CV3 chondrite matrix carbon, aliphatic carbon compounds, olivine (Fo_{99-59}), high- and low-Ca pyroxene, feldspars, magnetite, sulfides, lepidocrocite, carbonates, diamond, apatite and possibly the zeolite phillipsite [3]. Here we report organic analyses of these carbonaceous residues in Monahans halite using C-, N-, and O- X-ray absorption near edge structure (XANES).

Approximately 100 nm-thick sections were extracted with a focused ion beam (FIB) at JSC from solid inclusions from Monahans halite. The sections were analyzed using the scanning transmission X-ray microscope (STXM) on beamline 5.3.2.2 at the Advanced Light Source, Lawrence Berkeley National Laboratory for XANES spectroscopy. C-XANES spectra of the solid inclusions show micrometer-scale heterogeneity, indicating that the macromolecular carbon in the inclusions have complex chemical variations. C-XANES features include 284.7 eV assigned to aromatic C=C, 288.4-288.8 eV assigned to carboxyl, and 290.6 eV assigned to carbonate. The carbonyl features obtained by C-XANES might have been caused by the FIB used in sample preparation. No specific N-XANES features are observed. Various degrees of 1s-$\sigma*$exciton shown in the C-XANES spectra indicate that the solid inclusions contain macromolecular carbon which experienced various degree of thermal processing. The natures of the macromolecular carbon in the solid inclusions observed by C-XANES are consistent with the previous studies showing that the solid inclusions have not originated from Monahans parent body [1-3].

References: [1] Zolensky et al. 1999. Science 285: 1377-1379. [2] Fries et al. 2011. 74th MetSoc #5390. [3] Zolensky et al. 2013. 76th MetSoc #5200.

Keywords: C-XANES, Halite, Carbon, Chondrite, Organic matter

Japan Geoscience Union Meeting 2014
(28 April - 02 May 2014 at Pacifico YOKOHAMA, Kanagawa, Japan)

PPS25-15 Room:213 Time:May 2 14:15-14:30

3D shapes of Itokawa regolith particles: comparison with lunar regolith particles

TSUCHIYAMA, Akira[1*] ; MATSUSHIMA, Takashi[2] ; MATSUMOTO, Toru[3] ; NAKANO, Tsukasa[4] ; MATSUNO, Junya[1] ; SHIMADA, Akira[3] ; UESUGI, Kentaro[5] ; TAKEUCHI, Akihisa[5] ; SUZUKI, Yoshio[5] ; OHTAKE, Makiko[6] ; NAKAMURA, Tomoki[7] ; UESUGI, Masayuki[6] ; YADA, Toru[6] ; NISHIIZUMI, Kunihiko[8]

[1]Graduate School of Science, Kyoto University, [2]Graduate School of Systems and Information Engineering, [3]Graduate School of Science, Osaka University, [4]AIST/GSJ, [5]JASRI/SPring-8, [6]JAXA/ISAS, [7]Graduate School of Science, Tohoku University, [8]Space Sciences Laboratory, University of California

Regolith particles were returned from the surface of asteroid Itokawa by the Hayabusa spacecraft. The sample analysis elucidated a variety of surface processes on the asteroid (e.g., [1]): (1) Formation of regolith by impacts of small objects, with selective escape of the finest-scale particles. (2) Implantation of solar wind into the uppermost particle surfaces and formation of space-weathering rims. (3) Grain abrasion, probably due to seismic-induced particle motion. Processes (5) and (6) might have been repeated. (7) Final escape of particles from the asteroid by impact within the past 8 million years (1-3 million years [3]).

During the course of the analysis, 3D size and shape features of the Itokawa particles were obtained by SR-based x-ray microtomography to understand the origin and evolution of the regolith particles on Itokawa ' s surface [2,3]. In particular, the particle shape distribution with respect to their three-axial ratios was obtained and compared with that of fragments formed by high-speed impact in laboratory experiments [4,5] and of lunar regolith samples [6]. The 3D shapes of the lunar samples have been examined by tomography [6] but not grain-by-grain as performed for the Itokawa samples. In addition, the procedure for measuring the three axial lengths was different between the regolith particles and the impact fragments: the former was obtained from 3D external particle shapes by ovoid approximation [2,3,6], while the latter by bounding box method using a calliper [4,5]. In order to make strict comparison between them, lunar regolith particles were examined by the same method as the Itokawa particles, and the three axial lengths were measured from the tomography data by bounding box method that was newly developed in the present study.

The 3D shapes of 70 particles from 105-250 μm sieved fraction of Descartes highland (60501) and 74 particles from $<$1 mm sieved fraction of Mare Tranquillitatis (10084) were obtained by microtomography at BL47XU of SPring-8. Furthermore, the 3D shapes of new 24 Itokawa particles (3 of them are from Dr. M. Meier, personal communication) were also examined in addition to the previous 48 particles [3]. The three axial lengths were measured in the orders of short to long and long to short axes to compared with the data of [3] and [4], respectively. The shape distribution in a Zingg diagram was compared using the Kolmogorov-Smirnoff test.

The shape distribution of the Itokawa particles cannot be distinguished from that of the impact fragments of [4] but can be distinguished from that of [3]. This may suggest that the Itokawa particles resulted from mechanical disaggregation, as a response to impacts with a specific condition. In contrast, the shape distribution of the lunar regolith particles can be distinguished from that of the Itokawa particles and the impact fragments although lunar regolith is the product of impact on the lunar surface. The lunar particle shapes are more equant than the others. The both lunar samples examined are matured (Is/FeO = 80 and 78 for 60501 and 10084, respectively [7]). These regolith particles should become equant from the shapes similar to the impact fragments by mechanical disaggregation or abrasion due to repeated impacts during a long residence time in the regolith layer although a specific process for the shape change is not known.

[1] Tsuchiyama (2013) Elements, 10: in print. [2] Tsuchiyama et al. (2011) Science, 333: 1125. [3] Tsuchiyama et al. (2013) Meteor. & Planet. Sci., 1-16. doi: 10.1111/maps.12177. [4] Fujiwara et al. (1978) Nature 272: 602. [5] Capaccioni et al. (1984) Nature 308: 832. [6] Katagiri (2010) Proc. 12th Internat. Conf. Engin., Sci., Constr., Operat. in Challeng. Environ., 254?259. [7] Morris et al. (1978) Proc. Lunar Planet. Sci. Conf., 9th, 2287.

Keywords: Hayabusa mission, particle shape, SPring-8, x-ray tomography, Apollo mission, impact

Japan Geoscience Union Meeting 2014
(28 April - 02 May 2014 at Pacifico YOKOHAMA, Kanagawa, Japan)

PPS25-16 Room:213 Time:May 2 14:30-14:45

Surface micromorphology of regolith particles from Asteroid Itokawa: Implication for space weathering of regolith

MATSUMOTO, Toru[1*] ; TSUCHIYAMA, Akira[2] ; MIYAKE, Akira[2] ; NOGUCHI, Takaaki[3] ; NAKAMURA, Tomoki[4] ; NAKAMURA, Michihiko[4] ; MATSUNO, Junya[2] ; SHIMADA, Akira[1] ; UESUGI, Kentaro[5] ; NAKANO, Tsukasa[6]

[1]Osaka University, [2]Kyoto University, [3]Ibaraki University, [4]Tohoku University, [5]JASRI/SPring-8, [6]GSJ/AIST

Spectral features of airless bodies are known to be modified by processes called space weathering. From Analysis of lunar samples, the space weathering is considered to be caused by mainly nano phase iron (npFe^0) formed by mainly vapor deposition produced by micrometeorite bombardments and solar wind irradiation [1].Space weathering of asteroid is also considered to progress by mainly solar wind irradiation and micrometeorite bombardments [1]. Detailed Space weathering processes on asteroids are expected to be revealed by analysis of asteroidal regolith samples. Hayabusa spacecraft recovered regolith particles from S-type asteroid 25143 Itokawa. In previous study, implantation of solar wind to Itokawa regolith particles was detected by noble gas isotope analysis [2]. The space weathering rims including npFe^0 were observed on regolith particles using transmission electron microscopes [3][4]. Surface micromorphology of regolith particles are expected to have information to reveal space weathering processes related to surface activity on Itokawa and applied to. So far, general surface features of regolith particles have not yet been clearly understood. Therefore, this study investigates Itokawa regolith particles focusing on their surface micromorphology.

Three-dimensional (3D) external shapes of the regolith particles were analyzed by microtomography. Surface morphologies of the regolith particles were observed by field-emission scanning electron microscopy (FE-SEM). It is revealed that the regolith surfaces can be classified into fractured surfaces formed by impact and surfaces formed by condensation from vapor in microdruses of original chondritic materials. Regardless of these surface types, there are matured surfaces, which have rounded edges. The matured surfaces are considered to be formed by abrasion processes on Itokawa [5]. Internal structures of space weathering rim of regolith particles was observed by transmission electron microscopy (TEM/STEM) and this was compared with the surface morphologies of the same surface observed by FE-SEM. Observed space weathering rim have vesicles and form blister structures. The blisters can be identified by FE-SEM, indicating that space weathering rims with blisters can be observed by FE-SEM without any destructive methods. Space weathering processes related to the surface activities on Itokawa is considered from observation of blister distribution on the regolith particles. It is revealed that there is no correlation between blister distribution and the roundness of the surface morphologies, indicating that dominant mechanism of the abrasion process is not solar wind sputtering but mechanical abrasion. The abrasion processes can peel off the space weathering rims. In addition, there are heterogeneous distribution of blisters suggesting migration and fragmentation of regolith particles. Two distinct time-scales for the spectral reddening of S-type asteroids due to space weathering were proposed [7]: solar wind irradiation for about 10^6 years and micrometeorite bombardment for about 10^9 years. This study proposes that spectral change of Asteroid Itokawa by space weathering would have gradually occurred for 10^6 years at the latest by regolith activities on Asteroid Itokawa such as mechanical abrasion, migration and fragmentation of regolith particles, while space weathering rims are developed on local surface of individual regolith particles for 10^3-10^4 years[4].

[1]Clark B. E. (2002) Asteroid, 585-599. [2] Nagao K. et al. (2011) Science, 333, 1128-1131. [3] Noguchi T. et al. (2011) Science, 333, 1121-1125. [4] Noguchi T. et al. (2013) Met. Planet. Sci.27, 1-27 [5] Tsuchiyama A. et al. (2011) Science, 333, 1125-1128. [6] Matsumoto T. et al. (2013) LPSC XLIV, 1441. [7] Vernazza et al. (2009) Nature, 458, 993-995.

Keywords: Itokawa, regolith, space weathering

Japan Geoscience Union Meeting 2014
(28 April - 02 May 2014 at Pacifico YOKOHAMA, Kanagawa, Japan)

PPS25-17 Room:213 Time:May 2 14:45-15:00

Extraction and Identification of Primitive Grains Driven by Magnetic Volume Force.

HISAYOSHI, Keiji[1*] ; UYEDA, Chiaki[1]

[1]Institute of Earth and Space Science, Graduate School of Science, Osaka University

Magnetic volume force caused by a field gradient has been commonly used to extract ferro-(or ferri-) magnetic materials from weak magnetic materials. The separation was realized because the field-gradient forces that operated on the spontaneous magnetizations of the above category of materials were considerably large with respect to terrestrial gravity. It was considered that dynamic motion of a weak magnetic material generally require a strong field above B = 10T .

Primitive materials are generally obtained as an ensemble of grains with different elemental composition with heterogeneous origins. At an initial stage of investigating this type of material, it is important to extract and identify the material of individual particles included in the ensemble. Such method should be non-destructive and easily performed. Moreover, it should be based on a well-established physical or chemical concept. In the case of analyzing a fluid sample of organic molecules, the stage separation and identification has been established by introducing the technique of chromatography; such method has not been established as yet on mixture of solid samples. Here we propose a new principle of grain separation that is driven by magnetic volume force. By comparing the measured χ_{DIA} of a particle by their published values, material of the particle is identified. This is because an intrinsic χ_{DIA} value is assigned to a material.

Microgravity was generated using a compact drop shaft system, which can be introduced in an ordinary laboratory. The length of the shaft was 1.8m, and the duration of microgravity time was about 0.5 second. The sample is released in the field-gradient produced by a by a magnetic circuit composed by a NdFeB permanent magnet. Maximum field intensity of the circuit was 0.8 T. The experimental apparatus was set inside a rectangle box which had a size of 30x30x20cm. The vacuum chamber equipped with an electric actuator, sample releasing signal reception device, the sample holder controller, the magnet, the battery, and the high-vision video camera are installed in the above box. [1-3]

The present results achieved on sub-millimetre-sized diamagnetic grain have a large significance as a step to realize the extraction and identification of micron-sized grains that compose the primitive materials. The technique described is useful in the search for new types of pre-solar grains that are not identified as yet.

Reference

[1] K. Hisayoshi, S. Kanou and C. Uyeda : Phys.:Conf. Ser., 156 (2009) 012021.
[2] K. Hisayoshi, C. Uyeda, K. Kuwada, M. Mamiya and H. Nagai, : Phys.:Conf. Ser., 327 (2011) 012058.
[3] C. Uyeda, K. Hisayoshi, and S. Kanou : Jpn. Phys. Soc. Jpn. 79 (2010) 064709.

Keywords: magnetic ejection,, nondestructive identification, magnetic extraction, microgravity, translational motion, magnetic volume force

Japan Geoscience Union Meeting 2014
(28 April - 02 May 2014 at Pacifico YOKOHAMA, Kanagawa, Japan)

PPS26-01 Room:418 Time:April 30 09:00-09:15

Summay of the third stage of Next Decade Initiatives for Lunar Planetary Explorations

WATANABE, Sei-ichiro[1*]

[1]Dept. of Environmental Studies, Nagoya University

The Next Decade Initiatives for Lunar Planetary Explorations is now in the final phase of the third stage selection. The concept and progress of the third stage selection will be presented.

We have been discussed the mid-range (the next decade or two) future vision of planetary explorations providing the best mix of medium- to large-size flagship missions, small-size missions, and missions of opportunity for science payloads on foreign missions; the compelling concepts of the flagship missions that are central to the mid-range future vision, and strategy for unifying the planetary science community to the flagship missions. The final candidates for the flagship missions are (1) the lunar (or planetary) chronological mission based on the in-situ geochronology instruments, (2) the Mars lander and rover exploration with science payloads including the life-detection experiment system, and (3) the solar power sail mission for Trojan asteroids with cruising phase observation of the cosmic infrared background radiation. The selection committee are now reviewing the three mission concepts to polish up. I will report on the activity of the committee and discuss the relation to the ISAS's roadmap for space science approved by the Japanese Strategic Headquarter for Space Policy in September 2013.

Keywords: planetary science, Solar System exploration, Future missons

Japan Geoscience Union Meeting 2014
(28 April - 02 May 2014 at Pacifico YOKOHAMA, Kanagawa, Japan)

PPS26-02 Room:418 Time:April 30 09:15-09:30

A status report of future geospace satellite projects

MIYOSHI, Yoshizumi[1*] ; TERADA, Naoki[2] ; FUJIMOTO, Masaki[3]

[1]STEL, Nagoya University, [2]Graduate School of Science, Tohoku University, [3]ISAS/JAXA

In this presentation, we report several plans for future geospace exploration projects including magnetosphere and ionosphere, and discuss a possible roadmap for the future mission.

Keywords: future mission, solar-terrestrial physics, geospace exploration

Japan Geoscience Union Meeting 2014
(28 April - 02 May 2014 at Pacifico YOKOHAMA, Kanagawa, Japan)

PPS26-03 Room:418 Time:April 30 09:30-09:45

MELOS1 Mars Exploration for Life-Organism Search

SATOH, Takehiko[1*] ; KUBOTA, Takashi[1] ; FUJITA, Kazuhisa[1] ; YAMAGISHI, Akihiko[2] ; MIYAMOTO, Hideaki[3] ; HASHIMOTO, George[4] ; SENSHU, Hiroki[5] ; USUI, Tomohiro[6] ; KOMATSU, Goro[7] ; DEMURA, Hirohide[8] ; ISHIGAMI, Genya[9] ; OGAWA, Naoko[1] ; OKADA, Tatsuaki[1]

[1]Japan Aerospace Exploration Agency, [2]Tokyo University of Pharmacy and Life Sciences, [3]University of Tokyo, [4]Okayama University, [5]Chiba Institute of Technology, [6]Tokyo Institute of Technology, [7]Universita' d'Annunzio, [8]Aizu University, [9]Keio University

Mars exploration is uniquely significant as it includes all of "scientific", "engineering", and "exploration" importances almos equally. Visiting Mars is, therefore, an essential milestone to expand the frontier of human being. In this paper, as part of JSPS "next decade" activity, we discuss MELOS1 with view points of science and engineering.

The target of MELOS1 is direct detection of lives on Mars. It will be a simplified mission with just a rover plus a cruise stage, no orbiter at all. It may not be unreasonable to expect relay orbiters in Mars orbit when MELOS1 will arrive at the red planet as there are a number of mission plans from the U.S.A., Europe, and Russia.

The MELOS1 rover will weigh about 60 kg, equipped with a life-detection microscope (LDM) and meteorology sensors to monitor its environment. Details of LDM will be presented elsewhere. In brief, the LDM uses the highest possible sensitivity technique, dyeing cells with pigment and observe them by fluorescent light. This technique will give us 3 orders of magnitudes higher sensitivity of life detection than was done on Viking Landers.

If discovered, it should undoubtedly be the biggest discovery in science. The surface area of Mars is so wide and so different from one place to another. Yet, we had only 7 landers, basically at places similar to each other. The best places for life-detection experimetn, fluvial feasures or mud volcanoes (may be methane hot spots) are still intact. In MELOS1, we will perform high-precision landing to such a place and will search for lives for the first time. The current status of planning will be presented. In addition, the position in Japan's future missions will be discussed with

audience of greater variety.

Keywords: Mars, exploration, landing, life, rover

Japan Geoscience Union Meeting 2014
(28 April - 02 May 2014 at Pacifico YOKOHAMA, Kanagawa, Japan)

PPS26-04 Room:418 Time:April 30 09:45-10:00

Lunar chronological mission based on the in-situ geochronology instruments

MOROTA, Tomokatsu[1*] ; SUGITA, Seiji[2] ; CHO, Yuichiro[2] ; MIURA, Yayoi N.[2] ; WATANABE, Sei-ichiro[1] ; OHTAKE, Makiko[3] ; KOBAYASHI, Naoki[3] ; KAROUJI, Yuzuru[3] ; FURUMOTO, Muneyoshi[1] ; HONDA, Chikatoshi[4] ; SUGIHARA, Takamitsu[5] ; ISHIHARA, Yoshiaki[3] ; ISHIBASHI, Ko[6] ; ARAI, Tomoko[6] ; TAKEDA, Hiroshi[2] ; TERADA, Kentaro[7] ; KAMATA, Shunichi[8] ; SAIKI, Kazuto[7] ; KOBAYASHI, Shingo[9] ; KAMEDA, Shingo[10] ; YOSHIOKA, Kazuo[3] ; OKAZAKI, Ryuji[11] ; NAMIKI, Noriyuki[6] ; KOBAYASHI, Masanori[6] ; OHNO, Sohsuke[6] ; SENSHU, Hiroki[6] ; WADA, Koji[6] ; TACHIBANA, Shogo[8] ; TANAKA, Satoshi[3] ; MUKAI, Toshifumi[3]

[1]Nagoya Univ., [2]Univ. Tokyo, [3]JAXA, [4]University of Aizu, [5]JAMSTEC, [6]Chiba Institute of Technology, [7]Osaka Univ., [8]Hokkaido Univ., [9]NIRS, [10]Rikyo Univ., [11]Kyushu Univ.

In-situ geochronology measurements have long been a key goal for planetary science.We propose a mission, which is designed to determine formation age of young Aristillus crater of the Moon. The correlation of crater frequency measured with remote-sensing data with the obtained age provides information about the cratering history in the inner solar system.

Keywords: Lunar and Planetary explorations, Moon, chronology, crater, K-Ar dating

Japan Geoscience Union Meeting 2014
(28 April - 02 May 2014 at Pacifico YOKOHAMA, Kanagawa, Japan)

PPS26-05 Room:418 Time:April 30 10:00-10:15

Applicability of a laser-ablation in-situ K-Ar dating method on the Moon: insights from lunar samples

CHO, Yuichiro[1*] ; MIURA, Yayoi N.[2] ; MOROTA, Tomokatsu[3] ; SUGITA, Seiji[4]

[1]Department of Earth and Planetary Science, University of Tokyo, [2]Earthquake Research Institute, University of Tokyo, [3]Nagoya University, [4]Department of Complexity Science and Engineering, University of Tokyo

We have been developing an in-situ K-Ar isochron dating method for future landing missions. Potassium-argon ages are measured with the combination of laser-induced breakdown spectroscopy (LIBS) and mass spectrometry using a quadrupole mass spectrometer (QMS). In our previous studies, we reported that isochron ages for gneiss samples with 30% accuracy and 10-20% precision.

However, such experimental results using test samples do not guarantee the applicability of our LIBS-QMS isochron method for actual rock samples on planetary surfaces. Depending on geologic units, the types of rocks and K concentration vary greatly on planetary surfaces.

Thus, we assess the capability of our in-situ K-Ar dating method taking the petrologic properties including K abundance and possible age range of the lunar surfaces into account. First, we examined the global maps of K obtained with the Gamma Ray Spectrometers onboard remote sensing satellites. We found that the concentrations of K and Ar of KREEPy materials are well above the detection limits of our LIBS-QMS approach. Then, the elemental compositions and textures of KREEP basalt were investigated. We found that Si-rich glasses contained in mesostasis are measurable with K-Ar dating on the Moon because of the high K concentration (˜7 wt%), while other minerals (i.e., pyroxene, olivine, and plagioclase) contain virtually no K. Since the textures of these samples were heterogeneous at the scale of laser spot (˜500 microns), the ”isochron” ages would be obtained by measuring the different portions containing K-bearing phases in various ratios.

The major problem concerning in-situ K-Ar dating is partial 40Ar loss due to thermal events after crystallization. This suggests that K-Ar dating only yields the lower limit for the real crystallization age. Furthermore, brecciation by impacts and contamination by solar wind will inhibit accurate in-situ dating. In order to avoid such problems and obtain meaningful age data by in-situ dating, we aim to measure fresh impact melt rocks exposed by a very recent (tens of Ma) impact on the Aristillus crater floor.

Finally, we evaluated how our method can constrain the absolute chronology models of the Moon and Mars based on the precisions of age measurements achieved by this study. For example, the absolute age of impact melt rocks in Aristillus crater, whose ages correspond to the ”missing ages” of the current lunar crater chronology model (i.e., between 3.0 Ga and 0.1 Ga), would be measured with ˜20% precision when the K concentration of the glass in KREEP basalt is assumed. Then, our method would be able to discriminate the constant flux model [Neukum, 1983] and the decreasing flux model [Hartmann et al., 2007]. The implications of in-situ dating in Aristillus crater include refining the crater chronology model, determining the age of the youngest mare basalts, and understanding the dynamical evolution of the asteroids in the last three billion years.

Japan Geoscience Union Meeting 2014
(28 April - 02 May 2014 at Pacifico YOKOHAMA, Kanagawa, Japan)

PPS26-06 Room:418 Time:April 30 10:15-10:30

Exploration of Jovian Trojan asteroids by Solar Power Sail

NAKAMURA, Ryosuke[1] ; SEKINE, Yasuhito[2*] ; MATSUURA, Shuji[3] ; YANO, Hajime[3] ; MORI, Osamu[3] ; SOLAR SAIL, Working group[3]

[1]AIST, [2]Universit of Tokyo, [3]JAXA

Solar Power Sail is a novel concept with hybrid propulsion of large-area solar sail and ion engine driven by thin-film solar panel. It enables us to bring relatively large mission payloads to the outer solar system without nuclear technology. The Solar Power Sail spacecraft is currently planned in Japan to explore Jovian Trojan astereoids. There exist two competing hypotheses on their origin. The classic model suggests that Trojan asteroids are mainly survivors of building blocks of the Jupiter system, while NICE model claims that they must be intruders from outer regions after the planetary migration of gas planets settled. This mission will provide invaluable clues to the genesis of the planets, asteroids ana comets through remote sensing, in-situ sample analysis and comparison of the results with other small body missions, such as Dawn, Rosetta, Osiris-ReX and Hayabusa-2. Another target of this mission is novel astronomy; measurement of the infrared extragalactic background light without foreground contamination of the zodiacal light thanks to low-density environment at deep space, polarization measurement of the gamma-ray burst and accurate determination of its direction based on the interplanetary network technique. The Solar Power Sail mission will thus develop a new direction of space astronomy and planetary science providing us an interplanetary telescope site and will play an important roll to form a new interdisciplinary science field.

Keywords: Jupiter, Trojan, asteroids, exploration, Solar Sail

Japan Geoscience Union Meeting 2014
(28 April - 02 May 2014 at Pacifico YOKOHAMA, Kanagawa, Japan)

PPS26-07 Room:418 Time:April 30 11:00-11:15

Current status of mission study for small scale planetary exploration in JSPS

ARAKAWA, Masahiko[1*]

[1]Graduate School of Science, Kobe University

Recent success of launching a new Japanese rocket named as Epsilon gives us a new chance for planetary exploration. So, we just begin to discuss a new planetary exploration mission suitable for this Epsilon rocket in Japanese Society of Planetary Science (JSPS) . Future planning section in JSPS has examined the small size mission for planetary exploration since last summer, and the special working group for this purpose in this section was organized to submit our report showing the scientific feasibility in a small size mission to a vice-president of JSPS. The final report is shown on the web-site of https://www.wakusei.jp/~shourai/wiki/epsilon/. A new load map for space science in Japan by JAXA was released last september, and it showed that the exploration of solar system would be planned in a small scale mission in order to overcome technical problems and develop new devices for the future planetary exploration planned after 10 years. According to this new load map related to planetary science, we have decided to discuss a future mission of small scale planetary exploration by using Epsilon rocket in JSPS fall meeting. We are going to hold a symposium to discuss a future plan regularly in 2014, and our symposium is open not only for JSPS member but also for every scientist and engineer who are interested in a small scale planetary exploration.

Keywords: Epsilon rocket, small scale planetary exploration

Japan Geoscience Union Meeting 2014
(28 April - 02 May 2014 at Pacifico YOKOHAMA, Kanagawa, Japan)

PPS26-08 Room:418 Time:April 30 11:15-11:30

This is what I learned from the development of EXCEED

YOSHIKAWA, Ichiro[1*]

[1]University of Tokyo

I will present my plan for the next 10-year instrumental development based on my heritage on the Sprint-A/EXCEED.

An earth-orbiting Extreme Ultraviolet (EUV) spectroscopy (EXCEED) is the first mission of the Small scientific satellite Platform for Rapid Investigation and Test -A (Sprint-A) conducted by ISAS/JAXA. A single science instrument (EXCEED) is boarded on Sprint-A. EXCEED has started to observe the solar planets in the EUV spectral range, and will extend to the identification of extrasolar planet atmosphere.

Keywords: Sprint-A, EUV, Planetary airglow

Japan Geoscience Union Meeting 2014
(28 April - 02 May 2014 at Pacifico YOKOHAMA, Kanagawa, Japan)

PPS26-09 Room:418 Time:April 30 11:30-11:45

Deep Space Explorer DESTINY

KAWAKATSU, Yasuhiro[1*]

[1]ISAS/JAXA

DESTINY which stands for "**D**emonstration and **E**xperiment of **S**pace **T**echnology for **IN**terplanetary vo**Y**age" is a mission candidate for the next space science small program. The next mission is planned to be decided in 2014, and the select one is scheduled to be launched in 2018.

As illustrated in the Figure, DESTINY will be launched by an Epsilon launch vehicle and firstly placed into a low elliptical orbit, where then its altitude raised by the use of ion engine. When the orbit raising reaches the Moon, DESTINY subsequently is injected into transfer orbit for L_2 Halo orbit of the Sun-Earth system by using lunar gravity assist. Upon arrived at L_2 Halo orbit, DESTINY will conduct its engineering experiment as well as scientific observations for at least a half year. If conditions permit, DESTINY will leave L_2 Halo orbit, and transfer to the next destination.

On the way to L_2 Halo orbit, DESTINY will conduct demonstration and experiment on key advanced technologies for future deep space missions. Major items of the technology demonstration are listed as follows.

1) High energy mission by Epsilon rocket.

We investigate appropriate rocket configurations and flight path designs, and evaluate the performance of Epsilon rocket to insert spacecrafts into high energy orbits. It provides basic data of Epsilon rocket application to deep space missions.

2) Ultra-Lightweight solar panel.

In order to generate large electric power to run μ20 ion engine, "Ultra-Lightweight Solar Panel", which is under development at JAXA, is applied and its performance is evaluated. This solar panel is estimated to achieve power to mass ratio at least double to conventional ones. Future application is expected in outer planet probes (JMO, MELOS) or probes with large ion engines.

3) Large scale ion engine μ20.

DESTINY is inserted into an elliptical orbit and reaches to a Halo orbit by its own orbital maneuver. For this maneuver, a large ion engine (μ20) which is under R&D at JAXA will be adopted and its performance is evaluated. This ion engine has thrust five times as much as μ10 used by Hayabusa and will be expected to be applied to large probes such as SOLAR-D or Hayabusa Mk2.

4) Advanced thermal control.

In order to manage large amount of heat generated by the large ion engine, advanced thermal control techniques by way of Loop Heat Pipe will be adopted.

5) Orbit determination under low thrust operation.

DESTINY will reach to Halo orbit by running ion engine over long duration. In order to reduce burdens to shut down the ion engine each time of orbit determinations, orbit determination under ion engine operation is conducted and its performance is evaluated.

6) Automatic/autonomous onboard operation.

In order to increase the efficiency of operation, autonomous and highly functioned spacecraft management system is developed demonstrated on board. This technique is expected to be adopted especially in the deep space missions usually operated under severe communication condition.

7) Halo orbit transfer and maintenance.

DESTINY will reach to Halo orbit and maintains the orbit more than one period. In order to reduce the risks of Halo orbit insertion and suppress the amount of orbital maneuvers, the orbit control technique using dynamical system theory is used and its operability is evaluated. This technique will be adopted in SPICA, which will be operated in Halo orbit.

DESTINY itself is an engineering experiment probe which destines L_2. However, its mission profile is naturally applied to lunar missions and escape missions by forking the profile at the lunar encounter. Moreover, the spacecraft's high astronautic performance makes its application to other launch method attractive, such as dual launch with GEO satellite or another deep space probe. The significance of DESTINY from the point of its opening new opportunities for low-cost deep space mission is discussed in the presentation as well.

PPS26-09 Room:418 Time:April 30 11:30-11:45

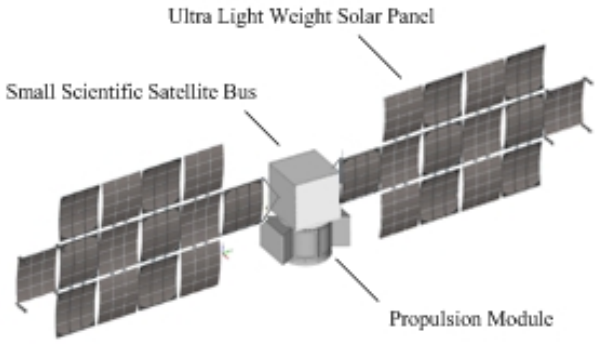

DESTINY Overview

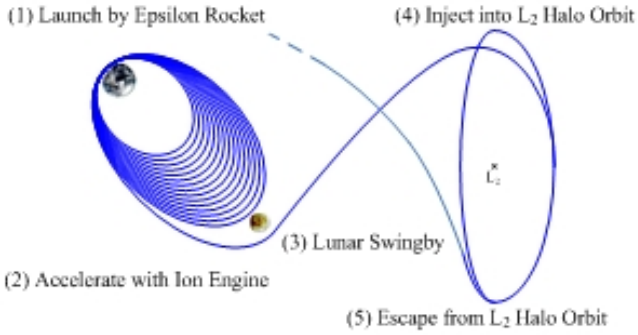

Mission Profile

Japan Geoscience Union Meeting 2014
(28 April - 02 May 2014 at Pacifico YOKOHAMA, Kanagawa, Japan)

PPS26-10 Room:418 Time:April 30 11:45-12:00

Introduction of SLIM, a small and pinpoint lunar lander

SAKAI, Shin-ichiro[1*] ; SAWAI, Shujiro[1] ; SLIM, Working group[1]

[1]ISAS/JAXA

Small experimental spacecraft ”SLIM” is proposed to demonstrate accurate ”pinpoint” landing technology on a celestial body with gravity. Conventional landing missions, such as Apollo or Chang’e achieved lunar landing with km-order accuracy. Since modern spacecraft provided extensive high-resolution data on the Moon, such as the fruits of SELENE spacecraft, now the place of interest comes to be ”exactly that point”, not ”somewhere on the Moon”. Marius Hill’s Hall (MHH), which is one of the candidates of SLIM landing target, is an interesting vertical hall, for example, and to carry out some exploration on MHH, pinpoint-landing with 100 meter-order accuracy is desired. To enable such 100 meter-order landing accuracy on a celestial body with gravity, several novel technologies has been researched and developed with the effort of SLIM working group members. Practical crater detection and recognition algorithms were proposed for image based guidance system, which can be implemented on an existing space qualified FGPA device. Novel landing radar system was newly developed, and was already evaluated with a bread board model in the field flight test. Detection and avoidance of harmful obstacles around the landing point based on camera image were also researched.

SLIM spacecraft is designed as a small 500 kg-class spacecraft, to pursue lower project cost and shorter development time. To realize lunar lander in this restricted size and weight, unique ideas have been also investigated. Improved ceramic thruster will be applied based on the heritage from AKATSUKI mission, and inherited one is now discussed to be a candidate main thruster for future ESA mission. Propellant tank is designed as a part of spacecraft main structure, to minimize the total weight of SLIM spacecraft. Unique aluminum foam based landing gear is also studied and experimentally demonstrated, and electrical power system is designed with novel ultra-lightweight space solar sheet. Numbers of these engineering researches have been carried out in many universities, and with these efforts, the SLIM is just proposed to the third mission of Epsilon launch vehicle.

SLIM mission is important for its original purpose, to demonstrate the accurate landing technology, and at the same time, key technologies to realize lunar lander in small size and light weight will contribute a lot to the future exploration missions based on Epsilon launcher. In the presentation, the detail of each technology researched and developed by the member of SLIM working group will be introduced, with the result of the system design of SLIM spacecraft. The future perspective on the Epsilon exploration missions based on the SLIM design will be also discussed.

Keywords: Moon and Planetary survey, Lunar landing, Guidance and Navigation for landing, Precise landing, Epsilon Rocket

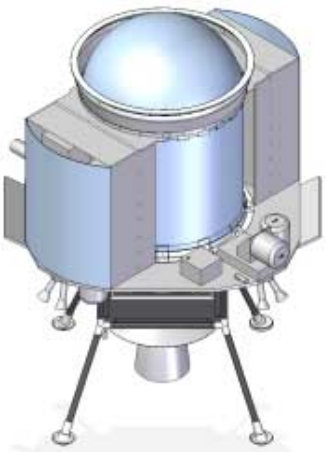

Japan Geoscience Union Meeting 2014
(28 April - 02 May 2014 at Pacifico YOKOHAMA, Kanagawa, Japan)

PPS26-11 Room:418 Time:April 30 12:00-12:15

Proposal for Demonstration of Penetrator Technology by Small Satellite and Epsilon Launch Vehicle

SHIRAISHI, Hiroaki[1*] ; YAMADA, Ryuhei[2] ; ISHIHARA, Yoshiaki[1] ; OGAWA, Kazunori[1] ; OKAMOTO, Taro[3] ; TAKEUCHI, Nozomu[4] ; ISHIHARA, Yasushi[5] ; MURAKAMI, Hideki[6] ; TANAKA, Satoshi[1] ; KOBAYASHI, Naoki[1] ; HAYAKAWA, Masahiko[1] ; HAYAKAWA, Hajime[1] ; ARAYA, Akito[4] ; GOTO, Ken[1] ; MIZUNO, Takahide[1] ; ISHII, Nobuaki[1] ; TSUDA, Yuichi[1] ; HABU, Hiroto[1] ; KAKEHASHI, Yuya[1] ; ISHIMURA, Kosei[1] ; TOKUDOME, Shinichiro[1]

[1]Department of Solar System Sciences, Institute of Space and Astronautical Science, JAXA, Japan, [2]National Astronomical Observatory of Japan, RISE project, [3]Department of Earth and Planetary Sciences, Tokyo Institute of Technology, [4]Earthquake Research Institute, University of Tokyo, [5]IFREE, JAMSTEC, [6]Department of Applied Science,Faculty of Science,Kochi University

A new mission to validate the penetrator technology and to investigate the shallow structure of the Moon, using a small satellite and a penetrator module developed for the former LUNAR-A project is proposed. The lunar penetrator module consists of a penetrator main body, a de-orbit motor and an attitude control system. The de-orbit motor attached at the rear end of the penetrator module is used to cancel the orbital velocity, and the attitude control system which consists of a small gas jet and a sun-sensor is also attached to the central part of the module. The penetrator probe is a missile-shaped instrument carrier and is about 75 cm in length, 14 cm in maximum diameter and about 14 kg in weight. The penetrator contains a two-component seismometer and a heat flow probe, together with electronics, primary batteries, a tiltmeter, an accelerometer, and radio communication system. The primary objective of this mission is to demonstrate the technical issues in penetrator system; (1) holding and separation mechanism, (2) sequence of de-orbit, attitude control and subsurface deployment, (3) data-relay and remote operation by way of an orbital spacecraft, and (4) long-term geophysical observation on the Moon. The flight-proven penetrator system could be applied to the future lunar mission for a full-scale network.

The Epsilon launch vehicle lifts off a spacecraft (or lunar orbiter) with a solid propellant motor newly developed as the upper stage. The spacecraft, which should be play roles of the carrier of penetrator module and of data-relay orbiter, is assumed to revolve in a near-circular orbit of 100-200 km by 25-45 km altitude around the Moon and to release the penetrator module to deploy on the low latitude zone of the lunar nearside or terminator. The penetrator will hit on the lunar surface with a velocity of 270 to 300 m/sec and penetrate into the regolith up to a depth of 2 or 3 meters, and then it will measure the acceleration record and the stop angle at the rest position. These data would be also useful for data reduction of seismic and heat-flow data. After that, it will observe the near-surface and internal structures on the geological unit different from the past Apollo and Luna landers. Ground-based optical telescopes will continuously monitor meteoroid impact flashes on the night side of the Moon, which should frequently occur during the observation period of penetrator seismometer. These landmarks detected in the vicinity of the penetrator will be available for seismological study as known moonquake foci.

This paper describes the spacecraft design, the mission profile from launch to deployment and an operational scenario of geophysical instruments.

Keywords: small satellite, Epsilon rocket, penetrator, seismometer, heat flow probe

Japan Geoscience Union Meeting 2014
(28 April - 02 May 2014 at Pacifico YOKOHAMA, Kanagawa, Japan)

PPS26-12 Room:418 Time:April 30 12:15-12:30

Lunar and planetary explorations in a coming decade: Summary of 4 years and problems remained

NAMIKI, Noriyuki[1*] ; KOBAYASHI, Naoki[2] ; DEMURA, Hirohide[3] ; OHTSUKI, Keiji[4]

[1]PERC/Chitech, [2]Department of Planetary Science, ISAS, [3]The University of Aizu, [4]Kobe University

Future Planetary Exploration Working Group of Japanese Planetary Science Society is discussing next generation of planetary explorations that need to be strongly supported by planetary science community. We started ”Planetary Exploration in a Coming Decade” activity in 2010 aiming to organize a new mission to be launched between 2017 and 2027. The first stage of the activity is ending in March, 2011. A summary of the first stage was reported by 5 panels; (1) terrestrial solid planets, (2) terrestrial atmosphere and magnetosphere, (3) minor body, (4) Jovian planets, icy satellites, and exoplanets, and (5) astrobiology. Each panel received proposals regarding ”top sciences” of each category from the community in the summer of 2010. On September 10 in 2010, an open meeting was held at Kobe University to discuss top sciences among the community of planetary scientists. From the summer of 2011, the second stage began. Proposals for new mission and instruments were submitted by 13 groups and were adivsed by the second-stage committee not only to improve the proposal, but also to raise and develop exploration groups. In 2012 May, the thrid stage started. The main purpose of the third stage is to polish up the proposls in the view of feasibility. In September 14 and 15, 2012, we held a workshop to integrate individual proposals into a few comprehensive mission plans, such as in-situ chronology and interior exploration of the moons and planets, primitive small body exploration, and sercha of life on Mars. The mission concepts of these comprehensive mission plans are now being discussed for later evaluation by the third stage committee. Thsi activity will be closing in the summer of 2014, and the final report will be published in October.

Keywords: moon, planets, exploration, road map

Japan Geoscience Union Meeting 2014
(28 April - 02 May 2014 at Pacifico YOKOHAMA, Kanagawa, Japan)

PPS26-13 Room:418 Time:April 30 12:30-12:45

Approach of the next decade panel

DEMURA, Hirohide[1*]

[1]University of Aizu

Report of the next decade panel.

Keywords: Planetary Science, Space Science, Future Planning, Exploration, Epsilon Launch Vehicle, JAXA

Japan Geoscience Union Meeting 2014
(28 April - 02 May 2014 at Pacifico YOKOHAMA, Kanagawa, Japan)

PPS26-P01 Room:Poster Time:April 30 18:15-19:30

Development and evaluation of heat flow probe for the precise measurement of lunar and planetary heat flow

HORIKAWA, Yamato[1*] ; TANAKA, Satoshi[2] ; SAKATANI, Naoya[1] ; TAKITA, Jun[3]

[1]The Graduate University for Advanced Studies, [2]Japan Aerospace Exploration Agency, [3]The University of Tokyo

The precise measurement of lunar and planetary heat flow contributes to a better understanding of bulk composition and thermal history of the solid bodies. In order to conduct the in situ measurement, a high speed penetration probe, penetrator, which can be buried into a depth of 1 to several meters, has been developed. Since the shock durability at the penetration and the weight saving are required prior to scientific measurements, the heat flow sensors are installed on the surface of the penetrator. However, the sensors must have an uncertainty by disturbances of temperature distribution around the penetrator due to a large difference of thermal conductivities between the penetrator and the surrounding regolith.

In this study, we propose to develop an extension mechanism of needle probes from the buried penetrator which can avoid the thermal disturbance and measure heat flux with an uncertainty better than 10%. The temperature sensing part is required to be placed at a distance as far as possible from the penetrator body. Although the theoretical solution has been obtained to estimate thermal conductivity of the particulate material at the tip part of the probe, no research has yet been carried out to measure thermal conductivity of regolith by the needle probes whose temperature sensing parts are at the tip part. We developed a prototype model of the probe and evaluated the measurement uncertainty of thermal conductivity of glass beads as the regolith simulant material under vacuum condition.

The prototype of the needle probe consists of a wire heater, a K-type thermocouple, a stainless pipe as the needle probe's sheath, and epoxy resin fixing the heater and the thermocouple in the pipe. The length of the probe is 10cm which is the equivalent size of inner diameter of the penetrator body. Thermal conductivity of the glass beads under 200Pa can be controlled to be about 0.02W/m/K, which is almost the same thermal conductivity of the lunar environment at a depth of 1 to several meters. The needle probe was placed at the center of the sample container and surrounded by three sets of line heat source conductivity sensors for reference calibration.

Under 200Pa, we obtained 0.0165W/m/K by the theoretical solution of the probe, and 0.0207W/m/K by the average values of three line heat source sensors. The measurement uncertainty of thermal conductivity by the probe was calculated to be about 31%. However, the thermal conductivity by the probe can't be estimated directly from the theoretical solution because the conditions of the solution differ from the properties of the actual probe, such as the diameter of the probe, the thermal contact between the probe and the glass beads, and the axial heat flow of the probe. Therefore, we conducted the heat-transfer simulation whose numerical model included the properties of the actual probe, and estimated the thermal conductivity by the probe from increases in temperature after heating of the simulation. In addition, we confirmed an agreement with the temperature profiles of the theory and the simulation whose model condition was the same as the condition of the theory.

As a result, the thermal conductivity by the probe was estimated to be 0.0212W/m/K, and the measurement uncertainty of thermal conductivity was calculated to be about 3%, which was well satisfied with the requirement uncertainty of better than about 5%. In future, in order to estimate thermal conductivity of the regolith in lunar and planetary surface layer by using our probe, the measurement uncertainties are required to determine for the probable thermal conductivities by using the heat-transfer simulation.

Keywords: heat flow, thermal conductivity, moon, planet, penetrator, needle probe

Japan Geoscience Union Meeting 2014
(28 April - 02 May 2014 at Pacifico YOKOHAMA, Kanagawa, Japan)

PEM04-01 Room:311 Time:April 28 11:00-11:15

ERG project

MIYOSHI, Yoshizumi[1*] ; TAKASHIMA, Takeshi[2] ; ASAMURA, Kazushi[2] ; SHIOKAWA, Kazuo[1] ; SEKI, Kanako[1] ; SHOJI, Masafumi[1] ; SHINOHARA, Iku[2] ; HIRAHARA, Masafumi[1] ; HIGASHIO, Nana[2] ; MATSUMOTO, Haruhisa[2] ; KASAHARA, Satoshi[2] ; MITANI, Takefumi[2] ; KASABA, Yasumasa[3] ; MATSUOKA, Ayako[2] ; KOJIMA, Hirotsugu[4] ; FUJIMOTO, Masaki[2] ; ONO, Takayuki[3]

[1]STEL, Nagoya University, [2]JAXA, [3]Graduate School of Science, Tohoku University, [4]RISH, Kyoto University

The ERG (Exploration of energization and Radiation in Geospace) is Japanese geospace exploration project. The project focuses on relativistic electron acceleration mechanism of the outer belt in the context of the cross-energy coupling via wave-particle interactions. The project consists of the satellite observation team, the ground-based network observation team, and integrated-data analysis/simulation team. The ERG satellite will be launched in FY2015. Comprehensive instruments for plasma/particles, and field/waves are installed in the ERG satellite to understand the cross-energy coupling system. In the ERG project, several ground-network teams join; magnetometer networks, radar networks, optical imager networks, etc. Cooperative observations between the in-situ satellite and ground-based observations are important. Some simulation codes including both macro-scale phenomena and micro-physics are developed in Japan, which are very helpful quantitatively to understand the observational results and to incorporate the observations. In this presentation, the overview of the projects will be presented and possible collaborations with other geospace satellite missions as well as the ground-based observations will be discussed.

Keywords: ERG project, inner magnetosphere, future mission

Japan Geoscience Union Meeting 2014
(28 April - 02 May 2014 at Pacifico YOKOHAMA, Kanagawa, Japan)

PEM04-02 Room:311 Time:April 28 11:15-11:35

Upper Atmosphere phenomena in Geomagnetic Anomaly Region in association with Magnetosphere Disturbances

MAKITA, Kazuo[1*]

[1]Takushoku University

Since 1999, we continuously study/observe upper atmosphere phenomena in Geomagnetic Anomaly Region (South Atlantic Anomaly: SAA) by using several equipments and obtained several interesting results. We show several remarkable phenomena in SAA on the basis of imaging riometer data and CCD imager data obtained at Southern Space Observatory (SSO; 29.4S, 307E) in Brazil and other stations.

(1) Particle precipitation in SAA seems to be related with polar disturbances. From imaging riometer data, enhancement of Cosmic Noise Absorption (CNA) occurs simultaneously with magnetic disturbances in polar region. On the other hand, CNA at Kakioka imaging riometer can be also seen during polar disturbance (not so frequently observed). It may suggest that particle precipitations are occurred in association with substorm at Kakioka as well as SAA.

(2) In sometimes, strong CNA is observed in association with sharply decreasing of electron flux (GOES satellite data) after moderate polar disturbance period. It may indicate that injection and drifting of electrons after polar disturbances precipitate in SAA during this period.

(3) It is well known that VLF waves trigger precipitation of radiation belt particles.

Although the longitudinal difference is 94 degrees (6 hours local times) between Syowa Station, Antarctica and SSO, CNA at SSO is nearly simultaneously observed with VLF emissions at Syowa Station. It may suggest that particles are more easily precipitating and observed in SAA through the wave particle interactions in radiation belt.

(4) Static multiple bands are singularly observed at SSO. The characteristics of static multiple bands are different from atmospheric gravity waves. They are fixed at the ground and rotate with earth rotation. This phenomena is very seldom and looks like occurs in winter season. The luminosity of these phenomena are not clear but less than 150R like airglow level..

We almost finished to construct South America Riometer Network (SARINET; 7 stations) and hope to collect data continuously during one solar cycle.

Keywords: South Atlantic Geomagnetic Anomaly, Cosmic noise absorption, Imaging riometer, Radiation belt, Airglow

South America Riometer Net work (SARINET)

Japan Geoscience Union Meeting 2014
(28 April - 02 May 2014 at Pacifico YOKOHAMA, Kanagawa, Japan)

PEM04-03 Room:311 Time:April 28 11:35-11:55

Loss of geosynchronous relativistic electrons by EMIC waves during quiet geomagnetic conditions

KIM, Khan-hyuk[1*] ; HYUN, Kiho[1] ; LEE, Ensang[1] ; LEE, Dong-hun[1]

[1]School of Space Research, Kyung Hee University, Gyeonggi, Korea.

We have examined relativistic electron flux losses at geosynchronous orbit under quiet geomagnetic conditions. Two 3-day periods, from 11 to 13 October and from 29 November to 1 December, in 2007 were chosen for analysis because geomagnetic conditions were very quiet (3-day average of Kp $<$1) and significant losses of geosynchronous relativistic electrons were observed. During both intervals, there were no geomagnetic storm activities. Thus, the loss processes associated with geomagnetic field modulations caused by ring current buildup can be excluded. The flux of geosynchronous relativistic electrons with energy $>$2 Mev shows typical diurnal variations with a maximum near noon and a minimum near midnight for each day. The flux level of the daily variation gradually decreased from first day to third day for each 3-day period. The total magnetic field strength (Bt), however, is relatively constant for each day. Unlike electron flux decreases, the flux of protons with energy between 0.8 and 4 MeV adiabatically responses to the daily variation of Bt. That is, there is no significant decrease of the proton flux when the electron flux decreases. During both 3-day periods, well-defined electromagnetic ion cyclotron (EMIC) waves were detected at geosynchronous spacecraft. Low-altitude polar orbiting spacecraft observed the precipitation of energetic electrons and protons in the interval of EMIC waves enhancement. From these observations, we suggest that the EMIC waves are a major factor to control the electron flux decrease under quiet geomagnetic conditions.

Keywords: Relativistic electron flux, geosynchronous orbit, EMIC waves

Japan Geoscience Union Meeting 2014
(28 April - 02 May 2014 at Pacifico YOKOHAMA, Kanagawa, Japan)

PEM04-04 Room:311 Time:April 28 11:55-12:10

Characteristics of dayside SAPS structures observed by the SuperDARN Hokkaido radar

NISHITANI, Nozomu[1*] ; HORI, Tomoaki[1] ; NAGANO, Hiroki[1]

[1]Solar-Terrestrial Environment Laboratory, Nagoya University

Sub-Auroral Polarization Streams (SAPS) are intense westward ionospheric flows in the subauroral ionosphere, and considered to be generated as a result of magnetosphere-ionosphere coupling during relatively disturbed periods. SAPSs are usually located in the evening to midnight sector, but occasionally it extends to earlier magnetic local times close to local noon. Owing to limitation of the observation techniques, no detailed studies of its local time extent have been made so far. In this study we use the data from the SuperDARN Hokkaido radar, one of the midlatitude SuperDARN radars located at the lowest geomagnetic latitude, to discuss the detailed characteristics of dayside SAPS, with focus on their relation to solar wind and geomagnetic parameters.

Keywords: dayside, SAPS, SuperDARN, Hokkaido radar, magnetosphere, ionosphere

Japan Geoscience Union Meeting 2014
(28 April - 02 May 2014 at Pacifico YOKOHAMA, Kanagawa, Japan)

PEM04-05 Room:311 Time:April 28 12:10-12:25

Amplification of EMIC waves by Pc3-4 waves

NOMURA, Reiko[1*] ; KEIKA, Kunihiro[2] ; TERAMOTO, Mariko[4] ; KLETZING, Craig[3]

[1]IGEP, TU Braunschweig, [2]Solar-Terrestrial Environment Laboratory, Nagoya University, [3]Japan Aerospace Exploration Agency, [4]Department of Physics and Astronomy, The University of Iowa

Electromagnetic ion cyclotron (EMIC) wave is one of the key phenomena for the dynamics of high energy electrons in the radiation belt, since EMIC waves can scatter particles and make them precipitate into the ionosphere from the inner magnetosphere. The EMFSIS of Van Allen Probes observed the proton-band EMIC wave with the frequencies 2-6Hz at ∼3RE in the GSM coordinates at 1110-1140UT on 29 June 2013. It was during the recovery phase of the magnetic storm started on 27 June. This event has significant enhancements of wave amplitudes up to ∼10nT at 1123 and 1130UT. At these times, the magnetic field variations in the Pc3-4 range are also observed. We present the relation between amplitudes of EMIC waves and Pc3-4 wave occurrences, and discuss the amplification mechanism of EMIC waves by ULF waves with longer periods.

Keywords: EMIC waves, Pc3-4

Japan Geoscience Union Meeting 2014
(28 April - 02 May 2014 at Pacifico YOKOHAMA, Kanagawa, Japan)

PEM04-06 Room:311 Time:April 28 12:25-12:40

Study of Pc1 pearl structures observed at multi-point ground stations at Russia, Japan and Canada

JUN, Chae-woo[1*] ; SHIOKAWA, Kazuo[1] ; SCHOFIELD, I.[2] ; CONNORS, M.[2] ; PODDELSKY, I.[3] ; SHEVTSOV, B.[3]

[1]Solar-Terrestrial Environment Laboratory, Nagoya University, Nagoya, Japan, [2]Center for Science, Athabasca University, Athabasca, Canada, [3]Institute of Cosmophysical Research and Radiowave Propagation, Far Eastern Branch of the Russian Aca

We have investigated possible generation mechanisms of pearl structures of Pc1 geomagnetic pulsations using ground-based multi-point induction magnetometers at Athabasca in Canada, at Magadan in Russia and at Moshiri in Japan. During 3-years of observation (January 1, 2009 to December 31, 2011), we found two Pc1 pulsations with similar dynamic spectrum shapes at three stations simultaneously. For the case 1, which occurred on April 8, 2010, Pc1 pulsations were clearly identified at the three stations in the frequency range of 0.4 to 1.2 Hz. Coherence between the two stations was high ($r > 0.8$). The cross-correlation of the upper envelope of Pc1 waves between the ATH and the MGD, which indicates amplitude modulation of Pc1 due to pearl structures, was also high ($r > 0.8$). In some time interval during the case 1, however, correlation decreased down to 0.5. The case 2 occurred on April 11, 2010 in the frequency range of 0.2 to 0.8 Hz showed that the coherence and cross-correlation between ATH and MGD were both high ($r > 0.8$) throughout the event. The high coherence indicates that the Pc1 pulsations observed at these different stations were propagated from the same source region. However, in case 1, the Pc1 pearl structures were slightly different for different stations. The case 1 showed polarization angle variation depending on frequencies, while the case 2 does not show such dependence, suggesting that the case 1 has a spatially-distributed ionospheric source at high latitudes. In order to understand these different features of Pc1 pearl structures, we made two model calculations of Pc1 peal structures under the different conditions. One model is that the Pc1 waves come from a north-south extended ionospheric source region with slightly different frequencies at different latitudes. This source distribution, causes the Pc1 pearl structure by beating during the duct propagation in the ionosphere. The other model is that the Pc1 waves with different frequencies are mixed at the point source in the ionosphere, assuming that the pearl structures were already made in the magnetosphere. The Pc1 from the point source shows an identical waveform among the different stations. On the other hand, the Pc1 from distributed source region shows slightly different waveforms at different stations. This result suggests that the distributed source region is able to create the different Pc1 pearl structures at different stations through the beating, as observed for the case 1. We conclude that the Pc1 pearl structures are created by both magnetospheric processes and ionospheric beating processes before they reach the ground-based magnetometer at low latitudes.

Keywords: Pc1 pulsation, Pearl structures, multi-point ground observations

Japan Geoscience Union Meeting 2014
(28 April - 02 May 2014 at Pacifico YOKOHAMA, Kanagawa, Japan)

PEM04-07 Room:311 Time:April 28 14:15-14:35

Gradual Diffusion and Punctuated Enhancements of Highly Relativistic Electrons: Van Allen Probes Observations

BAKER, Daniel N.[1*]

[1]University of Colorado Boulder

The dual-spacecraft Van Allen Probes mission has provided a new window into megaelectron Volt (MeV) particle dynamics in the Earth′ s radiation belts. Observations (up to E ˜10 MeV) show clearly the behavior of the outer electron radiation belt at different time scales: months-long periods of gradual inward radial diffusive transport and weak loss being punctuated by dramatic flux changes driven by strong solar wind transient events. Analysis of multi-MeV electron flux and phase space density (PSD) changes during March 2013 are presented in the context of the first year of Van Allen Probes operation. This March period demonstrates the classic signatures both of inward radial diffusive energization as well as abrupt localized acceleration deep within the outer Van Allen zone (L ˜4.0±0.5). This reveals graphically that both ″ competing ″ mechanisms of multi-MeV electron energization are at play in the radiation belts, often acting almost concurrently or at least in very rapid succession. It also shows in remarkable ways how the coldest plasmas in the magnetosphere intimately control the most highly energetic particles.

Keywords: Van Allen Probes, Radiation belts, Solar wind, Electron energization

Japan Geoscience Union Meeting 2014
(28 April - 02 May 2014 at Pacifico YOKOHAMA, Kanagawa, Japan)

PEM04-08 Room:311 Time:April 28 14:35-14:55

Particle Acceleration in Kinetic Eigenmodes from the Van Allen Probes

CHASTON, Christopher[1*] ; BONNELL, John[2] ; WYGANT, John[3] ; KLETZING, Craig[4] ; MOZER, Forrest[2] ; BALE, Stuart[2] ; KURTH, William[4] ; HOSPARDARSKY, George[4] ; KERSTEN, Kris[3] ; BRENEMAN, Aaron[3] ; SMITH, Charles[5] ; MACDONALD, Elizabeth[6]

[1]School of Physics, University of Sydney, Sydney, NSW, Australia, [2]Space Sciences Laboratory, University of California, Berkeley, CA, USA, [3]School of Physics and Astronomy, University of Minnesota, Minneapolis, MN, USA, [4]Department of Physics and Astronomy, University of Iowa, Iowa City, IA, USA, [5]Department of Physics and IEOS, University of New Hampshire, Durham, NH, USA, [6]Los Alamos National Laboratory, Los Alamos, NM, USA

The Van Allen Probes have revealed the presence of a broad spectrum of narrow scale Alfvén eigenmodes in the inner magnetosphere during geomagnetic storms. Here we use observations from the Van Allen Probes to build a reduced MHD model for these waves in a dipolar geomagnetic field. This model is then used to explore the manner through which particles may be accelerated in these wavefields. Test particle simulations show that the narrow perpendicular scale and parallel electric fields carried by these waves lead to the violation of the 1st and 2nd adiabatic invariants for ions. This can drive the heating of the thermal ion population to multi-keV temperatures and the acceleration of a small fraction of these particles to energies exceeding 100 keV. This process has obvious implications for the storm time ring current, but also for the acceleration/loss of radiation belt electrons.

Keywords: Particle acceleration, Alfven waves, van allen probes, field lines resonances, ring current, radiation belts

Japan Geoscience Union Meeting 2014
(28 April - 02 May 2014 at Pacifico YOKOHAMA, Kanagawa, Japan)

PEM04-09 Room:311 Time:April 28 14:55-15:10

Van Allen Probes observations of oxygen torus in the inner magnetosphere

NOSE, Masahito[1*] ; KEIKA, Kunihiro[2] ; KLETZING, C. A.[3] ; SMITH, C. W.[4] ; MACDOWALL, R. J.[5] ; KURTH, W. S.[3] ; DE PASCUALE, S.[3]

[1]Graduate School of Science, Kyoto University, [2]Solar-Terrestrial Environment Laboratory, Nagoya University, [3]Department of Physics and Astronomy, University of Iowa, [4]Institute for the Study of Earth, Oceans and Space, University of New Hampshire, [5]NASA Goddard Space Flight Center

The oxygen torus is found in the deep inner magnetosphere as enhancements of O^+ ion density in a limited L range. It was first reported by Chappell [1982] who used the DE-1/RIMS instrument. Horwitz et al. [1984, 1986] showed that the O^+ density sometimes becomes comparable to or exceeds the H^+ density at L=3-4. Following studies revealed that the oxygen torus is observed just inside the plasmasphere at all local time with higher occurrence frequency in the late evening and morning sectors. A recent study by Nosé et al. [2010] cast a new light on the oxygen torus as a one of essential factors of O^+-rich ring current generation. They proposed that thermal O^+ ions preexisting in the oxygen torus are locally and nonadiabatically accelerated by fluctuations associated with dipolarization in the deep inner magnetosphere and contribute to ring current O^+ ions. Therefore investigation of the oxygen torus is important to understand the dynamics of ions of ionospheric origin in the inner magnetosphere.

We study the oxygen torus, using the magnetic field and plasma wave data obtained by the Electric and Magnetic Field Instrument Suite and Integrated Science (EMFISIS) instrument onboard the Van Allen Probes. We examine a few events on the dawnside in which toroidal standing Alfven waves appear clearly. From the frequency of the toroidal waves, the magnetospheric local mass density (ρ) is estimated by solving the MHD wave equation for realistic models of the magnetic field and the field line mass distribution. We also estimate the local electron number density (n_e) from the plasma wave spectrograms by identifying narrow-band emission at the upper-hybrid resonance frequency. Assuming the quasi-neutral condition of plasma, we infer the local average ion mass (M) by ρ/n_e. It is found that M is generally less than 4 amu in the plasma trough, while it shows an enhancement of $>$6 amu near the plasmapause. This indicates an existence of the oxygen torus in the vicinity of the plasmapause. We will present the result and discuss possible formation mechanisms of the oxygen torus. Possible contribution of the oxygen torus to the formation of the O^+-rich ring current will be also discussed.

Japan Geoscience Union Meeting 2014
(28 April - 02 May 2014 at Pacifico YOKOHAMA, Kanagawa, Japan)

PEM04-10 Room:311 Time:April 28 15:10-15:25

Akebono observations of EMIC waves in the slot region of the radiation belts

SAKAGUCHI, Kaori[1*] ; KASAHARA, Yoshiya[2] ; SHOJI, Masafumi[3] ; OMURA, Yoshiharu[4] ; MIYOSHI, Yoshizumi[3] ; NAGATSUMA, Tsutomu[1] ; KUMAMOTO, Atsushi[5] ; MATSUOKA, Ayako[6]

[1]National Institute of Information and Communications Technology, [2]Information Media Center, Kanazawa University, [3]Solar-Terrestrial Environment Laboratory, Nagoya University, [4]Reserach Institute for Sustainable Humanosphere, Kyoto University, [5]Department of Geophysics, Graduate School of Science, Tohoku University, [6]Institute of Space and Astronautical Science, Japan Aerospace Exploration Agency

We present a unique observation of electromagnetic ion cyclotron (EMIC) waves in the deep inner magnetosphere at L = 2.5-5 made by the Akebono satellite at altitudes of 3,300-8,700 km. The mode conversion, i.e., L mode (He+ band)→R mode (He+ band)→L mode (O+ band) was clearly identified from the equator to high latitudes. In addition, we found rising tone structures, recently identified as EMIC triggered emissions, which could lead to bursty precipitation of relativistic electrons. First, we estimated the ion composition ratio (H+, He+, O+) = (83%, 16%, 1%) from polarization analysis. Second, we estimated minimum resonant electron energies with the observed EMIC waves and triggered emissions to be 1?10 MeV. The satellite trajectory during the wave observation was primarily through the slot region of electron radiation belts. The collocation implies possible contribution of EMIC waves to formation of the slot region of radiation belts after a magnetic storm.

Keywords: EMIC wave, slot region of the radiation belt, mode conversion, triggered emission, ion compotision ratio, Akebono satellite

Japan Geoscience Union Meeting 2014
(28 April - 02 May 2014 at Pacifico YOKOHAMA, Kanagawa, Japan)

PEM04-11 Room:311 Time:April 28 15:25-15:40

Oxygen ion acceleration and transport in the near-Earth plasma sheet during an isolated substorm

NAKAYAMA, Yohei[1*] ; EBIHARA, Yusuke[1] ; TANAKA, Takashi[2]

[1]Research Institute for Sustainable Humanosphere (RISH), Kyoto university, [2]SERC, Kyushu University

Rapid enhancements of energetic ions during a substorm are one of the unsolved issues in the inner magnetospheric research (<7 Re). Previously, two distinct processes have been suggested to explain the enhancements. The first one is transport from the near-earth plasma sheet, and the other one is local acceleration. To test the both process, we performed test particle simulation under the electric and magnetic fields that are self-consistently obtained by the global MHD simulation developed by Tanaka et al. (2010, JGR). Oxygen ions are released in the lobe region with an interval of 1 minutes. The distribution function in the lobe is assumed to be drifting Maxwellian. The temperature is assumed to be 20 eV, the density is 105 cm-3, and the parallel velocity is given by the MHD simulation. In total, a few hundreds of millions of particles are traced. Each test particle carries the real number of particles in accordance with the Liouville theorem. After tracing particles, we reconstruct 6-dimensional phase space density of the oxygen ions, as well as the directional differential number flux so as to be able to make a direct comparison with in-situ satellite observations. Just after a substorm onset, the differential flux of the ions is rapidly enhanced in the energy range from 50 to 150 keV at radial distance R greater than 7 on the nightside in the equatorial plane. The region of the enhanced flux propagates duskward, then to dayside because of grad-B and curvature drift of the ions. We also plotted energy versus time spectrograms of the differential flux at a fixed position to make a direct comparison with the CRRES satellite observation. At 7.2 Re and at 22.4 MLT, the ion flux is suddenly enhanced about 10 minutes after the onset. The enhancement appears first at 120 keV, followed by lower energy as time proceeds. The energy-time dispersion is similar to that observed by CRRES [Fu et al., 2002]. The steepness of the energy-time dispersion depends on the source location of the ions. After a while, a high energy ion flux appears first, followed by that at lower energies. This is a called a drift echo, arising from the ions that encircled the Earth by the grad-B and curvature drift. We will discuss the acceleration processes in more detail, the role of pre-existing ions, and the total kinetic energy of the oxygen ions and its dependence on the source distribution function in terms of the ring current development.

Reference:

Fu, S. Y., Q. G. Zong, T. A. Fritz, Z. Y. Pu, and B. Wilken, Composition signatures in ion injections and its dependence on geomagnetic conditions, J. Geophys. Res, 107(A10), 1299, doi:10.1029/2001JA002006, 2002.

Tanaka, T., A. Nakamizo, A. Yoshikawa, S Fujita, H. Shinagawa, H. Shimizu, T. Kikuchi, and K. K. Hashimoto, Substorm convection and current system deduced from the global simulation, J. Geophys. Res. 115, A05220, doi:10.1029/JA014676, 2010.

Japan Geoscience Union Meeting 2014
(28 April - 02 May 2014 at Pacifico YOKOHAMA, Kanagawa, Japan)

PEM04-12 Room:311 Time:April 28 15:40-15:55

On the formation of overshielding triggered by a substorm onset: Global MHD simulation study

EBIHARA, Yusuke[1*] ; TANAKA, Takashi[2] ; KIKUCHI, Takashi[3]

[1]RISH, Kyoto Univerisity, [2]Emeritus Professor, Kyushu University, [3]Emeritus Professor, Nagoya University

The dawn-dusk convection electric field is a significant driver of transport of charged particles in the inner magnetosphere. When the dawn-disk convection electric field is enhanced, the ring current is developed, and the plasmasphere is shrunk. Ground-based observations have shown that, sometimes, the polarity of the convection electric field is reversed after a substorm onset. The presence of the dusk-dawn electric field is called an overshielding condition. Here, we demonstrate that the overshielding condition can appear after a substorm onset on the basis of a global MHD simulation. Immediately after the substorm onset manifested by a sudden decrease in the AL index and auroral brightening, the plasma pressure is enhanced in the inner magnetosphere. The simulated magnetic field on the ground shows a negative excursion in the polar cap, a positive excursion at auroral latitudes, and a negative excursion at sub-auroral latitudes at dusk. At noon and at equator (0 MLAT), the eastward electrojet starts to decrease just after the onset, and the westward electrojet appears about 10 min after the onset. All these variations are consistent with the observations. We discuss generation mechanisms, evolution of the overshielding condition in the ionosphere and the magnetosphere, and the redistribution of the charged particles trapped in the inner magnetosphere during the overshielding condition on the basis of the simulation solving drift transport equations.

Japan Geoscience Union Meeting 2014
(28 April - 02 May 2014 at Pacifico YOKOHAMA, Kanagawa, Japan)

PEM04-13 Room:311 Time:April 28 16:15-16:30

Nonlinear wave particle interactions in oblique whistler-mode chorus emissions

NUNN, David[2] ; OMURA, Yoshiharu[1*]

[1]RISH, Kyoto University, [2]ECS School, Southampton University

The highly nonlinear phenomena of VLF chorus and triggered VLF emissions are of great interest due to their role in electron heating and precipitation, and are widely believed to be due to nonlinear cyclotron resonance between the narrow band wavefield and the anisotropic energetic electron population (∼keV), the dominant mechanism being identified as nonlinear phase trapping. Considerable advances have been made in the theory and numerical simulation by assuming parallel (ducted) propagation [Nunn et al., 1997, 2009;Omura et al., 2008, 2009; Omura and Nunn, 2011]. Here we address the important issue of nonlinear wave particle interaction in oblique VLF wavefields. The treatment is of necessity non self-consistent. The narrow band wavefield is arbitrarily, but here chosen to be a CW field or a sophisticated model of a VLF chorus element based upon the theory of Omura et al.[2008, 2009]. We develop the electron equations of motion and then by backward trajectory integration compute resonant particle distribution function , resonant currents and thus local nonlinear growth rates. This may be done for any resonance order n and any field. As shown in Omura et al. [2008] nonlinear trapping for n=1 cyclotron resonance gives rise to a phase space hole in distribution function at the trap. Such a hole is also noted at higher order resonances (e.g. n=2) for sufficient wave amplitude and obliquity. For n=1 we find a marked saturation effect due to adiabatic effects, growth maximising at about 25pT and 2000km from the equator. For moderate obliquity ϑ<20 degrees the n=1 resonance is relatively unaffected but growth rolls off sharply at high obliquity. For the n=0 resonance for obliquity ϑ >20 degrees nonlinear trapping may occur giving a peak in phase space density. As trapped electrons are moving away from the equator adiabatic effects do not occur and maximum damping rates are at ∼6000kms and at obliquities ∼55 degrees. For the lower band rising chorus element model maximum n=1 growth is close to the equator, but maximum n=0 damping is found at the top of the frequency band at ∼10000km downstream. Due to the coincidence of group and resonance velocities particles may be trapped near the equator and dragged a long way before detrapping.

References

Nunn, D., Y. Omura, H. Matsumoto, I. Nagano, and S. Yagitani (1997), The numerical simulation of VLF chorus and discrete emissions observed on the Geotail satellite using a Vlasov code, J. Geophys. Res., 102, 27,083?27,097.

Nunn, D., O. Santolik, M. Rycroft, and V. Trakhtengerts (2009), On the numerical modelling of VLF chorus dynamical spectra, Ann. Geophys., 27, 2341?2359.

Y. Omura,Y. Katoh, and D. Summers (2008), Theory and simulation of the generation of whistler-mode chorus, J. Geophys. Res., 113, A04223.

Y. Omura, , M. Hikishima, Y. Katoh, D. Summers, and S. Yagitani (2009), Nonlinear mechanisms of lower band and upper band VLF chorus emissions in the magnetosphere, Journal Geophysical Research, 114, A07217.

Omura, Y., and D. Nunn (2011), Triggering process of whistler mode chorus emissions in the magnetosphere, J. Geophys. Res., 116, A05205.

Keywords: whistler wave, wave-particle interaction, simulation, nonlinear, inner magnetosphere, chorus emissions

Japan Geoscience Union Meeting 2014
(28 April - 02 May 2014 at Pacifico YOKOHAMA, Kanagawa, Japan)

PEM04-14 Room:311 Time:April 28 16:30-16:45

Relativistic electron microbursts induced by EMIC triggered emissions in the dipole magnetic field

KUBOTA, Yuko[1*] ; OMURA, Yoshiharu[1]

[1]Research Institute for Sustainable Humanosphere, Kyoto University

We perform test particle simulations of relativistic electrons interacting with electromagnetic ion cyclotron (EMIC) triggered emissions with rising-tone frequencies. We assume that the geomagnetic field is dipole because EMIC triggered emissions and radiation belt electrons are observed in the inner magnetosphere [1]. EMIC triggered emissions are generated by energetic protons injected into the inner magnetosphere and drifting westwards in the longitudinal direction. We study trajectories of relativistic electrons drifting eastwards interacting with EMIC triggered emissions over different longitudinal ranges. When relativistic electrons in the radiation belt interact with EMIC triggered emissions, some of them are trapped by a wave potential and efficiently guided down to lower pitch angles. Repeated interactions result in scattering of relativistic electrons into the loss cone [2]. Counting relativistic electrons which fall into the polar region, we find that half of the relativistic electrons interacting with EMIC triggered emissions are precipitated. We derive conditions of kinetic energies and pitch angles for efficient precipitation of relativistic electrons.

References

[1] Pickett, J. S., et al. (2010), Cluster observations of EMIC triggered emissions in association with Pc1 waves near Earth's plasmapause, Geophys. Res., 37, L09104.

[2] Omura, Y., and Zhao, Q., (2013), Relativistic electron microbursts due to nonlinear pitch-angle scattering by EMIC triggered emissions, J.Geophys.Res., 118, 5008-5020.

Japan Geoscience Union Meeting 2014
(28 April - 02 May 2014 at Pacifico YOKOHAMA, Kanagawa, Japan)

PEM04-15 Room:311 Time:April 28 16:45-17:00

Investigating the upper and lower energy cutoffs of EMIC-wave driven precipitation events

HENDRY, Aaron[1*] ; RODGER, Craig[1] ; CARSON, Bonar[1] ; CLILVERD, Mark[2] ; RAITA, Tero[3]

[1]University of Otago, New Zealand, [2]British Antarctic Survey, UK, [3]SGO, Sodankyla, Finland

For some time theoretical modelling has shown that electromagnetic ion cyclotron (EMIC) waves should play an important role in the loss of relativistic electrons from the radiation belts, through precipitation of the electrons into the polar ionosphere. However, there are limited direct experimental observations of relativistic electron precipitation occurring, despite the indirect evidence for its importance.

Relativistic electron resonance takes place through ”anomalous resonance” where the electron overtakes the wave. Until recently, it was through that EMIC wave scattering interactions were limited to electrons with energies greater than 1-2 MeV. Recent theoretical modelling [Omura et al., JGR, 2012] has suggested that this lower limit may be as small as 100 keV when considering EMIC waves more like those experimentally observed (i.e. non-constant frequency which ramps with time on one second timescales). Using data from the POES satellites we confirm the presence of lower energy ($<$1 MeV) electron precipitation most likely driven by EMIC waves.

We report on a continuing study that determines the typical flux impacting the ionospheric D-region during EMIC-driven precipitation events, and the effect this has on ionospheric conditions. We examine a very large set of EMIC-driven electron precipitation events detected using data from the POES satellite constellation [Carson et al., JGR, 2013] and determine the typical precipitating electron and proton fluxes.

As part of this study, we investigate the response of the MEPED instruments on-board the POES satellites to better characterise the EMIC-driven precipitation. Using the results of a previously reported Monte-Carlo simulation of the MEPED electron and proton telescopes [Yando et al., JGR, 2011], we characterise the typical energy range and flux for both the precipitating electrons and protons observed in these events. We go on to show that such events will produce very significant D-region changes detectable using the ground-based Antarctic-Arctic Radiation-belt (Dynamic) Deposition - VLF Atmospheric Research Konsortium (AARDDVARK) worldwide VLF receiver network.

Keywords: EMIC waves, electron precipitation, POES spacecraft, AARDDVARK, radiation belts, particle precipitation

Japan Geoscience Union Meeting 2014
(28 April - 02 May 2014 at Pacifico YOKOHAMA, Kanagawa, Japan)

PEM04-16 Room:311 Time:April 28 17:00-17:15

Plasmaspheric Content as Revealed by Spaceborne GPS Observations

TSAI, Ho-fang[1*] ; CHOU, Min-yang[1] ; CHEN, Chao-yen[2] ; LIN, Charles[1] ; LIU, Jann-yenq[2]

[1]Dept. of Earth Sciences, National Cheng Kung University, Taiwan, [2]Institute of Space Science, National Central University, Taiwan, [3]National Space Organization, Taiwan

The FORMOSAT-3/COSMIC (F3/C) mission has been operating for more than seven years. The F3/C low earth orbit (LEO) satellites receive the signals from the global positioning system (GPS) for sounding of the atmosphere and the ionosphere of the earth, including the plasmasphere. The plasmasphere above ionosphere acts like a reservoir; it takes plasma from the ionosphere by day, stores it in a loss-free environment, and returns it to the ionosphere at night. For the non-radio occultation observation of the F3/C, we study the morphology of the plasmaspheric electron content (PEC) derived from F3/C raw observation data, which includes the diurnal variations of the time-series PEC, two-dimensional distribution and the interaction with the ionosphere.

Keywords: plasmasphere, FORMOSAT-3/COSMIC, GPS

Japan Geoscience Union Meeting 2014
(28 April - 02 May 2014 at Pacifico YOKOHAMA, Kanagawa, Japan)

PEM04-17 Room:311 Time:April 28 17:15-17:30

Polarization and occurrence statistics of VLF/ELF chorus waves at sub-auroral latitudes at Athabasca, Canada.

MARTINEZ CALDERON, Claudia[1*] ; SHIOKAWA, Kazuo[1] ; MIYOSHI, Yoshizumi[1] ; OZAKI, Mitsunori[2] ; SCHOFIELD, Ian[3] ; CONNORS, Martin[3]

[1]Solar-Terrestrial Environment Laboratory, Nagoya University, Nagoya, Japan, [2]Kanazawa University, Kanazawa, Japan, [3]Athabasca University, Athabasca, Canada

Chorus waves are whistler-mode emissions in the very low frequency (VLF) range that are one of the most intense and common natural emissions. They are generated in the inner magnetosphere at the geomagnetic equator and follow the geomagnetic field lines into the ionosphere and the ground. They are believed to be *one of the major contributions to the acceleration and scattering of radiation belt particles* (e.g., Inan et al., 1982; Omura et al., 2007). Consequently we are interested in the *spatial and temporal motion of the acceleration region of radiation belt electrons*, which might be directly linked to the motion of the Ionospheric footprints of VLF/ELF waves.

For a period of 9 days, from February 17 to 25, 2012, the VLF-CHAIN campaign observed VLF/ELF emissions at sub-auroral latitudes using two loop antennas at Athabasca (MLAT=61.31, L=4.3) and Fort Vermillion (MLAT=64.51, L=5.4), Canada.

Several interesting features of chorus emissions have been observed such as quasi-periodic emissions, falling-tone and rising-tone chorus, as well as *Bursty-Patch* emissions. We have applied polarization and spectral analysis to make **the first comprehensive study of the physical properties of VLF/ELF chorus waves at sub-auroral latitudes**. Combining these analyses with a triangulation method we have also identified the location and motion of the Ionospheric exit points of these various types of chorus waves.

Furthermore, after September 24, 2012, continuous measurements of VLF/ELF waves with a sampling rate of 100 kHz have been made at Athabasca. Based on this data we show in this presentation the preliminary results of a one-year statistical analysis of frequency and occurrence rate of VLF/ELF chorus waves at sub-auroral latitudes.

Keywords: VLF, Chorus Waves, Polarization analysis, Ionospheric exit point, Sub-auroral latitudes

Japan Geoscience Union Meeting 2014
(28 April - 02 May 2014 at Pacifico YOKOHAMA, Kanagawa, Japan)

PEM04-18 Room:311 Time:April 28 17:30-17:45

Nonlinear analysis of magnetospheric wave-particle interactions

SUMMERS, Danny[1*] ; TANG, Rongxin[2] ; OMURA, Yoshiharu[3]

[1]Memorial University of Newfoundland,St John's,Canada, [2]Nanchang University,China, [3]Kyoto University,Japan

The dynamics of the Earth's radiation belts are largely controlled by wave-particle interactions. Gyro-resonant whistler-mode chorus - electron interactions can generate relativistic (MeV) electrons in the outer zone during magnetic storms. Whistler-mode waves can pitch-angle scatter electrons and induce precipitation loss from the inner magnetosphere. Here we analyze the growth of magnetospheric whistler mode waves with particular emphasis on the nonlinear growth phase. We show that nonlinear wave growth can only take place over a restricted parameter space. We examine the conditions under which chorus wave growth can take place,and discuss how the results can be compared with computer simulations and experimental observations.

Keywords: wave-particle interactions, whistler-mode waves, radiation belts, nonlinear cyclotron resonance, chorus wave growth

Japan Geoscience Union Meeting 2014
(28 April - 02 May 2014 at Pacifico YOKOHAMA, Kanagawa, Japan)

PEM04-P01 Room:Poster Time:April 28 18:15-19:30

Retrieval of plasmaspheric He+ density field-aligned distributions from EUV imaging data

KEIKA, Kunihiro[1*] ; BRANDT, Pontus C.[2] ; TOIGO, Anthony[2] ; ROBERT, Demajistre[2]

[1]Solar-Terrestrial Environment Laboratory, Nagoya University, [2]The Johns Hopkins University Applied Physics Laboratory

We retrieve the spatial distributions of He+ density (n_{He+}) in the Earth ' s plasmasphere from EUV imaging data, by using a forward modeling technique. We use a parametric model for the density distribution to simulate line-of-sight integrated He+ densities (i.e., EUV images), and then find parameters that give the best fit to real EUV images. The parametric model used in this study is described as a function of L and magnetic latitude (λ): $n_{He+} = n_0 (L_0/L)^{alpha\_L} \times (r_0/L_0 \cos\lambda^2)^{alpha\_f}$, where n_0 and L_0 are He^+ density and L value at the inner boundary of this model (i.e., the topside ionosphere), and α_L and α_f are parameters that represent L and field-aligned dependence of He^+ density, respectively.

In this paper, we evaluated how well our forward model can retrieve the He^+ density spatial distribution, by performing the following analysis. (1) EUV emission intensities were simulated through the EUV camera response function, given a vantage point of the IMAGE satellite. (2) EUV images were simulated for a large number of (α_L, α_f) pairs: α_L was chosen from 4.0 to 6.0 with 0.1 increment, and α_f was from 0.0 to 2.0 with 0.1 increment. (3) The EUV image corresponding to the (α_L, α_f)=(5.0, 1.0) pair was chosen as our synthetic EUV image. After noise was added to the synthetic image, the forward modeling was applied to all simulated images made in (2). The reduced χ^2 ($\chi_r{}^2$) was used to determine how well simulated image data fit to the synthetic image. The results of this analysis confirm that the He^+ density distributions can be retrieved with good certainty within |40 deg.|MLAT. However, beyond this magnetic latitude it is difficult to determine the L dependence or field-aligned dependence of plasmaspheric He^+ density.

Next, in order to decouple the synthetic data from the parametric formula, we will use density distributions provided by physics-based ionosphere/plasmasphere models as our synthetic data. We will also apply our forward simulation model to real EUV image data from the EUV imager onboard the IMAGE spacecraft.

Keywords: Plasmasphere, Helium ion density, Inner magnetosphere, Plasma refilling, Forward modeling

Japan Geoscience Union Meeting 2014
(28 April - 02 May 2014 at Pacifico YOKOHAMA, Kanagawa, Japan)

PEM04-P02 Room:Poster Time:April 28 18:15-19:30

Solar-cycle variation of the plasmasphere observed from the Akebono PWS data

HASEGAWA, Shuhei[1*] ; MIYOSHI, Yoshizumi[1] ; KITAMURA, Naritoshi[1] ; KEIKA, Kunihiro[1] ; SHOJI, Masafumi[1] ; KUMAMOTO, Atsushi[2] ; MACHIDA, Shinobu[1]

[1]Solar-Terrestrial Environmment Laboratory, Nagoya University, [2]Department of Geophysics, Graduate School of Science, Tohoku University

Plasmaspheric density structures have been studied for a long time. Although it has been clarified that the density is roughly constant along field lines in the outer plasmasphere, field-aligned density distributions of the inner plasmasphere has not been studied intensively. Moreover, continuous observations longer than one-solar cycle have not been reported. Consequently, long-term variations of the plasmaspheric density over a solar cycle remain unknown. In this study, using electron density data based on plasma wave observations from the PWS experiments on board the Akebono satellite from 1989 to 2008, we conduct statistical analyses on variations of structures of the plasmasphere and plasmatrough. In order to investigate the latitudinal distribution of the electron density, we assumed that electron density distribution along field lines are described by a power law form N_e = $N_{e0}(LR_E/R)\alpha, where N_{e0}$ is the equatorial electron density. Using the dataset during geomagnetically quiet periods and altitude higher than 4000 km, we derived solar cycle variations of the equatorial density N_{e0} and field-aligned density distributions α. N_{e0} and α are almost constant for the solar cycle ($N_{e0} \approx$ 2000 cm^{-3} and α = 0 – 1) in the inner plasmasphere at L = 2.1 – 2.3, which distribution is close to diffusive equilibrium. In contrast, $N_{e0}\sim$200 cm^{-3} and α=0 – 1 at solar minimum which distribution is close to diffusive equilibrium and N_{e0} $\sim$30 cm^{-3} and α= 2 – 3 at the solar maximum which distribution is close to collisionless in the outer plasmasphere at L = 4.2 – 4.7.

Keywords: plasmasphere, electron density, akebono satellite, solar-cycle

Japan Geoscience Union Meeting 2014
(28 April - 02 May 2014 at Pacifico YOKOHAMA, Kanagawa, Japan)

PEM04-P03 Room:Poster Time:April 28 18:15-19:30

Statistical analysis of EMIC waves in the inner magnetosphere from the Akebono observations

KATO, Yuichi[1*] ; MIYOSHI, Yoshizumi[1] ; SAKAGUCHI, Kaori[2] ; KASAHARA, Yoshiya[3] ; KEIKA, Kunihiro[1] ; KITAMURA, Naritoshi[1] ; SHOJI, Masafumi[1] ; HASEGAWA, Shuhei[1] ; KUMAMOTO, Atsushi[4] ; SHIOKAWA, Kazuo[1]

[1]Solar-Terrestrial Environment Laboratory, Nagoya University, Japan, [2]National Institute of Information and Communications Technology, [3]Information Media Center, Kanazawa University, [4]Department of Geophysics, Graduate School of Science, Tohoku University

Electromagnetic ion cyclotron (EMIC) waves in the inner magnetosphere are important since EMIC waves cause the pitch angle scattering of ring current ions as well as relativistic electrons of the radiation belts. Although the spatial distributions of EMIC waves have been investigated by several spacecraft such as CRRES, THEMIS and AMPTE, there have been little studies on their latitudinal distributions. Up to this point, we developed the automatic detection algorithm to use the magnetic field data observed by the ELF instrument on board the Akebono satellite, and demonstrated that EMIC waves exist inside the plasmasphere. Since the Akebono satellite measures the thermal plasma density, we investigate the fp(plasma frequency)/fc(cyclotron frequency) dependence and derive the resonance energies of the observed EMIC waves. In this presentation, we report the spatial distributions of EMIC waves, and discuss the dependence of fp/fc and the resonant energy.

Keywords: Electromagnetic Ion Cyclotron, EMIC wave, Statistical analysis, inner magnetosphere

Japan Geoscience Union Meeting 2014
(28 April - 02 May 2014 at Pacifico YOKOHAMA, Kanagawa, Japan)

PEM04-P04 Room:Poster Time:April 28 18:15-19:30

Dispersion relation of Pc1 geomagnetic pulsations using ground-magnetometer observations

NOMURA, Reiko[1*] ; PLASCHKE, Ferdinand[2] ; NARITA, Yasuhito[2] ; GLASSMEIER, Karl-heinz[1] ; FUJITA, Shigeru[3] ; MANN, Ian[4]

[1]IGEP, TU Braunschweig, [2]Space Research Institute Austrian Academy of Sciences, [3]Meteorological College, Japan Meteorological Agency, [4]University of Alberta

Pc1 geomagnetic pulsation (Pc1) observed on the ground at subauroral latitudes (L∼4) is the signature of ion cyclotron waves with frequencies 0.2-5.0Hz near the plasmapause. When the waves reach onto the ionosphere, they induce the Pedersen and Hall currents which generate both Alfven and fast mode waves in the ionospheric duct. On the ground we observe the variations of the magnetic field caused by both of the Alfven and the fast mode wave in the ionospheric duct. Previous studies based on the theoretical models showed the frequency dependence of attenuations, and the spatial distribution of wave polarisations, and furthermore, predicted the dispersion relation in the ionospheric duct. Especially for the characteristics of attenuations and polarisations, previous studies have been established using ground magnetometer observations. Yet, no study has demonstrated the Pc1 dispersion relation experimentally. In our presentation, we show the Pc1 dispersion relation obtained by the wave telescope analysis using CARISMA ground magnetometers.

Keywords: Pc1, EMIC waves, dispersion relation, ionospheric duct

Japan Geoscience Union Meeting 2014
(28 April - 02 May 2014 at Pacifico YOKOHAMA, Kanagawa, Japan)

PEM05-01 Room:424 Time:May 2 09:00-09:15

A Brief History of Collaborative Study on Equatorial MLT Dynamics using Meteor and MF Radars in Indonesia

TSUDA, Toshitaka[1*] ; DJAMALUDDIN, Thomas[2] ; YATINI, Clara[2] ; BUDIYONO, Afif[2] ; VINCENT, Robert[3] ; REID, Iain[3]

[1]Research Institute for Sustainable Humanosphere (RISH), Kyoto University, [2]Indonesian National Institute of Aeronautics and Space (LAPAN), [3]Department of Physics, University of Adelaide

In the tropics active cumulus convection generates various atmospheric waves, such as Kelvin waves, planetary waves, tides, and gravity waves. The wave energy and momentum are transported upward though propagating of these waves. Wave-mean flow interactions are crucially important for understanding of dynamical processes in the equatorial atmosphere, including the formation of peculiar long-term variations such as quasi-biennial oscillation (QBO) and semi-annual oscillation (SAO) in both the stratosphere and the MLT (mesosphere and lower thermosphere) region (70-120 km).

We constructed a total of five meteor and medium frequency (MF) radars in Indonesia since 1992 under close collaboration between RISH, LAPAN and the University of Adelaide. The MLT radar network has been expanded in India, Central and Eastern Pacific, and China. These radars have clarified the behavior of atmosphere dynamics in the MLT region. This paper gives an overview of our collaborative studies as well as highlights of scientific achievements using the MLT radar network

Keywords: mesosphere and lower thermosphere, equaotrial atmosphere, atmospheric waves, meteor radar, medium frequency radar, Indonesia

Japan Geoscience Union Meeting 2014
(28 April - 02 May 2014 at Pacifico YOKOHAMA, Kanagawa, Japan)

PEM05-02 Room:424 Time:May 2 09:15-09:45

Atmospheric Waves in the MLT: A Review

VINCENT, Robert[1*]

[1]University of Adelaide

Through their efficient transfer of energy and momentum, atmospheric waves propagating up from the lower atmosphere play an important role in determining the structure of the Mesosphere/Lower Thermosphere (60-100 km). A wide range of wave types are involved, with periods ranging from minutes to days. Here we review developments in our understanding of wave coupling and impacts on the MLT, with an emphasis on developments in the past decade.

Keywords: MLT Dynamics, Gravity Waves, Atmospheric Tides, Planetary Waves

Japan Geoscience Union Meeting 2014
(28 April - 02 May 2014 at Pacifico YOKOHAMA, Kanagawa, Japan)

PEM05-03 Room:424 Time:May 2 09:45-10:00

Behavior of non-migrating tides in the MLT region

MIYOSHI, Yasunobu[1*] ; FUJIWARA, Hitoshi[2]

[1]Kyushu University, [2]Seikei University

It is well established that non-migrating tides have significant amplitudes in the mesosphere and lower thermosphere (MLT). Using a general circulation model that contain the region from the ground surface to the upper thermosphere, behavior and excitation sources of non-migrating tides are examined. In this study, behaviors of the westward moving semidiurnal tide with zonal wavenumber 1 (SW1), the semidiurnal tide with zonal wavenumber 0 (S0) and the diurnal tide wit zonal wavenumber 0 (D0) are examined in detail. There are two main sources for non-migrating tides. One is latent heat release due to the cumulus convection in the troposphere. The other is the nonlinear interaction between the migrating tide and the stationary planetary wave in the middle atmosphere. Our results indicate that the amplitudes of SW1, S0 and D0 are enhanced when the stationary planetary wave in the stratosphere and mesosphere is active. This means that SW1, S0 and D0 are mainly excited by the nonlinear interaction between the migrating tide and the stationary planetary wave. Furthermore, we discuss excitation sources of other non-migrating tides, such as the eastward moving diurnal tide with zonal wavenumber 3 (DE3) and the eastward moving semidiurnal tide with zonal wave number 2 (SE2).

Keywords: Tides, General Circulation Model

Japan Geoscience Union Meeting 2014
(28 April - 02 May 2014 at Pacifico YOKOHAMA, Kanagawa, Japan)

PEM05-04 Room:424 Time:May 2 10:00-10:15

Long-term observations of MLT zonal wind variations in relation to stratospheric zonal winds over low-latitudes

GRANDHI, Kishore kumar[1*] ; KARANAM, Kishore kumar[2] ; SINGER, Werner[1] ; ZULICKE, Christoph[1] ; S, Gurubaran[3] ; GERD, Baumgarten[1] ; RAMKUMAR, Geetha[2] ; S, Sathishkumar[4] ; RAPP, Markus[5]

[1]Leibniz Institute of Atmospheric Physics, University of Rostock, Kuhlungsborn, Germany, [2]Space Physics Laboratory, Vikram Sarabhai Space Center, Trivandrum, India, [3]Indian Institute of Geomagnetism, Navi Mumbai, India, [4]Equatorial Geophysical Research Laboratory, Indian Institute of Geomagnetism, Tirunelveli, India, [5]German Aerospace Center Institute of Atmospheric Physics (IPA), Oberpfaffenhofen, Wessling, Germany

Long-term observations from medium-frequency and meteor radars (1993-2012) and rocket soundings (1979-1990 and 2002-2007) are used to study mesosphere lower thermosphere (MLT) zonal wind variations in relation to the stratospheric winds over Northern low-latitudes. The combined dataset provide a complete height profile of amplitude of semiannual oscillation (SAO) up to 100 km, with an exception around 75-80 km. The SAO signal has maxima around 50 km and 82 km and a minimum around 65 km. The MLT zonal winds show remarkable inter-annual variability during spring equinox and much less during fall equinox. Zonal wind mesospheric spring equinox enhancements (MSEE) appear with a periodicity of 2-3 years suggesting a modulation by the quasi-biennial oscillation, which we identified with the strength of stratospheric westward winds. Out of 20 years of observations, the stratospheric westward winds are strong during 11 years (non-MSEE) and weak during 9 years. Six of these years show large MLT winds (MSEE) and 3 years (1999, 2004 and 2006) show small MLT winds (missing-MSEEs). These unexpected small winds occur in years with global circulation anomalies as identified with strong sudden stratospheric warmings and an early spring transition of zonal winds, along with a minor enhancement in the tidal amplitudes.

Keywords: MLT winds, MSAO, Meteor radar, MF radar, QBO

Japan Geoscience Union Meeting 2014
(28 April - 02 May 2014 at Pacifico YOKOHAMA, Kanagawa, Japan)

PEM05-05 Room:424 Time:May 2 10:15-10:30

The saturation of gravity waves traveling from the lower to the upper atmosphere observed by the MU radar and understood

KATO, Susumu[1*] ; TSUDA, Toshitaka[1] ; YAMAMOTO, Mamoru[1] ; NAKAMURA, Takuji[2]

[1]Research Institute for Sustainable Humanosphere, Kyoto University, [2]National Polar Research Institute)

The MU radar of Kyoto University was constructed in 1984. One of the main purpose of the radar construction is to observe atmospheric gravity waves particularly to find how gravity waves saturate in traveling from the lower atmosphere to the upper atmosphere. In the 1980s Matsuno, Geller and others put forwards an idea suggesting that the gravity wave saturation may release momentum for driving the mesosphere general circulation. Their idea is based on rocket and satellite global- observation of winds and temperature varying peculiarly with seasons in the mesosphere.

Our MU radar observation has been successful in proving the gravity wave momentum release to be in a good agreement with the required quantity for the mesosphere general circulation. Also our success of precise measurements of the saturated gravity wave power spectrum strongly supports to explain the gravity wave saturation idea in terms of a simple theory based on the linear or monochromatic gravity wave theory by Hines in 1960.

Our theory on the basis of our MU radar observation shows that the gravity wave saturation is attained for each gravity wave in amplitude reaching the phase speed due to a balance between the increasing amplification expected by the linear theory and non-linear braking effects. We can consider that the original gravity wave dispersion relation is maintained upon the saturation.

Gravity waves should experience a number of such saturations before
reaching the thermosphere on the way.

Japan Geoscience Union Meeting 2014
(28 April - 02 May 2014 at Pacifico YOKOHAMA, Kanagawa, Japan)

PEM05-06 Room:424 Time:May 2 10:30-10:45

Ducted Concentric Gravity Wave Observed by IMAP/VISI Associated with Super Typhoon Haiyan

PERWITASARI, Septi[1*] ; SAKANOI, Takeshi[1] ; YAMAZAKI, Atsushi[2] ; OTSUKA, Yuichi[3] ; HOZUMI, Yuta[4] ; AKIYA, Yusuke[4] ; SAITO, Akinori[4] ; SUZUKI, Shin[3]

[1]PPARC, Tohoku University, [2]JAXA/ISAS, [3]STEL, Nagoya University, [4]Geophysics Dept., Kyoto University

Although the convection activity in the troposphere is generally accepted as one of important source of gravity waves in the mesosphere and lower thermosphere, however it is still uncertain how these waves can reach these regions and what types of waves are generated. For decades, the study of gravity waves has been classified into two categories; first is that the waves travel directly from the source and the second is that the waves are ducted or trapped. Many studies tried to explain both categories yet all studies focused on gravity waves produced by transient events. There were almost no observation reports of airglow emissions during a large storm and what type of gravity waves and typical wavelength can be produced from such event. To address this issue, a space-based observation is more preferable since it covers wider area. Until recently, IMAP/VISI is the only space-based instrument that capable of imaging gravity waves above the troposphere in the nadir direction. The Visible and near-Infrared Spectral Imager (VISI) of the IMAP mission was launched successfully on July 21, 2012 with H-IIB/HTV-3 and installed onto the International Space Station (ISS). IMAP/VISI is now operated in the night side hemisphere with a range of +/- 51 deg. GLAT. IMAP/VISI is measuring three different airglow emissions of OI at 630 nm, the OH Meinel band at 730 nm and the O_2 (762 nm) atmospheric band at 762 nm at an altitude of ˜400 km with the typical spatial resolution of 16-50 km.

We found concentric gravity waves events in the southeastern part of Australia that was observed around 13-15 UT for 3 days from 6-8 November 2013 in O_2 (0-0) airglow emission by IMAP/VISI. The waves have horizontal wavelength vary from 80 – 210 km. By using the least squares method, the curvature of the waves was fitted to a perfect circle. The center of the wave was found to be around 155^0E; -42^0S with the radius varies from 400-1200 km. From the meteorological satellite, we cannot locate any convective source around the center of the wave. The nearby local convective source was located a few hundreds km to the south of the wave center and the rainfall rate was less than 10 mm/hr. Therefore, we rule out the possibility of local convective activity as the source of these waves. From the past studies, there were evidences that the gravity waves may be ducted and traveled a great distance away from a specific convective source (e.g. Nakamura et al., 1999; Walterscheid et al., 1999; Hecht et al., 2001). Their studies suggested that the gravity waves observed in Australia were originated from convective activity several thousands km north of Australia. During the observed events, the Typhoon Haiyan was underway. On November 6, the typhoon was categorized as 5 – equivalent of super typhoon and reached its peak on November 7 and then made a landfall in Philippine on November 8. In this study, we argue that the concentric gravity waves seen by IMAP/VISI could be generated by the intense convective activity associated with the Haiyan Typhoon event. Background wind data from TIDI (TIMED Doppler Interferometer) and MF Radar will be used to examine the plausibility for the formation of a ducted/trapped region that can explain the long distance propagation of these waves. The temperature profile from MSISE-90 model will also be used to examine the mesospheric inversion layer and if it ′ s possible to get the data, we will also use the ground-based airglow imager data from Adelaide and Alice Spring.

Keywords: IMAP/VISI, O2 (0-0), concentric gravity wave, ducted, typhoon Haiyan

Japan Geoscience Union Meeting 2014
(28 April - 02 May 2014 at Pacifico YOKOHAMA, Kanagawa, Japan)

PEM05-07 Room:424 Time:May 2 11:00-11:30

The MF Radar Technique: a Review

REID, Iain[1*]

[1]Department of Physics, University of Adelaide, [2]ATRAD Pty Ltd

The Medium Frequency (MF) radar technique has been applied for more than five decades to measure winds and turbulence in the upper atmosphere in the region between 60 and 100 km during the day, and between 80 and 100 km at night. It is one of the few techniques able to provide winds reliably in the 60 to 80 km height region during the day. Although some care is needed in interpretation of the results, it remains a powerful and very useful technique. In this paper, we review the technique and highlight some recent recent results.

Keywords: Radar, Medium Frequency, Spaced Antenna, Mesosphere Lower Thermosphere, Winds, Turbulence

Japan Geoscience Union Meeting 2014
(28 April - 02 May 2014 at Pacifico YOKOHAMA, Kanagawa, Japan)

PEM05-08 Room:424 Time:May 2 11:30-11:45

Tidal periodicity of mesospheric gravity waves observed with MF radar at Poker Flat, Alaska and at Tromso, Norway

MURAYAMA, Yasuhiro[1*] ; KINOSHITA, Takenari[1] ; KAWAMURA, Seiji[1] ; NOZAWA, Satonori[2] ; HALL, Chris[3]

[1]National Institute of Information and Communicatoins Technology, [2]Solar-Terrestiral Physics Laboratory, [3]Toromso University

The interaction between gravity waves and tidal waves has been studied by using observations, although the phase relation between them was not fully understood (e.g., Saskatoon, Canada (Manson et al. 1998), Rothera, Antarctica (Beldon and Mitchell, 2010)). The neutral wind velocity data from mesosphere to lower thermosphere observed by MF radars at Poker Flat in Alaska and Tromso in Norway has been observed since the late 1990s. The long-term wind velocity data at Poker Flat and Tromso was analyzed for 10 years of 1999 ? 2008 to show daily and seasonal behaviors and climatology of mesospheric gravity waves and horizontal wind of the 12 and 24 hour components. First, we extracted these waves from the MF radar observation data. In this study, harmonic analysis was carried out for periods of 48, 24, 12, and 8 hours, which are extracted from the 5 day time series of wind velocity using. Gravity waves are defined as the 1 ˜12 hour period component of difference between observed wind velocity and these harmonic components. The method is applied to 30-minute-average data to calculate the 5 day running mean amplitude and phase of zonal wind of the 12 and 24 hour components. We made 1- day composite plots of kinetic energy of gravity waves for periods of 1 ˜4 hours and harmonic components. The results show that the kinetic energy of gravity waves in Tromso has a peak in 6UT from November to February which tends to coincide with the time when zonal wind of 24 hour component is easterly maximum and easterly wind of 12 hour components is switched westerly. This feature is different from results in Poker Flat and Saskatoon. On the other hand, the phase relation between 12 hour components of zonal wind and kinetic energy of gravity waves shows that their phase agrees for more than 10 days in several years in both observation points. We confirmed the phase agreement in Tromso continued about 10 days at the same time when that in Poker Flat is continued more than 20 days from November to December in 2000. However, the phase of gravity wave kinetic energy is shifted 90 degrees between Tromso and Poker Flat. We plan to discuss more detail of underlying physical processes, focusing on migrating and non-migrating tidal waves and background state of horizontal wind velocities.

Japan Geoscience Union Meeting 2014
(28 April - 02 May 2014 at Pacifico YOKOHAMA, Kanagawa, Japan)

PEM05-09 Room:424 Time:May 2 11:45-12:00

Characteristics of Short Period Tidal Components in Antarctic MLT above Syowa and Davis

TSUTSUMI, Masaki[1*] ; MURPHY, Damian[2]

[1]National Institute of Polar Research, Japan, [2]Australian Antarctic Division

The behaviour of short period atmospheric tidal components in the Antarctic mesosphere and lower thermosphere is studied based on long term observations over Syowa (69.0S, 39.6E) and Davis (68.6S, 78.0E) stations. Semidiurnal tides in the Antarctic mesosphere and lower thermosphere have been extensively studied through the recently established Antarctic radar network [e.g., Murphy et al., 2006; 2008]. However, details of shorter period components such as terdiurnal and six-hour tides are less investigated and poorly known because of their smaller amplitudes compared to the semidiurnal and diurnal tides in the height region of conventional MF radar observations of around 70-90 km. These short period tides also fall in the frequency range of inertial gravity waves and are often hard to distinguish from these waves.

The characteristics of the terdiurnal tide above Davis and Syowa have been measured on a short-term to seasonal basis in the mesosphere and lower thermosphere using long-term simultaneous MF radar data at the two sites (1999-). The terdiurnal tide achieves moderate amplitudes in the winter at these heights but there are subtle differences between the two stations. These differences are explored further by differencing tide phasors in local time and checking the amplitude of the result on a seasonal basis. If the terdiurnal tide was made up entirely of migrating components, this difference would yield a zero-average amplitude. However, the observed non-zero values suggest that the terdiurnal tide at these latitudes contains strong non-migrating tidal components.

The Syowa MF radar has a great advantage over other MF radars in that it has been conducting simultaneous meteor wind measurements together with the conventional correlation based measurements, which enables wind observations in a very wide height range of 65-120km [Tsutsumi and Aso, 2005]. A clear enhancement in terdiurnal amplitudes is seen in early winter months of March-June. The amplitudes can reach 20 m/s around 110 km even in the composite plot made with more than 10 years of data. These amplitudes can be comparable or sometimes even larger than those of diurnal and semidiurnal tides, and indicate a possible significant role of short period tidal components in the polar lower thermosphere.

Keywords: Antarctic, mesosphere and lower thermosphere, short period atmospheric tidal waves

Japan Geoscience Union Meeting 2014
(28 April - 02 May 2014 at Pacifico YOKOHAMA, Kanagawa, Japan)

PEM05-10 Room:424 Time:May 2 12:00-12:15

The SMILES observations of mesospheric ozone during the solar eclipse

IMAI, Koji[1*] ; AKIYOSHI, Hideharu[2] ; TAKAHASHI, Kenshi[3] ; YAMASHITA, Yousuke[2] ; IMAMURA, Takashi[2] ; SUZUKI, Makoto[1] ; EBISAWA, Ken[1] ; SHIOTANI, Masato[3]

[1]Institute of Space and Astronautical Science, Japan Aerospace Exploration Agency, Sagamihara, [2]National Institute for Environmental Studies, [3]Research Institute for Sustainable Humanosphere, Kyoto University

Solar eclipse temporally reduces the amount of solar radiation, providing an opportunity to verify the ozone photochemistry under changing solar radiation. During the longest annular solar eclipse in this millennium occurred on 15 January 2010, Superconducting Submillimeter-Wave Limb-Emission Sounder (SMILES) successfully captured increased ozone mostly in the mesosphere with a decrease in solar illuminations. The ozone increment shows altitude dependence in the mesosphere. Using an atmospheric chemistry box model, it is found that the dependence results from the difference in chemical reaction rates to the solar radiation change. The model also predicts the difference in the ozone concentration evolution between the sunlight decreasing and increasing phases, although SMILES observation does not resolve the difference.

Keywords: SMILES, ozone, mesosphere

Japan Geoscience Union Meeting 2014
(28 April - 02 May 2014 at Pacifico YOKOHAMA, Kanagawa, Japan)

PEM05-11 Room:424 Time:May 2 12:15-12:30

Contribution of the IUGONET data analysis system to upper atmospheric researches

SHINBORI, Atsuki[1*] ; YAGI, Manabu[2] ; TANAKA, Yoshimasa[3] ; SATO, Yuka[3] ; YATAGAI, Akiyo[4] ; UMEMURA, Norio[4] ; UENO, Satoru[5] ; KOYAMA, Yukinobu[6] ; ABE, Shuji[7]

[1]Research Institute for Sustainable Humanosphere (RISH), Kyoto University, [2]Planetary Plasma and Atmospheric Research Center, Graduate School of Science, Tohoku University, [3]National Institute of Polar Research, [4]Nagoya University Solar Terrestrial Environment Laboratory Geospace Research Center, [5]Kwasan & Hida Observatories, School of Science, Kyoto University, [6]Data Analysis Center for Geomagnetism and Space Magnetism Graduate School of Science, Kyoto Universi, [7]International Center for Space Weather Science and Education, Japan

Various kinds of atmospheric disturbances and long-term variation as seen in several parameters (temperature, mean wind etc.) in the upper atmosphere (mesosphere, thermosphere and ionosphere) is caused by energy input from solar radiation, momenta and energies from the lower atmosphere (stratosphere and troposphere) via atmospheric waves, and chemical reaction. Such atmospheric phenomena observed by ground-based and satellite instruments are the result of such complicated processes. In order to investigate the mechanisms of the atmospheric disturbances and long-term variations in the upper atmosphere, which may be affected by solar activities and global warming, researchers need to conduct comprehensive analyses with various kinds of long-term observation data that have been continued by means of a global network of MST (Mesosphere-Stratosphere-Troposphere) radars, optical sensors, radiosondes, etc. The IUGONET (Inter-university Upper atmosphere Global Observation NETwork) project initiated in 2009 aims at the establishment of a cross-reference system for various kinds of ground-based observation data. The IUGONET participants consist of five universities/institutes: the National Institute of Polar Research (NIPR), Tohoku University, Nagoya University, Kyoto University, and Kyushu University. We have developed a metadata database (MDB) of ground-based observations and IUGONET data analysis software (UDAS) in order to provide researchers in a wide range of disciplines with a seamless data environment to link databases spread across the IUGONET institutions. In particular, the MDB and UDAS will be of great help in data acquisition and integrated analyses to understand the dynamics on the mesosphere-lower thermosphere (MLT) throughout the Sun-Earth system. Therefore, the IUGONET MDB and UDAS will greatly contribute to upper atmospheric researches on the basis of integrated analysis of various kinds of long-term observation data covering a wide region from both the poles to the equator. In this talk, we introduce a brief overview of the IUGONET project and an application of the IUGONET products for upper atmospheric researches.

Keywords: Upper atmosphere, Grand-based observation data, IUGONET, metadata search system, IUGONET data analysis tool

Japan Geoscience Union Meeting 2014
(28 April - 02 May 2014 at Pacifico YOKOHAMA, Kanagawa, Japan)

PEM05-12 Room:424 Time:May 2 12:30-12:45

Vertical and lateral wave coupling observed with network of MLT/MST Radars over Indian region

M, Venkat ratnam[1*] ; S., Eswariah[2] ; N., Venkateswara rao[1] ; S., Vijayabhaskar rao[2] ; K., Kishore kumar[3] ; S., Sathish kumar[4] ; S., Gurubaran[4]

[1]National Atmospheric Research Laboratory, [2]Sri Venkateswara University, [3]Space Physical Laboratory, [4]Indian Institute of Geomagnetism

It is well known that gravity waves and tides play an important role in delineating the middle atmospheric structure and dynamics. There have been several studies in recent years, using different measurement techniques, to understand significant roles played by gravity waves and tides in the lower, middle and upper atmospheres. However, only a few studies addressed this problem with simultaneous observations of all the three regions. Moreover, no efforts have been made so far to understand the lateral forcing of these waves and tides since such a study needs a network of radars located nearby which was missing. With the establishment of an advanced meteor radar at Sri Venkateswara University, Tirupati (13.63oN, 79.4oE), India, and up gradation of MF radar at Kolhapur (16.8oN, 74.2oE) together with MST radar at Gadanki (13.5oN, 79.2oE), Meteor radar at Thumba (8.5oN, 77oE) and MF radar at Tirunalveli (8.7oN, 77.8oE) forms a unique network of radars in the tropical region. Importantly, all these radars are located within 1000 km distance. Accordingly, this network is suitable to study the lower atmospheric forcing and its impacts on middle and upper atmospheric structure and dynamics. For the present study, all these radars were simultaneously operated for a few days in September 2013. These observations show the presence of short period gravity waves and tides (diurnal, semi-diurnal and ter-diurnal) at all locations. Large day-to-day day variability in gravity waves and tides is observed within a station and among different stations providing insight on lateral coupling. Phase propagations of the three tidal components at different stations is used to further understand the lateral coupling. Using simultaneous MST radar, Rayleigh lidar and SVU meteor radar (which are nearly co-located), lower atmospheric forcing and its impacts on the mesosphere and lower thermosphere are investigated. This study showed need for long-term measurements, with simultaneous operation of all the above mentioned network of radars, to effectively address the problem of vertical and latitudinal wave forcing.

Keywords: Coupling, Meteor/MF radars, Tropical MLT region

Japan Geoscience Union Meeting 2014
(28 April - 02 May 2014 at Pacifico YOKOHAMA, Kanagawa, Japan)

PEM05-P01 Room:Poster Time:May 2 16:15-17:30

Diurnal tide and QTD wave in the tropical stratosphere and MLT region: Long-term trends and solar cycle influence

NARUKULL, Venkateswara rao[1*] ; M., Venkat ratnam[1] ; C., Vedavathi[2] ; S., Gurubaran[3] ; B.V., Krishna murthy[4] ; S., Vijaya bhaskara rao[2]

[1]National Atmospheric Research Laboratory, [2]Sri Venkateswara University, [3]Indian Institute of Geomagnetism, [4]B1, CEEBROS, 47/20, IIIrd Main Road, Chennai

In the present study, long-term trends and solar cycle influence on the diurnal tide (DT) and quasi two day wave (QTDW) in the stratosphere, mesosphere and lower thermosphere (MLT) region over a tropical station Tirununveli (8.7oN, 77.7oE) are investigated using ERA-Interim datasets and MF radar observations available since 1993. As no ground truth is available over Tirununveli, suitability of the ERA-Interim data for the present study is ascertained using simultaneous radiosonde and MST radar observations over Gadanki (13.5oN, 79.2oE) and good consistency is found between the two. Amplitudes of the DT and QTDW over Tirununveli show a long-term linear increasing trend, which becomes prominent in the MLT region. Role of solar cycle on the DT and the QTDW is investigated by separating them with respect to the solar activity (minimum and maximum of solar cycles). Both the DT and QTDW show higher amplitudes during solar minimum and vice versa. Significant higher amplitudes in the recent extended solar minimum are noticed in the MLT region. However, no consistent relation is found between solar activity and DT in the stratosphere although increasing trend is clearly observed. Though increasing trend in the tropical convection is noticed at nearby locations, similar to the DT, it varies from location to location which may be due to large scale circulation effects. This demands data from network of radars located across the globe to see the combined effects of lower atmospheric forcing, circulation and their effects on MLT region.

Keywords: Diurnal Tide, Quasi-two day wave, Long-term trends, Solar cycle, Extended minimum

Japan Geoscience Union Meeting 2014
(28 April - 02 May 2014 at Pacifico YOKOHAMA, Kanagawa, Japan)

PEM05-P02 Room:Poster Time:May 2 16:15-17:30

MQBE and Amplitude Modulation of SAO in the MLT

MATSUMOTO, Naoki[1*] ; SHINBORI, Atsuki[2] ; TSUDA, Toshitaka[2]

[1]Division of Earth and Planetary Sciences, Graduate School of Science, Kyoto University, [2]Research Institute for Sustainable Humanosphere (RISH), Kyoto University

Characteristics of various atmospheric waves in the mesosphere and lower thermosphere (MLT) have been investigated by long-term ground-based and satellite-based observation. In the equatorial region, the westward monthly mean wind is enhanced in March in 2 or 3 years in MLT, which is called Mesosphere Quasi-Biennual Enhancement (MQBE) [Rao et al., 2012]. Recently, They showed that MQBE appears once in 2 or 3 years until 2002, based on data analysis of meteor/MF radars in the Asia-Oceania region. However, the occurrence features remained unknown due to no sufficient wind data with high-time resolution from 50 to 80 km.

We analyzed the long-term wind data from 1990 to 2013 obtained from meteor/MF radars in the Asia-Oceania region, such as Kauai, Christmas island, Tirunelveli, Koto Tabang in order to identify the occurrence features and mechanism of MQBE. And also we investigated relationship of the monthly-mean wind between MLT stratosphere using MERRA retrospective-analyses data provided by NASA. We used integrated analysis tool " UDAS " provided by " IUGONET " (Inter-university Upper atmosphere Global Observation NETwork). And We use Stockwell-transform to detect the temporal variation of frequency and amplitude in time series data.

As a result, we found that MQBE occurred in spring of 2005, 2008 and 2011 with amplitude over 32 m/s in an altitude from 80 to 100 km . From an S-transform spectral analysis of zonal wind in MLT, MQBE coincides with the enhancement of the amplitude of 6-months component of zonal wind. Furthermore, comparing the 6-month component in the lower thermosphere at 90 km and stratosphere using retrospective-analyses data of MERRA, 6-months component of lower thermosphere(90 km) and stratopause (1 hPa) are well negative correlated. And also 6-months component of lower thermosphere and lower stratosphere (70 hPa) are well positive correlated. Their correlation coefficients are about 0.6, and lags are under 3 month. the former result is consistent with the fact that the phase of SAO are reversal in the lower thermosphere and in the stratosphere.

Although Rao et al.,[2012] reported that MQBE did not appear after 2002, the present results showed that MQBE takes place after 2002. Next, the SAO amplitude in MLT obtained from the S-transform analysis tends to be enhanced significantly, corresponding to the occurrence of MQBE. This relationship can be a clue of occurrence features of MQBE. Furthermore, the relationship of mean wind between in MLT and stratosphere indicates that MQBE is driven by coupling process of the mesosphere-stratosphere system. We can infer that MQBE is caused by atmospheric gravity waves, which is similar to the generation mechanism of QBO.

In addition, we need to detect and analyze the gravity wave in equatorial region to identify the mechanism of MQBE.

Keywords: meteor radar, MF radar, stratosphere, SAO, MQBE

Japan Geoscience Union Meeting 2014
(28 April - 02 May 2014 at Pacifico YOKOHAMA, Kanagawa, Japan)

PEM05-P03 Room:Poster Time:May 2 16:15-17:30

Meteor Wind Radar Application for the study the dynamics of the neutral winds above at Kototabang and Biak station

ACHMAD, Effendy[1] ; TSUDA, Toshitaka[2] ; SHINBORI, Atsuki[2*]

[1]National Institute of Aeronautics and Space Indonesia (LAPAN), [2]Research Institute for Sustainable Humanosphere

Currently for meteor observations is not only done with the naked eye and optical equipment such as a telescope, the latest development to detect natural phenomena meteor shower rained almost every day the Earth can be detected using radar technology. Meteor Wind Radar (MWR) is a radar system used to detect, analyse and display meteor entrance events to the Earth's atmosphere. By using of radar meteors (SKiYMET Meteor Radar) was used to observe the meteor trail (ionized air columns) that moves with the wind neutral layer of mesosphere. When a meteor enters the atmosphere it rapidly vaporises leaving behind a trail of ionised gas along its path of travel, this trail can form a target for a radar transmission. Generally the frequencies used for the detection of radar, located on the VHF band wave spectrum. The results of the analysis of radar data output consists of 7th meteor parameter can be used to study the behavior of neutral winds in the Mesosphere. In this paper the utilization of SKiYMet shown to detect Wind speed Meridional and Zonal Wind speed, Temperature in the Mesosphere and the number and received Flux meteor in the Earth, as a sources of data to better understand the dynamics of the neutral winds at an altitude of 70-110 km region of observation locations. Simultaneously measurement data will be shown at Kototabang observations that have been operating since year 2006 and in Biak Station since year 2011. All of the radar installation is a collaboration between LAPAN and RISH - Kyoto, NICT Japan.

Keywords: Meteor radar, Indonesia, Equatorial regiona, Koto Tabang, Biak

Japan Geoscience Union Meeting 2014
(28 April - 02 May 2014 at Pacifico YOKOHAMA, Kanagawa, Japan)

PEM05-P04 Room:Poster Time:May 2 16:15-17:30

Concentric structures in molecular oxygen emission observed by ISS-IMAP/VISI

AKIYA, Yusuke[1*] ; SAITO, Akinori[1] ; SAKANOI, Takeshi[2] ; HOZUMI, Yuta[1] ; YAMAZAKI, Atsushi[3] ; OTSUKA, Yuichi[4] ; NISHIOKA, Michi[5] ; TSUGAWA, Takuya[5]

[1]Department of Geophys., Kyoto Univ., [2]PPARC, Tohoku University, [3]ISAS/JAXA, [4]STE Lab., Nagoya Univ., [5]NICT

Concentric structures in airglow emissions were often observed from ground based imagers. Some of them were thought to be caused by the active clouds in the troposphere. It was not able to observe the overall structures from the imagers on the ground under the cloudy condition. Field of views of the imagers were not enough to observe whole structure. Space borne imagers are able to observe the structures caused by the disturbances in the lower atmosphere with wider field of view. Concentric structures of the O_2 airglow emission in 762-nm wavelength were found by the Visible and near-infrared imager on the International Space Station on June 1, 2013 over the U. S. This is the first case which took the image from edge to the center of the concentric structure. Spatial scale of this concentric structures were estimated to be 1,200 km. Fine structures with 80 km wavelength and no dumping in the intensity were observed in this VISI observation. Amplitude in these fine structures were about 10 % to the background intensity. Circular structures were also observed in the GPS-TEC observations before the VISI observation. These concentric structures were estimated to be caused from the active clouds after tornado and atmospheric gravity waves had propagated in horizontal direction in the emission layer.

Keywords: Near infrared, Airglow, Concentric structure, the Mesosphere, Atmospheric gravity waves

Japan Geoscience Union Meeting 2014
(28 April - 02 May 2014 at Pacifico YOKOHAMA, Kanagawa, Japan)

PEM05-P05 Room:Poster Time:May 2 16:15-17:30

Background Lamb waves coupled with thermospheric gravity waves

NISHIDA, Kiwamu[1*] ; KOBAYASHI, Naoki[3] ; FUKAO, Yoshio[2]

[1]ERI, Univ. of Tokyo, [2]IFREE, Jamstec, [3]ISAS, JAXA

Lamb waves of the Earth's atmosphere in the millihertz band have been considered as transient phenomena excited only by large events. Nishida et al. (2014) showed the first evidence of background Lamb waves in the Earth's atmosphere from 0.2 to 10 mHz, based on the array analysis of microbarometer data from the USArray in 2012. The observations suggest that the probable excitation source is atmospheric turbulence in the troposphere. Theoretically, their energy in the troposphere tunnels into the thermosphere at a resonant frequency via thermospheric gravity wave because the Lamb-wave branch intersects that of thermospheric gravity waves at 3.5 mHz and that of acoustic waves trapped near the mesopause at 6.5 mHz [Garrett 1969]. The observed FK spectrum shows a local minimum of Lamb-wave amplitudes at around 3.5 mHz, where the Lamb-wave branch is crossed by the thermospheric gravity-wave branch. Coupled Lamb waves leak a certain amount of energy from the troposphere to the thermosphere, reducing the Lamb-wave amplitudes at the crossover frequency relative to those at neighboring frequencies, when their excitation sources exist in the troposphere. The energy tunnels from the troposphere to the thermosphere at the resonant frequency, although Lamb waves themselves cannot induce an upward flux [Lindzen 1972]. The RMS amplitudes of the coupled modes are estimated to be 0.3 m/s at 150 km and 0.1 m/s at 120 km, respectively. These modes might contribute to the thermosphere energy balance by heating via viscous dissipation [Hickey et al. 2001]. The amplitude suggests that the Lamb waves partly contribute to the excitation of thermospheric wave activity associated with severe convection activity [Hunsucker1982].

Keywords: Atmospheric Lamb wave, Thermospheric gravity wave

Japan Geoscience Union Meeting 2014
(28 April - 02 May 2014 at Pacifico YOKOHAMA, Kanagawa, Japan)

PEM05-P06 Room:Poster Time:May 2 16:15-17:30

A proposal of simple resonance scattering lidar using an alkali metal vapor laser for monitoring the MLT region

ABO, Makoto[1*] ; MIURA, Natsumi[1] ; NAGASAWA, Chikao[1] ; SHIBATA, Yasukuni[1]

[1]Tokyo Metropolitan University

Many observations of metal atomic layers such as Na, Fe, K, Ca and Ca ion in the mesopause region have been conducted in many parts of the world. We have observed several mesospheric metallic layers at Tokyo and Indonesia using resonance scattering lidars consisting of a dye laser and a Ti:Sapphire laser [1]. Especially, in order to solve the formation mechanism of metallic sporadic layers occurred in the mesopause region, the simultaneous observation of Ca ion and the neutral metal atom is necessary. However since the output power of the Ti:Sapphire laser has a low damage threshold of a crystal, it is difficult to improve the output average power. We propose the resonance scattering lidar consisting of the alkali vapor laser for monitoring the MLT region. Optically pumped alkali vapor lasers have attracted increasing attention because of their potential of achieve high power in a high quality beam. The alkali vapor laser can easily realize narrow-linewidth and precise tuning.

Metal atomic layers in the mesosphere are an excellent tracer of the atmospheric wave motion in the region between 80 and 100km. sudden formation of thin metallic layers, superposed in the background mesospheric metallic layers was discovered and these enhanced layers are called the sporadic metallic layers. We have observed frequently the sporadic sodium layers (Nas) at Hachioji, Japan (35.6N, 139.4E) and the sporadic sodium and iron layers (Fes) at Kototabang, Indonesia (0.2S, 100.3E). The ion recombination mechanism invoking wind shear and sporadic E layers appears to be consistent with many observed characteristics, but their cause is still an open question.

Zhdanov et al. presented optically pumped continuous wave potassium vapor laser operating in a single longitudinal and a single transverse mode at 770 nm [2]. Zweiback et al. demonstrated a high efficiency potassium vapor laser using a 0.15nm bandwidth alexandrite laser as the pump source [3]. The alkali vapor laser operates in a three level scheme. The optical pump source excites the D2 line of alkali atom and lasing occurs on the D1 line. To provide a population inversion, fast quenching must be provided by using a buffer gas. We are developing a high peak power pulsed potassium vapor laser using alexandrite laser as the optical pump source. Sealed potassium vapor cell had AR coated windows, and filled with metallic potassium and helium. The cell was assembled inside an oven which had temperature controlled heaters. A pump beam polarized in the horizontal plane was focused through the polarizing beam splitting cube into the potassium vapor cell with a lens. A laser cavity was created for the vertical polarization by two mirrors and the beam splitting cube.

The development of these kinds of lasers is identified as one of the key topics for advancing the application of resonance scattering lidar systems.

References

[1] Y. Shibata et al., J. Meteor. Soc. Jap., 84A, 317-325, 2006.
[2] B. Zhdanov et al., Opt. Commun., 270, 353-355, 2007.
[3] J. Zweiback et al., Opt. Commun., 282, 1871-1873, 2009.

Keywords: mesopause, metal atomic layer, resonance scattering lidar, metal vapor laser

Japan Geoscience Union Meeting 2014
(28 April - 02 May 2014 at Pacifico YOKOHAMA, Kanagawa, Japan)

PEM06-01 Room:312 Time:April 30 11:00-11:30

Study of Coupling Processes in the Solar-Terrestrial System: Project Overview

TSUDA, Toshitaka[1*]

[1]Research Institute for Sustainable Humanosphere (RISH), Kyoto University

We promote a project named ”Coupling Process in the Solar-Terrestrial System” under close collaboration among universities and research institutess. We aim to study the solar energy inputs to the Earth, and responses of the Geospace (magnetosphere, ionosphere and atmosphere) to them. The solar energy can manly be divided into two parts; the solar radiation, involving infra-red, visible, ultra-violet and X-ray, and the solar wind, which is a high-speed flow of plasma particles.

The solar radiation becomes the maximum on the equator, then, atmospheric disturbances are actively generated near the Earth’s surface. They further excite various atmospheric waves, which propagate upward carrying energy and momentum. On the other hand, electro-magnetic energy associated with the solar wind converges into the polar regions. Disturbances are also generated there, and a part of the energy is transported toward lower latitudes and lower atmospheric regions. We propose to establish large atmospheric radars with active phased array antenna on the equator and the Arctic region. Among the equatorial regions, we focus on Indonesia where the atmospheric disturbances are most intense in the world, and we will establish a comprehensive observatory in Indonesia with the Equatorial MU radar as its main facility. While, we will also construct the state-of-the-art radar, called EISCAT-3D, in Scandinavia under international collaboration. An observation network of portable equipment for will be expanded in Asia and Africa to clarify the global flow of energy and materials.

Keywords: Equatorial fountain, Equatorial MU Radar, EISCAT_3D, Global observation network

Japan Geoscience Union Meeting 2014
(28 April - 02 May 2014 at Pacifico YOKOHAMA, Kanagawa, Japan)

PEM06-02 Room:312 Time:April 30 11:30-11:45

A Review on Equatorial Atmosphere Radar (EAR) Observations of Lower Atmosphere

HASHIGUCHI, Hiroyuki[1*] ; TSUDA, Toshitaka[1] ; YAMAMOTO, Mamoru[1] ; YAMAMOTO, Masayuki[1] ; SHIBAGAKI, Yoshiaki[2] ; SHIMOMAI, Toyoshi[3] ; EDDY, Hermawan[4]

[1]Research Institute for Sustainable Humanosphere (RISH), Kyoto University, [2]Osaka Electro-Communication University, [3]Shimane University, [4]National Institute of Aeronautics and Space (LAPAN), Indonesia

The Equatorial Atmosphere Radar (EAR) is an atmospheric radar located in Kototabang, West Sumatra in Indonesia (0.20S, 100.32E). The EAR has a circular antenna array of approximately 110 m in diameter, consisting of 560 three-element Yagis. It is an active phased array system with each Yagi driven by a solid-state transceiver module. It is operated by collaboration between the Research Institute for Sustainable Humanosphere (RISH), Kyoto University and National Institute of Aeronautics and Space of Indonesia (LAPAN), Indonesia since 2001. RISH has conducted a collaborative research program (EAR collaboration) by using the EAR and its related facilities since 2005. The EAR can observe winds and turbulence in the lower atmosphere and echoes from ionospheric irregularities. In the presentation, observation results of the lower atmosphere with the EAR are reviewed.

Keywords: Equatorial Atmosphere Radar, Equatorial MU Radar, Equatorial Atmosphere

Japan Geoscience Union Meeting 2014
(28 April - 02 May 2014 at Pacifico YOKOHAMA, Kanagawa, Japan)

PEM06-03 Room:312 Time:April 30 11:45-12:00

Ionospheric observations by SEALION and the Equatorial Atmosphere Radar

YOKOYAMA, Tatsuhiro[1*] ; TSUGAWA, Takuya[1] ; ISHII, Mamoru[1]

[1]National Institute of Information and Communications Technology

Equatorial spread F (ESF) is a well-known phenomenon in the equatorial ionoshperic F region. As it causes severe scintillation in the amplitude and phase of radio signals, it is important to understand and forecast the occurrence of ESF from a space weather point of view. Ionospheric observation with the 47-MHz Equatorial Atmosphere Radar (EAR) in West Sumatra, Indonesia (0.20S, 100.32E, 10.36S dip latitude) has been conducted since 2001, and its unique observational data has been obtained for more than one solar cycle. The EAR is sensitive to 3-m scale ionospheric irregularities, which can be regarded as a tracer of ESF. Along with the EAR observations, Southeast Asia Low-latitude Ionospheric Network (SEALION) project by NICT started in 2003 for the purpose of monitoring and forecasting ESF. The SEALION consists of multiple ionosondes, GPS receivers and several other instruments in the Southeast Asian region. Since the developed ESF usually drifts eastward, monitoring ESF in this region can provide important space weather information for the Japanese longitude sector. We will summarize observational results with the SEALION and EAR, and discuss future potential of the ionospheric observation in the Southeast Asian region.

Keywords: SEALION, EAR, equatorial spread F, equatorial ionosphere

Japan Geoscience Union Meeting 2014
(28 April - 02 May 2014 at Pacifico YOKOHAMA, Kanagawa, Japan)

PEM06-04 Room:312 Time:April 30 12:00-12:15

Development of Indonesian Monsoon Index (IMI) Based on EAR and other Facilities at Kototabang

EDDY, Hermawan[1] ; HASHIGUCHI, Hiroyuki[2*]

[1]National Institute of Aeronautics and Space (LAPAN), Indonesia, [2]Research Institute for Sustainable Humanosphere (RISH), Kyoto University

This study is mainly concerned on developing of the Indonesian Monsoon Index (IMI) based on the Equatorial Atmosphere Radar (EAR) at Kototabang, West Sumatera (0.2S; 100.32E, 865 m from MSL). We have analyzed the zonal and meridional wind data of EAR for period of July 2001 to July 2008. By applying the bandpass filtering method that we call as the Fast Fourier Transform (FFT) and Wavelet (WL) technique, we have identified the characteristics of meridional wind velocity in frequency domain. The predominant peak oscillation that appear is Annual Oscillation (AO) for the meridional wind velocity between 8 to 18 km above mean sea level (MSL). While, the strongest is located around 14.1 km from MSL (It's equal to 200 hPa). At the same time period observation of EAR, we analyzed also the Global Monsoon Index as represented by the Indian Summer Monsoon Index (ISMI), Western North Pacific Monsoon Index (WNPMI), and Australian Monsoon Index (AUSMI), respectively. We found a 12 months oscillation for Global Monsoon Index that we call as the AO. By comparing them with meridional wind velocity of EAR, we found a good agreement between AUSMI and the meridional wind velocity of EAR, especially. By this preliminary result, we suspect that we can use the AUSMI parameter to detect the Monsoon Signal over Indonesia, especially for the Western part of Indonesia region, especially at about the 200 hPa. We wish to develop these results by investigating the Monsoonal Onset, especially, including their anomalies, since we know that Monsoon is still a pre dominant peak oscillation at the Indonesian Maritime Continent (IMC) which have big effect to control the complexity of atmospheric dynamic over Indonesia. If it looks possible, we wish also to develop the IMI model that suitable for Indonesia region. Detailed information due to that preliminary results including the basic idea of this proposal research will be discussed at our presentation.

Keywords: IMI, EAR, AUSMI, Model

Japan Geoscience Union Meeting 2014
(28 April - 02 May 2014 at Pacifico YOKOHAMA, Kanagawa, Japan)

PEM06-05 Room:312 Time:April 30 12:15-12:30

Vertical and horizontal coupling processes in the equatorial atmosphere

YAMANAKA, Manabu D.[1*]

[1]JAMSTEC/Kobe U

Future targets of the equatorial atmosphere dynamics are discussed from viewpoints of recent progress of the lower-atmospheric parts including increase of climatological interests and rapid developments of tropical countries. From recognition of the importance of land-sea heat contrast on Earth we must consider again two types of diurnal cycles: sea-land breeze circulations and atmospheric tides, which have local and global phase structures, respectively. We must consider also two types of Earth rotation effects: solar radiation heating and Coriolis force, which are stronger and weaker, respectively, in the equatorial region. Furthermore, in the lower atmosphere, clouds govern winds in the equatorial region, in contrast to opposite relationship in middle and high latitudes. Because the equatorial convective clouds are dependent not only on dynamical and thermal instabilities but also by water and electrical budgets, we need to study again dynamical-chemical and atmosphere-ionosphere couplings.

Keywords: atmosphere vertical coupling, atmosphere observation network

Japan Geoscience Union Meeting 2014
(28 April - 02 May 2014 at Pacifico YOKOHAMA, Kanagawa, Japan)

PEM06-06 Room:312 Time:April 30 12:30-12:45

Vertical wind measurement in the equatorial troposphere by the Equatorial Atmosphere Radar: A review

YAMAMOTO, Masayuki[1*] ; HASHIGUCHI, Hiroyuki[1] ; YAMAMOTO, Mamoru[1]

[1]Research Institute for Sustainable Humanosphere, Kyoto University

Measurements of vertical wind are important not only for clarifying transportation processes of energy and momentums but also for quantifying dynamical processes of precipitation and clouds. Because 50-MHz atmospheric radars measure vertical and horizontal wind velocity by using scatterings caused by irregularities of radio refractive index, they can measure vertical wind both in clear and precipitation regions. Using the capability, EAR has resolved the fine-scale vertical wind motions in the equatorial troposphere. In the presentation, the measurement results of vertical wind obtained by the EAR are reviewed. Future plans of vertical wind measurement using the Equatorial MU radar are also proposed.

Keywords: Equatorial Atmosphere Radar, Equatorial MU Radar, equatorial atmosphere, vertical wind measurement

Japan Geoscience Union Meeting 2014
(28 April - 02 May 2014 at Pacifico YOKOHAMA, Kanagawa, Japan)

PEM06-07 Room:312 Time:April 30 14:15-14:45

Science and design overview of the EISCAT_3D radar

MCCREA, Ian[1*]

[1]STFC Rutherford Appleton Laboratory

For thirty years, the EISCAT Scientific Association (www.eiscat.se) has operated a network of leading facilities for ground-based research in solar-terrestrial physics. The UHF and VHF radars at Tromso in northern Norway, together with the receiver sites at Kiruna, Sweden and Sodankyla, Finland and the EISCAT Svalbard Radar near Longyearbyen, represent a uniquely capable group of instruments serving a worldwide user community. The EISCAT mainland radars in particular, however, are based on ageing transmitters and antennas which are slow-moving and increasingly hard to maintain. For several years now, EISCAT (with support from international partners including the European Union) has been planning to replace the current set of mainland radars with a new state-of-the-art radar system, better suited to the current needs of the research community. EISCAT_3D (www.eiscat3d.se) will be the next-generation radar for the high-latitude atmosphere and geospace, with capabilities going beyond anything currently available. The facility will consist of large phased arrays in three countries. EISCAT_3D will comprise tens of thousands, up to more than 100 000, antenna elements. The new facility combines volumetric imaging and tracking, aperture synthesis imaging, multistatic configuration, improved sensitivity and transmitter flexibility. EISCAT_3D will be the first multistatic phased array ISR. A network of five sites is planned, with receivers located around 120 km and 250 km from the active site, providing optimal geometries for vectors in the middle and upper atmosphere. At the passive sites, the design allows the transmitted beam to be imaged using multi-beam techniques. EISCAT_3D will be a modular system, allowing an array to be split into sections for imaging. The result will be a new data product, range-dependent images of small structures, with sizes down to a few tens of metres. The antenna gain and array size will deliver large increases in the figure-of-merit relative to the existing EISCAT radars. An active site comprising 16,000 elements will exceed the sensitivity of the present VHF radar by an order of magnitude. In this talk the technical specifications and science case for EISCAT_3D will be discussed and the current progress reviewed. Studies of the atmospheric energy budget, exploration of small-scale and large-scale processes, as well as geospace environment monitoring and potential space weather service applications will be presented.

Keywords: EISCAT, Incoherent Scatter, Radar, Ionosphere, Solar-Terrestrial Physics, Space Weather

Japan Geoscience Union Meeting 2014
(28 April - 02 May 2014 at Pacifico YOKOHAMA, Kanagawa, Japan)

PEM06-08 Room:312 Time:April 30 14:45-15:00

The EISCAT_3D System and Status

HEINSELMAN, Craig[1*]

[1]EISCAT Scientific Association

The EISCAT Scientific Association has been operating incoherent scatter radars in the arctic since the early 1980s. Those systems have been extremely productive over the decades, supporting a wide range of scientific topics within geospace research and resulting in more than 2000 publications in peer-reviewed journals. For the past several years the EISCAT community, with significant support from the European Commission, has been working toward a new set of radar systems to replace the now aging infrastructure. This distributed radar, called EISCAT_3D, will provide the scientific community with new measurement capabilities that far exceed, both quantitatively and qualitatively, those presently available.

EISCAT_3D, when it is fully implemented, will consist of five phased array antennas strategically positioned in northern Norway, Sweden, and Finland. One of the antennas will include a distributed 10 MW peak power transmitter with full polarization capabilities, rapid steering, and antenna aperture coding options. The receive antenna arrays will be capable of instantaneously covering the entire transmit beam, thus providing a large number of intersecting volumes for vector drift measurements. The overall system will, furthermore, have sufficient sensitivity to provide order of magnitude improvements in both spatial and temporal resolution over the present radars.

We will present an overview of the system in this talk along with an update on the present status of the overall project.

Keywords: Incoherent Scatter Radar, ionosphere

Japan Geoscience Union Meeting 2014
(28 April - 02 May 2014 at Pacifico YOKOHAMA, Kanagawa, Japan)

PEM06-09 Room:312 Time:April 30 15:00-15:15

Thermospheric neutral density observations using the EISCAT incoherent scatter radars

KOSCH, Michael[1*] ; VICKERS, Hannah[2] ; OGAWA, Yasunobu[3]

[1]Physics Dept., Lancaster University, Lancaster, UK, [2]Institute for Physics and Technology, University of Tromso, Norway, [3]National Institute of Polar Research, Tachikawa, Japan

We exploit a recently-developed technique, based on ion-neutral coupling, to estimate the thermospheric neutral density at ˜350 km using measurements of ionospheric plasma parameters made by the EISCAT radars. The passive version of the technique is applied to a 13-year long data set from the EISCAT Svalbard Radar (ESR). Here we show that the thermospheric density in the polar cap is decreasing, consistent with satellite drag estimates at lower latitudes. The active version of the technique requires the EISCAT Heater to artificially induce ion up-flow by heating the electrons, with observations from the EISCAT UHF radar. Here we show that ion up-flow is consistent with the plasma pressure gradient, and we extract the thermospheric neutral density. At an altitude of ˜500 km, where neutral composition is not always pure atomic oxygen, problems with the technique are discussed.

Keywords: Thermospheric density, Incoherent scatter radar

Japan Geoscience Union Meeting 2014
(28 April - 02 May 2014 at Pacifico YOKOHAMA, Kanagawa, Japan)

PEM06-10 Room:312 Time:April 30 15:15-15:30

3D ionospheric electron density determination in Scandinavia with TomoScand and EISCAT 3D

AMM, Olaf[1*] ; NORBERG, Johannes[1] ; VIERINEN, Juha[3] ; ROININEN, Lassi[4] ; LEHTINEN, Markku[4] ; NAKAMIZO, Aoi[1]

[1]Finnish Meteorological Institute, Arctic Research Unit, Helsinki, Finland, [2]STEL, Nagoya University, Japan, [3]Haystack Observatory, Massachusetts Institute of Technology, Westford, Massachusetts, USA, [4]Sodankyla Geophysical Observatory, University of Oulu, Finland

The TomoScand network for ionospheric tomography in Scandinavia consists of a network of newly designed Beacon receivers and an extensive, dense array of GPS receivers. A novel tomographic inversion technique allows for a multi-frequency analysis for reconstruction of ionospheric electron densities, and is also able to include information of a multitude of ground-based measurements into the inversion, such as data from ionosondes, from the EISCAT radar, and from the magnetometers of the MIRACLE network in Scandinavia. We present the current status of the TomoScand network, and show latest inversion results on 2D profiles in meridional direction, together with test results that allow to evaluate the performance of the inversion technique. Further, we discuss the future development into a full 3D inversion scheme, and how the TomoScand network can be used as a ”partner instrument” for the upcoming EISCAT 3D radar.

Keywords: ionospheric tomography, ionospheric electron density, ground-based observations, EISCAT 3D

Japan Geoscience Union Meeting 2014
(28 April - 02 May 2014 at Pacifico YOKOHAMA, Kanagawa, Japan)

PEM06-11 Room:312 Time:April 30 15:30-15:45

Advancement of geospace and atmospheric sciences with EISCAT_3D

MIYAOKA, Hiroshi[1*] ; NOZAWA, Satonori[2] ; OGAWA, Yasunobu[1] ; OYAMA, Shin-ichiro[2] ; NAKAMURA, Takuji[1] ; FUJII, Ryoichi[2] ; HEINSELMAN, Craig[3]

[1]National Institute of Polar Research, [2]STEL, Nagoya University, [3]EISCAT Scientific Association

The EISCAT(European Incoherent SCATter) Scientific Association is an international research organization, which operates incoherent scatter radars at 931MHz, 224MHz and 500MHz in northern Scandinavia and Svalbard for studies of physical and environmental processes in the middle/upper atmosphere and near-Earth space. Affiliated in the EISCAT scientific association in 1996, Japanese science community has jointly contributed to achieve further understanding of the magnetosphere-ionosphere-thermosphere coupling processes using the integrated ground-based instruments and rocket/satellite simultaneous observations with EISCAT radars.

EISCAT_3D is the major upgrade of the existing EISCAT radars in the northern Scandinavia.With a multi-static phased array system composed of one central active (transmit-receive) site and several receive-only sites, the EISCAT_3D system is expected to provide us 10 times higher temporal and spatial resolution and capabilities than the present radars.

In this presentation, we will overview our scientific activity and achievements with the EISCAT facility and our strategic plan of national funding for EISCAT_3D as well as the science targets which we expect to be unraveled by EISCAT_3D.

Keywords: Incoherent scatter radar, EISCAT, Ionosphere, Thermosphere, Mesosphere, 3D imaging observation

Japan Geoscience Union Meeting 2014
(28 April - 02 May 2014 at Pacifico YOKOHAMA, Kanagawa, Japan)

PEM06-12 Room:312 Time:April 30 15:45-16:00

Study on ion upflow and outflow based on EISCAT_3D and its related observations

OGAWA, Yasunobu[1*]

[1]National Institute of Polar Research, JAPAN

An important phenomenon of magnetosphere-ionosphere coupling is the formation of upwelling ions in the topside polar ionosphere. These upflows can be a significant loss of atmospheric gasses into interplanetary space and a significant source of magnetospheric plasma, which may also affect the dynamics of the magnetosphere. Key processes for upward ion flows in the topside ionosphere are suggested to be frictional heating, ambipolar diffusion driven by a heated electron gas, and transverse ion acceleration produced by plasma waves. It is critical to determine the relative importance of the different mechanisms in operation and to understand the 3D distribution and composition of the upflowing ions and neutrals. Moreover, there are several transitions of upflowing ions, for examples, from chemical to diffusion dominance at 500-800 km altitude, from subsonic to supersonic flow at 1000-2000 km altitude, and from collisional to collisionless region at 1500-2500 km altitude.

EISCAT_3D is one of the most suitable measurements to investigate such transitions because of its wider height coverage (up to about 2000 km) along the field line. EISCAT_3D will have more transmitter power density and higher sensitivity than those of the current Tromso UHF radar, and will give information of accurate thermal ion velocity, upward flux, and ion composition (O^+, H^+, and hopefully NO^+). A combination of the EISCAT_3D, ground-based optical instruments, and in-situ measurements is definitely essential to solve several key questions of ion upflow and outflow study. In this paper, we show potential investigations of ion upflow and outflow using the EISCAT_3D, and also discuss a desirable combination of the EISCAT_3D and its related observations for the ion upflow and outflow study.

Keywords: EISCAT, ionosphere, M-I coupling

Japan Geoscience Union Meeting 2014
(28 April - 02 May 2014 at Pacifico YOKOHAMA, Kanagawa, Japan)

PEM06-13 Room:312 Time:April 30 16:15-16:30

Meteor head echo observation with a high power large aparture (HPLA) radar and an open database of precise meteor orbit

NAKAMURA, Takuji[1*] ; KERO, Johan[2]

[1]National Institute of Polar Research, [2]Swedish Institute of Space Physics (IRF)

Mass influx from the space into the terrestrial atmosphere is mainly caused by meteors. Meteors delivers various elements into the atmosphere, but the meteoric dust particles are also of great importance in the terrestrial atmosphere, as they act as nucleus for condensation and clouds and affect the various atmospheric phenomena both in physical and chemical aspects. Thus, to investigate the meteor flux, orbits and their interactions in the upper atmosphere is very important but at the same time the method of investigation is limited, especially for the precise measurements.

A high power large aperture (HPLA) radar technique is one of the recent technique to provide useful information on meteor influx and orbital information, as well as interactions with atmosphere. The recent development of the technique carried out using the middle and upper atmosphere radar (MU radar) of Kyoto University at Shigaraki (34.9N, 136.1S), which is a large atmospheric VHF radar with 46.5 MHz frequency, 1 MW output transmission power and 8330 m^2 aperture array antenna, has established very precise orbit observations with meteor head echoes. Since 2009, orbital data of about 120,000 meteors have been collected. A database is now being created as an open database for research and education. In this

study, we present the physical quantities and precisions obtained by our radar meteor head echo observations and the detail of the database.

Keywords: meteor, upper atmosphere, high power large aperture radar

Japan Geoscience Union Meeting 2014
(28 April - 02 May 2014 at Pacifico YOKOHAMA, Kanagawa, Japan)

PEM06-14 Room:312 Time:April 30 16:30-16:45

Comparison of Cloud Propagation over Sumatera during CPEA-I and II

MARZUKI, Marzuki[1*] ; RAHAYU, Aulya[1] ; VONNISA, Mutya[1] ; HASHIGUCHI, Hiroyuki[2] ; K. YAMAMOTO, Masayuki[2] ; D. YAMANAKA, Manabu[3] ; MORI, Shuichi[3] ; KOZU, Toshiaki[4] ; SHIMOMAI, Toyoshi[4]

[1]Department of Physics, Andalas University, Padang, Indonesia, [2]Research Institute for Sustainable Humanosphere (RISH) Kyoto University, Gokasho, Uji, Kyoto 611-001, [3]Japan Agency for Marine-Earth Science and Technology (JAMSTEC), Yokosuka, Japan, [4]Interdisciplinary Faculty of Science and Engineering, Shimane University, Japan

Maritime Continent of the Indonesian (MCI) archipelago is one of the world's most convectively active areas and thereby affects the global climate system. It consists of thousands of islands with different size. The island coastlines' complex shape and geography, as well as their orientation, contribute to the uniqueness of this region. Not surprisingly, maritime continent receives a large amount of rainfall throughout the year, and the precipitation varies considerably across the region. Global climate models exhibit systematic errors in their mean precipitation over the MCI due to such variability. In this study, the behavior of convective activity over Sumatera during the Coupling Processes in the Equatorial Atmosphere (CPEA) campaign I and II is examined using 1-hourly satellite infrared data. Sumatra Island is elongated and oriented from northwest to southeast and its elevated orography temporarily blocked the eastward propagation of precipitation system. The dynamics of Sumatra weather systems remains poorly understood and part of the problem lies in the lack of atmospheric data and high-resolution gridded data analyses and realistic model simulations. Therefore, the data of two intensive observation periods as the international observation campaign of the CPEA will also be used. Cloud propagation statistics (speed, span, life time, size, etc.) of the individual cloud episodes and the physical basis behind the results will be discussed.

Keywords: Cloud propagation, Sumatra, CPEA

Japan Geoscience Union Meeting 2014
(28 April - 02 May 2014 at Pacifico YOKOHAMA, Kanagawa, Japan)

PEM06-15 Room:312 Time:April 30 16:45-17:00

SuperDARN global observation of energy input and coupling processes and recent technical development

YUKIMATU, Akira sessai[1*] ; NISHITANI, Nozomu[2] ; NAGATSUMA, Tsutomu[3]

[1]NIPR/SOKENDAI, [2]STEL, Nagoya Univ., [3]NICT

SuperDARN (Super Dual Auroral Radar Network) [Greenwald, et al., 1995] is an international collaborative HF-radar network [Greenwald, et al., 1985] operated by more than 15 institutions in over 10 countries, and the number of the radars is currently more than 30 and it is still growing and the fields-of-view (FOVs) have been expanding to both higher and mid-latitudes covering considerable portions of global upper atmosphere in both hemispheres.

SuperDARN was originally designed to measure line-of-sight plasma Doppler spectra and ionospheric electric field to obtain global large scale two-dimensional polar ionospheric plasma convection patterns and polar cap potential drop in both hemispheres with a temporal resolution of 1 to 2 minutes in real time since 1995, which have never been possible by any other observational techniques, and this capability provides us very important and essential information on solar energy input to our geospace, magnetosphere and polar ionosphere, which has greatly contributed to basic understanding of coupling processes in Sun-Earth system as well as space weather researches.

SuperDARN is a powerful tool to be applied to many scientific issues [Chisham, et al., 2007 and references therein]. It can be used not only to deduce dynamics of global large-scale convection patterns, but also to study dynamics of transient meso-scale phenomena like FTEs and TCVs, and polar cap boundary or open-closed field line boundary (OCB), to detect reconnection sites and to deduce reconnection rates, to study substorms, storms and phenomena related to subauroral regions like sub-auroral polarisation stream (SAPS), to deduce field aligned currents (FACs), to study MHD waves in a variety of frequency ranges, and also to study ionospheric irregularities in D-, E-, and F-regions. Moreover, it can be utilised not only to ionospheric researches but also to neutral atmospheric studies, e.g., on atmospheric waves like TIDs, tides and gravity waves, neutral winds around mesopause region, and also polar mesospheric summer echoes (PMSEs), etc.

These days, the fields-of-view (FOVs) of SuperDARN have been expanded to higher latitude (PolarDARN) and mid-latitude (StormDARN) which covers considerable portions of mid- and polar latitudes of earth's ionosphere in both hemispheres and enables us to address much wider ranges of scientific questions including inner magnetospheric physics. There are also ongoing discussions to expand the SuperDARN radars field of view to even lower latitudes, up to low latitude and equatorial regions.

SuperDARN has extensively evolved successfully and has been extremely productive by strong cooperation and competitions within the community and also by collaborative studies with other ground-based and satellite/rocket observations and theoretical researches, which has greatly contributed to a variety of studies especially on magnetosphere-ionosphere coupling processes and ionosphere and neutral atmosphere coupling.

As SuperDARN could have provided basic and important physical parameters in global upper atmosphere, collaborative studies with other projects like IS-radars like EISCAT and PANSY providing many detailed physical parameters at fix points as well as satellite missions like THEMIS, VAP, and ERG and rocket campaigns providing in-situ measurements will be particularly important to contribute to our deeper understanding of the Sun-Earth coupling processes.

Also some SuperDARN radars has developed new technical upgrade including imaging radar capabilities providing higher spatial resolution. New science targets with SuperDARN with new capabilities will also be discussed.

Keywords: SuperDARN, HF radar, coupling processes, imaging radar, MI coupling, neutral wind

Japan Geoscience Union Meeting 2014
(28 April - 02 May 2014 at Pacifico YOKOHAMA, Kanagawa, Japan)

PEM06-16 Room:312 Time:April 30 17:00-17:15

Low Latitude Ionospheric Scintillation Research Using GISTM Network over Indonesia

HUSIN, Asnawi[1*] ; ABADI, Prayitno[1] ; JIYO, Harjoswito[1] ; YAMAMOTO, Mamoru[2] ; OTSUKA, Yuichi[3]

[1]Space Science Center, LAPAN, [2]RISH, Kyoto University, [3]STEL, Natoya University

The ionosphere plays an active role in the space weather relationships, so the permanent monitoring of the ionosphere state on global and regional is required. The advancement of Global Navigation Satellite Systems (GNSS) such as GPS (Global Positioning System) receiver technology provides a low cost solution for monitoring and research the ionosphere on global and regional basis. National Institute of Aeronautics and Space (LAPAN) Indonesia has been installed GPS Ionospheric Scintillation and TEC Monitor (GSV4004b) to monitor and study ionospheric irregularities.

This paper reports a statistical study of the occurrences characteristic of GPS ionospheric scintillation and irregularity in low latitude Indonesia sector. These measurements were made by GPS Ionospheric Scintillation and TEC Monitor System (GISTM) at Pontianak (0.03S 109.33E), Bandung (6.93S 107.6E), Manado (1.34N 124.83E), Kupang (10.16S 123.66E), and Kototabang (0.12S 100.12E). For the GPS station at Kototabang, we use ISM (ionospheric scintillation monitor) under collaboration with STELAB Nagoya Univeristy. We distinguish scintillation occurrences rate between post sunset and after midnight by using S4 index during maximum solar activity period in 2013. We analyze the occurrence rate using azimuth-elevation coordinate (sky plot). The following figure is to show observation geometry which is used in this study.

Keywords: Ionospheric Scintillation, Indonesia, GPS receiver

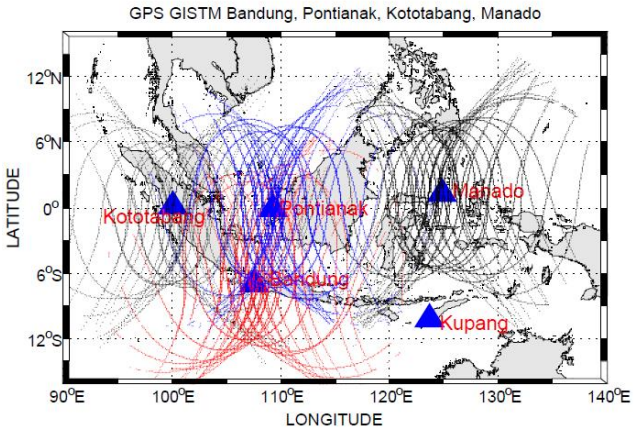

Japan Geoscience Union Meeting 2014
(28 April - 02 May 2014 at Pacifico YOKOHAMA, Kanagawa, Japan)

PEM06-17 Room:312 Time:May 1 09:00-09:30

Future direction of the ground-based network observations of the magnetosphere and the upper atmosphere

SHIOKAWA, Kazuo[1*] ; OTSUKA, Yuichi[1]

[1]Solar-Terrestrial Environment Laboratory, Nagoya University

Multi-point ground-based instruments are powerful tools to investigate global dynamics of the magnetosphere, ionosphere, and the upper atmosphere. Airglow imagers and multi-point GPS receivers provide two- and three-dimensional view of these regions. The ring-current and radiation-belt particles in the inner magnetosphere round the earth with a time scale from a few tens of minutes to a few hours. Interactions of these particles with Pc5 (times scale of ˜minutes), Pc1 (˜Hz) and VLF/ELF chorus (˜kHz) causes acceleration and loss of these particles. Thus, longitudinal chain of ground-based stations to observe these various waves and auroras is essentially needed to understand the acceleration and loss of the plasma in the inner magnetosphere. The auroral energy input from the solar wind and magnetosphere to the high-latitude ionosphere is a major energy source of the dynamic variation of the upper atmosphere. Intense convective activity in the equatorial troposphere gives another energy source of the dynamic variation of the upper atmosphere. Thus, meridional chain stations are essentially needed to understand these dynamic variations and their global coupling. In this presentation we discuss possible future directions of these ground-based network observations to understand the global dynamics of the magnetosphere, ionosphere, and the upper atmosphere.

Keywords: ground-based network observation, ionosphere, magnetosphere, upper atmosphere, future direction

Japan Geoscience Union Meeting 2014
(28 April - 02 May 2014 at Pacifico YOKOHAMA, Kanagawa, Japan)

PEM06-18 Room:312 Time:May 1 09:30-09:45

ICSWSE/ MAGDAS Project: Research for global electromagnetic coupling from polar to equatorial ionosphere

YOSHIKAWA, Akimasa[1*] ; NAKAMIZO, Aoi[2] ; OHTANI, Shinichi[3] ; TANAKA, Yoshimasa[4] ; IMAJO, Shun[5] ; MATSUSHITA, Hiroki[5] ; CARDINAL, Maria gracita[1] ; ABE, Shuji[1] ; UOZUMI, Teiji[1] ; YUMOTO, Kiyohumi[1]

[1]International Center for Space Science and Education, Kyushu University, [2]Finish Meteorological Institute, [3]The Johns Hopkins University Applied Physics Laboratory, [4]National Institute of Polar Research, [5]Earth and Planetary Science , Kyushu University

International Center for Space Weather Science and Education (ICSWSE) has developed a real time magnetic data acquisition system (the MAGDAS project) for space environment monitoring around the world. The number of observational sites is increasing every year with the collaboration of MAGDAS host countries. Now at this time, the MAGDAS Project has installed 73 real time magnetometers ? so it is the largest magnetometer array in the world.

Applying equivalent current method to this network data, we analyze a global ionospheric current system from polar to equatorial ionosphere. Our results suggest that Dp2 type disturbances excited by solar wind variation, Pi2 type pulsations accompanied by aouroral substorm onset process and Pc3 type pulsations accompanied by dayside cavity type oscillation show the same type of global current system, which are produced by primary bipolar electric field accompanied by field-aligned current system and Hall polarization electric field excited at the dawn-dusk conductivity terminator and at the magnetic dip equator.We will discuss how the electromagnetic coupling between polar and equatorial ionosphere is regulated by the formation of global Cowling channel in the ionosphere.

Keywords: Space Weather, Magnetosphere-Ionosphere-Atmosphere Coupling, Global Coupling

Japan Geoscience Union Meeting 2014
(28 April - 02 May 2014 at Pacifico YOKOHAMA, Kanagawa, Japan)

PEM06-19 Room:312 Time:May 1 09:45-10:00

Contribution of the IUGONET data analysis system to a study on coupling processes in the solar-terrestrial system

SHINBORI, Atsuki[1*] ; YAGI, Manabu[2] ; TANAKA, Yoshimasa[3] ; SATO, Yuka[3] ; YATAGAI, Akiyo[4] ; UMEMURA, Norio[4] ; HORI, Tomoaki[4] ; UENO, Satoru[5] ; KOYAMA, Yukinobu[6] ; ABE, Shuji[7]

[1]Research Institute for Sustainable Humanosphere (RISH), Kyoto University, [2]Planetary Plasma and Atmospheric Research Center, Graduate School of Science, Tohoku University, [3]National Institute of Polar Research, [4]Solar-Terrestrial Environment Laboratory, Nagoya University, [5]Kwasan & Hida Observatories, School of Science, Kyoto University, [6]Data Analysis Center for Geomagnetism and Space Magnetism Graduate School of Science, Kyoto Universi, [7]International Center for Space Weather Science and Education, Japan

Various kinds of disturbance phenomenon and long-term variation as seen in several observation parameters (electric and magnetic fields, temperature, mean wind etc.) in a wide area from space surrounding the Earth to the atmospheric layers are caused by energy input from solar radiation, solar wind, momenta and energies from the lower atmosphere via atmospheric waves, and chemical reaction. Such a disturbance phenomenon and long-term variation observed by various kinds of ground-based and satellite instruments are the result of such complicated processes. Then, in order to investigate the mechanisms of these phenomena in this region, researchers need to conduct comprehensive analyses with various kinds of long-term observation data that have been continued by means of a global network of radars, magnetometers, optical sensors, helioscopes, etc. The IUGONET (Inter-university Upper atmosphere Global Observation NETwork) project initiated in 2009 aims at the establishment of a cross-reference system for various kinds of ground-based observation data obtained from different techniques. The IUGONET participants consist of five universities/institutes: the National Institute of Polar Research (NIPR), Tohoku University, Nagoya University, Kyoto University, and Kyushu University. We have developed metadata database (MDB) and IUGONET data analysis software (UDAS) of ground-based observation data managed by these IUGONET universities/institutes with an international collaboration in order to promote a study on coupling process in the Sun-Earth system. The MDB provides researchers in a wide range of disciplines with a seamless data environment to link databases spread across the IUGONET universities/institutes. In particular, UDAS will be of great help in conducting integrated analyses and visualization of various kinds of solar-terrestrial observation data to investigate the long-term variation in the upper atmosphere throughout the Sun-Earth system. Then, the IUGONET products will greatly contribute to a study on coupling process in the Sun-Earth system on the basis of integrated analysis of various kinds of long-term observation data covering a wide region from both the pole to the equator. In this talk, we introduce a brief overview of the IUGONET project, and an application of the IUGONET products to typical examples of upper atmospheric researches.

Keywords: Upper atmosphere, Long-term variation, Solar activity, Metadata search system, Data analysis tool, Coupling process in the Sun-Earth system

Japan Geoscience Union Meeting 2014
(28 April - 02 May 2014 at Pacifico YOKOHAMA, Kanagawa, Japan)

PEM06-20 Room:312 Time:May 1 10:00-10:15

Statistical characteristics of nighttime MSTIDs observed by an airglow imager over sub-tropical site Yonaguni (19.3N dip)

VISWANATHAN, Lakshmi narayanan[1*] ; SHIOKAWA, Kazuo[1] ; OTSUKA, Yuichi[1] ; SAITO, Susumu[2]

[1]Solar Terrestrial Environment Laboratory, Nagoya University, Nagoya, Japan, [2]Electronic Navigation Research Institute, Tokyo, Japan

The nighttime medium-scale travelling ionospheric disturbances (MSTIDs) are frequently observed in the mid-latitude ionosphere. They very often moves toward the southwest direction in the northern hemisphere with phase fronts aligned along the northwest to the southeast. However they do not extend to the equatorial latitudes and are rarely sighted at dip latitudes below 15^o. In this study we investigate the characteristics of MSTID features observed over Yonaguni (24.5^oN, 123.0^oE; 19.3^oN dip latitude), Japan with all-sky imaging of OI 630.0 nm airglow emission. We selected two year period for analysis in which one year corresponds to the solar minimum conditions and another year corresponds to solar maximum conditions. It is found that the MSTIDs occur more frequently during solar minimum conditions. The observed range of wavelengths, phase speeds and directions of MSTIDs are similar to those observed at typical mid-latitude sites. On many occasions the phase fronts of the observed MSTIDs do not extend over the whole field of view of imager indicating that some process hinders their extension to further lower latitudes. Herein, we also investigate the possible reason for the disappearance of phase fronts when they reach lower latitudes.

Keywords: medium-scale travelling ionospheric disturbances, OI 630.0 nm airglow

Japan Geoscience Union Meeting 2014
(28 April - 02 May 2014 at Pacifico YOKOHAMA, Kanagawa, Japan)

PEM06-21 Room:312 Time:May 1 10:15-10:30

Thermospheric wind variations in the pulsating aurora measured with FPI and IS radars

OYAMA, Shin-ichiro[1*] ; KURIHARA, Junichi[2] ; TSUDA, Takuo[3] ; SHIOKAWA, Kazuo[1] ; MIYOSHI, Yoshizumi[1] ; WATKINS, Brenton J.[4]

[1]Solar-Terrestrial Environment Laboratory, Nagoya University, [2]Graduate School of Science, Hokkaido University, [3]National Institute of Polar Research, [4]Geophysical Institute, University of Alaska Fairbanks

Pulsating aurora is a typical phenomenon of the recovery phase of magnetic substorm and is frequently observed in the morning sector. While our understanding of pulsating aurora has not yet reached maturity, the widely accepted generation mechanism causing pulsations in precipitating electrons is related to wave-particle interactions around the equatorial plane in the magnetospheric tail. The closure current system in pulsating aurora may not be as strongly evolved as compared to that in the discrete arc because of smaller precipitation flux (or upward field-aligned current) and weaker perpendicular electric field (or the Pedersen current). Thus one may assume that Joule energy dissipation and/or Lorentz force does not play an important role for modifications of the thermospheric wind dynamics in pulsating aurora. However, we found thermospheric-wind variations in the pulsating aurora during simultaneous observations with a Fabry-Perot Interferometer (FPI; 557.7 nm), an all-sky camera (557.7 nm), and the European Incoherent Scatter (EISCAT) UHF radar. Of particular interest is that the location of the fluctuations was found in a darker area that appeared within the pulsating aurora. During the same time period, the EISCAT radar observed sporadic enhancements in the F-region backscatter echo power, which suggests the presence of low-energy electron (1 keV or lower) precipitation. Using other data sets archived by the EISCAT radar, a statistical analysis shows that the F-region enhancement tends to coexist with hard-particle precipitation or the pulsating aurora. This presentation will summarize our experimental evidences showing several events of the pulsating aurora, and discuss application of the phased-array IS radar to this study.

Keywords: pulsating aurora, thermosphere, FPI, IS radar

Japan Geoscience Union Meeting 2014
(28 April - 02 May 2014 at Pacifico YOKOHAMA, Kanagawa, Japan)

PEM06-22 Room:312 Time:May 1 10:30-10:45

Coordinated observation of space-borne imaging by ISS-IMAP and ground-based measurement by radars and GPS

SAITO, Akinori[1*] ; YAMAZAKI, Atsushi[2] ; SAKANOI, Takeshi[3] ; YOSHIKAWA, Ichiro[4] ; OTSUKA, Yuichi[5] ; YAMAMOTO, Mamoru[1] ; NAKAMURA, Takuji[6] ; AKIYA, Yusuke[1] ; HOZUMI, Yuta[1]

[1]Kyoto University, [2]JAXA/ISAS, [3]Tohoku University, [4]University of Tokyo, [5]Nagoya University, [6]National Institute of Polar Research

ISS-IMAP mission is a space-borne mission to investigate the mesoscale structures in the ionosphere, the mesosphere, and the plasmasphere by imaging observations of instruments on International Space Station. It consists of two imaging instruments. Visible-light and infrared spectrum imager (VISI) observes the airglow in the MTI region. Extra ultraviolet imager (EUVI) observes the resonant scattering from ions in the ionosphere and the plasmasphere. The objective of this mission is to clarify the upper atmospheric structures whose horizontal scale is 50-500km, and the effect of the structures on the space-borne systems in the low- and mid-latitude regions. VISI observes the airglow of 730nm (OH, Alt. 85km), 762nm (O2, Alt 95km), 630nm(O, Alt.250km) in the Nadir direction to investigate the mesoscale structures in the mesosphere and the ionosphere. The coordinated observations of ISS-IMAP with ground-based measurements have been carried out. The MU radar and Equatorial Atmosphere Radar (EAR) observe the ionosphric density structures and field-aligned irregularities while ISS-IMAP observe the large and mesoscale ionospheric structures with the 630nm airglow, and the atmospheric gravity waves in the mesosphere with the 762nm airglow. The two-dimensional distribution of total electron contents derived with the ground-base GPS receiver array is also compared with the ionospheric and mesospheric structures observed by ISS-IMAP. The results of the ISS-IMAP mission by VISI and EUVI, and its coordinated observations with the ground-based instruments will be introduced in the presentation.

Keywords: Ionosphere, Airglow, Atmospheric Gravity Wave, Plasma Bubble, Radar, GPS

Japan Geoscience Union Meeting 2014
(28 April - 02 May 2014 at Pacifico YOKOHAMA, Kanagawa, Japan)

PEM06-23 Room:312 Time:May 1 11:00-11:30

Current status of Program of the Antarctic Syowa MST/IS radar (PANSY)

SATO, Kaoru[1*] ; TSUTSUMI, Masaki[2] ; SATO, Toru[3] ; NAKAMURA, Takuji[2] ; SAITO, Akinori[3] ; TOMIKAWA, Yoshihiro[2] ; NISHIMURA, Koji[2] ; KOHMA, Masashi[1] ; YAMAGISHI, Hisao[2] ; YAMANOUCHI, Takashi[2]

[1]Dept Earth & Planetary Sci., The University of Tokyo, [2]National Institute of Polar Research, [3]Kyoto University

The PANSY radar is the first Mesosphere-Stratosphere-Troposphere/Incoherent Scatter (MST/IS) radar in the Antarctic. It is a VHF monostatic pulse Doppler radar operating at 47 MHz, consisting of an active phased array of 1,045 Yagi antennas and an equivalent number of transmit-receiver modules with a total peak output power of 500 kW. The first stage of the radar was installed at Syowa Station (69^{o}00'S, 39^{o}35'E) in early 2011, and is continuously operating with 228 antennas and modules since April 2012. The full radar system operation will start in 2015. This paper reports the project's scientific objectives, technical descriptions, and the preliminary results of observations made to date. The radar is designed to clarify the role of atmospheric gravity waves at high latitudes in the momentum budget of the global circulation in the troposphere, stratosphere and mesosphere, and to explore the dynamical aspects of unique polar phenomena such as polar mesospheric/stratospheric clouds. The katabatic winds as a branch of Antarctic tropospheric circulation and as an important source of gravity waves are also of special interest. Moreover, strong and sporadic energy inputs from the magnetosphere by energetic particles and field-aligned currents can be quantitatively assessed by the broad height coverage of the radar which extends from the lower troposphere to the upper ionosphere. From engineering points of view, the radar had to overcome restrictions related to the severe environments of Antarctic research, such as very strong winds, limited power availability, short construction periods, and limited manpower availability. We resolved these problems through the adoption of specially designed class-E amplifiers, lightweight and tough antenna elements, and versatile antenna arrangements. We will show highlights of several interesting results from the radar observations regarding severe snow storms, gravity waves, multiple tropopauses, and polar mesosphere summer/winter echoes.

Reference

Sato, K., et al., *J. Atmos. Solar-Terr. Phys.*, doi:10.1016/j.jastp.2013.08.022, 2013.

Keywords: MST/IS radar, polar atmosphere, middle atmosphere, gravity waves, general circulation

Japan Geoscience Union Meeting 2014
(28 April - 02 May 2014 at Pacifico YOKOHAMA, Kanagawa, Japan)

PEM06-24 Room:312 Time:May 1 11:30-11:45

Importance of coordinated ground-based, satellite observations

MIYOSHI, Yoshizumi[1*] ; OYAMA, Shin-ichiro[1] ; SAITO, Shinji[1]

[1]STEL, Nagoya University

The ERG (Exploration of energization and Radiation in Geospace) is Japanese geospace exploration project. The project focuses on the geospace dynamics in the context of the cross-energy coupling via wave-particle interactions. The project consists of the satellite observation team, the ground-based network observation team, and integrated-data analysis/simulation team. The ERG satellite will be launched in FY2015. Comprehensive instruments for plasma/particles, and field/waves are installed in the ERG satellite to understand the cross-energy coupling system. In the ERG project, several ground-network teams join; magnetometer networks, radar networks, optical imager networks, etc. Moreover, the modeling/simulations play an important role for the quantitative understanding. In this presentation, we will discuss the importance of coordinated observations toward the ERG era. As an example, we show the cooperative observations between the geospace satellite Van Allen Probes an EISCAT to observe the pulsating aurora. The EISCAT measured the height profile of the electron density that can provide the energy of the precipitating electrons. The Van Allen Probes measured the plasma waves in the magnetosphere, which can be used to investigate the origin of the pulsating aurora. In fact, the GEMSIS-RBW simulation that used the observed plasma waves as an input reproduces characteristics of the observed precipitation. Such coordinated observations including the modeling provide a comprehensive view on cause and result.

Keywords: satellite-ground observations, ERG project

Japan Geoscience Union Meeting 2014
(28 April - 02 May 2014 at Pacifico YOKOHAMA, Kanagawa, Japan)

PEM06-25 Room:312 Time:May 1 11:45-12:00

Synthetic Study on Solar-Terrestrial Phenomena with Widespread Observation Network in Antarctica

KADOKURA, Akira[1*] ; YAMAGISHI, Hisao[1] ; YUKIMATU, Akira sessai[1] ; MIYAOKA, Hiroshi[1] ; OKADA, Masaki[1] ; OGAWA, Yasunobu[1] ; TANAKA, Yoshimasa[1] ; KATAOKA, Ryuho[1] ; EBIHARA, Yusuke[2] ; MOTOBA, Tetsuo[3]

[1]National Institute of Polar Research, [2]Research Institute for Sustainable Humanosphere, Kyoto University, [3]Applied Physics Laboratory, Johns Hopkins University

A large observation network with the SuperDARN radars and other ground-based instruments at manned and unmanned stations is currently developed in the Antarctic area from sub-auroral latitudes to polar cap region and from nightside to dayside hours under international collaboration. Such a widespread circumpolar observation network is very unique and powerful for studies on the phenomena which occur due to the Sun-Earth interaction, e.g., direct entry of solar wind energy and momentum into the cusp and polar cap regions, explosive energy dissipation during substorm-time, highly energetic particle precipitation into the atmosphere during storm-time. Coordinated observations with several low-altitude satellites (e.g., NOAA, DMSP, etc.) and magnetospheric satellites (e.g., THEMIS/ARTEMIS, Geotail, MMS, ERG, etc.) can be also expected In our presentation, current status and future plan of NIPR-related project will be introduced, and importantce of such a widespread ground-based observation network in Antarctica will be explained and discussed.

Keywords: Antarctica, large area, observation network, Solar-Terrestrial Physics

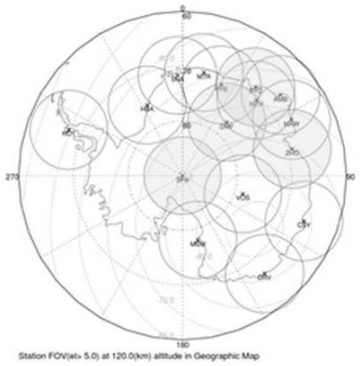

Figure 1. Field of views (FOVs) of Antarctic stations projected at 120 km altitude for elevation above 5 deg. The shaded FOV indicates the station where auroral optical observation is currently carried out. Geomagnetic latitudes are also shown in gray lines.

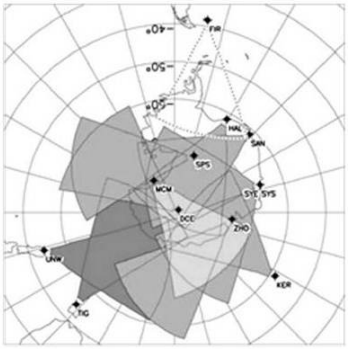

Figure 2. Field of views of the SuperDARN radars in the southern hemisphere in the magnetic coordinates, including two radars at Syowa Station (SYE and SYS).

Japan Geoscience Union Meeting 2014
(28 April - 02 May 2014 at Pacifico YOKOHAMA, Kanagawa, Japan)

PEM06-26 Room:312 Time:May 1 12:00-12:15

A review of selected data-analysis techniques for determining ionospheric electrodynamic parameters on mesoscales

VANHAMAKI, Heikki[1*] ; AMM, Olaf[1]

[1]Finnish Meteorological Institute, Helsinki, Finland

We present a review of selected data-analysis methods that are applied in studies of ionospheric electrodynamics and magnetosphere-ionosphere coupling using ground-based and space-based data sets. At present, there is no single measurement device that can measure all ionospheric electrodynamic parameters directly and simultaneously, with good spatial and temporal resolution and coverage. Therefore data-analysis techniques are needed to combine different types of measured data and to obtain unobserved ionospheric parameters from the observed ones, possibly using some additional assumptions in the process. We concentrate on methods that are data driven and applicable to single events (not simulations or statistical models), and which can be used in mesoscale studies, where the analysis area is typically some hundreds or thousands of km across.

The primary focus of this review is in ionospheric electrodynamics, so we do not include variables like chemical composition, temperature, etc. in our discussion. Furthermore we concentrate on analysis techniques that have been developed to be used with data from the MIRACLE network (Magnetometers - Ionospheric Radars - All-sky Cameras Large Experiment) situated in Northern Europe, possibly in combination with satellite observations, such as Cluster or CHAMP. However, the techniques can be applied to data from any other mesoscale network with similar observations.

The full set of ionospheric electrodynamic parameters that we are interested in consist of the ionospheric horizontal electric field, height integrated Hall and Pedersen conductances, horizontal sheet current and field aligned current (FAC). Additionally, the ground magnetic perturbation is an important input parameter in many analysis methods.

Most of the reviewed methods are used in 2-dimensional (latitude - longitude) regions of the ionosphere, but some methods have also 1-dimensional variants. In 1D analysis it is assumed that ionospheric parameters vary only in one horizontal direction (e.g. as a function of geomagnetic latitude), so input data is required along a single chain or a satellite track only. The 1D methods are especially useful when analyzing data from an overpassing satellite or from a meridional magnetometer chain.

Keywords: Ionosphere, Ionospheric electrodynamics, Ionospheric currents, Data-analysis methods

Japan Geoscience Union Meeting 2014
(28 April - 02 May 2014 at Pacifico YOKOHAMA, Kanagawa, Japan)

PEM06-27 Room:312 Time:May 1 12:15-12:30

Fine-scale electrodynamic structure behind auroral vortex street

HOSOKAWA, Keisuke[1*]

[1]University of Electro-Communications

One of the primary scientific objectives of the planned EISCAT_3D system would be “3D imaging of aurora”, especially 3D imaging of dynamically moving auroral arcs at the time of substorm expansion phase onset. In order to discuss the specification of the EISCAT_3D system in detail, we have to know how such an effort of multi-dimensional imaging of aurora has been made by using currently-working radar systems in the high-latitude region. For this purpose, I present a fine-scale electrodynamic structure behind an auroral vortex street observed immediately before substorm expansion phase onset, as inferred from high spatial and temporal resolution measurements of auroral breakup with an all-sky TV camera (ATV) and a coherent HF radar of Super Dual Auroral Radar Network (SuperDARN) in Iceland. During the interval of interest, the ATV observed eastward propagating auroral vortices in the initial brightening arc of a substorm just prior to the poleward expansion. During the sequential passage of the vortices across the radar beams, the radar detected large velocity flow shears whose magnitude was in excess of 1.5 km/s. The observations suggest that flow shears were located very close to the center of the vortices; thus, they corresponded to electric fields converging toward the vortices, which is consistent with the existence of upward field-aligned currents (FACs) flowing out of the vortices. The temporal and spatial resolutions of the current radar measurement were still insufficient for fully resolving the detailed electrodynamic structure behind the fast moving auroral vortices. At least, however, the observations suggest the existence of highly localized filamentary FAC structures behind the auroral vortex street. Such a fine-scale structuring process of an auroral arc would be one of the possible targets of the 3D imaging observations of the planned EISCAT_3D system.

Keywords: Aurora, Radar, Electric Field

Japan Geoscience Union Meeting 2014
(28 April - 02 May 2014 at Pacifico YOKOHAMA, Kanagawa, Japan)

PEM06-28 Room:312 Time:May 1 12:30-12:45

Study of the physical meanings of ionospheric tidal signatures using theoretical models

LIN, Charles[1*] ; CHEN, Yu-tsung[1] ; CHEN, Po-cheng[1] ; CHANG, Loren[2] ; LIN, Jia-ting[1] ; HUBA, Joseph[3] ; CHEN, Chia-hung[1]

[1]Department of Earth Science, National Cheng-Kung University, Tainan, Taiwan, [2]Institute of Space Science, National Central University, Chung-Li, Taiwan, [3]Plasma Physics Division, Naval Research Laboratory, Washington, D.C., USA

Variations the ionospheric electron density structures related to the tidal forcing propagating upward from the lower atmosphere have been studied intensively recently. The longitudinal variations of ionospheric electron density are related to the themospheric nonmigrating tidal signatures produced in-situ or propagating upward from below. During a stratospheric sudden warming, thermospheric migrating tidal signatures are modified and lead to the phase shift of ionospheric electron density structures at low latitudes. With the increasing number of global ionospheric observations, it is desirable to relate the thermospheric tidal signatures to corresponding tidal signatures of ionospheric electron density, since the neutral thermospheric temperature and wind observations are rather limited. In this paper we perform theoretical simulations to study the interconnections between tidal modes in thermospheric neutral parameters and ionospheric plasma. The migrating and nonmigrating tides of thermospehric winds output from NCAR GSWM/TIEGCM runs are incorporated to NRL SAMI-3 to investigate the responses of corresponding tidal modes in ionospheric electron density and their physical meanings.

Keywords: atmospheric tides, tidal signature of ionospheric electron density

Japan Geoscience Union Meeting 2014
(28 April - 02 May 2014 at Pacifico YOKOHAMA, Kanagawa, Japan)

PEM06-29 Room:312 Time:May 1 14:15-14:45

Wavelike Structures in the Low-Latitude F region Using Beacon Satellites

TSUNODA, Roland[1*]

[1]SRI International

The low-latitude F-region plasma is produced by solar radiation, and its gross structural features arise from plasma transport and re-distribution (1) along geomagnetic field (B) lines by a meridional neutral wind, and (2) in planes transverse to B by an electric field (E). The fundamental process is often referred to as the equatorial fountain, in which an eastward electric field, applied over the magnetic dip equator, drives the plasma upward; this transverse transport is accompanied by downward and outward transport along B, which is driven by gravity and diffusion. The enhancements in plasma density that form, one in each hemisphere, are known as the equatorial ionization anomalies. Embedded within these largest-scale structures is a hierarchy of smaller-scale wavelike perturbations that extend downward from perhaps 1000 km to nearly 10 cm. These structures include large-scale wave structure, traveling ionospheric disturbances, equatorial plasma bubbles, as well as the small-scale irregularities that are responsible for radio wave scintillations and radar backscatter. Because of the complex hierarchy of structures that can be present, comprehensive investigations require a network of sensors that can provide both spatial and temporal information with adequate spatial resolution, while providing the necessary geographical coverage. A brief review of some of the recent results regarding wavelike structures, obtained from studies using a broad network of instruments distributed throughout the Southeast Asian sector, is presented.

Keywords: Wavelike structures, Low Latitude F Region, Plasma Structures, Beacon Satellites

Japan Geoscience Union Meeting 2014
(28 April - 02 May 2014 at Pacifico YOKOHAMA, Kanagawa, Japan)

PEM06-30 Room:312 Time:May 1 14:45-15:00

Preliminary study of equatorial ionization anomaly characteristic from GRBR chain in southeast Asia

WATTHANASANGMECHAI, Kornyanat[1*] ; YAMAMOTO, Mamoru[1] ; SAITO, Akinori[2] ; MARUYAMA, Takashi[3]

[1]Research Institute for Sustainable Humanosphere, Kyoto University, [2]Department of Geophysics, Graduate School of Science, Kyoto University, [3]National Institute of Information and Communications Technology

To study the equatorial ionization anomaly (EIA) characteristic, comparison of total electron content (TEC) obtained from the GNU Radio Beacon Receiver (GRBR) network in southeast Asia with the data from SEALION ionosonde network, Equatorial Atmosphere Radar (EAR), and the SAMI2 model are employed. Five GNU Radio Beacon Receivers (GRBRs) were aligned along 100 degree geographic longitude. Their observations started in March 2012 to enable monitoring the ionosphere during the high solar activity. The GRBR network in southeast Asia is a unique observation network of which the field of view covers $\pm$ 20 degree magnetic latitude including the magnetic equator to capture the ionospheric irregularities including the EIA. As a preliminary result, the day-to-day variability of the EIA was captured by GRBR chain. The asymmetry of the EIA was investigated. As generally known, the neutral wind is a primary source of the EIA asymmetry, while the zonal electric field is the secondary one. Using the GRBR network, the EIA asymmetry is compared with the data from SEALION ionosonde network and from SAMI2 model to clarify the source mechanism of the EIA asymmetry.

Keywords: GRBR, EIA symmetry, Equatorial, Ionosphere, Ionosonde, SAMI2 model

Japan Geoscience Union Meeting 2014
(28 April - 02 May 2014 at Pacifico YOKOHAMA, Kanagawa, Japan)

PEM06-31 Room:312 Time:May 1 15:00-15:15

Performance evaluation of plasma bubble monitoring by VHF radars for GNSS augmentation systems

SAITO, Susumu[1*] ; YAMAMOTO, Mamoru[2] ; OTSUKA, Yuichi[3] ; YOSHIHARA, Takayuki[1]

[1]Electronic Navigation Research Institute, [2]RISH, Kyoto University, [3]STEL, Nagoya University

For global navigation satellite systems (GNSS), ionospheric plasma is one of the most serious error sources. Especially in air navigation where safety is extremely important, augmentation systems corresponding to flight phases are used. Even with augmentation systems of current design, such as ground-based augmentation system (GBAS) or satellite-based augmentation system (SBAS), probability of miss-detection of ionospheric anomalies prevent them from more advance operations. In the low latitude region, ionospheric anomaly detection is a challenge because of frequent occurrence of plasma bubbles.

In this study, plasma bubble detection by a VHF backscatter radar is proposed as an external ionospheric monitor. Multi-beam observation of plasma bubbles can detect two dimensional shapes of plasma bubbles in a plane perpendicular to the magnetic field. When satellite-receiver path of GNSS signals pass crosses the magnetic field line, the signals shall be discarded because it may be affected by plasma bubble.

To evaluate the performance of this system, a VHF radar-GNSS receivers combined experiment has been conducted. The Equatorial Atmosphere Radar (EAR) is used to detect plasma bubbles. Sets of GNSS receivers around the EAR and in Bangkok are used as the pseudo-user and reference station. The observation started from
October 2012, and continues with some technical interruptions.

At the meeting, first results of the experiment will be presented.

Keywords: Equatorial Atmosphere Radar, GNSS augmentation system, plasma bubble, ionospheric monitoring

Japan Geoscience Union Meeting 2014
(28 April - 02 May 2014 at Pacifico YOKOHAMA, Kanagawa, Japan)

PEM06-32 Room:312 Time:May 1 15:15-15:30

Future direction of operational ionospheric research

ISHII, Mamoru[1*]

[1]NICT

We are now facing new aspect of oprational ionospheric research. International Civil Aviation Organization (ICAO) is planning to revise their protocol and in near future all civil aviation must use space weather information for their operation.

Space weather information is important for aviation mainly in the following three factors; HF communication, aviation and radiation. Space weather phenomena in polar region are tend to be focused on in many cases, however, it is important also in equatorial region, e.g., equatorial plasma bubbles.

There are still some unknown process in space weather and they make the forecast difficult and low precision. We are required two different approach; understand the unknows process, and make empirical forecast methods which works even though we have still unknown process. Especially we need domestic/international cooperation in the former approach e.g., EISCAT-3D and Equatorial MU radar, because it is impossible to cover these ovservation in only one institute. ICAO issue is one of the important outcome for space weather and we should unify our activity to contribute the operation.

Keywords: space weather, ionosphere, ICAO

Japan Geoscience Union Meeting 2014
(28 April - 02 May 2014 at Pacifico YOKOHAMA, Kanagawa, Japan)

PEM06-33 Room:312 Time:May 1 15:30-15:45

Importance of EISCAT 3D as space weather reseach

NAGATSUMA, Tsutomu[1*]

[1]National Institute of Information and Communications Technology

These days, importance of space weather is significantly realized by international community, such as ICAO, WMO etc. NICT has been responsible for national space weather forecast in Japan for a long time. Since NICT's space weather forecast center belongs to the International Space Environment Service (ISES) as the Regional Warning Center (RWC) Japan, our operational activities are supported by international cooperation. To understand the current conditions of "space weather", monitoring networks of space weather observations are operated and used. For future objective and advanced space weather monitoring, we have been developing a space weather numerical simulation codes, too. These activities are strongly related to the space weather research for improving space weather forecasting.

EISCAT 3D is a quite unique facility to measure many kinds of physical parameters which cannot be obtained from other instruments. Therefore, it is expected that the EISCAT 3D can contirbute to the evaluation and improvement of space weather models. The future perspective of space weather research and our expectation to EISCAT 3D are introduced in our presentation.

Keywords: Space Weather, EISCAT 3D, Ground-Based Observation

Japan Geoscience Union Meeting 2014
(28 April - 02 May 2014 at Pacifico YOKOHAMA, Kanagawa, Japan)

PEM06-34 Room:312 Time:May 1 15:45-16:00

Thunderstorm Activity in Asia Maritime Continent and Global Cloud Variation

TAKAHASHI, Yukihiro[1*] ; SATO, Mitsuteru[1] ; YAMASHITA, Kozo[2]

[1]Department of Cosmosciences, Hokkaido University, [2]Salesian Polytechnic

Global relationship among the thunderstorm activities especially in Asia Maritime Continent, cloud variations in tropical regions and solar parameters was examined based on lightning data measured by Global ELF observation Network (GEON) operated by Hokkaido University and Outgoing Longwave Radiation (OLR) intensity. A correlated analysis between the number of the lightning strokes, cloud variation in the tropical regions, and solar parameters was examined, looking into the variation with ˜one month periodicity. It was found that the number of lightning stokes in Asia Maritime Continent (AMC) varies with about month periodicity in the period from February to June 2004 and shows positive correlation (R= ˜0.8) with OLR in the Western Pacific Warm Pool (WPWP). On the other hand, OLR in the central Africa shows negative correlation with the number of lightning stokes in the AMC in that period. It is also found that the galactic cosmic rays or UV intensity associated with solar activity shows good correlation with tropical OLR or lightning activity in AMC. One explanation to connect such global variations in thunderstorm / cloud amount with solar parameters would be the electrical circuit between lower and upper atmospheres. The radars distributed globally would provide some essential information for this hypothesis, such as conductivity in the lower ionosphere, which may determine the strength of electrical connection in the vertical and horizontal directions.

Keywords: Maritime Continent, thunderstorm, tropical region, cloud amount, OLR, solar activity

Japan Geoscience Union Meeting 2014
(28 April - 02 May 2014 at Pacifico YOKOHAMA, Kanagawa, Japan)

PEM06-P01 Room:Poster Time:April 30 18:15-19:30

Equatorial MU Radar project

YAMAMOTO, Mamoru[1*] ; HASHIGUCHI, Hiroyuki[1] ; TSUDA, Toshitaka[1]

[1]RISH, Kyoto University

Research Institute for Sustainable Humanosphere, Kyoto University (RISH) has been studying the atmosphere by using radars. The first big facility was the MU (Middle and Upper atmosphere) radar installed in Shiga, Japan in 1984. This is one of the most powerful and multi-functional radar, and is successful of revealing importance of atmospheric waves for the dynamical vertical coupling processes. The next big radar was the Equatorial Atmosphere Radar (EAR) installed at Kototabang, West Sumatra, Indonesia in 2001. The EAR was operated under close collaboration with LAPAN (Indonesia National Institute for Aeronautics and Space), and conducted the long-term continuous observations of the equatorial atmosphere/ionosphere for more than 10 years. The MU radar and the EAR are both utilized for inter-university and international collaborative research program for long time. National Institute for Polar Research (NIPR) joined EISCAT Scientific Association together with Nagoya University, and developed the PANSY radar at Syowa base in Antarctica as a joint project with University of Tokyo. These are the efforts of radar study of the atmosphere/ionosphere in the polar region. Now we can find that Japan holds a global network of big atmospheric/ionospheric radars. The EAR has the limitation of lower sensitivity compared with the other big radars shown above. RISH now proposes a plan of Equatorial MU Radar (EMU) that is to establish the MU-radar class radar next to the EAR. The EMU will have an active phased array antenna with the 163m diameter and 1055 cross-element Yagis. Total output power of the EMU will be more than 500kW. The EMU can detect turbulent echoes from the mesosphere (60-80km). In the ionosphere incoherent-scatter observations of plasma density, drift, and temperature would be possible. Multi-channel receivers will realizes radar-imaging observations. The EMU is one of the key element in the project ”Study of coupling processes in the solar-terrestrial system” for Master Plan 2014 of the Science Council of Japan (SCJ). We show the EMU project and its science in the presentation.

Keywords: Atmospheric radar, ionosphere observation, Indonesia, MST radar

Japan Geoscience Union Meeting 2014
(28 April - 02 May 2014 at Pacifico YOKOHAMA, Kanagawa, Japan)

PEM06-P02 Room:Poster Time:April 30 18:15-19:30

Development of a configurable digital receiver for atmospheric radars

YAMAMOTO, Masayuki[1*] ; GAN, Tong[1] ; FUJITA, Toshiyuki[1] ; NOOR HAFIZAH BINTI, Abdul aziz[1] ; OKATANI, Yoshikazu[1] ; HASHIGUCHI, Hiroyuki[1] ; YAMAMOTO, Mamoru[1]

[1]Research Institute for Sustainable Humanosphere, Kyoto University

Recent progress in radar imaging techniques enables high-resolution measurements of wind and turbulence by atmospheric radars. In order to implement radar imaging techniques to existing atmospheric radars, a cheap multi-channel receiver needs to be developed. Further, for improving and verifying radar imaging techniques, a digital receiver which can change its real-time signal processing is highly useful. We are now developing a low-cost configurable digital receiver. Because the digital receiver comprises a general-purpose software-defined radio receiver and a personal computer, its purchase cost is low and its real-time signal processing is easy to be implemented. In the presentation, we report the current development status of the digital receiver.

Keywords: atmospheric radar, wind profiler radar, digital receiver, software-defined radio technique, Universal Software Radio Peripheral (USRP)

Japan Geoscience Union Meeting 2014
(28 April - 02 May 2014 at Pacifico YOKOHAMA, Kanagawa, Japan)

PEM06-P03 Room:Poster Time:April 30 18:15-19:30

Statistical study of F-region field-aligned irregularities based on Equatorial Atmosphere Radar in Indonesia

DAO, Tam[1*] ; OTSUKA, Yuichi[1] ; SHIOKAWA, Kazuo[1] ; YAMAMOTO, Mamoru[2]

[1]STEL, Graduate School of Science, Nagoya University, [2]Research Institute for Sustainable Humanosphere, Kyoto University

I examined the statistical characteristics of Field-Aligned Irregularities (FAIs) echoes from the F-region of Ionosphere using Equatorial Atmosphere Radar (EAR) in Indonesia during three years from 2010 to 2012. We investigated the differences between post-sunset and post-midnight FAIs. Some results are analyzed in the daily and monthly average of echo power, spectral width, and Doppler velocity. We found that post-midnight FAIs occurred mostly in summer solstices from May to August in 2010 and 2011, and only in June and July in 2012. We realized some different characteristics between post-sunset and post-midnight FAIs observed from EAR as follow. (1) Echo intensity of the post-midnight FAIs is weaker than that of post-sunset FAIs. (2) The post-sunset FAIs often exceed an altitude of 450 km, whereas the post-midnight FAIs mostly occur in a range from 200 to 450 km in F-region. (3) Spectral width of the post-midnight FAIs is smaller than that of the post-sunset FAIs. These results suggest that plasma instability operates more actively at post-sunset than at post-midnight.

Keywords: F-region Ionosphere, Field-Aligned Irregularities (FAIs), VHF radar

Japan Geoscience Union Meeting 2014
(28 April - 02 May 2014 at Pacifico YOKOHAMA, Kanagawa, Japan)

PEM06-P04 Room:Poster Time:April 30 18:15-19:30

Statistical study of ionospheric irregularities by using Equatorial Atmosphere Radar

MARTININGRUM, Dyah rahayu[1*] ; YAMAMOTO, Mamoru[1]

[1]RISH, Kyoto University

The equatorial region is the source of many unique atmospheric processes that couple the entire atmosphere vertically from bottom to top and horizontally from equator to pole. The dynamical, electrodynamical, and electrical process of lower and upper atmosphere of equatorial region contribute to ionospheric irregularities through propagation of atmospheric waves, and magnetosphere-ionosphere interaction. Those process are responsible for the large degree of variabilities observed in the low latitude ionosphere.

Study of ionospheric irregularities was made during 2008-2013 by using 47 MHz Equatorial Atmosphere Radar (EAR) in Kototabang, Indonesia (0.20S, 100.32E; 10.36S dip latitude). Characteristic of echoes from ionospheric Field Aligned Irregularities (FAI) classified based on structure of E and F backscattered echoes power of EAR radar both of spatially and temporally. The results base on intermittent observations (2008-2010) and continuous observations (2011-2013). During the observations were obtained percentage of Equatorial Spread F (ESF) occurrences, diurnal and seasonal characteristics of ionospheric irregularities from the E region and also from F region. Furthermore, occurrence correlation between E and F region irregularities are also observed.

Keywords: Ionospheric Irregularity, Equatorial Atmosphere Radar, Statistical Study

Japan Geoscience Union Meeting 2014
(28 April - 02 May 2014 at Pacifico YOKOHAMA, Kanagawa, Japan)

PEM06-P05 Room:Poster Time:April 30 18:15-19:30

Lidar observations for study of coupling processes over the equatorial region

ABO, Makoto[1*] ; NAGASAWA, Chikao[1] ; SHIBATA, Yasukuni[1]

[1]Tokyo Metropolitan University

Stratosphere-troposphere exchange is important for the budget of ozone in the lower stratosphere as well as in the troposphere. Upward transport occurs in the tropical region (Brewer-Dobson circulation), but the exact mechanism controlling the transport is not clear. We have constructed the lidar facility for survey of atmospheric structure over troposphere, stratosphere, mesosphere and low thermosphere over Kototabang (100.3E, 0.2S), Indonesia in the equatorial region [1]. The lidar system consists of the Mie and Raman lidars for tropospheric aerosol, water vapor and cirrus cloud measurements, the Rayleigh lidar for stratospheric and mesospheric temperature measurements and the Resonance lidar for metallic species such as Na, Fe, Ca ion measurements and temperature measurements in the mesopause region. The laser system included in this lidar facility consists of three pulsed Nd:YAG lasers, a pulsed Ti:Sapphire laser seeded by a ring Ti:Sapphire laser and a dye laser. The most parts of this lidar system are remotely controlled via the Internet from Japan. The full lidar observations started from 2004. The routine observations of clouds and aerosol in the troposphere and stratosphere are continued now.

We found the top height of the stratospheric aerosol layer descend with time, synchronized with the QBO in the zonal wind. The QBO signals of the aerosol layer are noticed in the altitude range from 30 to 40 km. In addition, the tropospheric aerosol amount observed around the tropopause over Kototabang is much more than at mid-latitudes. They suspect that this is an evidence of active material exchange between the troposphere and the stratosphere over the equatorial region.

We have installed DIAL (differential absorption lidar) system for high-resolution measurements of vertical ozone profiles in the equatorial tropopause region over Kototabang, Indonesia. We will contribute to the elucidation of the climate change by getting observational information about high-resolution ozone density profiles, and the wave-propagation and material transportation using ozone as a tracer from the troposphere to the lower stratosphere over the equator.

There were many ozone DIAL systems in the world, but almost systems are optimized for stratospheric ozone layer measurement [2] or tropospheric ozone measurement [3]. Because of deep ozone absorption in the UV region, the wavelength selection is important. Simulation results show that we can measure above 20km with height resolution of 500m within 5% random error.

Acknowledgments

This work was financially supported by Grants-in-Aid for Scientific Research (No. 233401043).

References

1. Nagasawa C., M. Abo, Y. Shibata 23rd International Laser Radar Conference, No.2O-8, 43-46, 2006.
2. Megie G. J., G. Ancellet,, J. Pelon, Lidar measurements of ozone vertical profiles, Applied Optics 24, 3454-3463, 1985.
3. Nakazato M., T. Nagai, T. Sakai, Y. Hirose, Applied Optics, 46, 2269-2279, 2007.

Keywords: coupling process, equatorial region, lidar

Japan Geoscience Union Meeting 2014
(28 April - 02 May 2014 at Pacifico YOKOHAMA, Kanagawa, Japan)

PEM06-P06 Room:Poster Time:April 30 18:15-19:30

Microstructure of Precipitation over Indonesia from a Network of Parsivel disdrometers

MARZUKI, Marzuki[1*] ; HASHIGUCHI, Hiroyuki[2] ; YAMAMOTO, Masayuki[2] ; MORI, Shuichi[3] ; TAKAHASHI, Yukihiro[4]

[1]Department of Physics, Andalas University, Padang, Indonesia, [2]Research Institute for Sustainable Humanosphere (RISH) Kyoto University, Gokasho, Uji, Kyoto 611-001, [3]Japan Agency for Marine-Earth Science and Technology (JAMSTEC), Yokosuka, Japan, [4]Hokkaido University, Sapporo, Japan

Insight into the regional variability of raindrop size distribution (DSD), is of primary importance for estimation of rainfall using remote sensing techniques, cloud/precipitation microphysical processes and numerical weather modeling. In order to quantify the regional variability of the DSD over Indonesia, a network of 4 Parsivel disdrometers along equatorial Indonesia has been designed. The disdrometers were installed at Kototabang (KT; 100.32E, 0.20S), Pontianak (PT; 109.37E, 0.00S), Manado (MN; 124.92E, 1.55N) and Biak (BK; 136.10E, 1.18S). It was found that the DSD at PT has more large drops than at the other three sites. The DSDs at the four sites are influenced by both oceanic and continental systems, and majority of the data matched the maritime-like DSD that was reported in a previous study. Continental-like DSDs were somewhat dominant at PT and KT. The combination of World Wide Lightning Location Network, wind profiler and the Tropical Rainfall Measuring Mission (TRMM) Precipitation Radar (PR) allows a discussion on physical basis behind the regional variability of DSD over Indonesia.

Keywords: Indonesia, Parsivel, Raindrop

Japan Geoscience Union Meeting 2014
(28 April - 02 May 2014 at Pacifico YOKOHAMA, Kanagawa, Japan)

PEM06-P07 Room:Poster Time:April 30 18:15-19:30

Feature studies of the polar lower thermosphere by EISCAT_3D

NOZAWA, Satonori[1*]

[1]STEL, Nagoya University

The new EISCAT_3D radar will give us with great opportunities. Its 3D volumetric observations of ion velocity will provide high quality neutral wind data in the lower thermosphere. Furthermore, its continuous observations will make it possible to study planetary waves in the lower thermosphere in more detail as well as day-to-day variabilities of tides. In this talk, we will describe our future study targets.

The lower thermospheric wind dynamics has been paid great attention for several decades to understand the Magnetosphere-Ionosphere-Thermosphere coupling, since the neutral atmosphere plays a key role. In particular, it has been an issue how the lower thermosphere will response to the solar wind energy input. IS radar measurements of the polar lower thermosphere begun about 40 years ago by a pioneer work of Brekke et al. [JGR, 78, 8235, 1973], and significant number of studies have been conducted since then. However, our understanding of the lower thermosphere is still limited. One of reasons is that the lower thermosphere is significantly influenced by atmospheric waves propagating from below. Thus, the day-to-day variability is very prominent. Owing to high running cost, long term datasets are hard to be obtained by IS radar a decade ago. In 2007-2008, EISCAT Svalbard radar was operated almost continuously for 1 year. However, only about 20% of the data sets can be used for deriving the ion velocity vector. If we have wind velocity datasets on daily basis like meteor and MF radars usually made for the mesospheric wind measurements (70-100 km), our understanding of the lower thermosphere wind dynamics will be much more progressed. EISCAT_3D will make it possible.

Furthermore, the EISCAT_3D radar will give us higher temporal resolution data sets of neutral winds in the lower thermosphere with multi volumes. The observations will allow us to distinguish the temporal and spatial variations of winds. One of scientific targets is to investigate wind variations nearby the auroral arc in the E-region. By combining sodium and Rayleigh LIDARs as well as meteor and MF radars, which provide neutral temperature and wind velocity, respectively, we expect we can investigate dissipation process of gravity waves in more details as well as effects of auroral precipitation on the middle atmosphere.

Keywords: EISCAT_3D, polar ionosphere, lower thermosphere, planetary wave, tidal wave, gravity wave

Japan Geoscience Union Meeting 2014
(28 April - 02 May 2014 at Pacifico YOKOHAMA, Kanagawa, Japan)

PEM06-P08 Room:Poster Time:April 30 18:15-19:30

Observation of non-thermal planetary radio emissions with EISCAT 3D

TSUCHIYA, Fuminori[1*] ; MISAWA, Hiroaki[1]

[1]Tohoku University

EISCAT 3D is developing as incoherent scatter radar to study the terrestrial ionosphere and atmosphere. Due to large aperture area and low noise temperature of the receiving system of EISCAT 3D and the uniqueness of the receiving frequency of 233 MHz, it can also be a useful tool to study non-thermal radio emissions from the solar system planets. In this paper, feasibility and advantage of EISCAT 3D for observing non-thermal planetary radio emissions are presented. Following topics will be discussed. (1) Time variability of Jovian synchrotron radiation, (2) Radio emissions from lightning discharges occurred in the atmospheres of Mars and Saturn, and (3) Recent trials to detect incoherent radio emissions from extra-solar planets.

Japan Geoscience Union Meeting 2014
(28 April - 02 May 2014 at Pacifico YOKOHAMA, Kanagawa, Japan)

PEM06-P09 Room:Poster Time:April 30 18:15-19:30

Numerical simulation of Generalized Auroral Computed Tomography toward its application to the EISCAT_3D project

TANAKA, Yoshimasa[1*] ; OGAWA, Yasunobu[1] ; KADOKURA, Akira[1] ; GUSTAVSSON, Bjorn[2] ; ASO, Takehiko[3] ; BRANDSTROM, Urban[4] ; MIYAOKA, Hiroshi[1] ; UENO, Genta[5] ; SAITA, Satoko[6]

[1]National Institute of Polar Research, [2]University of Tromso, [3]The Graduate University for Advanced Studies (Sokendai), [4]Swedish Institute of Space Physics, [5]The Institute of Statistical Mathematics, [6]Research Organization of Information and Systems

The EISCAT_3D is a next-generation phased-array incoherent scatter radar, which is capable of measuring three-dimensional (3D) ionospheric plasma parameters at ten-times higher temporal and spatial resolution. Thus, it is expected that the EISCAT_3D will provide new insights into auroral physics. On the other hand, optical imaging observation will be still useful for studying the auroral dynamics, because high-sensitivity camera can generally measure horizontal 2D distribution of the aurora at higher temporal resolution than the radars. We demonstrate by numerical simulation how useful monochromatic auroral images taken at multi-point camera network are for the study of aurora dynamics in the EISCAT_3D project. We apply the generalized - aurora computed tomography (G-ACT) to simulated observational data from real instruments, that is, the Auroral Large Imaging System (ALIS) and the EISCAT_3D radar. The G-ACT is a method to reconstruct three dimensional (3D) distribution of auroral emission and ionospheric electron density (corresponding to horizontal 2D distribution of energy spectra of precipitating electrons) from multi-instrument data. It is assumed that a core site of the EISCAT_3D radar is located at Skibotn (69.35N, 20.37E), Norway, and scans an area of 0.8 degrees in geographic latitude and 3 degrees in longitude at 130km altitude with 21x21 beams. Two neighboring discrete arcs are assumed to appear in the observation region of the EISCAT_3D radar. The reconstruction results from the G-ACT are compared with those from the normal ACT as well as those from only the electron density observed by the EISCAT_3D radar. It is found that the G-ACT can interpolate the ionospheric electron density at much higher spatial resolution than the original one observed by the EISCAT_3D radar. Furthermore, the multiple arcs reconstructed by the G-ACT are more precise than those by the normal ACT. Even for the case that the reconstruction by the ACT is difficult due to unsuitable location of the camera sites relative to the discrete arcs and/or a small number of available images, the G-ACT allows us to achieve the reconstruction.

Keywords: aurora computed tomography, EISCAT_3D, simulation, multi-point camera observation

Japan Geoscience Union Meeting 2014
(28 April - 02 May 2014 at Pacifico YOKOHAMA, Kanagawa, Japan)

PEM06-P10 Room:Poster Time:April 30 18:15-19:30

Aurora-induced sodium layer variation detected by coordinated observation with sodium lidar and EISCAT radar

TSUDA, Takuo[1*] ; NOZAWA, Satonori[2] ; KAWAHARA, Takuya[3] ; KAWABATA, Tetsuya[2] ; SAITO, Norihito[4] ; WADA, Satoshi[4] ; OGAWA, Yasunobu[1] ; OYAMA, Shin-ichiro[2] ; HALL, Chris[5] ; TSUTSUMI, Masaki[1] ; EJIRI, Mitsumu K.[1] ; SUZUKI, Shin[2] ; TAKAHASHI, Toru[2] ; NAKAMURA, Takuji[1]

[1]National Institute of Polar Research, [2]Solar-Terrestrial Environment Laboratory, Nagoya University, [3]Faculty of Engineering, Shinshu University, [4]RIKEN, [5]University of Tromsoe

Sodium atom layer is generally distributed at 80-100 km. One of mysterious subjects on high-latitude sodium layers is relationship between auroral particle precipitation and sodium atom layer variation. A previous study suggested a sodium column density decrease during a geomagnetic active period due to that the particle precipitation accompanied by electron density enhancement could induce ionization of sodium atom through their ion-molecule chemistry. Another study pointed a possibility of sodium density increase. For this reason, it is suggested that auroral precipitating particle bombardment on meteoric smoke particles can sputter sodium atoms from the smoke particles. On the other hand, ionospheric electric field, which may become more significant near auroral precipitating regions, could induce ion motions (i.e. can generate sodium ion convergence and/or divergence), and then also could affect generation and/or loss processes of sodium atoms through their ion-molecule chemistry. Thus, for the examination of the causality, it is vitally important to distinguish the effects of auroral particle precipitation and ionospheric electric field. Using a sodium lidar (which was installed in early 2010) and European incoherent scatter (EISCAT) radar at Tromsoe, Norway (69.6N, 19.2E), we have investigated, for the first time, that the actual effect of the particle precipitation to the sodium density variations without electric filed injection. In the nighttime observation on 24-25 January 2012, we detected a significant decrease of sodium atom density coincied with electron density enhancements (implying strong particle precipitations) and low ion temperatures (implying no electric field injections). These results strongly suggested that auroral particle precipitations induced sodium atom density decrease. Furthermore we discuss observed time response in the sodium density decrease.

Keywords: Na lidar, EISCAT radar, Na layer, Auroral particle precipitation, Ionospheric electric field

Japan Geoscience Union Meeting 2014
(28 April - 02 May 2014 at Pacifico YOKOHAMA, Kanagawa, Japan)

PEM06-P11 Room:Poster Time:April 30 18:15-19:30

The spatial and temporal evolution of equatorial plasma bubble observed using ground based GPS TEC measurement.

M BUHARI, Suhaila[1*] ; ABDULLAH, Mardina[2] ; HASBI, Alina marie[3] ; OTSUKA, Yuichi[4] ; NISHIOKA, Michi[5] ; TSUGAWA, Takuya[5]

[1]Physics Department, Universiti Teknologi Malaysia, [2]Space Science Centre, Universiti Kebangsaan Malaysia, [3]Department of Electrical, Electronics & Systems Engineering, Universiti Kebangsaan Malaysia, [4]Solar-Terrestrial Environment Laboratory, Nagoya University, [5]National Institute of Information and Communications Technology

The equatorial plasma bubble (EPB) commonly occurs near the equatorial region after post sunset period. The generation process of EPB has been well understood where it is commonly developed near the magnetic equator and elongated along magnetic field lines through Rayleigh-Taylor instability mechanism. However, the source of seeding perturbation leads to the generation of Rayleigh-Taylor instability is still unknown. The temporal and spatial properties of EPB have been well studied using airglow imager. However, the observation using airglow imager is impossible during sunset time where the EPB starts to develop due to light from the sun while the observation during night time is always interfered by moon and clouds.

In this study, we obtain the GPS data from Malaysia Real-Time Kinematics GNSS Network (MyRTKnet), International Ground Station (IGS) network and Sumatera GPS Array (SUGAR) network. The networks contains 127 receivers in South East Asia (SEA) region covers 8^{o}N to -8^{o}S latitude and 92^{o}E to 120^{o}E longitude geographic coordinates. In this study, we detected the structure of EPB using two-dimensional map of rate of TEC index (ROTI) calculated from ground based GPS TEC measurement in. The average ROTI value for all visible satellites at 300 km altitude is binned into 0.45^o x 0.45^o grid in geographic latitude and longitude. The advantage of this technique is the GPS data is always available and we are able to observe the spatial and temporal properties of EPBs continuously without distracted by light.

On the 17th March 2011, we observed the appearance of EPB structure pass through the SEA territory for 5 hours from 1300 UT (2100 LT) - 1900 UT (0200 LT). The initial ROTI-enhancement region is at 1300 UT is propagating to eastward direction and the information of the structure is lost due to the limited coverage of GPS receiver. At 1340 UT, a new ROTI-enhancement region appeared as a point source at geographic coordinate 2^{o}N and 98^{o}E as shown in Figure (a). After 20 minutes, the point source of ROTI-enhancement region expand to ˜600 km in the North and ˜200 km South direction as shown in Figure (b) while the zonal size ˜50 km remains the same. The perturbation region is expanding faster towards dip magnetic equator might associated with field-aligned irregularities. The structure travelled in eastward direction with velocity ˜133 ms^{-1} until the development process stopped. After 60 minutes, we assumed the structure is fully developed as illustrated in Figure (c) when no development in zonal size and ROTI value is observed anymore. The developed structure has 200 km zonal size continuously moves to eastward directions with slower velocity ˜111 ms^{-1}. The slower velocity incidentally with no development in zonal size and ROTI value might indicates the ”fossil” bubble where the plasma density is equal with background density and the structure velocity following the background plasma density. At 1440 UT the second structure is coming ˜600 km away from the first structure with velocity ˜111 ms^{-1} and zonal size 200 km same as the previous structure as shown in Figure (d). The first and second structure has the same zonal sizes and velocities might due to the same temporal and spatial evolution during the generation process.

The two-dimensional structure of EPB has been presented using GPS networks in SEA region is an alternative tool to observe the temporal and spatial properties of EPB structure from the initial perturbation until the decaying process without being distracted by light. The temporal and spatial properties of EPB can contribute towards understanding the generation mechanism of the Rayleigh-Taylor instability process.

Keywords: equatorial plasma bubble, rate of TEC index, GPS TEC measurement

PEM06-P11 Room:Poster Time:April 30 18:15-19:30

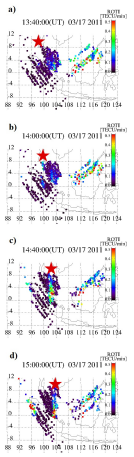

Japan Geoscience Union Meeting 2014
(28 April - 02 May 2014 at Pacifico YOKOHAMA, Kanagawa, Japan)

PEM06-P12 Room:Poster Time:April 30 18:15-19:30

Relationship between Latitudinal Extension of Scintillation and Pre-reversal Enhancement in the Southeast Asian Region

ABADI, Prayitno[1*] ; OTSUKA, Yuichi[2] ; HUSIN, Asnawi[1] ; JIYO, Jiyo[1] ; YAMAMOTO, Mamoru[3] ; TSUDA, Toshitaka[3]

[1]National Institute of Aeronautics and Space (LAPAN), [2]STEL, Ngoya University, [3]RISH, Kyoto University

We have investigated the relationship between the maximum latitude extension of observed scintillations (Lmax) and the maximum altitude of the equatorial F-region bottomside (h'Fmax), peak of eastward electric field (Emax), and time duration of eastward electric field (TE) during PRE period in the equatorial region. We used three GPS receivers installed in Kototabang (0.2S, 100.3E; 10.0N magnetic latitude), Pontianak (0.02S, 109.3E; 8.9S magnetic latitude), and Bandung (6.9S, 107.6E; 17.5S magnetic latitude), Indonesia for observing scintillation activity in period 18.00-22.00 LT (LT=UT+7h) and two frequency modulated-continues wave (FM-CW) ionosondes installed near equator magnetic, Chumphon (10.7N, 99.4E; 3.3N magnetic latitude), Thailand and Bac Lieu (9.3N, 105.7E; 1.7N magnetic latitude), Vietnam for measuring PRE parameters, such as h'F, vertical drift (dh'F/dt) which indicates eastward electric field, and TE. Our observation period is during equinox months (March, April, September, and October) in 2010, 2011, and 2012. We divide the relationships into two groups; 1) the relationships between PRE parameters obtained from Chumphon ionosonde and Lmax observed by Kototabang and Bandung GPS receivers and 2) PRE parameters obtained from Bac Lieu ionosonde and Lmax observed by Pontianak and Bandung GPS receivers. The following table is to show the coefficient correlation (R) of the relationships for each group. The results indicate that duration of eastward electric field does not play an important role for extension of the plasma bubble or latitudinal extension of scintillation, and that the peak of h'F and magnitude of E at the initial phase of plasma bubble generation (PRE period) is a primary factor for the plasma bubble extension. Therefore, the maximum latitude of scintillation is determined at the initial phase of plasma bubble generation (PRE period) in the equatorial region.

Relationship	R (group 1)	R (group 2)
h'Fmax vs Lmax	0.596	0.471
Emax vs Lmax	0.489	0.270
TE vs Lmax	0.054	0.090

Keywords: Ionosphere, Scintillation, Pre-reversal enhancement

Japan Geoscience Union Meeting 2014
(28 April - 02 May 2014 at Pacifico YOKOHAMA, Kanagawa, Japan)

PEM06-P13 Room:Poster Time:April 30 18:15-19:30

Geolocation of lightning discharge in the Maritime Continent based on radio observation in 0.1-40 kHz band

YAMASHITA, Kozo[1*] ; OHYA, Hiroyo[2] ; TAKAHASHI, Yukihiro[3] ; TSUCHIYA, Fuminori[4] ; MATSUMOTO, Jun[5]

[1]Salesian Polytechnic, [2]Chiba University, [3]Hokkaido University, [4]Tohoku University, [5]Tokyo Metropolitan University

Recent researches based on observation and data assimilation of lightning discharge indicate a possibility of now-cast and forecast of severe weather such as torrential rain. In these works, lightning data is focused on as a proxy for the presence or absence of deep convection which generates thunderstorm.

In previous works, occurrence of cloud-to-ground (CG) lightning discharges has been mainly used due to the ease of data availability. However, lighting observation based on electromagnetic measurement shows that there is extremely huge scale lightning whose scale is more than hundreds times bigger than that of averaged event. Lightning data including ″ occurrence ″ and ″ scale ″ enable us to evaluate not only existence but also intensity of atmospheric convection. Quantitative evaluation of atmospheric convection would make it possible to make a now-cast and forecast for intensity distribution of precipitation.

The Maritime Continent (MC) is one of the most important regions for lightning observation in the world. Thunderstorm activity causes enormous human and economic damage to countries in MC. However, until now, only few statistical studies on the lightning activity with scale information of lightning discharge have been done.

In this works, lightning observation network in the MC based on electromagnetic measurement in 0.1-40 kHz band is summarized. This network is developed to estimate not only spatial distribution but also scale one of lightning discharges. We have already constructed observation stations at Tainan in Taiwan (23.1N, 121.1E), Saraburi in Thailand (14.5N, 101.0E), Pontianak in Indonesia (0.0N, 109.4E), Los Banos in Philippines (14.2N, 121.25E) and Son Tay in Viet Nam (21.1N, 105.5E). Data obtained by multipoint observation is synchronized by GPS receiver installed at each station.

At the presentation, we show evaluation of accuracy for geolocation and detection efficiency of signal radiated from lightning discharge based on comparisons with World Wide Lightning Location Network (WWLLN) data.

Keywords: lightning discharge, thunderstorm, severe weather, VLF, the Maritime Continent

Japan Geoscience Union Meeting 2014
(28 April - 02 May 2014 at Pacifico YOKOHAMA, Kanagawa, Japan)

PEM06-P14 Room:Poster Time:April 30 18:15-19:30

A study on a low Earth orbit (LEO) satellite mission using radio propagation characteristics

TAKEDA, Yuji[1*] ; TSUDA, Toshitaka[1]

[1]Research Institute for Sustainable Humanosphere, Kyoto University

We study in this paper an Earth observation mission with a low Earth orbit (LEO) satellite using radio propagation characteristics on L (1.2-1.6 GHz for GPS) and Ka (17.3-20.2 GHz for O3b satellite) bands . In particular, applying GPS radio occultation (GPS RO) technique, we aim to obtain profiles of atmospheric parameters (humidity, temperature and electron density) with a good height resolution, covering a wide area. We also measure cloud water content and vapor distribution by using radiometer technique on Ka-band.

Radio occultation employs propagation delay and bending of radio waves in the atmosphere. Though GPS satellites hitherto has been used for observing radio occultation, we use not only GPS but also other GNSS satellites (GLONASS, Galileo, Beidou, and QZSS), moreover we further use O3b(Other 3 billion people), which is a communications satellite, then, we can increase number of observation points of RO.

Because the observation point of RO is determined by the relative location between the LEO satellite and transmitting satellites, we used a numerical model to investigate the data distribution of RO and proposed an optimal satellite orbit for a new LEO satellites mission. The model analysis shows that using GNSS and O3b satellites for RO the total number of RO data becomes approximately three times larger than those by using only GPS satellites. The analysis also shows that the longitudinal distribution of RO data does not depend on orbit of the LEO satellite, but, the latitudinal distribution is largely affected by an inclination angle of LEO satellite. Data distribution as function of local time varies by inclination and longitude of ascending node of LEO satellite.

We also investigate application of O3b operated on Ka-band, which is approximately ten times higher than L-band. So Ka-band is less sensitive to the ionosphere, but it is greatly attenuated by cloud water and vapor. In GPS RO on L band, atmospheric profiles at high-altitude (50km-) are not determined accurately because of influence of ionosphere. But using Ka-band of O3b we will be able to increase the maximum height of the profiles. Moreover, we expect to measure cloud water content and vapor distribution by using attenuation of Ka-band.

Keywords: GPS radio occultation, Low Earth orbit satellite, Global Navigation Satellite System, Ka-band

Japan Geoscience Union Meeting 2014
(28 April - 02 May 2014 at Pacifico YOKOHAMA, Kanagawa, Japan)

PEM07-01 Room:213 Time:April 30 14:15-14:30

Introdution to GLIMS mission

USHIO, Tomoo[1*] ; SATO, Mitsuteru[2] ; MORIMOTO, Takeshi[3] ; SUZUKI, Makoto[4] ; YAMAZAKI, Atsushi[4] ; HOBARA, Yasuhide[5] ; KIKKUCHI, Masayuki[6]

[1]Osaka University, [2]Hokkaido University, [3]Kinki University, [4]JAXA, [5]University of Electro Communications, [6]NIPR

The Global Lightning and sprIte MeasurementS (GLIMS) on the International Space Station (ISS) is a mission to detect and locate optical transient luminous events (TLEs) and its associated lightning simultaneously from the non-sun synchronous orbit, and was launched successfully in July, 2013 as part of the multi-mission consolidated equipment on Japanese Exposure Module (JEM). Our mission goals are to identify temporal and spatial evolutions of lightning and TLEs and to clarify the occurrence conditions of TLEs and global occurrence locations and rates of TLEs from the nadir observation. To achieve these goals, two CMOS cameras, six Photometers, VLF receiver, and VHF interferometer with two antennas, are installed at the bottom of the module to observe the TLEs as well as causative lighting discharges at nadir direction during day and night time. Though the luminous events so-called sprite, elves and jets have been investigated by numerous researchers all over the world based mainly on the ground observations, some important problems have not been fully understood yet such as generation mechanisms of columniform fine structure and horizontal offset of some sprites from the parent lightning discharges. In the JEM-GLIMS mission, observations from our synchronized sensors are going to shed light on above-mentioned unsolved problems regarding TLEs as well as causative lighting discharges.

The optical instruments are two CMOS cameras (LSI-1, LSI-2) and six-channel spectrophotometers (PH1 - PH6). The FOV of LSI is 28.3 deg. x 28.3 deg., and LSI-1 (LSI-2) equips a 766-832 nm wide band filter (a 762+/-7 nm narrow band filter). Each PH channel equips the optical band-pass filter, and these photometers measure the N2 1P, N2 2P, N2 LBH, and N2+ 1N emissions of lightning and TLEs. The radio receivers consist of one VLF receiver (VLFR) and two sets of VHF receivers (VITF). In order to detect TLE-associated whistler waves, VLFR employs a nadir-directing monopole antenna and an electronics unit recording waveform data with a sampling frequency of 100 kHz with 14-bit resolution. VITF consists of two patch-type antennas separated by 1.5 m and an electronics unit, and VITF mainly observes VHF pulses in the frequency range of 70-100 MHz excited by lightning discharges with a sampling frequency of 200 MHz with 8-bit resolution.

JEM-GIMS was successfully launched and transported to the ISS by the H-II Transfer Vehicle (HTV) No.3 cargo transporter at the end of July 2012, and started its operation from December 2013. So far, more than one thousand events were recorded. In this presentation, mission history and overview will be given as an introdution.

Keywords: Lightning, Sprite, ISS

Japan Geoscience Union Meeting 2014
(28 April - 02 May 2014 at Pacifico YOKOHAMA, Kanagawa, Japan)

PEM07-02 Room:213 Time:April 30 14:30-14:45

Estimating lightning characteristics by spaceborne spectrophotometric observation

ADACHI, Toru[1*] ; SATO, Mitsuteru[2] ; USHIO, Tomoo[3] ; YAMAZAKI, Atsushi[4] ; SUZUKI, Makoto[4] ; KIKUCHI, Masayuki[5] ; TAKAHASHI, Yukihiro[2] ; INAN, Umran[6] ; LINSCOTT, Ivan[6] ; HOBARA, Yasuhide[8] ; COHEN, Morris[6] ; LU, Gaopeng[9] ; CUMMER, Steven[9] ; HSU, Rue-ron[10] ; CHEN, Alfred[10] ; FREY, Harald[7]

[1]Waseda Institute for Advanced Study, Waseda University, [2]Department of Cosmosciences, Hokkaido University, [3]Division of Electrical, Electric and Information Engineering, Osaka University, [4]ISAS, JAXA, [5]NIPR, [6]Electrical Engineering Department, Stanford University, [7]Department of Electronic Engineering, The University of Electro-Communications, [8]Electrical and Computer Engineering Department, Duke University, [9]Physics Department, National Cheng Kung University, [10]SSL, University of California at Berkeley

The present study analyzes satellite optical data to evaluate the effectiveness of spaceborne spectrophotometric measurement in characterizing properties of lightning flash. The main data analyzed here are those obtained by FORMOSAT-2/ISUAL limb observation and ISS/GLIMS nadir observation. While ISUAL spectrophotometer observes optical emissions of 150-280, 316, 337, 392, 762, 600-900 nm at a sampling rate of 10 kHz, GLIMS observes emissions of 150-280, 337, 762, 600-900, 316, 392 nm at a rate of 20 kHz. These data for the first time derive fine spectral and temporal properties of lightning emission observed from space. By analyzing the ISUAL optical data and ground-based radio data, we found that spectral intensity ratio is a new parameter to discriminate intra-cloud (IC) and cloud-to-ground (CG) lightning discharges: the blue/red intensity ratio of CG strokes tends to be lower than that of IC pulses. We also found similar tendency in GLIMS lightning events. A case study showed that the color of lightning turned to red when a very bright impulsive emission, which is consistent with a ground return stroke, occurred. These results consistently suggest that the color of CG component is redder than that of IC component, and we explain this as a result of the Rayleigh scattering which effectively attenuates blue light emissions in the case of light sources located at lower-altitudes such as CGs. Using this technique, we will further examine the lightning characteristics on a global level, focusing on latitudinal dependences and land/ocean contrast for example.

Keywords: lightning, CG, IC, satellite, remote sensing

Japan Geoscience Union Meeting 2014
(28 April - 02 May 2014 at Pacifico YOKOHAMA, Kanagawa, Japan)

PEM07-P01 Room:Poster Time:April 30 18:15-19:30

VLF subionospheric disturbances and electrical properties of lightning discharges observed by JEM-GLIMS mission

KAKINUMA, Kanata[1*] ; HOBARA, Yasuhide[1] ; USHIO, Tomoo[2] ; SATO, Mitsuteru[3] ; MORIMOTO, Takeshi[4] ; TAKAHASHI, Yukihiro[5] ; SUZUKI, Makoto[6]

[1]Graduate School of Informatics and Communication Eng., The University of Electro-Communications, [2]Information and communication engineering department, Osaka University, [3]Department of Cosmoscience, Hokkaido University, [4]Faculty of Science and Engineering, Kinki University, [5]Department of Cosmosciences, Graduate School of Science, Hokkaido University, [6]Institute for Space and Astronautical Sciences, Japan Aerospace Exploration Agency

In this paper we report the preliminary results of ionospheric perturbation and causative lightning discharges observed by JEM-GLIMIS mission to study the electromagnetic coupling mechanism between the tropospheric lightning and overlaying ionosphere. Continuous nadir optical observations of lightning discharges are performed by ISS JEM-GLIMS mission and many lightning images have been observed globally. Ionospheric perturbations and electrical properties of causative lightning discharges such as polarity and vertical charge moment changes are derived by the data from UEC's ground-based observation networks of VLF/LF transmitter signal reception and of ELF waveforms respectively. We discuss the electrical coupling efficiencies from the tropospheric lightning to the ionosphere by comparing the area of the lightning flash and corresponding subionospheroic VLF disturbances and lightning properties.

Keywords: Transient Luminous Events, lightning discharges, GLIMS, ionospheric perturbation, charge moment

Japan Geoscience Union Meeting 2014
(28 April - 02 May 2014 at Pacifico YOKOHAMA, Kanagawa, Japan)

PEM07-P02 Room:Poster Time:April 30 18:15-19:30

The building of multipoint measurement network for observing electrostatic field changes caused by lightning discharge

SAKAI, Rikuma[1*] ; TAKAHASHI, Yukihiro[1] ; SATO, Mitsuteru[1] ; KUDO, Takeshi[1]

[1]Cosmosciences, Hokkaido Univ.

It’s not easy to understand the developing process of thunderstorm only with existing meteorological measurements because of its small spatial scale (less than an order of 1 km) and rapid change of the complicated structure. Electrostatic field under the thundercloud or its predecessor reflects the distribution of electrical charges, which is the result of frictions between ice crystal and hail due to strong vertical wind inside the thundercloud. If we measure the vertical electric field at multipoints on the ground, we could estimate the 3 dimensional distribution or the changes of the distribution of electrical charges, from which we may know the detailed development of thunderstorm. The traditional equipment for atmospheric electrostatic filed measurement is filed-mill sensor, which costs an order of 1 M JPY. In order to increase the number of observing stations, we should reduce the price of the instrument. Here we introduce a thunderstorm observation campaign, carried out in mountain area of Yamanashi prefecture, August 2013.We developed new plate-type electric filed sensor, which costs about 0.2 M JPY or less including recording device and battery for one site.This sensor was placed at seven locations in every 4 km with recording system and GPS clock.As a result, we succeeded to record the electrostatic field changes at the same time in multi points, which occured due to lightning strikes for three days.

Keywords: lightning discharge, electrostatic field, multipoint measurement

Japan Geoscience Union Meeting 2014
(28 April - 02 May 2014 at Pacifico YOKOHAMA, Kanagawa, Japan)

PEM07-P03 Room:Poster Time:April 30 18:15-19:30

Preliminary results of global lightning study by the DEMETER satellite

SUTO, Yushi[1*] ; NAKAMURA, Maho[1] ; KAMOGAWA, Masashi[1]

[1]Dpt. of Phys., Tokyo Gakugei Univ.

We investigate statistical property of global lightning activity by means of the DEMETER satellite. The DEMETER satellite which was launch by CNES, France, was operated from 2004 to 2010. In the study, we use electric field data to measure Whistler waves generated by lightning. In this presentation, we show preliminary results of this study.

Keywords: Ionosphere, Lightning, Whistler waves

Japan Geoscience Union Meeting 2014
(28 April - 02 May 2014 at Pacifico YOKOHAMA, Kanagawa, Japan)

PEM07-P04 Room:Poster Time:April 30 18:15-19:30

VHF lightning observations by digital interferometry on JEM-GLIMS

MORIMOTO, Takeshi[1*] ; KIKUCHI, Hiroshi[2] ; SATO, Mitsuteru[3] ; USHIO, Tomoo[2] ; YAMAZAKI, Atsushi[4] ; SUZUKI, Makoto[4]

[1]Kinki University, [2]Osaka University, [3]Hokkaido University, [4]ISAS/JAXA

Global Lightning and sprIte Measurements (GLIMS) mission is now ongoing on Exposed Facility of Japanese Experiment Module (JEM-EF) of the International Space Station (ISS). This paper focuses on an electromagnetic (EM) payload of JEM-GLIMS mission, very high frequency (VHF) broadband digital InTerFerometer (VITF). JEM-GLIMS mission is designed to conduct comprehensive observations with both the EM and the optical payloads for lightning activities and related transient luminous events (TLEs) expecting to give us many scientific impacts to the field.

VITF consists of two sets of antennas, band-pass filters, amplifiers, and 2-channel-AD-converter. Impulsive EM radiations received by the antennas are digitized by the AD converter synchronizing with another channel through the filters and the amplifiers. A patch type antenna is developed within the size of 200∗200 mm. It is mounted on the antenna base made of aluminum alloy and Teflon block with the total height of 100 mm to gain its bandwidth and to reduce the interference from other structural objects. The same two units of antennas are installed with the separation of 1.6 m. Their bandwidths with the higher return loss than -3 dB are from 70 to 100 MHz. The signals received by the antenna are transmitted along cables with the same lengths to the electronics. The AD converter records 130 waveforms as maximum of one dataset with the duration of 2.5 μs with 200 MS/s. The developments of VITF are based on the heritage of VHF sensor on Maido-1 satellite.

JEM-GIMS mission payload was successfully launched at the end of July 2012, and transported and installed to the ISS. After the initial checkout and maintenance, its nominal operation is continued from December 2012. Through the operation period, VITF corrects numerous VHF EM data synchronized with optical signals. About 650 VITF datasets were obtained in January and February 2013, for instance. The estimations of the EM direction-of-arrival (DOA) are attempted using the broadband digital interferometry. Some results agree with the optical observations, even though DOA estimation has difficulties caused by its very short baseline of the antennas and multiple pulses in short time, namely burst-type EM waveforms. VITF is designed expecting to estimate the DOA with about 10 km resolution that is equivalent to the scale of a thundercloud. The results on narrow bipolar pulses (NBPs) and/or transionospheric pulse pairs (TIPPs) are also expected as well as TLEs. The recorded VHF EM signals and the results of their DOA estimations, and the comparisons with optical observations will be introduced in the presentation.

Keywords: lightning, VHF radio observations, GLIMS, International Space Station

Japan Geoscience Union Meeting 2014
(28 April - 02 May 2014 at Pacifico YOKOHAMA, Kanagawa, Japan)

PEM08-01 Room:411 Time:May 1 16:15-16:30

Numerical Modeling of the Three-Dimensional Magnetic Fields and Eruption in the Solar Active Region 11158

INOUE, Satoshi[1*]

[1]School of Space Research, Kyung Hee University

Solar flares and coronal mass ejections (CMEs) are considered as sudden liberation of magnetic energy in the solar corona, which affect geospace in the form of electromagnetic disturbance called geomagnetic storms. Unfortunately, measurement based on vector field observations only provide the two-dimensional information of magnetic field on the photosphere, therefore, we could not reach on a common understanding yet regarding to the three-dimensional (3D) magnetic structure causing the eruptive phenomena and associated dynamics. In order to clarify them, in this study we first extrapolate a 3D coronal magnetic field under the Nonlinear Force-Free Field (NLFFF) approximation based on the vector field, using the Magnetohydrodynamic (MHD) relaxation method developed by Inoue et al. 2014, and then compare the 3D structures before and after the flare. Next we perform an MHD simulation to clarify the dynamics during the flare where the NLFFF prior to the flare is set as an initial condition. Photospheric vector field was observed at 00:00 UT and 03:00 UT on February 15 corresponding to before and after the X2.2-class flare taking place around at 01:50 UT, taken by the Helioseismic And Magnetic Imager (HMI) on board the Solar Dynamics Observatory (SDO) satellite.

As a result, we found that the NLFFF has strongly twisted field lines; most of them are in the range from half-turn to one turn twist, being resided above the polarity inversion line. Furthermore, we found that a distribution of these footpoints well captures the flare ribbons observed by Hinode where Ca II emission is strongly enhanced. On the other hand, because the most of these strongly twisted lines disappear after the flare, consequently the twisted field lines having more than half-turn twist play an important role on causing the large flare. The MHD simulation successfully shows an eruption of the more strongly twisted lines whose values are over one-turn twist, which are produced through the magnetic reconnection in strongly twisted lines of the NLFFF. Eventually, we found that they exceed a critical height at which the flux tube becomes unstable to the torus instability determining the condition that whether a flux tube might escape from the overlying field lines or not. In addition to these, during the eruption, we found that the distribution of the observed two-ribbon flares is similar to the spatial variance of the footpoints caused by the reconnection of strongly twisted lines with more than half-turn twist. Furthermore, because the post flare loops obtained from MHD simulation well capture that in EUV image taken by SDO, these results support the reliability of our simulation.

Keywords: Active Region, Coronal Magnetic Field, Solar Flare, Coronal Mass Ejections, Numerical Modeling

Japan Geoscience Union Meeting 2014
(28 April - 02 May 2014 at Pacifico YOKOHAMA, Kanagawa, Japan)

PEM08-02 Room:411 Time:May 1 16:30-16:45

Study on Triggering Process of Solar Flare on the basis of Satellite Observation

BAMBA, Yumi[1*] ; KUSANO, Kanya[1] ; IMADA, Shinsuke[1]

[1]STEL, Nagoya Univ.

Solar Flares are explosive phenomena driven by magnetic energy stored in the solar corona. Because interplanetary disturbances associated with solar flares sometimes impact terrestrial environments and infrastructure, understanding the flare-triggering process is important not only from a solar physics perspective but also for space weather forecasting. There are numerous observational studies and simulations which attempted to reveal the onset mechanism of solar flares. Because different observations support different models, the underlying mechanism of flare onset remains elusive. Thus the predictability of flare occurrence remains limited.

We have analyzed several flare events obtained by the Solar Optical Telescope (SOT) onboard the Hinode Satellite in order to elucidate flare trigger mechanism [*Bamba et al.* 2013]. We investigated the spatio-temporal correlation between the detailed magnetic field structure and the chromospheric pre-flare emission at the central part of flaring regions for several hours prior to the onset of flares. We observed that the magnetic shear angle in the flaring regions exceeded 70 degrees, as well as that characteristic magnetic disturbances developed at the centers of flaring regions in the pre-flare phase. The observed signatures strongly support the idea of flare trigger mechanism presented by *Kusano et al.* (2012), which proposed that solar flares can be triggered by the interaction between the sheared arcade and one of the two types of small magnetic disturbances. Hence, we could classify the events into two groups depending on the structure of their magnetic polarity inversion lines; to the so-called " Opposite-Polarity (OP) " and " Reversed-Shear (RS) " magnetic field. Furthermore, we studied how small magnetic field can work for triggering flares based on the Hinode observations. The results indicate that the critical amount of magnetic flux for the small magnetic field to trigger flares, depends on the magnetic connectivity in the flaring site, and it varies even within an active region.

However, only four Hinode data sets habe been utilizable for the analyze of this study because of the SOT ' s limited field of view (FOV) (328 " × 164 " for Narrow-band Filter Imager, 218 " × 109 " for Broad-band Filter Imager). Therefore, we applied the analysis method of *Bamba et al.* (2013) to the data obtained by the Helioseismic and Magnetic Imager (HMI) and the Atmospheric Imaging Assembly (AIA) onboard the Solar Dynamics Observatory (SDO), which has a full-disk FOV (2000 " × 2000 ") in order to increase the number of event analysis. We chose the flare events observed by SDO until 31 Jan. 2014, larger than M5.0 GOES class. Eleven X-class and twenty M-class events meet this condition, and we classified these events into independent 6 types by using following three conditions: (1) whether the initial flare kernels has obvious and sheared two-ribbon structure, (2) whether the chromospheric brightening was observed at the center of sheared ribbon, (3) the results of measurement of the magnetic shear angle θ and the azimuth of flare trigger field ϕ.

In this presentation, we would like to report the result of comparative study of Hinode and SDO. We would like to also introduce our preliminary result of statistical flare trigger study using SDO/HMI and AIA.

References:
[1] *Study on Triggering Process of Solar Flares Based on Hinode/SOT Observations,*
Y. Bamba, K. Kusano, T. T. Yamamoto, and T. J. Okamoto,
2013 ApJ 778 48 doi:10.1088/0004-637X/778/1/48
[2] *Magnetic Field Structures Triggering Solar Flares and Coronal Mass Ejections,*
K. Kusano, Y. Bamba, T. T. Yamamoto, Y. Iida, S. Toriumi, and A. Asai,
2012 ApJ 760 31 doi:10.1088/0004-637X/760/1/31

Keywords: Sun, solar flare, magnetic field, SDO, Hinode, space weather

Japan Geoscience Union Meeting 2014
(28 April - 02 May 2014 at Pacifico YOKOHAMA, Kanagawa, Japan)

PEM08-03 Room:411 Time:May 1 16:45-17:00

X5.4 flare on 7 March 2012: magnetic and velocity properties at the solar surface

SHIMIZU, Toshifumi[1*] ; LITES, Bruce[2] ; BAMBA, Yumi[3]

[1]ISAS/JAXA, [2]HAO/NCAR, [3]Nagoya University

Solar flares abruptly release the free energy stored as a non-potential magnetic field in the corona and may be accompanied by eruptions of the coronal plasma. Formation of non-potential magnetic field and the mechanisms on triggering the onset of flares are still unclear; Especially, dynamical behaviors observed around polarity inversion lines producing major flares observationally. This presentation will discuss X5.4 flare on 7 March 2012 with emphasis on magnetic and velocity field properties at the solar surface. The coronal mass ejection launched at the same time as the X5.4 flare propagated through interplanetary space and caused a large geomagnetic storm on 9 March. One of remarkable properties to be discussed is a high-speed material flow existing along the polarity inversion line located between flare ribbons at the main energy release side. The high-speed material flow was observed in the horizontally oriented magnetic field formed nearly in parallel to the polarity inversion line and it existed at least from 6 hours before the onset of the flare and continued at least for several hours after the onset of the flare. Observations suggest that the observed material flow represents neither the emergence nor convergence of the magnetic flux. It may be rather considered as material flows working for increasing the magnetic shear along the polarity inversion line and for developing the magnetic structures favorable for the onset of the eruptive flare.

Keywords: solar flare, Hinode, X-ray, Optical, magnetic field, Doppler shift

Japan Geoscience Union Meeting 2014
(28 April - 02 May 2014 at Pacifico YOKOHAMA, Kanagawa, Japan)

PEM08-04 Room:411 Time:May 1 17:00-17:15

Estimation of Astronaut Dose inside the Kibo Module during Large Solar Flare Events

SATO, Tatsuhiko[1*] ; KATAOKA, Ryuho[2] ; NAGAMATSU, Aiko[3]

[1]Japan Atomic Energy Agency, [2]National Institute of Polar Research, [3]Japan Aerospace Exploration Agency

Forecast of radiation doses for astronauts as well as aircrews due to the exposure to solar energetic particles (SEP) is one of the greatest challenges in space weather research. In last 3 years, we have developed a warning system of aviation exposure to solar energetic particles: WASAVIES, which can predict the SEP doses at any flight conditions within 2.5 hours after the onset of ground level enhancements (GLE). In this system, the SEP fluxes incident to the atmosphere are calculated by physics-based models [1,2], and they are converted to radiation doses using a database developed on the basis of air-shower simulation [3]. In this study, we applied the same physics-based models to the estimate of the SEP fluxes on the orbit of International Space Station, and converted the fluxes to radiation doses for astronauts staying inside the Kibo module. For this conversion, we performed Monte Carlo cosmic-ray transport simulation, using the Particle and Heavy Ion Transport code System PHITS [4] in combination with the realistic 3D model of the Kibo module. A brief outline of WASAVIES together with the results of the astronaut dose estimation will be presented at the meeting.

[1] Y. Kubo, submitted to Space Weather
[2] R. Kataoka et al. submitted to Space Weather
[3] T. Sato et al. (2013) Radiat. Prot. Dosim. doi:10.1093/rpd/nct332
[4] T. Sato et al. (2013) J. Nucl. Sci. Technol. 50, 913-923. http://phits.jaea.go.jp/

Keywords: solar flare, radiation dose, solar energetic particle, astronaut, space weather, PHITS

Japan Geoscience Union Meeting 2014
(28 April - 02 May 2014 at Pacifico YOKOHAMA, Kanagawa, Japan)

PEM08-05 Room:411 Time:May 1 17:15-17:30

WASAVIES: Warning System for Aviation Exposure to Solar Energetic Particles

KATAOKA, Ryuho[1*] ; SATO, Tatsuhiko[2] ; KUBO, Yuki[3] ; SHIOTA, Daikou[4] ; KUWABARA, Takao[5] ; YASHIRO, Seiji[6] ; YASUDA, Hiroshi[7]

[1]NIPR, [2]JAEA, [3]NICT, [4]Nagoya University, [5]Delaware University, [6]CUA, [7]NIRS

Solar energetic particles (SEP) sometimes induce air shower that significantly increase the radiation dose at flight altitudes. In order to inform the situation of such a space radiation hazard to aircrews, a physics-based forward model is developed as WASAVIES (Warning System for Aviation Exposure to SEP) based on focused transport equation and Monte Carlo particle transport simulation code PHITS. WASAVIES gives the fastest and simplest way to predict the time profile of dose rate during ground-level enhancements (GLEs).

Keywords: solar proton, radiation dose, flares, air shower

Japan Geoscience Union Meeting 2014
(28 April - 02 May 2014 at Pacifico YOKOHAMA, Kanagawa, Japan)

PEM08-06 Room:411 Time:May 1 17:30-17:45

Plan of large SPE search by the 14C content measurement in Japanese trees for the past 5000 years

MIYAKE, Fusa[1*] ; MASUDA, Kimiaki[1] ; HAKOZAKI, Masataka[2] ; NAKAMURA, Toshio[2] ; KIMURA, Katsuhiko[3]

[1]Solar-Terrestrial Environment Laboratory, Nagoya University, [2]Center for Chronological Research, Nagoya University, [3]Faculty of Symbiotic Systems Science, Fukushima University

Radiocarbon (^{14}C) is produced by incoming cosmic rays to the Earth. Produced ^{14}C becomes $^{14}CO_2$ and is absorbed by trees by photosynthesis. Then,tree-rings record the past cosmic ray intensity. Rapid yearly increases in the ^{14}C content have been detected for the period from AD 774 to AD 775 and from AD 993 to AD 994. Althogh some candidates for the cause of these cosmic-ray invents have been considered, it has been considered that the solar activity (large SPE) is the most plausible cause.

There is the possibility that a lot of ^{14}C increase events like the AD 775 one are hidden in the periods when the ^{14}C content has not been measured with a 1-year resolution. If we detect such events, we are able to discuss a detailed occurrence rate of large SPE which is very important factor to prepare for future large SPEs.

We are planning to search for ^{14}C increase events by the measurements of ^{14}C content in Japanese trees for this 5000 years. In this thesis, we are going to explain the plan and problems.

Keywords: radiocarbon, tree-rings, cosmic-ray, SPE

Japan Geoscience Union Meeting 2014
(28 April - 02 May 2014 at Pacifico YOKOHAMA, Kanagawa, Japan)

PEM08-07 Room:411 Time:May 1 17:45-18:00

End-Cretaceous mass extinction driven by the encounter with a dark cloud

NIMURA, Tokuhiro[1*] ; EBISUZAKI, Toshikazu[2] ; MARUYAMA, Shigenori[3]

[1]Okayama Astronomical Museum, [2]RIKEN, [3]Earth-Life Science Intitute, Tokyo Institute of Technology

We found that a significant positive broad component of iridium in a pelagic deep sea sediment core (886C) around an iridium peak by asteroid impact corresponds at the K-Pg boundary. The 886C is core sample was taken by the Ocean Drilling Program (ODP) in the central portion of the North Pacific. This site has been in Pelagic from the End-Cretaceous periods. The accumulation rate is 0.5 m Myr^{-1}. Kyte et al., (1995) measured iridium density in the 886C core of 0.75-72.2 m which corresponds of $\sim$80 Ma from the present. In this data, there is one sharp peak around 65.5 m correspond at K-Pg boundary. In addition, we found that there are broad components across $\sim$20 m above the back ground which have some sharp peak component. The Ir value of the broad component which is about dozen times of back ground. This broad component is difficult to be explained by the materials on the surface of the Earth, and requires the contribution from the iridium-rich extraterrestrial materials, such as CI chondrite. And it is difficult to explain the broad component by diffusion and bioturbation of an iridium peak by asteroid impact. Platinum-group-element such as Pt, Re and Ir are redistributed by changes in sedimentary redox condition. However such change can probably account for many of small $<$10 cm (Colodner et al., 1992) and the mean global depth of marine bioturbation was calculated to be 9.8$\pm$4.5 cm (Boudreau, 1994). And also an evidence of bioturbation was not found from lithofacies (Proc. ODP, Init. Repts., 145).

We consider that the broad component can be caused by an encounter of the solar system with a dark cloud with a size of $\sim$100 pc and the central density of over 2000 protons/cc in the galactic disk and estimated that the flux of exosolar material began $\sim$73 Ma and has run through $\sim$8 Myr. By the Kataoka's "Nebula Winter model" (Kataoka 2013), dark cloud can lead to an environmental catastrophe to the Earth from a few kiloannum to megaannum. The dark cloud encounter enhances a flux of cosmic dust particles and cosmic rays which lead to global cooling and destruction of the ozone layer.

The solid particles from the dark cloud accrete on the Earth and in the stratosphere, stay for a several months; their sunshield effect is as large as -9.3 W m^{-2}. The climate cooling in the End-Cretaceous period is also suggested by the variations of stable isotope rations in oxygen and strontium (Brian and Huber, 1990; Barrera and Savin, 1999; Li and Keller, 1998). Any photosynthetic plants had heavy damaged, and loss of biodiversity began to the top of food chain.

The mass extinction at K-Pg boundary, which is widely thought to be caused by an impact of an asteroid (e. g., Schulte et al., 2010). However, a complete extinction of level of family by asteroid impact seems rather difficult. First, a severe environment turn-over would finish few years after impact, the solid particles and sulphate launched by the asteroid impact was settled down for only few month (troposphere) to few years (stratosphere) and negative radiative forcing became negligible after a few years from the impact (Pierazzo, 2001).The number of individuals would recover completely after the environmental catastrophe was over, if a few percent of individuals of one species survived.

Second, in spite of there were similar impacts without catastrophic on the Earth, for example, Alamo, Woodleigh, and Popigai crater, there are no evidences of association for extinction. However, because the encounter with the dark cloud perturbs the orbit of asteroid or comet by its gravitational potential and may lead an asteroid or comet shower, the asteroid impact at K-Pg may be one of the consequences of the dark cloud. For a certainly, only an asteroid impact cannot involve mass extinction, however may be role cruncher. The multiple impact and volcanism in a short period of time (Keller, 2005) may have been caused by encounter the dark nebula and attendant cosmic ray, respectively.

Keywords: Nebula Winter, dark cloud, mass extinction, End-Cretaceous, K-Pg boundary, Ocean Drilling Program

Japan Geoscience Union Meeting 2014
(28 April - 02 May 2014 at Pacifico YOKOHAMA, Kanagawa, Japan)

PEM08-08 Room:411 Time:May 2 09:00-09:15

Update on the US GIC activities and generation of benchmark geomagnetic disturbance (GMD) scenarios

PULKKINEN, Antti[1*]

[1]NASA GSFC

The awareness about potential major impacts of geomagnetically induced currents (GIC) has drawn a high level action in the US and in Canada. More specifically, regulatory process has been launched to generate standards for GIC hazard assessments and mitigation procedures. All US high-voltage power transmission-related entities need to follow the standards in the near future. One of the central GIC activities in the US has been the North the American Electric Reliability Corporation's (NERC) GMD Task Force that has allowed in-depth communication and collaboration between US federal organizations, power transmission operators and scientific research community. I will discuss these activities in this paper and outline the road ahead for some of the key US GIC activities.

As a part of the GMD standards drafting process and the US GIC hazards assessments, substantial effort has been made for generating benchmark GMD scenarios. These scenarios that quantify extreme geoelectric field magnitudes and temporal waveforms of the field fluctuations are the foundation for subsequent engineering analyses. The engineering analyses will include the transmission system voltage stability and transformer heating assessments. The work on the GMD scenarios has been a major collaboration between a number of US and Canadian entities involved in GMD research and transmission system operations. I will discuss in this paper also the key elements of the benchmark GMD generation process and show the latest results from our NASA GSFC work on the topic.

Keywords: Space weather, geomagnetically induced currents, Extreme events

Japan Geoscience Union Meeting 2014
(28 April - 02 May 2014 at Pacifico YOKOHAMA, Kanagawa, Japan)

PEM08-09 Room:411 Time:May 2 09:15-09:30

Spatial distribution of nonthermal electrons in an X-class flare on 13 May 2013

MASUDA, Satoshi[1*]

[1]STEL, Nagoya Univeristy

Four X-class flares took place in May 2013. Fortunately three of four were observed with Nobeyama Radioheliograph (NoRH). One of them occurred behind the east limb on 13 May 2013. It is a good chance to investigate the height distribution of nonthermal electrons in the solar corona. In the framework of the standard flare model based on magnetic reconnection, Minoshima et al. (2011) showed that the height distribution of accelerated/heated electrons depends on the energy of the electrons. NoRH has a capability to observe a solar flare in 17 and 34 GHz with a high time resolution (100 ms). The energy of electrons emitting microwaves is very high (˜MeV), and the mean-energy emitting 34 GHz is higher than that for 17 GHz. Hard X-rays are emitted by relatively lower-energy (˜100 keV) electrons. So this dataset can cover a wide energy range of accelerated electrons. In order to understand the electron acceleration/transport/loss processes, multi-wavelength observation is crucially important. The 13 May 2013 flare was simultaneously observed with NoRH and RHESSI (The Reuven Ramaty High Energy Solar Spectroscopic Imager). Investigating the distribution of these emission sources in the solar corona, we discuss the electron acceleration/transport/loss processes.

Keywords: solar flare, particle acceleration, microwave, hard X-ray, solar corona, magnetic recconection

Japan Geoscience Union Meeting 2014
(28 April - 02 May 2014 at Pacifico YOKOHAMA, Kanagawa, Japan)

PEM08-10 Room:411 Time:May 2 09:30-09:45

An energetics study of X-ray jets using Hinode/XRT observation

SAKO, Nobuharu[1*] ; SHIMOJO, Masumi[2] ; WATANABE, Tetsuya[2] ; SEKII, Takashi[2]

[1]The Graduate University for Advanced Studies, [2]National Astronomical Observatory of Japan

For plasma acceleration in X-ray jets in the solar corona, three mechanisms have been considered, based on the model of X-ray jets by magnetic reconnection (Shibata et al. 1992); The reconnection jet produced by magnetic tension, the evaporation flow produced by pressure gradient, and the twisted jet produced by magnetic pressure. There are some evidences of X-ray jets in active regions (ARs) produced by pressure gradient. On the other hands, there is no observational evidence of X-ray jets by the other forces except the result of a high-speed jet. In order to distinguish the evaporation flow from the other types of jets, I have studied the energetics of the X-ray jets.

Using over 100 X-ray jets greater than 3×104 km in length in ARs, quiet regions (QRs), and coronal holes (CHs), I have found no large differences in the life time, the width of the jets, and the area of the footpoint flares in such regions. On the other hands, the plasma number density of the X-ray jets and flares in ARs is ten times larger than those in QRs and CHs. Assuming the energy balance between conductive flux and heat flux by the footpoint flare, we estimate the temperature of the jets. The AR jets has a wide range of the temperature (1 MK-9 MK), while the temperature of most X-ray jets in CH and QR is $1\sim2$ MK. In my presentation, I will discuss a relationship of the speed with the temperature of the jets.

Keywords: Sun, Solar Corona, X-ray jet, Energy release, Hinode

Japan Geoscience Union Meeting 2014
(28 April - 02 May 2014 at Pacifico YOKOHAMA, Kanagawa, Japan)

PEM08-11 Room:411 Time:May 2 09:45-10:00

Lower temperature response of an EUV wave observed by Hinode/EIS and SDO/AIA

LEE, Kyoung sun[1*] ; KWON, Ryun young[2] ; BROOKS, David[2] ; SHIMIZU, Toshifumi[1]

[1]ISAS/JAXA, [2]George Mason University

We investigate an EUV wave observed by Hinode/EIS and SDO/AIA on 2011 August 04. The EUV wave propagates across the solar disk and the wave front passing through a remote active region (AR 11263) is observed by EIS. This EUV wave has already been analyzed using coronal lines, but the lower temperature response to the EUV wave has not been investigated. Using multi-wavelength observations from EIS and AIA, we determined the intensity and Doppler velocity variation of different temperature lines and compared them. From the comparison, we found an enhancement of the intensity at lower temperatures before the intensity increase seen in the coronal filters of AIA. And a significant enhancement of the red shift (10 km/s) in the lower temperature line (Si VII, log T ˜5.8) compared to the increase of the red shift (˜3 km/s) in coronal lines (Fe XII, FeXIII, and Si X, log T ˜6.1-6.2) when the EUV wave interacts with the active region. We will discuss the impact of the EUV wave on the lower temperature emission.

Keywords: Spectroscopy, Corona, EUV wave

Japan Geoscience Union Meeting 2014
(28 April - 02 May 2014 at Pacifico YOKOHAMA, Kanagawa, Japan)

PEM08-12 Room:411 Time:May 2 10:00-10:15

Imaging, spectroscopic and stereoscopic observations of the bi-directional inflow in the solar flare

MATSUI, Yuki[1*] ; YOKOYAMA, Takaaki[1]

[1]University of Tokyo

The standard model of solar flares based on the magnetic reconnection includes bi-directional inflow toward the reconnection point. Corresponding to the bi-directional inflow, high temperature loops like a cusp shape are formed due to the magnetic reconnection. By combination of imaging, spectroscopic and stereoscopic observations, we succeeded in capture the three-dimensional structure of a bi-directional reconnection inflow of a solar flare.

We analyzed a C-class flare that occurred on 2012 September 11 beyond the solar limb. The bi-directional inflow was found in the images of coronal temperature filter taken by AIA onboard SDO. Hinode EUV Imaging Spectrometer (EIS) also observed this flare and provide the Doppler velocity of the bi-directional inflows. At the same time, cusp loops were observed with the raster scans of FeXXIV emission line (over 10 MK) at the region surrounded by the bi-directional inflow. This is clear evidence that 1MK loops are heated over 10MK by the magnetic reconnection. STEREO A/SECCHI was observing this flow from a different line of site. Inflowing angle in STEREO A/SECCHI images is consistent with the angle speculated by apparent velocity of SDO/AIA and line of sight velocity of Hinode/EIS. By combining these data sets, we constructed a self-consistent three-dimensional picture of the flows.

Keywords: solar flare, reconnection

Japan Geoscience Union Meeting 2014
(28 April - 02 May 2014 at Pacifico YOKOHAMA, Kanagawa, Japan)

PEM08-13 Room:411 Time:May 2 10:15-10:30

Diagnosis of coronal shock strength using the activation of large amplitude prominence oscillation

TAKAHASHI, Takuya[1*] ; ASAI, Ayumi[2] ; SHIBATA, Kazunari[3]

[1]Graduate School of Science, Kyoto University, [2]Unit of Synergetic Studies for Space, Kyoto University, [3]Kwasan and Hida Observatories, Kyoto University

X5.4 class solar flare occurred on March 7,2012 which was the second largest flare in this solar cycle. The flare was associated with very fast coronal mass ejection(CME) with the velocity of over 2500km/s. Associated with this flare, a wave-like coronal disturbance(known as EUV wave) was observed to propagate along the solar surface. The observed EUV wave propagated with the average speed of about 670km/s towards the north and 'hit' a polar prominence leading to its large amplitude oscillation. The activated prominence strongly brightened when EUV wave 'pushed' it.

Because of the difficulty in direct observation of physical quantities in the corona, the physical nature of the EUV waves is still under discussion. Two main interpretations of EUV waves are the 'fast mode MHD wave/shock' interpretation, and 'non-wave' interpretations.

In the images taken with Inner coronagraph(COR1) of the Sun Earth Connection Corona and Heliospheric Investigation(SECCHI) on board *Solar Terrestrial Relations Observatory(STEREO)-Behind*, we could see a coronal disturbance detached from expanding CME plasma. The time evolution of the disturbance seen in COR1 images was consistent with that of observed EUV wave. Also, Type II radio burst which is thought to be evidence of coronal shock wave was observed simultaneously. Because of that observational evidence, we regard the observed EUV wave as MHD fast mode shock front. Assuming the shock nature of the observed EUV wave, we could also explain prominence acceleration and brightening consistently.

Using the initial velocity of activated prominence, we could estimate the coronal shock strength of the EUV wave with the help of linear wave theory. We also check the applicability of linear theory to the shock problem with one dimensional numerical model and ascertained that it is applicable when the shock strength is not strong. Estimated fast mode mach number of the EUV wave was between 1.20 and 1.42, and we could say that the EUV wave was a weak shock front in the corona.

Keywords: solar flare, coronal mass ejection(CME), shock waves, solar prominence, magnetohydrodynamics(MHD)

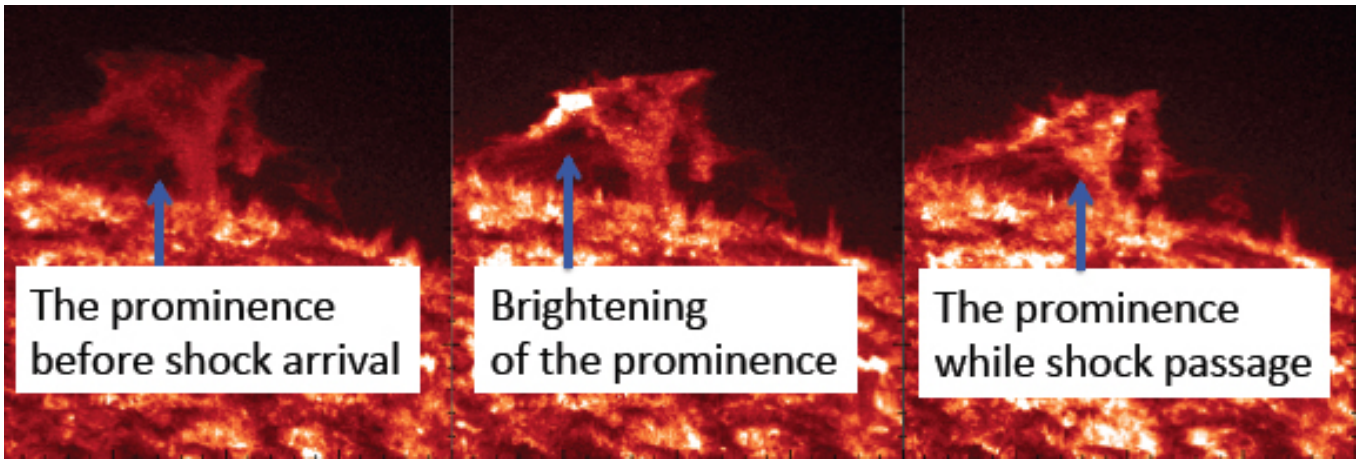

Japan Geoscience Union Meeting 2014
(28 April - 02 May 2014 at Pacifico YOKOHAMA, Kanagawa, Japan)

PEM08-14 Room:411 Time:May 2 10:30-10:45

Influence of interplanetary solar wind sector polarity on the ionosphere

LIU, Jing[1*]

[1]Beijing National Observatory of Space Environment, Institute of Geology and Geophysics, CAS

Knowledge of solar sector polarity effects on the ionosphere may provide some clues in understanding of the ionospheric day-to-day variability and 'hysteresis' effect on foF2. In this study, a solar-terrestrial connection ranging from solar sector boundary crossings, geomagnetic disturbances and ionospheric perturbations has been demonstrated. The increases in interplanetary solar wind speed within three days are seen after SB crossings, while the decreases in solar wind dynamic pressure and magnetic field intensity immediately after SB crossings are confirmed by the superposed epoch analysis results. Furthermore, the interplanetary magnetic field (IMF) Bz component turns from northward to southward in March equinox and June solstice as the Earth passes from a solar sector of outward to inward directed magnetic fields, whereas the reverse situation occurs for the transition from toward to away sectors. The IMF Bz component for the same solar sector polarity has opposite signs between March equinox and September equinox, and also between June solstice and December solstice. In order to know how the ionosphere reacts to the interplanetary solar wind variations linkage of SB crossings, the F2 region critical frequency (foF2) covering about four solar cycles and total electron content (TEC) during 1998?2011 are utilized to extract the related information, revealing that they are not modified significantly and vary within the range of 15% on average. The responses of the ionospheric TEC to SB crossings exhibit complex temporal and spatial variations and have strong dependencies on season, latitude, and solar cycle. This effect is more appreciable in equinoctial months than in solstitial months, which is mainly caused by larger southward Bz components in equinox. In September equinox, latitudinal profile of relative variations of foF2 at noon is featured by depressions at high latitudes and enhancements in low-equatorial latitudes during IMF away sectors. The negative phase of foF2 is delayed at solar minimum relative to it during other parts of solar cycle, which might be associated with the difference in longevity of major interplanetary solar wind drivers perturbing the near-Earth environment in different phases of solar cycle.

Japan Geoscience Union Meeting 2014
(28 April - 02 May 2014 at Pacifico YOKOHAMA, Kanagawa, Japan)

PEM08-15 Room:411 Time:May 2 10:55-11:15

Ensemble Data Assimilation for Thermospheric Mass Density Specification and Forecasting

MATSUO, Tomoko[1*] ; LEE, Ite[3] ; ANDERSON, Jeffrey[4]

[1]University of Colorado at Boulder, CO, USA, [2]National Oceanic and Atmospheric Administration, CO, USA, [3]National Central University, Taiwan, [4]National Center for Atmospheric Research, CO, USA

Even though the Earth's upper atmosphere density is tenuous, it is substantial enough to exert significant drag on orbiting spacecraft and debris. The largest uncertainty in low-Earth orbit prediction is aerodynamic drag estimation. Thermospheric mass density variation is the major source of drag estimation errors at altitudes below about 700 km. This paper demonstrates how the limit of predictability of thermospheric mass density variability can be extended by means of ensemble data assimilation.

To assimilate observations of the thermosphere and ionosphere, we use an ensemble data assimilation procedure constructed with the Data Assimilation Research Testbed and the Thermoshere-Ionosphere Electrodynamics General Circulation Model, two sets of community software offered by NCAR. An important attribute of our approach is that the ionosphere-thermosphere coupling is self-consistently treated in both the forecast model and the assimilation scheme. This enables the inference of unobserved thermospheric states from the relatively plentiful observations of the ionosphere. Given the ever-expanding global navigation satellite infrastructure, this is indeed a promising prospect for upper atmosphere data assimilation. Another relevant strategy is using data assimilation to estimate the model forcing parameters that control states of the thermosphere and ionosphere. In comparison to the lower atmosphere, the upper atmosphere is a dissipative, strongly forced dynamical system, so estimation of model forcing parameters can have a dramatic impact on the quality of ensemble forecasting and assimilation of the upper atmosphere.

In this paper, we present results from our ensemble assimilation experiments with thermospheric mass densities obtained from the accelerometer on board the CHAMP satellite, and electron density profiles obtained from the COSMIC/FORMOSAT-3 mission.

Keywords: thermosphere-ionosphere coupling, data assimilation, parameter and state estimation, thermospheric mass density, aerodynamic drag estimation, LEO orbit prediction

Japan Geoscience Union Meeting 2014
(28 April - 02 May 2014 at Pacifico YOKOHAMA, Kanagawa, Japan)

PEM08-16 Room:411 Time:May 2 11:15-11:30

Forecast of ionospheric disturbances using a high-resolution atmosphere-ionosphere coupled model

SHINAGAWA, Hiroyuki[1*] ; JIN, Hidekatsu[1] ; MIYOSHI, Yasunobu[2] ; FUJIWARA, Hitoshi[3] ; YOKOYAMA, Tatsuhiro[1]

[1]NICT, [2]Kyushu University, [3]Seikei University

Space weather forecasts are about to enter a stage incorporating numerical forecasts based on realistic numerical simulation, in addition to conventional methods used by forecasters to make predictions based on observational data and experience. At the National Institute of Information and Communications Technology (NICT) of Japan, we have developed an atmosphere-ionosphere coupled model, which includes the whole neutral atmosphere and the ionosphere. The model is called GAIA (Ground-to-topside model of Atmosphere and Ionosphere for Aeronomy). The present version has spatial resolution of about 1 degree in horizontal direction. In addition, we are also developing a high-resolution regional ionospheric model, which has a horizontal resolution of about 10 km. We plan to combine GAIA and the regional model to reproduce mesoscale ionospheric phenomena, such as plasma bubbles and SED (storm enhanced density). The model will be a useful tool for space weather forecast. We will report previous results, and a plan for the new model.

Keywords: space weather, ionosphere, atmosphere, simulation, model, disturbance

Japan Geoscience Union Meeting 2014
(28 April - 02 May 2014 at Pacifico YOKOHAMA, Kanagawa, Japan)

PEM08-17 Room:411 Time:May 2 11:30-11:45

Projection of substom processes from the plasma sheet to the polar ionosphere

TANAKA, Takashi[1*]

[1]Emeritus Professor, Kyushu University

It has been believed that auroras observed in the ionosphere have their corresponding counterpart in the plasma sheet (Haerendel, 2011). Localized auroral breakup should reveal the location of explosive dissipation in the plasma sheet. Similar correspondence is supposed even during the growth phase. While it is well known that the prebreakup arc breakups first during the substorm, the equatorial location and relating formation mechanism of equatormost arc are long-standing questions in the understanding of the growth phase (Sergeev et al., 2012). Another aurora during the growth phase is the poleward bright arc that is believed to be an ionospheric projection of the reconnection separatrix. Also the equatorward extension of the N-S auroral arc has been suggested to be associated with eathward fast bursty flows (Nishimura et al., 2010). The region of aurora indicates that the width of oval is 7^o (64^o to 71^o), near midnight just prior to the breakup. Pich angle isotropy boundary at 65.5^o is critical for the prebreakup arc, since the isotropy boundary coincides with the prebreakup arc. Seen from the structure of isotropy boundary, the breakup arc is somewhere in the transition region between the dipole-like region and the current sheet region. A phenomenon closely related to the projection of the aurora is the distribution of FAC and its tracing. A traditional understanding for the driver of disturbances is the fast flow, both for the growth phase and the onset. The BBF was expected for a wide range of activity including localized auroral brightenings, N-S auroras and streamers (Nakamura et al., 2001). At the same time, the BBF can be a source of the FAC. The cross-tail current is diverted via downward FAC into the ionosphere on the eastward side of the bubble and is connected to upward FACs west of the bubble. The overall region 1-sense FACs is expected to emerge from 64^o to 70^o (Yang et al., 2012). The plasma ahead of the bubble is compressed, resulting in a high plasma pressure and the region 2-sense FACs that are as thin as 1^o, centered at 63^o.

Recent M-I coupling simulation reproduces almost all signatures of the substorm, including the preonset arc, and the onset that start from the low-latitude side of the oval (Tanaka et al., 2010). From the numerical solution just prior tp the onset, the BBF region from x=-10 Re to x=-20 Re in the plasma sheet is projected down along the magnetic filed to a quite narrow region in the ionosphere from 65.7^o to 66.8^o latitudes. Even the outmost field line of the plasma sheet is traced down to 68^o latitude in the ionosphere. So that the observed high-latitude part of the oval (68^o~71^o) is outside the plasma sheet. The N-S arc that usually starts from higher latitude than 70^o cannot be the reflection of the BBF. Near the midnight, in the numerical solution, the region 1 FAC distributes from 65^o to 69^o (with strong part 67^o~68^o) and the region 2 FAC distributes from 62^o to 64^o latitude. From this result, the growth phase region 1 FAC cannot be from the plasma sheet. The result of current line tracing shows that the growth phase region 1 FAC extends into the magnetosphere as far as x=-20Re through the east-west flow shear between the tail plasma sheet and the lobe. If we look at only the latitude it is barely possible that the onset FAC strating from the lowest-latitude area of the region 1 FAC around 65^o could be from the CW that should to be inside x=-10 Re (65.7^o). However, it is implausible from the current line tracing. The onset region 1 FAC is mapped to the cusp-mantle region through the near earth flow shear between the plasma sheet and the lobe. Correspondence beween the plasma sheet and the ionosphere so far believed is quite confusing. It is doubtful to consider that all auroras observed in the ionosphere have their corresponding counterpart in the plasma sheet.

Keywords: substorm

Japan Geoscience Union Meeting 2014
(28 April - 02 May 2014 at Pacifico YOKOHAMA, Kanagawa, Japan)

PEM08-18 Room:411 Time:May 2 11:45-12:00

One-month periodicity in thunderstorm, OLR and solar parameters

TAKAHASHI, Yukihiro[1*] ; SATO, Mitsuteru[1]

[1]Department of Cosmosciences, Hokkaido University

Recently the relationship between the global circuit and solar-climate connection was pointed out. Here we introduce an example, which indicates the roles of thunderstorm or its resultant electric circuit in solar-climate connection. Global relationship between thunderstorm/cloud activities and solar parameters are examined based on lightning measurement by Global ELF observation Network (GEON) operated by Hokkaido University and Outgoing Longwave Radiation (OLR) intensity. It was found that the number of lightning stokes in Asia Maritime Continent (AMC) varies with about month periodicity in the period from February to June 2004 and shows positive correlation (R= ˜0.8) with OLR in the Western Pacific Warm Pool (WPWP). On the other hand, OLRs in the central Africa and some other tropical areas show negative correlation with the number of lightning stokes in the AMC in that period. It is also found that the galactic cosmic rays or UV intensity associated with solar activity indicates good correlation with tropical OLR or lightning activity in AMC. One explanation to connect such global variations in thunderstorm / cloud amount with solar parameters would be the electrical circuit involving lower and upper atmospheres. Global electric circuit model was proposed log time ago, in 1930s, in which thunderstorm plays a role of generator, and the ground and the ionosphere work as a spherical capacitor. However, now we need to reconstruct this simple model, taking into account 3 aspects: 1) global-scale nonuniformities both of ionospheric conductivity and of the distribution of the generators, 2) connections between the troposphere and D-region, considering the effects of TLEs, such sprites and blue jets, 3) establishing the observational methodology for global electric field, excluding the effect of cloud existing just above the observation sites. If the ionospheric electric field modulates the potential gradient in the lower atmosphere, it could cause the re-distribution of ionized atmospheric particles, which may, in turn, change the generation / reduction speed of cloud particles.

Keywords: thunderstorm, OLR, solar activity, one-month periodicity

Japan Geoscience Union Meeting 2014
(28 April - 02 May 2014 at Pacifico YOKOHAMA, Kanagawa, Japan)

PEM08-19 Room:411 Time:May 2 12:00-12:15

Influence of solar wind on climate: On the factors such as Quasi Biennial Oscillation

ITOH, Kiminori[1*] ; MATSUO, Shinya[1] ; YAMASHITA, Kazuyoshi[1]

[1]Yokohama National University, Graduate School of Env. & Inf. Sciences

In spite of long history of research, the influence of solar changes on the climate is not convincing enough yet. We have employed solar wind parameter (e.g., Pα (energy flowing into magnetosphere) and aa index) to successfully show their correlation with the temperatures of the stratosphere, troposphere and surface. For further analyses, OLR (outgoing longwave radiation) and the participation of QBO etc. are studied. For instance, January OLR during 1975-2011 showed high correlation with Pα at particular regions. At the QBO westerly phase, high correlation coefficient (r = 0.76) was found near Indonesia. The correlation map at the easterly phase resembled that for the Arctic Oscillation, and r = 0.81 at the Siberia region.

Keywords: Solar wind, climate, QBO, OLR, temperature

Japan Geoscience Union Meeting 2014
(28 April - 02 May 2014 at Pacifico YOKOHAMA, Kanagawa, Japan)

PEM08-20 Room:411 Time:May 2 12:15-12:30

Laboratory experiment with various radiation sources for verification of cloud condensation nucleation by cosmic rays

SUZUKI, Asami[1*] ; MASUDA, Kimiaki[1] ; TAKEUCHI, Yuya[1] ; ITOW, Yoshitaka[1] ; SAKO, Takashi[1] ; MATSUMI, Yutaka[1] ; NAKAYAMA, Tomoki[1] ; UEDA, Sayako[1] ; MIURA, Kazuhiko[2] ; KUSANO, Kanya[1]

[1]Solar-Terrestrial Environment Laboratory,Nagoya University, [2]Tokyo university of science

It is considered that the solar activity may affect the global climate,but the correlation mechanism is still not understood.

One of the possible mechanisms for the correlation is the cloud formation by the galactic cosmic rays, which are modulated by the variation of solar activity. This relation was clearly indicated by the good correlation observed for the galactic cosmic-ray intensity and the global low-cloud amount.

This hypothesis includes the ion-induced nucleation model, in which new particles in the atmosphere are created efficiently through atmospheric ions produced by cosmic rays, and finally these particles grow up to the size of

cloud condensation nuclei.

In this study, a laboratory experiment for verification of the hypothesis has been conducted with a reaction chamber. A flow of clean air, water vapor, ozone and sulfuric dioxide was introduced to a metallic chamber, where we irradiated UV light for solar irradiance and beta-rays or accelerator beam for cosmic rays. The beam of the heavy ion accelerator HIMAC at National Institute of Radiological Sciences was used in the present experiment.

As a result, ions produced by the ionizing radiation and increased particle density were observed for beta rays.

Some results with the accelerator beam are the following.

Ion density in the chamber increased as the beam intensity and particle density increased with ion density.

Particle size distribution was measured and the peak particle size and the particle density became to larger with time after start irradiation, but the density stopped to increase or decreased after irradiation stopped although the peak size continued to increase.

It is shown that our system is ready for more detailed measurements.

Keywords: cosmic rays, cloud, cosmoclimatology, cloud condensation nuclei

Japan Geoscience Union Meeting 2014
(28 April - 02 May 2014 at Pacifico YOKOHAMA, Kanagawa, Japan)

PEM08-21 Room:411 Time:May 2 14:15-14:30

Study on symmetry-breaking between the northern and southern hemispheres of the solar dynamo

SHUKUYA, Daishi[1*] ; KUSANO, Kanya[1]

[1]Solar-Terrestrial Environment Laboratory, Nagoya University

Solar dynamo is a mechanism whereby the kinetic energy of the plasma in the sun is converted to the magnetic energy. This mechanism works to generate and maintain all solar magnetic activities. Because the Earth's climate can be influenced by solar activities, variability of the solar dynamo is an important issue to understand long-term evolution of the Earth's climate.

Comparisons of the solar activities in each solar hemisphere show hemispheric asymmetry. Sunspots were found preferentially in one hemisphere and not the other in often long periods of time (Spoerer, 1889; Maunder, 1890, 1904). This asymmetry was extended to other measures of activity including faculae, prominences and flares (Waldmeier, 1971; Roy, 1977). The asymmetry happens in the solar polar magnetic field reversals. The polarity of the solar magnetic fields on the north and south poles periodically reverses at every sunspot maxima. However, the reversals at both poles actually don't occur at the same time. In other words, the reversal at one pole is followed by that on the other pole. This time difference of magnetic field reversals between the poles was first noted by Babcock (1959) from the very first observation of polar field. Recently, it was confirmed by detailed observations with the HINODE satellite (Shiota et al. 2012). As above, we have ever obtained many observation facts. However, the mechanisms of hemispheric asymmetry of the solar dynamo haven't been revealed theoretically yet.

In this paper, we study the asymmetric feature of the solar dynamo based on the flux transport dynamo model (Chatterjee et al. 2004) to explain the time difference of magnetic polarity reversal between the north and south poles. In order to calculate long-term variations of solar activities, we use the mean field kinematic dynamo model, which is derived from magnetohydrodynamics (MHD) equation through the mean field and other approximations. We carried out the mean field dynamo simulations using the updated SURYA code which was developed originally by Choudhuri and his collaborators (2004). We decomposed the symmetric and asymmetric components of magnetic field, which correspond respectively to the quadrupole and dipole-like components (Nishikawa and Kusano 2008), and analyzed the phase relation between them. As a result, we found that the two components are mixed even if the dipole-like component is predominant and that the two components spontaneously form 90 or -90 degree out of phase oscillation. The solutions with 90 and -90 degree out of phase oscillation form the different attracters of dynamo solutions. We found that the time difference of the polar field reversals between the different hemispheres can be explained by the out of phase relation between the different components of magnetic field.

Keywords: polar field reversal, solar dynamo, numerical simulation, hemispheric asymmetry

Japan Geoscience Union Meeting 2014
(28 April - 02 May 2014 at Pacifico YOKOHAMA, Kanagawa, Japan)

PEM08-22 Room:411 Time:May 2 14:30-14:45

Climate responses in central Japan and Taiwan to the cosmic ray intensifications during the Maunder Minimum

SAKASHITA, Wataru[1*] ; YOKOYAMA, Yusuke[1] ; MIYAHARA, Hiroko[2] ; AZE, Takahiro[3] ; YONENOBU, Hitoshi[4] ; OHYAMA, Motonari[5] ; HOSHINO, Yasuharu[6] ; NAKATSUKA, Takeshi[7]

[1]Atmosphere and Ocean Research Institute, The University of Tokyo, [2]College of Art and Design, Musashino Art University, [3]Interactive Research Center of Science, Tokyo Institute of Technology, [4]Graduate School of Education, Naruto University of Education, [5]The Center for Academic Resources and Archives, Botanical Gardens, Tohoku University, [6]National Research Institute for Cultural Properties, Nara, [7]Research Institute for Humanity and Nature

Relationship between solar variations and climate has been long discussed for various time scales. It is difficult to distinguish the impacts of the multiple solar parameters (total solar irradiance (TSI), solar ultraviolet (UV) radiation, and galactic cosmic rays (GCRs)) on climate, because these variations are nearly synchronized. However, GCR fluctuations related to solar magnetic activity have slightly different features compared to the other external forcing factors (TSI, UV). According to previous studies, the cosmic ray fluctuation was particularly unique during the Maunder Minimum (A. D. 1645-1715), when almost no sunspots were observed. Annually measured tree-ring Δ^{14}C and ice-core ^{10}Be data have shown that decadal variations of GCRs had been remarkably amplified during the Maunder Minimum. This characteristic amplification may be utilized to shed light on the GCR influence on climate.

In this study, we employ tree rings that can reconstruct both annual climate (δ^{18}O) and cosmic ray fluctuations (Δ^{14}C) during the Maunder Minimum. By using these proxies, we can directly compare these reconstructions without any dating error. Annually measured tree-ring δ^{18}O records from central Japan have shown significant wet climate at every remarkable GCRs enhancement. On the other hand, there is no significant climate response in tree-ring δ^{18}O record from Taiwan. We suggest that these climate responses may be related to a stationary position of the Baiu front. Recent satellite observations have shown that GCRs may cause the increase of low cloud amount at tropical western Pacific region. It can be suggested that cooling of tropical western Pacific region caused by GCR enhancement might have caused the weakening of Pacific high and indirectly brought wet rainy seasons in central Japan.

Keywords: Solar Magnetic Activity, Galactic Cosmic Ray, The Maunder Minimum, Tree-ring isotope

Japan Geoscience Union Meeting 2014
(28 April - 02 May 2014 at Pacifico YOKOHAMA, Kanagawa, Japan)

PEM08-23 Room:411 Time:May 2 14:45-15:00

Dynamical estimation of external/internal acceleration processes of the outer radiation belt using data assimilation

MIYOSHI, Yoshizumi[1*] ; TOYAMA, Haruto[1] ; UENO, Genta[2] ; KOSHIISHI, Hideki[3] ; MATSUMOTO, Haruhisa[3] ; SHIOKAWA, Kazuo[1]

[1]STEL, Nagoya University, [2]The Institute of Statistical Mathematics, [3]JAXA

Dynamical evolution of the outer belts should be a delicate balance among several processes. It has been believed that there exist two different acceleration mechanisms: the radial diffusion as the external source process, and the non-adiabatic wave particle interactions as the internal source process. In order to discriminate when and where these processes are dominant for the large flux enhancement of the outer belt electrons, we have developed a data assimilation code on the outer belt electrons. In our data assimilation, the particle filter and the particle smoother are used which are effective for non-linear/non-Gaussian distribution problems. We include the radial diffusion coefficient and the internal source model in the state vector and estimate the dynamical variations of these parameters. The Tsubasa satellite electron data are used as the observation vector. The results indicate that only the radial diffusion process is always too small to explain the observed flux enhancement and the internal source process should be necessary. The assimilation result suggests that the internal source process tend to take place around the storm recovery phase, which is consistent with the observations.

Keywords: radiation belts, data assimilation

Japan Geoscience Union Meeting 2014
(28 April - 02 May 2014 at Pacifico YOKOHAMA, Kanagawa, Japan)

PEM08-24 Room:411 Time:May 2 15:00-15:15

Evaluation of Relativistic Electron Flux Forecast at GEO Satellite

NAGATSUMA, Tsutomu[1*] ; SAKAGUCHI, Kaori[1] ; SAITO, Shinji[2] ; MIYOSHI, Yoshizumi[2] ; SEKI, Kanako[2]

[1]National Institute of Information and Communications Technology, [2]Solar Terrestrial Environment Laboratory, Nagoya University

We have developed near real time prediction model for relativistic electron flux at GEO satellite. This model is based on a multivariate autoregressive model with using solar wind speed, north-south component of the magnetic field and dynanmic pressure as inputs. Detailed description of this model can be found in Sakaguchi et al. [2013]. We have started relativistic electron flux forecast service as a test product since Apr. 2013. Forecast information can be found in the following web pages (URL: http://seg-web.nict.go.jp/radi/).

There are several difficulties in operating a near-real time forecast model. One is the quality of the real-time solar wind data. Because quality of real-time solar wind density data is quite poor, we avoid using solar wind density data for our operational model. The other one is the lead-time of the solar wind data. Currently, we can use only ACE data for solar wind input. The lead-time of this data is only about one hour. Threfore, we also 'predict' solar wind condition for two or three days in advance from current solar wind information. Anyway, prediction efficiencies of our forecast for 1day, 2day, and 3day ahead in 2013 are 81%, 63%, 48%, respectively. Evaluation and future parspective of our forecasting model will be introduced in our presentation.

Reference:

Sakaguchi, K., Y. Miyoshi, S. Saito, T. Nagatsuma, K. Seki and K. T. Murata (2013), Relativistic electron flux forecast at geostationary orbit using Kalman filter based on multivariate autoregressive model, Space Weather, 11, 79?89, doi:10.1002/swe.20020.

Keywords: Space Weather Forecast, Solar Wind - Magnetosphere Interaction, Magnetosphere, Radiation Belt, Inner Magnetosphere, Modeling

Japan Geoscience Union Meeting 2014
(28 April - 02 May 2014 at Pacifico YOKOHAMA, Kanagawa, Japan)

PEM08-25 Room:411 Time:May 2 15:15-15:30

Maps of ionospheric conductances, currents, and convection from the Swarm multi-satellite mission

AMM, Olaf[1*] ; VANHAMAKI, Heikki[1] ; KAURISTIE, Kirsti[1] ; STOLLE, Claudia[4] ; CHRISTIANSEN, Freddy[3] ; HAAGMANS, Roger[5] ; MASSON, Arnaud[6] ; TAYLOR, Matt[5] ; FLOBERGHAGEN, Rune[7] ; ESCOUBET, Philippe[5]

[1]Finnish Meteorological Institute, Arctic Research Unit, Helsinki, Finland., [2]STEL, Nagoya University, Japan, [3]Technical University of Denmark, DTU Space, Lyngby, Denmark, [4]Helmholtz-Centre Potsdam, GFZ German Research Center for Geosciences, Germany, [5]ESTEC, Noordwijk, The Netherlands, [6]ESAC, Madrid, Spain, [7]Directorate of Earth Observation Programmes, ESRIN, Frascati, Italy

The recently launched ESA Swarm spacecraft mission is the first dedicated multi-satellite ionospheric mission with two low-orbiting spacecraft that are flying in parallel in a distance of ˜100 km, thus allowing to derive spatial gradients of ionospheric parameters not only along the orbits, but also in the direction perpendicular to them. In addition, a third satellite with a slightly higher orbit regularly crosses the paths of the lower spacecraft pair. Using the Swarm magnetic and electric field instruments, we present a novel technique that allows to derive 2-dimensional (2D) maps of ionospheric conductances, currents, and convection in the area between the trajectories of the two parallel flying spacecraft, and even to some extent outside of it. This technique is based on Spherical Elementary Current Systems (SECS). We present several test cases of modelled ionospheric situations from which we calculate virtual Swarm data, and show that the technique is able to reconstruct the model electric field (or convection), horizontal currents, and conductances with very good to excellent accuracy. Larger errors arise for the reconstruction of the 2D field-aligned currents (FAC) map, especially in the area outside of the spacecraft orbits. However, even in this case the general pattern of the model FAC is recovered, and the magnitudes are valid in an integrated sense. Finally, using an MHD model run, we show how our technique allows to estimate the ionosphere-magnetosphere coupling parameter K, if conjugate multi-point observations of the magnetospheric magnetic and electric field are available, as they can be obtained, e.g., from the ESA Cluster mission.

Keywords: ionosphere, ionospheric electrodynamics, ionospheric currents, ionospheric convection, magnetosphere-ionosphere coupling, Swarm mission

Japan Geoscience Union Meeting 2014
(28 April - 02 May 2014 at Pacifico YOKOHAMA, Kanagawa, Japan)

PEM08-26 Room:411 Time:May 2 15:30-15:45

MLT and seasonal dependence of auroral electrojets: IMAGE magnetometer network observations

GUO, Jianpeng[1*] ; LIU, Huixin[2]

[1]SIGMA Weather Group, State Key Laboratory of Space Weather, CSSAR, Chinese Academy of Sciences, [2]Department of Earth and Planetary Sciences, Faculty of Sciences, Kyushu University

Total eastward and westward electrojet currents (EEJ and WEJ) and their central latitudes derived from the IMAGE network magnetic measurements are analyzed for the combined MLT and seasonal dependence during the period 1995-2009. EEJ shows a strong MLT variation with significant dependence on season. During summer months the maxima occur around 1600-1800 MLT, whereas during winter months the maxima occur at a later local time sector around 1800-2000 MLT. Moreover, the summer maxima are much larger than the winter maxima, and appear at higher latitudes. The summer maxima are mainly associated with the solar EUV conductivity effect, while the winter maxima are mainly due to the contribution of northward convective electric field. EEJ exhibits a dominant annual variation with maximum in summer and minimum in winter. WEJ also exhibits a strong MLT variation with significant dependence on season. The maxima occur around 0200-0400 MLT during summer months, around 0000-0200 MLT during winter months, and around 0000-0400 MLT during equinoctial months. Moreover, the equinoctial maxima are much larger than the summer and winter maxima, and appear at relatively lower latitudes. The seasonal variations in WEJ are the combinations of annual variations and semiannual variations. Both annual and semiannual variations show significant dependence on MLT. These results increase our knowledge on what factors contribute to the auroral electrojets as well as their magnetic signatures, and hence help us better understand the limitations of global auroral electrojet indices, such as the AE and SME indices.

Japan Geoscience Union Meeting 2014
(28 April - 02 May 2014 at Pacifico YOKOHAMA, Kanagawa, Japan)

PEM08-27 Room:411 Time:May 2 15:45-16:00

Temporal variations of nitric oxide in the mesosphere and lower thermosphere over Syowa station, Antarctica

ISONO, Yasuko[1] ; MIZUNO, Akira[1*] ; NAGAHAMA, Tomoo[1] ; MIYOSHI, Yoshizumi[1] ; NAKAMURA, Takuji[2] ; KATAOKA, Ryuho[2] ; TSUTSUMI, Masaki[2] ; EJIRI, Mitsumu[2] ; FUJIWARA, Hitoshi[3] ; MAEZAWA, Hiroyuki[4] ; UEMURA, Miku[1]

[1]Solar-Terrestrial Environment Laboratory, Nagoya University, [2]National Institute of Polar Research, [3]Seikei University, [4]Osaka Prefecture University

Energetic particle precipitation (EPP) related to solar proton events or geomagnetic storms induce ion-neutral reactions and change abundance of some minor molecules such as NO_x and HO_x in the mesosphere and lower thermosphere. To investigate the temporal variations of NO by EPP, we installed a millimeter-wave spectroscopic radiometer at Syowa Station (69.00S, 39.85E), and we have carried out ground-based observations of spectral line of nitric oxide (NO) at 250.796 GHz since January 2012.

We obtained 197 and 172 daily averaged NO spectra in 2012 and 2013 (until 30 September; DOY 273), respectively. The daily NO spectra are characterized by narrow line width with a Full-Width-at-Half-Maximum (FWHM) of about 0.5 MHz. These NO spectra are well fitted by a single Gauss function or by a single Lorenz function. From the spectral line shape, we conclude that the NO emitting region is between 75 and 100 km.

We found two temporal variation patterns of NO column density. One is a seasonal variation with a maximum in the winter and a minimum in the summer. The column density of NO during the winter was about 4 times larger than that during the summer. This seasonal variation is considered to be related to the atmospheric transport and the NO dissociation by solar radiation. The other is the short-term variation in a timeframe of 5-10 days associated with EPP events such as solar proton events and geomagnetic storms. At Syowa Station, short-term variations were caused mainly by the precipitation of electrons rather than that of protons. In the electron precipitation events, the column density of NO gradually increases just after the main phase of the geomagnetic storm and gradually decreases soon after its peak.

One of the short-term events related to a large geomagnetic storm in April 2012 was the most prominent single event among those observed at Syowa Station since January 2012. From the high time resolution (~ 3-hour) data, we revealed a diurnal tendency that NO column density increased about twice at UT 0, which is interpreted to be caused by the dawn-dusk asymmetry of the precipitated electrons with energies 30-300 keV.

Keywords: Nitric oxide, mesosphere and lower thermosphere, energetic particle precipitation, geomagnetic storm, solar proton event, Antarctica

Japan Geoscience Union Meeting 2014
(28 April - 02 May 2014 at Pacifico YOKOHAMA, Kanagawa, Japan)

PEM08-28 Room:411 Time:May 2 16:10-16:30

The Impacts of Space Weather on Society and the Economy

BAKER, Daniel N.[1*]

[1]University of Colorado Boulder

This presentation describes possible extreme space weather impacts and their economic and societal costs. Modern society depends heavily on a variety of technologies that are vulnerable to the effects of intense geomagnetic storms and solar energetic particle (SEP) events. Strong currents flowing in the ionosphere can disrupt and damage Earth-based electric power grids and contribute to the accelerated corrosion of oil and gas pipelines. Magnetic storm-driven ionospheric disturbances interfere with high-frequency radio communications and navigation signals from Global Positioning System (GPS) satellites. Exposure of spacecraft to solar particles and radiation belt enhancements can cause temporary operational anomalies, damage critical electronics, degrade solar arrays, and blind optical systems such as imagers and star trackers. Moreover, intense SEP events present a significant radiation hazard for astronauts during the high-latitude segment of the International Space Station (ISS) orbit as well as for future human explorers of the Moon and Mars. In addition to such direct effects as spacecraft anomalies or power grid outages, a thorough assessment of the impact of severe space weather events on present-day society must include the collateral effects of space-weather-driven technology failures. For example, polar cap absorption events due to solar particles can degrade — and, during severe events, completely black out — radio communications along transpolar aviation routes, requiring aircraft flying these routes to be diverted to lower latitudes. This can add considerable cost to the airlines and can greatly inconvenience passengers. Modern technological society is characterized by a complex set of interdependencies among its critical infrastructures. A complete picture of the socioeconomic impact of severe space weather must include both direct as well as collateral effects of space-weather-driven technology failures on dependent infrastructures and services.

Keywords: Space weather, Electric power grids, Radiation hazards, Infrastructure interdependencies, Socioeconomic impact of severe space weather

Japan Geoscience Union Meeting 2014
(28 April - 02 May 2014 at Pacifico YOKOHAMA, Kanagawa, Japan)

PEM08-29 Room:411 Time:May 2 16:30-16:45

GEMSIS-Sun Numerical Model of Sun-Earth System (SUSANOO): Application for Extremely Strong IMF CMEs

SHIOTA, Daikou[1*] ; KATAOKA, Ryuho[2] ; MIYOSHI, Yoshizumi[1] ; KUSANO, Kanya[1]

[1]STEL, Nagoya University, [2]National Institute of Polar Research

Solar wind including coronal mass ejections (CMEs) is a main driver of various space weather disturbances. MHD modeling of the solar wind is a powerful tool to understand the solar-terrestrial environment and to forecast space weather accurately. Recently, we developed an MHD model of the inner heliosphere on the basis of minimal input, namely, time series of daily synoptic observation of the photospheric magnetic field. The time series of MHD parameters at the Earth position is passed to a radiation belt model [Miyoshi et al. 2004] for forecasting of the radiation belt energetic electron flux. These programs are executed everyday on a server in STEL, Nagoya University and the results are uploaded on the web site (http://st4a.stelab.nagoya-u.ac.jp/susanoo/). This system is named as Space-weather-forecast-Usable System Anchored by Numerical Operations and Observations (SUSANOO).

Carrington event that occurred in September 1859 is the most violent solar storm in the human records. Since the magnetic storm associated with the event influenced globally, aurora was observed in wide area in the world. The magnetic response recorded in Bombay shows a rapid decrease of -1600 nT / h (Tsurutani et al. 2003). The induced electric field to explain the rapid decrease in the ground level is estimated to be 355 mV/m associated with a magnetic cloud influence. The time lag between onsets of solar flare and sudden commencement is 17.5 hours, and therefore shock propagation speed is estimated as 2380 km/s. The magnetic field strength in the associated magnetic cloud is needed to be 150nT. However, it is not clear how such a strong magnetic field can be kept while the strength of ordinary interplanetary magnetic field (IMF) is the order of 10 nT at 1 au.

In order to examine which condition of coronal mass ejections (CMEs) associated with an extreme event such as the Carrington event should be satisfied, we modeled a series of CMEs with the inner heliosphere MHD simulation (used in SUSANOO). In the model, multiple CMEs are injected as a twisted magnetic flux rope accompanying with a velocity pulse through the inner boundary of the simulation and propagate into the solar winds. Because there is almost no information associated with the Carrington event and the solar wind, instead, we used observational data of CMEs associated recent large-scale active regions: NOAA 10486 in October to November 2003 (Halloween event) and NOAA 11520 in July 2012 (far side STEREO event, Russell et al. 2013). Only fast (V $>\tilde{}$1000 km/s) and wide (angular width $>$60 degree) CME data are extracted from LASCO CME catalog (http://cdaw.gsfc.nasa.gov/CME_list/). As a result, the strength of compressed magnetic field becomes as high as about four times of background IMF when a CME interacts with the background solar wind. However, successive CMEs interact with each other to form much stronger magnetic filed due to compression of the magnetic cloud of the preceding CME by shock associated the following CME.

Keywords: MHD, coronal mass ejection, solar wind, IMF, geomagnetic storm, radiation belt

Japan Geoscience Union Meeting 2014
(28 April - 02 May 2014 at Pacifico YOKOHAMA, Kanagawa, Japan)

PEM08-30 Room:411 Time:May 2 16:45-17:00

Discovery of Two Sun-like Superflare Stars Rotating as Slow as the Sun

NOGAMI, Daisaku[1*] ; NOTSU, Yuta[1] ; HONDA, Satoshi[2] ; MAEHARA, Hiroyuki[3] ; NOTSU, Shota[1] ; SHIBAYAMA, Takuya[1] ; SHIBATA, Kazunari[1]

[1]Kyoto University, [2]University of Hyogo, [3]The University of Tokyo

We report on the results of high dispersion spectroscopy of two ‘superflare stars’, KIC 9766237, and KIC 9944137 with Subaru/HDS. Superflare stars are G-type main sequence stars, but show gigantic flares compared to the Sun, which have been recently discovered in the data obtained with the Kepler spacecraft. Though most of these stars are thought to have a rotation period shorter than 10 days on the basis of photometric variabilities, the two targets of the present paper are estimated to have a rotation period of 21.8 d, and 25.3 d. Our spectroscopic results clarified that these stars have stellar parameters similar to those of the Sun in terms of the effective temperature, surface gravity, and metallicity. The projected rotational velocities derived by us are consistent with the photometric rotation period, indicating a fairy high inclination angle. The average strength of the magnetic field on the surface of these stars are estimated to be 1-20 G, by using the absorption line of Ca II 8542. We could not detect any hint of binary in our spectra, although more data are needed to firmly rule out the presence of an unseen low-mass companion. These results claim that the spectroscopic properties of these superflare stars are very close to those of the Sun, and support the hypothesis that the Sun might cause a superflare.

Keywords: Sun-like stars, superflares, high dispersion spectroscopy

Japan Geoscience Union Meeting 2014
(28 April - 02 May 2014 at Pacifico YOKOHAMA, Kanagawa, Japan)

PEM08-P01 Room:Poster Time:May 2 16:15-17:30

Cosmic-ray exposure Space weather information during aircraft operation

AKUTSU, Retsu[1*] ; ASADA, Kazuaki[1]

[1]Airline Pilots' Association of Japan

Effects of exposure to cosmic-ray during aircraft operation are divided into exposure of aircrew and operational impact.

International Commision on Radiological Protection (ICRP) issued a recommendation to include occupational exposure of aircrew with a jet operated exposure from natural radiation source in 1990. Radiation Council consists of the Ministry of Education, Culture, Sports, Science and Technology, the Ministry of Health, Labour and Welfare, the Ministry of Land, Infrastructure, Transport and Tourism establised Guidelines for management of aircrew exposure to cosmic radiation in 2006. In response to this, airlines keep record of assessed doses on each aircrew using Japanese Internet System for Calculation of Aviation Route Doses (JISCARD-EX) developed by National Institute of Radiological Sciences (NIRS).

Impacts of space weather on aircraft operations can be classified into communications and navigations.

For communicaton, it includes difficulties on HF radio due to Dellinger Phenomenon while flying out of range of VHF coverages as international flight. And also includes difficulties on SATCOM voice communication and Controller Pilot Data Link Communication (CPDLC) in oceanic region.

Modern navigation by Global Navigation Satellite System (GNSS) is becoming mainstream. GNSS are used all phase of aircraft operation during on the ground, depareture, en-route, and approach. Future of operations aim high category precision approach using automatic approach and landing by GNSS even extremely low visibility until stop on runway. Cosmic-ray re-write the data in memory known as soft error on electronic equipment onboard aircrafts.

Use of SpaceWeather forecast, how to provide the information to aircrew and how to make decisions are urgent consideration.

For these problems International Airways VolcanoWatch Operations Group (IAWOPSG) which one of operations group of International Civil Aviation Organization (ICAO) is making draft Concept of Operations (ConOps) for international space weather information in support of international air navigation. Adoption of ConOps is targeted for ICAO/WMO divisional meeting in 2014.

Japan Geoscience Union Meeting 2014
(28 April - 02 May 2014 at Pacifico YOKOHAMA, Kanagawa, Japan)

PEM08-P02 Room:Poster Time:May 2 16:15-17:30

Rdiation exposure management for astronauts

MATSUMURA, Chiemi[1*] ; SATO, Masaru[1] ; KANEKO, Yuki[1] ; OGATA, Katsuhiko[1]

[1]JAXA

On the International Space Station (ISS), a habitable artificial satellite that orbits the Earth at an altitude of about 400 km, astronauts receive space radiation exposure 0.5-1.0mSv in one day which is equivalent to what humans on the Earth receive in six months.

The Japan Aerospace Exploration Agency (JAXA) employs radiation exposure management for JAXA astronauts to minimize the health damage caused by space radiation exposure.

Because of we must take action at space environment anomaly, the space environment monitoring and space weather is important information.

In this report, we introduce space radiation exposure management by JAXA.

Keywords: Astronaut, Space radiation exposure

Japan Geoscience Union Meeting 2014
(28 April - 02 May 2014 at Pacifico YOKOHAMA, Kanagawa, Japan)

PEM08-P03 Room:Poster Time:May 2 16:15-17:30

On a new antenna system for reception of real-time solar wind data

WATARI, Shinichi[1*] ; KUBO, Yuki[1] ; ISHII, Mamoru[1]

[1]National Institute of Information and Communications Technology

In-situ solar wind data are important for space weather to estimate effects of solar wind disturbances on magnetosphere and ionosphere of the Earth and investigate their solar sources. Since 1997, National Institute of Information and Communications Technology (NICT) contributes reception of real-time solar wind data from Advanced Composition Explorer (ACE), which observes solar wind at L1 point, for 24-hour data coverage. Deep Space Climate Observatory (DSCOVR) following on mission of ACE is plan to be launched in the end of 2014. NICT renews the antenna system, which enables to receive real-time data from DSCOVR. We will report on details of the new antenna system completed in March, 2014 and our application of real-time solar wind data in the presentation.

Keywords: solar wind, space weather, L1, ACE, DSCOVR

Japan Geoscience Union Meeting 2014
(28 April - 02 May 2014 at Pacifico YOKOHAMA, Kanagawa, Japan)

PEM08-P04 Room:Poster Time:May 2 16:15-17:30

Solar cell degradation of Akebono satellite due to space radiation and effect of temperature variation

MIYAKE, Wataru[1*] ; MIYOSHI, Yoshizumi[2] ; MATSUOKA, Ayako[3]

[1]Tokai University, [2]Solar Terrestrial Environment Laboratory, Nagoya University, [3]Institute of Space and Astronautical Science

Solar cells on any satellite degrade gradually due to severe space radiation environment. We have analyzed the degradation of the solar cells of the Akebono satellite, and found a fair correlation between the decrease rate of the solar cell output current and the trapped proton flux between 1989 and 1996. The previous studies demonstrated that we can deduce information of proton radiation belt from degradation of solar cells of the Akebono satellite. The relationship cannot be discernible after 1996. The previous studies suggested more prominent temperature effect in the later years because of progress of the degradation. In order to expand studies by using solar cells as a radiation monitor, we must separate exactly the contribution of temperature and of proton radiation. Since the sensor for solar cell temperature failed in 1991 and no temperature is available after 1991, we try to model the temperature variation at solar cells from the temperature of other surface parts. Once we establish the method, we correlate the temperature with solar cell output current and deduce the contribution of proton radiation.

Keywords: Akebono satellite, proton radiation belt

Japan Geoscience Union Meeting 2014
(28 April - 02 May 2014 at Pacifico YOKOHAMA, Kanagawa, Japan)

PEM08-P05 Room:Poster Time:May 2 16:15-17:30

Development of space weather prediction algorithm using big data analysis

HADA MURANUSHI, Yuko[1*] ; MURANUSHI, Takayuki[1] ; SHIBAYAMA, Takuya[1] ; ISOBE, Hiroaki[1] ; NEMOTO, Shigeru[2] ; SHIBATA, Kazunari[1]

[1]Kyoto University, [2]BroadBand Tower, Inc.

To predict and forecast the occurrence of solar flares and coronal mass ejections automatically without human power is one of the major goals in the space weather forecast research. Many studies have been performed in space weather prediction until today; For example, there are heuristics studies from the correlation of flares and the physical quantity being observed from the shape of the each sunspot. We always have required human power in such studies.

In recent years, the accuracy of the satellite and observation equipment has been increasing with the development of technology. Given that observation data is fast increasing, it is difficult for us to directly survey all data. On the other hand, big data analysis has developed rapidly in the field of information processing technology; Methods of machine learning and processing of unstructured large amounts of data by the parallel/distributed processing have been widely adopted in various fields of science. Therefore, we began to research fully automated flare prediction methods, in aim to utilize entire exhaustively large amount of data available for space weather forecast research. We set our goal to predict the X-ray flux with GOES satellites (Geostationary Operational Environmental Satellite.) More specifically, our goal is to predict the maximum of the X-ray flux from the present to 24 hours in the future.

First, we tried to predict GOES X-ray flux from past data of GOES X-ray flux and magnetic field data (Helioseismic and Magnetic Imager HMI) with SDO (Solar Dynamics Observatory), then evaluated the flare prediction accuracy using HSS (Heidke Skill Score) and TSS (True Skill Statistic) (see figure). Next, we added the extreme ultraviolet data observed with SDO/AIA (Atmospheric Imaging Assembly, wavelength: 193$\mathring{A}$) to the original dataset that consists of HMI and GOES data, and evaluated the flare prediction accuracy in the same way.

The reason for adding the AIA data is twofold. First, flare prediction studies using extreme ultraviolet full-disk image data with SOHO (Solar and Heliospheric Observatory) have revealed that we can construct a good indicator of flare activity of active regions by integrating over only pixels brighter than certain threshold in extreme ultraviolet images (threshold integral). Second, we expected to improve prediction accuracy by adding the AIA data, because magnetic field data cannot capture precursory phenomena of flare occurring in the rim of the sun, while AIA data can.

By our comparison study we found that adding full-disk integral of the AIA images to the data set improve the prediction accuracy, particularly that of X- class flares. In this presentation, we will try flare prediction based on the data set with additional features obtained by preprocessing AIA images, such as the threshold integral values, and report the results. This study is a joint research program with BroadBand Tower, Inc.

Keywords: Space weather, Solar flare, Active region, SDO/AIA, SDO/HMI, GOES

		GOES+MHI	AIA+GOES+MHI
X class Flare	HSS*1	0.209	0.215
	TSS*2	0.551	0.581
M class flare	HSS	0.439	0.402
	TSS	0.500	0.470
C class flare	HSS	0.521	0.542
	TSS	0.627	0.605

*1HSS=Heidke Skill Score

*2TSS=True Skill Statistic

Japan Geoscience Union Meeting 2014
(28 April - 02 May 2014 at Pacifico YOKOHAMA, Kanagawa, Japan)

PEM08-P06 Room:Poster Time:May 2 16:15-17:30

Statistical study on generating factors of white light solar flares

KITAGAWA, Jun[1*] ; MASUDA, Satoshi[1] ; WATANABE, Kyoko[2]

[1]STEL. Nagoya University, [2]JAXA/ISAS

'White Light Flare' is a flare with enhancement of visible continuum and is mainly associated with energetic flares like GOES X-class flares. But it could not be always observed in energetic flares and recently it is observed in relatively weak flares like GOES C-class flares (Matthews et al. 2003; Hudson et al. 2006). Its occurring mechanism has not been well understood yet and hence a key question remains; "What is needed to enhance white light emission in solar flares?"

In this study, we chose 37 events observed with Hinode/SOT and RHESSI among M- and X-class flares from January 2011 to August 2013. Out of the 37 events, Using running difference images of SOT three continuum bands (red, green, blue), we identified 13 White Light (WL) events. Remaining 24 events are classified into No White Light (NWL) events. We compare these two groups in several parameters (e.g., duration, distance between flare ribbons, and so forth) to find a generating factor of White Light event.

We found the following characteristics of WL events. (1) Most of WL events show a short duration within 20 minutes in GOES soft X-rays. (2) WL events show high (>15MK) temperature and relatively low emission measure at the peak of GOES soft X-rays. (3) The distance between two ribbons in WL events is short as 10arcsec. (4) Assuming the thick-target model, the mean dissipation rate of non-thermal energy in WL events is larger than that of NWL events. (5) WL events do not tend to coincide with CME comparing to NWL. These results indicate that precipitation of large amount of accelerated electrons into a compact area within a short time plays a key role to generate a WL event.

Keywords: solar flare, white light, hinode

Japan Geoscience Union Meeting 2014
(28 April - 02 May 2014 at Pacifico YOKOHAMA, Kanagawa, Japan)

PEM08-P07 Room:Poster Time:May 2 16:15-17:30

Influence of solar wind and ozone on the temperatures of the troposphere and stratosphere

YAMASHITA, Kazuyoshi[1*]

[1]YOKOHAMA National University

The correlation between global atmosphere and solar magnetic activity is evident though the cause is not clear. In this presentation, we analyze the influence that solar wind and ozone give to the global atmosphere to examine the cause on the basis of the previous observations [1].

The AE and Dst index data were used to detect the influence of the solar wind on the total ozone and the air temperature change of the troposphere and stratosphere.

In the analysis, the following factors were taken into account: 1)EPP-NOx effects on ozone at low latitudes may be comparable to the effects of solar UV radiation [Callis et al., 2000, 2001; Langematz et al., 2005; Rozanov et al., 2005]. 2) Since the ozone generated at low latitude is conveyed to the pole aria of the winter hemisphere, EPP-NOx has affected the ozone reduction of the pole area.

Thus, changes in the stratospheric ozone due to the influence of the solar wind appears to affect the climate of the troposphere.

References
[1]K.Itoh,JpGU 2008-2013

Keywords: troposphere, stratosphere, temperature, ozone, solar wind, geomagnetic activity

Japan Geoscience Union Meeting 2014
(28 April - 02 May 2014 at Pacifico YOKOHAMA, Kanagawa, Japan)

PEM08-P08 Room:Poster Time:May 2 16:15-17:30

On the influence of the luni-solar oscillation on the climate

ITOH, Kiminori[1*] ; AI, Yang[1] ; KAWANO, Shoh[1]

[1]Yokohama National University, Graduate School of Env. & Inf. Sciences

We have demonstrated a close relation between solar wind and regional temperatures, and suggested the participation of the Arctic oscillation. On the other hand, a link between the luni-solar oscillation and the Arctic oscillation has also been suggested [1]. Thus, both the sun and the moon appear to be important climatic factors to consider.

An interesting mechanism was proposed recently for the luni-solar oscillation cycle associated with the population change of the snowshoe hare in Canada [2]; that is, the position of the moon changes the intensity of the ionizing cosmic ray to induce changes in the activity of plants, which results in the changes in the forage quality.

This mechanism suggests a combination between the influences of the sun and the moon on the climate while their mutual independence is also possible. Thus, we try to examine the possible contribution of the luni-solar oscillation for establishing the effect of the solar wind on the climate.

1) Renato Ramos da Silva and Roni Avissar, The impacts of the Luni-Solar oscillation on the Arctic oscillation, Geophys. Res. Lett., VOL. 32, L22703 (2005)

2) Vidar Selås, Linking ’10-year’ herbivore cycles to the lunisolar oscillation: the cosmic ray hypothesis, Oikos, Volume 123, 194?202 (2014)

Keywords: Luni-solar oscillation, Arctic oscillation, Solar wind, Climate

Japan Geoscience Union Meeting 2014
(28 April - 02 May 2014 at Pacifico YOKOHAMA, Kanagawa, Japan)

PEM09-01 Room:211 Time:April 28 09:00-09:15

VarSITI - Variability of the Sun and Its Terrestrial Impact

SHIOKAWA, Kazuo[1*] ; GEORGIEVA, Katya[2]

[1]Solar-Terrestrial Environment Laboratory, Nagoya University, [2]Space Research and Technologies Institute, Bulgarian Academy of Sciences

The Scientific Committee on Solar Terrestrial Physics (SCOSTEP) is an interdisciplinary body of the International Council for Science (ICSU) to run international interdisciplinary scientific programs and promotes solar-terrestrial physics research. The last solar minimum in 2008-2009 and the current solar maximum of sunspot cycle 24 show much lower activities compared with the previous two solar cycles 22 and 23. The scientists in the solar-terrestrial physics are watching very low solar activities and their consequences on Earth, which have never been observed since modern scientific measurements become available. The SCOSTEP program "Variability of the Sun and Its Terrestrial Impact (VarSITI)" (2014-2018) will focus on this particular low solar activity and their consequences on Earth, for various times scales from the order of thousands years to milliseconds, and for various locations and their connections from the solar interior to the Earth's atmosphere. In order to elucidate various sun-earth connections, we encourage communication between solar scientists (solar interior, sun, and the heliosphere) and geospace scientists (magnetosphere, ionosphere, and atmosphere). Campaign observations will be promoted for particular interval in collaboration with relevant satellite and ground-based missions as well as modeling efforts. Four scientific projects will be carried out in VarSITI as (1) Solar Evolution and Extrema (SEE), (2) International Study of Earth-Affecting Solar Transients (ISEST/Minimax24), (3) Specification and Prediction of the Coupled Inner-Magnetospheric Environment (SPeCIMEN), and (4) Role Of the Sun and the Middle atmosphere/thermosphere/ionosphere In Climate (ROSMIC).

Keywords: VarSITI, solar activity, climate change, magnetosphere, ionosphere, atmosphere

Japan Geoscience Union Meeting 2014
(28 April - 02 May 2014 at Pacifico YOKOHAMA, Kanagawa, Japan)

PEM09-02 Room:211 Time:April 28 09:15-09:30

Specification and Prediction of the Coupled Inner-Magnetospheric Environment (SPeCIMEN)

MIYOSHI, Yoshizumi[1*] ; OMURA, Yoshiharu[2] ; KATOH, Yuto[3] ; JACOB, Bortnik[4] ; CRAIG, Rodger[5]

[1]Solar-Terrestrial Environment Laboratory, Nagoya University, [2]RISH, Kyoto University, [3]Graduate School of Science, Tohoku University, [4]UCLA, US, [5]University of Otago, NZ

Specification and Prediction of the Coupled Inner-Magnetospheric Environment (SPeCIMEN) is a focus group of next SCOSTEP project: VarSITI. The goals and objectives are the quantitative prediction and specification of the Earth inner magnetospheric environment based on Sun/solar wind driving inputs. Our question is how the inner magnetosphere responds as a coupled system to Sun/solar-wind driving, which will be solved by a combination of physical and statistical modeling, theory and observations from various platforms under this project. The satellite missions such as NASA/Van Allen Probes (US), JAXA/ERG (Japan) and ground-based network observations provide a comprehensive picture on the dynamical evolutions of geospace and reveal processes and consequences of the inner magnetosphere. Anticipated outcome should be a series of coupled, related models that quantitatively predict the dynamical evolution of the inner magnetospheric state including radiation belts, ring current, plasmasphere, plasma sheet. In this presentation, we give an overview of the SpeCIMEN project and the strategy of the project to gain the science output.

Keywords: future mission, inner magnetosphere

Japan Geoscience Union Meeting 2014
(28 April - 02 May 2014 at Pacifico YOKOHAMA, Kanagawa, Japan)

PEM09-03 Room:211 Time:April 28 09:30-09:45

Geotail observation of magnetic reconnection

NAGAI, Tsugunobu[1*] ; SHINOHARA, Iku[2]

[1]Tokyo Institute of Technology, [2]Institute of Space and Astronautical Science/JAXA

The spacecraft Geotail was launched on July 24, 1992. The main objective of the Geotail mission is to explore magnetic reconnection with in situ observations, and the Geotail mission has revealed various physical processes of magnetic reconnection. The ion-electron decoupling region where electron outflow speed differs from ion outflow speed is formed in the magnetic reconnection site. Ion and electron dynamics in the ion-electron decoupling region is derived with magnetic field and plasma observations by the spacecraft Geotail in near-Earth magnetotail magnetic reconnection. The ion-electron decoupling region has a spatial extent of approximately 11 ion inertial length along the GSM x direction, and the dawn-dusk current sheet with main current carriers of electrons exists over this region. An intense electron current layer with a spatial extent of 0.5?1 ion inertial length occupies in its center around the X line. High-speed electron outflow jets are formed just outside the central intense electron current layer. They are decelerated and become non-jet outflows with speed slightly higher than ion outflow speed. Electrons have flattop distribution functions indicating heating and acceleration in both the outflow jets and the non-jet outflows; however, heating and acceleration are weak in the central intense current layer. Inflowing ions enter the central intense electron current layer, and these ions are accelerated up to 10 keV inside the electron outflow jet regions. Ion acceleration beyond 10 keV and thermalization operate mostly in the non-jet electron outflow regions. Electrons show thermal distributions without any heating/acceleration signatures immediately beyond the edge of the ion-electron decoupling region, while higher-energy ions pervade even beyond the edge and hot MHD plasma flows are produced.

Keywords: magnetic reconnection, space plasma, substorm, magnetotail

Japan Geoscience Union Meeting 2014
(28 April - 02 May 2014 at Pacifico YOKOHAMA, Kanagawa, Japan)

PEM09-04 Room:211 Time:April 28 09:45-10:00

Global dynamics of the inner magnetosphere derived from long term observation by Akebono

KASAHARA, Yoshiya[1*] ; MATSUOKA, Ayako[2] ; NAGAI, Tsugunobu[3] ; KUMAMOTO, Atsushi[4] ; ABE, Takumi[2]

[1]Kanazawa University, [2]JAXA/ISAS, [3]Tokyo Inst. Tech., [4]Tohoku Univ.

Akebono is a Japanese scientific spacecraft which was launched in February, 1989 for observations of the Earth's magnetosphere, and has been operated successfully for 25 years. The regular data acquisition of MGF, PWS, VLF, TED, and RDM is still continued at stations in Japan and Sweden. The operation of the Akebono will be extended until March, 2015 (FY2014) in order to realize collaborative measurements with the Van Allen Probes, and further extension to the end of FY2016 is expected as an optional mission. Because of its unique orbit, the stored data is quite valuable for studying plasma physics in the auroral region as well as the radiation belt. In the present paper, we introduce important achievements of Akebono observation and discuss future science to be obtained from the long term observation data.

Keywords: Akebono, Inner Magnetosphere, Radiation belt, Aurora, Plasma wave

Japan Geoscience Union Meeting 2014
(28 April - 02 May 2014 at Pacifico YOKOHAMA, Kanagawa, Japan)

PEM09-05 Room:211 Time:April 28 10:00-10:15

ERG Science Center

KEIKA, Kunihiro[1*] ; MIYOSHI, Yoshizumi[1] ; SEKI, Kanako[1] ; HORI, Tomoaki[1] ; MIYASHITA, Yukinaga[1] ; SHOJI, Masafumi[1] ; SEGAWA, Tomonori[1] ; SHINOHARA, Iku[2] ; TAKASHIMA, Takeshi[2] ; TANAKA, Yoshimasa[3] ; ERG, Science center team[4]

[1]Solar-Terrestrial Environment Laboratory, Nagoya University, [2]Institute of Space and Astronautical Science, Japan Aerospace Exploration Agency, [3]National Institute of Polar Research, [4]ERG Science Center Team

ERG (Exploration of energization and Radiation in Geospace) is a Japanese geospace exploration project, and the ERG satellite will be launched in Japanese FY 2015. The project consists of the satellite observation team, the ground-based network observation team, and the integrated data analysis/simulation team. Besides these research teams, the ERG Science Center has been organized to promote close collaborations of these teams and thereby maximize scientific output. For studies of geospace, where different plasma populations are dynamically coupled with one another via cross-energy and cross-regional couplings, the environment for integrated data analysis is critical for comprehensive understanding using various kinds of data sets including data from physics-based models developed by the GEMSIS (Geospace Environment Modeling System for Integrated Studies) project of the Solar-Terrestrial Environment Laboratory, Nagoya University.

A standard data format and integrated data analysis tools are essential to realize the seamless data analysis environment. The ERG project data after Level-2 will be open to the public in the NASA CDF format. The integrated data analysis tool is developed as a plug-in tool of SPEDAS (Space Physics Environment Data Analysis System) in collaboration with the THEMIS (Time History of Events and Macroscale Interactions during Substorms) and IUGONET (Inter-university Upper atmosphere Global Observation NETwork) teams. It should be noted that other project data, such as THEMIS and Van Allen Probes, can be easily analyzed with SPEDAS if the data are converted to the CDF format. Thus the integrated data analysis using many kinds of data is truly realized through SPEDAS. Other useful tools in the web browser have been developed by the science center: ERGWAT (ERG Web Analysis Tool) is an interactive visualization tool, and CEF (Conjunction Event Finder) is a web-based tool enabling users to easily find conjunctions between satellites and ground-based observations. These tools will contribute to a part of the capacity building activity of the SPeCIMEN (Specification and Prediction of the Coupled Inner-Magnetospheric Environment) project carried out under the VarSITI (Variability of the Sun and Its Terrestrial Impact) program for 2014-2018.

Keywords: ERG, GEMSIS, IUGONET, Integrated analysis tool, SPEDAS, SPeCIMEN

Japan Geoscience Union Meeting 2014
(28 April - 02 May 2014 at Pacifico YOKOHAMA, Kanagawa, Japan)

PEM09-06 Room:211 Time:April 28 10:15-10:30

ICSWSE/MAGDAS Research Projects During the VarSITI Program Interval

KAWANO, Hideaki[1*] ; YOSHIKAWA, Akimasa[1] ; ABE, Shuji[1] ; UOZUMI, Teiji[1] ; CARDINAL, Maria gracita[1] ; MAEDA, George[1] ; YUMOTO, Kiyohumi[1] ; MAGDAS/CPMN, Group[1]

[1]International Center for Space Weather Science and Education

International Center for Space Weather Science and Education (ICSWSE) has developed a real time magnetic data acquisition system (the MAGDAS project) to monitor the space environment around the world. The number of observational sites is increasing every year in collaboration with MAGDAS host countries. Up to now, the MAGDAS Project has installed 73 real time magnetometers: It is the largest magnetometer array in the world. Using data from this global network, we are developing many research projects. In this talk, we introduce our research projects planned during the VarSITI program interval, as follows:

(1) Global electromagnetic coupling from polar to equatorial ionosphere
(2) Vertical coupling among the atmosphere, the ionosphere and the magnetosphere
(3) Plasmaspheric diagnosis using the Field line resonance
(4) Magnetospheric diagnosis using geomagnetic disturbances
(5) Monitoring of Space weather phenomena using solar and magnetospheric indices
(6) Modeling of Space weather parameters
(7) Sun-atmosphere coupling

Keywords: VarSITI, MAGDAS, CPMN

Japan Geoscience Union Meeting 2014
(28 April - 02 May 2014 at Pacifico YOKOHAMA, Kanagawa, Japan)

PEM09-07 Room:211 Time:April 28 10:30-10:45

Energetic electron precipitation during magnetic storm and substorm: Subionospheric VLF/LF observation

TSUCHIYA, Fuminori[1*] ; OBARA, Takahiro[1] ; MORIOKA, Akira[1] ; MISAWA, Hiroaki[1] ; YAGI, Manabu[1] ; MIYOSHI, Yoshizumi[2] ; SHIOKAWA, Kazuo[2] ; OGAWA, Yasunobu[3] ; CONNORS, Martin[4]

[1]Tohoku University, [2]Solar-Terrestrial Environment Laboratory, Nagoya University, [3]National Institute of Polar Research, [4]Athabasca University

Subionospheric VLF/LF radio observation is useful probe to investigate precipitation of high-energy (>100keV) electrons into the atmosphere and the observation at Ny-Alsound, Norway (NAL) and Athabasca, Canada (ATH) are used to detect energetic electron precipitation in auroral and sub-auroral regions during storm and substorm. At the NAL station, radio signals which are transmitted in mid-latitude and propagate across the auroral and sub-auroral regions are recorded. During magnetic storms, the strong phase variation associated with the substorm induced electron precipitation has been detected and the phase change quantitatively corresponds to the precipitating energetic electron flux observed by the NOAA/POES satellites over the radio propagation path. Onsets of the phase change were delayed by ten to several tens of minutes from the substorm onset in the morning and noon sectors, which is consistent with the drift time of energetic electrons with energy of ˜100 keV. On the other hand, the phase change in the dusk sector occurred shortly after the substorm onset and is often accompanied by Pc1 or Pi1B observed on the ground station near the radio path. These results show that the energetic electron precipitation is strongly connected with the dynamics of energetic ions and electrons and wave generations in the inner magnetosphere. The ATH station is located in the subautoral region and subionospheric signals from lower latitude are measured. The phase fluctuations with time scales of Pc5 or longer period were sometimes found during main and early recovery phases of magnetic storms. The phase fluctuations found on 5 June 2011 show good correlation with the GOES magnetic field data, suggesting Pc5 modulation of either electron injection or precipitation rates. Subionospheric radio observation provides opportunities to investigate various kinds of energetic electron precipitation processes. Part of observed data is provided through the IUGONET metadata database.

Japan Geoscience Union Meeting 2014
(28 April - 02 May 2014 at Pacifico YOKOHAMA, Kanagawa, Japan)

PEM09-08 Room:211 Time:April 28 11:00-11:15

A longitudinal network of VLF/ELF antennas and induction magnetometers at subauroral latitudes - Contribution to VarSITI

SHIOKAWA, Kazuo[1*] ; MIYOSHI, Yoshizumi[1] ; OZAKI, Mitsunori[2] ; NAGATSUMA, Tsutomu[3] ; ISHII, Mamoru[3] ; CONNORS, Martin[4] ; PODDELSKY, Igor[5] ; SHEVTSOV, Boris[5]

[1]Solar-Terrestrial Environment Laboratory, Nagoya University, [2]Kanazawa University, [3]National Institute of Information and Communications Technology, [4]Athabasca University, [5]Institute of Cosmophysical Research and Radiowave Propagation (IKIR), FEB RAS

We report observations of VLF/ELF chorus waves (~kHz) using loop antennas and Pc1 waves (~Hz) using induction magnetometers at longitudinally-distributed stations at subauroral latitudes. Continuous measurements of VLF waves with a sampling rate of 100 kHz have been made since September 2012 to monitor daily variations of chorus waves and their detailed structures at Athabasca (54.72N, 246.69E, MLAT=61.3). We observe various chorus emissions, such as quasi-periodic (Q-P) emissions, patchy burst emissions, rising and falling tone emissions at Athabasca. New loop antennas will be installed at Fredericton in the east-coast of Canada and at Zhigansk in the east-Siberia in Russia in 2014-2015. The induction magnetometer chain observes Pc1 geomagnetic pulsation which corresponds to electromagnetic ion cyclotron (EMIC) waves in the inner magnetosphere. The magnetometers have deployed in Athabasca, Magadan and Paratunka in far-eastern Russia, Moshiri and Sata in Japan, and will be deployed at Fredericton in the east-coast of Canada in 2014. These chorus waves and EMIC waves are known to contribute to the acceleration and loss of radiation belt particles. The longitudinal network of these measurements will provide continuous monitor of global distribution of the occurrence of these waves. These observations will contribute the next SCOSTEP program VarSITI, particularly to the SPeCIMEN Project.

Keywords: chorus wave, EMIC wave, Pc1 geomagnetic pulsations, ground-based multi-point observation, subauroral latitudes

Japan Geoscience Union Meeting 2014
(28 April - 02 May 2014 at Pacifico YOKOHAMA, Kanagawa, Japan)

PEM09-09 Room:211 Time:April 28 11:15-11:30

Solar Evolution and Extrema (SEE) under VarSITI Scientific Program

SAKAO, Taro[1*] ; SUZUKI, Takeru[2] ; KUSANO, Kanya[2] ; MARTENS, Petrus C.[3] ; NANDI, Dibyendu[4] ; OBRIDKO, Vladimir N.[5] ; SHIOKAWA, Kazuo[2] ; GEORIEVA, Katya[6]

[1]ISAS/JAXA, [2]Nagoya University, [3]CfA-Harvard, USA, [4]Indian Institute of Science Education and Research, India, [5]IZMIRAN, Russia, [6]SRTI, Bulgaria

Following the recent unsual solar activities, the next SCOSTEP international scientific program 'Variability of the Sun and Its Terrestrial Impact (VarSITI)' was launched as a 5 years program covering 2014-2018. It will focus on the the unusual solar activities and their consequences on Earth, for various times scales from the order of thousands years to milliseconds, and for various locations and their connections from the solar interior to the Earth's atmosphere.

The program consists of four elements:

(1) Solar Evolution and Extrema (SEE), (2) International Study of Earth-Affecting Solar Transients (ISEST/Minimax24), (3) Specification and Prediction of the Coupled Inner-Magnetospheric Environment (SPeCIMEN), and (4) Role Of the Sun and the Middle atmosphere/thermosphere/ionosphere In Climate (ROSMIC).

Among these elements, SEE will address, by promoting coordination of various projects between the Sun and the Earth, the following scientific questions:

(a) Are we at the verge of a new grand minimum? If not, what is the expectation for cycle 25? (b) Does our current best understanding of the evolution of solar irradiance and mass loss resolve the "Faint Young Sun" problem? What are the alternative solutions? (c) What is the largest solar eruption/flare possible? What is the expectation for periods with absence of activity?

An overview of SEE element will be presented.

Keywords: VarSITI Program, SEE Element, SCOSTEP, solar evolution, extreme solar events

Japan Geoscience Union Meeting 2014
(28 April - 02 May 2014 at Pacifico YOKOHAMA, Kanagawa, Japan)

PEM09-10 Room:211 Time:April 28 11:30-11:45

Solar Magnetic Activity and Their Influence on the Earth's Environment

SAKURAI, Takashi[1*]

[1]National Astronomical Observatory of Japan

The Sun affects the environment of the Earth in diverse ways. In a time scale of a few days, XUV emission and energetic particles from solar flares and disturbances in the solar wind (coronal mass ejections) cause various phenomena in the ionosphere and the magnetosphere. In a time scale of 2-4 weeks, the rotation of the Sun modulates its irradiance and solar wind properties. In a time scale of 11-year solar cycle, total and spectral irradiance changes in phase with the sunspot number. In this presentation I will pick up new results obtained with the Hinode mission and other ground-based instruments.

Hinode, launched on 23 September 2006, is a Japan-US-UK joint mission with contributions for downlink connections from ESA. The three primary instruments on Hinode are

(1) solar optical telescope/magnetograph (SOT),

(2) soft X-ray telescope (XRT), and

(3) extreme ultraviolet imaging spectrometer (EIS).

Ulysses spacecraft showed in 1998 that fast and steady solar wind comes from polar regions, and slow and variable solar wind comes from low-latitude regions. Since low-latitude regions are basically characterized by closed magnetic field lines by the presence of active regions with bipolar magnetic field configuration, it was not clear how the solar wind could flow out of the regions. However, Hinode/XRT discovered continuous outflow from the edges of active regions. Later, EIS observations confirmed the outflow by its Doppler shift. Now this outflow is believed to be the long-sought source of the slow solar wind.

The fast solar wind originates from polar regions which are basically unipolar. Since quiet-sun magnetic field of 10 gauss or less was known to consist of intense flux tubes with a kilo-gauss field strength occupying 1% of the area, the same might be expected for polar fields. Hinode/SOT showed clearly with its high spatial resolution observations of vector magnetic fields that it is the case. Hinode/SOT observations also track the polar field reversal with an unprecedented accuracy. The time delay of the south pole reversal compared with the north pole is seen in Hinode/SOT polar field observations as well as other indices, and is speculated to be related to an unusually low activity of the present solar cycle.

Coronal mass ejections (CMEs) are the major source of geomagnetic disturbances. How such an ejection of plasma cloud takes place is explained by several models. In one scenario, a solar magnetic configuration evolves by supplies of magnetic flux and magnetic helicity from below the surface. The accumulation of magnetic helicity leads to abrupt instability of magnetic configuration, leading to a CME. Magnetic helicity is distributed basically anti-symmetrically with respect to the equator, but anomaly is often observed. Long-term observations of magnetic helicity by ground-based instruments and high accuracy measurements of helicity by Hinode/SOT are providing interesting information on the nature of magnetic field generation in the solar convection zone.

Keywords: Sun, solar activity cycle, solar wind, solar magnetic field, helicity

Japan Geoscience Union Meeting 2014
(28 April - 02 May 2014 at Pacifico YOKOHAMA, Kanagawa, Japan)

PEM09-11 Room:211 Time:April 28 11:45-12:00

Modeling of the geomagnetically induced electric field in Japan

FUJITA, Shigeru[1*] ; ENDO, Arata[2] ; FUJII, Ikuko[3]

[1]Meteorological College, [2]Meteorological College, [3]Magnetic Observatory

The geomagnetically induced current (GIC) happens to damage transformers of electrical power line systems in high-latitude countries like Canada and Sweden where the geomagnetic disturbances are enhanced. Thus, since it is important to evaluate the GICs associated with geomagnetic disturbances in these countries, there have been many works about GIC [Pulkkinen et al., 2005]. On the other hand, the low-latitude countries like Japan seem to be regarded to be free from dangers of the GIC disasters [Pulkkinen et al., 2008]. Indeed, Watari et al. [2009] revealed that the GICs measured along the power line in Hokkaido (the northernmost part of Japan) are as small as several Ampere. These values are negligibly small compared with the permissible current of a transformer. It is noted that the measurements by Watari et al. [2009] were carried out in the period of extremely quiet solar activity.

The result by Watari et al. [2009] seems to indicate that Japan is safe from the GIC disasters. However, it should be noted that the ground conductivity structure is quite different between Hokkaido and other Japanese areas like the most industrialized and highly-populated Kanto plain. This difference invokes the following geoelectric characters in Japan; the geomagnetically induced electric field at Kakioka in Kanto plain is sometimes about 10-times larger than that at Memambetus in Hokkaido. This difference probably comes from difference in the ground conductivity structure. As a result, we have to employ a realistic 3D ground conductivity model to present a reliable conclusion on the GIC.

In the talk, we will present the first numerical result of the geomagnetically induced electric field in Japan based on the 3D electric conductivity in the Earth. The conductivity is compiled after the resistivity suitable to the characteristic layers based on the crustal layer structure after the database on the bathymetry and that on the thickness of the sediment layer together. Our initial results reveal several localized enhancements of the induced electric field in the coastline regions when the induced electric current tends to converge into a bay-shaped area. The enhanced electric field appears in the different areas depending on the direction of the external source current in the magnetosphere. Combination of the induced electric field calculated and quantities of the severe space weather event yields the info for evaluation of the extreme severe GIC in Japan.

References

Pulkkinen, A. et al. (2005), Space Weather, 3, S08C03, doi:10.1029/2004SW000123.
Pulkkinen, A. et al. (2008), Space Weather, 6, S07001, doi:10.1029/2008SW000388.
Watari, S., et al. (2009), Space Weather, 7, S03002, doi:10.1029/2008SW000417.

Keywords: geomagnetically induced current, space weather, electric conductivity, numerical modeling, nonuniformity

Japan Geoscience Union Meeting 2014
(28 April - 02 May 2014 at Pacifico YOKOHAMA, Kanagawa, Japan)

PEM09-12 Room:211 Time:April 28 12:00-12:15

Role of magneto-convection from the point of view of large-scale magnetic structure formation on the solar surface

IIDA, Yusuke[1*]

[1]ISAS/JAXA

The roles of magneto-convection on the solar surface in the formation of large scale magnetic field, which are revealed by the recent observation, are reported in this presentation.

Many energetic activities on the solar surface, e.g. filament formation, solar jet, and slow solar wind etc., root in the large-scale magnetic configurations. The circumstances around the photosphere, e.g. actual visible surface, is at high plasma beta condition. So the magnetic field is transported mainly by the surface convection there. Simultaneously its configuration is significantly affected and changed from its birth to solar surface. Hence, understanding of magneto-convection on the solar surface is thought to be a basic but an important issue in the solar physics for long time.

Despite of its importance, it is very difficult to give the conclusion to roles of solar surface convection to global structure, namely to answer how does it transport magnetic field and how does it change states of magnetic field. The difficulties come from the smallness and short time scale of the element structures of magneto-convection on the solar surface (<1,000km and order of minutes). The first difficulty is its smallness and short time scale in absolute value. We need stable high spatial and temporal resolution to catch up their element structure. We can say this difficulty is nearly solved thanks to the recent satellite observation. However, there is the second difficulty, smallness and short time scale compared to large scale structure (˜700,000km and order of years). We need a new method of analysis to overcome the problem, huge scale difference.

To solve this problem, we develop auto-recognition and tracking method of patches and apply it to the actual data. In the presentation, we report the results about reformation of patch structures by surface convection, especially the frequency distribution of flux content in each patch structure. We find that it is re-formed in 30 minutes, which is much shorter than flux supply time scale. This result indicates that most magnetic structures on the solar surface is decided by the local convection nature.

Keywords: the Sun, magnetic field, convection

Japan Geoscience Union Meeting 2014
(28 April - 02 May 2014 at Pacifico YOKOHAMA, Kanagawa, Japan)

PEM09-13 Room:211 Time:April 28 12:15-12:30

Solar Magnetism: Exploration with Local Convective Dynamo Modeling

MASADA, Youhei[1*]

[1]Department of Computational Science, Kobe University

A grand challenge in astrophysics is the origin of self-organizing properties of the magnetic field in highly turbulent flows. The solar magnetism is the front line in this area. The solar magnetic field shows a remarkable spatiotemporal coherence though it is generated by turbulent convective dynamo operating within its interior. Our understanding on the solar magnetism has been accelerated over the past decade in response to broadening, deepening and refining of numerical dynamo modelings. However, it is still unclear what dynamo mode is excited in the solar interior and how it regulates magnetic cycle with equatorward sunspot migration and periodicity of 22 years. To gain a deeper understanding of the solar dynamo mechanism, we are currently working on the convective dynamo simulation in a local stratified system.

Here we report a successful direct numerical simulation (DNS) of oscillatory large-scale dynamo spontaneously excited in a rotating stratified convection. The figure shown below is the simulation result; the time-radius diagram of the mean horizontal magnetic fields. Our simulation model consists of three layers like as the solar interior: bottom and top stably stratified layers and mid-convection zone (the area between white-dashed lines). It is found that the large-scale magnetic field is organized in the bulk of the convection zone and shows a well-regulated oscillatory behavior. The mean-field component is the strongest at around the mid-convection zone and propagates from there to top and base of the convection zone. The polarity is then gradually reversed over the period of about 200 convective turn-over time. It is noteworthy that there is a phase difference of about $\pi/2$ between B_x and B_y . The simulated spatiotemporal evolution of the large-scale magnetic field is quite reminiscent of the solar butterfly diagram although there is a difference in the propagation direction between the simulated field and the sunspot field.

To explore the underlying dynamo mechanism, we construct a mean-field electrodynamics model with dynamo coefficients directly computed from the DNS. The nonlinear back-reaction of the mean-field on the dynamo coefficients (both α- and η-quenching) is self-consistently taken into account. We demonstrate that the simulated large-scale dynamo is quantitatively reproduced by our DNS-driven mean-field dynamo model, and is interpreted as a manifestation of oscillatory α^2-dynamo mode. We will describe the basic physics which characterizes the cycle period and amplitude of the large-scale magnetic field sustained by the α^2-dynamo, and then discuss its playing role in the solar magnetism. This is the first to quantitatively demonstrate the presence of the oscillatory α^2-dynamo mode as a natural outcome of the rotating stratified convection, and raises an unignorable question about the conventional solar dynamo model relying strongly on the profiles of the mean flows, such as the differential rotation and meridional circulation.

Keywords: Sun, MHD, Convection, Dynamo

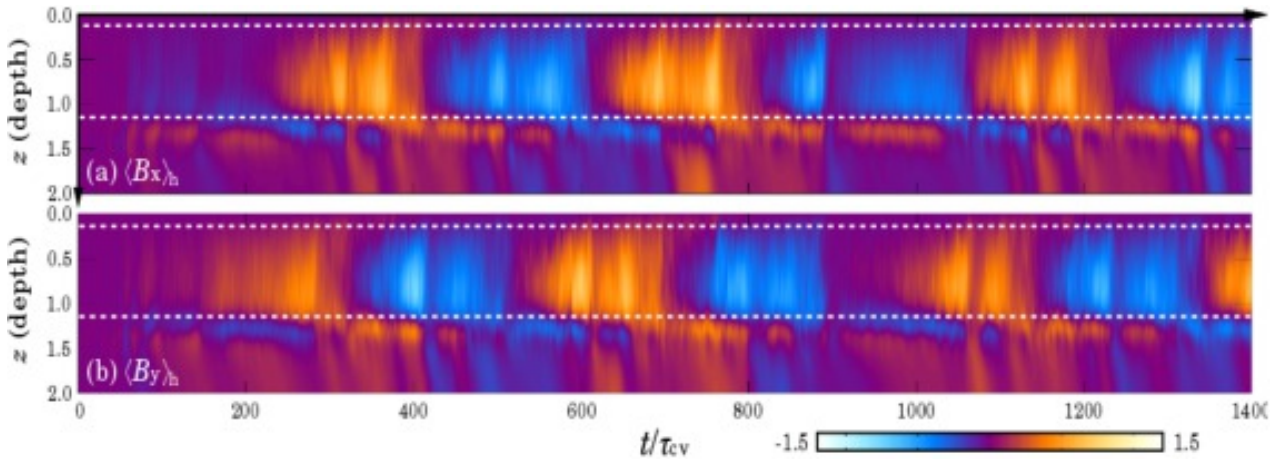

Japan Geoscience Union Meeting 2014
(28 April - 02 May 2014 at Pacifico YOKOHAMA, Kanagawa, Japan)

PEM09-14 Room:211 Time:April 28 12:30-12:45

From Deep Space Explorer DESTINY towards Solar Polar Region Observer SOLAR-D

KAWAKATSU, Yasuhiro[1*]

[1]ISAS/JAXA

DESTINY which stands for "**D**emonstration and **E**xperiment of **S**pace **T**echnology for **IN**terplanetary vo**Y**age" is a mission candidate for the next space science small program. The next mission is planned to be decided in 2014, and the select one is scheduled to be launched in 2018.

As illustrated in the Figure, DESTINY will be launched by an Epsilon launch vehicle and firstly placed into a low elliptical orbit, where then its altitude raised by the use of ion engine. When the orbit raising reaches the Moon, DESTINY subsequently is injected into transfer orbit for L_2 Halo orbit of the Sun-Earth system by using lunar gravity assist. Upon arrived at L_2 Halo orbit, DESTINY will conduct its engineering experiment as well as scientific observations for at least a half year. If conditions permit, DESTINY will leave L_2 Halo orbit, and transfer to the next destination.

On the way to L_2 Halo orbit, DESTINY will conduct demonstration and experiment on key advanced technologies for future deep space missions. Major items of the technology demonstration are listed as follows.

1) Ultra-Lightweight solar panel.

In order to generate large electric power to run μ20 ion engine, "Ultra-Lightweight Solar Panel", which is under development at JAXA, is applied and its performance is evaluated. This solar panel is estimated to achieve power to mass ratio at least double to conventional ones. Future application is expected in outer planet probes (JMO, MELOS) or probes with large ion engines.

2) Large scale ion engine μ20.

DESTINY is inserted into an elliptical orbit and reaches to a Halo orbit by its own orbital maneuver. For this maneuver, a large ion engine (μ20) which is under R&D at JAXA will be adopted and its performance is evaluated. This ion engine has thrust five times as much as μ10 used by Hayabusa and will be expected to be applied to large probes such as SOLAR-D or Hayabusa Mk2.

3) Advanced thermal control.

In order to manage large amount of heat generated by the large ion engine, advanced thermal control techniques by way of Loop Heat Pipe will be adopted.

4) Orbit determination under low thrust operation.

DESTINY will reach to Halo orbit by running ion engine over long duration. In order to reduce burdens to shut down the ion engine each time of orbit determinations, orbit determination under ion engine operation is conducted and its performance is evaluated.

5) Automatic/autonomous onboard operation.

In order to increase the efficiency of operation, autonomous and highly functioned spacecraft management system is developed demonstrated on board. This technique is expected to be adopted especially in the deep space missions usually operated under severe communication condition.

The technologies demonstrated by DESTINY will be applied to various future solar system exploration programs. One of them is a solar polar region observer, SOLAR-D, which is planned to be launched in 2020s.

SOLAR-D aims at the observation of the polar region of the Sun from out-of-ecliptic view point. It requires the observation from the high latitude point of the Sun, namely 45deg. To observe the Sun from the high latitude point, the space observatory (spacecraft) must be on the orbit largely inclined with the ecliptic plane. It is not an easy task to inject the spacecraft into the orbit largely inclined with the ecliptic plane. The mission plan under consideration supposes the use of solar electric propulsion, whose major technology challenges are going to be demonstrated in DESTINY.

The over view of DESTINY mission, and its effect on the future SOLAR-D mission will be introduced in the presentation.

PEM09-14 Room:211 Time:April 28 12:30-12:45

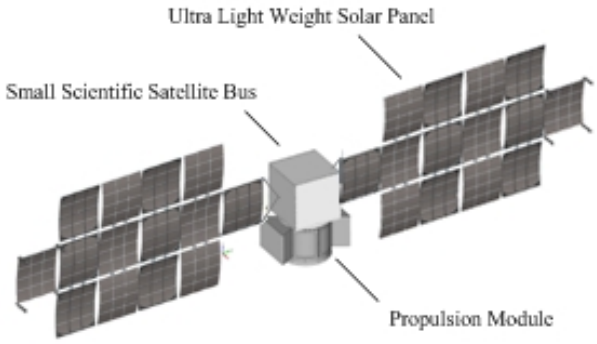

DESTINY Overview

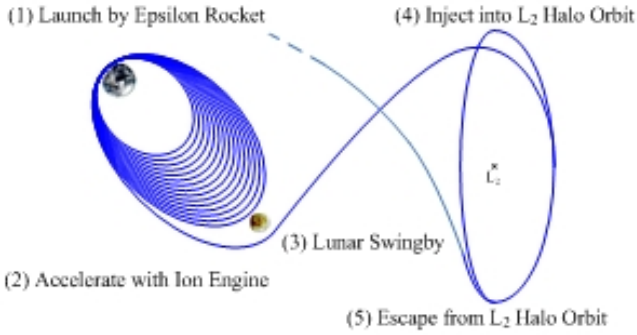

Mission Profile

Japan Geoscience Union Meeting 2014
(28 April - 02 May 2014 at Pacifico YOKOHAMA, Kanagawa, Japan)

PEM09-15 Room:211 Time:April 28 14:15-14:30

Overview of CAWSES II: Advancing the understanding of the Sun-Earth interaction

TSUDA, Toshitaka[1*]

[1]Research Institute for Sustainable Humanospherer (RISH), Kyoto University

CAWSES (Climate and Weather of the Sun-Earth System) was established as an international program by SCOSTEP (Scientific Committee on Solar-Terrestrial Physics) in order to enhance our understanding of the Solar Terrestrial relations, which impacts on life and society. In particular, we put special emphasis on the short and long-term variability of solar activity and its effects on the geospace and Earth's environment.

We carried out the first five-year project of CAWSES in 2003-2007. On the basis of its successful achievements, we conducted the second phase of CAESES during 2009-20013. CAWSES-Phase II especially promoted science and application of the following four themes, which are related to the fundamental questions of the Sun-Earth system.

TG1: What are the solar influences on the Earth's climate?
TG2: How will geospace respond to an altered climate?
TG3: How does short-term solar variability affect the geospace environment?
TG4: What is the geospace response to variable waves from the lower atmosphere?

We have enhanced international collaboration of ground-based observations, numerical modeling and satellite missions. Database is also very important for CAWSES-II. We also help capacity building activities to involve researchers in developing countries as well, and provide educational opportunities for students of all levels. We review in this talk recent achievements of CAWSES-II.

Keywords: CAWSES, SCOSTEP

Japan Geoscience Union Meeting 2014
(28 April - 02 May 2014 at Pacifico YOKOHAMA, Kanagawa, Japan)

PEM09-16 Room:211 Time:April 28 14:30-14:45

The Role of ICSU World Data System in VarSITI

WATANABE, Takashi[1*]

[1]Solar-Terrestrial Environment Laboratory, Nagoya University, [2]ICSU-WDS International Programme Office (NICT)

Solar-terrestrial physics is a typical example of interdisciplinary science, covering a wide variety of research fields. Interdisciplinary usage of observational data and information are essential in the research works to be conducted under VarSITI. ICSU has a long history to promote international collaborations in long-term provision of interdisciplinary data and information. In the IGY era (1957-58), the initial World Data Center (WDC) System was created under the policy of Full and Open Access to data and information. By the early 2000s, about 50 data centers were registered as WDCs, mainly for geophysical researches. ICSU also had another international data-oriented service under the name of Federation of Astronomical and Geophysical data-analysis Services (FAGS), which was created also in the IGY era, including ten services, e.g. International Space Environment Service (ISES). The World Data System (WDS) has been created by the 29th General Assembly of ICSU in 2008 as an Interdisciplinary Body to expand the range of data and information activities conducted by WDC and FAGS to much wider research fields, including social sciences. WDS strives to become a world-wide community of excellence providing trusted data services for global science with searchable common data directories and catalogues, which ensures the long-term stewardship and provision of quality-assessed data and data services. The VarSTEP will be one of the important partners of WDS because WDS includes many data centers came from former WDC and FAGS communities.

Keywords: VarSITI, Database, International collaboration, Interdisciplinary collaboration

Japan Geoscience Union Meeting 2014
(28 April - 02 May 2014 at Pacifico YOKOHAMA, Kanagawa, Japan)

PEM09-17 Room:211 Time:April 28 14:45-15:00

International Study of Earth-affecting Solar Transients (ISEST)/MiniMax24

KATAOKA, Ryuho[1*] ; SHIMIZU, Toshifumi[2] ; ASAI, Ayumi[3] ; ZHANG, Jie[4] ; MANUELA, Temmer[5] ; GOPALSWAMY, Nat[6]

[1]NIPR, [2]JAXA, [3]Kyoto University, [4]George Mason University, [5]University of Graz, [6]NASA/GSFC

We introduce the project ISEST (International Study of Earth-affecting Solar Transients)/Minimax24 of VarSITI, internationally led by Jie Zhang (USA), Manuela Temmer (Austria), and Nat Gopalswamy (USA). Goals and objectives are to understand the propagation of solar transients through the space between the Sun and the Earth, and develop space weather prediction capability. How do coronal mass ejections (CMEs) and corotating interaction regions (CIRs) propagate and evolve, drive shocks and accelerate energetic particles in the heliosphere? To answer this question, we need data/theory/modeling as follows: Establish a database of Earth-affecting solar transient events including CMEs, CIRs, flares, and energetic particle events based on remote sensing and in-situ observations from an array of spacecraft, run observation campaigns such as MiniMax24, develop empirical, theoretical, and numerical models of CME propagation and prediction, validate models using observations. As anticipated outcome, a comprehensive database of Earth-affecting solar transients will be created, and space weather prediction capability will be significantly improved.

Keywords: coronal mass ejection, corotating interaction region, flares, solar energetic particles

Japan Geoscience Union Meeting 2014
(28 April - 02 May 2014 at Pacifico YOKOHAMA, Kanagawa, Japan)

PEM09-18 Room:211 Time:April 28 15:00-15:15

The next-generation space solar observatory SOLAR-C

HARA, Hirohisa[1*]

[1]National Astronomical Observatory of Japan

The SOLAR-C is a planned satellite mission that is led by the JAXA SOLAR-C working group as the 4th Japanese space solar observatory that follows the 3rd satellite mission, Hinode. Hinode equips three major science payloads to cover from the photosphere to the corona simultaneously and has revealed the ubiquitous emergence/submergence of small-scale bipolar fields and the formation of kilo Gauss magnetic flux tubes from vector magnetic field measurements on the photosphere, unexpected dynamical phenomena in the chromosphere, spectral signatures of small-scale coronal heating events near the chromosphere below its spatial resolution, and so forth. These are the universal magnetized plasma activity in the nearest star, and the essential energy source of the phenomena is of magnetic-field origin coupled with photospheric convective motion. To elucidate the newly-found solar active phenomena and the problems that have been tackled for a long time in solar physics, we try to understand the causal linkage between solar magnetic fields and active phenomena on the Sun in the true sense by high-resolution (0.1-0.3 arcsecs) instruments in space. SOLAR-C will observe photospheric and chromospheric activity by imaging and measure chromospheric magnetic fields by spectro-polarimetry, in addition to photospheric magnetic fields. It visualizes the site of dynamical events for chromospheric and coronal heating by imaging and spectroscopy with comparable resolution and by high-resolution chromospheric magnetometry. In addition, SOLAR-C essentially contributes to space weather by estimating the stored magnetic energy in the corona via measurements of chromospheric magnetic fields.

Japan Geoscience Union Meeting 2014
(28 April - 02 May 2014 at Pacifico YOKOHAMA, Kanagawa, Japan)

PEM09-19 Room:211 Time:April 28 15:15-15:30

Statistical analysis of the gyroresonance sources using Nobeyama Radioheliograph and sunspot sketches

OTSUJI, Kenichi[1*] ; SHIBASAKI, Kiyoto[1] ; TANAKA, Yuuki[2] ; MIYAGOSHI, Takehiro[3]

[1]NAOJ, [2]Kyoto University, [3]JAMSTEC

Nobeyama Solar Radio Observatory of National Astronomical Observatory of Japan has continued the solar fulldisk observation using Radioheliograph (NoRH) since 1992. NoRH can measure the intensity and circular-polarization intensity of solar radio waves and identify the regions where the gyroresonance occurs. Gyroresonance is the mechanism in which the strongly circular-polarized radio waves are emitted from the resonance of the electrons gyrating around the magnetic field lines of sunspots. The radio flux coming from the gyroresonance mechanism depends on the magnetic field strength of its source and the observing wavelength. NoRH adopts 17 GHz radio waves and detects the gyroresonance emission from the strong magnetic field region with more than 2000 gauss. The statistical analysis combining gyroresonance sources and their magnetic field, or identifying them as the NOAA (National Oceanic and Atmospheric Administration) active region, however, has not been done sufficiently. So, the database including these informations is urgently needed.

In this study, we developed the database which combines the gyroresonance sources with NOAA active region number and the photospheric field strength. We listed up the location, radio flux and the circular-polarization ratio of each gyroresonance source with its area, using NoRH observation data. We also examined the area, McIntosh sunspot group classification, sunspot number and the magnetic classification of sunspots of each active region corresponding to the gyroresonance source. We used the sunspot sketches from Mt.Wilson and Crimea observatories because of the merits of covering solar fulldisk and being free from the saturation effect at the strong field. The temporal coverage of our database is from 1992 to 2013, which corresponds to almost two solar cycles.

The statistical analysis using our database clarified that the ratio of the active regions accompanied by the gyroresonance emissions increases in the latter half of cycle 23 (2002-2007). This phenomenon is not confirmed in cycle 22. There is a quadratic correlation between the number of occurrences of gyroresonance and the total number of active regions. This means that the ratio of the active regions accompanied by the gyroresonance emissions is proportional to the total number of active regions. Furthermore, we classified the active regions with the gyroresonance by their magnetic classification of sunspots and found that the complex magnetic configurations (beta-gamma-delta etc.) were predominant. Our statistical analysis provides new diagnostics to the past solar cycles and the prediction for the future solar activities.

Keywords: Sun, Radio, Sunspot

Japan Geoscience Union Meeting 2014
(28 April - 02 May 2014 at Pacifico YOKOHAMA, Kanagawa, Japan)

PEM09-20 Room:211 Time:April 28 15:30-15:45

Particle acceleration in a 3D current sheet of a Solar flare and comparison with solar radio observations

NISHIZUKA, Naoto[1*] ; NISHIDA, Keisuke[2]

[1]National Astronomical Observatory of Japan, [2]Kwasan and Hida observatories, Kyoto Uni.

Solar flares show intermittent time variability in nonthermal emissions, because particles are impulsively accelerated in small acceleration regions, i.e. multiple X-points, reconnection outflows, colliding plasmoids and internal shocks in a fragmented current sheet. We performed 3D MHD simulation of a solar flare, in which a horizontal flux rope in an unstable but equilibrium state are triggered by small amplitude of perturbation to be flown upward. The eruption of a flux rope forms a current sheet just below the flux rope, and when the width of a current sheet becomes enough thin, it becomes unstable for the tearing instability and generate small scale plasmoid inside. The formation and interaction of the plasmoids make the current sheet complex and turbulent structure. When a small scale plasmoid is ejected out or when two plasmoids collide with each other, the electric field in a current sheet is locally and intermittently enhanced.

In this 3D MHD simulation result, we inserted test particles, which are forced by electromagnetic field varying in time. Particles are trapped in the turbulent current sheet, or more exactly between multiple plasmoids, and accelerated by locally enhanced electric field along the current sheet. At that time, particles are intermittently accelerated at several heights and repeat multistep acceleration moving to other X-points. Sometimes, particles escape upward into the erupting flux rope and propagate along the field line of the flux rope. Particles are slightly accelerated by the curvature drift acceleration in the erupting flux rope and finally precipitate to another X-point connected to the different pair of loop-foot points. We also compared this simulation result with radio spectrograph data observed in Ondrejov observatory in Czech Republic. The radio spectrograph data shows similar intermittent time variability of type III bursts, i.e. electron beams, and sometimes slowly drifting pulsating structures, i.e. trapped electron beams in a plasmoid.

In this talk, we mainly talk about the test particle acceleration in 3D MHD simulation of an erupting solar flare and the comparison with the radio observation data. We are also aiming at simulating the propagation of a flux rope eruption into the interplanetary space, i.e. coronal mass ejection, forming a shock at the propagation front and reconnecting with open field in the interplanetary space. We welcome discussion and collaboration in VarSITI.

Keywords: Solar Flare, Coronal Mass Ejection, Particle Acceleration, Space Weather, Numerical Simulation, Radio Observation

Japan Geoscience Union Meeting 2014
(28 April - 02 May 2014 at Pacifico YOKOHAMA, Kanagawa, Japan)

PEM09-21 Room:211 Time:April 28 15:45-16:00

Role of the Japanese SuperDARN network in the VarSITI Program

NISHITANI, Nozomu[1*] ; YUKIMATU, Akira sessai[2] ; NAGATSUMA, Tsutomu[3]

[1]Solar-Terrestrial Environment Laboratory, Nagoya University, [2]National Institute of Polar Research, [3]National Institute of Information and Communications Technology

The Super Dual Auroral Radar Network (SuperDARN) is a network of HF radars operated under the international collaboration of 12 countries. At present, total of 33 radars have been operating in both hemispheres, monitoring important ionospheric parameters such as the global convection pattern and plasma density perturbations with high time (1 to 2 min) resolution. In addition to normal operaration modes, SuperDARN frequently operates special observation modes for conjunction studies with spacecraft programs, such as THEMIS, VAP and ERG missions. Japan has been operating total of 4 radars in Antarctica, Alaska and Hokkaido, contributing to the operation of the network. Judging from the characteristics of the network, it is expected to play important roles in several projects of the VartSITI programs, such as: ISEST (International Study of Earth-affecting Solar Transients/MiniMax24), SPeCIMEN (Specification and Prediction of the Coupled Inner-Magnetospheric Environment), and ROSMIC (Role Of the Sun and the Middle atmosphere/ thermosphere/ionosphere In Climate). Details of the SuperDARN network's role in the VarSITI program will be presented.

Keywords: SuperDARN, midlatitude, ionosphere, thermosphere, dynamics, VarSiti

Japan Geoscience Union Meeting 2014
(28 April - 02 May 2014 at Pacifico YOKOHAMA, Kanagawa, Japan)

PEM09-22 Room:211 Time:April 28 16:15-16:30

What determines the severity of space weather?

NANAN, Balan[5*] ; SKONG, R.[2] ; TULASI RAM, S.[3] ; RAJESH, P. K.[5] ; SHIOKAWA, Kazuo[1] ; HSU, R.[5] ; SU, T. H.[5] ; LIU, J. Y.[4]

[1]Solar-Terrestrial Environment Laboratory, Nagoya University, [2]Los Alamos National Laboratory, [3]Indian Institute of Geomagnetism, [4]National Central University, [5]National Cheng Kung University

Thanks to the works of a number of scientists it is known that severe space weather can cause extensive social and economic disruptions in the modern high-tech society. It is therefore important to understand what determines the severity of space weather, and whether it can be predicted. We present the results obtained from the analysis of solar-geophysical data during 30 space weather events that occurred since 1957 and produced geomagnetic storms of intensity less than -275 nT, and the Carrington event of 1859. The results seem to indicate that (1) space weather can become severe occasionally (7 since 1957) as experienced by satellite systems, Earth-based systems and Earth's environment. (2) It is the impulsive energy (or power) at the leading edge of the CMEs (coronal mass ejections) mainly due to impulsive leading edge velocity and partly due to density that determines the severity of space weather in the heliosphere; the higher the impulsive velocity (sudden increase by over 275 km s-1 over the background), the more severe the space weather. (3) Such CMEs with IMF Bz also southward from the leading edge cause severe space weather on Earth though the magnitude of southward Bz does not seem important, and the minimum impulsive velocity for severe space weather on Earth seems higher than that for severe space weather in heliosphere. (4) CMEs having northward IMF Bz at the leading edge do not seem to cause severe space weather on Earth though they can lead to geomagnetic storms of long duration main phase with intensity less than even -420 nT. Measurements of the rate of energy release during CME eruption (or measurements of the velocity and density of CMEs as close to the Sun as possible) and orientation of IMF Bz in CMEs may be used for predicting severe space weather.

Keywords: Severe space weather, solar flare, CME, geomagnetic storm

Japan Geoscience Union Meeting 2014
(28 April - 02 May 2014 at Pacifico YOKOHAMA, Kanagawa, Japan)

PEM09-23 Room:211 Time:April 28 16:30-16:45

Research and operatoinal activity of NICT space weather

ISHII, Mamoru[1*]

[1]NICT

ICT has been managing operational space weather forecast
since 1988 as a member of Inernational Space Environment Services (ISES). We provide the space weather forecast information every day including holidays with email and web site, and the number of subscribers is over 9,000.

In addition to these operational activity, we have research activities for improving the performance of space weather forecast.
We have three research projects, (1)sun and solar wind (2)magnetosphere, and (3)ionosphere with three approaches as follows: observation, simulation and informatics. These activities are progressing under the cooperation with domestic/international organizations which is suitable to the concept of VarSITI. Especially the connection to the operational users of space weather is important but very few institute only works for that including NICT. In this meaning we NICT can contribute to the activity of VarSITI.

Keywords: space weather

Japan Geoscience Union Meeting 2014
(28 April - 02 May 2014 at Pacifico YOKOHAMA, Kanagawa, Japan)

PEM09-24 Room:211 Time:April 28 16:45-17:00

Researches on solar eruptive phenomena and solar activities using chromospheric imaging data with the CHAIN

UENO, Satoru[1*] ; SHIBATA, Kazunari[1] ; ASAI, Ayumi[1] ; KITAI, Reizaburo[1] ; MORITA, Satoshi[2] ; OTSUJI, Kenichi[2] ; CABEZAS, Denis P.[3] ; G. ESCATE, Maria V.[3] ; ISHITSUKA I., Jose K.[4] ; YAMAGUCHI, Masashi[1] ; WATANABE, Hiroko[1] ; KIMURA, Goichi[1] ; ICHIMOTO, Kiyoshi[1] ; NAGATA, Shin'ichi[1] ; NAKATANI, Yoshikazu[1]

[1]Kyoto University, Japan, [2]NAOJ, [3]Presbiteriana Mackenzie University, Brazil, [4]Institute of Geophysics in Peru

In 2010, Kyoto University moved the Flare Monitoring Telescope (FMT) from Japan to Peru, and currently we are technically supporting two projects of building new solar telescopes in Saudi Arabia and Algeria under the Continuous H-Alpha Imaging Network (CHAIN) project. We also held international data analysis workshops three times during this four years to train foreign and domestic young researchers to analyze the data obtained by the FMT and Solar Magnetic Research Telescope (SMART) at Hida Observatory in Japan.

Current main scientific themes of the CHAIN project are

(1) 3D velocity field measurement of eruptive phenomena on the solar surface:
By applying "cloud model fitting" to multi-wavelength H-alpha chromospheric images, we can calculate physical parameters of moving features on the chromosphere. We especially focus on the 3D velocity field of erupting filaments to understand the process of growth and propagation of CMEs. Morimoto & Kurokawa (2003) statistically investigated time evolution of 3D velocity field of disappearing phenomena of chromospheric H-alpha filaments, and they observationally showed that if H-alpha filaments actually erupted, then CMEs necessary appears. On the other hand, however, when filaments are disappeared without eruption, sometimes CMEs occur. We have to know how to CMEs are generated in such a case, comparing with other observational data or MHD simulations. Moreover, we will statistically investigate relationship between characteristics of filament eruptions and geo-effectiveness of the CMEs .

(2) Detection of shock waves (Moreton wave) generated by solar explosive phenomena:
The FMT is quite effective to detect Moreton wave that was explained as the intersection of coronal shock wave on the solar chromosphere. Narukage et al. (2002) and Asai et al. (2012) observationally showed that Moreton waves detected in H-alpha chromospheric images actually correspond to foot-point of coronal shock waves observed with X-ray telescope or EUV telescope on satellites. On the other hand, even if flares that has almost the same intensity, sometimes they are accompanied by Moreton waves and sometimes they are not accompanied by them. We are investigating what are differences between flares "with" and "without" Moreton waves. According to our preliminary statistical study, the angle of filament eruption from the solar surface seems to be the most important parameter. We promote more investigation for more cases more accurately by combining with other satellite data or MHD simulations. Moreover, after that, we want to compare with characteristics of radio bursts and to investigate time evolution of various shock waves from solar surface to interstellar space.

(3) Estimation of solar UV radiation and comparison with ionospheric variation:
Solar radiation is also one of very important element for understanding the change of space weather. Especially solar UV around from 50 to 140 nm has strong influence for the ionosphere of the earth. One of good index of the change of ionosphere is the "geomagnetic solar daily quiet variation (Sq)". It basically changes well obeying the variation of solar UV radiation. When we investigate long-term variation of solar component and terrestrial component of Sq, currently we usually use F10.7 flux, sunspot number etc. as indexes of solar activity, because actual UV observations started just after around 1995. However, the indexes such as F10.7 do not accurately express variation of UV radiation and we cannot know accurate variation of terrestrial component of Sq. Therefore, we are currently trying to reproduce UV intensity from chromospheric images that have been obtained during longer-term than UV data. After this, by using estimated variation of solar UV radiation, we want to investigate relationship between solar activities and other physical parameters of ionosphere, too.

In this talk, we introduce our recent results and plans in VarSITI period on these themes.

Keywords: CHAIN, solar flare, filament eruption, Moreton wave, chromosphere, solar UV radiation

Japan Geoscience Union Meeting 2014
(28 April - 02 May 2014 at Pacifico YOKOHAMA, Kanagawa, Japan)

PEM09-25 Room:211 Time:April 28 17:00-17:15

The EISCAT_3D project

NOZAWA, Satonori[1*] ; MIYAOKA, Hiroshi[2] ; OGAWA, Yasunobu[2] ; OYAMA, Shin-ichiro[1] ; NAKAMURA, Takuji[2] ; FUJII, Ryoichi[1]

[1]STEL, Nagoya University, [2]NIPR

The EISCAT (European Incoherent SCATter) Scientific Association is an international research organization, which operates incoherent scatter (IS) radars in northern Scandinavia and Svalbard for studies of physical and environmental processes in the middle/upper atmosphere and near-Earth space. Since 1996, National Institute of Polar Research, in collaboration with STEL, Nagoya University, has promoted EISCAT collaborations for the user community in Japan to utilize the EISCAT facility as well as EISCAT data for their scientific subjects. Japanese scientists have been studying several scientific topics such as 3-D ionospheric current system, aurora dynamics, ion upflow, neutral wind dynamics, using EISCAT data, and published 110 papers from1995 to 2013.

EISCAT_3D is the major upgrade of the existing EISCAT radars in northern Scandinavia. The EISCAT_3D radar is a new phased array IS radar using the center frequency 233 MHz. The idea was firstly presented as 'E-prime' in 2003. The EISCAT community has been doing large efforts to make it happen since then. The design study was conducted from 2005 to 2009, and the preparatory phase program has been conducting since 2009 (until September 2014). With a multi static phased array system composed of one central active (transmiter-receiver) site and four receiver sites, the EISCAT 3D system is expected to provide us 10 times higher temporal and spatial resolution and capabilities than the present EISCAT radars. Furthermore, continuous observations can be made, and will provide us with long-term data sets of the polar ionosphere, which can be used to investigate variations of the ionosphere as well as the neutral wind dynamics (in particular, studies of planetary waves and tidal waves). In this presentation, we will overview the EISCAT_3D project, and present our strategic plan of national funding for the EISCAT_3D as well as science targets.

Keywords: EISCAT_3D, Incoherent Scatter radar, polar ionosphere, Magnetosphere-Ionosphere-Thermosphere coupling, 3D imaging observation, Mesosphere

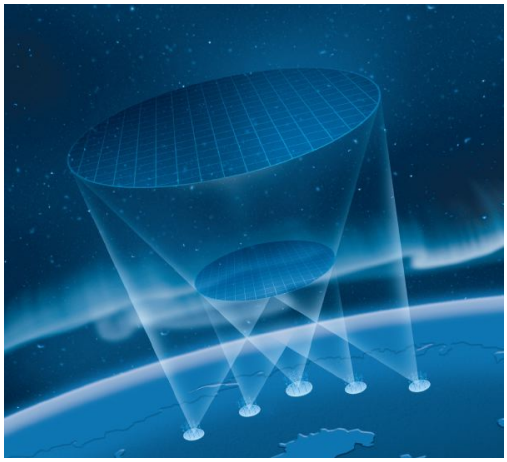

Japan Geoscience Union Meeting 2014
(28 April - 02 May 2014 at Pacifico YOKOHAMA, Kanagawa, Japan)

PEM09-26 Room:211 Time:April 28 17:15-17:30

Introduction of ROSMIC project in SCOSTEP/VarSITI program

OTSUKA, Yuichi[1*] ; NAKAMURA, Takuji[2] ; TAKAHASHI, Yukihiro[3] ; LUEBKEN, Franz-josef[4] ; WARD, William[5] ; SEPPALA, Annika[6]

[1]Nagoya University, [2]National Institute of Polar Research, [3]Hokkaido University, [4]Leibniz Institute of Atmospheric Physics, Germany, [5]University of New Brunswick, Canada, [6]Finnish Meteorological Institute, Finland

ROSMIC (Role Of the Sun and the Middle atmosphere/thermosphere/ionosphere In Climate, co-leaders: F.-J. Luebken, A. Seppala, W. Ward) is one of the four projects in VarSITI started in 2014 as a five year project. The goal of the project is to understand the impact of the Sun on the terrestrial middle atmosphere/lower thermosphere /ionosphere (MALTI) and Earth's climate and its importance relative to anthropenic forcing over various time scales from minutes to centuries. ROSMIC project consists of four sub-projects: 1) Coupling through solar variability (radiative, electrodynamics, ionospheric and photochemical effects), 2) Coupling by dynamics, 3) Trends in Mesosphere and Lower Thermosphere, 4) Trends and solar cycle effects in the thermosphere (incl. technological aspects). The project will be conducted under close collaborations between observations and modelings. Observations include both usage of existing data records and new measurements from a wide range of ground based (lidars, radars, mappers), in-situ (rockets, balloons, aircraft), and satellite (e.g., AIM, TIMED) instruments. Dedicated models are used and developed for a better understanding of specific processes (e.g. gravity wave breaking, ice formation). Global scale models will be modified and applied from the ocean to the thermosphere. Through the five year projects, we expect better understanding of the impact of solar activity on the entire atmosphere, relative to anthrogenic forcing and natural long term variability. In the paper, we will introduce outline of ROSMIC project and discuss how Japanese activities contribute to the ROSMIC project.

Keywords: Sun, middle atmosphere, thermosphere, ionosphere, climate

Japan Geoscience Union Meeting 2014
(28 April - 02 May 2014 at Pacifico YOKOHAMA, Kanagawa, Japan)

PEM09-27 Room:211 Time:April 28 17:30-17:45

Contribution of IUGONET to the VarSITI program

TANAKA, Yoshimasa[1*] ; YATAGAI, Akiyo[2] ; SHINBORI, Atsuki[3] ; KOYAMA, Yukinobu[4] ; ABE, Shuji[5] ; UMEMURA, Norio[2] ; SATO, Yuka[1] ; YAGI, Manabu[6] ; UENO, Satoru[7] ; HORI, Tomoaki[2]

[1]National Institute of Polar Research, [2]Solar-Terrestrial Environment Laboratory, Nagoya University, [3]Research Institute for Sustainable Humanosphere, Kyoto University, [4]World Data Center for Geomagnetism, Kyoto University, [5]International Center for Space Weather Science and Education, Kyushu University, [6]Planetary Plasma and Atmospheric Research Center, Tohoku University, [7]Kwasan and Hida Observatories, School of Science, Kyoto University

The Variability of the Sun and Its Terrestrial Impact (VarSITI) program aims at understanding the current extremely low solar activity and its influence on the Earth for various time scales and locations. In order to achieve these goals, it is necessary to conduct an interdisciplinary study that uses various types of data from multiple regions, such as solar interior, solar surface, heliosphere, magnetosphere, ionosphere, and atmosphere. The Inter-university Upper atmosphere Global Observation NETwork (IUGONET) project has developed the research infrastructure to promote such an interdisciplinary study. The IUGONET is an inter-university project by five Japanese institutes and universities (Tohoku University, Nagoya University, Kyoto University, Kyushu University, and the National Institute of Polar Research) that have been developing a worldwide ground-based observation network of the upper atmosphere, Sun and planets. The main tools developed by the IUGONET are metadata database and data analysis software.

The IUGONET metadata database (IUGONET-MDB) enables cross-searching of data distributed across the member institutes/universities of IUGONET. The metadata of various ground-based observational data have already been registered not only by the members of IUGONET but also by the other Japanese institutes, for example, the National Institute of Information and Communications Technology (NICT), the Solar Observatory of National Astronomical Observatory of Japan (NAOJ), and the Kakioka magnetometer observatory, Japan Meteorological Agency. We also consider including data from the satellites and the numerical simulation in the future. The iUgonet Data Analysis Software (UDAS) is a plug-in software of Space Physics Environment Data Analysis System (SPEDAS), which is an integrated analysis platform for visualizing and analyzing the ground-based and satellite observation data. The UDAS has provided many routines to load the ground-based observational data from various types of instruments, including solar telescope, solar radio telescope, ionosphere and atmosphere radars, imagers, magnetometers, and so on. The SPEDAS also includes a plug-in tool from a Japanese satellite mission, Energization and Radiation in Geospace (ERG), which will explore the dynamics of the radiation belts in the Earth's inner magnetosphere. Thus, they will be powerful tools for four projects of the VarSITI, in particular, Specification and Prediction of the Coupled Inner-Magnetospheric Environments (SPeCIMEN) and Role Of the Sun and Middle atmosphere thermosphere/ionosphere in Climate (ROSMIC). In the presentation we will show some examples of scientific researches that the IUGONET has done using the upper atmospheric data and discuss our possible contribution to the VarSITI program.

Keywords: IUGONET, upper atmosphere, ground-based observation, metadata database, data analysis software, interdisciplinary study

Japan Geoscience Union Meeting 2014
(28 April - 02 May 2014 at Pacifico YOKOHAMA, Kanagawa, Japan)

PEM09-28 Room:211 Time:April 28 17:45-18:00

Characteristics of airglow and auroral emissions in the lower- and upper-thermosphere obtained with IMAP/VISI on ISS

SAKANOI, Takeshi[1*] ; PERWITASARI, Septi[1] ; SAKAMOTO, Daiki[1] ; SAITO, Akinori[2] ; OTSUKA, Yuichi[3] ; AKIYA, Yusuke[2] ; HOZUMI, Yuta[2] ; YAMAZAKI, Atsushi[4] ; SUZUKI, Shin[3]

[1]Grad. School of Science, Tohoku University, [2]Grad. School of Science, Kyoto University, [3]STEL, Nagoya University, [4]ISAS / JAXA

We report the recent highlights of results on airglow and auroral distribution in the lower- and upper-thermosphere based on IMAP/VISI measurement data, and also report the current status of the operation VISI. IMAP/VISI is a visible imaging spectrometer which aims to measures nightglow emissions from ISS (˜400 km altitude) covering the wide range from +51 deg. to ? 50 deg. in geographical latitude. VISI adopts two field-of-views (+/-45 deg. to nadir) to make a stereoscopic measurement of the airglow and aurora emission to subtract background contaminations from clouds and ground structures. Each field-of-view has 90 deg width faced perpendicular to the orbital plane, which is mapped to ˜600 km width at 100 km altitude and ˜300 km width at 250 km altitude. A continuous line-scanning for all emissions lines in the nightside hemisphere in the latitudinal range from +51 deg. to -51 deg. is carried out by VISI with the successive exposure cycle with a time interval of 1 - several sec, which corresponds to a spatial resolution of 10 km ? a few tens km. From VISI data, we obtain the global distribution of airglow emissions (O 630 nm at 250 km alt., OH Meinel band 730 nm at 87km alt., and O2 (0-0) atmospheric band 762 nm at 95 km alt.) and auroral emissions (O 630 nm at 250 km alt., N2 1P 730 nm at ˜110 km alt. and O2 762 nm at ˜120 km alt.).

Since the successful launch of IMAP on August 2012, we found that meso-scale (˜10 - 50 km) wave pattern is always seen in the airglow emission at O2 762 nm mainly at mid-latitudes. The typical O2 airglow intensity is several hundreds R to several kR. Most of O2 airglow shows straight-shaped pattern, which indicates plane atmospheric gravity waves. In addition, we found more than 30 events on the concentric gravity wave (CGW) pattern in O2 airglow emission, which suggests that the local generation source in the lower-atmosphere. 26 CGW events out of total 30 events happened in March and April in 2013, which suggests its seasonal effect.

VISI sometimes measured auroral emissions at high-latitudes during geomagnetically disturbed period. One of major purposes of auroral measurement with VISI is to understand the generation process of gravity wave by auroral activity. However, we could not obtain the gravity wave event caused by aurora so far. Another target of VISI high-latitude measurement is SAR arc in the sub-auroral region. Even though the solar activity is expected to be maximum in 2012 ? 2013, we could not obtain the SAR arc data so far. However, we still expect to measure the SAR arc event caused with a major storm during a solar declining phase.

In addition, in the low-latitude region around the magnetic equator, we frequently obtained the enhanced O630 nm emission associated with equatorial ionization anomaly (EIA) overlapped with small-scale dark filament pattern, i.e., plasma bubble. We found the seasonal dependence of O630 nm intensity in the EIA which is consistent with the vertical motion of ionospheirc plasma due to the dragged by thermospheric day-to night tidal winds. The O630 nm intensity associated with EIA significantly decreased during the main phase of magnetic storm when the Dst index is larger than 90 nT. This fact suggests that the westward electric field associated with Region-2 current system penetrates to the ionosphere in the lower latitude that reduce the upwelling of EIA. We also obtained the MSTID pattern in O 630 nm emission in the eastside of North America on August 1 2013 by comparing the O 630 nm emission and TEC map. We carried the special operation for the measurement of MSTID last winter, and will summarize the result.

Acknowledgements

We thank the IMAP science team and the MCE team for their kind support.

Keywords: ISS, airglow, thermosphere, ionosphere, JEM, gravity wave

Japan Geoscience Union Meeting 2014
(28 April - 02 May 2014 at Pacifico YOKOHAMA, Kanagawa, Japan)

PEM09-29 Room:501 Time:April 29 11:00-11:15

The effect of Solar radiation on the Climate of Yakushima

MURAKI, Yasushi[1*] ; SHIBATA, Shoichi[2] ; SHIBATA, Takashi[3]

[1]Solar-Terrestrial Environment Laboratory, Nagoya University, [2]Department of Engeneering, Chubu University, [3]Graduate School of Environment Studies, Nagoya University

Yakushima (Yaku-island) is located to the south of Kyushu in Japan and is known as one of the world natural heritages of UNESCO. There are mountains on the island with heights of about 2,000m where cedar trees have lived for more than 2000 years. We analyzed meteorological data for the island from 1938 to 2013 and found several interesting results:

(1) Eleven and 20-30-year-periodicities are present in the data on daylight hours. Similar periodicities are, however, not seen in the data on temperature or water vapor pressure.
(2) The 11-year-periodicty appears strongly in June, the rainy season of the island, while the 20-30-year-periodicty is seen throughout the year except in April.
(3) An 11-year-periodicty can be also seen in the data for June and July at the other remote island Hachijyojima situated 300km to the south of Tokyo. Both islands are located on the Kuroshio warm current.
(4) The daylight hour data for January increased systematically around 1976. This may be related to the change of the North Hemisphere Temperature (NHT) in 1976.

In order to explain the observations, we examined the following hypothesis. Ocean waves produce large numbers of tiny salty droplets which contain plankton on the sea surface. These droplets (aerosols) are winded up and reach at the top of the mountain. They may act as cloud condensation nuclei (CCN).
It is known that the intensity of the UV light from the Sun is modulated by solar activity. It is also possible that the growth rate of CCN is affected by the solar UV radiation in the early stage of the aerosol formation process.
We speculate that this may be why solar activity is recognized in the daylight hour data. We have not accounted for the 20-30-year-periodicity in the data, but we speculate that this could be related to the Pacific Decadal Oscillation (PDO).
Details will be presented at the conference.

Keywords: solar activity, solar Ultra-Violet light, cloud, daylight hours, aerosols, Passific Decadal Oscillation

PEM09-29 Room:501 Time:April 29 11:00-11:15

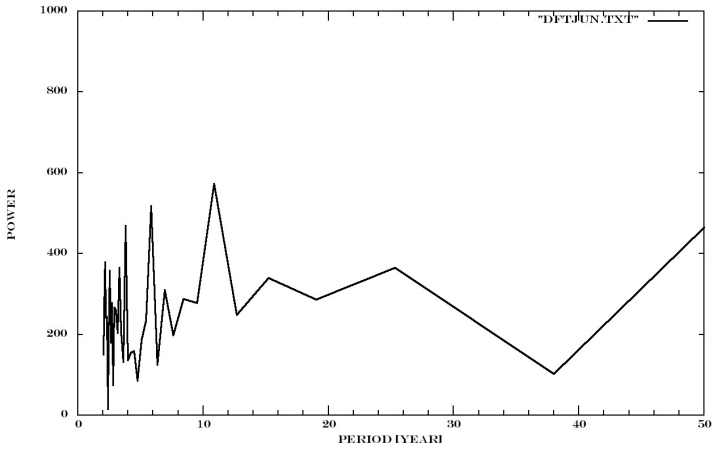

Japan Geoscience Union Meeting 2014
(28 April - 02 May 2014 at Pacifico YOKOHAMA, Kanagawa, Japan)

PEM09-30 Room:501 Time:April 29 11:15-11:30

Sounding rocket observation of the thermosphere-ionosphere-magnetosphere coupling

ABE, Takumi[1*] ; SAITO, Yoshifumi[1]

[1]Japan Aerospace Exploration Agency

The polar ionosphere is an open window of the Earth atmosphere to the outside space such as the magnetosphere and the solar wind, because energy and/or mass tends to be injected along the magnetic fields via various physical processes. In this connection, there exist numerous unique and unrevealed phenomena in the polar ionosphere.

Sounding rocket is a powerful platform which provides opportunity to make a vertical sounding through the lower thermosphere, ionosphere and magnetosphere while satellite generally flies in a horizontal direction, and it has an advantage so that it can enable us to make a brief survey of the upper atmosphere in the vertical direction. The Institute of Space and Astronautical Science (ISAS) of Japan Aerospace Exploration Agency (JAXA) has conducted sounding rocket experiments in Norway to investigate the upper atmospheric dynamics and chemistry induced by the auroral energy input. The primary objectives of these experiments include various topics; pulsating aurora, ozone chemistry affected by the auroral activity, fine structure of the auroral arc, and the cusp ion outflow. These subjects arise from phenomena that is caused by interaction between the solar wind or magnetospheric plasma and the upper atmosphere. It is necessary to make a comprehensive observation of the energy input, the response and consequences for better understanding of the causal relationship.

There are several candidates of the sounding rocket experiment which should be conducted in the auroral region for a direct measurement of the energy input from higher altitudes and the ionospheric response. To obtain the high-time resolution data of the ionospheric ion outflow which is one of the most significant phenomena of the magnetosphere-ionosphere coupling, it is necessary for the sounding rocket equipped with plasma and field instruments to reach up to 1000 km altitude. For such an experiment, it will be a key to get information on the wave-particle interaction which may play an important role in accelerating ionospheric ions. It is well known that the polar lower thermosphere has a significant response to auroral energy input from higher altitudes. This indicates an existence of energy inputs from the magnetosphere probably in the form of electric fields or energetic particles. It is important to understand quantitatively the momentum transfer between the neutrals and plasma by observing the neutral wind and ion drift simultaneously. The sounding rocket experiment to elucidate such a neutral-plasma coupling is also under consideration.

Thus, we are considering several candidates of the sounding rocket experiments which should be conducted in the auroral region to investigate the upper atmospheric response against the energy input from higher altitudes. In this presentation, we will briefly introduce some of the promising experiments.

Keywords: sounding rocket, thermosphere, M-I coupling, in-situ observation, aurora

Japan Geoscience Union Meeting 2014
(28 April - 02 May 2014 at Pacifico YOKOHAMA, Kanagawa, Japan)

PEM09-31 Room:501 Time:April 29 11:30-11:45

Trend of SST anomalies and Solar Activity

YAMASHIKI, Yosuke[1*]

[1]GSAIS, Kyoto University, [2]APL, JAMSTEC

The tendency of anomalies of SST during the fluctuation of Sunspot numbers are studied using composite SST and fluctuation of SSN.

In general, El Nino tendency is observed during Sunspot numbers (SSN) minimum, while La Nina tendency is observed in SSN maximum. It is generally accepted that the frequency of Solar Activity varies in 11 years, during those years there are SSN maximum and minimum. On the other hand, SST anomalies do not correspond well to the frequency of the solar activity. In addition, the thermal structure of sea surface temperature (SST) varies during El Nino and La Nina. Moreover, the impact of large-scale solar flare on the SST has not been clearly evident for the 4 days backward and forward comparison for the flare event on 2 April 2001 and 28 October 2003 on SST, wind velocity and OLR. Since the ocean has higher heat capacity, this might prevent the appearance of immediate SSN effect through the surge of any frequency in any band of electromagnetic waves from the SUN. The subtle impact might be confirmed either through cloud or wind. The long-term impact should also be considered by precise integration of the total energy on each wavelength. Numerical simulation is also expected to validate this issue.

Keywords: Solar activity, SST, Anomalies

Japan Geoscience Union Meeting 2014
(28 April - 02 May 2014 at Pacifico YOKOHAMA, Kanagawa, Japan)

PEM09-32 Room:501 Time:April 29 11:45-12:00

Recent observations by Rayleigh/Raman lidar and developments of tunable resonance scattering lidar system in JARE

EJIRI, Mitsumu K.[1*] ; TSUDA, Takuo[1] ; NISHIYAMA, Takanori[1] ; ABO, Makoto[2] ; TOMIKAWA, Yoshihiro[1] ; SUZUKI, Hidehiko[3] ; KAWAHARA, Takuya[4] ; TSUTSUMI, Masaki[1] ; NAKAMURA, Takuji[1]

[1]National Institute of Polar Research, [2]Graduate School of System Design, Tokyo Metropolitan University, [3]College of Science, Rikkyo university, [4]Faculty of Engineering, Shinshu University

The National Institute of Polar Research (NIPR) is leading a six year prioritized project of the Antarctic research observations since 2010. One of the sub-project is entitled ”the global environmental change revealed through the Antarctic middle and upper atmosphere”. Profiling dynamical parameters such as temperature and wind, as well as minor constituents is the key component of observations in this project, together with a long term observations using existent various instruments in Syowa, Antarctica (69S, 39E). As a part of the sub-project, Rayleigh/Raman lidar was installed at Syowa Station in January, 2011 and has been operated at more than 350 nights ($>$3000 hours clear sky) by February, 2014. The Rayleigh/Raman lidar observes temperature and clouds in the mesosphere, the stratosphere and part of the troposphere, and providing seasonal and yearly variations of temperature profiles and data of gravity wave characteristics in the middle atmosphere, as well as high altitude clouds of PMC (polar mesospheric clouds) and PSC (polar stratospheric clouds). In order to extend the height coverage to include mesosphere and lower thermosphere region, and also to extend the parameters observed, a new resonance scattering lidar system with tunable wavelengths is developed at NIPR in Tachikawa (36N, 139E). The lidar transmitter is based on injection-seeded, pulsed alexandrite laser for 768-788 nm (fundamental wavelengths) and a second-harmonic generation (SHG) unit for 384-394 nm (second harmonic wavelengths). The laser wavelengths are tuned in to the resonance wavelengths by a wavemeter that is well calibrated using a wavelength-stabilized He-Ne laser. The new lidar has capabilities to measure density variations of minor constituents such as atomic iron (Fe, 386 nm), atomic potassium (K, 770 nm), calcium ion (Ca^+, 393 nm), and aurorally excited nitrogen ion ($N_2{}^+$, 390-391 nm) and temperature profiles in the mesosphere and lower thermosphere (MLT) region using resonance scatter of K. Currently, the fundamental laser pulses are transmitted with 120-160 mJ/pulse at approximately 25 Hz (i.e., $\sim$3-4 W) and the backscattered signal is received with a 35 cm diameter telescope. The new lidar system will be installed two years later at Syowa Station and provide information on the mesosphere and lower thermosphere as well as the ionosphere. This unique observation is expected to make important contribution to studies on the atmospheric vertical coupling process and the neutral and charged particle interaction. In this talk, current status of the research, observations, and system developments will be presented.

Keywords: Lidar, Resonance scatter, Rayleigh/Raman, Antarctic observation, Syowa Station

Japan Geoscience Union Meeting 2014
(28 April - 02 May 2014 at Pacifico YOKOHAMA, Kanagawa, Japan)

PEM09-33 Room:501 Time:April 29 12:00-12:15

400 years interval of amplification in quasi bi-decadal climate variability: a case of summer precipitation in Japan

NAKATSUKA, Takeshi[1*]

[1]Research Institute for Humanity and Nature

Introduction

Quasi bi-decadal climate variability, often found in palaeoclimatological time series, should be not only attributed to internal climate variation such as ocean-atmosphere interaction, but also owing to astronomical climate forcing like 22 year cycle of solar activity. In long human history, the multi-decadal climate variations are sometimes enhanced to cause long abnormal meteorological conditions and result in numerous famines, wars and political regime shifts. Why does the amplitude of natural climate variation change? If we can understand mechanism of the amplitude modulation in climate variability and predict its future, it must be very helpful for improvement of our adaptability to climate change. In this presentation, I will discuss climatic mode of 400 year intervals of amplification in quasi bi-decadal climate variability found in last two millennial records of summer precipitation which were reconstructed annually by tree-ring cellulose isotope ratios.

Reconstruction of summer precipitation by tree-ring oxygen isotope ratio

Until recently, paleoclimatologists in Japan could not reconstruct precipitation before Edo era when weather descriptions in numerous diaries enable us to discuss climate change precisely. However, it is now possible to elucidate historical changes in summer precipitation with annual time resolution using tree-ring cellulose oxygen isotope ratios all over Asia monsoon area including Japan. Last two millennial summer precipitation variations have been reconstructed in central Japan using many wood samples of Japanese cypress from living trees, old architectures, archaeological remains and buried logs.

Amplification of quasi bi-decadal variability occurring at 400 years intervals.

By wavelet analysis of the two millennia length of summer precipitation record in central Japan, I have found that there are distinct periods of amplitude modulation for the multi-decadal variability, especially at quasi bi-decadal periodicity, in 2nd, 6th, 10th, 14th and 18th centuries when long lasting flood and drought occurred. In fact, 2nd, 6th and 14th centuries correspond to the end of Yayoi, Kofun eras and the medieval upheaval period (Namboku-cho, twin dynasty, era) in Japan, respectively. 10th and 18th centuries are also known as periods of the collapse of centralized political system and the occurrence of giant famines all over Japan, respectively. The amplitude modulation in quasi bi-decadal periodicity occurring at 400 years intervals always started with sudden decrease in tree ring d18O, accompanied with sudden increase and decrease in its d13C and 14C content, respectively. At present, I can propose the sudden enhancement of summer monsoon activity bringing tropical air mass to explain all signals of sudden changes in tree-ring isotope records. Especially, sudden increases in temperature during 14th century, which is corresponding to the precipitation increase in Japan, are found at low and middle latitudinal areas in both hemispheres, illustrating that they are actually owing to the summer monsoon enhancement originating from tropical areas. If the amplification in quasi bi-decadal variability at 400 year intervals is related to the periodical change in solar activity such as 800 year cycle, it must be very important to elucidate astronomical and climatic mechanisms combining cause (solar cycle) and effect (amplitude modulation) precisely.

Keywords: tree ring, oxygen isotope, bi-decadal change, precipitation

Japan Geoscience Union Meeting 2014
(28 April - 02 May 2014 at Pacifico YOKOHAMA, Kanagawa, Japan)

PEM09-34 Room:501 Time:April 29 12:15-12:30

Ionospheric studies using high-resolution GPS total electron content observations

TSUGAWA, Takuya[1*] ; NISHIOKA, Michi[1] ; SAITO, Akinori[2] ; OTSUKA, Yuichi[3] ; ISHII, Mamoru[1]

[1]National Institute of Information and Communications Technology, [2]Graduate School of Science, Kyoto University, [3]Solar-Terrestrial Environment Laboratory, Nagoya University

Two-dimensional total electron content (TEC) observations using dense GPS receiver networks have been applied to studies of various ionospheric disturbances since mid-1990s. For the purpose of monitoring and researching the ionospheric disturbances, we have developed high-resolution TEC maps using dense GPS receiver networks. We have been collecting all the available GNSS receiver data in the world to expand the TEC observation area. These GNSS data are provided by IGS, UNAVCO, SOPAC, and other regional data centers. Currently, we are providing global and regional maps of absolute TEC, detrended TEC, and rate of TEC change index (ROTI). These data and quick-look maps are archived and available in DRAWING-TEC website (http://seg-web.nict.go.jp/GPS/DRAWING-TEC/).

These high-resolution GPS-TEC maps have been applied to studies of various ionospheric disturbances. Sudden increase in TEC caused by solar flares were studied using global TEC observations. Regional TEC observations have revealed new characteristics of large- and medium-scale traveling ionospheric disturbances (LSTIDs and MSTIDs). Recently, clear concentric waves and short-period oscillations were observed after huge earthquakes/tsunamis and massive tornadoes, indicating that acoustic and/or gravity waves propagate upward from the lower atmosphere and reach the ionosphere.

These GPS-TEC observations will contribute the next SCOSTEP program VarSITI, particularly to the ROSMIC (Role Of the Sun and the Middle atmosphere/thermosphere/ionosphere In Climate) project.

Keywords: ionosphere, GPS, TEC, thermosphere

Japan Geoscience Union Meeting 2014
(28 April - 02 May 2014 at Pacifico YOKOHAMA, Kanagawa, Japan)

PEM09-35 Room:501 Time:April 29 12:30-12:45

Modulation of Greenland temperature through changes in solar activity

KOBASHI, Takuro[1*] ; KAWAMURA, Kenji[1] ; GOTO-AZUMA, Kumiko[1]

[1]National Institute of Polar Reseaerch

During the past decades, Greenland climate has undergone rapid warming and ice sheet ablation in coastal region with a nearly 1 mm/y sea level contribution. For sea level projection, it is critical to understand the mechanisms of Greenland temperature variability. Greenland temperature is known to be affected by the North Atlantic Oscillation (NAO), and it is also highly correlated with North Atlantic average temperature. Using the Greenland temperature reconstructed from argon and nitrogen isotopes in occluded air in GISP2 ice core (Kobashi et al., 2011), we found Greenland temperature deviated negatively (positively) from North Hemispheric (NH) temperature trend during stronger (weaker) solar activity over the past 800 years (Kobashi et al., 2013b). We also confirmed this effects continued over the past 4000 years (Kobashi et al., 2013a). Climate modeling suggests that the deviation was caused by solar induced atmospheric circulation changes (like NAO). The model also suggests that Atlantic meridional circulation weakens during the stronger sun by similar processes as enhanced greenhouse effect (Kobashi et al., 2013b). From the past relation between Greenland temperature anomaly and solar variability, it can be speculated that future gland solar minimum may induce additional 2 ^{0} C warming in Greenland with increased melting of the ice-sheet.

Kobashi, T., Kawamura, K., Severinghaus, J. P., Barnola, J.-M., Nakaegawa, T., Vinther, B. M., Johnsen, S. J., and Box, J. E.: High variability of Greenland surface temperature over the past 4000 years estimated from trapped air in an ice core, Geophysical Research Letters, 38, 10.1029/2011GL049444, 2011.

Kobashi, T., Goto-Azuma, K., Box, J. E., Gao, C.-C., and Nakaegawa, T.: Causes of Greenland temperature variability over the past 4000 years: Implications for Northern Hemispheric temperature change Climate of the Past, 9, 2299-2317, 2013a.

Kobashi, T., Shindell, D. T., Kodera, K., Box, J. E., Nakaegawa, T., and Kawamura, K.: On the origin of Greenland temperature anomalies over the past 800 years, Climate of the Past, 9, 583-596, 2013b.

Keywords: solar activity, Greenland, temperature, ice core, climate change

Japan Geoscience Union Meeting 2014
(28 April - 02 May 2014 at Pacifico YOKOHAMA, Kanagawa, Japan)

PEM09-36 Room:501 Time:April 29 14:15-14:30

Study of equatorial atmosphere/ionosphere under RISH/LAPAN collaboration

YAMAMOTO, Mamoru[1*] ; YATINI, Clara[2] ; BUDIYONO, Afif[2] ; HERMAWAN, Eddy[2] ; HASHIGUCHI, Hiroyuki[1]

[1]RISH, Kyoto University, [2]National Institute of Aeronautics and Space (LAPAN)

The Earth's atmosphere is vertically coupled with atmospheric waves. Momentum/energy transfer from lower to upper atmosphere through wave propagation plays an big role of determining the dynamics of the atmosphere. The energy input from the sun is the maximum at the equator that leads to the intense convection, and then variety of atmospheric waves are generated in the region. The equatorial atmosphere could be regarded as an engine for dynamics of the whole atmosphere. RISH-LAPAN started collaboration for the study of equatorial atmosphere/ionosphere since mid 1980s, and conducted radiosonde observation campaigns, meteor and MF radars, etc. The Equatorial Atmosphere Radar (EAR) was installed over the geographic equator on Sumatra Island in 2001. We continued long-term experiment for more than 10 years, and have found that troposphere-stratosphere airmass exchange is controlled by the modulation of the tropopause by Kelvin waves. Turbulent structures of the tropopause region is also revealed by the EAR. In the ionosphere, spatial and temporal variability of the equatorial Spread-F are clearly observed by the multibeam experiment. With research collaboration with other Japanese university/institutes, the EAR site now became a complete observatory that consists of many instruments, i.e., a meteor radar, a boundary-layer radar, a meteorological radar, lidars, an ionosonode, GPS receivers, etc. The next big project of our own is to improve the EAR ability by building the Equatorial MU radar (EMU) aside of the EAR, which is now included in the Japanese Master Plan. RISH-LAPAN recently obtained a fund of "JSPS Bilateral Joint Research Projects" for FY2014-2016. We will have more chances to discuss collaborative research program for the equatorial atmosphere/ionosphere. In the presentation we summarize our collaboration, and discuss future direction of research including the new EMU.

Keywords: Atmosphere, Ionospphere, Indonesia, Equatorial Atmosphere Radar

Japan Geoscience Union Meeting 2014
(28 April - 02 May 2014 at Pacifico YOKOHAMA, Kanagawa, Japan)

PEM09-37 Room:501 Time:April 29 14:30-14:45

Monitoring of molecular compositions in mesosphere with a network of ground-based millimeter-wave radiometers

NAGAHAMA, Tomoo[1*] ; MIZUNO, Akira[1] ; NAKAJIMA, Tac[1] ; OHYAMA, Hirofumi[1] ; ISONO, Yasuko[1] ; KOJIMA, Yasusuke[1] ; TSUTSUMI, Masaki[2] ; NAKAMURA, Takuji[2] ; MAEZAWA, Hiroyuki[3] ; OGAWA, Hideo[3]

[1]Solar-Terrestrial Environment Laboratory, Nagoya University, [2]National Institute of Polar Research, [3]Osaka Prefecture University

Chemical composition in mesosphere and lower thermosphere (MLT) region is strongly affected by changes of solar-terrestrial environment; for example, energetic particle precipitation into the earth atmosphere induces composition change in the mesosphere and lower thermosphere. Changes of gravity-wave activities also make the composition changes caused by temperature variations in various timescales.

To investigate these changes related to environment changes in the altitude region, we have started a project of network measurements of the distribution of mesospheric minor constituents, such as ozone, by using ground-based millimeter-wave spectral radiometers with a high-sensitivity superconducting (SIS) mixer receiver. We have been operating three millimeter-wave radiometers in the southern hemisphere; Atacama highland in Chile (23S, 68W), Rio Gallegos in Argentina (52S, 69W), and Syowa station in Antarctica (69S, 39E), and one radiometer in Rikubetsu, Japan(44N, 144E). Especially, at Syowa station, we have been monitoring ozone and nitric oxide (NO) spectra in 250 GHz band, and we have clearly detected temporal variations of NO column density in the MLT region including sudden enhancements of NO suggested to be associated with the energetic electron precipitation events.

In the presentation, we report features of observed variations of mesospheric ozone and NO as well as details of instruments, data validation and future extensions.

Keywords: mesosphere, composition change, millimeter-wave measurement

Japan Geoscience Union Meeting 2014
(28 April - 02 May 2014 at Pacifico YOKOHAMA, Kanagawa, Japan)

PEM09-38 Room:501 Time:April 29 14:45-15:00

Observations and modeling studies for understanding atmospheric responses to unusual solar activities

FUJIWARA, Hitoshi[1*] ; MIYOSHI, Yasunobu[2] ; JIN, Hidekatsu[3] ; SHINAGAWA, Hiroyuki[3] ; NOZAWA, Satonori[4] ; OGAWA, Yasunobu[5] ; KATAOKA, Ryuho[5]

[1]Faculty of Science and Technology, Seikei University, [2]Department of Earth and Planetary Sciences, Faculty of Sciences, Kyushu University, [3]National Institute of Information and Communications Technology, [4]Solar Terrestrial Environment Laboratory, Nagoya University, [5]National Institute of Polar Research

As pointed out by many researchers, the recent solar activities are very unusual; the solar activity during the last minimum in 2008-2009 was extremely low and that during the next maximum of sunspot cycle 24 shows much lower activities compared with the previous two solar maximums in cycle 22 and 23. In order to understand the complex system of the Earth's middle and upper atmosphere, these solar activities will give us important information and/or good opportunities for searching the basic states of the system both from the observations and GCM simulations. Comprehensive studies by observations from space, ground-based ones, and numerical simulations will enable us to understand the polar mesosphere, thermosphere, and ionosphere quantitatively. In order to understand variations of the polar ionosphere from the solar minimum to maximum periods, we have made EISCAT experiments in January 2011, March, 2012, and March 2013. For example, ionospheric variations were observed during solar flare and CME events on March 12, 2012. These EISCAT data clearly show an example of the solar wind, magnetosphere, and ionosphere coupling. In addition to the EISCAT observations, we have also investigated variations of the polar thermosphere during periods of significant solar activities from GCM simulations. In this presentation, we will introduce our research activities mainly related to the "Role Of the Sun and the Middle atmosphere/thermosphere/ionosphere In Climate (ROSMIC)" project in VarSITI.

Keywords: thermosphere, ionosphere, middle atmosphere, GCM, radar, aeronomy

Japan Geoscience Union Meeting 2014
(28 April - 02 May 2014 at Pacifico YOKOHAMA, Kanagawa, Japan)

PEM09-39 Room:501 Time:April 29 15:00-15:15

Enhancing our understanding of the atmosphere-ionosphere coupling with Low Earth Orbiting satellite missions

LIU, Huixin[1*] ; LUEHR, Hermann[2]

[1]Kyushu University, Japan, [2]GFZ, Germany

Low Earth Orbiting (LEO) satellites provide unique opportunities to observe the near-Earth space environment. Recent LEO satellite mission have been making rapid contribution to our understanding of the coupled atmosphere-ionosphere system by providing unprecedented observational evidences for the connection between ionospheric/thermosphric phenomena and their meteorological causes. This talk will briefly summarize the achievements of the decade-long CHAMP mission from the vertical coupling point of view, which is followed by a scientific perspective on the newly launched 3-satellite constellation SWARM mission.

Japan Geoscience Union Meeting 2014
(28 April - 02 May 2014 at Pacifico YOKOHAMA, Kanagawa, Japan)

PEM09-40 Room:501 Time:April 29 15:15-15:30

Multipoint airglow imaging measurements of mesospheric gravity waves over Japan

SUZUKI, Shin[1*] ; SHIOKAWA, Kazuo[1] ; OTSUKA, Yuichi[1]

[1]Solar-Terrestrial Environment Laboratory, Nagoya University

Atmospheric gravity waves significantly contribute to the wind/thermal balances in the mesosphere and lower thermosphere (MLT) through their vertical transport of horizontal momentum. It has been reported that the gravity wave momentum flux preferentially associated with the scale of the waves; the momentum fluxes of the waves with a horizontal scale of 10-100 km are particularly significant. Airglow imaging is a useful technique to observe two-dimensional structure of small-scale (<100 km) gravity waves in the MLT region and has been used to investigate global behavior of the waves. The Solar-Terrestrial Environment Laboratory, Nagoya University, has made long-term airglow imaging observations with ground-based all-sky airglow imagers using the Optical Mesosphere and Thermosphere Imager (OMTI) system. Each airglow imager of OMTI has interference filters on rotating wheels to observe airglow emissions in the vicinity of the mesopause (OI 557.7-nm, emission height ∼96 km; OH Meinel-bands, ∼86 km) and the ionosphere (OI 630.0-nm, ∼250 km). Four airglow imagers, which each has the field-of-view with a size of 5 deg x 5 deg in longitude and latitude at the mesopause height, has been in operation in Japan and, as a whole system, they nearly cover all part of Japan. This multipoint network enables us to detect propagation signatures and the spatial extent of MLT waves over a much wide range than ever.

In the presentation, we will report recent results of the MLT gravity waves having a very large spatial extent based on the OMTI multipoint measurements, such as a coherent gravity wave ducting and large concentric gravity wave rings possibly induced by a typhoon; these results offer new insight into dynamical coupling process between the lower and upper atmosphere.

Japan Geoscience Union Meeting 2014
(28 April - 02 May 2014 at Pacifico YOKOHAMA, Kanagawa, Japan)

PEM09-41 Room:501 Time:April 29 15:30-15:45

Exploration into evolution of solar-planetary environments: Solar variation and a variation and atmospheric escape

SEKI, Kanako[1*] ; TERADA, Naoki[2] ; YOKOYAMA, Takaaki[3] ; SUZUKI, Takeru[4] ; IMAMURA, Takeshi[5] ; NAKAMURA, Takuji[6] ; NAKAGAWA, Hiromu[2] ; KURODA, Takeshi[2] ; FUJIMOTO, Masaki[5] ; ESPE, Project team[1]

[1]Solar-Terrestrial Environment Laboratory, Nagoya University, [2]Graduate School of Science, Tohoku University, [3]School of Science, University of Tokyo, [4]School of Science, Nagoya University, [5]Institute of Space and Astronautical Science, JAXA, [6]National Institute of Polar Research

How has the atmosphere of terrestrial planets responded to the evolution of the sun, a center star of our solar system? In order to answer the question of the coevolution of our sun and the planetary environment " planetosphere ", planetary exploration missions have been promoted and related interdisciplinary researches are rapidly developing worldwide. It is scheduled that NASA ' s Mars mission MAVEN arrives at Mars in September 2014 and Venus weather explorer AKATSUKI arrives at Venus at the end of 2015. These missions will provide us new observations and insights in this field. Moreover, the solar evolution is included in one of the next emphasized problems in VarSITI program that starts in 2014, and the time of international collaborations is expected to come. On the other hand, the past researches in the solar-terrestrial sciences have had large emphasis on understanding of dynamic variations of the present sun and planetary environment. The interdisciplinary researches of understanding the coevolution of the sun and planetosphere over past four billion years or so are in the incunabula but start to develop rapidly. In this presentation, we will introduce an attempt to investigate the coevolution of the sun and planetosphere by combining large-scale numerical simulations and the latest observations based on international collaborations and cooperation of solar physics, solar-terrestrial physics, aeronomy, and meteorology.

Keywords: solar evolution, planetosphere, atmospheric escape, coupling of lower and upper atmosphere, climate change, evolution of planetary atmosphere

Japan Geoscience Union Meeting 2014
(28 April - 02 May 2014 at Pacifico YOKOHAMA, Kanagawa, Japan)

PEM09-42 Room:501 Time:April 29 15:45-16:00

Role of global electric circuit in solar-climate connection

TAKAHASHI, Yukihiro[1*] ; SATO, Mitsuteru[1]

[1]Department of Cosmosciences, Hokkaido University

Global electric circuit model was proposed log time ago, in 1930s, in which thunderstorm plays a role of generator, and the ground and the ionosphere work as a spherical capacitor. We need to reconstruct this simple model, taking into account 3 aspects: 1) global-scale nonuniformities both of ionospheric conductivity and of the distribution of the generators, 2) connections between the troposphere and D-region, considering the effects of TLEs, such sprites and blue jets, 3) establishing the observational methodology for global electric field, excluding the effect of cloud existing just above the observation sites. Recently, the relationship between the global circuit and solar-climate connection was pointed out. Here we introduce an example, which indicates the roles of thunderstorm or its resultant electric circuit in solar-climate connection. Global relationship between thunderstorm/cloud activities and solar parameters are examined based on lightning measurement by Global ELF observation Network (GEON) operated by Hokkaido University and Outgoing Longwave Radiation (OLR) intensity. It was found that the number of lightning stokes in Asia Maritime Continent (AMC) varies with about month periodicity in the period from February to June 2004 and shows positive correlation (R= ˜0.8) with OLR in the Western Pacific Warm Pool (WPWP). On the other hand, OLRs in the central Africa and some other tropical areas show negative correlation with the number of lightning stokes in the AMC in that period. It is also found that the galactic cosmic rays or UV intensity associated with solar activity indicates good correlation with tropical OLR or lightning activity in AMC. One explanation to connect such global variations in thunderstorm / cloud amount with solar parameters would be the electrical circuit involving lower and upper atmospheres. If the ionospheric electric field modulates the potential gradient in the lower atmosphere, it could cause the re-distribution of ionized atmospheric particles, which may, in turn, change the generation / reduction speed of cloud particles.

Keywords: global electric circuite, solar-climate connection, TLEs, thunderstorm activity, Asia Maritime Continent

Japan Geoscience Union Meeting 2014
(28 April - 02 May 2014 at Pacifico YOKOHAMA, Kanagawa, Japan)

PEM09-43 Room:501 Time:April 29 16:15-16:30

A Realistic Whole Atmosphere-Ionosphere Modeling and Collaboration with Observations

JIN, Hidekatsu[1*] ; MIYOSHI, Yasunobu[2] ; FUJIWARA, Hitoshi[3] ; SHINAGAWA, Hiroyuki[1] ; MATSUO, Tomoko[4]

[1]National Institute of Information and Communications Technology, [2]Kyushu University, [3]Seikei University, [4]National Oceanic and Atmospheric Administration

There has been an increasing number of collaboration between modeling and observation for the study of upper atmospheric variability and its relation to the lower atmosphere. Observations are used as the forcing inputs to models as well as for their validation. Outputs from models can be useful for the interpretation of observed phenomena owing to their sufficient spatial and temporal coverage, especially for the analysis of phenomena whose effects extend beyond the several atmospheric layers. Recently, we have examined the effects of a prominent stratospheric sudden warming (SSW) in January 2009 on the upper atmospheric variability, by using a whole atmosphere-ionosphere coupled model called GAIA. The model used the meteorological reanalysis data as realistic lower atmospheric forcing, and we compared the model outputs with the satellite observations of upper atmosphere [Jin et al., 2012; Liu et al., 2012]. The comparison suggests that the model can reproduce the overall major features of the observed perturbed variations in the upper atmosphere during the SSW period, which ensures the usage of model output for the detail analysis of vertical coupling mechanism during the event.

In this study, we applied the same method for the inclusion of realistic lower atmospheric forcing and carried out a whole atmosphere-ionosphere simulation for longer period. We will show the relation of ionospheric variability to the climatological and irregular variations in the lower atmosphere including several SSW events. Initial results from data assimilation experiment will also be shown as an example of model-observation collaboration.

Keywords: ionosphere, thermosphere, atmospheric vertical coupling, simulation, data assimilation, space weather

Japan Geoscience Union Meeting 2014
(28 April - 02 May 2014 at Pacifico YOKOHAMA, Kanagawa, Japan)

PEM09-44 Room:501 Time:April 29 16:30-16:45

Contribution of the Optical Mesosphere Thermosphere Imagers (OMTIs) to VarSITI

OTSUKA, Yuichi[1*] ; SHIOKAWA, Kazuo[1]

[1]Solar-Terrestrial Environment Laboratory, Nagoya University

The Optical Mesosphere Thermosphere Imagers (OMTIs) consist of thirteen all-sky cooled-CCD imagers, five Fabry-Perot interferometers (FPIs), three meridian scanning photometers, and four airglow temperature photometers. They measure two-dimensional pattern, Doppler wind, and temperature through airglow emissions from oxygen (wavelength: 557.7 nm) and OH (near infrared band) in the mesopause region (80-100 km) and from oxygen (630.0 nm) in the thermosphere/ionosphere (200-300 km). They are in automatic operation at Australia, Indonesia, Thailand, far-east Russia, Japan, Canada, Hawaii, and Norway. Station information and quick look plots are available at http://stdb2.stelab.nagoya-u.ac.jp/omti/. We show recent results obtained by OMTIs particularly focusing on the penetration of short-period gravity wave from the lower atmosphere to the thermosphere and the ionosphere, which are often recognized as meridum-scale traveling ionospheric disturbances (MSTIDs) in the ionosphere. We also show some results obtained by the multi-point Fabry-Perot interferometers. These observations will contribute the next SCOSTEP program VarSITI, particularly to the ROSMIC Project.

Keywords: airglow, ionosphere, thermosphere, mesosphere, gravity wave, traveling ionospheric disturbance

Japan Geoscience Union Meeting 2014
(28 April - 02 May 2014 at Pacifico YOKOHAMA, Kanagawa, Japan)

PEM10-01 Room:414 Time:April 29 14:15-14:35

Modeling Turbulence in Space Plasmas

CHO, Jungyeon[1*]

[1]Chungnam National University

Space plasmas are magnetized and in turbulent states. I will briefly introduce properties of turbulence in a strongly magnetized medium. Turbulence in space plasmas is involved with various length scales. In general, different descriptions should be used for different scales. On large scales, plasma turbulence can be described in the framework of magnetohydrodynamics (MHD). In the first par of the talk, I will focus on MHD turbulence in the presence of a strong mean field. I will discuss energy cascade and structure of turbulence in this regime. On the other hand, on small scales near the proton gyro-scale, we cannot use MHD. In the second part of the talk, I will discuss how we can treat magnetized turbulence on small scales. I will also discuss properties and scaling relations of waves and turbulence in this regime.

Keywords: turbulence, MHD, waves, magnetic field

Japan Geoscience Union Meeting 2014
(28 April - 02 May 2014 at Pacifico YOKOHAMA, Kanagawa, Japan)

PEM10-02 Room:414 Time:April 29 14:35-14:50

Nonlinear evolution of envelope-modulated Alfvenic turbulence in expanding accelerating solar wind plasmas

NARIYUKI, Yasuhiro[1*] ; HADA, Tohru[2] ; TSUBOUCHI, Ken[3]

[1]Faculty of Human Development, University of Toyama, [2]E.S.S.T., Kyushu University, [3]Tokyo Institute of Technology

It is well known that low-frequency Alfvenic turbulence is ubiquitously observed in solar wind plasmas. There is great interest in nonlinear evolution of the Alfvenic turbulence, since the observational studies clarified that the Alfvenic turbulence disappear with the increasing heliocentric distance and the fully-developed turbulence becomes dominant. Although most past studies on Alfvenic turbulence assumes uniform background plasmas and magnetic fields, the effects of the inhomogeneity may not be negligible in the inner-heliosphere, in which several future spacecraft missions are planned. It is important that even if the wave reflection due to the inhomogeneity is negligible, the inhomogeneity of background plasmas and magnetic field may affect the nonlinear interaction among waves through contraction and reflection of the waves and the radial dependence of the back ground parameters such as the Alfven velocity and the ion cyclotron frequency. In the present study, the nonlinear evolution of low-frequency, quasi-parallel propagating Alfvenic turbulence is studied by using the two-dimensional hybrid accelerating expanding box model. The dependence of the nonlinear evolution of Alfvenic turbulence on the effects of the inhomogeneity is discussed.

Keywords: solar wind, Alfvenic turbulence, ion kinetics

Japan Geoscience Union Meeting 2014
(28 April - 02 May 2014 at Pacifico YOKOHAMA, Kanagawa, Japan)

PEM10-03 Room:414 Time:April 29 14:50-15:10

Development and Properties of Compressible MHD Turbulence in High-Beta Plasmas

JONES, Thomas[1*] ; RYU, Dongsu[2] ; PORTER, David[1] ; EMMERICK, Andrew[1] ; CHO, Jungyeon[3]

[1]University of Minnesota, [2]Ulsan National Institute of Science and Technology, [3]Chungnam National University

Many cosmic plasmas, including those in the solar wind and extra-galactic environments, are high beta = P_g/P_B>1, so that as turbulence develops, magnetic stresses are, at least initially, weak. As the turbulence evolves, magnetic stresses become increasingly important on scales below the driving scales. Depending on the initial field strength and topology this evolution can take many large-scale eddy times to reach saturation. Even in subsonic turbulence, shocks can form and influence turbulence evolution and properties. We have carried out an extensive set of high resolution compressible MHD simulations of the evolution of such turbulence for a range of initial magnetic field strengths and topologies. Here we report on their properties and the astrophysical implications of those properties. This work is supported at the University of Minnesota by the US National Science Foundation and the Minnesota Supercomputing Institute.

Keywords: MHD Turbulence, High Beta Plasma

Japan Geoscience Union Meeting 2014
(28 April - 02 May 2014 at Pacifico YOKOHAMA, Kanagawa, Japan)

PEM10-04 Room:414 Time:April 29 15:10-15:30

Instabilities and turbulence near the heliopause

POGORELOV, Nikolai[1*] ; BOROVIKOV, Sergey[2] ; ZANK, Gary[1] ; ZHANG, Ming[3]

[1]Department of Space Science, University of Alabama in Huntsville, [2]CSPAR, University of Alabama in Huntsville, [3]Department of Physics and Space Sciences, Florida Institute of Technology

Recent observations from the Voyager 1 spacecraft show that it is sampling the local interstellar medium (LISM). This is quite surprising because no realistic, steady-state model of the solar wind (SW) interaction with the LISM gives the inner heliosheath width as narrow as 30. This includes such models that assume a strong redistribution of the ion energy to the tails in the pickup ion distribution function. We show that the heliopause (HP), which separates the SW from the LISM, is not a smooth tangential discontinuity, but rather a surface subject to Rayleigh-Taylor-type instabilities which can result in the LISM material penetration deep inside the SW. We also show that the HP flanks are always subject to a Kelvin-Helmholtz instability. The instabilities are considerably suppressed near the HP nose by the heliospheric magnetic field in steady-state models, but reveal themselves in the presence of solar cycle effects. We argue that Voyager 1 may be in one of such instability regions and therefore observing plasma densities much higher than those in the pristine SW. These results may be an explanation of the Voyager 1 early penetration into the LISM. We also show that there is a possibility that the spacecraft may enter the SW again before it finally leaves the heliosphere.

We demonstrate a spontaneous transition to chaotic behavior in the heliosheath region covered by the heliospheric current sheet. Additionally, we analyze the behavior of the heliopause in the heliotail and show that it becomes violently unstable beyond 1000 AU, which results in the interpenetration of the solar and interstellar plasma.

Keywords: ISM: kinematics and dynamics, ISM: magnetic fields, solar wind, Sun: heliosphere, turbulence

Japan Geoscience Union Meeting 2014
(28 April - 02 May 2014 at Pacifico YOKOHAMA, Kanagawa, Japan)

PEM10-05 Room:414 Time:April 29 15:30-15:45

Wave reflection-driven accretion in active solar-type star winds

SUZUKI, Takeru[1*] ; TERANISHI, Yasumasa[1]

[1]Nagoya University

In MHD simulations for winds from active solar-type stars by Suzuki et al.(2013), intermittent but long-time accretion phenomena were observed even though the Poynting flux associated with Alfven waves is directed outward. In this talk, we present the detailed mechanism how this counter-streaming accretion takes place. Alfven waves generated from a stellar surface are stochastically trapped in a transient density hole, and the magnetic pressure with the waves further dig the density hole. Eventually, this hole works as an efficient mirror against out-going Alfven waves. As a result, out-going waves are reflected and the reflected component excites counter streaming flow.

Keywords: Wave, MHD, stellar wind, accretion

Japan Geoscience Union Meeting 2014
(28 April - 02 May 2014 at Pacifico YOKOHAMA, Kanagawa, Japan)

PEM10-06 Room:414 Time:April 29 15:45-16:00

Physical Picture of 2-1/2D Driven Collisionless Magnetic Reconnection

CHENG, Chio[1*] ; INOUE, S.[2] ; ONO, Y.[3] ; HORIUCHI, R.[4]

[1]Plasma and Space Science Center, National Cheng Kung University, Taiwan, [2]Graduate School of Engineering, Universty of Tokyo, Japan, [3]Department of Advanced Energy, University of Tokyo, Japan, [4]National Institute of Fusion Science, Japan

The physical picture of how electrons and ions flow, how the electric and magnetic fields change, and how particles gain energy will be presented for the 2-1/2D collisionless driven magnetic reconnection. The 2-1/2 dimensional collisionless reconnection studies are performed using the particle simulation PASMO code [1] and theoretical analysis. In particular, we will provide the physical mechanism of how the poloidal current (including the Hall current in the downstream region) is generated and how the electrostatic potential is produced in the poloidal plane. The physical picture of how the quadrupole magnetic field and electrostatic potential are generated in the 2-dimensional (poloidal) plane is different from the one presented by Uzdensky and Kulsrud.[2]

[1] H. Ohtani and R. Horiuchi, Plasma Fusion Res., 4, 024 (2009)
[2] D. A. Uzdensky and R. M. Kulsrud, Phys. Plasma, 13, 062305 (2006)

Keywords: magnetic reconnection, numerical simulation, space plasma, laboratory experiment

Japan Geoscience Union Meeting 2014
(28 April - 02 May 2014 at Pacifico YOKOHAMA, Kanagawa, Japan)

PEM10-07 Room:414 Time:April 29 16:15-16:35

Turbulence and shocks in high-beta plasmas

RYU, Dongsu[1*]

[1]Department of Physics, UNIST

High-beta plasmas are common in astrophysical environments, such as the intracluster medium (ICM) of galaxy clusters and the interplanetary medium (IPM) of the solar system. Observations and theoretical arguments suggest that the plasmas in such environments are in the state of turbulence, where highly nonlinear and complex physics is involved. Here we report high-resolution simulations to study the turbulence in high-beta plasmas. Along with the properties of the turbulence, we discuss the role of shocks and the energy dissipation.

Keywords: turbulence, shock wave, high-beta plasma

Japan Geoscience Union Meeting 2014
(28 April - 02 May 2014 at Pacifico YOKOHAMA, Kanagawa, Japan)

PEM10-08 Room:414 Time:April 29 16:35-16:50

Acceleration and Diffusion of Cosmic Rays in Supernova Remnants in a Multi-Phase interstellar Medium

ROH, Soonyoung[1*] ; INUTSUKA, Shu-ichiro[2] ; INOUE, Tsuyoshi[3]

[1]Graduate School of Science, Nagoya University, [2]Graduate School of Science, Nagoya University, [3]Department of Physics and Mathematics, Aoyama Gakuin University

Supernova remnants (SNRs) are one of the most powerful cosmic phenomena and are thought to be the dominant source of Galactic cosmic rays (CRs). A recent report by Funk et al. (2013) has shown an unequivocal signature of pion-decay in the gamma-ray spectra of SNRs. This provides strong evidence that high-energy protons are accelerated in SNRs. On the other hand, Fukui et al. (2012) showed that pion-decay from protons dominates in emission from SNR RX J1713 based on the spatial correlation of gamma-rays and molecular line emission. The actual gamma-ray emission from pion-decay should depend on the diffusion of CRs in a multi-phase interstellar medium with molecular clouds (Inoue et al. 2012). In order to quantitatively describe the diffusion of high energy CRs from acceleration sites, we have performed test particle numerical simulations using a three-dimensional magnetohydrodynamics (MHD) simulation data cube provided by Inoue et al. (2012). In this presentation, we analyze a realistic diffusion coefficient of cosmic rays in simulated SNRs, and discuss the possible implications for X-ray and gamma-ray observations.

Keywords: Supernova Remnants, Diffusion of Cosmic Rays, Acceleration of Cosmic Rays, Pion-decay

Japan Geoscience Union Meeting 2014
(28 April - 02 May 2014 at Pacifico YOKOHAMA, Kanagawa, Japan)

PEM10-09 Room:414 Time:April 29 16:50-17:05

Superdiffusion in turbulence and shock acceleration

YAN, Huirong[1*]

[1]Kavli Institute of Astronomy & Astrophysics, Peking U

Cosmic ray (CR) transport and acceleration are determined by the properties of turbulent magnetic field. We use the models of magnetohydrodynamic turbulence that were tested in numerical simulation, in which turbulence is injected at large scale and cascades to to small scales. I shall address, in particular, the cross field transport of CRs. I shall demonstrate both analytically and numerically that particles are superdiffusive on small scales. We consider both super- and sub-Alfvenic cases. In the sub-Alfvenic case, the transport in the perpendicular direction is proportional with M_Aˆ4, consistent with our earlier analytical prediction. Implication for shock acceleration is discussed and we show that the difference between acceleration at perpendicular shock and parallel shock is marginalized in the presence of superdiffusion.

Keywords: turbulence, superdiffusion, particle, shock, acceleration, transport

Japan Geoscience Union Meeting 2014
(28 April - 02 May 2014 at Pacifico YOKOHAMA, Kanagawa, Japan)

PEM27-01 Room:421 Time:May 1 16:15-16:30

Micro-TypeIII radio bursts and outer corona

MORIOKA, Akira[1*] ; MIYOSHI, Yoshizumi[2] ; KASABA, Yasumasa[3] ; MASUDA, Satoshi[2] ; IWAI, Kazumasa[4] ; MISAWA, Hiroaki[1]

[1]PPARC, Tohoku University, [2]STEL, Nagoya University, [3]Dep. of Gephys. Tohoku University, [4]NSRO, NAOJ

We presents detailed features of micro-typeIII radio bursts and its relation to the outer corona, by using long-term observations made by the Geotail satellites. Micro-typeIII radio bursts are elements of the so-called type III storm, and are characterized by short-lived, continuous, and weak emissions. Their average power is estimated to be well below that of the largest type III burst by 6 orders of magnitude. The activity of micro-typeIII bursts with respect to the solar activity, lower frequency limit of the bursts and its relation to the solar activity, and the configuration of magnetic field line of which source electrons are trapped are investigated. The relationship between streamers and micro-typeIII bursts are discussed by using STEREO observations.

Keywords: micro-type-III burst, outer corona, solar radio burst, interplanetary space, inner-heliosphere

Japan Geoscience Union Meeting 2014
(28 April - 02 May 2014 at Pacifico YOKOHAMA, Kanagawa, Japan)

PEM27-02 Room:421 Time:May 1 16:30-16:45

Coronal vector magnetic field and the plasma beta determined from the NoRH and multiple satellites observations

IWAI, Kazumasa[1*] ; SHIBASAKI, Kiyoto[1] ; NOZAWA, Satoshi[2] ; TAKAHASHI, Takuya[3] ; SAWADA, Shinpei[2] ; KITAGAWA, Jun[4] ; MIYAWAKI, Shun[2] ; KASHIWAGI, Hirotaka[5]

[1]Nobeyama Solar Radio Observatory, National Astronomical Observatory of Japan, [2]Department of Science, Ibaraki University, [3]Graduate School of Science, Kyoto University, [4]Solar-Terrestrial Environment Laboratory, Nagoya University, [5]Planetary Plasma and Atmospheric Research Center, Tohoku University

In the solar corona, there are various kinds of eruptive phenomena, such as flares and coronal mass ejections, which are caused by interactions between the coronal magnetic field and plasma. Hence, it is important to precisely measure the coronal plasma parameters, including the magnetic field, plasma density, and temperature, in order to understand the mechanisms that generate these eruptive coronal phenomena.

The solar coronal vector magnetic field, plasma density, and temperature is derived from coordinated observations of the radio thermal free-free emission using the Nobeyama Radioheliograph (NoRH) and multiple line-of-sight extreme ultraviolet observations using the Solar Dynamic Observatory (SDO) and the Solar Terrestrial Relations Observatory (STEREO). We observed a post-flare loop on the west limb on 2013 April 11. The line-of-sight magnetic field was derived from the circularly polarized free-free emission observed by NoRH, which was combined with the tilt angle toward the Earth observed with STEREO and converted to a vector magnetic field. The emission measure and temperature were derived from the Atmospheric Imaging Assembly (AIA) onboard SDO. The derived temperature was used to estimate the emission measure from the NoRH radio free-free emission observations. The derived density from NoRH was 40% larger than that determined using AIA, which is due to the fact that the low temperature plasma is not within the temperature coverage range of the AIA filters used in this study. The derived plasma parameters (vector magnetic field, plasma density, and temperature) were used to derive the plasma beta, which is a ratio between the magnetic pressure and the plasma pressure. The derived plasma beta is about 6.2×10^{-3} at the pool top region. The plasma parameters derived in this study were all based on observational results, and the calculated vector magnetic field presented herein is one of the least affected by assumptions or modeling ever derived.

Keywords: Sun, corona, magnetic fields, polarization observation, Nobeyama Radioheliograph

Japan Geoscience Union Meeting 2014
(28 April - 02 May 2014 at Pacifico YOKOHAMA, Kanagawa, Japan)

PEM27-03 Room:421 Time:May 1 16:45-17:00

Relationships among cosmic ray intensity, the photospheric magnetic field, and solar wind speed

HAKAMADA, Kazuyuki[1*] ; TOKUMARU, Munetoshi[2] ; FUJIKI, Ken'ichi[2] ; KOJIMA, Masayoshi[2]

[1]Chubu University, [2]Solar-Terrestrial Environment Laboratory

We visualize three-dimensional structure of the coronal magneic field by using the Radial-Field model for the coronal magnetic field devised by Hakamada with synoptic maps of photospheric magnetic field observed by the NSO/Kitt Peak, USA. As the rsults, we obtained the radial component of the photospheric magnetic field (Br_pho) and the one of the coronal magnetic field (Br_sou) on the source surface on the same field line in the coronal magnetic field. We estimate the solar wind speed (SWS) by using IPS technique divised by STE Lab, Nagoya Univiersity. According to our previous analysis on the Carrignton rotation bases, Log10|Br_pho|, Log10|Br_sou|show good correlations with the SWS for the data of [-1.0 <= Log10|Br_pho|<= 1.5, (0.1 G <= |Br_pho|<= 31.6 G), -1.5 <= Log10|Br_sou|<= 0.0, (0.0316 G <= |Br_sou|<= 1.0 G)]. In this study, we add the intensity of Oulu neutorn monitor (NM), and study relations among rotation averages of these NM, SWS, and Log10|Br_pho|. We found good simple correrations coefficients between Log10|Br_pho|-NM (r=-0.773), and SWS-NM (r=0.703), as well as, a good multiple correlaion (r = 0.785) among them by using the regression equation in the form of NM = a + b ∗SWS + c ∗log10|Br_pho|with a = 6363, b = 1.186, and c = -1400.0. However, Log10|Br_pho|-SWS also shows good simple correlation (r=-0.802). We calculated partial correlation coefficients between (a) Log10|Br_pho|-NM, (b) SWS-NM, (c) Log10|Br_pho|-SWS and obtained (a) r=-0.294, (b) r=0.130, (c) r=-0.364. These results suggest that, althogh the cosmic ray intensities shown by NM is determined by the intensity of photospheric magnetic fields on the open field lines and the solar wind speed occupied by these field lines, the dpendence of magnetic field is stronger than the one of wind speed.

Keywords: cosmic ray intensity, photoshpheric magnetic field, solar wind speed

Japan Geoscience Union Meeting 2014
(28 April - 02 May 2014 at Pacifico YOKOHAMA, Kanagawa, Japan)

PEM27-04 Room:421 Time:May 1 17:00-17:15

Does a Plasma Tail of Comet ISON (C/2012 S1) Cause the Interplanetary Scintillation?

IJU, Tomoya[1*] ; ABE, Shinsuke[2] ; TOKUMARU, Munetoshi[3]

[1]Particle and Astrophysical Science, Nagoya-University, [2]Aerospace Engineering, CST, Nihon-University, [3]Solar-Terrestrial Environment Laboratory, Nagoya-University

C/2012 S1 (ISON) (referred to as Comet ISON) showed a well-developed plasma tail (longer than 0.1 AU) before its perihelion passage on November 28, 2013. A plasma tail consists of ionized gases emitted from a cometary nucleus and orients itself in the anti-solar direction by an interaction with the solar wind. In this study, we investigated the plasma tail of Comet ISON with interplanetary scintillation (IPS) data. The IPS is a scattering phenomenon of radio waves by density fluctuations of the solar wind, and it is well known that interplanetary disturbances such as coronal mass ejections (CMEs) cause an abrupt increase in IPS. A cometary plasma tail may also be a potential cause for the IPS enhancement, while observational studies for C/1972 E1 (Kohoutek), 1P/Halley and other are still controversial (*e.g.* Ananthakrishnan *et al.*, 1975, 1987; Slee *et al.*, 1987; Abe *et al.*, 1997; Roy *et al.*, 2007). We identified radio sources whose lines-of-sight approached to Comet ISON's plasma tail between November 1 and 28, and obtained their IPS data using the Solar Wind Imaging Facility (Tokumaru *et al.*, 2011) of the Solar-Terrestrial Environment Laboratory, Nagoya University. From examinations for them, we confirmed four IPS enhancement events, which is likely to be related to the plasma tail passage. In this session, we report this preliminary result for them and discuss an IPS of a cometary plasma tail origin.

Keywords: Comet ISON (C/2012 S1), Cometary plasma tail, Radio scintillation

Japan Geoscience Union Meeting 2014
(28 April - 02 May 2014 at Pacifico YOKOHAMA, Kanagawa, Japan)

PEM27-05 Room:421 Time:May 1 17:15-17:30

Effects of phase and group velocities on wave spectra observed in the solar wind

TSUGAWA, Yasunori[1*] ; KATOH, Yuto[1] ; TERADA, Naoki[1]

[1]Department of Geophysics, Tohoku University

Waves propagating in a plasma medium which has a relative velocity to the observer are differently observed in the spectra from those in the plasma rest frame. As known in general, the observed frequency is Doppler shifted by the relative velocity between the medium and the observer, V_{rel}. The frequency shift is the result of the difference of the phase velocities of the waves in the medium rest frame and in the observer frame. When the wave vector has a finite angle with respect to V_{rel} and the component of V_{rel} parallel to the wave vector is considerable to the phase velocity, the difference of the phase velocities between the frames and the frequency shift become significant.

We note that the observed spectral density is also modified by V_{rel}. The modification of the spectral density is the result of the difference of the group velocities of the waves in the medium rest frame and in the observer frame. When the component of V_{rel} parallel to the group velocity vector is considerable to the group velocity, the difference of the group velocities between the frames and the modification of the spectral density become significant. In order to estimate the amount of the modification, we derive the analytical expression of the modified spectral density in the observer frame.

It is important to consider not only the frequency shift but also the modification of the spectral density of waves observed by spacecraft in a moving plasma, such as the solar wind. Indeed, the phase and group velocities of whistler-mode waves cause significant frequency shift and modification of the spectral density in the solar wind. By the modification of the spectral density, we can explain the characteristic properties of '1 Hz waves', which have been generally observed in the upstream regions of various bodies, and suggest that the broadband upstream whistlers are the same source waves. The understanding of the effects is necessary to reveal the true nature of waves propagating in a moving plasma and to discuss their generation processes.

Japan Geoscience Union Meeting 2014
(28 April - 02 May 2014 at Pacifico YOKOHAMA, Kanagawa, Japan)

PEM27-06 Room:421 Time:May 1 17:30-17:45

Monochromatic whistler waves at 8 Hz observed by Kaguya above the terminator of the Moon

HASHIMOTO, Akira[1] ; NAKAGAWA, Tomoko[1*] ; TSUNAKAWA, Hideo[2] ; TAKAHASHI, Futoshi[2] ; SHIBUYA, Hidetoshi[3] ; SHIMIZU, Hisayoshi[4] ; MATSUSHIMA, Masaki[2]

[1]Information and Communication Engineering,Tohoku Institute of Technology, [2]Deparment of Earth and Planetary Sciences, Tokyo Institute of Technology, [3]Department of Earth and Environmental Sciences, Graduate School of Science and Technology, Kumamoto, [4]Earthquake Research Institute, University of Tokyo

Magnetic fluctuations around the moon are characterized with 2 major categories: (1) large amplitude monochromatic waves of 0.01 Hz and (2) monochromatic or non-monochromatic whistler waves, both observed on the dayside surface of the moon or above the terminator. Their generation is associated with (1) the solar wind ions or (2) electrons, respectively, reflected at the surface of the moon or the local crustal magnetic field. The monochromatic whistler waves are found at 1-2 Hz with left-handed polarization due to the Doppler shift caused by the solar wind flow. The frequency range is determined by the group velocity of the whistler waves that can overcome the solar wind speed.

Differently from the previously known characteristics, a new type of monochromatic waves was found at 8 Hz in the magnetic field data obtained by MAP/LMAG onboard Kaguya. They concentrated above the terminator. They propagated in the direction of the background magnetic field and showed right-hand polarization. They are thought to be whistler waves propagating down-stream, and the frequency was up-shifted due to the Doppler shift.

Keywords: moon, SELENE, KAGUYA, MAP/LMAG, whistler wave, solar wind

Japan Geoscience Union Meeting 2014
(28 April - 02 May 2014 at Pacifico YOKOHAMA, Kanagawa, Japan)

PEM27-P01 Room:Poster Time:May 1 18:15-19:30

Measurement result of the neutron monitor onboard the Space Environment Data Acquisition Equipment(SEDA-AP)

KOGA, Kiyokazu[1*] ; MURAKI, Yasushi[2] ; SHIBATA, Shoichi[3] ; YAMAMOTO, Tokonatsu[4] ; MATSUMOTO, Haruhisa[1] ; OKUDAIRA, Osamu[1] ; KAWANO, Hideaki[5] ; YUMOTO, Kiyohumi[5]

[1]JAXA, [2]Nagoya University, [3]Chubu University, [4]Konan University, [5]Kyushu University

To support future space activities, it is crucial to acquire space environmental data related to the space-radiation degradation of space parts and materials, and spacecraft anomalies. Such data are useful for spacecraft design and manned space activity.
SEDA-AP was mounted on ”Kibo” of the ISS (International Space Station) to measure the space environment at a 400-kilometer altitude.

Neutrons are very harmful radiation, with electrical neutrality that makes them strongly permeable. SEDA-AP measures the energy of neutrons from thermal to 100 MeV in real time using a Bonner Ball Detector (BBND) and a Scintillation Fiber Detector (FIB). BBND detects neutrons using He-3 counters, which have high sensitivity to thermal neutrons. Neutron energy is derived using the relative response function of polyethylene moderators of 6 different thicknesses. FIB measures the tracks of recoil protons caused by neutrons within a cubic arrayed sensor of 512 scintillation fibers. The charged particles are excluded using an anti-scintillator which surrounds the cube sensor, and the neutron energy is obtained from the track length of a recoil proton.

There are three sources of neutrons in space;
1. Albedo Neutrons
Produced by reactions of galactic cosmic rays or radiation belt particles with the atmosphere
2. Local Neutrons
Produced by the reactions of galactic cosmic rays or radiation belt particles with spacecraft
3. Solar Neutrons
Produced by accelerated particles in solar flares
An accurate energy spectrum of the solar neutrons includes important information on high-energy particle generation mechanism in a solar flare, because neutrons are unaffected by interplanetary magnetic fields. These data will become useful to forecast solar energetic particles in future. Some candidate events involving solar neutrons were found as a result of analyzing data of the solar flare of M>2 since September 2009.

Moreover, it is important to measure albedo neutrons, since protons generated by neutron decays are thought to originate from the radiation belt. This theory is called CRAND (Cosmic Ray Albedo Neutron Decay). Our observation result is consistent with the CRAND theory prediction in the case of low-energy parts. Moreover, the flux and angular distribution of local neutrons were estimated using the nuclear simulation code ”PHITS” to evaluate the influence of local neutrons on the structure of SEDA-AP and ”Kibo”.

The results of our analyses on solar and albedo neutrons are reported in this paper.

Japan Geoscience Union Meeting 2014
(28 April - 02 May 2014 at Pacifico YOKOHAMA, Kanagawa, Japan)

PEM27-P02 Room:Poster Time:May 1 18:15-19:30

Interplanetary emission observed by HISAKI (SPRINT-A) satellite

YAMAZAKI, Atsushi[1*] ; YOSHIOKA, Kazuo[1] ; MURAKAMI, Go[1] ; KIMURA, Tomoki[1] ; TSUCHIYA, Fuminori[2] ; KAGITANI, Masato[2] ; SAKANOI, Takeshi[2] ; TERADA, Naoki[3] ; KASABA, Yasumasa[3] ; YOSHIKAWA, Ichiro[4]

[1]Institute of Space and Astronautical Science / Japan Aerospace Exploration Agency, [2]Planetary Plasma and Atmospheric Research Center, Graduate School of Science, Tohoku University, [3]Dep. Geophysics Graduate School of Science Tohoku University, [4]The University of Tokyo

The HISAKI (SPRINT-A) satellite, which was launched last summer, has been observing the extreme ultraviolet emission around planets, such as Venus and Jupiter. In addition to the main observational target of Venus and Jupiter, HISAKI has detected the emission from interplanetary space. In this presentation the HISAKI observation of interplanetary emission is shown and its potential on the interplanetary issue is argued.

Keywords: HISAKI (SPRINT-A) satellite, extreme ultra violet emission, interplanetary, resonance scattering

Japan Geoscience Union Meeting 2014
(28 April - 02 May 2014 at Pacifico YOKOHAMA, Kanagawa, Japan)

PEM27-P03 Room:Poster Time:May 1 18:15-19:30

The Behavior of Distributions for Magnetic Polarities on the Surface of the Sun and Solar Minimum

SEINO, Mitsuhiro[1*] ; SHIMABUKURO, Tomomi[1]

[1]Department of Physics and Earth Sciences, Faculty of Science, University of the Ryukyus

Time series of satellite image data for SOHO/MDI Continuum and Magnetogram from 1997 to 2010, and for SDO/HMI Continuum and Magnetogram from 2011 to 2013 are analyzed. The new time series data derived from fractal analysis of the time series images illustrated in 1200x1200 pixels from 1997 to 2013 are generated and fractal measures and packing exponents are analyzed by box-counting method. Then the occupancies of sunspot pixels in Continuum and of pixels for the positive and negative magnetic polarities in Magnetogram are calculated and packing exponents for sunspot pixels in Continuum and packing exponents for positive polarity pixels and negative polarity pixels in Magnetogram are evaluated. For packing exponents of Continuum and Magnetogram from 1997 to 2013, power spectra with peaks are calculated by using Fourier transform, respectively. A first peak which appears the power spectra is determined, and time intervals between nearest neighbor peaks are valued. The correlations between sunspot numbers and occupancies of the positive and negative magnetic polarities for 17 years are anatomized. As the correlation coefficients are calculated by using the least squares method, the correlation between sunspot number and occupancy of positive magnetic polarities has a very high correlational relationship because the correlation coefficient is 0.86 and it for negative magnetic polarities is low.

Furthermore, the behavior of occupancies of sunspot pixels in Continuum and of pixels for the positive and negative magnetic polarities in Magnetogram and the packing exponents represented with time series are described in detail and discussed. Fluctuations for occupancies of positive magnetic polarities are similar to it for Zurich number from 1997 to 2013. As observing the occupancies and packing exponents of positive and negative magnetic polarities, the two and three different fluctuations appear in (1) 1997-2005 and 2009 and (2) 2006-2008 including the time period that solar cycle 24 began on January 4, 2008, respectively. In addition, the occupancies and packing exponents of them have a single fluctuation in (3) 2010-2013. Therefore, the periods for characterizing solar activity from 1997 to 2013 are divided into three periods in (1), (2), and (3). Specially, for 2 years before solar minimum on 2008, the packing exponents start fluctuating suddenly and sharply in 2006 and the fluctuation disappear in the end of 2009.

Keywords: Time Series Analysis, Fourier Analysis, SOHO/MDI Continuum, Magnetogram, Solar Minimum

Japan Geoscience Union Meeting 2014
(28 April - 02 May 2014 at Pacifico YOKOHAMA, Kanagawa, Japan)

PEM27-P04 Room:Poster Time:May 1 18:15-19:30

Fine spectral structures of a solar radio type-II burst observed with AMATERAS

SATO, Shintaro[1] ; MISAWA, Hiroaki[1*] ; TSUCHIYA, Fuminori[1] ; OBARA, Takahiro[1] ; IWAI, Kazumasa[2] ; MASUDA, Satoshi[3] ; MIYOSHI, Yoshizumi[3]

[1]PPARC, Tohoku Univ., [2]Nobeyama Solar Radio Observatory, NAOJ, [3]STE Lab., Nagoya Univ.

Solar radio type-II bursts are metric to hectometric radio bursts that show frequency drifting spectral structures caused by the plasma emission from shock-accelerated electrons. The bursts are known to sometimes show rapidly drifting fine structures; for example, about 20% of type-II bursts are composed of both negative and positive rapidly drifting elements, which are called as ”herringbone” structure (hereafter HB) [Roberts, 1959]. Such the drifting fine structures are interpreted as the motion of non-thermal energetic electron beams accelerated by the shock. However, their particle acceleration mechanisms and regions have not been understood well. The purpose of this study is to extract characteristics of the fine spectral structures of type-II bursts from high-resolution observations and investigate their acceleration processes.

AMATERAS is a ground-based solar radio receiving system developed in 2010 by Tohoku University [Iwai et al., 2012]. This system enables us to observe radio phenomena in 150 - 500 MHz with the 10 ms accumulation time and 61 kHz bandwidth. So far some type-II bursts with fine spectral structures have been observed. Among them, a type-II burst observed on November 12, 2010 around 200MHz showed distinctive fine structures whose spectral characteristics were different from those of HB. The fine structures showed no core structure which were normally confirmed in HB, but showed various rapidly drifting nature and composed whole body of a slowly negative-drifting type-II burst. The statistical drift rate analysis showed that negative drift cases were dominant and some of them indicated more than 100MHz/s. The particle speed for the drift rate by assuming a general coronal plasma density model, for example the Newkirk model [Newkirk, 1961], is estimated to be unrealistically fast. This implies that the rapidly drifting fine structures were generated by energetic electron beams in an outward moving steep density gradient region such as a shock front.

In this presentation, we will show revealed statistical characteristics of the fine structures and discuss inferred generation processes of the type-II burst. We will also introduce characteristics of fine spectral structures of the other events of type-II burst.

Keywords: Sun, radio wave, type-II burst, fine structure, generation process

Japan Geoscience Union Meeting 2014
(28 April - 02 May 2014 at Pacifico YOKOHAMA, Kanagawa, Japan)

PEM27-P05 Room:Poster Time:May 1 18:15-19:30

Spectral fine structure of solar radio bursts observed with IPRT/AMATERAS: Characteristics of Zebra Pattern

KANEDA, Kazutaka[1*] ; MISAWA, Hiroaki[1] ; TSUCHIYA, Fuminori[1] ; OBARA, Takahiro[1] ; IWAI, Kazumasa[2]

[1]PPARC, Tohoku University, [2]NSRO/NAOJ

It is known that there are a variety of complex fine structures in solar radio bursts in the meter to decimeter wave bands such as broadband pulsations, narrowband spikes, fiber bursts and zebra patterns (hereafter ZP). Since they are thought to be caused by some inhomogeneities or modulations of wave generation and/or radio propagation processes, they have significant information about plasma parameters and dynamical plasma processes in the solar corona. Among the various fine structures, ZP has a particularly characteristic spectral pattern with parallel drifting narrow stripes of enhanced emission. Although several models for generating ZP have been proposed so far, the generation mechanisms have not been revealed well yet.

AMATERAS (the Assembly of Metric-band Aperture Telescope and Real-time Analysis System) is a radio spectro-polarimeter installed in a large radio telescope named IPRT in Fukushima, which was developed for solar radio observations in 2010 by Tohoku University (Iwai et al., 2012). The specifications of this system are time resolution of 10 ms, frequency resolution of 61 kHz and the minimum detectable flux of 0.7 s.f.u. in the frequency range of 150 MHz to 500 MHz, which are enough to observe fine structures of solar radio bursts and analyze their spectral characteristics. In this study we focus on an event on June 21, 2011 associated with C7.7 class flare. In this event enhanced ZP appeared around 200MHz with about 30 stripes in fast drifting envelopes like type III bursts or broadband pulsations. The emission was strongly polarized in right-handed and shows a distinctive time delay of the left-handed component relative to the right-handed component by several tens msec increasing with emission frequency. In the presentation, we will show the characteristics of ZP precisely and also discuss the expected generation processes.

Keywords: solar radio, AMATERAS, zebra pattern

Japan Geoscience Union Meeting 2014
(28 April - 02 May 2014 at Pacifico YOKOHAMA, Kanagawa, Japan)

PEM27-P06 Room:Poster Time:May 1 18:15-19:30

Upgrade of the multi-station IPS system and solar wind observations at the cycle 24 maximum

TOKUMARU, Munetoshi[1*] ; FUJIKI, Ken'ichi[1] ; MARUYAMA, Kazuo[1] ; MARUYAMA, Yasushi[1] ; YAMASAKI, Takayuki[1] ; IJU, Tomoya[1]

[1]Solar-Terrestrial Environment Laboratory, Nagoya University

Since interplanetary scintillation (IPS) serves as a useful method to determine global distribution of the solar wind, IPS observations have been regularly conducted over more than 30 years using the multi-station system of the Solar-Terrestrial Environment Laboratory (STEL) of Nagoya University. Such long-term data collection is made possible by continuous maintenance and improvement of the system. The STEL has four antennas dedicated for IPS observations at Toyokawa, Fuji, Kiso, and Sugadaira. The system at Toyokawa was upgraded to a new antenna (called the Solar Wind Imaging Facility Telescope, SWIFT, Tokumaru et al., 2011) in 2008. After that, the observation control and data acquisition systems at Fuji and Kiso were upgraded in 2010 to enable 3-station IPS observations using Toyokawa, Fuji and Kiso antennas. However, the low-noise phased-array receivers of Fuji and Kiso antennas, which are a vital part to archive high sensitivity, remained unchanged, and some other parts such as reflectors, gears, motors, became superannuated. In order to improve these problems, we have performed extensive work for upgrading Fuji, Kiso and Sugadaira antennas since 2013.

The items for this upgrade are as follows; (1) installation of low-noise amplifiers using HEMTs (FE327-V5) and the phased-array control system, (2) development of the phase/gain calibration system using the loop method and the receiver temperature measurement system using a noise source for Fuji and Kiso antennas, (3) fabrication of reflector and replacement of gears and motors (for Kiso). The work at Fuji almost completed by the end of 2013, and that at Kiso will be made in this spring.

Owing to the upgrade project, IPS observations for 2013 was made for the period between April and August. Obtained IPS data clearly show that the fast wind reappears over the northern pole. This is not the case for the southern pole, and the slow wind is found to be dominant in the southern hemisphere. The disappearance and reappearance of the fast wind over the northern pole preceding that over the southern pole have been observed in solar maxima of two previous cycles, so that this is regarded as a common feature of the solar dynamo activity. While our IPS data for this cycle show good correlation between fast wind areas and polar fields, they reveal that the slope for this cycle differs from the ones for past cycle. This fact suggests that higher-order magnetic moments for this cycle may have more contribution for formation of fast winds than past cycles. The solar wind structure is expected to significantly change with declining solar activity toward the next minimum, and we intend to finish work for the upgrade project as soon as possible in order to miss observing this change.

Keywords: solar wind, interplanetary scintillation, heliosphere, solar cycle, space weather

Japan Geoscience Union Meeting 2014
(28 April - 02 May 2014 at Pacifico YOKOHAMA, Kanagawa, Japan)

PEM28-01 Room:413 Time:April 29 11:00-11:15

MLT dependence in the response of ionospheric electric fields at mid-low latitude during geomagnetic sudden commencement

TAKAHASHI, Naoko[1*] ; KASABA, Yasumasa[1] ; SHINBORI, Atsuki[2] ; NISHIMURA, Yukitoshi[3] ; KIKUCHI, Takashi[4] ; NAGATSUMA, Tsutomu[5]

[1]Graduate School of Science, Tohoku University, [2]Research Institute for Sustainable Humanosphere (RISH), Kyoto University, [3]University of California, Los Angeles, [4]Solar-Terrestrial Environment Laboratory, Nagoya University, [5]National Institute of Information and Communications Technology

The geomagnetic sudden commencement (SC) is one of the geomagnetic disturbance phenomena triggered by an enhancement of the magnetopause current associated with the compression of the magnetosphere due to solar wind disturbances [e.g., Araki, 1994]. Detailed evolution and propagating processes of the electromagnetic field associated with SCs are observed three-dimensionally in the entire geospace. Unlike magnetic storms and substorms which involve complex plasma physical processes, SCs can be identified as distinct magnetic variations that sharply change on a global scale. However, the characteristics of SCs have been extensively investigated mainly by means of the magnetic field variations obtained by ground-based observations, which could be affected by conductivities when deducing electric fields. Thus, investigating the electric field variations is needed to understand the transport of electromagnetic energy (Poynting fluxes, E$\times$B/μ) associated with SCs. In this study, we examined two critical subjects about the ionospheric electric field associated with SCs using the in-situ electric field data.

The in-situ ionospheric electric field was derived from the drift velocity observed by the Ionospheric Plasma and Electrodynamics Instrument (IPEI) onboard ROCSAT-1, which orbited at an ionospheric altitude (about 600 km), with magnetic field from the IGRF-10 model. We also used the geomagnetic field data from ground stations at the subauroral region, mid and low latitudes, and dip equator with a high time resolution of 1 second.

The first subject is the transmission time of the ionospheric electric field from the subauroral region to the dip equator. We found the simultaneous SC onset between the ionospheric electric field by the ROCSAT-1 observations and geomagnetic fields by ground-based observations, and the time delay in the peak amplitudes of the preliminary impulse (PI) and main impulse (MI) occur irrespective of the magnetic local time (MLT). In statistical analyses, we showed that peak signatures of the ionospheric electric field at the low latitude appeared simultaneously with that of the geomagnetic field at the subauroral region. We also found that the peak signature at the equatorial region was observed with the time delay, and its value is about 20-40 seconds in the PI peak and 80-140 seconds in the MI peak. The instantaneous onset can be explained by means of the TM_0 mode waves propagating at the speed of light in the Earth-ionosphere waveguide, while the time delay in the peaks is interpreted as the difference of the time constant L/R of an equivalent circuit. From these results, we demonstrated the transmission of the electric field from the subauroral region and the common energy transport process for both the PI and MI.

The second subject is the global structure of the ionospheric field. Ground-based observations are limited to mid and low latitudes, and provide only the horizontal component (E_{phi}) of the electric field. Thus, it is difficult to estimate the global electric field variation, especially at the terminator sector where SC signatures tend to appear in the radial component (E_r) of the electric field. We found the MLT dependence of the SC amplitude both the PI and MI signatures in the E_r and E_{phi} electric fields. In addition, the dayside characteristics of the PI signature extended to the evening terminator sector (18-21 h MLT) with an enhancement around 20 h MLT. This tendency is consistent with previous results obtained by the ground-based observations and model calculations. We consider that enhancements associated with SCs are influenced by the non-uniform ionospheric conductivity.

In the present study, we revealed the global instant response of the ionospheric electric field during SCs based on the in-situ ionospheric electric field observations. Our results can serve as a basis for understanding energy transmission paths during rapid reconfigurations of ionospheric convection.

Japan Geoscience Union Meeting 2014
(28 April - 02 May 2014 at Pacifico YOKOHAMA, Kanagawa, Japan)

PEM28-02 Room:413 Time:April 29 11:15-11:30

Evolution of convection vortices associated with sudden impulses observed by SuperDARN

HORI, Tomoaki[1*] ; SHINBORI, Atsuki[2] ; NISHITANI, Nozomu[1] ; FUJITA, Shigeru[3]

[1]STE lab, Nagoya Univ, [2]RISH, Kyoto Univ, [3]Meteorological College

Spatial evolution of transient ionospheric convection induced by sudden impulses (SIs) recorded by ground magnetometers is studied statistically by using SuperDARN (SD) data. An advantage of using SD data instead of ground magnetic fields is that ionospheric flows measured by the radars are not virtually biased by the spatially-varying ionospheric conductance or the magnetospheric currents. First we surveyed the Sym-H index for Jan., 2007 to Dec., 2012 to identify SI events with a peak amplitude |dSym-H|greater than 10 nT. Next we searched all SD data over the northern hemisphere during the SI events for ionospheric backscatters which give us the light-of-sight velocity of horizontal ionospheric flows. For each SI event, the collected ionospheric flow data were sorted into the four periods: the pre-SI period, the pre-Main Impulse (MI), middle-MI, and post-MI periods. In the present study, we examine the differences in flow velocity between the pre-SI period and the three MI periods to clarify how ionospheric flows change in association with SIs. As a result, the ionospheric flow shifts eastward on the dusk side and westward on the dawn side at the higher latitudes during positive SIs (SI+), while it shows a roughly westward/eastward shift on the dusk/dawn side, respectively, during negative SIs (SI-). These polarities of flow shifts are basically consistent with the higher latitude portions of the DP current for the MI phase as shown by Araki [1994] and Araki and Nagano [1988]. The high latitude flow shifts are basically larger for SI events with larger Sym-H variations, in the same fashion as ground magnetic field variations at high latitudes. In addition to the major dependence on SI amplitude, the flow shift magnitude shows a minor dawn-dusk asymmetry particularly under strong IMF-By conditions. We speculate that the interaction with pre-existing convection cells might cause the selective enhancement of either side of flow shifts.

Keywords: sudden impulse, SuperDARN, ionospheric convection

Japan Geoscience Union Meeting 2014
(28 April - 02 May 2014 at Pacifico YOKOHAMA, Kanagawa, Japan)

PEM28-03 Room:413 Time:April 29 11:30-11:45

Global distributions of storm-time ionospheric currents as seen in geomagnetic field variations

SHINBORI, Atsuki[1*] ; HORI, Tomoaki[2] ; TANAKA, Yoshimasa[3] ; KOYAMA, Yukinobu[4] ; KIKUCHI, Takashi[2] ; NAGATSUMA, Tsutomu[5]

[1]Research Institute for Sustainable Humanosphere (RISH), Kyoto University, [2]Nagoya University Solar Terrestrial Environment Laboratory Geospace Research Center, [3]National Institute of Polar Research, [4]Data Analysis Center for Geomagnetism and Space Magnetism Graduate School of Science, Kyoto Universi, [5]National Institute of Information and Communications Technology

To investigate temporal and spatial evolution of global geomagnetic field variations from high-latitude to the equator during geomagnetic storms, we analyzed ground geomagnetic field disturbances from high latitudes to the magnetic equator. The daytime ionospheric equivalent current during the storm main phase showed that twin-vortex ionospheric currents driven by the Region 1 field-aligned currents (R1 FACs) are intensified significantly and expand to the low-latitude region of ˜30 degrees magnetic latitude. Centers of the currents were located around 70 and 65 degrees in the morning and afternoon, respectively. Corresponding to intensification of the R1 FACs, an enhancement of the eastward/westward equatorial electrojet occurred at the daytime/nighttime dip equator. This signature suggests that the enhanced convection electric field penetrates to both the daytime and nighttime equator. During the recovery phase, the daytime equivalent current showed that two new pairs of twin vortices, which are different from two-cell ionospheric currents driven by the R1 FACs, appear in the polar cap and mid latitude. The former led to enhanced northward Bz (NBZ) FACs driven by lobe reconnection tailward of the cusps, owing to the northward interplanetary magnetic field (IMF). The latter was generated by enhanced Region 2 field-aligned currents (R2 FACs). Associated with these magnetic field variations in the mid-latitudes and polar cap, the equatorial magnetic field variation showed a strongly negative signature, produced by the westward equatorial electrojet current caused by the dusk-to-dawn electric field.

Keywords: geomagnetic storm, convection electric field, shielding electric field, ionospheric disturbance dynamo, interplanetary magnetic field, solar wind

Japan Geoscience Union Meeting 2014
(28 April - 02 May 2014 at Pacifico YOKOHAMA, Kanagawa, Japan)

PEM28-04 Room:413 Time:April 29 11:45-12:00

The forenoon-afternoon asymmetry of DP2 electric field penetrated to the dip equator

MATSUSHITA, Hiroki[1*] ; YOSHIKAWA, Akimasa[2] ; UOZUMI, Teiji[3] ; IKEDA, Akihiro[4] ; OHTANI, Shinichi[5]

[1]Department of Earth and Planetary Sciences, Graduate School of Science, Kyushu university, [2]Department of Earth and Planetary Sciences, Graduate School of Science, Kyushu university, [3]International Center for Space Weather Science and Education, Kyushu University, [4]Kagoshima National College of Technology, [5]The Johns Hopkins University Applied Physics Laboratory

DP2 oscillation is quasi-periodic disturbance whose period is from 30 min to a few hours, and it is well known that DP2 synchronize with IMF Bz oscillation [Nishida, 1968] and can be observed globally from polar to equator [Nishida, 1968], [Kikuchi et al., 1996]. These two characteristics indicate that the disturbance associated with solar wind comes into ionosphere at polar region and M-I coupled current system like penetrating to dip equator is produced, however, this mechanism of the inversion of electric field from polar to equator is not well understood.

The purposes of this study are to clarify how the electric field at polar region is penetrated to dip equator region and to identify the global distribution of DP2 current system. To attain these goals, we analyzed longitudinal and latitudinal distribution of DP2 oscillation observed at dip equator region that is the final destination of M-I coupling system. The electric field is calculated from magnetic field and electric conductivity based on Ohm ' s law, and magnetic field data used in this study are MAGDAS data [K. Yumoto et al., 2006 and 2007] and electric conductivity data are calculated using data of WDC for geomagnetism. We analyzed the real local time distribution of the electric field during DP2 event in 2007 and 2008 using these data. It is used the data Equatorial Magnetometer Network [T.-I. Kitamura, 1985] to derive latitudinal distribution of DP2 oscillation.

The result of this analysis shows that there is an asymmetry of electric field between forenoon and afternoon. It is difficult to explain this asymmetry from the view point of only the electric field at polar region on northern and southern hemisphere which makes global DP2 current system, so this result indicates that there is some mechanism to produce this asymmetry of electric field when the polar electric field is penetrated to equator. As this mechanism, we suggest that the polarization electric field along dip equator and the terminator line of day and night can change global potential structure by Cowling channel model [Yoshikawa et al., 2012, AGU], and the electrostatic potential distribution assumed from our observational result is consistent with the distribution derived from the calculation result based on this model.

Keywords: DP2 oscillation, dip equator, ionospheric current

Japan Geoscience Union Meeting 2014
(28 April - 02 May 2014 at Pacifico YOKOHAMA, Kanagawa, Japan)

PEM28-05 Room:413 Time:April 29 12:00-12:15

Substorm electric fields at nightside low latitude

HASHIMOTO, Kumiko[1*] ; KIKUCHI, Takashi[2] ; TOMIZAWA, Ichiro[3] ; NAGATSUMA, Tsutomu[4]

[1]Kibi International University, [2]Nagoya University, [3]University of Electro-Communications, [4]National Institute of Information and Communications Technology

The convection electric field penetrates from the polar ionosphere to low latitude and drives the DP2 currents in the global ionosphere with an intensified equatorial electrojet (EEJ). The electric field often reverses its direction, that is, the overshielding occurs and causes the equatorial counterelectrojet (CEJ) during storm and substorms. In this paper we report that the overshielding electric field is detected by the HF Doppler sounders at low latitude on the nightside. We analyzed the Doppler frequency of the HF radio signals propagated over 120 km in Japan at frequencies of 5 and 8 MHz and compared with the equatorial EEJ/CEJ during the substorm expansion phase. We found that the overshielding electric field reaches around 2 mV/m during major substorms (AL <-1800 nT). Taking the geometrical attenuation into account, we estimate the equatorial electric field to be about 1.5 mV/m. We also found that the electric field drives the eastward electrojets in the equatorial ionosphere on the night side. It is to be noted that the overshielding electric field is observed on the nightside at low latitude during the major substorms, while the convection electric field is dominant during smaller size substorms, as the CEJ flows on the dayside. These results suggest that the overshielding electric field associated with the Region-2 field-aligned currents becomes dominant during substorms at low latitude on the nightside as well as on the dayside. On the other hand, we found strong seasonal dependence of the overshielding in the sub-auroral latitudes. Although the substorm CEJs at Huancayo do not depend on season, the overshielding frequently occurs at subauroral latitudes during the winter period from November to February. In contrast, the convection electric field is dominant at the subauroral and low-latitudes during the summer period from April to August. The strong seasonal dependence may suggest that the Region-1 field aligned currents (FACs) have a constant voltage source, while the Region-2 FACs have a constant current source, which results in the convection and overshielding electric fields being dominant in summer and winter, respectively.

Keywords: subsotm, midlatitude ionosphere, convection electric field, overshielding, equatorial counter electrojet

Japan Geoscience Union Meeting 2014
(28 April - 02 May 2014 at Pacifico YOKOHAMA, Kanagawa, Japan)

PEM28-06 Room:413 Time:April 29 12:15-12:30

Comparing the ionospheric plasma drift obtained from the global MHD simulation and that measured by SuperDARN radars

SAITA, Satoko[1*] ; FUJITA, Shigeru[2] ; KADOKURA, Akira[3] ; TANAKA, Takashi[4] ; YUKIMATU, Akira sessai[3] ; TANAKA, Yoshimasa[3] ; OHTANI, Shinichi[5] ; MURATA, Ken T.[6] ; HIGUCHI, Tomoyuki[7]

[1]Research Organization of Information and Systems, [2]Meteorological College, [3]National Institute of Polar Research, [4]International Center for Space Weather Science and Education, Kyushu University, [5]Johns Hopkins University Applied Physics Laboratory, [6]National Institute of Information and Communications Technology, [7]The Institute of Statistical Mathematics

We present a parameter study of simulated processes of the magnetosphere-ionosphere (M-I) coupling using the global MHD simulation code developed by *Tanaka* (2010).

The boundary conditions for the M-I coupling include some scaling factors. These factors are adjustable and are determined through trial and error. The main goal of this study is optimization of these scaling factors in the boundary condition by use of a data assimilation technique.

In this paper, we combine the MHD simulation and solar wind parameters derived from the ACE satellite, and compare the ionospheric E x B plasma drift obtained from the global MHD simulation and that obtained from the SuperDARN HF Radar Network.

References:

Tanaka, T., A. Nakamizo, A. Yoshikawa, S. Fujita, H. Shinagawa, H. Shimazu, T. Kikuchi, and K. K. Hashimoto (2010), Substorm convection and current system deduced from the global simulation, J. Geophys. Res., 115, A05220, doi:10.1029/2009JA014676.

Keywords: the ionospheric convection, SuperDARN, simulation

Japan Geoscience Union Meeting 2014
(28 April - 02 May 2014 at Pacifico YOKOHAMA, Kanagawa, Japan)

PEM28-07 Room:413 Time:April 29 12:30-12:45

Toward construction of comprehensive proton and electron auroral substorm model: Ground-based observation at Syowa

KADOKURA, Akira[1*] ; FUKUDA, Yoko[2] ; I, Tomofumi[3] ; MIYAJI, Kohei[4] ; MIYAOKA, Hiroshi[1] ; SATO, Natsuo[1]

[1]NIPR, [2]Department of Earth and Planetary Science, Graduate School of Science, The University of Tokyo, [3]Kakioka Magnetic Observatory,Japan Meteorological Agency, [4]Graduate School of Science, Nagoya University

National Institute of Polar Research (NIPR) has been constructing an auroral optical observation system at Syowa Station during the 8th project term of 6 years of the Japanese Antarctic Research Expedition (JARE) program. Instruments categorized in the ”Monitoring observation” are (1) 4 sets of All-sky monochromatic digital CCD imagers (427.8, 557.7, 485.0, 481.0 nm) and (2) All-sky color digital camera, and those categorized in the ”Specific purpose observation” are (1) All-sky TV camera and (2) 8-color Scanning Photometer (SPM). Simultaneous observations with 2 electron and 2 proton CCD monochromatic imagers will be carried out in 2014. Interval of the 4 imagers are the same as each other, 15 sec, although the spatial resolution of the 2 proton imagers are reduced into 64x64, comparing with the full resolution of 512x512 of the electron imager.

Center (FWHM) wavelengths of the SPM are 482.5(0.6), 483.5(0.6), 484.5(0.6), 485.5(0.6), 486.5(0.6), 487.5(0.6),670.5(5.0), 844.6(0.6) nm.

Scanning speed and sampling rate are 180 deg/10 sec and 20 Hz, respectively.

Using these electron and proton auroral data observed with all-sky imager and scanning photometer, we would like to construct a comprehensive model of substorm including the information on energy characteristics of precipitating auroral electrons and protons.

Keywords: aurora, substorm, ground-based observation, Syowa Station

Japan Geoscience Union Meeting 2014
(28 April - 02 May 2014 at Pacifico YOKOHAMA, Kanagawa, Japan)

PEM28-08 Room:413 Time:April 29 14:30-14:45

Characteristics of Pi 2 pulsations around the dawn and dusk terminator

IMAJO, Shun[1*] ; YOSHIKAWA, Akimasa[2] ; UOZUMI, Teiji[2] ; OHTANI, Shinichi[3] ; NAKAMIZO, Aoi[4] ; MARSHALL, Richard[5] ; SHEVTSOV, Boris M.[6] ; AKULICHEV, Victor A.[7] ; SUKHBAATAR, Usnikh[8] ; YUMOTO, Kiyohumi[2]

[1]Dept. Earth Planet. Sci., Kyushu Univ., [2]ICSWSE, Kyushu Univ., [3]APL, Johns Hopkins Univ., [4]FMI, Arctic Research Unit, [5]IPS Radio and Space Services, Bureau of Meteorology, Australia, [6]Institute of Cosmophysical Researches and Radio Wave Propagation, [7]Pacific Oceanological Insititude, FEB RAS, [8]The Research Center of Astronomy and Geophysics of Mongolian Academy of Sciences

We statistically investigate low-latitude Pi 2 pulsations observed around the dawn and dusk terminator. The main observational results of this study are: (1) Pi 2 pulsations tended to have east-west polarity in the sunlit side of the dawn terminator, while these in the sunlit side of the dusk terminator tended to have north-south polarity. (2) Phase reversals of D-component oscillations occurred near the dawn terminator and 2-3 hours before the dusk terminator. (3) Peaks of D/H (maximum amplitude ratio between D and H component) appear 3 hours after the dawn terminator and near the dusk terminator.

We suggest that there is the dawn-dusk asymmetry of meridional ionospheric currents connecting between equatorial Cowling current and oscillating nightside FACs; meridional currents around dawn is more intense than around dusk. This asymmetry current system can be qualitatively explained by the deformation of potential pattern caused by polarization charges at the terminator.

Keywords: Pi 2 pulsations, The dawn and dusk terminator, Ionospheric currents, FACs

Japan Geoscience Union Meeting 2014
(28 April - 02 May 2014 at Pacifico YOKOHAMA, Kanagawa, Japan)

PEM28-09 Room:413 Time:April 29 14:45-15:00

Automatic identification of Pc5 waves using RBSP mode data from the SuperDARN Hokkaido HF radar

MATSUSHITA, Toshinori[1*] ; SEKI, Kanako[1] ; NISHITANI, Nozomu[1] ; HORI, Tomoaki[1]

[1]STEL, Nagoya University

Ultra-low-frequency Pc5 waves have been observed by many methods such as ground-based magnetometers, HF radars and satellites. It has been demonstrated by numerical experiments that magnetospheric Pc5 waves are globally and directly generated on the dayside by solar wind dynamic pressure variations and/or on the dawn/dusk flank by Kelvin-Helmholtz surface waves. In addition, there are storm-time Pc5 waves on the dusk side magnetosphere that are associated with instabilities in the storm time ring current caused by the particle injection. The Pc5 waves can play an important role in mass and energy transport within the inner magnetosphere such as the radial diffusion of outer radiation belt electrons, as suggested by previous studies. Outstanding problems in Pc5 studies include clarification of their global characteristics and distribution, generation mechanisms, and especially their dependence on the solar wind parameters.

In this study, we try to develop a new automatic identification method of Pc5 waves using ˜20-sec time resolution data obtained by the SuperDARN Hokkaido HF radar operated in the RBSP mode. In this method, we use the Doppler velocity data and the power spectrum density calculated by the wavelet transformation. We set criteria which can detect Pc5 waves even when harmonic oscillations coexist. We show an example for the identification method using the Doppler velocity data obtained by the SuperDARN Hokkaido HF radar in details. Then, the candidates of Pc5 event are verified by inspection. From the rate of error identification, we evaluate the accuracy of the automatic identification method statistically. In the presentation we will also report on the preliminary results of mid-latitude Pc5 characteristics such as frequency distribution and MLT dependence.

Keywords: SuperDARN, Pc5 waves

Japan Geoscience Union Meeting 2014
(28 April - 02 May 2014 at Pacifico YOKOHAMA, Kanagawa, Japan)

PEM28-10 Room:413 Time:April 29 15:00-15:15

A Simultaneous Observation of Pc 4 pulsation by Hokkaido HF Radar and Ground-Based Magnetometers

OBANA, Yuki[1*] ; NISHITANI, Nozomu[2] ; HORI, Tomoaki[2] ; TERAMOTO, Mariko[3] ; NOSE, Masahito[4] ; YOSHIKAWA, Akimasa[5]

[1]Department of Engineering Science, Osaka Electro-Communication University, [2]Solar-Terrestrial Environment Laboratory, Nagoya University, [3]Japan Aerospace Exploration Agency, [4]Graduate School of Science, Kyoto University, [5]Department of Earth and Planetary Sciences, Kyushu University

We studied a Pc 4 (6.7-22.2 mHz) oscillation of ionospheric Doppler plasma velocity observed around the dawn terminator on 16 Jul 2013 on an east-northeast pointing beam 14 of SuperDARN Hokkaido HF radar in Japan. We compared this ionospheric Pc 4 oscillation with magnetic field variation at St. Paratunka (PTK) in Russia, Kakioka (KAK) in Japan, Guam (GUA), Middlemarch (MDM) and Te Wharau (TEW) in New Zealand. PTK and conjugate points of MDM and TEW are located almost under the radar beam. The waveforms showed high similarity among the HF Doppler, the D (east-west) component of magnetic field at stations in the middle latitude of northern hemisphere (PTK and KAK). While, at the other stations (MDM, TEW, and GUA) the H (north-south) component of magnetic field showed high similarity to the HF Doppler. Using the value of the peak-to-peak amplitude of the HF Doppler velocity, we estimated amplitude of magnetic field variation with assuming a horizontal current sheet infinitely extended in the ionosphere. The estimated amplitude was comparable to the observed amplitude at PTK. We also studied longitudinal variation in amplitude using magnetic field data at Amsterdam Isl. (AMS) in South Indian Ocean and Fredericksburg (FRD) in the United States. The maximum amplitude was found at AMS which located around the midnight.

These results can be interpreted as follows. This event had its source from night side and the Doppler velocity oscillation was caused by an oscillating electric field in the east-west direction. In the northern hemisphere (PTK and KAK), the ionosphere above the observatory was sunlit, thus the ionospheric Hall current induced by the electric field makes D component of magnetic filed oscillation on the ground. On the other hand, in the southern hemisphere (MDM and TEW) and GUA, the ionosphere above the stations was still in the darkness, thus effective ionospheric current could not be induced due to low conductivity. The H component of magnetic field oscillation may reflect direct incidence of magnetic field oscillation from the magnetosphere to the ground.

Keywords: ULF, HF radar, M-I coupling, magnetic pulsation

Japan Geoscience Union Meeting 2014
(28 April - 02 May 2014 at Pacifico YOKOHAMA, Kanagawa, Japan)

PEM28-11 Room:413 Time:April 29 15:15-15:30

Solar zenith angle dependence of relationships between energy inputs to the ionosphere and O+ and H+ ion outflows

KITAMURA, Naritoshi[1*] ; SEKI, Kanako[1] ; KEIKA, Kunihiro[1] ; NISHIMURA, Yukitoshi[2] ; HORI, Tomoaki[1] ; STRANGEWAY, Robert J.[3] ; MCFADDEN, James P.[4] ; LUND, Eric J.[5]

[1]STEL, Nagoya University, [2]Dept. of Atmos. and Oceanic Science, UCLA, [3]Inst. of Geophys. and Planetary Phys.,UCLA, [4]Space Science Laboratory, UCBerkeley, [5]SSC, Univ. of New Hampshire

Recent satellite observations and simulations have clarified that plasma outflows play an important role in abrupt changes in the ion composition in the plasmasheet and ring current during geomagnetic storms. Statistical studies by Strangeway et al. [2005] and Brambles et al. [2011] indicated that the flux of ion outflows is correlated well with soft electron precipitation (precipitating electron density and electron density in the loss cone), and DC and Alfvenic Poynting fluxes using the data obtained by the FAST satellite near the cusp region in the dayside during the 24-25 September 1998 geomagnetic storm. To distinguish between O^+ and H^+ ion outflows, we performed statistical studies using the ion composition data in addition to the ion and electron data obtained by the FAST satellite at 3000-4150 km altitude during January 1998 and January 1999. The long-term dataset enables us to identify empirical formulas between the outflowing O^+ and H^+ ion fluxes and the precipitating electron density, the electron density in the loss cone, the net electron number flux, and the DC and Alfvenic Poynting fluxes in a wide solar zenith angle (SZA) range (for dayside, 50-110 degree; and for nightside, 90-150 degree). In the SZA range of 90-110 degrees, the above formulas in the dayside are almost similar to those in the nightside. While SZA dependence of the relationshps between the outflowing O^+ and H^+ ion fluxes and the DC and Alfvenic Poynting fluxes are weak, the empirical formulas between the outflowing O^+ and H^+ ion fluxes and soft electron precipitation, especially the precipitating electron density and the electron density in the loss cone, depend on SZA. Although the precipitating electron density and the electron density in the loss cone that correspond to the outflowing O^+ ion flux of about 10^7 /cm^2/s increase with decreasing SZA, the outflowing O^+ and H^+ ion fluxes become more sensitive to an increase in soft electron precipitation with decreasing SZA.

Keywords: ion outflow, polar ionosphere

Japan Geoscience Union Meeting 2014
(28 April - 02 May 2014 at Pacifico YOKOHAMA, Kanagawa, Japan)

PEM28-12 Room:413 Time:April 29 15:30-15:45

Inversion method for estimating the helium ion density distribution in the plasmasphere based on IMAGE/EUV data

NAKANO, Shin'ya[1*] ; FOK, Mei-ching[2] ; BRANDT, Pontus C.[3] ; HIGUCHI, Tomoyuki[1]

[1]The Institute of Statistical Mathematics, [2]NASA Goddard Space Flight Center, [3]The Johns Hopkins University Applied Physics Laboratory

The plasmasphere exhibits a variety of shapes as a result of the variation in the electric field in the inner magnetosphere due to the coupling processes between the solar wind, the magnetosphere, and the ionosphere. Global imaging observations from outside the plasmasphere provide striking evidence of the variability of the plasmasphere. In particular, the EUV imager on board the IMAGE satellite obtained global EUV images of the plasmasphere, which have provided important insights into the variation of the plasmasphere. Our aim is to obtain the information on the ion density distribution for individual events rather than simply the averaged distribution from IMAGE/EUV data. For this purpose, we propose a linear inversion technique by which to estimate the helium ion density distribution. We applied this technique to a synthetic EUV image generated from a numerical model. This technique was confirmed to successfully reproduce the helium ion density that generated the synthetic EUV data. We also demonstrate how the proposed technique works for real data using real EUV images.

Keywords: plasmasphere, inverse problem, magnetosphere

Japan Geoscience Union Meeting 2014
(28 April - 02 May 2014 at Pacifico YOKOHAMA, Kanagawa, Japan)

PEM28-13 Room:413 Time:April 29 15:45-16:00

Current availability and utilization prospect of data obtained by AKEBONO for the research on lightning whistler

OIKE, Yuta[1*] ; KASAHARA, Yoshiya[1] ; GOTO, Yoshitaka[1]

[1]Kanazawa University

The AKEBONO spacecraft (EXOS-D) was launched in 1989 to observe particles and plasma waves in the auroral region and the plasmasphere of the Earth. It covers the altitude region from 300 km to about 10,000 km with an orbital inclination of 75 degree, and has been operated for more than 25 years which exceed 2 cycles of solar activity or 1 cycle of solar magnetic polarity reversal. Therefore analyses of the data obtained by AKEBONO enable us to study how the magnetosphere varies comprehensively.

The WBA (Wide Band Analyzer) is one of subsystems of the VLF instruments onboard AKEBONO. It measures 1 component of electric or magnetic analogue waveform in the frequency band of 50 Hz - 15 kHz. Typical waves such as chorus, hiss and whistler were frequently observed by the WBA. Huge amounts of data obtained by the WBA for more than 25 years are originally recorded as analogue waveform format in the magnetic audio tapes. Data conversion from analogue to digital is now carried out and the converted data are stored in our computer storage as digital WAVE format. Total number of the data files of digital WAVE format is more than 6,000, the total file size exceeds 10 terabytes and the processable data amount corresponds to more than 5,000 hours observation.

An automatic detection system to detect lightning whistlers from spectrograms of the WBA was developed. The spectrum intensity is automatically calibrated inside the system referring to the status of automatic gain controller of the receiver before detecting lightning whistlers. The system can output observed time, frequency band and dispersion of each detected lightning whistler. Some statistics of the lightning whistlers such as spatial and local time dependence of the occurrence frequency were already performed and the comparison with lightning activities are now under study. Because the dispersion of lightning whistler strongly depends on the electron density profile along the propagation path of the wave so that global electron density profile can be estimated using trend of dispersions of lightning whistlers. It is also pointed out that the propagation behavior of lightning whistlers is important clue to understand the wave-particle interaction. Thus these data and statistics have potential to achieve more valuable knowledge of the plasma physics in the magnetosphere.

In this presentation, we introduce the current status of data availability of the WBA and the derived results so far. We also discuss prospect of the data utilization.

Keywords: AKEBONO (EXOS-D), VLF, wide band receiver, lightning whistler

Japan Geoscience Union Meeting 2014
(28 April - 02 May 2014 at Pacifico YOKOHAMA, Kanagawa, Japan)

PEM28-14 Room:413 Time:April 29 16:15-16:30

Simultaneous ground-based and satellite observations of MF/HF auroral radio emissions

SATO, Yuka[1*] ; KUMAMOTO, Atsushi[2] ; KATOH, Yuto[2] ; SHINBORI, Atsuki[3] ; KADOKURA, Akira[1] ; OGAWA, Yasunobu[1]

[1]National Institute of Polar Research, [2]Department of Geophysics, Graduate School of Science, Tohoku University, [3]Research Institute for Sustainable Humanosphere, Kyoto University

Ground-based and satellite observations have revealed that the Earth is a distinct radio source. The terrestrial auroral ionosphere emits electromagnetic waves in the MF/HF ranges (about 1-6 MHz) as well as well-known intense auroral kilometric radiation (AKR) and auroral hiss in the VLF/LF ranges. Terrestrial Hectometric Radiation (THR) is observed by satellite observations in a frequency range of 1-4.5 MHz at high latitudes during geomagnetic disturbances and is regarded as a counterpart of auroral roar which is one type of MF/HF auroral radio emissions observable from the ground. Both THR and auroral roar are attributed to mode conversions of upper hybrid waves favorably generated under the matching condition, $f_{UH} \sim nf_{ce}$, where previous studies confirmed n = 2,3,4 and 5 for auroral roar, and n = 2 for THR. However, no previous studies have tested the simultaneous appearance. In this study, we survey long-term observation data obtained by the ground-based passive receivers installed at the Husafell station, Iceland (after September 2005, latitude 64.67^{o}N, longitude -21.03^{o}E, 65.3^o magnetic latitude) and the Kjell Henriksen Observatory (KHO), Svalbard (after August 2008, latitude 78.15^{o}N, longitude 16.04^{o}E, 75.2^o magnetic latitude) and by the Plasma Waves and Sounder experiment (PWS) mounted on the Akebono satellite. This data set includes several simultaneous appearance events, while the frequency of aurora roar is different from that of THR observed by the Akebono satellite passing over the ground-based stations. This frequency difference supports the previously proposed idea that auroral roar and THR are generated at different altitudes near 250 km and 1000 km, respectively. There is hardly any possibility that simultaneous observations indicate the identical generation region of auroral roar and THR. We also find that auroral roar appearing during the time when the Akebono satellite passes over the ground-based stations tends to be accompanied by THR. However, when the Akebono satellite passing over the stations detects THR, auroral roar does not always appear. This tendency is explained in terms of the fact that the Akebono satellite can detect THR emissions coming from a wider region, and a considerable portion of auroral roar emissions generated in the F region is absorbed in the D/E regions.

Japan Geoscience Union Meeting 2014
(28 April - 02 May 2014 at Pacifico YOKOHAMA, Kanagawa, Japan)

PEM28-15 Room:413 Time:April 29 16:30-16:45

Spatiotemporal distribution of auroral brightening in the cusp

TAGUCHI, Satoshi[1*] ; HOSOKAWA, Keisuke[1] ; OGAWA, Yasunobu[2]

[1]University of Electro-Communications, [2]National Institute of Polar Research

Previous studies have shown that mesoscale auroral forms occur near the equatorward edge of the background, stable cusp aurora, and that they move in a direction that is consistent with the motion of the magnetic field line after reconnection on the dayside magnetopause. In this study we pay attention to its initial brightening using data from a high-sensitivity all-sky imager at Longyearbyen, Svalbard. The imager has a field-of-view that spans more than 4 hours in MLT, and can observe auroral brightenings that are widely separated in MLT. We determined the position of dayside auroral brightening using the 630-nm auroral images, and examined how these positions are distributed in the cusp, focusing on intervals when IMF was extremely stable. Results of analyses show that brightening occurs over a wide dayside MLT range. We show detailed spatiotemporal patterns for successive brightening events, and discuss the patterns in terms of the formation of intermittent reconnection on the dayside magnetopause.

Keywords: aurora, cusp, particle precipitation, magnetic reconnection, all-sky imager

Japan Geoscience Union Meeting 2014
(28 April - 02 May 2014 at Pacifico YOKOHAMA, Kanagawa, Japan)

PEM28-16 Room:413 Time:April 29 16:45-17:00

Height measurement from stereo imaging of aurora

KATAOKA, Ryuho[1*] ; SHIGEMATSU, Kai[2] ; MIYOSHI, Yoshizumi[2] ; MIYAHARA, Hiroko[3] ; ITOYA, Satoru[4]

[1]NIPR, [2]Nagoya University, [3]MAU, [4]JSF

A new stereoscopic measurement technique is developed (Kataoka+2013) to obtain an all-sky altitude map of aurora using two ground-based digital single-lens reflex (DSLR) cameras. Two identical full-color all-sky cameras were set with an 8 km separation across the Chatanika area in Alaska (Poker Flat Research Range and Aurora Borealis Lodge) to find localized emission height with the maximum correlation of the apparent patterns in the localized pixels applying a method of the geographical coordinate transform. It is successfully estimated that a typical ray structure of discrete aurora shows the broad altitude distribution above 100 km, while a typical patchy structure of pulsating aurora shows the narrow altitude distribution of less than 100 km. Recent new findings about the time variation of the emission height and further new challenges of February/March 2014 will also be reported.

Reference: Kataoka, R., Y. Miyoshi, K. Shigematsu, D. Hampton, Y. Mori, T. Kubo, A. Yamashita, M. Tanaka, T. Takahei, T. Nakai, H. Miyahara, and K. Shiokawa (2013), Stereoscopic determination of all-sky altitude map of aurora using two ground-based Nikon DSLR cameras, Ann. Geophys, 31, 1543-1548.

Keywords: aurora, ground-based imaging, digital single-lens reflex camera

Japan Geoscience Union Meeting 2014
(28 April - 02 May 2014 at Pacifico YOKOHAMA, Kanagawa, Japan)

PEM28-17 Room:413 Time:April 29 17:00-17:15

Statistical analysis of auroral structures related to the plasma instability based on ground optical observations

HASHIMOTO, Ayumi[1*] ; SHIOKAWA, Kazuo[1] ; OTSUKA, Yuichi[1] ; OYAMA, Shin-ichiro[1] ; NOZAWA, Satonori[1]

[1]Solar-Terrestrial Environment Laboratory, Nagoya University, Nagoya, Japan

Auroral complex shapes are formed due to the connection of the ionosphere and magnetosphere by geomagnetic field lines which project disturbance of the magnetosphere onto the ionosphere through auroral particles. Thus, study of the auroral dynamics is important in considering the disturbance of the magnetosphere. Shiokawa et al. [JGR, 2010] reported observations of small-scale finger-like auroral structures which appeared on the west side of auroral patches, using a high-resolution narrow field-of-view CCD camera at Gillam (geomagnetic latitude: 65.5 N), Canada. At the recovery phase of substorm in the night side, these structures appeared when the speed of the patches moving to the east was slowed down, due to the macroscopic Rayleigh-Taylor type instability in the magnetosphere. However, statistical characteristics of this phenomenon have not been investigated yet. In this study, based on observations by an all-sky imager at Tromso (magnetic latitude: 67.1 N), Norway from January 2009 to November 2012, we made statistical analysis of the occurrence conditions of 19 events of auroral structures that seem to be driven by pressure-driven plasma instability. We found fourteen large-scale finger-like structures which developed from auroral arcs and six small-scale finger-like structures which appeared in auroral patches. We investigated MLT dependence of the start time of these finger-like structures, their relationship with auroral substorms, scale sizes, eastward drift speeds, development speeds, and so on. The large- scale structures were seen from midnight to dawn and small-scale structures were seen at dawn mainly. Large-scale structures tend to appear at the beginning of substorms' recovery phase and small-scale structures tend to occur at the late recovery phase of substorms. The scale sizes of these large and small structures are larger than the gyro radius of the ions in the magnetospheric equatorial plane, indicating that the finger-like structures are caused by MHD instabilities. The eastward propagation speeds are slower than the typical midnight auroral drift speed. This fact indicates that the low-energy plasma may be source of the structures. However, this consideration may contradict with the idea that the high-energy particles lead to the pressure-driven instability.

Keywords: aurora, pressure-driven plasma instability, ground optical observation

Japan Geoscience Union Meeting 2014
(28 April - 02 May 2014 at Pacifico YOKOHAMA, Kanagawa, Japan)

PEM28-18 Room:413 Time:April 29 17:15-17:30

Auroral vortex street formation and cavity trapping of Alfven waves

HIRAKI, Yasutaka[1*]

[1]National Institute of Polar Research

The structuring of auroral arc has been studied to be understood in the context of magnetohydrodynamic (MHD) instabilities and their nonlinear evolution in the magnetosphere-ionosphere (MI) coupling system. It was demonstrated that feedback instability of field-line resonant and ionospheric Alfven resonant modes occurs, by means of linear analysis with non-uniformity of the Alfven velocity (v_A) in the dipole magnetic field and the convection electric field [Hiraki and Watanabe, 2011; 2012, Hiraki, 2013]. We performed 3D reduced-MHD simulations in the MI coupling system to examine nonlinear behavior of the initially assumed arc structure, where v_A is constant along the field line. Results show that i) the initial arc splits, intensifies, and just after that deforming into a vortex street, and ii) the transition of the growth pattern exists at the convection electric field of 20-40 mV/m. We also performed 3D simulations with non-uniformity of v_A, though without the initial arc, to examine changes in auroral structure and properties of Alfven waves due to the magnetospheric and ionospheric cavities. It was found that, if the ionospheric cavity becomes deep, the secondary instability in the magnetic equator side [Watanabe, 2010] is suppressed, alternatively, large-amplitude waves are trapped in the ionospheric cavity. In this talk, we report the initial results of the above two simulations. Furthermore, we would discuss on auroral electron acceleration in the cavity region, by means of extended analyses with two-fluid effects and parallel electric field.

Keywords: Auroral vortex street, Alfven wave, Ionospheric Alfven resonator, Electron acceleration, MHD simulation

Japan Geoscience Union Meeting 2014
(28 April - 02 May 2014 at Pacifico YOKOHAMA, Kanagawa, Japan)

PEM28-19 Room:413 Time:April 29 17:30-17:45

Relative timing of substorm-associated magnetic reconnection in the magnetotail and formation of auroral onset arc

MIYASHITA, Yukinaga[1*] ; IEDA, Akimasa[1] ; MACHIDA, Shinobu[1] ; HIRAKI, Yasutaka[2] ; ANGELOPOULOS, Vassilis[3] ; MCFADDEN, James P.[4] ; AUSTER, H. uli[5] ; MENDE, Stephen B.[4] ; DONOVAN, Eric[6] ; LARSON, Davin[4]

[1]STEL, Nagoya Univ., [2]NIPR, [3]Univ. of California, Los Angeles, [4]SSL, Univ. of California, Berkeley, [5]Technischen Universitat Braunschweig, [6]Univ. of Calgary

We have studied the relative timing of magnetic reconnection in the near-Earth magnetotail and formation of auroral onset arc, based on substorm events observed by the THEMIS spacecraft and ground-based all-sky imagers. The THEMIS all-sky imagers can observe auroras over a wide area with temporal and spacial resolutions higher than spacecraft-borne cameras. This enables us to investigate the timing of auroral development in more detail than before. A few min after the appearance and intensification of an auroral onset arc, it begins to form wave-like structure. Then auroral poleward expansion begins another few min later. Based on observations of plasmoids in the near-Earth magnetotail, we clearly show that magnetic reconnection is initiated at X∼-20 Re at least 1-3 min before the appearance of the auroral onset arc. This result suggests that magnetic reconnection plays some role in the formation of auroral onset arc.

Keywords: substorm, auroral onset arc, magnetotail, magnetic reconnection, plasmoid, GEMSIS

Japan Geoscience Union Meeting 2014
(28 April - 02 May 2014 at Pacifico YOKOHAMA, Kanagawa, Japan)

PEM28-20 Room:413 Time:April 29 17:45-18:00

Characteristics of eastward propagating aurora vortices obtained by aurora tomography

TANAKA, Yoshimasa[1*] ; OGAWA, Yasunobu[1] ; KADOKURA, Akira[1] ; MIYAOKA, Hiroshi[1] ; GUSTAVSSON, Bjorn[3] ; PARTAMIES, Noora[2] ; BRANDSTROM, Urban[4] ; WHITER, Daniel[2] ; ENELL, Carl-fredrik[5]

[1]National Institute of Polar Research, [2]Finnish Meteorological Institute, [3]University of Tromso, [4]Swedish Institute of Space Physics, [5]EISCAT Scientific Association

We investigate characteristics of three mesoscale aurora vortices observed in the Northern Scandinavia by aurora campaign observation in March, 2013, which was conducted in collaboration with the Swedish Institute of Space Physics (IRF) and the Finnish Meteorological Institute (FMI). The aurora vortices propagated eastward intermittently at about 15-minute intervals in the post-midnight sector (0:00-0:40 UT; 2:30-3:10 magnetic local time) after the substorm onset. They were simultaneously observed by three monochromatic (427.8nm wave length) all-sky EMCCD imagers at Tromso (69.6N, 19.2E), Norway, Kilpisjarvi (69.0N, 20.9E), Finland, and Abisko (68.4N, 18.8E), Sweden, with an exposure time of about 2 seconds and a sampling rate of about 10 seconds. In addition to these optical data, geomagnetic field data from the IMAGE magnetometer chain were also available.

The propagation speed of these vortices was approximately 3 to 10 km/s at 100 km altitude. The ionospheric equivalent current system accompanied by the aurora vortices indicated a two-vortex structure. By applying tomographic inversion analysis to the events, we also obtained 3D distributions of volume emission rate and ionospheric electron density, as well as horizontal distribution of auroral precipitating electrons. It is also possible to estimate horizontal distribution of the ionospheric conductivity from the electron density distribution at every 10-second interval. In the presentation we will discuss the magnetosphere - ionosphere coupling process of the aurora vortices and the relationship with the omega bands that are generally observed in the post-midnight sector.

Keywords: aurora, tomography, substorm, vortex structure, imager, ionospheric current

Japan Geoscience Union Meeting 2014
(28 April - 02 May 2014 at Pacifico YOKOHAMA, Kanagawa, Japan)

PEM28-P01 Room:Poster Time:April 29 18:15-19:30

Observation of 630 nm auroral polarization with a newly-developed imaging spectrograph

TAKASAKI, Shimpei[1*] ; SAKANOI, Takeshi[1] ; KAGITANI, Masato[1]

[1]PPARC, Tohoku University

From the recent result of observation of OI 630nm auroral emission related to polar rain at high-latitudes using a polarization photometer, linear polarization parallel to geomagnetic field with 2-7% was reported [Lilensten et al., 2013]. From a theoretical approach, OI 630nm emission can be polarized up to 17% [Bommier et al., 2011]. However, these past measurements were limited in the polar cap region and its polarimetry characteristics is not clear. Therefore, we developed an imaging spectrograph which can measure auroral polarization in the wide field-of-view of 130 deg. from 420 nm to 680 nm with a accuracy of 1% polarization degree, which enable us to obtain polarization degrees at 557.7 nm aurora and 630 nm auroral emission simultaneously at various geomagnetic angle configuration. Here we consider that 557.7nm aurora is useful as a standard light source because a theory predicts 557.7nm emission does not produce polarization. We installed it in the middle of auroral region at Poker Flat Research range in November 2013and carried out precise calibration to extract artificial polarization which may be produce inside the optical system using an LED light source with a linear polarizer. From the calibration, we found the acrylic dome does not produce serious artificial polarization. Since then, automatic operation is continuously going on till the beginning of April 2014.

From the result on January 1st 2014, we obtain the polarization of 630 nm aurora with degree of 10%. Then, there was elevation angle dependence in both degree and direction. But, we also observed the polarization of no polarized 557.7nm emission. It has same elevation angle dependence as former. So, it is indicated that they are polarized by same processes like atmospheric scattering on the path from emission region to instrument. In this presentation, we report these results.

Keywords: aurora, polarimetry

Japan Geoscience Union Meeting 2014
(28 April - 02 May 2014 at Pacifico YOKOHAMA, Kanagawa, Japan)

PEM28-P02 Room:Poster Time:April 29 18:15-19:30

Development of polarization photometer and observation of OI 630 nm auroral polarization

MONJI, Hiroyuki[1*] ; KAGITANI, Masato[1] ; SAKANOI, Takeshi[1]

[1]PPARC, TOHOKU Univ.

Auroral O630 nm emission is theoretically expected to be polarized due to the velocity anisotropy of precipitating electrons. On the other hand, auroral O557.7 nm emission should not be polarized because it is quadrupole transition [Lilensten et al., 2006].

Recent ground-based measurement data showed that auroral emission at OI 630 nm probably polarized with a degree of 1-4%, and the polarization is maximized in the magnetic perpendicular direction [Lilensten et al., 2008, Barthelemy et al., 2011]. This fact suggest that it would be possible to investigate auroral physical processes, like electron anisotropy, by remote-sensing the auroral polarization.

In this study, we aim to establish the procedures of polarimetry observation of aurora, and obtain its polarization degree by developing a new polarization photometer.

We developed the polarization photometer which measures the polarization parameters (Stokes vector) using a quartz waveplate mounted on rotation stage and a polarization beam splitter. We adopt a narrow band 630 nm for wavelength selection. The field-of-view of this photometer is 3 deg. Observation of OI 630 nm auroral polarimetry was performed at Poker Flat Research Range in Alaska for three weeks in January 2013. We rotated the waveplate and took data at nine positions in one rotation. The time resolution for one rotation is 30 s. In addition, we carried out the calibration at Polar Flat with a linear polarizer and LED lamp. Using the auroral polarization data set and calibration data, we estimated the linear polarization degree and circular polarization simultaneously for the world first time.

On January 17, aurora appeared in the whole sky around 14:00 UT. During this period, we estimated the auroral polarization degree at various points along geomagnetic meridian. The estimated polarization degree maximized at the point parallel to the local geomagnetic field, which is inconsistent with the past result. On January 18, the auroral linear polarization degree increased correlated with auroral enhancement at 11:30 UT. This fact suggest that auroral polarization may increase due to the change in anisotropy in precipitating electrons.

Keywords: aurora ground observation, polarization

Japan Geoscience Union Meeting 2014
(28 April - 02 May 2014 at Pacifico YOKOHAMA, Kanagawa, Japan)

PEM28-P03 Room:Poster Time:April 29 18:15-19:30

Approximate formula of daytime ionospheric conductance ratio

IEDA, Akimasa[1*] ; OYAMA, Shin-ichiro[1] ; FUJII, Ryoichi[1] ; NAKAMIZO, Aoi[2] ; HORI, Tomoaki[1] ; YOSHIKAWA, Akimasa[3] ; NISHITANI, Nozomu[1]

[1]STEL, Nagoya University, [2]Finish meteological institute, [3]Kyushu University

Solar zenith angle (SZA) dependences of daytime ionospheric conductances are studied. In particular, we developed a simple theoretical form for the Hall to Pedersen conductance ratio against SZA. The European incoherent scatter (EISCAT) radar observations located at Tromso (67 MLAT) on 30 March 2012 were used to calculate conductances.

Daytime electric conductances in the ionosphere are associated with plasmas created by Solar extreme ultraviolet radiation into the neutral atmosphere of Earth. Previous conductance models have been either consistent or not with the ideal Chapman theory of such plasma productions.

Our results indicate that the SZA dependence of the Pedersen conductance can be consistent with the Chapman theory after modifications. Such modifications include an approximation of vertically-uniform plasma densities in the topside E region, and taking atmospheric temperature upward gradient into account. The Hall conductance decreases with increasing SZA more rapidly than the Pedersen conductance does. This is because that the Hall conductivity layer thins from noon toward night.

Keywords: ionospheric conductivity, ionosphere, conductance, EISCAT, incoherent scatter radar

Japan Geoscience Union Meeting 2014
(28 April - 02 May 2014 at Pacifico YOKOHAMA, Kanagawa, Japan)

PEM28-P04 Room:Poster Time:April 29 18:15-19:30

Temporal variation of electron density in the vicinity of the ionospheric trough

ISHIDA, Tetsuro[1*] ; OGAWA, Yasunobu[2] ; KADOKURA, Akira[2] ; HOSOKAWA, Keisuke[3] ; OTSUKA, Yuichi[4]

[1]The Graduate University for Advanced Studies, [2]National Institute of Polar Research, [3]The University of Electro-Communications, [4]Nagoya University

The purpose of this study is to examine temporal variation of electron density in the vicinity of the ionospheric trough, and to understand its physical mechanisms on different geomagnetic activities.

Basu et al. [2008] showed that Subauroal Polarization Stream (SAPS) enhances in the south of the trough during storm main phase. At the same time, GPS-TEC map showed that the trough also extends longitudinally throughout the Northern American continent. In addition, they pointed out that the plasma density irregularities in the trough/SAPS region impact the GPS-based navigation systems.

So far, it remains unclear how the trough and such irregularities develop in a shorter time scale and what determines their spatial structure because adequate observation with sufficient temporal resolution has not been operated. Therefore, we had conducted EISCAT SP experiment (high speed meridional scans which take only 60-80 seconds to scan elevation angles from 25 to 89 degrees) in duskside-nightside (1630-2030 MLT) on Oct. 2013 - Dec. 2013, and obtained totally 9 events including 7 quiet-moderate events and 2 disturbed events.

We have been investigating on the following topics: (1) the difference of temporal variation of electron density between inside and outside the trough, (2) the characteristic of temporal variation of electron density in the vicinity of the trough. We have obtained the following results so far.

1. The quasi-periodic variations in electron density, on the time scale of 5-40 minutes, have been found outside the trough, which varies with time and altitude. Oh the other hand, such structures less occurs within the trough. This tendency is independent on geomagnetic activity.

2. The quasi-periodic variations in electron density, on the time scale of 5-10 minutes, have been found within the trough boundary, which is nearly consistent toward altitude in magnetically quiet-moderate condition. However, this cyclic pattern is inconsistent toward altitude in magnetically disturbed condition.

Keywords: ionosphere, trough

Japan Geoscience Union Meeting 2014
(28 April - 02 May 2014 at Pacifico YOKOHAMA, Kanagawa, Japan)

PEM28-P05 Room:Poster Time:April 29 18:15-19:30

Classification and occurrence characteristics of subauroral rapid plasma flows observed by SuperDARN Hokkaido HF radar

NAGANO, Hiroki[1*] ; NISHITANI, Nozomu[1] ; HORI, Tomoaki[1]

[1]STEL, Nagoya Univ.

The rapid ionospheric plasma flows equatorward of the auroral zone are called Sub-Auroral Polarization Stream (SAPS). As a result of the past studies of SAPS, Kataoka et al. [2009] reported that positions of SAPS shift toward lower latitude with developing Dst index using the SuperDARN Hokkaido HF radar.

In this study we investigate the occurrence characteristics of SAPS, with focus on the relationship between SAPS occurrence and solar wind / geomagnetic parameters, using the SuperDARN Hokkaido HF radar with the field of view covering the Far East region, which began its operation in 2006. In order to discuss characteristics of SAPS extensively, we take a wider range of velocity (>10 m/s) and MLAT (>40 deg) than the previous studies. As a result of the statistical analysis we identified two kinds of flows with a threshold of 150 - 200 m/s. MLAT of faster flows has correlation with SYM-H and AL index, whereas the slower ones have no such correlation. We will report on the details of correlation between flow characteristics of solar wind and geomagnetic parameters, including substorm and storm phases.

Japan Geoscience Union Meeting 2014
(28 April - 02 May 2014 at Pacifico YOKOHAMA, Kanagawa, Japan)

PEM28-P06 Room:Poster Time:April 29 18:15-19:30

Magnetic latitude and MLT dependence of the bandwidth of MF/HF auroral radio emissions in the topside ionosphere

SAKAI, Masataka[1*] ; KUMAMOTO, Atsushi[1] ; KATOH, Yuto[1] ; SATO, Yuka[2]

[1]Department of Geophysics, Tohoku University, [2]National Institute of Polar Research

In the ionosphere, auroral radio emissions are generated by precipitating auroral particles. Previous studies reported that the MF/HF auroral radio emissions emitted from the bottomside ionosphere were observed on the ground. The narrowband emissions are called auroral roar, and the broadband emissions are called MF burst. On the other hand, Sato et al. [2010] showed the spectrum and polarization of two events of MF/HF radio emissions observed in the topside ionosphere by the Akebono satellite. Based on the event studies, they suggested that the observed narrowband emissions are generated by the mode conversion of UHR waves enhanced in the auroral ionosphere where the upper hybrid frequency matches the harmonics of the electron cyclotron frequency as suggested for generation mechanism of the auroral roar observed on the ground [Weatherwax et al., 1995; Yoon et al., 1998; Weatherwax et al., 2002].

In this study, we have focused on broadband emissions observed in the topside ionosphere which are similar with broadband MF burst observed on the ground. We analyzed MF/HF broadband emissions (with wider bandwidth of $>$0.5 kHz) observed by the Akebono satellite. Because it is difficult to observe broadband emissions on the ground and in the topside ionosphere at the same time, we have performed statistical analysis. We found that the bandwidth of the MF/HF emissions was larger in the high latitude and in the dusk side. The bandwidth of the MF/HF emissions was greater than 1 MHz in higher geomagnetic latitude than 70 degree in the sector from 12 to 24 MLT. Previous studies suggested that the MF bursts observed on the ground were generated by the mode conversion of upper hybrid waves stimulated by the energetic auroral electrons [e.g. Sato et al., 2008]. Therefore, we can expect that the bandwidth of MF bursts depend on the generation processes of upper hybrid waves, mode conversion processes of upper hybrid waves, and propagation processes of converted electromagnetic waves in the auroral ionosphere.

Japan Geoscience Union Meeting 2014
(28 April - 02 May 2014 at Pacifico YOKOHAMA, Kanagawa, Japan)

PEM28-P07 Room:Poster Time:April 29 18:15-19:30

Time Variability of Characteristics of Pc5 during Passage of CIRs

KITAMURA, Kentarou[1*] ; SAITA, Satoko[2] ; TANAKA, Yoshimasa[3] ; KADOKURA, Akira[3] ; YAMAGISHI, Hisao[3]

[1]Tokuyma college of Technology, [2]The Institute of Statistical Mathematics, [3]National Institute of Polar Research

In this study, we analyzed the magnetic data observed at the high-latitude magnetic stations in Antarctica, H057 (-66.42, L=6.25), and Skallen (-66.42) to compare with the >2Mev electron flux observed by GOES 10 satellite. The pair of stations is located at the same latitude and within 1.7 degrees in longitude, which are quite suitable to estimate the azimuthal wave number.

We statistically analyzed the wave characteristics of the Pc5 pulsations by the superposed epoch (SPE) analysis for 14 magnetic storm events caused by the passage of CIRs (Corotating Interaction Region). The epoch time is defined as days from the passage of the stream interface (SI) of the CIR. The Pc5 power suddenly increases at 3-6 MLT sector from 0 day which is much stronger than that at dusk sectors. During 1-2 days, which is correspond to the recovery phase of the storms, the Pc5 power at the afternoon sectors (12-21 MLT) increases with the peak frequency of 2.5-3 mHz, whereas the Pc5 power at the morning sector does not become stronger.

On the other hand, the phase delay between the Pc5s at H057 and SKAL also shows the local time dependence especially during the epoch time of 1-2 day. At the noon and afternoon sectors, the Pc5 shows the eastward propagation and the phase lags between H057 and SKAL are less than 5 seconds. In contrast, at the morning sector, the Pc5 shows westward propagation with small azimuthal wave numbers.

These features indicate that the sources and generation mechanisms of Pc5 in the two periods (0-1 day and 1-2 day) are quite different. The premiere intensification of the Pc5 corresponds to the main phase of the moderate magnetic storm and can thought to be the forced oscillation caused by the strong disturbance of the solarwind dynamic pressure. In this case, the local time dependence of the phase structure does not show the obvious regularities. In the latter intensification of the Pc5 corresponds to the recovery phase of the storm (1-2 days). The westward (eastward) propagation at the morning (afternoon) sector and local time distribution of the Pc5 power could well correspond with the previous perception which could explain the Pc5 pulsations caused by the KH instability on the magnetopause.

The present result implies that the difference of the wave characteristics of Pc5s closely related the drift bounce resonance with the relativistic electrons. The drift bounce resonance might occur at the afternoon sector during the recovery phase of the moderate magnetic storm by the KH instability due to the passage of the high speed solar wind.

Keywords: Raadiation Belt, ULF wave

Japan Geoscience Union Meeting 2014
(28 April - 02 May 2014 at Pacifico YOKOHAMA, Kanagawa, Japan)

PEM29-01 Room:503 Time:April 30 09:00-09:25

Spontaneous excitation of Alfven waves and their interactions with high-energy ions in a magnetic mirror configuration

ICHIMURA, Makoto[1*] ; IKEZOE, Ryuya[1]

[1]Plasma Research Center, Univ. of Tsukuba

In laboratory fusion plasmas, high-energy ions are produced with DD and DT fusion reactions and are also created with high-energy neutral beam injection and electromagnetic waves for plasma heating. Special emphasis is given to plasma waves excited by such high-energy ions and their interactions with particles. For example, energetic alpha particles produced with DT fusion process can interact resonantly with shear Alfven waves during slowing-down process, and excite plasma instabilities, that is, so-called Alfven eigenmodes (AEs). Recently, enhancement of energetic ion transport caused by these instabilities has been remarked on its deleterious effects. When a small fraction of alpha particles is transported to the first wall in burning plasma devices, plasma facing materials can be damaged seriously. Many kinds of the experimental observations related to such wave-particle interactions are reported. In this report, spontaneously excited waves in Ion Cyclotron Range of Frequency (ICRF) and their interactions with high-energy ions in a mirror magnetic field configuration are presented.

The ICRF waves are frequently used for the plasma heating in laboratory fusion devices with the mirror magnetic field configuration. When the ICRF power and consequent wave energy levels are increased, it will become important to understand the detailed physics of wave-wave and wave-particle interactions. It is required to consider both linear and nonlinear processes for deposition of ICRF powers. In the ICRF heating experiments on the GAMMA 10 tandem mirror, the maximum ion temperature in the perpendicular direction has reached 10 keV and the temperature anisotropy (which is defined as the temperature ratio of perpendicular to parallel to the magnetic field line) becomes more than 10 in the central cell. Alfven-ion- cyclotron (AIC) waves are spontaneously excited owing to such the strong temperature anisotropy. The excitation of the AIC wave is one of the common physical phenomena in space plasmas with an anisotropic velocity distribution. High energy ions, of which energy is more than 50 keV, have been observed along the magnetic field line at the open end of the mirror magnetic field configuration. The transport of high-energy ions along the magnetic field line owing to the loss processes other than the classical Coulomb scattering has been suggested. The existence of considerable energy transport along the magnetic field line owing to the AIC waves is discussed theoretically. The AIC waves in GAMMA 10, which has several discrete peaks in the frequency spectrum, are excited as eigenmodes. Their spatial structures are measured with a microwave reflectometer inside the plasma and magnetic probes in the peripheral region. Low-frequency fluctuations around 0.1 MHz, which is a differential frequency between discrete peaks of the AIC waves, are observed in the central cell. These fluctuations are also observed in the high-energy ion signal detected by a semiconductor detector installed at the end for measuring ions along the magnetic field line. Pitch angle scattering in the velocity space owing to the spontaneously excited Alfven waves are indicated. The radial transport of high-energy ions owing to the low-frequency MHD instability has been observed, however, the transport across the magnetic field line owing to the AIC waves has not yet been detected.

Observations of spontaneously excited waves in ICRF in the large tokamak experiments are also reported as Ion Cyclotron Emissions (ICE). The fluctuations in ICRF are driven by the presence of non-thermal ion distribution in magnetically confined plasmas and plasmas with the strong anisotropy. Waves owing to fusion products of ^{3}He and T ions are clearly detected in D-plasma and alpha particles in DT-plasma experiments.

Keywords: magnetic mirror configuration, Alfven wave, wave-particle interaction, Alfven Ion Cyclotron wave

Japan Geoscience Union Meeting 2014
(28 April - 02 May 2014 at Pacifico YOKOHAMA, Kanagawa, Japan)

PEM29-02 Room:503 Time:April 30 09:25-09:45

Nonlinear wave particle interaction of electromagnetic ion cyclotron wave

SHOJI, Masafumi[1*] ; OMURA, Yoshiharu[2]

[1]Solar-Terrestrial Environment Laboratory, Nagoya University, [2]Research Institute for Sustainable Humanosphere, Kyoto University

Spacecraft observations and simulations show generation of coherent electromagnetic ion cyclotron (EMIC) triggered emissions with rising-tone frequencies. In the inner magnetosphere, the spontaneously triggered EMIC waves are generated by the energetic protons with large temperature anisotropy. We reproduced EMIC triggered emissions in the Earth's magnetosphere by real scale hybrid simulations with cylindrical magnetic geometry. We perform parametric analyses of electromagnetic ion cyclotron (EMIC) triggered emissions on the gradient of the non-uniform ambient magnetic field using a hybrid simulation. According to nonlinear wave growth theory, as the gradient of the ambient magnetic field becomes larger, the theoretical threshold of the wave amplitude becomes larger although the optimum wave amplitude for nonlinear wave growth does not change. With a larger magnetic field gradient, we obtain coherent rising tone spectra because the triggering process of the EMIC triggered emission takes place only under the limited condition of the wave amplitude. On the other hand, with a smaller magnetic field gradient, triggering of the emissions can be caused with various wave amplitudes, and then the sub-packets are generated at various locations at the same time. The concurrent triggerings of emissions result in incoherent waves, observed as "broadband" EMIC bursts. Broadband emissions induce rapid precipitation of the energetic protons into the loss cone since the scattering by the concurrent triggering takes place faster than that of the coherent emissions. The coherent triggered emission causes efficient proton acceleration around the equator because of the stable particle trapping by the coherent rising tone emission.

Keywords: triggered emission, electromagnetic ion cyclotron wave, wave particle interaction, acceleration, scattering

Japan Geoscience Union Meeting 2014
(28 April - 02 May 2014 at Pacifico YOKOHAMA, Kanagawa, Japan)

PEM29-03 Room:503 Time:April 30 09:45-10:00

Solar energetic particle spectrum at the Sun and the Earth

KUBO, Yuki[1*]

[1]National Institute of Information and Communications Technology

It is well accepted that high-energy solar energetic particles are accelerated at reconnection regions in a solar flare and coronal shock waves driven by a coronal mass ejection. The coronal shock waves accelerate particles through the first-order Fermi process. The original Fermi acceleration theory predicts a power law particle distribution in momentum with index depending on shock compression ratio. Solar energetic particle spectra have been well investigated and it is found that the observed spectra are represented by almost power law (with high energy rollover). This looks like natural results at first glance. However, the observed spectrum is the spectrum at the observation location not at the acceleration site, and it is not trivial if the observed spectrum is as same as the source spectrum. There are some evidences that typical observed power law index will be about 6 in ground level enhancement (GLE). If the source spectrum of accelerated particle at a coronal shock is assumed to be as same as observed one, a compression ratio of the coronal shock accelerating particles should be about 1.6 according to the Fermi acceleration theory. This shock strength may not be enough to accelerate particles to GeV energy range in a short time. This implies that the spectrum at the source may not be as same as one at the observation location. While a power law spectrum predicted by Fermi process is a steady state solution, a lot of study show that a shock accelerated particle spectrum is time dependent manner. This fact may also imply a different spectrum between at the Sun and at the Earth. In this study, we investigate an energetic particle spectrum difference between at the source region and at the observation location by the interplanetary particle transport simulations.

Keywords: Solar energetic particles, Spectra

Japan Geoscience Union Meeting 2014
(28 April - 02 May 2014 at Pacifico YOKOHAMA, Kanagawa, Japan)

PEM29-04 Room:503 Time:April 30 10:00-10:15

Coupling between ULF waves and high-energy particles in the inner geomagnetosphere based on a drift-kinetic simulation

SEKI, Kanako[1*] ; AMANO, Takanobu[2] ; SAITO, Shinji[3] ; MIYOSHI, Yoshizumi[1] ; KEIKA, Kunihiro[1] ; MIYASHITA, Yukinaga[1] ; MATSUMOTO, Yosuke[4] ; UMEDA, Takayuki[1] ; EBIHARA, Yusuke[5]

[1]Solar-Terrestrial Environment Laboratory, Nagoya University, [2]Graduate School of Science, University of Tokyo, [3]Graduate School of Science, Nagoya University, [4]Graduate School of Science, Chiba University, [5]Research Institute for Sustainable Humanosphere, Kyoto University

Understanding of acceleration mechanisms of electrons to cause drastic variation of the Earth's outer radiation belt is one of outstanding issues of the geospace researches. While the radial diffusion of the electrons driven by ULF waves has been considered as one of the candidate mechanisms, efficiency of the mechanism under realistic ULF characteristics and distribution is far from understood. GEMSIS (Geospace Environment Modeling System for Integrated Studies) of STEL, Nagoya University, is the observation-based modeling project for understanding energy and mass transportation from the Sun to the Earth in the geospace environment. The GEMSIS-Magnetosphere working team has developed a new physics-based model for the global dynamics of the ring current (GEMSIS-RC model). The GEMSIS-RC model is a self-consistent and kinetic numerical simulation code solving the five-dimensional collisionless drift-kinetic equation for the ring-current ions in the inner-magnetosphere coupled with Maxwell equations. In contrast to previous ring current models assuming a force-balanced equilibrium, the new model allows the force-imbalance to exist, which generates induced electric field through the polarization current. The most prominent advantage of the new model is the capability of describing fast time scale phenomena such as injections during substorms and MHD-time scale (ULF) waves.

We applied the GEMSIS-RC model for simulation of global distribution of ULF waves. Comparison between runs with/without ring current ions show that the existence of hot ring current ions can deform and amplify the original sinusoidal waveforms. The deformation causes the energy cascade to higher frequency range (Pc4 and Pc3 ranges). The cascade is more pronounced in the high beta case. It is also shown that the existence of plasmapause strengthens ULFs outside the plasmapause and widens the MLT region where the E_r (toroidal) component is excited from initially-given E_phi (poloidal) component. We also report the basic characteristics of the ring current driven ULF waves and its effects on the electron transport in the inner magnetosphere.

Keywords: drift-kinetic approximation, ring current, radiation belt, MHD wave, inner magnetosphere, drift resonance

Japan Geoscience Union Meeting 2014
(28 April - 02 May 2014 at Pacifico YOKOHAMA, Kanagawa, Japan)

PEM29-05 Room:503 Time:April 30 10:15-10:30

Radiation spectra from relativistic electrons moving in a Langmuir turbulence

TERAKI, Yuto[1*]

[1]Osaka University / RIKEN

We examine the radiation spectra from relativistic electrons moving in a Langmuir turbulence expected to exist in high energy astrophysical objects by using numerical method. The spectral shape is characterized by the spatial scale λ, field strength σ, and frequency of the Langmuir waves, and in term of frequency they are represented by {s:0188$_0$ $2\pi c/\lambda$, ω_{st} = eσ/mc, and ω_p, respectively. We normalize ω_{st} and ω_p by ω_0 as a $\equiv \omega_{st}/\omega_0$ and b $\equiv \omega_p/\omega_0$, and examine the spectral shape in the a ? b plane. An earlier study based on Diffusive Radiation in Lang- muir turbulence (DRL) theory by Fleishman & Toptygin showed that the typical frequency is $\gamma^2\omega_p$ and that the low frequency spectrum behaves as F$\omega\overline{\Gamma}\omega^1$ for b $>$1 irrespective of a. Here, we adopt the first principle numerical approach to obtain the radiation spectra in more detail. We generate Langmuir turbulence by superposing Fourier modes, inject monoenergetic electrons, solve the equation of motion, and calculate the radiation spectra using Lienard-Wiechert potential. We find different features from the DRL theory for a $>$b $>$1. The peak fre- quency turns out to be $\gamma^2\omega_{st}$ which is higher than $\gamma^2\omega_p$ predicted in the DRL theory, and the spectral index of low frequency region is not 1 but 1/3. It is because the typical deflection angle of electrons is larger than the angle of the beaming cone $\approx$ 1/γ. We call the radiation for this case " Wiggler Radiation in Langmuir turbulence " (WRL).

Keywords: Radiation mechanism, Relativistic particle, Turbulent electromagnetic field

Japan Geoscience Union Meeting 2014
(28 April - 02 May 2014 at Pacifico YOKOHAMA, Kanagawa, Japan)

PEM29-06 Room:503 Time:April 30 10:30-10:45

Fine Spectral Structures and Their Generation Mechanisms for Solar Radio Bursts Observed by AMATERAS

IWAI, Kazumasa[1*] ; MIYOSHI, Yoshizumi[2] ; MASUDA, Satoshi[2] ; TSUCHIYA, Fuminori[3] ; MORIOKA, Akira[3] ; MISAWA, Hiroaki[3]

[1]Nobeyama Solar Radio Observatory, NAOJ, [2]STEL, Nagoya University, [3]PPARC, Tohoku University

The solar corona contains many particle acceleration phenomena that are caused by the interactions between the coronal magnetic field and plasma. Non-thermal electrons accelerated in the corona emit radio waves in the metric range. As a result, many types of solar radio bursts are observed. There are many types of complex fine spectral structures in the solar radio bursts. They are thought to be caused by some inhomogeneity of particle acceleration, wave generation, radio emission, and radio propagation processes. Hence, metric solar radio bursts are very important to understand coronal plasma processes such as the particle acceleration and wave-particle interaction.

The fine spectral structures of solar radio type-I bursts were observed by the solar radio telescope AMATERAS. The spectral characteristics, such as the peak flux, duration, and bandwidth, of the individual burst elements were satisfactorily detected by the highly resolved spectral data of AMATEAS with the burst detection algorithm that is improved in this study. The peak flux of the type-I bursts followed a power-law distribution with a spectral index of 2.9?3.3, whereas their duration and bandwidth were distributed more exponentially. There were almost no correlations between the peak flux, duration, and bandwidth. That means there were no similarity shapes in the burst spectral structures. We defined the growth rate of a burst as the ratio between its peak flux and duration. There was a strong correlation between the growth rate and peak flux. These results suggest that the free energy of type-I bursts that is originally generated by non-thermal electrons is modulated in the subsequent stages of the generation of non-thermal electrons, such as plasma wave generation, radio wave emissions, and propagation. The variation of the time scale of the growth rate is significantly larger than that of the coronal environments. These results can be explained by the situation that the source region may have the inhomogeneity of an ambient plasma environment, such as the boundary of open and closed field lines, and the superposition of entire emitted bursts was observed by the spectrometer.

Keywords: Sun, Solar radio burst, corona, wave-particle interaction, radio emission processes

Japan Geoscience Union Meeting 2014
(28 April - 02 May 2014 at Pacifico YOKOHAMA, Kanagawa, Japan)

PEM29-07 Room:503 Time:April 30 11:00-11:15

Co-evolution of upstream waves and accelerated particles around parallel shocks

SUGIYAMA, Tooru[1*] ; FUJIMOTO, Masaki[2]

[1]JAMSTEC, [2]JAXA

We have investigated the co-evolution of upstream waves and the accelerated particles around the parallel shock. Hybrid particle simulations are performed in the exactly parallel shock configuration with Mach number of ˜10. The upstream waves convecting into the shock surface contribute the particles acceleration as reported in Sugiyama et al. (2001). The appropriate wave-length exists for the particle energization, that is, the longer wave-length wave leads the higher energy particles. Simultaneously, the higher energized particles excite the longer wave-length waves in the upstream region. Here we report that the higher energy particles and longer wave-length waves are observed as the time elapses later in the simulation runs. Therefore, the present process is ”co-evolution” of the upstream waves and accelerated particles.

Keywords: collisionless shock, particle acceleration, wave-particle interaction

Japan Geoscience Union Meeting 2014
(28 April - 02 May 2014 at Pacifico YOKOHAMA, Kanagawa, Japan)

PEM29-08 Room:503 Time:April 30 11:15-11:30

Colliding Two Oblique Shocks: Shock Structures and Particle Acceleration

NAKANOTANI, Masaru[1*] ; MATSUKIYO, Shuichi[1] ; HADA, Tohru[1]

[1]ESST, Kyushu univ.

Mechanisms of the particle acceleration at a collisionless shock have been intensively studied analytically, numerically, and observationally. Most of the previous studies assume that energetic particles interact with a single shock. However, shock waves are ubiquitous in space, and two shocks frequently come close to or even collide with each other. For instance, it is observed that a CME (coronal mass ejection) driven shock collides with the earth's bow shock [H. Hietala et al., 2011], or interplanetary shocks pass through the heliospheric termination shock [J. Y. Lu et al., 1999]. The detailed structures of such colliding shocks and the accompanied particle heating/acceleration processes have not been understood.

Cargill et al. [1986] performed one dimensional hybrid simulations to discuss the dynamic structure of colliding shocks and the accompanied ion acceleration. They showed that some ions are efficiently accelerated at the time of the collision of two supercritical shocks. However, since electron dynamics are neglected in a hybrid simulation, the microstructures of the colliding shocks, which may affect the early stage processes of particle acceleration, cannot be resolved.

Here, we perform full Particle-in-Cell (PIC) simulations to examine colliding two shocks. In particular, the following three points interacting with two colliding oblique shocks is discussed in detail.

1. Energetic electrons are observed upstream of the two shocks before their collision. These energetic electrons are efficiently accelerated through multiple reflections at the two shocks (Fermi acceleration). Moreover, a part of the accelerated electrons are farther energized by interacting with increasing magnetic field during the collision and/or one of the shocks after the collision.

2. Before two shocks collide, there is a large amplitude wave excited by electrons flowing out to the upstream. We discuss the excitation mechanism and the influence on particle propagation or shock structures.

3. After two shocks collide, we find that a plasma density and pressure in the downstream is lower than the value calculated by MHD. The reason is that energetic electrons run away to the upstream. In addition to this, we discuss kinetic influences by comparing PIC simulation's results with the value after two shocks collide (magnetic fields, the shock velocity and etc.) calculated by MHD.

Keywords: collisionless shock, multi-shock waves, particle acceleration, numerical simulation

Japan Geoscience Union Meeting 2014
(28 April - 02 May 2014 at Pacifico YOKOHAMA, Kanagawa, Japan)

PEM29-09 Room:503 Time:April 30 11:30-11:45

Particle acceleration in high Mach number quasi-parallel shocks

KATO, Tsunehiko[1*]

[1]Hiroshima University

We study particle acceleration process of electrons and protons in high Mach number (M_A~30) quasi-parallel collisionless shocks by particle-in-cell (PIC) simulation. We found that a fraction of protons which consist of the plasma are injected into acceleration mechanisms and efficiently accelerated around the shock. The energy spectrum of the accelerated protons becomes power-law like distribution. A part of electrons are also accelerated around the shock although they are roughly two orders of magnitude fewer than the accelerated protons. For both protons and electrons, the acceleration processes are often not diffusive and their time-scales are even shorter than the respective gyration times. We also found that protons reflected at the shock generate circularly polarized Alfven waves with very large amplitude in the upstream region of the shock and that, because of the strong perpendicular magnetic field of these waves, the structure of the collisionless shock itself is in fact similar to that of quasi-perpendicular shocks.

Keywords: particle acceleration, plasma, collisionless shocks

Japan Geoscience Union Meeting 2014
(28 April - 02 May 2014 at Pacifico YOKOHAMA, Kanagawa, Japan)

PEM29-10 Room:503 Time:April 30 11:45-12:00

Particle simulations on electron acceleration at Quasi-Perpendicular Shocks

SHINOHARA, Iku[1*] ; FUJIMOTO, Masaki[1] ; NAKAMURA, Takuma[2]

[1]Institute of Space and Astronautical Science / Japan Aerospace Exploration Agency, [2]Los Alamos National Laboratory

We found efficient production of non-thermal electrons up to $\gamma\sim20$ in results of three-dimensional full kinetic simulations of quasi-perpendicular shocks. The seed acceleration occurs in large-amplitude electromagnetic wave excited in the most front region of the shock foot. A small portion of electrons keeps staying in the foot region due to the scattering by the large-amplitude electromagnetic wave, and these electrons can get energy from the motional electric field in the shock rest frame. Since the large-amplitude electromagnetic wave is only possible in 3-D simulations, no electron acceleration is observed in previous 1-D and 2-D simulations. After the seed acceleration, these electrons can be further accelerated at the shock lamp region by the shock drift acceleration. The acceleration process occurs during the steepen phase of the self-reformation, and the acceleration efficiency depends on the phase of the shock self-reformation. In contrast to the standard Fermi acceleration at quasi-parallel shocks, the electron acceleration process at quasi-perpendicular shocks is much quicker (order of the ion cyclotron period); however, electrons cannot experience effective acceleration again and again so that there would be an energy limitation of the acceleration. In this presentation, we will discuss the energy limit of electron acceleration at quasi-perpendicular shocks by using simulation results obtained from the K computer.

Keywords: shock acceleration, particle simulation

Japan Geoscience Union Meeting 2014
(28 April - 02 May 2014 at Pacifico YOKOHAMA, Kanagawa, Japan)

PEM29-11 Room:503 Time:April 30 12:00-12:15

The fast acceleration of particles scattered by MHD wave in parallel shock

MURAKI, Koudai[1*] ; AMANO, Takanobu[2] ; HOSHINO, Masahiro[2]

[1]EPS. Univ. of Tokyo, [2]University of Tokyo

The origin of the galactic cosmic ray is believed to be generated around the supernova remnant shocks (SNR), and the first-order Fermi acceleration is widely recognized as the standard theory of cosmic ray acceleration. Yet this acceleration mechanism is not always efficient enough to explain high energy cosmic ray particles extending to the knee. The maximum attainable energy expected by the first-order Fermi acceleration is less than the observations. To overcome this problem, additional acceleration and/or other efficient acceleration processes are needed.

Scattering process is important to investigate diffusive shock acceleration(DSA). In the previous numerical simulations, scattering is often treated as just numerical way like Monte-Carlo methods or electromagnetic perturbation. Among these researches, a special attention is paid to the particle acceleration for the particles scattered by magnetohydrodynamic (MHD) waves around the shock wave front. In the uniform system, when the wave phases are strongly correlated spatially localized traveling wave packets can efficiently large angle scatter charged particles (*Kuramitsu & Hada, 2000*). The scattering process through monochromatic large amplitude MHD waves around the parallel shock (*Sugiyama et al. 2001*) is regarded as a possible pre-acceleration process injecting the thermal particles into the Fermi acceleration process and the subsequent fast Fermi acceleration process.By extending the previous researches, we study a fast particle acceleration process for MHD turbulence around the parallel shock. By using the test particle simulation, we argue about the particle acceleration in the quasi-linear regime and also about the case of strongly coherent waves and large amplitude waves.

Keywords: acceleration of particles, cosmic ray, shock, Alfven wave, coherence, large amplitude

Japan Geoscience Union Meeting 2014
(28 April - 02 May 2014 at Pacifico YOKOHAMA, Kanagawa, Japan)

PEM29-12 Room:503 Time:April 30 12:15-12:30

On statistics of a plasma in a nonuniform flow

HADA, Tohru[1*]

[1]IGSES, Kyushu University

It is well known that energetic particles such as cosmic rays can efficiently be accelerated by scatterers convected by a compressional flow (Fermi acceleration). Scatterers convected by an expanding flow decelerate the particles, but this is not the reverse process of the acceleration. Plasma in space is never uniform, but is rather composed of different plasmas with different propagation speeds. We analyze statistics of energetic particles in such nonuniform plasma flow analytically and numerically. Results will be compared with non-equilibrium plasma distributions in the solar wind.

Keywords: Fermi acceleration, Nonequilibrium distribution

Japan Geoscience Union Meeting 2014
(28 April - 02 May 2014 at Pacifico YOKOHAMA, Kanagawa, Japan)

PEM29-13 Room:503 Time:April 30 14:15-14:30

Helicon wave propagation, mode conversion, and plasma heating

ISAYAMA, Shogo[1*] ; HADA, Tohru[1] ; TANIKAWA, Takao[2] ; SHINOHARA, Shunjiro[3]

[1]Graduate School of Engineering Sciences, Kyushu University, [2]Research Institute of Science and Technology Tokai University, [3]Tokyo University of Agriculture and Technology, Institute of Engineering

Helicon plasma is a high-density (number density ˜10^{19} /m^3) and low-temperature (electron temperature ˜a few eV) plasma generated by the helicon wave, i.e., electromagnetic whistler wave in a bounded plasma. Helicon plasma is thought to be useful for various applications including plasma processing and electric thrusters. On the other hand, there remain a number of unsolved fundamental issues regarding how the plasma is generated. Some of the key processes involved are the wave propagation (dispersion relation), mode conversion, collisional and non-collisional damping and resultant plasma heating, ionization and re-combination of neutral particles due to electrons accelerated by the wave, and modification of the dispersion relation due to addition of newly produced plasma.

In this presentation, as a first step to understand the helicon plasma production mechanism, we study the helicon wave propagation, mode conversion, and the plasma heating. According to Shamrai (1996), the helicon wave is linearly mode converted to an electrostatic Trivelpiece-Gould (TG) wave, which can accelerate electrons efficiently. However, the mode conversion and the production of the TG wave strongly depend on the dissipation included in the plasma. Using fluid and particle-in-cell (PIC) simulations, we discuss the mode conversion efficiency, wave damping, and plasma heating due to wave-particle interactions. We show that direct damping of the helicon waves can play major roles in the plasma heating under circumstances relevant to actual laboratory experiments.

Keywords: Helicon plasma, Helicon wave, TG(Trivelpiece-Gould) wave, Mode conversion, PIC simulation

Japan Geoscience Union Meeting 2014
(28 April - 02 May 2014 at Pacifico YOKOHAMA, Kanagawa, Japan)

PEM29-14 Room:503 Time:April 30 14:30-14:45

Hamilton-Jacobi equation based on exterior derivative

NAKAMURA, Tadas[1*]

[1]Fukui Prefectural University

Analytical Mechanics of fields usually singles out the temporal coordinate as an independent parameter and calculates the time evolution regarding fields as dynamical parameters with infinite degree of freedom. Spatial coordinates are treated as infinit number of indexes of dynamical parameters. This approach has a disadvantage when applied to electromagnetism: the resulting equations are not manifestly covariant. Moreover, when applied to gauge fields, the canonical theory with this approach has extra degree of freedom, which need to be eliminated with some constraints. One must fix the gauge at the price of loosing manifest covariance, or introduce some
complicated technique such as Dirac brackets.

The author reported the way to treat four (time 1 + space 3) parameters equally to construct analytical mechanics at the fall SGEPPS meeting. The expression obtained is manifestly covariant, and there is no need for gauge fixing when applied to gauge fields. The present study is to extend it to Hamilton-Jacobi theory. Also, possible application to the fluid dynamics will be discussed at the presentation.

The name of Hamilton-Jacobi equation is well known by name, however, not many researchers try to understand its detail because it is not quite useful to solve actual problems. However, it is conceptually important for the deep understanding of analytical mechanics. Also, it is essential to introduce quantum mechanics based on the knowledge of classical mechanics.

Several attempts have been made to establish classical mechanics of relativistic fluid dynamics, but fully covariant expressions are yet to come. Kambe (2010) has reported the Euler equation can be cast into the form of Maxwell equation with appropriate definitions of variables. The present study has been successfully applied to the analytical mechanics of electromagnetism, therefore, it may be applicable to fluid dynamics based on Hasimoto's representation.

References:
T.K. Nakamura 2003 (http://hdl.handle.net/2433/97295)[In Japanese]
T. Kambe 2010, Fluid Dyn. Res.
Y. Kaminaga, Electronic Journal of Theoretical Physics, 2012 (http://www.ejtp.com/ejtpv9i26)

Keywords: exterior derivative, analytical mechanics, Hamilton-Jacobi Equation, fluid dynamics

Japan Geoscience Union Meeting 2014
(28 April - 02 May 2014 at Pacifico YOKOHAMA, Kanagawa, Japan)

PEM29-P01 Room:Poster Time:April 30 18:15-19:30

Study of the slowly drifting narrowband structure in type-IV solar radio bursts observed by AMATERAS

KATOH, Yuto[1*] ; IWAI, Kazumasa[2] ; NISHIMURA, Yukio[1] ; KUMAMOTO, Atsushi[1] ; MISAWA, Hiroaki[3] ; TSUCHIYA, Fuminori[3] ; ONO, Takayuki[1]

[1]Department of Geophysics, Graduate School of Science, Tohoku University, [2]Nobeyama Solar Radio Observatory, National Astronomical Observatory of Japan, [3]Planetary Plasma and Atmospheric Research Center, Graduate School of Science, Tohoku University

We show the type-IV burst event observed by AMATERAS on June 7, 2011, and reveal that the main component of the burst was emitted from the plasmoid eruption identified by the EUV images of SDO. The slowly drifting narrowband structure (SDNS) appear in the spectra of the burst. By a statistical analysis, we reveal that SDNS appeared with the duration of tens to hundreds of millisecond and with the typical bandwidth of 3 MHz. For the generation mechanism of SDNS, we propose the wave-wave coupling between Langmuir waves and whistler-mode chorus emissions generated in a post-flare loop, inferred from the similarities of the plasma environments between a post-flare loop and the equatorial region of the Earth's inner magnetosphere. We assume that a chorus element with a rising tone is generated at the loop-top of a post-flare loop. By referring to the propagation properties of chorus in the magnetosphere, we assume that the chorus element propagates downward along the magnetic field line and then propagates away from the central region of the flare-loop toward the outer edge of the loop where the plasma density is relatively small. By the magnetic field and plasma density models, we quantitatively estimate the expected duration of radio emissions generated through the coupling between Langmuir waves and chorus during its propagation in the post-flare loop and find that the observation properties of duration and bandwidth of SDNS are consistently explained by the proposed generation mechanism. The characteristics of SDNS are its intermittency in time and the negative frequency drift in the limited frequency band. While observation in the terrestrial magnetosphere shows that chorus is a group of large amplitude wave elements naturally generated intermittently, the mechanism proposed in the present study can explain both intermittency and slowly drifting narrowband structure in the observed spectra.

Keywords: solar radio burst, solar corona, wave-particle interaction

Japan Geoscience Union Meeting 2014
(28 April - 02 May 2014 at Pacifico YOKOHAMA, Kanagawa, Japan)

PEM29-P02 Room:Poster Time:April 30 18:15-19:30

Numerical simulation of magnetic field generation by relativistic effect in high intensity laser experiments

KAWAZURA, Yohei[1*] ; YOSHIDA, Zensho[1]

[1]Graduate School of Frontier Sciences, The University of Tokyo

It has been a big mystery how the seed (primordial) magnetic field is generated in the universe. In fluid description of plasma, a magnetic filed is coupled with a mechanical vorticity then represented as curl of canonical vorticity. Recently, Mahajan and Yoshida proposed a novel mechanism of vorticity generation by relativistic effect [1, 2]. The relativistic plasma have two vorticity generating terms, one is so-called baroclinic term(S_T). The baroclinic term is known to be weak except for strongly thermal nonequilibrium state (e.g. shock front). Mahajan and Yoshdia proposed that, even if the system is barotropic, there appears another term available to generate vorticity due to the relativistic effect (S_R).

Recent progress in high intensity laser experiment enables us to obtain relativistic electron plasma, and some of the workers established high accuracy measurement of the generated magnetic field [3]. The relativistic vorticity generation (RG) is expected to be verified in such high intensity laser experiments.

In this study, we conducted numerical simulation for the proposal of the experimental verification. We have following objectives; is RG sufficiently working in actual experiment? If not, in what parameters will RG effectively work? What is the characteristics of the magnetic field given by RG? We calculated for parameters relevant to the experiment in Ref. 3. Observing the ratio of relativistic baroclinicity to thermodynamic baroclinicity, we can state that thermal baroclinic effect is governing and RG is not sufficiently working. By raising the hot electron temperature or decreasing the ratio of skin depth to scale length, the ratio is improving (Fig).

[1] S. M. Mahajan and Z. Yoshida, Phys. Rev. Lett. 105, 095005 (2010).
[2] S. M. Mahajan and Z. Yoshida, Phys. Plasmas 18, 055701 (2011).
[3] S. Mondal et al., PNAS 109, 8011 (2012).

Keywords: relativistic plasma, high intensity laser experiment, magnetic field generation

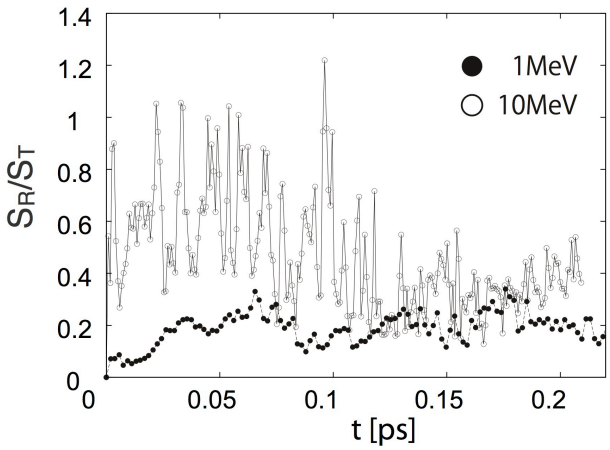

Japan Geoscience Union Meeting 2014
(28 April - 02 May 2014 at Pacifico YOKOHAMA, Kanagawa, Japan)

PEM29-P03 Room:Poster Time:April 30 18:15-19:30

The acceleration rate of cosmic rays in the cosmic ray modified shocks

SAITO, Tatsuhiko[1*] ; HOSHINO, Masahiro[1] ; AMANO, Takanobu[1]

[1]EPS, The University of Tokyo

It is a still controversial matter whether the production efficiency of cosmic rays (CRs) is relatively efficient or inefficient (e.g. Helder et al. 2009; Hughes et al. 2000; Fukui 2013). In upstream region of SNR shocks (the interstellar medium), the energy density of CRs is comparable to a substantial fraction of that of the thermal plasma (e.g. Ferriere 2001). In such a situation, CRs can possibly exert a back-reaction to the shocks and modify the global shock structure. These shocks are called cosmic ray modified shocks (CRMSs). In CRMSs, as a result of the nonlinear feedback, there are almost always up to three steady-state solutions for given upstream parameters, which are characterized by CR production efficiencies (efficient, intermediate and inefficient branch).

We evaluate qualitatively the efficiency of the CR production in SNR shocks by considering the stability of CRMS, under the effects of i)magnetic fields and ii)injection, which play significant roles in efficiency of acceleration.

By adopting two-fluid model (Drury & Völk, 1981), we investigate the stability of CRMSs by means of time-dependent numerical simulations. As a result, we show explicitly the bi-stable feature of these multiple solutions, i.e., the efficient and inefficient branches are stable and the intermediate branch is unstable, and the intermediate branch transit to the inefficient one. This feature is independent of the effects of i) shock angles and ii) injection.

Furthermore, we investigate the evolution from a hydrodynamic shock to CRMS in a self-consistent manner. From the results, we suggest qualitatively that the CR production efficiency at SNR shocks may be the least efficient.

Keywords: shocks, particle acceleration, feedback from cosmic rays

Japan Geoscience Union Meeting 2014
(28 April - 02 May 2014 at Pacifico YOKOHAMA, Kanagawa, Japan)

PEM29-P04 Room:Poster Time:April 30 18:15-19:30

2D Full Particle-In-Cell Simulation on a High Beta Collisionless Shock and Particle Acceleration

MATSUKIYO, Shuichi[1*] ; MATSUMOTO, Yosuke[2]

[1]Kyushu University, [2]Chiba University

High beta and relatively low Mach number shocks are commonly present in a vriety of space and astrophysical environments, like the earth's bow shock, the heliospheric termination shock (effective beta is rather high due to the presense of pickup ions), galaxy cluster merger shocks, etc. Even such high beta shocks show some evidences that high energy particles are possibly accelerated there. Voyager 2 spacecraft revealed that the fluxes of non-thermal electrons and ions (the latter are called as termination shock particles) are enhanced at the crossings of the termination shock. Radio synchrotron emissions from relics of galaxy cluster mergers imply the presence of relativistic electrons accelerated in the merger shocks. In this study we perform two-dimensional full particle-in-cell simulation to discuss structure of the shock as well as the acceleration process of electrons. The one-dimensional simulations performed in the past showed that under the high beta and relatively low Mach number conditions the shock is more or less laminar and time stationary and electron acceleration occurs through the so-called shock drift mechanism. Here, we reveal that two-dimensional structure of the shock is highly complex even for such a high beta and a low Mach number and further that some electrons are accelerated to high energy but their acceleration mechanism appears not to be so simple as that reproduced in one-dimensional simulations.

Keywords: collisionless shock, numerical simulation, particle acceleration

Japan Geoscience Union Meeting 2014
(28 April - 02 May 2014 at Pacifico YOKOHAMA, Kanagawa, Japan)

PEM30-01 Room:503 Time:April 30 14:45-15:10

Kelvin-Helmholtz turbulence in space and astrophysical plasmas

MATSUMOTO, Yosuke[1*]

[1]Graduate School of Science, Chiba University

Solar wind interactions with magnetized or un-magnetized planets destabilize planetary boundaries such as the magnetopause of the Earth magnetosphere and the ionopause of Mars and Venus. The Kelvin-Helmholtz (K-H) instability arising at a velocity shear layer has been considered to be important for momentum transport of the solar wind across the boundary layers, and been a universal nature of the planetary interactions. Linear and nonlinear growths of the instability depend on background plasma and magnetic field configurations. At the Martian ionopause, where the ionospheric ion escape is expected by the K-H instability, a fast (˜400 km/s), delute (˜1 /cc) plasma flow directly interacts with a high density (10^4-10^5 /cc), low temperature (a few thousand K) plasma. The situation can be found similarly at the terrestrial magnetopause, where in-situ observations have often indicated growth of the instability and resultant transport of the solar wind plasma into the magnetosphere, in the sense that the K-H instability grows in a strongly inhomogeneous plasma.

In this presentation, we review nonlinear evolutions of the K-H instability in strongly inhomogeneous plasmas. The evolutions are characterized by the secondary instabilities such as the Rayleigh-Taylor instability and the magnetic reconnection, by which a coherent eddy structure are destroyed and the energy is transported to smaller scales. Recent kinetic plasma simulations have shown that electron-scale structures are spontaneously generated as a consequence of the secondary instabilitties (Karimabadi et al., 2013). The micro-scale structure accompanied with the MHD-scale evolution enhanced mixing of collisionless plasmas. It was also found that the spatial size of the turbulent area was quickly broaden when coupled with a coalescence of large scale K-H modes, that is, the inverse energy cascade (Matsumoto & Seki, 2010). When nonlinear mode coupling was considered the time scale of the inverse energy cascade can be even faster than the fastest growing mode of the K-H instability. These nonlinear features in micro and macro scales have large impact on plasma transport process in the solar wind - planetary interactions as well as in astrophysical plasmas.

Keywords: Kelvin-Helmholtz instability, turbulence, Earth’s magnetosphere, Planetary atmosphere

Japan Geoscience Union Meeting 2014
(28 April - 02 May 2014 at Pacifico YOKOHAMA, Kanagawa, Japan)

PEM30-02 Room:503 Time:April 30 15:10-15:30

Experimental Study on Turbulent Transport using ElectroHydroDynamics Convection Turbulence

NAGAOKA, Kenichi[1*] ; YOSHIMURA, Shinji[1] ; HIDAKA, Yoshiki[2] ; TERASAKA, Kenichiro[2] ; YOKOI, Nobumitsu[3] ; MASADA, Yohei[4] ; MIURA, Hideaki[1] ; TSUNETA, Saku[5] ; KUBO, Masahito[6] ; ISHIKAWA, Ryoko[6]

[1]National Institute for Fusion Science, [2]Kyushu Univ., [3]Tokyo Univ., [4]Kobe Univ., [5]ISAS, [6]NAOJ

Turbulent transport is a very general subject in a wide area of physics research. The phenomena that we are interested in are very complex ones associated with structure formations in turbulence. It is well known that the Kolmogorov scaling appears in three-dimensional isotropic turbulence. However, it is less interested because nothing happens. In many cases of our interest, some structures appear in turbulence due to symmetry breaking such as temperature gradient, density gradient, intensity gradient of turbulence, rotation, velocity shear, magnetic field, etc. We have proposed a new experimental approach to turbulent transport using ElectroHydrodynamic Convection (EHC).

The EHC is a convection motion driven by the electric field in a liquid crystal, where the gravity and the temperature gradient in a Rayleigh Bernard convection (RBC) system can be replaced by the electric field alone. When the electric field is increased, the EHC becomes turbulent, which is the same feature as RBC with stronger buoyant force. Non-dimensional parameters characterizing EHC turbulence can be easily controlled with the biased voltage. The Rayleigh number is proportional to voltage squared and the Prandtl number is inversely proportional to the frequency of biased ac voltage, respectively. When the EHC turbulence experiment on a rotating table becomes possible in future, the Rossby number can be also controllable.

In the first step of the EHC turbulence experiment, particle transport in homogeneous EHC turbulence without rotation (symmetric case) was evaluated with a particle tracing technique. The small particles put in the liquid crystal can visualize local flow velocity in the EHC turbulence and the particle transport can be evaluated by the orbit tracing of particles. The diffusive nature (random walk process, the Hurst number ˜0.5) of particle transport was observed in the EHC turbulence. The effective diffusivity increases with the Rayleigh number with the power index of ˜0.85. These results are very similar to turbulent transport properties in viscos fluids (Navier-Stokes system).

The details of EHC turbulence experiment in laboratory frame without symmetry breaking and three experimental plans will be discussed. One is an investigation of non-uniformity effects on turbulent transport with inhomogeneity of turbulence intensity (spatial gradient of the Rayleigh number). Second one is an investigation of rotation effect on turbulent transport. These experiments on turbulent transport may reveal some general effects of symmetry breaking of scalar field and vector field, respectively. The last one is a laboratory simulation of the convection zone in stars and/or planet atmosphere with three-dimensional geometry identical to the real geometry (rotating spherical shell with radially driven convection). The radially-driven turbulence in rotating spherical shell have never realized in laboratory. Using ECH turbulence, turbulence can be driven in the radial direction with radial electric field. The convective zone in the Sun is the first target because of relatively large Rossby number˜0.1-1.

Keywords: turbulent transport experiment, symmetry breaking, EHC, liquid crystal

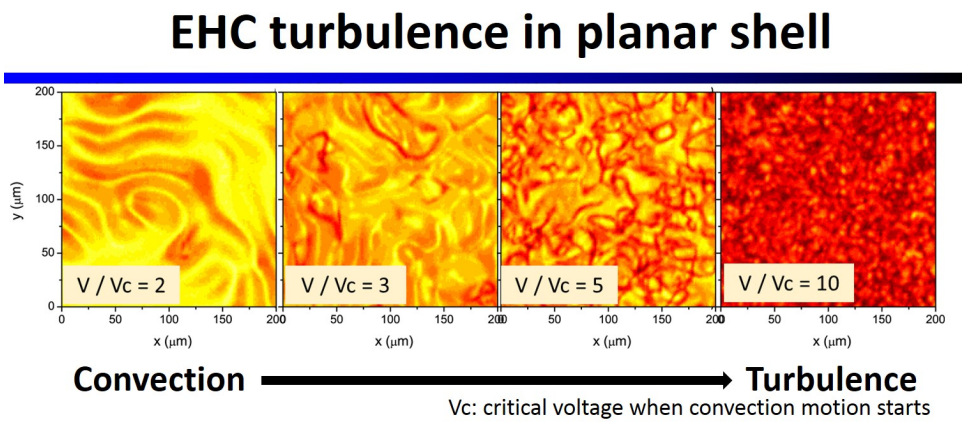

Japan Geoscience Union Meeting 2014
(28 April - 02 May 2014 at Pacifico YOKOHAMA, Kanagawa, Japan)

PEM30-03 Room:503 Time:April 30 15:30-15:45

Investigation of magnetic flux transport on the solar surface based on satellite data and auto-tracking technique

IIDA, Yusuke[1*]

[1]ISAS/JAXA

Spatial displacement of patch structure on the solar surface is investigated based on satellite data and auto-tracking technique.

Magento-convection system on the solar surface is thought to be important not only as a cause of various solar activities but also as an actual observable magneto-convection on the stellar surface. One important issue is how magnetic flux is transported there. In global scale, the transport of magnetic field is treated as a diffusion now. However it is not clear that diffusion treatment is appropriate in magneto-convection system. The aim of this study is to understand if the diffusion treatment of magnetic field transport in global scale is good or not.

I investigate the dependence of mean-square displacement on elapsed time by using auto-tracking technique, which is thought to be one of the critical characteristics for global-scale description of transport.

The longest magnetogram data obtained by Hinode/FG is used. In that data, number of tracked patches is enough for statistical study, more than 40000. The obtained dependence show a different character above and below the point of L˜10^4 km. Below that scale, it has a power-law dependence with an index of ˜-1.4, namely super-diffusion scheme. However, in the larger scale, the power-law dependence becomes ˜-0.6, namely sub-diffusion scheme. These characters can be explained by the network flow pattern qualitatively. Below the network scale, patch is transported by constant flow (˜0.3km s^{-1}) from center of network cell to edge of the cell addition to the large (˜1km s^{-1}) perturbing flow of granulation. On the other hand, above the network scale, patches experience the trapping around stagnation point of network flow, which makes displacement of patch shorter than that only by diffusion motion.

Keywords: the Sun, magnetic field, convection, diffusion, feature recognition

Japan Geoscience Union Meeting 2014
(28 April - 02 May 2014 at Pacifico YOKOHAMA, Kanagawa, Japan)

PEM30-04 Room:503 Time:April 30 15:45-16:00

Dynamic structure of convective motion depending on the height with line profile originating at solar photosphere

OBA, Takayoshi[1*] ; IIDA, Yusuke[2] ; SHIMIZU, Toshifumi[2]

[1]The Graduate University for Advanced Studies, [2]ISAS/JAXA

On the solar surface, there are bright cellular patterns which are called granules, separated by narrow dark regions named intergranular lanes. These spatial patterns result from surface convection. The surface convection induces the magnetic field dynamics and it is considered as an energy source of corona heating problem. Therefore, it is important to understand a convective motion in revealing the mechanism of corona heating problem. However, the smallness of its spatial structure prohibits us from resolving granular patterns in the observation. Furthermore, though the vertical structure is important in convection mechanism, it is difficult to observe it because there are few methods for a direct observation of solar interior. In this study, we investigate the height dependence of the vertical velocity and its spatial correlation with granular pattern based on the analysis of spectrum obtained by Solar Optical Telescope (SOT) on board the Hinode satellite. SOT/Spectropolarimeter (SP) obtains the spectrum including the Fe I 630.13/630.25nm lines, which corresponds the solar photosphere. The high spatial resolution of SP enables us to obtain spectra in granule and intergranular lanes separately. In addition, the seeing free condition in space observation enables the long time observation with high resolution, in this study, which is difficult for ground base observation. Consequently, we can remove the 5-min oscillation, which affects the radiative intensity and Doppler velocity, and then reduce errors of the analysis.

In this study, we focus on line profile of Stokes I originating in quiet region. Vertical velocity of convection is obtained from the Doppler shift of the line profile. We also analyze the wavelength structure of the line profile. Because of the dependence of absorption coefficient on wavelength, the intensity at different wavelength position reflects the structure at different height. The intensity at the line center reflects the structure in the higher layer, while the intensity at the line wings reflects the structure in the lower layer. We found that the difference of convective velocity between upper and lower level are typically 300 m s-1. At some locations, it exceeds 1km s-1. Taking into account that the speed of sound is approximately 7km s-1, it means that there are remarkable acceleration or deceleration around the solar surface. Further, there is a tendency between convective motion and acceleration, that granular region has upward motion with deceleration and intergranular region has downward motion with acceleration. In the presentation, we will discuss about the description of typical convective structure on the solar surface and what happens where has the different structure.

Keywords: sun, convection, spectrum, phtosphere

Japan Geoscience Union Meeting 2014
(28 April - 02 May 2014 at Pacifico YOKOHAMA, Kanagawa, Japan)

PEM30-05 Room:503 Time:April 30 16:15-16:30

Particle acceleration and magnetic field generation in the relativistic jet-plasma interactions

ARDANEH, Kazem[1*] ; CAI, Dongsheng[1]

[1]Department of Computer Science, University of Tsukuba, Ibaraki 305-8573, Japan

The aim of the current work is to analyze particle acceleration and magnetic field generation related to propagation of a relativistic electron-ion jet front into an unmagnetized ambient electron-ion plasma. We have focused on the earliest evolution in shock formation. The analysis is on the basis of a three-dimensional relativistic electromagnetic particle-in-cell (PIC) code. The results demonstrate that the Weibel instability is responsible for generation of strong small-scale magnetic fields and subsequent particles acceleration. In agreement with previous studies the majority of the particles acceleration occurs behind the jet front. Initially, the incoming electrons respond to field fluctuations growing as a result of the Weibel instability. Therefore, the electron channels are generated and the total magnetic energy grows linearly due to the mutual attraction between the channels, and downstream advection of the magnetic field fluctuations. When the magnetic fields become strong enough to deflect the much heavier ions, the linear growth rate of instability decreases as a result of oppositely directed electron-ion currents and topological change in the structure of magnetic fields. The Ion channels are then merged and magnetic energy increases more slowly at the expense of the energy stored in ion stream. It has been clearly illustrated that the ion channels develop through a larger scale in the longitudinal direction, while extension of the electron filaments is limited. Hence, the ions channels are the sources of deeply penetrating magnetic fields. Our results are in valid agreement with those reported in the literature.

Keywords: Relativistic jets, Particle acceleration, Magnetic field generation, Weibel instability

Japan Geoscience Union Meeting 2014
(28 April - 02 May 2014 at Pacifico YOKOHAMA, Kanagawa, Japan)

PEM30-06 Room:503 Time:April 30 16:30-16:45

Magnetohydrodynamic evolutions of the Richtmyer-Meshkov instability in astrophysical and laboratory plasmas

SANO, Takayoshi[1*]

[1]Institute of Laser Engineering, Osaka University

The Richtmyer-Meshkov instability (RMI) in magnetohydrodynamics is of great interest in many fields such as astrophysical phenomena, laboratory experiments, and inertial confinement fusion. The RMI occurs when an incident shock strikes a corrugated contact discontinuity. A strong shock wave traveling through the density inhomogeneity of magnetized interstellar medium is a promising site of the RMI. This astrophysically common event plays a key role in determining the dynamics of supernova remnants and gamma ray bursts. Recent laboratory experiments are designed to test the magnetic field amplification due to the RMI by the use of laser-induced shock waves. In inertial confinement fusion, the RMI excited at several capsule interfaces amplifies the perturbations that seed the Rayleigh-Taylor instability. For the fast ignition approach, the utilization of an external magnetic field to guide the fast electrons is discussed proactively and sheds light on the impact of magnetohydrodynamic (MHD) instabilities during the implosion.

The inclusion of a magnetic field brings two important consequences into the RMI, which are the amplification of an ambient field and the suppression of the unstable motions. The magnetic field can be amplified by the stretching motions at the interface associated with the RMI. A strong magnetic field inhibits the nonlinear turbulent motions of the RMI. The vorticity generated by the interaction between a shock front and a corrugated contact discontinuity is the driving mechanism for the RMI. For the cases of MHD parallel shocks, the role of the magnetic field is to prevent the deposition of the vorticity on the interface, and stabilize the RMI.

We have investigated that the critical strength of a magnetic field required for the suppression of the RMI numerically by using a two-dimensional single-mode analysis. For the cases of magnetohydrodynamic parallel shocks, the RMI can be stabilized as a result of the extraction of vorticity from the interface. A useful formula describing a critical condition for magnetohydrodynamic RMI is introduced and is successfully confirmed by direct numerical simulations. The critical field strength is found to be largely dependent on the Mach number of the incident shock. If the shock is strong enough, even low-beta plasmas can be subject to the growth of the RMI.

Keywords: MHD instability, astrophysical plasmas, laboratory plasmas

Japan Geoscience Union Meeting 2014
(28 April - 02 May 2014 at Pacifico YOKOHAMA, Kanagawa, Japan)

PEM30-07 Room:503 Time:April 30 16:45-17:00

Gyrokinetic simulation of multi-scale plasma turbulence

WATANABE, Tomo-hiko[1*]

[1]Graduate School of Science, Nagoya University

As is well known, spatio-temporal scales of plasma phenomena are characterized by multiple scale-lengths. As the scale-separation may not necessarily hold, multi-scale phenomena have been regarded as a common subject in the space and laboratory plasma studies. Magnetic reconnection is discussed as one of the examples. On the other hand, turbulence involves macro- and micro-scale structures simultaneously, and shows the fluctuation spectrum in a wide wavenumber range. Here, we discuss plasma turbulence with multiple scale-lengths, focussing on turbulent transport in magnetic fusion plasma.

By means of the gyrokinetic simulation, we have investigated transport phenomena in case with the electron temperature gradient (ETG) turbulence and the trapped electron mode (TEM) driven by a density gradient, where two scale-lengths characterizing the turbulence are involved. If both the two modes are unstable, after development of the ETG turbulence with a short spatio-temporal scale, the TEM instability grows with a long spatio-temporal scale. We have found an interesting case where the TEM drives a shear (zonal) flow with a longer spatio-temporal scale by which ETG and TEM fluctuations are regulated. The obtained result implies a possibility of turbulent transport reduction with a different driving source with a help of cross-scale interaction through zonal flows.

Furthermore, we have carried out a large-scale gyrokinetic simulation of multi-scale turbulence including the ion temperature gradient mode, where a turbulence spectrum from ion to electron scales as well as its dynamical evolution is studies. In the presentation, we will discuss characteristics of the multi-scale plasma turbulence and related transport.

∗This work is based on collaboration studies with Y. Aasahi (TiTech), S. Maeyama, M. Nakata, Y. Idomura (JAEA), A. Ishizawa, M. Nunami, and H. Sugama (NIFS). Under supports for the research collaborations, the numerical simulations are carried out by utilizing Plasma Simulator (NIFS), Helios (IFERC-CSC), and K (AICS, Riken). This work is also partly supported by by the MEXT grant for HPCI Strategic Program Field No.4, and by grants-in-aid of MEXT.

Keywords: turbulence, transport, kinetics, simulation

Japan Geoscience Union Meeting 2014
(28 April - 02 May 2014 at Pacifico YOKOHAMA, Kanagawa, Japan)

PEM30-08 Room:503 Time:April 30 17:00-17:15

Plasma heating by nonlinear development of a finite amplitude whistler wave

SAITO, Shinji[1*] ; NARIYUKI, Yasuhiro[2] ; UMEDA, Takayuki[3]

[1]Graduate School of Science, Nagoya University, [2]Faculty of Human Development, University of Toyama, [3]Solar-Terrestrial Environment Laboratory, Nagoya University

A two-dimensional, three-velocity (2D3V) particle-in-cell simulation has been done in order to study nonlinear development of a finite amplitude and long wavelength R-mode wave propagating parallel to the mean magnetic field, where the fluctuation energy is 10% of the mean magnetic field and the wavelength is about the ion inertial length. The simulation has shown that the bulk motion associated with the finite amplitude wave triggers the modified-two-stream instability that generates electrostatic field in the quasi-perpendicular direction. The electrostatic field scatters ions in the perpendicular direction and electrons in the parallel direction. About 70% of fluctuation energy of the initially imposed R-mode decreases in one gyro-period of ion. The dissipation through the modified-two-stream instability in the two-dimensional system is more effective than the parametric instability in the one-dimensional system. Further the simulation found that quasi-perpendicular-propagating electromagnetic fluctuations are enhanced through the nonlinear development of the R-mode. Discussion will focus on both the plasma heating and the nonlinearly enhanced fluctuations propagating quasi-perpendicular directions.

Keywords: Whistler wave, Solar wind, Nonlinear development, Plasma heating, Particle-in-cell simulation

Japan Geoscience Union Meeting 2014
(28 April - 02 May 2014 at Pacifico YOKOHAMA, Kanagawa, Japan)

PEM30-09 Room:503 Time:April 30 17:15-17:30

A theoretical model of nonlinear Alfven waves in expanding accelerating solar wind plasmas

NARIYUKI, Yasuhiro[1*]

[1]Faculty of Human Development, University of Toyama

During about forty years, a lot of studies have discussed the linear and nonlinear dynamics of Alfven waves in solar wind plasmas. Although the uniform plasmas are assumed in most past studies, the effects of the inhomogeneity of background plasmas cannot be negligible in the inner heliosphere, in which several future spacecraft missions are planned. In the present study, a nonlinear evolution equation of envelope-modulated Alfven waves is derived from the magnetohydrodynamic accelerating expanding box model by using the reductive perturbation method. The effects of the acceleration of solar wind to nonlinear evolution are discussed in detail.

Keywords: solar wind, Alfvenic turbulence

Japan Geoscience Union Meeting 2014
(28 April - 02 May 2014 at Pacifico YOKOHAMA, Kanagawa, Japan)

PEM30-P01 Room:Poster Time:April 30 18:15-19:30

Alfven wave resonance in density profile structure and the effect for nonlinear phenomenon

TSUTSUMI, Akihiro[1*] ; SUZUKI, Takeru[1]

[1]Nagoya University

Wave transport in plasma (e.g. Alfven wave) is a universal phenomenon for astrophysical fluid which is effected by electromagnetic force. Presence of

density structure in plasma causes these wave reflection, and prevents smooth transport for one direction. However, it is known that if the density structure is like square well form, Alfven wave is trapped in the structure and wave reflection does not occur. It seems that this wave trapping is a ordinary case and concerns with physical phenomenon, because density valley usual exist in plasma. For example, it is pointed out that Alfven wave energy is dissipated at low-density area which is located in surface of the sun, and this mechanism is relate to coronal heating.

At linear phase, we can understand analytically the property of Alfven wave transport on square well density profile. Therefore, we can also understand the condition that wave trapping and no reflection occurs. At this phase, the flow is well-regulated and steady state, and compressibility effect (e.g. pressure or density vary) doesn't appear because Alfven wave is essentially transverse wave. However, as the wave injection continues, the amplitude increases and nonlinear effect turns important. At this phase, the flow is complicated due to trapped wave's collision, and square well density profile can not keep the form. As a result, the resonance condition will change voluntarily. This density profile is universal in the plasma gas, so above physical mechanism is important for understanding plasma phenomenon.

In our numerical simulation, we pay attention voluntarily structural change due to linear phase shift to nonlinear phase. Consequently, the linear phase resonance condition directly affects the time evolution in nonlinear phase. We will introduce the result.

Japan Geoscience Union Meeting 2014
(28 April - 02 May 2014 at Pacifico YOKOHAMA, Kanagawa, Japan)

PEM30-P02 Room:Poster Time:April 30 18:15-19:30

The effect of the ion gyro motion to nonlinear processes of the Kelvin-Helmholtz instability

UENO, Satoshi[1*] ; UMEDA, Takayuki[1] ; NAKAMURA, Takuma[2] ; MACHIDA, Shinobu[1]

[1]Solar-Terrestrial Environment Laboratory, [2]Los Alamos National Laboratory

Nonlinear evolution of the Kelvin-Helmholtz instability (KHI) at a transverse velocity shear layer in an inhomogeneous space plasma is investigated by means of a four-dimensional (two spatial and two velocity dimensions) electromagnetic Vlasov simulation. When the rotation direction of the primary KH vortex and the direction of ion gyro motion are same, there exists a strong ion cyclotron damping. In this case, spatial inhomogeneity inside the primary KH vortex is smoothed and the secondary Rayleigh-Taylor instability is suppressed. The ion gyro motion also suppresses the formation of secondary vortices in the spatial scale smaller than the ion gyro radius, when the rotation direction of the vortex and the direction of ion gyro motion are same. As a result, the secondary instabilities take place at different locations in the primary KH vortex, where the rotation direction of the secondary vortex and the direction of ion gyro motion are opposite. These results indicate that secondary instabilities occurring in the nonlinear stage of the primary KHI at the Earth's magnetospheric boundaries might show dawn-dusk asymmetries.

Keywords: the Kelvin-Helmholtz instability, Vlasov simulation, space plasma, nonlinear processes, secondary instabilities

Japan Geoscience Union Meeting 2014
(28 April - 02 May 2014 at Pacifico YOKOHAMA, Kanagawa, Japan)

PEM30-P03 Room:Poster Time:April 30 18:15-19:30

Magnetohydrodynamic and Radiation Hydrodynamic Simulations of Tidal Disruption Events by a Supermassive Black Hole

KAWASHIMA, Tomohisa[1] ; OHSUGA, Ken[2] ; MATSUMOTO, Ryoji[3*]

[1]Shanghai Astronomical Observatory, [2]NAOJ, [3]Chiba University

Gas clouds or a star approaching a supermassive black hole can be disrupted by its tidal force. Such tidal disruption events enable us to observe the luminosity variations and state transitions triggered by the increase of the accretion rate, and give us hints to understand the transitions between different types of active galactic nuclei. Furthermore, the interval between the state transitions restricts the angular momentum transport rate, which determines the time scale of viscous evolution of an accretion disk. In 2014, tidal disruption flares are expected in two objects. One is the Galactic center supermassive black hole Sgr A$*$. A gas cloud named G2, whose mass is three times of the Earth mass is now approaching Sgr A$*$, and its pericenter passage will be in March, 2014. Since the distance from the black hole is well inside the radius of the accretion disk around Sgr A$*$, the tidally disrupted gas cloud will interact with the accretion disk. We carried out three-dimensional magnetohydrodynamic simulations of this interaction by applying a MHD code CANS+ based on the HLLD scheme. We found that the accretion rate increases more than 10 times during this outburst, and that magnetically driven jets are ejected. Increase of the X-ray and radio luminosity takes place within 1 month after the passage. The second object we expect an outburst is Swift J1644+57, which showed extremely high energy outburst in March 2011. This object locates at the center of a galaxy at redshift z=0.35. The energy released in this outburst indicates that the outburst was triggered by a disruption of a star. The luminosity of this source exceeded the Eddington luminosity for a 1-million solar mass black hole for period longer than a year but the X-ray luminosity decreased 100 times in August 2012. This darkening can be interpreted as the transition from a supercritically accreting slim disk state to a sub-critically accreting standard disk state. We carried out radiation hydrodynamic simulations of this event and showed that mass of the stellar debris is accumulating in the outer disk. When the surface density of the outer disk exceeds the threshold for the transition from a standard disk to a slim disk, the disk mass will accrete supercritically onto the black hole. Numerical results indicate that the luminosity of Swift J1644+57 may exceed the Eddington luminosity again in 1-2 years from the darkening.

Keywords: accretion disk, MHD, radiation hydrodynamics, black hole, tidal disruption, state transition

Japan Geoscience Union Meeting 2014
(28 April - 02 May 2014 at Pacifico YOKOHAMA, Kanagawa, Japan)

PEM31-01 Room:503 Time:May 1 15:15-15:40

Physics of weakly ionized dusty plasmas in planet formation

OKUZUMI, Satoshi[1*]

[1]Graduate School of Science and Engineering, Tokyo Institute of Technology

Planets form in gas disks around young stars. These protoplanetary disks are a typical example of weakly ionized plasmas in space: they are cool (∼10-1000 K) but are nonthermally ionized by galactic cosmic rays and stellar X-rays. The disks can also viewed as dusty plasmas as they contain micron-size dust particles from which planets form.

In this talk, we highlight interesting aspects of protoplanetary disks as weakly ionized dusty plasmas, and discuss their importance in planet formation as well as the MHD of the disks themselves. In particular, we focus on the interplay between charged dust particles and disk's MHD turbulence. Ionized accretion disks are prone to become turbulent because of the magnetorotational instability (MRI; Balbus & Hawley 1991). In protoplanetary disks, the activity of MRI strongly depends on how much dust has grown to larger solid bodies, as small dust particles determine the ionization degree of the disk gas. Meanwhile, turbulence, if present, drives the relative velocity of solid particles, which in turn affects how far the particles can grow by collisions. We briefly review recent developments in the numerical study of MRI-driven turbulence, and then discuss possible coevolution of MRI turbulence and dust particles as predicted by our latest self-consistent simulation (Okuzumi & Hirose 2012).

We will also highlight the importance of plasma heating by turbulent electric fields. A simple order-of-magnitude estimate shows that electric fields in MRI turbulence can significantly heat up electrons in the gas. This implies that Ohm's law can become *nonlinear* in the field strength. To study the nonlinearity of Ohm's law, we construct a gas-dust charge reaction model that takes into account the heating of ionized gas particles as well as impact ionization by hot electrons (Okuzumi & Inutsuka, in prep.). We find that the heating gives rise to negative differential resistivity at a high electric field strength. This occurs because heated electrons more frequently adsorb onto dust particles. The reduced conductivity will lead to suppressed MHD turbulence. Our ionization balance calculations predict that this effect become important in realistic protoplanetary disks (Mori & Okuzumi, in prep.).

Keywords: weakly ionized plasma, dust, planet formation, MHD, turbulence

Japan Geoscience Union Meeting 2014
(28 April - 02 May 2014 at Pacifico YOKOHAMA, Kanagawa, Japan)

PEM31-02 Room:503 Time:May 1 15:40-16:00

Ionospheric disturbances studied by high-resolution GPS total electron content observations

TSUGAWA, Takuya[1*] ; NISHIOKA, Michi[1] ; SAITO, Akinori[2] ; OTSUKA, Yuichi[3] ; ISHII, Mamoru[1]

[1]National Institute of Information and Communications Technology, [2]Graduate School of Science, Kyoto University, [3]Solar-Terrestrial Environment Laboratory, Nagoya University

The Global Positioning System (GPS) is a worldwide precise radio-navigation system formed from a constellation of at least 24 satellites at 20,200 km altitude, 4.2 R_E from the center of the Earth. GPS orbit configuration ensures that 5-10 satellites are visible from any single point on the Earth. The dual-frequency signals from the GPS satellites pass through the ionosphere to reach ground-based GPS stations. The phase and group velocities of radio waves vary in the ionosphere depending on the integrated electron density, that is total electron content (TEC), along the ray path and on the frequency of the radio waves. Using these characteristics, the TEC integrated along the ray path between a GPS satellite and a receiver can be accurately measured using two GPS signals in different frequencies. The TEC strongly reflects variations in the ionosphere at an altitude of about 300 km, where is the peak height of ionospheric electron density.

We have developed high-resolution TEC maps using dense GPS receiver networks. We have been collecting all the available GNSS receiver data in the world to expand the TEC observation area. These GNSS data are provided by IGS, UNAVCO, SOPAC, and other regional data centers. Currently, we are providing global and regional maps of absolute TEC, detrended TEC, and rate of TEC change index (ROTI). These data and quick-look maps are archived and available in DRAWING-TEC website (http://seg-web.nict.go.jp/GPS/DRAWING-TEC/).

These high-resolution GPS-TEC maps have been applied to studies of various ionospheric disturbances. Sudden increase in TEC caused by solar flares were studied using global TEC observations. Regional TEC observations have revealed new characteristics of large- and medium-scale traveling ionospheric disturbances (LSTIDs and MSTIDs). Recently, clear concentric waves and short-period oscillations were observed after huge earthquakes/tsunamis and massive tornadoes, indicating that acoustic and/or gravity waves propagate upward from the lower atmosphere and reach the ionosphere.

In this presentation, we will introduce recent studies of ionospheric disturbances using high-resolution GPS-TEC observations.

Keywords: ionosphere, GPS, TEC, thermosphere

Japan Geoscience Union Meeting 2014
(28 April - 02 May 2014 at Pacifico YOKOHAMA, Kanagawa, Japan)

PEM31-03 Room:503 Time:May 1 16:15-16:30

Observation of Lightning in Protoplanetary Disks by Ion Lines

MURANUSHI, Takayuki[1*] ; AKIYAMA, Eiji[2] ; INUTSUKA, Shu-ichiro[3] ; NOMURA, Hideko[4] ; OKUZUMI, Satoshi[4]

[1]Kyoto University, [2]The National Astronomical Observatory of Japan, [3]Nagoya university, [4]Tokyo Institute of Technology

Lightning in protoplanetary disks is an important elementary process in protoplanetary disk science. It has been studied as a candidate mechanism for chondrule formation, and it provides unique window to probe the electromagnetic state of the protoplanetary disks. As a consequence, multiple lightning models has proposed for protoplanetary disks, and it is important for protoplanetary disk astrophysics to observationally distinguish which model is correct. Here we study the possibility of observationally distinguishing lightning models in protoplanetary disks.

Lightning on Earth is discharge phenomenon in the air, and the gas discharge physics in air has been studied for centuries and is well understood process. But it has been observed that lightning takes place under electric field amplitude well below the dielectric strength of the air, the fact that has been a long standing mystery. Here, dielectric strength of an insulating material is the maximum amplitude of the electric field the subject material does not cause the electric breakdown. It is physical property of central importance for discharge physics.

In attempt to solve the mystery, traditional Townsend breakdown model has been challenged by new discharge models such as Druyversteyn-Penning breakdown model and runaway breakdown model. The values of the dielectric strength according to the latter two model are much smaller than it by Townsend breakdown model.

We can distinguish the breakdown models by their dielectric strength. Dielectric strength is the point where the electrons accelerated by the electric field reaches certain ionization energy. The electric field also accelerates the positively-charged ion species to the energy comparable to the electrons. Because the ionization energy is a universal constant, the accelerated ion energies are also constant. Observationally, this means that we will observe ion velocities much faster than the thermal velocity, and the observed velocities will be independent of the local density nor temperature among the lightning regions. This will be unique observational feature to detect and distinguish breakdown models in protoplanetary disks. For example, under disk gas that consists of 92% H_2 and 8% He, the characteristic ion speed of HCO^+ is 7.1km/s, 2.9km/s and 0.49km/s, respectively, for Townsend breakdown model, Druyversteyn-Penning breakdown model, and runaway breakdown model.

We have calculated the velocity distribution of the three ion species HCO^+, DCO^+ and N_2H^+, taking the lightning models into consideration. We have simulated the line profile and two-dimensional position-velocity images. We found lightning features of 10-100mJy appear in line profile. Recent ALMA observations e.g. by Mathews et al. (2013) and Qi et al. (2013) achives ˜10mJy sensitivity. Therefore we can reject some of the lightning models based on ALMA archive data, and distinguish lightning models by future ALMA observations.

Keywords: Protoplanetary disks, Discharge phenomena, Lightning, Weakly-ionized plasma, astrophysical plasma

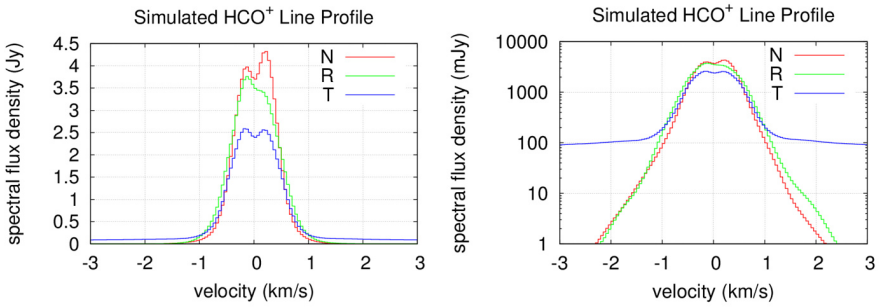

Simulated HCO^+ line profile of an MMSN disk located at distance d=56pc, inclination i = 7(deg). The three curves indicate disk without lightning (N), disk with runaway breakdown model (R), and with Townsend breakdown model (T), respectively.

Japan Geoscience Union Meeting 2014
(28 April - 02 May 2014 at Pacifico YOKOHAMA, Kanagawa, Japan)

PEM31-04 Room:503 Time:May 1 16:30-16:45

Investigation of attractive forces associated with overlapping Debye spheres using N-body simulations

ITOU, Hotaka[1*] ; AMANO, Takanobu[1] ; HOSHINO, Masahiro[1]

[1]Department of Earth and Planetary Science, Graduate School of Science, The University of Tokyo

Dust grains are quite common in space. They are thought to exist in, e.g., molecular clouds, protoplanetary disks, Earth's magnetosphere, and planetary rings. In addition, also in laboratories, the lattice formation of dust grains is the well-known phenomena and called Coulomb crystallization. Dust grains immersed in plasmas usually acquire large amount of charges due to several charging processes such as collisions with plasma partilcles and photoemission. Then the charged grains and the ambient plasma are strongly coupled with each other, and such plasmas are called dusty plasmas or complex plasmas. Since in situ observations in the solar system or Ikezi's prediction of Coulomb crystallization, dusty plasmas have been studied for not only astrophysical applications but also industrial applications.

When collisions between dust grains and plasma particles dominate charging processes, the dust grains are nagatively charged because generally the flux of electrons is larger than that of ions. Thus we expect that they repel each other. However, in realty, the force on dust grains is quite complex due to the interaction with the ambient plasma and several types of forces have been proposed (e.g., Shukla and Eliasson [2009]). Interestingly, some attractive forces may also exist and play important roles in aggregation or crystallization of dusty plsamas.

One of proposed attractive forces is that of due to the overlapping of Debye spheres (ODS). Resendes et al. [1998] showed that the potential between two dust grains is similar to Lennard-Jones potentials, which is repulsive at short distance and weakly attractive at longer distance. Moreover, Hou et al. [2009] showed that this type of attractive interaction has, if indeed it exists, the drastic aggregation and crystallization effect in dusty plasmas. On the other hand, it was suggested that the ODS attractive force does not exist when particles electrically trapped by grains are negligible ,i.e., the orbital motion limited (OML) theory is valid (Lampe et al. [2000]), and it has not been confirmed experimentally.

The aim of our study is to investigate the possibility of the ODS potential, by using direct N-body simulations, which allow us to investigate the electrostatic potential structure around the dust grains with minimun assumptions. By using a newly developed N-body simulation code implementing Ewald's sum algorithm, in which the short-range part of the potential is calculated in real space and the long-range part is calculated in wavenumber space, we have shown that in plasmas with a low plasma parameter there does not exist the ODS attractive force. In this study, we introduce the mesh and extend the code to implement the PM (particle-mesh) or PPPM (particle-particle particle-mesh) method allowing us to perform simulations with a much more particles to attempt the investigation of plasmas with the large plasma palameter.

Japan Geoscience Union Meeting 2014
(28 April - 02 May 2014 at Pacifico YOKOHAMA, Kanagawa, Japan)

PEM31-05 Room:503 Time:May 1 16:45-17:00

Test-particle simulation of electron-H2O elastic collision along the magnetic field line around Enceladus

TADOKORO, Hiroyasu[1*] ; KATOH, Yuto[2]

[1]Tokyo University of Technology, [2]Department of Geophysics, Graduate School of Science, Tohoku University

Saturn's inner magnetosphere is dominated by water group neutrals originated from Enceladus' water plume [e.g., Shemansky et al., 1993; Richardson et al., 1998; Esposito et al., 2005]. The neutrals in the inner magnetosphere contribute to one of the important loss processes of plasma through plasma-neutral collisions. However, little has been reported on a quantitative study of the electron loss process due to electron-neutral collisions. In this paper, we will focus on the collisional loss process with neutrals.

We examine the variation of equatorial electron pitch angle distribution and loss rate of precipitated electrons into Saturn's atmosphere through pitch angle scattering due to elastic collisions with neutral H_2O along Saturn's magnetic field line around Enceladus. We focus on 1 keV electrons as a typical energy in the present study. To examine the variation of those, we perform one-dimensional test-particle simulation when the co-rotating electron flux tube passes the dense H_2O region in the vicinity of Enceladus (˜6.4 minutes). Results show that the equatorial electron pitch angle distribution near the loss cone ($<$20 degrees and $>$160 degrees) decreases with time through pitch angle scattering due to elastic collisions. It is found that the electrons of ˜19 % to the total number of equatorial electrons at the initial condition are lost in ˜380 seconds. The calculated loss time is twice faster than the loss time under the strong diffusion.

Keywords: plasma-neutral collision, Saturn, Enceladus, elastic collision, pitch angle scattering

Japan Geoscience Union Meeting 2014
(28 April - 02 May 2014 at Pacifico YOKOHAMA, Kanagawa, Japan)

PEM31-06 Room:503 Time:May 1 17:00-17:15

MHD wave-driven mass loss from gas giants and effects on atmospheric structure

TANAKA, Yuki[1*] ; SUZUKI, Takeru[1] ; INUTSUKA, Shu-ichiro[1]

[1]Department of Physics, Nagoya University

Recently a number of exoplanets have been found, and some of them are close-in gaseous planets. Such planets are called hot Jupiters, and their surface temperatures are ˜1000K due to strong irradiation from central stars.

Information of radius and orbital period of exoplanet can be observed by transit method which is the one of method to detect exoplanets. Additionally, atmospheric composition can be estimated by variation of spectrum between transiting and non-transiting, and atmospheric structure can be estimated by multi-wavelength transit observation. From these observations, inflated hydrogen atmosphere of hot Jupiters and atmospheric escape are suggested. It is observed that escaping atmospheric flow is very fast, and mass loss rate is also estimated. However, detailed mechanism of mass loss from hot Jupiters are still unknown.

We propose a new mechanism of mass loss, which is mass loss driven by magneto-hydrodynamic wave, same as solar wind. Atmosphere is weakly ionized because surface temperatures of hot Jupiters are about 1000K, but it is good to treat as ideal MHD at upper atmosphere. If gas giant have magnetic field and turbulence exist on the surface of planet, magneto-hydrodynamic wave will be generated. The wave propagates upward and dissipates in upper atmosphere, then gas flow is accelerated. In this work, we apply numerical calculation of solar wind to mass loss from hot Jupiters. In consequence, mass loss by this magnetically driven wind is comparable to observed mass loss rate, therefore magnetically driven wind can be important role in mass loss from hot Jupiters.

We also derive an analytical solution for radius and mass dependence of mass loss rate, and it shows a good agreement with numerical results. Dissipation of MHD wave in the atmosphere also affects on atmospheric structure. The gas flow is accelerated to supersonic at upper atmosphere, and temperature become several tens of thousand kelvin. In this talk, we will discuss the possibility of mass loss from general gaseous planet and effects on atmospheric structure.

Keywords: exoplanet, atmospheric escape

Japan Geoscience Union Meeting 2014
(28 April - 02 May 2014 at Pacifico YOKOHAMA, Kanagawa, Japan)

PEM31-07 Room:503 Time:May 1 17:15-17:30

Group motion of heteromorphic fine particles in HF discharge plasma

MIENO, Tetsu[1*] ; MASUDA, Risa[2] ; MORIBAYASHI, Takashi[2] ; HAYASHI, Yasuaki[3]

[1]Grad. School Sci. Technol, Shizuoka Univ., [2]Dept. Phys., Shizuoka Univ., [3]Grad. School Eng., Kyoto Inst. Technol.

Related with complex systems, fine-particle plasmas have much attention to scientists and engineers [1, 2]. Hence, we are trying to make fine-particle plasmas with heteromorphic particle distributions by using a high-frequency (HF) Ar plasma. And the motions of charged particles are observed. In a stainless steel chamber (150 mm in diam, 150 mmh), 100 mm in diam disk electrodes and a 80 mm in diam metal ring are set. In this experiment, HF argon discharge is produced at 10˜13 Pa by applying HF voltage of about 270˜290 V_{rms} to the lower disk-electrode with respect to the upper grounded disk-electrode. And a ring is added on the lower electrode to confine fine-particles. The particles used are silicon carbide, which has diameter of about 8 um, or silicon-nitride (about 8 um), or short hemp (about 25 um diam. 10 ? 1500 um long). They are injected from a dust dropper. A digital microscope camera (SELMIC LWD100) and a CCD video camera are used to investigate the particle behaviors. Under a condition of discharge voltage V_d= 280 V_{rms}, discharge current I_d= 0.2 A_{rms} and pressure p(Ar)= 13 Pa, a disk-shaped cloud is generated as shown in Fig. 1. Each particle motion and the particle-group motion are recorded by the cameras. We could observe planet-like motions like Fig. 2 (track of a SiC particle). In case of the short hemp, there are spin motions and planet-like motions. We conjecture that these motions are activated by the dust-acoustic perturbation.

[1] Y. Hayashi, K. Tachibana, J. Vac. Sci. Technol. A 14 (2) (1996) 506.
[2] H. Thomas, G.E. Morfill, V. Demmel, Phys. Rev. Lett. 73 (1994) 652.

Keywords: fine particle plasma, heteromorphic particles, self organization, planetary motion, spin, dust plasma

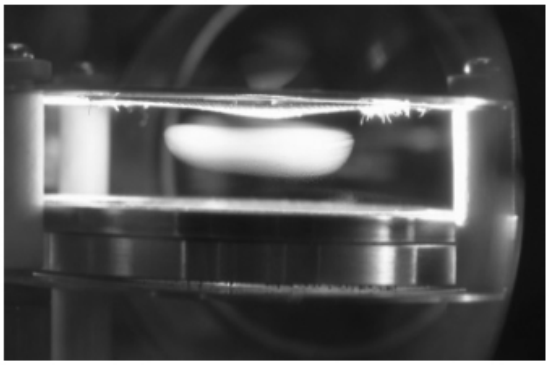

Fig. 1 Fine particles in the HF plasma.

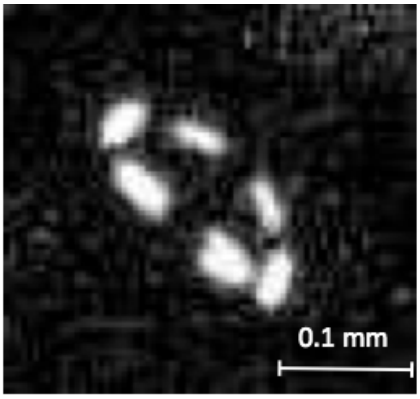

Fig. 2 Planet-like motion of a particle.

Japan Geoscience Union Meeting 2014
(28 April - 02 May 2014 at Pacifico YOKOHAMA, Kanagawa, Japan)

PEM32-01 Room:503 Time:May 2 09:00-09:15

A new instability along toroidal magnetic field in differentially rotating plasmas

HIRABAYASHI, Kota[1*] ; HOSHINO, Masahiro[1]

[1]Department of Earth and Planetary Science, The University of Tokyo

We discuss a new type of instability expected to take place in an accretion disk, which has a differentially rotating plasma threaded by a weak magnetic field, by performing linear eigenvalue analysis. We study the linear stability of a disk with a localized, toroidal magnetic field in the radial direction, which can be expected in an accretion disk during the nonlinear evolution of the magneto-rotational-instabilities (MRI).

The MRI is believed to be a strong source of magneto-hydro-dynamic (MHD) turbulence and the resultant angular momentum transport in the accretion disk, which is required for the gas to accrete onto the central object. Once the MRI grows, the system is chiefly governed by the toroidal and radial magnetic field newly generated by the dynamo action of MRI. Such a configuration allows the Alfven waves to propagate along toroidal direction.

In this talk, we study the linear stability of the Alfven wave in the local Cartesian coordinate, the so-called shearing periodic box, and show that the toroidally propagating Alfven wave can become unstable if its wavelength is larger than the length scale of the localized magnetic field gradient. We investigate our results of the linear eigenvalue analysis by changing the structure of the localized magnetic field, and discuss some properties of the instability with examining the eigenvectors and eigenvalues. It is revealed that this type of instability may also appear in non-rotating plasma, but it is highly suppressed in a rigid body rotating plasma. In addition to the linear analysis, the corresponding nonlinear behavior will also be discussed by using MHD numerical simulations. This instability plays an important role in the plasma transport because it probably couples with the magnetic reconnection occurring in the equatorial plane and then to contributes to the saturation mechanism of the MRI.

Japan Geoscience Union Meeting 2014
(28 April - 02 May 2014 at Pacifico YOKOHAMA, Kanagawa, Japan)

PEM32-02 Room:503 Time:May 2 09:15-09:30

Particle acceleration and angular momentum transport during magnetorotational instability in kinetic accretion disks

HOSHINO, Masahiro[1*]

[1]The University of Tokyo

Magneto-rotational instability (MRI) in a gravitational rotating system is known to play an important role on the formation of the astrophysical accretion disk and the angular momentum transport, and the nonlinear time evolution of magneto-rotational instability has been extensively investigated by using MHD simulations so far. The mean free path of plasma, however, is not necessarily smaller than the characteristic scale length for some classes of astrophysical accretion disks, and the collisionless behavior of MRI beyond the MHD approximation needs to be understood. In this talk, we study momentum transport and particle acceleration of the kinetic (collisionless) MRI by focusing on magnetic reconnection. We discuss that a strong pressure anisotropy is associated with the formation of the channel flow, and the anisotropic channel flow can lead to a rapid magnetic reconnection, that can occurs sporadically in three-dimensional system. As a result of the reconnection, non-thermal power law distribution with a hard spectral index p=1-1.5 is quickly formed. We also discuss that the so-called alpha parameter in the standard accretion disk model, which is numerically measured from the Reynolds and Maxwell stresses, can be dramatically enhanced during the nonlinear time evolution of MRI. The kinetic MRI is one of plausible mechanisms to explain much more efficient angular momentum transport and high-energy particle emissions observed from massive black holes such as Sgr A$*$.

Keywords: Space and astrophyiscal plasmas, accretion disk, particlle acceleration, magnetic reconnection, angular momentum transport

Japan Geoscience Union Meeting 2014
(28 April - 02 May 2014 at Pacifico YOKOHAMA, Kanagawa, Japan)

PEM32-03 Room:503 Time:May 2 09:30-09:45

Numerical Simulation of Kinetic Magnetorotational Instability using a new Hybrid Technique

SHIRAKAWA, Keisuke[1*] ; AMANO, Takanobu[1] ; HOSHINO, Masahiro[1]

[1]Faculty of Science, University of Tokyo

The evolution of Magnetorotational instability (MRI) is considered to be important in the context of efficient angular momentum transport in the accretion disks in our universe. Conventionally, the nonlinear evolution of MRI is studied under the MHD approximation which assumes the mean free path of the plasma is sufficiently small compared to the actual size of the disk. However some classes of the accretion disks, for example the disk around SgrA∗, are found to be constituted with a collision less plasma and therefore the kinetic effect of the plasma, such as generation and relaxation of the pressure anisotropy, should be taken into account.

For the inclusion of the kinetic plasma effects, hybrid code, which treats ions as particles and electrons as massless charge neutralizing fluid, may provide a robust approach resolving the ion scale physics and integrating over the Keplerian time scale. However in the 2 dimensional simulation of the MRI, it is well known that the system eventually grows to a set of channel flows. In this state, the density of the plasma is found to be extremely low in the region where the magnetic field is enhanced as a result of a strong dynamo effect of the differential rotation of the disk. In this low density, strong magnetic field region, the CFL condition determined by the R-mode wave is found to be severe. Moreover, since the extremely low density region is generated in the channel flow, the division-by-density operation in the conventional hybrid code leads to an unexpected termination of the calculation.

In this study we adopted a new approach of hybrid simulation to a differentially rotating system. In this approach, the finite electron inertia is taken into account which gives a upper bound in the phase velocity of the R-mode wave, providing a reduced CFL condition. In addition, the new approach is almost free from the division-by-density operation and the extremely low density region generated in the channel flow can then be calculated appropriately. With this new code we would like to discuss the nonlinear evolution of the 2 dimensional kinetic MRI.

Keywords: Magnetorotational Instability, Kinetic Plasmas, Accretion disks, Collisionless Plasmas, Hybrid code

Japan Geoscience Union Meeting 2014
(28 April - 02 May 2014 at Pacifico YOKOHAMA, Kanagawa, Japan)

PEM32-04 Room:503 Time:May 2 09:45-10:10

Self-organization and flow in high-beta magnetized plasmas

NAGATA, Masayoshi[1*]

[1]University of Hyogo, Graduate School of Engineering

The self-organized plasmas with high-beta such as spheromaks have the common features as magnetic reconnection, kinking behavior, particle acceleration and shock wave which are observed in space phenomena. Dynamical process of explosive plasmoid ejection, magnetic field's twisting and reconnection could account for the various phenomena called astrophysical jets, solar coronal loops and Jupiter's zonal flow driven by thermal convection. As for fusion plasmas, to control externally plasma flow or rotation plays an important role on maintaining high-beta confinements with an optimized pressure gradient. It is well known that for example, the H-mode transition in tokamak plasmas is created by inward radial electric field and poloidal shear flow. The diamagnetic configuration like Field Reversed Confinement (FRC) with super high beta, in which ion flows generate currents, is normally analyzed based on two-fluid MHD relaxation model. In helicity-driven system, non-axisymmetric dynamic processes create current due to the dynamo action in the plasmas and relax them toward certain minimum energy equilibria. The non-axisymmetric behavior, which arises from a helical kink instability on the open flux, could be responsible for the formation and sustainment of the configurations by helicity injection [1]. In this conference, we will present recent topics about dynamics and relaxed states relevant to MHD relaxations, plasmoid ejection, dynamo and kinking behavior which are recognized as analogical phenomena in astrophysical and fusion plasmas.

It is possible to replicate astrophysical plasma phenomena in the laboratory because MHD has no intrinsic scale. The governing MHD equations can be expressed in a dimensionless form that is equally applicable to systems having scale lengths with many orders of range. Now, a point is how to produce flexibly plasmoid eruptions like solar flares by taking critical issues of geometry and topology into consideration. We will introduce the magnetized coaxial plasma gun (MCPG) to make it possible to investigate such a bubble burst-like behavior. The MCPG is often used to produce spheromaks with poloidal and toroidal magnetic fields generated by internal current. Historically the spheromak was for the first time produced by Alfven et al. by using the MCPG.

The driven-relaxed configurations with open field lines, as well as closed systems, are described by the force-free equilibrium (Jensen-Chu) equation, $\nabla \times B = \lambda B$, where λ is the force-free parameter. The nature of the relaxed states in helicity-driven systems is characterized by the strength of the external toroidal field and the value of λ determined by coupling to the MCPG. Note that in the doubly connected helicity-driven system, the flipped spherical torus (ST) state appears in the regime of $\lambda < \lambda e$, where λe is the lowest eigenvalue, so that it could be observed in laboratory experiments. The structural formation of the flipped field configuration incorporates the self-reversal process of the toroidal and poloidal fields. This self-organizing phenomenon may have some analogy to reversal of the dipole field of Earth generated by a dynamo action. It is fundamentally important to elucidate a current-reversal phenomenon occurring in space and laboratory plasmas. We have observed this novel current-reversal phenomenon in our HIST experiment [2, 3]. The most important discovery of this experiment is that spherical torus plasmas tend to self-organize to the flipped states while reversing the direction of the external toroidal field [2, 3]. This experimental finding provides, for the first time, evidence for the existence of the relaxed states which were theoretically predicted.

References

[1] M. Nagata et al., Phys. Rev. Lett. 71, 4342 (1993)
[2] M. Nagata et al., Phys. Rev. Lett. 90, 225001 (2003)
[3] M. Nagata et al., Phys. Plasmas 10, 2932 (2003)

Keywords: plasmoid, spheromak, flow, self-organization, MHD relaxation, dynamo

Japan Geoscience Union Meeting 2014
(28 April - 02 May 2014 at Pacifico YOKOHAMA, Kanagawa, Japan)

PEM32-05 Room:503 Time:May 2 10:10-10:30

Observations of Alfvenic waves in the solar atmosphere

OKAMOTO, Joten[1*]

[1]ISAS/JAXA

Coronal heating and the acceleration of the solar wind are unsolved problems in solar physics. The propagation of Alfven waves along magnetic field lines is one of the candidate mechanisms to carry energy to large distances from the surface and heat the coronal plasma. However, such waves had not been observed for years.

The solar physics satellite, Hinode, was launched in 2006, and it opened the door to the world of coronal waves. Hinode observations have directly resolved small-scale transverse oscillations of field lines as a result of Alfven/Alfvenic waves in prominences (Okamoto et al. 2007) and spicules (De Pontieu et al. 2007) which are typical chromospheric features embedded in the corona. These waves had a period of 2-5 minutes (low frequency) and the velocity amplitudes are up to 20 km/s. If we assume these are propagating waves, the waves have enough power to heat the corona. However, since the wavelength of these waves is as long as or longer than the observed structures, it is difficult to resolve the phase difference along the field lines. This means we cannot know whether they are propagating or standing waves.

More recently, we had a challenge to detect ”propagating” waves (Okamoto and De Pontieu 2011). In this study, we developed an algorithm to detect spicules and phase difference of waves along them automatically. As a result, upward- and downward-propagating waves as well as standing waves were successfully detected. With statistical analyses, it is found that the behaviour of waves depends on the evolution of spicules, and numerous waves are reflected at the top of spicules. These waves detected in this study are high-frequency ones, and the energy is not larger than that of low-frequency ones. Hence, it is suggested that low-frequency waves are more important for coronal heating.

Finally, oscillations/waves shown here are ubiquitous in the solar atmosphere and ”wave hunting” is getting more active after the Hinode launch. In addition, investigation of coronal waves is important for the derivation of physical parameters such as coronal magnetic field strength, which it is difficult to measure in observations. In this talk, I will show these studies with Hinode and introduce a new result with a new satellite ”IRIS”.

Keywords: Sun, corona, wave, Hinode

Japan Geoscience Union Meeting 2014
(28 April - 02 May 2014 at Pacifico YOKOHAMA, Kanagawa, Japan)

PEM32-06 Room:503 Time:May 2 10:30-10:45

2.5D MHD Simulations of Solar Filament Formation by Condensation

KANEKO, Takafumi[1*] ; YOKOYAMA, Takaaki[1]

[1]Department of Earth and Planetary Science, The University of Tokyo

We investigate the formation mechanism of solar filaments by two-dimensional magnetohydrodynamic (MHD) simulations. Solar filaments are cool dense plasma clouds in the hot tenuous corona. Filaments abruptly erupt with flares, hence, they are the important objects to comprehend the explosive events in the solar atmosphere. On the other hand, their formation mechanism is still unclear as well as the mechanism for eruptions.

Filaments always appear inside the coronal arcade fields, and the cool dense plasma is sustained by the magnetic forces. Observations show that filaments are categorized as normal polarity filaments or inverse polarity filaments. The normal polarity filaments have the same polarity with the surrounding coronal magnetic fields, while the inverse polarity filaments have opposite polarity. One candidate to explain the origin of the cool dense plasma is condensation by the radiative cooling in the corona. The current condensation model can reproduce the normal polarity filaments, but not the inverse polarity filaments. We propose a new condensation model to reproduce the inverse polarity filaments, and demonstrate it by two-dimensional MHD simulations including radiative cooling, thermal conduction along the magnetic field and gravity. Our model starts from the formation of the magnetic flux rope. The relatively dense plasma at the lower corona is trapped inside the flux rope and lifted up to the upper corona. The dense plasma causes imbalance between the radiative cooling and the background heating, while the thermal conduction along the closed field line of the flux rope does not suppress the thermal imbalance. Consequently, the condensation process is triggered and the cool dense plasma is formed. We test two types of heating term (one depends on magnetic pressure and the other depends on density) and two types of formation mechanisms of the flux rope (one is the conversing motion at the footpoints of the coronal arcade field and the other is the interaction between the emerging flux and the coronal arcade field). As a result, the cool dense plasma is formed inside the flux rope in every case. We also show that our model has a possibility to reproduce the density of solar filaments, which is 10 -100 times larger than that of the surrounding corona, qualitatively.

Keywords: solar filament, prominence

Japan Geoscience Union Meeting 2014
(28 April - 02 May 2014 at Pacifico YOKOHAMA, Kanagawa, Japan)

PEM32-07 Room:503 Time:May 2 11:00-11:15

Comparative study of Observation and Calculation of Hot Fast Flow above a Solar Flare Arcade

IMADA, Shinsuke[1*]

[1]Nagoya Univ. STEL

Solar flares are one of the main forces behind space weather events. However, the mechanism that drives such energetic phenomena is not fully understood. The standard eruptive flare model predicts that magnetic reconnection occurs high in the corona where hot fast flows are created. However, there is not enough observational knowledge of the physical parameters in the reconnection region. The inflow into the reconnection region, the temperature of the plasma in the reconnection region, and the temperatures and densities of the plasma jets predicted by reconnection, have not been quantitatively measured in sufficient. First, we will show a flare that occurred on the west solar limb on 2012 January 27 observed by the Hinode EUV Imaging Spectrometer (EIS) and found that the hot (?30MK) fast (>500 km s?1) component was located above the flare loop and discuss how extent we understand the key-region of solar flare. Second, it is important to answer why the most observation cannot detect the predicted flow or temperature in the reconnection region. One of the reasons why we cannot observe inside the magnetic reconnection region is due to its darkness. Generally we can see the bright cusp-like structure during solar flare, although the reconnection region is faint/blind. One may think that the temperature in the reconnection region is enough higher than that of cusp-like flare loops. Thus the wavelength of emission from reconnection region is different from flare loops. However, this is not entirely true. Magnetic reconnection causes rapid heating. Thus ionization cannot reach to the equilibrium stage. We have calculated the ionization process in the down stream of Petschek type magnetic reconnection. From our result, we can clearly see that plasma cannot reach the ionization equilibrium in the down stream of slow-mode shock. The typical emissions from magnetic reconnection region are FeIXX or FeXX, although the plasma temperature is equal to 40MK. The typical temperature and density of post flare loops are 10 MK and 10ˆ11 /cc, and the dominant emissions from post flare loops are from FeIXX to FeXXIII. Thus the wavelength of emission from reconnection region is not so much different from post flare loops. We will discuss how the emissions from reconnection region looks like by using several ionization calculations of magnetic reconnection.

Keywords: flare, corona, non-equilibrium ionization, sun

Japan Geoscience Union Meeting 2014
(28 April - 02 May 2014 at Pacifico YOKOHAMA, Kanagawa, Japan)

PEM32-08 Room:503 Time:May 2 11:15-11:30

Magnetic Evolutions at Extremely High Latitude Region during Polarity Reversal Observed with Hinode

SHIOTA, Daikou[1*] ; SHIMOJO, Masumi[2] ; SAKO, Nobuharu[3] ; KAITHAKKAL, Anjali john[3] ; TSUNETA, Saku[4]

[1]STEL, Nagoya University, [2]National Astronomical Observatory of Japan, [3]The Graduate University for Advanced Studies, [4]ISAS, JAXA

The magnetic field in the Sun's polar region is a key ingredient of the solar dynamo mechanism because the polar field strength at a solar minimum has a correlation with solar activity of the following cycle. The evolution processes of the polar field (its polarity reversal and its build-up after the reversal) are thought to be caused by magnetic flux transport due to meridional flow and diffusion by turbulent convection. Nevertheless, our understanding of the meridional flow and diffusion in the polar region is still poor because of many difficulties in magnetic observation near the limb.

We recorded time evolution of magnetic polarity distribution within the whole of both polar regions derived from the high-accuracy spectropolarimetric observation with Solar Optical Telescope aboard Hinode. In the north polar region, the latitudinal polarity inversion line (PIL) between the preexisting negative polarity region and transported positive polarity region migrates from 60 degrees latitude at January 2012 to 68 degrees latitude at September 2012. Then the whole of the north polar region becomes positive at September 2013. The migration speed of the PIL is 5 m s^{-1} (January - September 2012) and then becomes 8.5 m s^{-1} (September 2012 - September 2013). According to a flux transport model, the speed-up is understood as a result of a diffusion process. In contrast, the whole of the south polar region observed in March 2013 has still ample positive field. The PIL locates out of the observed region (over 67 degrees latitude).

We examined a few parameter sets of the meridional flow pattern and the diffusion coefficient with an advection-diffusion model. The observed PIL migration in the north polar region can be explained well if there is slightly strong diffusion without the meridional flow.

Keywords: photosphere, magnetic fields, spectropolarimetry, polarity reversal, dynamo

Japan Geoscience Union Meeting 2014
(28 April - 02 May 2014 at Pacifico YOKOHAMA, Kanagawa, Japan)

PEM32-09 Room:503 Time:May 2 11:30-11:45

Properties of small-scale jets in a sunspot chromosphere revealed through spectroscopic observations

KATSUKAWA, Yukio[1*] ; OI, Akihito[2] ; REARDON, Kevin[3] ; TRITSCHLER, Alexandra[3]

[1]National Astronomical Observatory of Japan, [2]Kyoto University, [3]National Solar Observatory

High-resolution observations with HINODE Solar Optical Telescope (SOT) revealed that small-scale jets frequently occur in a sunspot chromosphere though their driving mechanism is not well understood yet because of lack of spectroscopic information, such as temperatures and Doppler velocities, in the chromospheric observations with Hinode SOT. Spectroscopic observations of the small-scale jets were attempted using an Interferometric BIdimensional Spectrometer (IBIS) at the National Soar Observatory (NSO), and suggested that temperature enhancements associated with the jets happened in the lower chromosphere though their upward flows were not clearly detected (Reardon, Tritschler, Katsukawa 2013). We've tried obtaining another spectroscopic data set of a sunspot chromosphere with better spectral resolution with IBIS, and carried out careful analysis of spectral profiles and their temporal evolution. The study shows majority of the heated plasma in the lower chromosphere has a bulk flow slower than the sound speed in the chromosphere. The spectral profiles indicate enhancements in the blue wing, which suggests a part of the heated plasma has a supersonic upflow. In addition, small temperature enhancements are also found in the upper chromosphere near the end of the duration of the jets. The supersonic upflows are possibly responsible for heating in the upper chromosphere. This study provides an important observational support for slow-mode waves as acceleration and heating mechanism in the chromospheric jets. We are going to present a new spectroscopic observation of chromospheric jets made by the Interface Regiong Imaging Spectrograph (IRIS) spacecraft that has just started observations since 2013.

Keywords: the Sun, chromosphere, jet, spectroscopy, HINODE, IRIS

Japan Geoscience Union Meeting 2014
(28 April - 02 May 2014 at Pacifico YOKOHAMA, Kanagawa, Japan)

PEM32-10 Room:503 Time:May 2 11:45-12:00

Fast magnetic reconnection with a moving X-point in resistive MHD

MIYOSHI, Takahiro[1*] ; KUSANO, Kanya[2]

[1]Graduate School of Science, Hiroshima University, [2]STEL, Nagoya University

Fast magnetic reconnection in high magnetic Reynolds number plasmas is one of the most important physical process of explosive phenomena in space and astrophysical plasmas. In recent years, using high-resolution MHD simulations with high magnetic Reynolds numbers, it has been indicated that fast magnetic reconnection may be triggered by the plasmoid instability in a thin current sheet [1]. Moreover, a state-of-the-art high-resolution MHD simulation revealed that some of multiple secondary reconnection are developed as Petschek-like reconnection [2]. However, the detailed structure and dynamics of individual secondary reconnection is not clarified yet.

The objective of this study is to reveal the structure and dynamics of resistive magnetic reconnection with a moving X-point paying attention to the motion of the secondary reconnection. Particularly, we propose an asymmetric reconnection model where a local anomalous resistivity including a shifting motion is added to the two-dimensional Harris equilibrium. A high-resolution MHD simulation for the asymmetric resistive reconnection was performed using the HLLD approximate Riemann solver and analyzed with respect to the structure in detail. Besides, we discussed the possibility of a self-sustaining mechanism of the asymmetric reconnection due to the flow driven by the reconnection itself.

[1] e.g, N. F. Loureiro, et al., Phys. Plasmas, 19, 042303 (2012)
[2] K. Kusano, K. Nakabou, et al., in preparation

Keywords: magnetic reconnection, MHD, anomalous resistivity model

Japan Geoscience Union Meeting 2014
(28 April - 02 May 2014 at Pacifico YOKOHAMA, Kanagawa, Japan)

PEM32-11 Room:503 Time:May 2 12:00-12:15

Dynamical Petscheck Reconnection

KUSANO, Kanya[1*] ; NAKABOU, Takashi[1] ; MIYOSHI, Takahiro[2] ; VEKSTEIN, Grigory[3]

[1]STEL, Nagoya University, [2]Graduate School of Science, Hiroshima University, [3]Manchester University

Magnetic reconnection is the major mechanism for explosive energy liberation in various plasmas. However, the mechanism of fast reconnection in high magnetic Reynolds number (S) plasmas like the solar corona, in which $S>10^{10}$, is still unclear. The observations suggested that the reconnection rate in solar flares is as large as 10^{-2}, although the classical theory by Sweet (1958) and Parker (1963) predicted that the reconnection rate is limited by $S^{-1/2}$. While Petscheck (1964) proposed the fast reconnection model driven by slow mode shock, the previous simulation study suggested that the Petscheck-type reconnection is not stable in uniform resistivity and some anomalous resistivity or non-MHD effects are needed for fast reconnection.

In this paper, we developed the high-resolution magnetohydrodynamics (MHD) simulation of magnetic reconnection for the high-S (S~10^4-10^6) regime aiming at revealing the acceleration mechanism of magnetic reconnection in the MHD regime of uniform resistivity. We applied the HLLD Riemann solver developed by Miyoshi and Kusano (2005) to the high resolution two-dimensional MHD simulation of current sheet dynamics. The initial state is given by the Harris sheet equilibrium plus perturbation, and the uniform and constant resistivity model is adopted.

As a result, we found a new type of fast reconnection. When S is larger than 10^4, multiple X-line reconnection appears as a result of the secondary tearing instability and magnetic reconnection is accelerated through the formation of multiple plasmoids. Furthermore, we found that the electric current sheets between some particular magnetic island bifurcate to V-shape current layers and that the reconnection at the apex of bifurcated current layers is preferentially accelerated. The bifurcated current layers create slow mode shocks which more increase the reconnection rate up to about 0.05. The slow mode shocks are repeatedly created and dissolved corresponding to the formation and transportation of plasmoids. These results indicate that, even though resistivity is uniform, when the magnetic Reynolds number is high enough, the multiple X-line reconnection of Sweet-Parker current sheets (plasmoid reconnection) is switched to a new regime called ”dynamical Petschek reconnection”. The mechanism of transition from the conventional plasmoid reconnection to the dynamical Petscheck reconnection will be discussed.

Keywords: reconnection, Petscheck reconnection, MHD, simulation, slow mode shock

Japan Geoscience Union Meeting 2014
(28 April - 02 May 2014 at Pacifico YOKOHAMA, Kanagawa, Japan)

PEM32-12 Room:503 Time:May 2 12:15-12:30

Thermal conduction effect on the Petschek magnetic reconnection

KONO, Shunya[1*] ; YOKOYAMA, Takaaki[1]

[1]University of Tokyo

We simulated the magnetic reconnection including the nonlinear thermal conduction effect with two-dimensional MHD equations. Magnetic reconnection is considered to be the basic process of the solar explosive phenomena. In the atmosphere with high temperature and low density like solar corona, time-scale of the nonlinear heat conduction becomes shorter and can become comparable to the Alfven time-scale. Thermal conduction effect should be considered. Previous studies have showed that, in the model of magnetic reconnection produced by Petschek, adiabatic slow mode shock wave generated from the localized diffusion region is dissociated into isothermal shock wave and conduction front due to the thermal conduction. However, the effect of the thermal conduction on the energy release rate in the magnetic reconnection is not explained enough in the past.

Here we investigated how the thermal conduction influences the energy conversion rate. We calculated the energy release rate in different magnitude of the magnetic diffusivity to see the dependence on the Lundquist number. As a result, due to the thermal conduction effect, adiabatic shock wave is dissociated into isothermal shock wave and conduction front and this makes temperature in the reconnection outflow jet smaller. In the outflow region with small temperature, density becomes larger. Considering mass conservation between the mass flux in the reconnection inflow and that in the outflow, inflow velocity is accelerated because of larger density in the outflow region. This causes increase of the energy release rate in the magnetic reconnection. That increase rate tends to become larger as the magnitude of magnetic diffusivity becomes smaller. Smaller magnetic diffusivity correponds to the larger Lundquist number. In the real solar atmosphere, plasma gas has larger Lundquist number than that in this numerical simulation. This means that thermal conduction effect on the energy release rate in magnetic reconnection might become more effective in the real solar atmosphere.

Keywords: solar flare, magnetic reconnection, thermal conduction, corona

Japan Geoscience Union Meeting 2014
(28 April - 02 May 2014 at Pacifico YOKOHAMA, Kanagawa, Japan)

PEM32-13 Room:503 Time:May 2 12:30-12:45

Analysis on turbulent reconnection of three-dimensional resistive MHD simulation

WANG, Shuoyang[1*] ; YOKOYAMA, Takaaki[1] ; ISOBE, Hiroaki[2]

[1]The University of Tokyo, [2]Kyoto University

This study starts from a three-dimensional current sheet with random perturbation on velocity, in order to understand more on the 3D reconnection in a more general way.

Due to the periodic boundary condition, the core of current sheet quickly develops a resonance netlike pattern under tearing instability. Small reconnection site mainly form two chains on either side of the current sheet center and constitute a zigzag arrangement. The outflow from one reconnection site is fed into the counterpart on the other side thus composes a positive feedback system resembles even double tearing mode. As the inflow being enhanced, slow-mode shocks are identified along the current sheet. The conversion of the magnetic energy is further raised. Total kinetic energy of the current sheet presents 4 steps of development while first 3 exhibit linear growing tendency. At the same time, reconnection rate increases by 5 times compared with the early phase. Thus we have achieved faster reconnection without localized resistivity in a more universal idea.

Japan Geoscience Union Meeting 2014
(28 April - 02 May 2014 at Pacifico YOKOHAMA, Kanagawa, Japan)

PEM32-14 Room:503 Time:May 2 14:15-14:30

Ion Acceleration Mechanisms in the Exhaust Region of Magnetic Reconnection

TAKAMOTO, Makoto[1*] ; FUJIMOTO, Keizo[2]

[1]Max-Planck-Institute for Nuclear Physics, [2]National Astronomical Observatory of Japan

Magnetic reconnection is considered to be a key mechanism to convert magnetic field energy into plasma kinetic and thermal energy in various plasma phenomena, in particular, in many astrophysical systems. In collisional plasma, many works assuming magnetohydrodynamic approximation have revealed that plasma jets can be accelerated up to the upstream Alfven velocity. However, in the case of the collisionless plasma, which is common in many astrophysical phenomena, there is still no conclusive theory of the ion acceleration mechanism and the maximum plasma jet velocity because of the complexities of plasma phenomena and the associated high numerical cost.

In this study, we performed a large-scale 2D particle-in-cell simulations with adaptive mesh refinement under an open boundary condition. The simulation was performed until the MHD condition is well-satisfied in the exhausts,
which allows us to study a long-time dynamical evolution of the structure of the diffusion region and exhausts.
To analyze the detailed mechanisms of the ion acceleration in the exhausts, we also performed test particle simulations on the dynamical background plasma. We found that the ions are accelerated mainly by the electric field perpendicular to the reconnection plane. However, effects from other electric field components are not negligible;
in particular, the contribution from the electric field along the exhausts becomes significant as the ions are accelerated. We also compared the results with the velocity distribution functions inside of the exhausts.

In this talk, we present our numerical results of the particle-in-cell simulation, and discussed its physical interpretations of the structure. We also discuss the ion kinetic mechanisms leading to the formation of reconnection jets.

Keywords: magnetic reconnection, ion acceleration

Japan Geoscience Union Meeting 2014
(28 April - 02 May 2014 at Pacifico YOKOHAMA, Kanagawa, Japan)

PEM32-15 Room:503 Time:May 2 14:30-14:45

Waves and particle acceleration around the separatrices of magnetic reconnection

FUJIMOTO, Keizo[1*]

[1]National Astronomical Observatory of Japan

Understanding the properties of waves in magnetic reconnection is very important in collisionless plasmas. The waves can transport the momentum and energy between the different species in plasmas, which results in the anomalous magnetic dissipation, particle heating, and formation of non-thermal particles. Therefore, the wave activities relevant to the kinetic interactions can have a significant impact on the dynamical behaviour of magnetic reconnection. Theoretical modeling of waves in the reconnection region is also beneficial to reveal the reconnection dynamics using in-situ satellite observations where wave properties are obtained in much higher time resolution than plasma distribution functions.

Recent satellite observations in the Earth's magnetotail have shown that the wave activities are significantly enhanced in a broad range of frequency around the separatrices of anti-parallel magnetic reconnection. The waves were recognized as lower hybrid waves, Langmuir waves, electrostatic solitary waves (ESWs), and whistler waves. In most cases, they were associated with cold electron beams and density cavity. However, because of the limited space-time resolutions of the observations, it has been difficult to identify the generation mechanisms of the waves and their roles in magnetic reconnection.

In this study, large-scale 2D particle-in-cell simulations with adaptive mesh refinement have been performed under an open boundary condition. The simulations use a set of more realistic parameters than those in most other simulations, achieving lower plasma beta in the upstream region that leads to stronger electron beams in the reconnection region. The wave activities are dominant in the inflow side of the separatrices. The waves are generated mainly due to the electron beams that constitute the Hall current. The relatively weak beams before strong acceleration trigger the Buneman instability which results in the waves with a frequency of the lower hybrid range. The strong acceleration occurs along the field line due to a localized potential hump and causes the density cavity. The intense electron beams excite the electron two-stream instability and the beam driven whistler instability. The former mode gives the Langmuir waves and the flat-top electron distributions in the parallel direction, both of which have been observed frequently in the Earth's magnetotail. The latter mode, on the other hand, scatters the electrons in the perpendicular direction, forming isotropic distribution with non-thermal high-energy tail. Both the Buneman and electron two-stream instabilities evolve the ESWs in the nonlinear phases.

In this talk, we present the generation mechanisms of the waves around the separatrices and their roles in magnetic reconnection. The mechanism of the intense electron acceleration along the field line will be discussed.

Keywords: magnetic reconnection, plasma waves, particle acceleration, particle-in-cell simulations

Japan Geoscience Union Meeting 2014
(28 April - 02 May 2014 at Pacifico YOKOHAMA, Kanagawa, Japan)

PEM32-16 Room:503 Time:May 2 14:45-15:00

Minimum spatial scale for maintaining vigorous magnetic reconnection

SHIMIZU, Kenya[1*] ; FUJIMOTO, Masaki[2] ; SHINOHARA, Iku[2]

[1]University of Tokyo, [2]Institite of Space and Astronautical Science, Japan Aerospace Exploration Agency

Magnetic reconnection drives the fast release of magnetic energy in explosive events such as magnetic substorms in the Earth's magnetosphere and flares in the solar corona. On the large scale, reconnection is an MHD-scale process but its rate is controlled by the compact electron diffusion region (EDR), where electrons are not magnetized. Recent kinetic simulations have revealed the structure of EDR in a quasi-steady reconnection rate. In some works, it is suggested that an elongated electron jet in the outflow region does not affect the reconnection rate. However, it is not clear the spatial scale for determining the rate. We find that the minimum spatial scale for maintaining magnetic reconnection by using kinetic simulations on periodic and reflective wall boundary conditions. On the periodic condition, an outflow jet extends a large distance downstream from the X-line with the fast rate of reconnection. However, the influence of periodicity shortens the jet to a narrow structure though the rate of reconnection is still fast. This structure is the minimum spatial scale for maintaining magnetic reconnection. On the other hand, asymmetric reconnection is performed on the reflective wall condition to lead a slow motion of the diffusion region away from the wall, the so called 'X-line retreat.' During the retreat motion an outflow jet is blocked by the wall though the rate of reconnection is maintained. The structure of the blocked jet is very similar to the minimum spatial scale on the periodic condition. We quantitatively show the minimum structure for maintaining magnetic reconnection by comparing the result on these periodic and reflective conditions. We also find the minimum structure is independent of domain sizes but gets smaller with decreasing electron mass.

Keywords: magnetic reconnection, electron diffusion region

Japan Geoscience Union Meeting 2014
(28 April - 02 May 2014 at Pacifico YOKOHAMA, Kanagawa, Japan)

PEM32-P01 Room:503 Time:May 2 16:15-17:30

Magnetothermal instability in the solar outer corona

YOKOYAMA, Takaaki[1*]

[1]The University of Tokyo

We discussed an application of the magnetothermal instability (MTI) to the solar atmosphere. This instability proposed by Balbus (2000) occurs in weakly collisionless plasmas where non-isotropic thermal conduction plays a role in a magnetized atmosphere. The time scale of the maximum growth is given as approximately sqrt(H/g) where H is the scale height, and g is the gravity. The magnetic field must be weak enough since its tension force contributes as a restoring force.

The solar corona is a dilute hot atmosphere where the thermal conduction is non-isotropic. The MTI is possible to work in the upper corona around a few solar radii above the photosphere where the temperature is decreasing outward and the scale height is about one solar radius. The condition for weak horizontal magnetic field might be satisfied above a closed loop in the lower corona. If the MTI is effective in such regions, it might contribute to generate the waves or perturbations in the solar wind.

We found that the MTI is unlikely to work in the upper corona because of its strong magnetic field that suppress the growth of the geometrically possible wavelength modes. It is found that when the field strength is 0.1 times the real corona, the wavelength for the maximum growth is comparable with the geometrical radius. The growth time for this setup can be consistent with the low frequency fluctuations in the solar wind.

Keywords: Sun, corona, plasma, magnetohydrodynamics

Japan Geoscience Union Meeting 2014
(28 April - 02 May 2014 at Pacifico YOKOHAMA, Kanagawa, Japan)

PEM32-P02 Room:503 Time:May 2 16:15-17:30

Cosmic-ray Parker Instability and Galactic Plane Symmetry

KUDOH, Takahiro[1*] ; YOKOYAMA, Takaaki[2] ; KUDOH, Yuki[3] ; MATSUMOTO, Ryoji[3]

[1]National Astronomical Observatory of Japan, [2]University of Tokyo, [3]Chiba University

We study two-dimensional MHD numerical simulations of the Parker instability with the cosmic-ray pressure under the circumstance of the galactic disk. Instead of the symmetric boundary conditions on the galactic plane as often used, we solve the entire region of the disk. Numerical simulations show that the symmetric mode on the disk also grows when the cosmic-ray pressure is relatively large, while the glide reflection symmetric mode dominates on the disk when the cosmic-ray pressure is small. We confirm that the results are consistent with those of the liner analyses: the growth rate of the symmetric mode approaches that of the glide reflection symmetric mode as the cosmic-ray pressure becomes relatively large.

In the nonlinear stage, some loop structures of the magnetic field lines expand rapidly and grow into large structure when the cosmic-ray pressure is relatively large. Other loops, which start to grow a little later, are suppressed by faster growing loops located nearby and do not reach the nonlinear expansions. Eventually, the loop structure at the nonlinear stage is larger than that is expected form the linear analysis when the cosmic-ray pressure is relatively large.

When the nonlinear fast growing loops collide with another loops, the high density thin gas layers are formed by the compression between the loops. The figure shows the logarithmic density at that stage. Some of the high density gas shows filament structures and some of them look like high density loops. Similarities of these structures with some observational features and the relation of star formation activities can be studied further.

Keywords: MHD, Interstellar gas, Cosmic rays

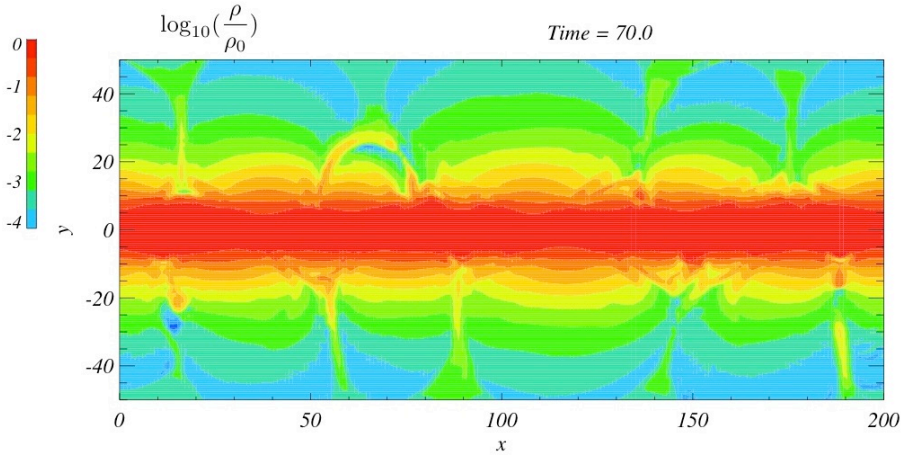

Japan Geoscience Union Meeting 2014
(28 April - 02 May 2014 at Pacifico YOKOHAMA, Kanagawa, Japan)

PEM32-P03 Room:503 Time:May 2 16:15-17:30

Formation of Dense, Cold Loops by Parker Instability in Galactic Gas Disks

PENG, Chih-han[1*] ; KUDOH, Yuki[1] ; ASAHINA, Yuta[1] ; MATSUMOTO, Ryoji[1]

[1]Faculty of Science, Chiba University

We performaced two dimensional numerical simulations of Parker instability taking into account the cooling and heating functions of the interstellar medium (Inoue et al. 2006). Our numerical experiment is based on the simulation code ”CANS+” in which the HLLD Riemann solver (Miyoshi & Kusano 2005) is used to solve the MHD equations. We found that the cold, dense filaments formed at the valley of magnetic field lines by Parker instability coupled with the cooling instability are deformed into loops of dense, cold gas when the Ram pressure at the left- and right-hand side of the filament is different. The maximum number density and the lowest temperature of cold, dense filament at 100Myrs is about 200 per cubic cm and 50K, respectively. These results support the model in which thermal instability triggered in the dense region formed by Parker instability is responsible for the formation of molecular loops found in the Galactic center region (e.g., Fukui et al. 2006).

Japan Geoscience Union Meeting 2014
(28 April - 02 May 2014 at Pacifico YOKOHAMA, Kanagawa, Japan)

PEM33-01 Room:503 Time:May 1 09:00-09:25

Effects of cosmological infall of galaxies: its discovery, plasma physical implications, and verification with ASTRO-H

MAKISHIMA, Kazuo[1*]

[1]Department of Physics, University of Tokyo

Clusters of galaxies are a system consisting of hundreds of galaxies that are gravitationally bound together. About 10% of the mass of each cluster is in the form of X-ray emitting hot plasmas, called Intra-Cluster Medium (ICM), that constitute the most dominant form of known baryonic components in the universe. The ICM is tenuous, hot, and magnetized, and is hence considered as the most ideal classical plasma ever known.

At central regions of many clusters, the ICM was considered to cool over the Hubble time by emitting X-rays, and lose its pressure. Then, the ICM would flow from outer to inner regions, and enhance the radiative cooling by raising the density. This catastrophy, called cooling flows, were long thought to be actually taking place, as X-ray observations kept discovering its evidence.(3) the energy is then transported to the cool ICM phase via Alfven waves and reconnection, (4) the two ICM phases are kept thermally stable by a mechanism known in Solar corona; and (5) the moving galaxies will gradually fall to the potential center as they transfer their dynamical energies to the ICM (Makishima et al., Publ. Astro. Soc. J. 53, 401, 2001). We have been striving to observationally enhance this novel scenario.

At central regions of many clusters, the ICM was considered to cool over the Hubble time by emitting X-rays, and lose its pressure. Then, the ICM would flow from outer to inner regions, and enhance the radiative cooling by raising the density. This catastrophy, called cooling flows, were long thought to be actually taking place, as X-ray observations kept discovering its evidence.

Through observations of clusters of galaxies with the 4th Japanese X-ray satellite ASCA launched in 1993, we found that the cooling flows are not taking place anywhere, even though the ICM ubiquitously shows mild temperature decrease towards the cluster center: there must be some unknown plasma heating source. We have hence proposed a novel plasma physical scenario; (1) the central galaxy has a magnetosphere, where the cooler plasma is confined and insulated from the surrounding hot ICM; (2) other galaxies, all moving in the cluster space, will receive resistance from the ICM and excite MHD turbulence therein; (3) the energy is then transported to the cool ICM phase via Alfven waves and reconnection, (4) the two ICM phases are kept thermally stable by a mechanism known in Solar corona; and (5) the moving galaxies will gradually fall to the potential center as they transfer their dynamical energies to the ICM (Makishima et al., Publ. Astro. Soc. J. 53, 401, 2001). We have been striving to observationally enhance this novel scenario.

Recently, we have obtained crucial evidence supporting (5). That is, we studied 34 clusters with various redshifts (0.1-0.9) with X-ray and optical wavelength. Then, galaxies in nearby clusters were confirmed to be much concentrated than the ICM, while these two components are nearly co-spatial at distant clusters (Gu et al., Astrophys. J. 767, id 157, 2013). That is, galaxies in each luster have been falling, on the Hubble time scale, to the center. This result not only provides the long-sought heating mechanism of the ICM and strengthen our hypothetical view, but means the discovery of a very large energy flow that has not been known. Furthermore, it can explain many other puzzles with clusters of galaxies.

We are now developing, under an extensive international collaboration, the innovative X-ray satellite ASTRO-H, to be launched in 2015. With ASTRO-H, we will be able to detect X-ray Doppler effects which is caused when moving galaxies drag the ICM around them, and study possible particle acceleration phenomena as a consequence of energy loss by galaxies.

Keywords: galaxies and their clusters, intra-cluster medium, X-ray emission, magnetoplasma effects, ASTRO-H satellite

Japan Geoscience Union Meeting 2014
(28 April - 02 May 2014 at Pacifico YOKOHAMA, Kanagawa, Japan)

PEM33-02 Room:503 Time:May 1 09:25-09:45

Direct measurement of the plasma momentum in a magnetic nozzle helicon plasma for electric propulsion

TAKAHASHI, Kazunori[1*] ; CHARLES, Christine[2] ; BOSWELL, Rod[2] ; CHIBA, Aiki[1] ; ANDO, Akira[1]

[1]Department of Electrical Engineering, Tohoku University, [2]Space Plasma, Power and Propulsion Laboratory, The Australian National University

The ion and electron energy distribution functions of a low-pressure, current-free helicon plasma in a magnetic nozzle configuration are experimentally investigated by electrostatic Langmuir probes including a radiofrequency compensated probe and a retarding field energy analyzer; the ions are electrostatically accelerated by a spontaneous potential drop of a double layer and/or ambipolar electric field, and only the energetic electrons can overcome the potential structure. The results indicate that the accelerated ions are spontaneously neutralized by the energetic electrons. These findings propose that the source system is applicable to an electrodeless and neutralizer-free plasma thruster.

Momentum of the plasma flow is one of essential physical parameters dominating the particle acceleration in both laboratory and space. Especially their interaction with magnetic fields have been significant subject associated with natural plasmas (astrophysical jets, magnetospheric physics, solar dynamics, aurora dynamics, etc.) and artificial plasmas (thermonuclear fusion devices, electric propulsion systems, plasma devices for material processing, etc.). The plasma momentum is equal in magnitude and opposite in direction to a thrust imparted from a plasma thruster for the electric propulsion device. The direct measurement of the thrust imparted from a magnetic nozzle helicon plasma thruster is successfully measured by using a pendulum thrust balance immersed in vacuum, where the thrust components arising from the presence of the physical boundaries and magnetic nozzle are also independently measured by attaching each component to the thrust balance. Further a laboratory experiment of a helicon plasma thruster is established to control only a plasma cross-field diffusion in a rapidly-divergent magnetic nozzle while maintaining a constant plasma injection into a magnetic nozzle. The thrust component due to a plasma pressure force inside the source cavity is constant and that due to the magnetic nozzle increases when inhibiting the cross-field diffusion in the nozzle. The latter force is well explained by an electron-diamagnetic-induced plasma momentum derived from two-dimensional momentum equations and approaches the theoretical limit derived from a one-dimensional model assuming an ideal magnetic nozzle with no plasma loss. Further a new source system approaching the ideal magnetic nozzle and the recent progress of the thruster performance will also be shown. It is noted that the above-described phenomena are occuring in current-free source system. These insights into the plasma thruster dynamics might include a common physics relating to the plasma acceleration in a non-uniform magnetic field in both the laboratory and space.

Keywords: plasma momentum, magnetic nozzle, helicon plasma, electric propulsion

Japan Geoscience Union Meeting 2014
(28 April - 02 May 2014 at Pacifico YOKOHAMA, Kanagawa, Japan)

PEM33-03 Room:503 Time:May 1 09:45-10:00

Laboratory in-situ experiments for plasma wave-particle interaction in linear magnetized plasma machine

KOGISO, Shun[1*] ; KATOH, Yuto[2] ; SHIMOYAMA, Manabu[1] ; KANEKO, Toshiro[3] ; MOON, Chanho[3] ; HIRAHARA, Masafumi[1]

[1]Solar-Terrestrial Environment Laboratory, Nagoya University, [2]Graduate School of Science, Tohoku University, [3]Graduate School of Engineering, Tohoku University

Wave-particle interactions are thought to play important roles to generate MeV electrons in the radiation belt. “ Wave-Particle Interaction Analyzer (WPIA) ” , which derives energy flaxes between wave and particle from simultaneous measurements of an electric field and particle velocity vector, has been developed to observe the interaction between wave and particle in space plasma. We have been conducting laboratory in-situ experiments of plasma wave-particle interaction.

We have carried out the laboratory simulation using the Q_T-Upgrade Machine in Tohoku University, which is linear magnetized plasma machine. The Q_T-Upgrade Machine consists of a vacuum chamber of 0.2 m in diameter and 4.5 m in length, and plasma sources, which generates high-temperature electrons using electron cyclotron resonance (ECR) and low-temperature thermal electrons. Thus, an electron temperature gradient (ETG) is formed in the apparatus by superimposing low temperature thermal electrons on the high temperature electrons of the ECR plasma. Moon et al. [Rev. Sci. Instrum., 2010] reported that low-frequency fluctuations of drift-wave mode with a frequency of 7 kHz were excited with ETG mode of 0.5 MHz. We focus on the low-frequency fluctuations and simultaneously measures an electric field vector (**E**) and current vector (**J**). Energy flaxes between wave and particle can be calculated from inner products of **E** and **J** vectors. For the simultaneous measurements, we have developed a combination probe, which is a combination of Mach probe for ion flow measurements and Twin probe for electric field measurements. Three-dimensional vector are measured by turning and moving the probe in the chamber.

In this presentation, we will report the performance of the combination probe, the phase relationship between the electric field fluctuation and the current fluctuation, and transient response of fluctuation growth in detail.

Japan Geoscience Union Meeting 2014
(28 April - 02 May 2014 at Pacifico YOKOHAMA, Kanagawa, Japan)

PEM33-04 Room:503 Time:May 1 10:00-10:15

Weibel instability mediated collisionless shock generation using large-scale laser systems

SAKAWA, Youichi[1*] ; MORITA, Taichi[1] ; KURAMITSU, Yasuhiro[2] ; KATO, Tsunehiko[3] ; MORITAKA, Toseo[1] ; SANO, Takayoshi[1] ; TOMITA, Kentaro[4] ; MATSUKIYO, Shuichi[4] ; OHNISHI, Naofumi[5] ; MIZUTA, Akira[6] ; WOOLSEY, N[7] ; GREGORI, G[8] ; KOENIG, M[9] ; SPITKOVSKY, A[10] ; HUNTINGTON, C[11] ; KUGLAND, N l[11] ; ROSS, J s[11] ; PARK, H-s[11] ; REMINGTON, B[11] ; TAKABE, Hideaki[1]

[1]ILE Osaka Univ, [2]National Central University Taiwa, [3]Hiroshjima Univ, [4]Kyushu Univ, [5]Tohoku Univ, [6]RIKEN, [7]York Univ UK, [8]Oxford Univ UK, [9]LULI France, [10]Princeton Univ USA, [11]LLNL USA

Collisionless shocks are considered to be sources of high-energy particles or cosmic rays, and occur when a coulomb mean-free-path is longer than the shock-front thickness. In such plasmas wave-particle interactions and collective effects play an essential role in the shock formation. In addition to local observations of spaces plasmas by spacecraft and global emission measurements of astrophysical plasmas, a laboratory experiment can be an alternative approach to study the formation of collisionless shocks.

In this paper, we investigate the formation of Weibel-instability mediated collisionless shocks in counter-streaming plasmas produced by large-scale laser systems. Kato and Takabe investigated the collisionless Weibel shock in two-dimensional PIC simulation using the injection method [1]. A scaling-law derived in simulation revealed that high-density (electron density $\sim 10^{20}$ cm^{-3}), high-flow velocity ($\sim$1000 km/s) plasmas are required to produce the collisionless Weibel shock. In order to achieve these plasma parameters, a MJ-class high-power laser system or the word largest laser, the NIF laser (LLNL, USA), is required. Before starting the NIF experiment, we conducted OMEGA laser (LLE, USA) experiment and measured plasma parameters such as electron and ion temperatures, electron density, and flow velocity of counter-streaming plasmas using collective Thomson scattering, and current filaments produced by the Weibel instability using proton-radiography.

[1] T. N. Kato and H. Takabe, The Astophys. J. Lett. 681, L93 (2008).

Keywords: collisionless shock, weibel instability, large-scale laser experiment

Japan Geoscience Union Meeting 2014
(28 April - 02 May 2014 at Pacifico YOKOHAMA, Kanagawa, Japan)

PEM33-05 Room:503 Time:May 1 10:15-10:30

Experimental study on collisionless shocks with high-power laser system ”Gekko-XII”

MORITA, Taichi[1*] ; SAKAWA, Youichi[1] ; ISHIKAWA, Taishi[1] ; YAMAURA, Yuta[1] ; SANO, Takayoshi[1] ; MORITAKA, Toseo[1] ; TOMITA, Kentaro[2] ; SHIMODA, Ryo[2] ; SATO, Yuta[2] ; MATSUKIYO, Shuichi[2] ; ISAYAMA, Shogo[2] ; HARADA, Daisuke[2] ; OYAMA, Tatsuya[2] ; FUJINO, Ryosuke[2] ; KURAMITSU, Yasuhiro[3] ; YONEDA, Hiroki[10] ; NAGAMINE, Kazuyoshi[10] ; KOENIG, Michel[4] ; YURCHAK, Roman[4] ; MICHAUT, Claire[5] ; WOOLSEY, Nigel[6] ; CROWSTON, Robert[6] ; PELKA, Alexander[7] ; LI, Yutong[8] ; YUAN, Dawei[8] ; YIN, Chuanlei[8] ; ZHONG, Jiayong[9] ; ZHANG, Kai[9] ; TAKABE, Hideaki[1]

[1]Institute of Laser Engineering, Osaka University, [2]Kyushu University, [3]National Central University, [4]LULI, Ecole Polytechnique, [5]LUTH, Observatoire de Paris, [6]University of York, [7]Helmholtz-Zentrum Dresden-Rossendorf, [8]Institute of Physics, Chinese Academy of Science, [9]National Astronomical Observatory, Chinese Academy of Science, [10]Institute for Laser Science, University of Electro-communications

Collisionless shocks play significant roles in particle acceleration, for example, in Earth’s bow shock and Supernova remnant shocks. In collisionless shocks, collisions between particles can not account for the formation mechanism and particle?field interactions are essential. Therefore, the shock thickness is much smaller than ion-ion mean free path and a large electromagnetic field exists at the vicinity of the shock. Laboratory experiments with high-power laser systems can be alternative to observations or in-situ measurements by satellites. Collisionless shocks have been produced and investigated in counter-streaming laser-produced plasmas. To investigate collisionless shocks, the measurements of an electric or magnetic field and of fundamental plasma parameters are required. Shocks have been measured by optical diagnostics such as interferometry, shadowgraphy, optical pyrometry, and Thomson scattering to obtain the fundamental plasma parameters: density, temperature, charge state, and flow velocity. We will present recent results from series of our experiments on collisionless shocks with Gekko-XII laser system.

Keywords: collisionless shock, laser, plasma, diagnostics

Japan Geoscience Union Meeting 2014
(28 April - 02 May 2014 at Pacifico YOKOHAMA, Kanagawa, Japan)

PEM33-06 Room:503 Time:May 1 10:30-10:45

Current status and issues of a study on collisionless shocks by using laser experiment

MATSUKIYO, Shuichi[1*] ; SAKAWA, Youichi[2] ; KURAMITSU, Yasuhiro[3] ; TOMITA, Kentaro[1] ; MORITA, Taichi[2] ; YAMAZAKI, Ryo[4] ; TAKABE, Hideaki[2]

[1]Kyushu University, [2]Osaka University, [3]National Central University, [4]Aoyama Gakuin University

Collisionless shocks are ubiquitous in various space and astrophysical environments like a termination shock of a stellar wind, planetary bow shocks, supernova remnant shocks, etc. Recently, collisionless shocks have been able to be experimentally generated by using high power laser facilities. One of the advantages in an experimental study is that both the global and the local structures of the phenomenon are simultaneously accessible in principle, which is inherently difficult in-situ or remote sensing observations in space. However, the shocks produced in the laser experiments and the method for measuring them are quite different from those in space. A majority of the shocks produced in laser experiments are unmagnetized shocks. The methodology for measuring their local quantities in the transition region has not been established.

On the other hand, basic structures and dissipation mechanisms in an unmagnetized shock have not been well understood theoretically. So far high Mach number electrostatic shocks are thought to be generated by the counter streams of two non-identical plasmas. In this study microstructures of such electrostatic shocks are studied by using a full particle-in-cell simulation. In addition, characteristics and issues of currently adopted method of measuring local quantities in shock transition region, known as Thomson scattering measurement, are also discussed.

Keywords: collisionless shock, laser experiment, numerical simulation

Japan Geoscience Union Meeting 2014
(28 April - 02 May 2014 at Pacifico YOKOHAMA, Kanagawa, Japan)

PEM33-07 Room:503 Time:May 1 11:00-11:15

Electromagnetic Field Excitation in Magnetized Plasmas by External Electrodes: 1D PIC Simulation Studies

OTSUKA, Fumiko[1*] ; HADA, Tohru[1] ; SHINOHARA, Shunjirou[2] ; TANIKAWA, Takao[3]

[1]Interdis. Grad. Sch. Eng. Sci., Kyushu Univ., [2]Inst. Eng.,TUAT, [3]RIST, Tokai Univ.

We perform one-dimensional particle-in-cell (PIC) simulation of external electromagnetic field excitation into magnetized plasmas. We consider two models for the electromagnetic field excitation: electrostatic excitation by electrodes and electromagnetic excitation by current antenna. Here, the external electrodes are placed outside plasma region, background magnetic field is perpendicular to the one-dimensional direction, and the externally applied field frequency is chosen in a range below the lower-hybrid frequency. For both models, we will discuss the electromagnetic field excitation processes by varying the externally applied field frequency and the plasma radius.

Keywords: external electromagnetic field, external electrodes, magnetized plasmas, electric thruster, electrodeless electric thruster

Japan Geoscience Union Meeting 2014
(28 April - 02 May 2014 at Pacifico YOKOHAMA, Kanagawa, Japan)

PEM33-08 Room:503 Time:May 1 11:15-11:30

Numerical simulation of satellite potential control using charged particle beam emission

HOSHI, Kento[1*] ; MURANAKA, Takanobu[2] ; KOJIMA, Hirotsugu[3] ; USUI, Hideyuki[4] ; SHINOHARA, Iku[5] ; YAMAKAWA, Hiroshi[3]

[1]Graduate School of Engineering Kyoto University, [2]School of Engineering Chukyo University, [3]Research Institute for Sustainable Humanosphere, Kyoto University, [4]Graduate school of system informatics Kobe University, [5]Japan Aerospace Exploration Agency/Institute of Space and Astronautical Science

It is known that a satellite is charged by plasma in space.

Satellite charging on surface is a cause of discharge and malfunction electric equipment, and affect plasma diagnostics by the satellite potential accelerate ambient plasma, therefore a satellite is designed to mitigate surface charging. However, a perfect mitigation of satellite charging is difficult.

Thereby, a charging mitigation technique using electron emitter and ion emitter is often adopted. Satellite charging will be caused due to collisions with charged particles in plasma. In general, surface potential is determined by the balance of inflow current and outflow current. It becomes a positive value in the sunshine, and a negative value in the shade. The potential balance point can be controlled using charged particle beam emission.

We investigate a feasibility of satellite potential control under various environments using numerical simulation.

Keywords: satellite charging, spacecraft charging, charged particle beam

Japan Geoscience Union Meeting 2014
(28 April - 02 May 2014 at Pacifico YOKOHAMA, Kanagawa, Japan)

PEM33-P01 Room:503 Time:May 1 18:15-19:30

New solar radio telescope in NICT - II

KUBO, Yuki[1*] ; WATARI, Shinichi[1] ; ISHII, Mamoru[1] ; ISHIBASHI, Hiromitsu[1] ; IWAI, Kazumasa[2]

[1]National Institute of Information and Communications Technology, [2]Nobeyama Solar Radio Observatory, National Astronomical Observatory of Japan

Solar radio burst is one of the most important events for not only space weather forecasting but also investigating high-energy phenomena in solar corona. The GHz solar radio waves are synchrotron radiation emitted by high energy electrons at lower corona. On the other hand, the MHz solar radio bursts, especially type II and III bursts, are radiated via mode conversion of Langmuir waves excited by high energy electrons. These high energy electrons are accelerated at reconnection regions in solar flare and shock waves in solar corona. Therefore, MHz and GHz solar radio waves are closely related each other through the accelerated high energy electrons. So, wide frequency range (MHz to GHz) radio wave observations with high time resolution are required to comprehensively understand high energy phenomena in solar corona. We have been operating solar radio spectrograph called HiRAS for over twenty years in Hiraiso Solar Observatory, National Institute of Information and Communications Technology (NICT), but the system has been decrepit and radio wave environment in Hiraiso is getting worse. So, we have developed a new solar radio telescope in Yamagawa radio observation facility, NICT. The frequency range and time resolution in the system is 70MHz to 9.0GHz and 8 msec. In this presentation, we introduce situation in progress for our new solar radio telescope.

Keywords: Solar radio waves, Solar corona, Radio spectrograph, Space weather

Japan Geoscience Union Meeting 2014
(28 April - 02 May 2014 at Pacifico YOKOHAMA, Kanagawa, Japan)

PEM34-01 Room:503 Time:May 1 11:30-11:55

Frontier of space plasma observations expanding from interplanetary space to interstellar medium

TOKUMARU, Munetoshi[1*]

[1]Solar-Terrestrial Environment Laboratory, Nagoya University

The Sun emits the super-sonic plasma flow, called the solar wind, to form the heliosphere in the ambient interstellar medium. The spatial scale of the heliosphere is about 100 AU. Since interesting physical phenomena such as the solar wind formation, excitation and propagation of shocks, acceleration of energetic particles arises through interaction between plasma and fields in the heliosphere, it is used as an experiment site to make various observational studies of the space plasma. Remote sensing measurements of the solar wind with the interplanetary scintillation (IPS) method are one of those studies. The obtained IPS data revealed the global distribution of the solar wind drastically changes its global distribution over short- and long-timescales being closely associated with the solar activities (Tokumaru, 2013).

At present, marked progress occurs in the heliospheric sciences, being driven by new observational facts. One of progress has been brought about by exploration of heliospheric boundary region by Voyager-1, 2 (V1,V2) and IBEX spacecraft (Gurnett et al., 2013, McComas et al., 2009). The V1 encountered the termination shock (TS) at 94 AU in 2004, and reached the heliopause at 120 AU in 2012, then entered the interstellar medium. The V2 encountered the TS at 87 AU in 2007, being expected to reach the heliopause in a few years. The IBEX revealed the large-scale ribbon structure surrounding the heliosphere from imaging observations of energetic neutral atoms (ENAs). In order to interpret those observations, information on 3-diminensional (3D) structure of the heliospheric boundary region is needed. Since IPS observations mentioned above give global distribution of the solar wind in the inner heliosphere, 3D structure of the heliospheric boundary region can be determined precisely by MHD simulation based on the IPS data. The IPS-based MHD simulation data are provided to both Voyager and IBEX teams to make collaborative studies of the heliospheric boundary region.

Another driver for progress in the heliospheric science is arrival of the peculiar solar activity. The level of the current solar cycle is 100 years low, and IPS observations revealed that significant changes including marked drop of the solar wind density and different distribution of fast and slow solar winds occurs in this cycle (Tokumaru et al., 2009, 2010, 2012). These facts are important not only for studies of the heliospheric boundary region and influence on the planetary magnetospheres (i.e. the space weather), but also for elucidating enigma of the solar wind acceleration mechanism. Besides, observations during the current peculiar activity provide a clue to understand a hidden process for cooling of the Earth's climate during the Maunder minimum in the 17th century.

The V2 encounter for the interstellar medium which is expected to occur within a few years will enable detailed investigation of plasma environment in the local interstellar cloud surrounding the heliosphere. Furthermore, the heliopshere is immersed in the low-density (but high-beta) region called the local bubble, whose plasma properties have been investigated from radio observations using pulsars (Spangler, 2009). In the future, space plasma study for the integrated region ranging from the heliosphere to the local bubble will significantly advance by using in situ and remote sensing observations.

Keywords: solar wind plasma, interplanetary scintillation, heliosphere, interstellar medium, solar cycle

Japan Geoscience Union Meeting 2014
(28 April - 02 May 2014 at Pacifico YOKOHAMA, Kanagawa, Japan)

PEM34-02 Room:503 Time:May 1 11:55-12:15

Scale hierarchy and self-organization in magnetospheric plasma

YOSHIDA, Zensho[1*]

[1]Graduate School of Frontier Sciences, University of Tokyo

Inhomogeneous magnetic field gives rise to interesting properties of plasmas which are degenerate in homogeneous (or zero) magnetic fields. Magnetospheric plasmas, as observed commonly in the Universe, are the most simple, natural realization of strongly inhomogeneous structures created spontaneously in the vicinity of magnetic dipoles. In this talk, we describe the experimental results form a ”laboratory magnetosphere” RT-1, and theoretical modeling of its spontaneous confinement.

The RT-1 device produces a magnetospheric plasma by a levitated superconducting magnet. Stable confinement (particle and energy confinement time = 0.5 s) of high-beta (local electron beta $>$0.7); electron temperature $>$10 keV) plasma has been demonstrated (which are promising characteristics for an innovative concept of advanced fusion; it is also applicable as a particle trap for experimental particle physics or atomic physics). The radial profile of the electron density n(r) is highly peaked. Fitting the data by a function $n(r) = n_0\ r^{-p}$,we estimate p=2.8$\pm$0.4 for a wide range of operating parameters. Multiplying n(r) by the magnetic flux tube volume, we can estimate the particle number N(r) in a unit magnetic-flux tube. While n(r) is a steep increasing function towards the center of the dipole magnetic field, N(r) is a decreasing function, hence interchange modes are stable. Whereas the simple kinetic model predicts a flat distribution of N(r) [1], the model of grand-canonical equilibrium explains the observed equilibrium state [2].

Theoretically, we can describe the self-organized confinement of the magnetospheric plasma as a grand-canonical equilibrium in a ”foliated phase space” of magnetized particles [3]. What makes the distribution function fundamentally different from the conventional Boltzmann distribution is the topological constraints on the phase space which limits the actual domain where the particles can occupy; the adiabatic invariants pose such constraints. Taking into account the constancy of the magnetic moment and the parallel action, we obtain a foliated phase space of coarse-grained variables, on with the invariant measure is distorted by the inhomogeneous magnetic field. The grand-canonical equilibrium has an inhomogeneous density when it is immersed in the laboratory flat space. Hence, the creation of a steep-density clump is a natural consequence of equipartition in the magnetic-coordinate phase space.

[1] A. Hasegawa, Phys. Scr. T116 (2005) 72.

[2] Z. Yoshida et al., Plasma Phys. Control. Fusion 55 (2013), 014018.

[3] Z. Yoshida and P.J. Morrison, in ”Nonlinear physical systems: spectral analysis, stability and bifurcation”, (ISTE and John Wiley and Sons, 2014) Chap. 18; http://arxiv.org/abs/1303.0887

Keywords: inward diffusion, adiabatic invariant, foliation, high-beta plasma, dipole magnetic field, non-neutral plasma

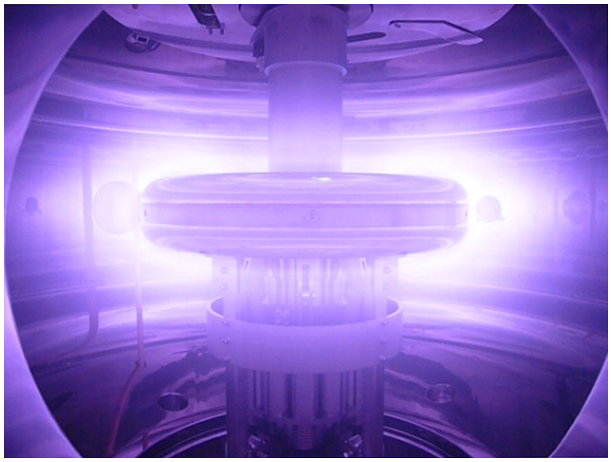

Japan Geoscience Union Meeting 2014
(28 April - 02 May 2014 at Pacifico YOKOHAMA, Kanagawa, Japan)

PEM34-03 Room:503 Time:May 1 12:15-12:30

Solar wind plasma entry into the wake behind an unmagnetized obstacle

NAKAGAWA, Tomoko[1*]

[1]Information and Communication Engineering, Tohoku Institute of Technology

Plasma entry into a wake downstream of a non-magnetized obstacle in the supersonic flow of the solar wind is studied by using a two-dimensional, electromagnetic particle-in-cell simulation. Importance of negative charging of the downstream-side surface of the obstacle is examined by comparing the simulation results of 3 different ratios 8, 16, 32 of the obstacle size to the Debye length.

Keywords: wake, solar wind, surface charging, electron thermal speed, Debye length, particle-in-cell simulation

Japan Geoscience Union Meeting 2014
(28 April - 02 May 2014 at Pacifico YOKOHAMA, Kanagawa, Japan)

PEM34-04 Room:503 Time:May 1 12:30-12:45

Global Vlasov simulation of a small body with a magnetic anomaly with the K-computer

UMEDA, Takayuki[1*]

[1]Solar-Terrestrial Environment Laboratory, Nagoya University

The interaction between a plasma flow and a small dielectric body with a weak intrinsic global magnetic field is studied by means of a five-dimensional (5D) full electromagnetic Vlasov simulation with two configuration spaces and three velocity spaces. In the present study, entry processes of ions into the nightside wake tail are examined. The simulation result shows that the bow shock and the magnetopause are formed on the dayside. However, most of solar-wind ions are reflected at the dayside magnetopause and are picked up by the interplanetary magnetic field. Then, a small part of the reflected ions are taken into the deep wake tail near the body by the E cross B cycloid motion. The present result, in which the spatial resolution is low and the Debye-scale charge separation on the dayside surface is not solved, is obtained by using a recent cluster computer system. Currently we are performing a 5D high-resolution global Vlasov simulation by using the K-computer. The direct comparison between the low- and high-resolution runs would show importance of fully kinetic global simulations.

Keywords: simulation, plasma, small geophysical body, magnetosphere, Vlasov code, K computer

Japan Geoscience Union Meeting 2014
(28 April - 02 May 2014 at Pacifico YOKOHAMA, Kanagawa, Japan)

PEM34-05 Room:503 Time:May 1 14:15-14:30

Dependence of Jovian Magnetopause Location on Solar Wind Dynamic Pressure

KITAGAWA, Hirotaka[1*] ; KASAHARA, Satoshi[2] ; TAO, Chihiro[3] ; KIMURA, Tomoki[2] ; FUJIMOTO, Masaki[2]

[1]Earth and Planetary Science, School of Science, University of Tokyo, [2]Institute of Space and Astronautical Science, Japan Aerospace Exploration Agency, [3]Research Institute in Astrophysics and Planetology

Past observations revealed that the probability density distribution of Jovian magnetopause stand-off distance has double-peak. The probability between two peaks is very low. Thus the stand-off distance of Jovian magnetopause changes from the peak distance to the other peak by solar wind dynamic pressure. However, the scatter plot of stand-off distance versus solar wind dynamic pressure was nearly on one line. But the solar wind dynamic pressure was considered by magnetic pressure in the Jovian magnetosphere, due to the absence of the solar wind monitor at the Jovian orbit. We approached the double-peaked distribution by using the calculated solar wind parameters via MHD equations whose input parameters are based on the observation at Earth's orbit. Referring the propagated solar wind parameters, we investigated the location of Jovian magnetopause observed by the Galileo spacecraft. We found that the peaks of the distribution seem to be a result of probability density distribution of solar wind dynamic pressure. The very low probability stand-off distance between the peaks seemed to be caused by unusual distribution of solar wind dynamic pressure.

Keywords: Jovian Magnetopause, Solar Wind Dynamic Pressure

Japan Geoscience Union Meeting 2014
(28 April - 02 May 2014 at Pacifico YOKOHAMA, Kanagawa, Japan)

PEM34-06 Room:503 Time:May 1 14:30-14:45

Pickup ion acceleration via multiple reflection between two successive CIRs

TSUBOUCHI, Ken[1*]

[1]Tokyo Institute of Technology

Interstellar neutral particles, during their propagation inside the heliosphere, become ionized by the charge exchange with the solar wind (SW) plasma. The interplanetary magnetic field picks up these newborn ions, called ”pickup ions” (PUIs), and carries them away into the outer heliosphere with SW. The gyrating velocity of PUIs around the magnetic field is equivalent to the SW flow speed, hundreds of km/s, which is much faster than the SW thermal velocity. This property enables PUIs to be accelerated more efficiently at the shock than the thermal SW particles. Thus PUIs are considered to be the dominant source of anomalous cosmic rays (ACRs) generated at the heliospheric termination shock.

However, the well-known diffusive shock acceleration (DSA) process alone is insufficient to raise the PUI energy up to the ACR range, typically in the order of MeV. This is because the primary PUI energy (10 keV at most) is still too low to be injected into DSA, where at least hundreds of keV is necessary. Therefore, some preacceleration should take place inside the heliosphere before SW and PUI reach the termination shock. Interplanetary shocks are the most possible source for it. In the present study, we focus on the shocks driven by the interaction of the fast SW with the ahead-flowing slow SW. The regions bounded by these shocks are called corotating interaction regions (CIRs); forward shock in the slow SW side and reverse shock in the fast SW side.

We demonstrate how particles are accelerated at this CIR system by performing hybrid simulations. The simulation results show that more efficient acceleration is identified in the PUI reflected at the shock than in those transmitted through the shock. The acceleration takes place while the PUI stays close to the shock surface. This situation is similar to the shock-drift or surfing acceleration mechanism. However, our results indicate that the acceleration is not dominant in the component transverse to the magnetic field, i.e., the direction of motional electric field. Rather, the net acceleration is confirmed in the field-aligned component. The mechanism will be discussed in terms of the characteristic of the Lorentz force balance acting on PUIs.

The periodic boundary condition applied in the present simulation virtually allows the successive appearance of two CIRs. After the reflected PUI travels the ”inter-CIR” space, it encounters the shock of another CIR, where the reflection again takes place. While one reflection increases the PUI energy only a few times, this multiple reflection process yields the most energetic PUI with its maximum energy up to 100 keV, probably enough for the injection into DSA. Recent CIR observations have confirmed the presence of the energetic PUI in the solar wind between two CIRs, which may prove the present results.

Japan Geoscience Union Meeting 2014
(28 April - 02 May 2014 at Pacifico YOKOHAMA, Kanagawa, Japan)

PEM34-07 Room:503 Time:May 1 14:45-15:00

Study on The Difference Between Proper-Motion of Balmer hydrogen line emission and Non-Thermal X-Ray emission in SNRs

SHIMODA, Jiro[1*] ; INOUE, Tsuyoshi[2] ; OHIRA, Yutaka[1] ; YAMAZAKI, Ryo[1] ; SOEDA, Masanobu[1]

[1]Aoyama Gakuin University, [2]National Astronomical Observatory of Japan

Balmer line emission (Hα) by neutral hydrogen and X-ray synchrotron emission by accelerated electrons are observed from some supernova remnants (SNRs), which are thought as accelerators of galactic cosmic rays (CRs). From these observations, the cosmic ray acceleration eciency is estimated. According to the theory of diusive shock acceleration (DSA), electrons are accelerated around the shock front, and emit the synchrotron radiation. Measurement of proper motion of the synchrotron X-rays gives the shock velocity. At the same time, we can estimate the post shock temperature from the line width of Hα emission, because neutral hydrogen collide with downstream hot protons and exchange their charge, so that the hot neutral component arises.

In the specific case of a SNR RCW86, measured expansion speed of Hα filament is about 1200km/s(Helder et al. 2013), while 6000km/s in X-rays (Helder et al. 2009). It is expected that the emission regions of the Hα and the synchrotron X-rays are dierent. However, they are overlaid in the same line of sight.

In this study, using three dimensional magnetohydrodynamics (MHD) simulations, we consider propagation of super

nova blast wave shock in realistic inhomogeneous interstellar medium. Interaction between the upstream density inhomogeneity and the shock wave causes rippled shock structure and uctuation of local shock velocity. We show that our synthetic observations of the MHD simulation data are consistent with actual observation results for RCW86.

Keywords: supernova remnants, shock wave, cosmic ray

Japan Geoscience Union Meeting 2014
(28 April - 02 May 2014 at Pacifico YOKOHAMA, Kanagawa, Japan)

PEM34-08 Room:503 Time:May 1 15:00-15:15

Magnetohydrodynamic Simulations of the Interaction of a Jet with Interstellar Neutral Hydrogen Clumps

ASAHINA, Yuta[1*] ; OGAWA, Takayuki[1] ; MATSUMOTO, Ryoji[1]

[1]Graduate School of Science, Chiba University

An astrophysical jet transfers the energy released near the gravitating object and interact with the interstellar medium. When the jet propagates in the interstellar medium interacting with its environment. We carried out magnetohydrodynamic simulations of the jet propagation in neutral hydrogen (HI) clumps taking into account the interstellar cooling. At the initial state, HI clumps are assumed to be in thermal equilibrium. As the clumps are compressed by the bow shock ahead of the jet, the shocked cloud is heated up but since the density enhancement increases cooling rate, the cloud is subsequently cooled down. As a result, cold, dense sheath is formed around the jet. The enhanced density triggers the cooling instability and prompts the formation of the cold, dense gas.

We studied the dependence of numerical results on the volume filling factor of the HI clumps. We found that when the volume filling factor is large, the propagation speed of the jet is slow and arc-shaped cold dense region is formed. When the volume filling factor is small, propagation speed does not decrease so much and dense cloud distribution is more elongated. The distribution of the cold, dense gas and the length of the jet propagation speed depend on the filling factor.

We report the application of this model to molecular clouds toward the stellar cluster Westlund 2 and TeV γ-ray source HESS J1023-575 observed by NANTEN2 and Mopra telescope. HESS J1023-575 is located between these molecular clouds. The shape of molecular cloud on the right of HESS J1023-575 is like an arc and molecular clouds on the other hand distribute linearly. The difference of the filling factor can explain the difference of the shape of these molecular clouds.

Keywords: jet, interstellar medium, magnetohydrodynamics

Japan Geoscience Union Meeting 2014
(28 April - 02 May 2014 at Pacifico YOKOHAMA, Kanagawa, Japan)

PEM34-P01 Room:503 Time:May 1 18:15-19:30

High beta plasma production and their diagnostics in magnetosphere RT-1 device

NISHIURA, Masaki[1*] ; YOSHIDA, Zensho[1] ; SAITOH, Haruhiko[1] ; YANO, Yoshihisa[1] ; KAWAZURA, Yohei[1] ; NOGAMI, Tomoaki[1] ; YAMASAKI, Miyuri[1]

[1]Graduate school of frontier sciences, The Univeristy of Tokyo

The magnetosphere plasma device is one of new concepts for nuclear fusion devices. A ring trap 1(RT-1) realizes the concept as a laboratory magnetosphere using a superconducting magnet levitated in a vacuum vessel, which produces a dipole magnetic field. We study the characteristics of confined plasmas in RT-1. In recent experiments, the RT-1 experiment has demonstrated the self-organization of a plasma clump with a steep density gradient; a peaked density distribution is spontaneously created through ”up-hill diffusion”.

The operation regime of RT-1 is extended into the electron density from 10^{17} to 10^{18} m^{-3} by optimizing the electron cyclotron heating (ECH) system. The line integrated density measured by an interferometer achieved 6.2x$10^{17}m^{-3}$ and diamagnetic flux 5.6 mWb. It is considered that the beta value (the ratio of plasma pressure to magnetic pressure) exceeds 100%. In such situation, a millimeter wave reflectometer is implemented to measure the density peaking and spatial structure. We observed the initial results and started the analysis of acquired signals.

When we use the electron heating by ECH system, the ion remains cold due to a collisionless situation. Therefore we installed three turn antenna into RT-1 to heat ions by a slow wave (ion cyclotron heating: ICH) in a MHz range. In the case of ˜$10^{18}m^{-3}$ as a target plasma of ICH by only use of ECH, the heating efficiency of ICH increases, and then leads to the increase of ion temperature. The effect has been observed by an electrostatic energy analyzer, which located at the plasma edge of RT-1.

We designed an ion probe to diagnose energies and pitch angles of ions in ICH experiments of RT-1. The principle of the ion probe is the same as that of fast ion loss measurement in a fusion machine, and is applied to the ion diagnostic in RT-1 plasmas. A scintillator is mounted inside the probe head with a pin hole. Ions with gyro motion enter into the probe head, and then hit the scintillator. We can know the energies and pitch angle simultaneously from the scintillation image.

We report the extension of plasma parameters by ECH optimization, progress on the installation of ion probe, and future perspective.

References

[1] Z. Yoshida et al., Phys. Rev. Lett. 104 (2010) 235004.
[2] H. Saitoh et al., Nucl. Fusion 51 (2011) 063034.

Keywords: plasma, magnetosphere, plasma diagnostics, plasma heating

Japan Geoscience Union Meeting 2014
(28 April - 02 May 2014 at Pacifico YOKOHAMA, Kanagawa, Japan)

PEM34-P02 Room:503 Time:May 1 18:15-19:30

Hybrid simulations of the interaction between the solar wind and the ion scale magnetosphere

NAKAMURA, Masao[1*]

[1]Osaka Prefecture University

The interaction between the solar wind and the ion scale magnetosphere with a dipole magnetic field is investigated by a three-dimensional hybrid simulation. In the present study, the ion scale magnetosphere has a dayside stand-off distance which is several to a hundred times larger than the ion Larmor radius of the solar wind proton in the magnetic field strength at the dayside magnetopause boundary. The hybrid simulation treats the ions as kinetic super particles via particle-in-cell method and the electrons as a massless fluid. In the interaction between the solar wind and the magnetosphere, the interplanetary magnetic field (IMF) condition controls not only the reconnection regions but also the subsolar sheath flow due to the ion kinetic effects. Those influence the structures of the bow shock and the magnetopause boundary layer. We will also discuss the momentum transfer process from the solar wind into the magnetosphere and to the magnetized object.

Keywords: Ion scale magnetosphere, Interaction between solar wind and mini-magnetosphere, 3D hybrid simulation

Japan Geoscience Union Meeting 2014
(28 April - 02 May 2014 at Pacifico YOKOHAMA, Kanagawa, Japan)

PEM35-01 Room:503 Time:May 2 15:00-15:25

Full PIC simulations on plasma electromagnetic disturbance in the vicinity of spacecraft

USUI, Hideyuki[1*] ; MIYAKE, Yohei[1]

[1]Graduate School of System Informatics, Kobe University

Space exploration has been rapidly increasing, and a strong demand arises regarding comprehensive understanding of spacecraft-plasma (SP) interactions [1]. This is clearly required to ensure survivability and proper operations of space-based systems, and also for correct interpretation of measurements and other information collected in situ by scientific spacecraft.

In space environments, spacecraft are electrically charged due to plasma contact to spacecraft surface and its floating potential is basically determined by the current balance at spacecraft surface. The current consists of incident background plasma, emission of photoelectrons/secondary electrons from spacecraft surface as well as active emission of plasma beam in electric propulsion system such as ion engine. Due to the spacecraft charging, plasma environment near spacecraft is influenced. Non-uniform plasma distributions such as sheath and wake structures are formed near spacecraft surface and in the downstream region with respect to the solar wind, respectively. Field components near spacecraft can be also disturbed by the plasma response to spacecraft. Understanding of the SP interactions is important from a view point of spacecraft observation of plasma environment as well as its data analysis. To discriminate plasma phenomena artificially disturbed by spacecraft from observational data, quantitative understanding of SP interactions is necessary. In designing science instruments such as electric field sensor, plasma disturbance near spacecraft has to be minimized as much as possible to obtain reliable and valuable data. To obtain self-consistent solution of these plasma disturbances near spacecraft, we perform plasma simulations including spacecraft body in a simulation domain.

For solving SP problems, we have developed the EMSES plasma particle simulation code [2]. EMSES is based on the standard electromagnetic PIC method, and also has the capability to include the conducting bodies of a spacecraft, based on the capacitance matrix method. In addition, a number of crucial physics such as the photoelectron emission and the secondary emission are modeled numerically in the latest version of EMSES. The code has been applied so far to some specific spacecraft, e.g., Geotail, Cluster, BepiColombo/MMO, and Solar Probe Plus.

In this talk, first we will briefly explain the numerical treatment of spacecraft in EMSES. Then we will show a few examples of EMSES applications to scientific spacecraft. One of such applications is an enhanced wake formed behind the Cluster satellite in tenuous streaming plasma [3]. In the simulation we have included the conducting surfaces of very thin (in an order of mm) wire booms by using the fictitious surface technique. We found that even the extremely thin wire booms can contribute substantially to the formation of an electrostatic wake because of highly positive spacecraft charging in the tenuous plasma environment. We will also show a recent research topic on the SP interactions in the near-Sun environment. Large photoelectron emission current caused by an intense solar flux forms a negative potential barrier on the spacecraft surface, leading to negative charging of the spacecraft. Electromagnetic environments around these specific spacecraft will be presented in the talk.

[1] D. Hastings and H. Garrett, Spacecraft-Environment Interactions, Cambridge University Press, 2004.

[2] Y. Miyake and H. Usui, A new electromagnetic particle code for the analysis of conductive spacecraft-plasma interactions, Physics of Plasmas 16, 062904, 2009.

[3] Y. Miyake, C. M. Cully, H. Usui and H. Nakashima, Plasma particle simulations of wake formation behind a spacecraft with thin wire booms, Journal of Geophysical Research: Space Physics, Volume 118, Issue 9, pages 5681-5694, September 2013.

Keywords: Spacecraft plasma environment, Spacecraft-plasma interactions, Electromagnetic Particle simulation, Spacecraft charging, electromagnetic disturbance

Japan Geoscience Union Meeting 2014
(28 April - 02 May 2014 at Pacifico YOKOHAMA, Kanagawa, Japan)

PEM35-02 Room:503 Time:May 2 15:25-15:45

General relativistic simulations of magnetized binary neutron star merger on K

KIUCHI, Kenta[1*] ; KYUTOKU, Koutarou[2] ; SEKIGUCHI, Yuichiro[1] ; SHIBATA, Masaru[1]

[1]Yukawa Institute for Theoretical Physics, [2]University of Wisconsin-Milwaukee

Binary neutron stars are a binary which is composed of two neutron stars and nine binaries have been observed so far. They gradually lose the orbital energy and angular momentum due to gravitation wave emission and merge in the end. Within the observed binaries, six of them will merger within the Hubble time. Gravitational waves emitted during the merger would be detectable with the ground-based gravitational wave detectors such as KAGRA, advanced LIGO, and advanced VIRGO at a frequency of about ten times per year. If we could observe the gravitational waves, they would tell us the validity of General Relativity in a strong gravitational field and the equation of state of neutron star matter which is poorly known to date as well.

This situation facilitates a theoretical study of binary neutron star mergers. During the merger, the density is as high as 10^{15} g/cc and the temperature rises as high as 10^{10} degrees. Therefore, any analytical approaches break down and we need a numerical modeling. Our group is approaching this problem in the framework of Numerical Relativity. It is a research field whose aim is figuring out phenomena in a strong gravitational field by solving the Einstein equation as well as the hydrodynamical equation and neutron radiation transfer.

The observations of the pulsars have revealed that the neutron stars are magnetized with about 10^{12} Gauss in general. Moreover, some of them could have 10^{14} Gauss. However, it is still unknown what the role of magnetic field during binary neutron star mergers is. There are several hydrodynamical instabilities which amplify the magnetic field and a short wavelength mode is essential in all cases. Therefore, it is mandatory to perform a high-resolution simulation. In the previous studies of this subject, it is hard to say that enough resolution is assigned to resolve these instabilities. Our group is performing a numerical simulation with the highest resolution on the supercomputer K and figuring out the role of the magnetic field during the merger of binary neutron stars. We summarize the result as follows.

When the two stars come into contact, the shear layer between the stellar surface becomes unstable against the Kelvin-Helmholts instability. The vortices are produce by this instability and the shorter the wavelength is, the larger the growth rate of the instability is. If there exists magnetic field lines, they are curled by these vortices and are expected to be amplified exponentially. By performing the convergence study against the numerical resolution, we have found the maximum magnetic field is amplified by the factor of about thirty at least at the merger.

After the merger, a hypermassive (HMNS) neutron star is transiently formed, which is supported by a rapid and strong differential rotation in addition to the thermal pressure. Although this star is unstable against the magnetorotational instability (MRI), it is difficult to resolve the MRI because the wavelength of the unstable mode is quite short due to the high density and high angular velocity of the HMNS neutron star. In our simulation, we have resolved this unstable mode and we have shown that the HMNS neutron star has the magnetic field as large as 10^{16}-10^{17} Gauss as a result.

In the HMNS neutron star, the angular momentum transport due to the non-axisymmetric structure as well as due to the MRI works. In addition, the star loses a significant amount of the angular momentum due to the gravitational wave emission. Then, the star collapses to a black hole which is surrounded by the accretion disk. Inside the accretion disk, the magnetohydrodynamical turbulence transports the angular momentum and its surface is unstable against the Kelvin-Helmoholts instability. Vortices produced by these two mechanisms transport the energy outwardly and the disk wind activates as a result. In this talk we will introduce the simulation result in details.

Japan Geoscience Union Meeting 2014
(28 April - 02 May 2014 at Pacifico YOKOHAMA, Kanagawa, Japan)

PEM35-03 Room:503 Time:May 2 15:45-16:00

Electromagnetic Vlasov simulations of magnetized plasma with a finite-volume multi-moment advection scheme

MINOSHIMA, Takashi[1*] ; MATSUMOTO, Yosuke[2] ; AMANO, Takanobu[3]

[1]Institute for Research on Earth Evolution, Japan Agency for Marine-Earth Science and Technology, [2]Graduate School of Science, Chiba University, [3]Department of Earth and Planetary Science, University of Tokyo

The Vlasov simulation, which directly discretizes the Vlasov equation on grid points in phase space, has been proposed as an alternative method to the common Particle-In-Cell simulation, to improve the accuracy of kinetic plasma simulations. Although the electrostatic Vlasov simulations have been successfully carried out thus far, the electromagnetic Vlasov simulation of magnetized plasma is still limited, owing to numerical difficulty in solving the distribution function in velocity space.

To overcome the difficulty, we develop a new numerical scheme, specifically designed to solve the Vlasov equation in magnetized plasma. The scheme advances multiple piecewise moments of a physical profile based on their governing equations, to preserve the profile with high accuracy. The scheme allows us to perform a long-time calculation of the distribution function of magnetized plasma with small numerical diffusion.

In this talk, we first present the scheme and its performance. Then, we report the application of the scheme to two-dimensional (2D3V) electromagnetic Vlasov simulations. Long-time simulations of the linear wave propagation in magnetized plasma are conducted with quite small numerical errors. We also conduct the simulation of collisionless magnetic reconnection. The simulation resolves macroscopic structure without numerical noise, and is in good agreement with previous studies. Furthermore, the simulation resolves microscopic structure of the non-Maxwellian plasma velocity distribution around the reconnection site, e.g., acceleration by the reconnection electric field at the X-point, high energy beams around the boundary layer, and heating by the magnetic compression at the downstream. Since the simulations have been successfully carried out with the grid size much larger than the Debye length, the Vlasov simulation is a powerful technique to treat global-scale kinetic plasma phenomena.

Keywords: Advection equation, Vlasov simulations, Magnetic reconnection

Japan Geoscience Union Meeting 2014
(28 April - 02 May 2014 at Pacifico YOKOHAMA, Kanagawa, Japan)

PEM35-04 Room:503 Time:May 2 16:15-16:30

Generalization of Plasma Hybrid Simulation Model

AMANO, Takanobu[1*] ; HIGASHIMORI, Katsuaki[1] ; SHIRAKAWA, Keisuke[1]

[1]Department of Earth and Planetary Science, University of Tokyo

The hybrid simulation model has been widely used as one of the self-consistent simulation methods in investigating nonlinear space plasma phenomena, which treats ions as kinetic macro-particles whereas electrons are assumed to be an inertialess fluid. It can correctly simulate from magnetohydrodynamic to the ion inertia length scale. However, the assumption of the inertialess electron makes it sometimes numerically difficult to handle high-frequency whistler waves. We have recently shown that the problem may be resolved by appropriately including finite electron inertia effect, which also makes it possible to handle vacuum regions in a hybrid code. In this report, we discuss extension of the model which may be able to incorporate electron kinetic effect. Ignoring the displacement current and assuming charge neutrality, we adopt the Vlasov-Ampere system of equations. An equation to determine the electric field is derived from the basic equation without any approximations. We demonstrate that by using the equation, the electron cyclotron resonance can be properly included.

Keywords: plasma, numerical simulation

Japan Geoscience Union Meeting 2014
(28 April - 02 May 2014 at Pacifico YOKOHAMA, Kanagawa, Japan)

PEM35-05 Room:503 Time:May 2 16:30-16:45

Optimization of Magnetohydrodynamic Simulation Code for Planetary Magnetosphere to Xeon Phi

FUKAZAWA, Keiichiro[1*]

[1]Research Institute for Information Technology, Kyushu University

For investigating the global structures of plasma, such as the planetary magnetospheres, the Magnetohydrodynamic (MHD) equations are often used, in which full kinetics of plasma are neglected by taking the moments of the Vlasov equations. The MHD equations are highly nonlinear and are very complex to solve by hand calculations. Thus computer simulations play essential roles in studies of global magnetosphere.

The numerical MHD code for the magnetosphere has been optimized for vector-type supercomputers for a long time because the MHD code is a kind of fluid code and most of supercomputers with vector processors have high performance to solve the fluid codes in 1990's. These codes often have achieved a very high computational efficiency (the ratio of the effective performance to the theoretical performance). However, almost 100% of the "Top 500" supercomputer systems in the world adopt the massively parallel scalar type processors and more than 85% of systems consist of the x86 processor architecture in these days. The other scalar type computers are POWER and SPARC architectures. Recently the new coprocessor Xeon Phi which has many cores (˜60 cores) of X86 architecture is introduced to the supercomputer system and achieved good performance of the Linpack benchmark.

In this study I evaluate the performance of MHD code for the planetary magnetosphere on the single Xeon Phi coprocessor. For the performance evaluation, I use the three-dimensional domain decomposition method and a cache-hit type of three-dimensional domain decomposition method with the flat MPI and hybrid MPI. As the results, I found that normal three-dimensional decomposition of the MHD model with the hybrid MPI is suitable for Xeon Phi coprocessor and achieved computing performance efficiency of ˜7%. Furthermore, I add the optimization to the MHD code based on the Xeon Phi architecture and obtained the computing performance efficiency of almost 10% which is the double performance of FX10 single node.

Japan Geoscience Union Meeting 2014
(28 April - 02 May 2014 at Pacifico YOKOHAMA, Kanagawa, Japan)

PEM35-06 Room:503 Time:May 2 16:45-17:00

A Study of Fluid Element Tracing in Global MHD Simulations via Parallel Data Processing on the NICT Science Cloud

MURATA, Ken T.[1*] ; FUKAZAWA, Keiichiro[2] ; GUO, Zhihong[3] ; EBIHARA, Yusuke[4] ; SAITA, Satoko[5] ; FUJITA, Shigeru[6] ; TANAKA, Takashi[7] ; KUBOTA, Yasubumi[1] ; WATANABE, Hidenobu[1] ; TATEBE, Osamu[8] ; TANAKA, Masahiro[8] ; KIMURA, Eizen[9]

[1]National Institute of Information and Communications Technology, [2]Kyushu University, [3]SURIGIKEN Co.,Ltd., [4]Kyoto University, [5]Research Organization of Information and Systems, [6]Meteorological College, Japan Meteorological Agency, [7]SERC, Kyushu University, [8]University of Tsukuba, [9]Ehime University

The NICT Science Cloud is a cloud system designed for scientific researches, and expected as a new infrastructure for big data sciences. Not only parallelization of CPU as in super-computers, but I/O and network throughput parallelization are crucial for the big data science. A high-performance visualization system is constructed on the NICT Science Cloud using Gfarm/Pwrake middleware. We examined performance of this parallel visualization environment for a set of computer simulation with 1000 files (2.3TB in all). After setting higher priority to access to local file on local disk, we finally achieved 124 times higher visualization using 192 core cpu.

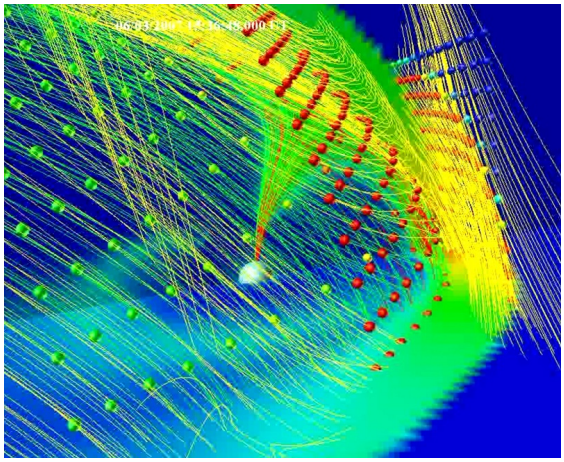

Japan Geoscience Union Meeting 2014
(28 April - 02 May 2014 at Pacifico YOKOHAMA, Kanagawa, Japan)

PEM35-P01 Room:503 Time:May 2 16:15-17:30

Development of magnetic field tracking module for analyzing a decaying sunspot

KATO, Shota[1*] ; IMADA, Shinsuke[1] ; MACHIDA, Shinobu[1]

[1]Solar-Terrestrial Environment Laboratory, Nagoya University

In order to analyze the structures of magnetic fields using the data from Solar Optical Telescope (SOT) on board the Hinode satellite, we have developed the automatic tracking module, which detects the magnetic region and tracks the time variation of each region.

The module, based on three thresholds, intensity, size, and distance, has main three functions: (1) detect the magnetic fields based on the intensity threshold, (2) remove the micro region by the size threshold, (3) based on move distance by time variation, detect the same regions and track them.

We made simple sample data for test and checked on the accuracy of our tracking module.

We applied the module to sunspot and analyzed the time variation of decaying sunspot which is one of the sources of magnetic element in the solar surface.

We have use the magnetograph data which was observed by Hinode/SOT from 29 Dec 2009 to 2 Jan 2010. We also discuss the north-south/east-west asymmetry of the decaying process in the active region.

Keywords: sunspot, development of module, auto detection, auto tracking

Japan Geoscience Union Meeting 2014
(28 April - 02 May 2014 at Pacifico YOKOHAMA, Kanagawa, Japan)

PEM35-P02 Room:503 Time:May 2 16:15-17:30

Application of feature recognition technique in the investigation of magneto-convection on the solar surface

IIDA, Yusuke[1*] ; HOTTA, Hideyuki[2]

[1]ISAS/JAXA, [2]High Altitude Observatory/JSPS

We show the recent feature recognition technique and its benefits in the investigation of magneto-convection on the solar surface using observational and numerical approaches.

The magneto-convection on the solar surface is important not only as a trigger of many surface energetic events, e.g. solar flare, jet, and X-ray bright point, but also as an actual example of the most detailedly observed and numerically simulated magneto-convection on the stellar surface owing to its closeness to the earth. However, the elements of magneto-convection (<1,000km), the basic convective cells and magnetic patches formed by convective motion, are much smaller than solar global scale(~70,0000km). It means that we need large field of view to catch up enough number of structures simultaneously with high spatial resolution to capture such small scale structures. Thanks to the improvement of engineering technique for satellite observation and computers for numerical calculation, we are now able to catch such a large scale structure at the same time. However, the new difficulty, how to investigate statistical characters of convective cells and magnetic structures in such huge data sets, has just shown up in the analysis.

Because of this situation, feature recognition and tracking technique is now focussed on. In this presentation, we want to introduce the auto-recognition and tracking code of magnetic patches and convective cells on the solar surface. Further it is shown that the statistical characters obtained through the analysis of observational data and numerical calculation data based on the auto-recognition and tracking code. We want to note that the feature tracking technique drastically improve statistics of the analysis drastically. We also want to discuss about the applicants of feature tracking technique with the scientists in the other fields though this collaborative session.

Keywords: the Sun, magneto-convection, feature recognition

Japan Geoscience Union Meeting 2014
(28 April - 02 May 2014 at Pacifico YOKOHAMA, Kanagawa, Japan)

PEM35-P03 Room:503 Time:May 2 16:15-17:30

On stability properties of the numerical Cherenkov instability in relativistic plasma flows

IKEYA, Naoki[1*] ; MATSUMOTO, Yosuke[1]

[1]Graduate School of Science, Chiba University

We examined stability properties of the numerical Cherenkov instability in relativistic plasma flows. Particle-in-cell simulation code package, pCANS, was used for the numerical analysis. With the implicit FDTD method for Maxwell equations, we found that the instability was greatly inhibited with the CFL number of 1.0. Numerical tests with various CFL numbers ranging from 0.5 to 1.0 showed that the growth rate remarkably decreased at CFL = 1.0 following a gradual decrease from the value at CFL=0.5. The implicitness factor (alpha=0.5 for Clank-Nicolson method) was also found to control the width of the dip. The present result contrasts with the recently reported results (Vay et al., 2011, Godfrey & Vay, 2013) in which the magical CFL number were 0.5 and 0.7 respectively for their different explicit field solvers. We present the result with the detailed dispersion relation of the implicit field solver and its application to relativistic collisionless shock simulations.

Keywords: particle-in-cell simulation, relativistic plasma, numerical Cherenkov radiation, shocks

Japan Geoscience Union Meeting 2014
(28 April - 02 May 2014 at Pacifico YOKOHAMA, Kanagawa, Japan)

PEM35-P04 Room:503 Time:May 2 16:15-17:30

Electron hybrid code simulations with OhHelp load balancer

KATOH, Yuto[1*] ; MIYAKE, Yohei[2] ; NAKASHIMA, Hiroshi[3] ; USUI, Hideyuki[2] ; OMURA, Yoshiharu[4]

[1]Department of Geophysics, Graduate School of Science, Tohoku University, [2]Graduate School of System Informatics, Kobe University, [3]Academic Center for Computing and Media Studies, Kyoto University, [4]Research Institute for Sustainable Humanosphere, Kyoto University

A spatially one-dimensional electron hybrid code has been developed for the study of the generation process of whistler-mode chorus emissions and relativistic electron acceleration in the Earth's inner magnetosphere [1-3]. In the electron hybrid code, we treat cold electrons as a fluid and energetic electrons as particles by the Particle-in-Cell (PIC) method. Since we assume an inhomogeneous background magnetic field in the simulation system so as to treat the bounce motion of energetic electrons along a magnetic field line, the distribution of energetic electrons in the system is non-uniform and energetic electrons move around the magnetic equator assumed at the center of the simulation system. While the electron hybrid code has been parallelized through the particle decomposition method, we need to improve the scalability of the electron hybrid code so as to use a large simulation system and billions of particles for simulations under initial conditions corresponding to the real magnetosphere.

In the present study, we have developed a spatially one-dimensional electron hybrid code domain-decomposed by OhHelp [4]. The OhHelp is a library which enables us to conduct PIC simulations by achieving both dynamic load balancing and scalability. The efficiency and scalability of OhHelp have been confirmed by a 3D full PIC simulations [5]. We show the efficiency and scalability of the developed code tested on the system A (Cray XE6) of Academic Center for Computing and Media Studies, Kyoto University. We compare the performance of the developed code and those of the code with the particle decomposition.

[1] Katoh Y., Y. Omura, Computer simulation of chorus wave generation in the Earth's inner magnetosphere, Geophys. Res. Lett., 34, L03102, doi:10.1029/2006GL028594, 2007.

[2] Katoh, Y., Y. Omura, and D. Summers, Rapid energization of radiation belt electrons by nonlinear wave trapping, Ann. Geophys., 26, 3451–3456, 2008.

[3] Katoh, Y. and Y. Omura, Effect of the background magnetic field inhomogeneity on generation processes of whistler-mode chorus and hiss-like broadband emissions, J. Geophys. Res. Space Physics, 118, 4189-4198, doi:10.1002/jgra.50395, 2013.

[4] Nakashima, H., Y. Miyake, H. Usui, and Y. Omura, OhHelp: A Scalable Domain-Decomposing Dynamic Load Balancing for Particle-in-Cell Simulations, Proc. 23rd Intl. Conf. Supercomputing, 90-99, 2009.

[5] Miyake, Y., H. Usui, and H. Nakashima, Development of a Scalable PIC Simulator and Its Application to Spacecraft-Plasma Interaction Problems, Proc. JSST 2012, OS6-8, pp. 262?267, 2012.

Keywords: dynamic load balancer, PIC simulation

Japan Geoscience Union Meeting 2014
(28 April - 02 May 2014 at Pacifico YOKOHAMA, Kanagawa, Japan)

PEM36-01 Room:312 Time:April 28 09:00-09:15

Effect of Surface BRDF on the Geostationary and Low Orbit Observations of Tropospheric NO_2

NOGUCHI, Katsuyuki[1*] ; RICHTER, Andreas[2] ; ROZANOV, Vladimir[2] ; ROZANOV, Alexei[2] ; BURROWS, John[2] ; IRIE, Hitoshi[3] ; KITA, Kazuyuki[4]

[1]Nara Women's University, [2]University of Bremen, [3]Chiba University, [4]Ibaragi University

We investigated the effect of surface reflectance anisotropy, Bidirectional Reflectance Distribution Function (BRDF), on geostationary and low orbit satellites' retrievals of tropospheric NO_2. We first develop an empirical model of the three BRDF coefficients for each land cover type over Tokyo, and then apply the model to the calculation of land cover type dependent AMFs and BAMFs. Results show that the variability of AMF among the land types is up to several tens percent, and if we neglect the reflectance anisotropy, the difference from BRDF's AMF reaches 10% or more. The evaluation of the BAMFs calculated shows that not to consider variations in BRDF will cause large errors if the concentration of NO_2 is high close to the surface, although the importance of BRDF for AMFs decreases for large AOD.

Japan Geoscience Union Meeting 2014
(28 April - 02 May 2014 at Pacifico YOKOHAMA, Kanagawa, Japan)

PEM36-02 Room:312 Time:April 28 09:15-09:30

R&D of passive radar -Water vapor estimation with digital terrestrial broadcasting wave-

KAWAMURA, Seiji[1*] ; OHTA, Hiroki[1] ; HANADO, Hiroshi[1]

[1]National Institute of Information and Communications Technology

In general, radars retrieve some information by transmitting radio waves and by receiving their scatted echoes. On the other hand, passive radars never transmit radio waves. They retrieve some information by receiving radio waves which are transmitted by others for other purposes. Passive radars do not need new radio wave frequencies, and just consist of rather simple and low cost receivers because they do not transmit radio waves. We, National Institute of Information and Communications Technology (NICT), are developing passive radar measurement systems whose targets are environmental monitoring.

In this study, we are developing a water vapor measurement system using digital terrestrial broadcasting wave as one of passive radars. Localized heavy rain in the urban area is a social issue in these days. Water vapor is an essential parameter for weather forecast because it is a state before rain drop. And it is one of the most difficult physical quantity to measure with remote sensing technique. If we can monitor water vapor around the ground surface with precise time and spacial resolutions, the weather forecast might be able to predict the localized heavy rain.

Radio waves are delayed due to water vapor through propagation. If we can measure this time delay, water vapor can be retrieved from it. Since delay doe to water vapor is quite small, very precise (sub-nano second order) measurements are needed. Radio waves used for digital terrestrial broadcasting are modulated with OFDM, and known signals are embedded. Complex delay profiles are calculated using these known signals. Using the phase of delay profile, we can measure propagation delay with precise accuracy (pico-second order).

When we consider the accuracy with order of sub-nano seconds, phase fluctuations of local oscillators at radio tower and receivers are essential error factors. We have developed a real-time delay (phase of delay profiles) measurement system with software-defined radio technique. Using this system, we can also measure phase fluctuations of local oscillator at each TV station by just receiving radio waves. With these systems at two receiving points on the same line including the radio tower, and with synchronization between their local oscillators, we can measure water vapor between two receiving points. After proving test of estimation of water vapor, we will distribute many small receivers and develop water vapor monitoring system in collaboration with many observations and data assimilations.

Keywords: passive radar, digital terrestrial broadcasting wave, water vapor, propagation delay

Japan Geoscience Union Meeting 2014
(28 April - 02 May 2014 at Pacifico YOKOHAMA, Kanagawa, Japan)

PEM36-03 Room:312 Time:April 28 09:30-09:45

Observation of local circulation in north area of Fukui prefecture by using two adjoining 1.3-GHz wind profiler radars

NAKAJO, Tomoyuki[1*] ; YAMAMOTO, Masayuki[2] ; AOYAMA, Takashi[1] ; HASHIGUCHI, Hiroyuki[2] ; UJIHASHI, Yasuyuki[3]

[1]Department of Electrical, Electronic and Computer Engineering, Fukui University of Technology, [2]Research Institute for Sustainable Humanosphere, Kyoto University, [3]Department of Architecture and Environmental Engineering, Fukui University of Technology

Global impact of our lifestyle to our own has been pointed out previously. In the field of atmospheric environment, it has been considered that heavy rainfall, of which occurrence and damages are increasing in recent years, to be related with global warming. In addition to influence of yellow dust and PM 2.5 on our health, it has been known that photochemical oxidant tends to increase again since 1980's. Furthermore, the severe accident of Fukushima Daiichi Nuclear Power Station has caused us the interest about diffusion of radioactivity.

Above atmospheric problems are not only global but also local because they are strongly affected by local circulation. Local circulation occurs in atmospheric boundary layer (ABL) which has different characteristics in each local area, therefore, it is essential to reveal the detailed characteristics of ABL for resolution of the atmospheric problems.

Under such a situation, Fukui University of Technology started a project named as "Formation of research base for measurement and conservation of environment in Hokuriku area" (H23 - H27) supported by MEXT. In the project, a 1.3-GHz wind profiler radar (FUT-WPR), which is same type atmospheric radar as that of JMA WINDAS network, was installed in the coastal area of northern part of Fukui prefecture in 2012. In Fukui prefecture, a WPR of WINDAS has worked at Fukui local meteorological observatory (WINDAS-FUKUI), and the distance between FUT-WPR and WINDAS-FUKUI is only 24 km. There is no area in Japan where two WPRs are located within such a short distance, which enables more detailed study of the local circulation in Fukui plain than previous studies.

The observation results of FUT-WPR have revealed the detailed characteristics of see and land breeze (SLB) which is well known local circulation in coastal areas; its temporal variation, structure in altitude, relation with ABL, occurrence probability, and effect on generating area of clouds. Especially, the comparison with WINDAS-FUKUI not only confirms the observation results by FUT-WPR but also shows the SLB reaches from the seashore to a few 10 km inland. Although the observation results are fundamental in meteorology, this is the first time that the real picture of SLB in Fukui plain was revealed in detail so far. The comparison with WINDAS-FUKUI also shows the horizontal winds under about 1 km in altitude often differs between FUT-WPR and WINDAS-FUKUI, which indicates the importance of measurement of ABL.

We also carried out the data analyses in the case of heavy rain. On September 3 in 2013, passage of the stationary front accompanying the typhoon No. 17 brought about the heavy rain reaching to 10 mm/10min in Fukui prefecture from 14:00 to 16:00 (JST). FUT-WPR observed not only a typical structure and temporal variation of horizontal wind followed by the passage of stationary front but also intermittent upward flow, of which velocity reaches 1 m/s in the altitude from 200 m to about 4 km, from 7 hours before the passage of front. Especially, a strong upward flow with the velocity of 4 m/s was observed around 12:00 in the altitude from 3.5 to 5 km although the duration was relatively short. The observations of MTSAT from 10:00 to 14:00 have shown that optically thick clouds, of which top altitude was estimated to reach about 10 km, had arrived over Fukui prefecture. Therefore, the upward flows observed by FUT-WPR should be a part of cumulonimbi system which brought about the heavy rain. On the other hand, upward flows observed by WINDAS-FUKUI was weaker than that of FUT-WPR, which indicates the horizontal scale of upward flow accompanying the cumulonimbi system was under 24 km at least.

The results of observations and data analyses obtained so far indicates the observation of ABL by adjoining WPRs will be useful in early detection of arriving cumulonimbi system or local weather prediction.

Keywords: atmospheric boundary layer, local circulation, see and land breeze, heavy rain, wind profiler radar

Japan Geoscience Union Meeting 2014
(28 April - 02 May 2014 at Pacifico YOKOHAMA, Kanagawa, Japan)

PEM36-04 Room:312 Time:April 28 09:45-10:00

Relationship between solar activity and disturbance in the middle atmosphere during Arctic winter

SAKANOI, Kazuyo[1*] ; KINOSHITA, Takenari[2] ; MURAYAMA, Yasuhiro[2]

[1]Komazawa Univ., [2]National Institude of Information and Communications Technology

Purpose of this research is to clarify relationship between solar activity and disturbance in the middle atmosphere during Arctic winter. In this research we consider stratospheric sudden warming (SSW), which is typical phenomenon in Arctic winter, as disturbance in the middle atmosphere including the mesosphere. Previous research reported effect of 11-year solar cycle on thermal structure only in the Stratosphere.

To get thing started, we selected daily bottom altitude of easterly wind area, which corresponds to SSW, in the zonal mean horizontal wind. Averaged value of those during one SSW event is used for quantitative comparison with solar activity and QBO index. No clear relationship was found between the selected new value (ZEW index) and two indexes. However we confirm that the ZEW index represents well the degree of disturbance. Next, we calculate AO index in the altitude range from 1000 hPa to 0.1 hPa (65km alt). AO index also represents the degree of disturbance.

In this presentation, we will examine and discuss in more detail about ZEW and AO index as those which indicate the degree of disturbance in the middle atmosphere for quantitative comparison with solar activity.

Keywords: Middle atmosphere disturbance, Solar activity, Arctic Oscillation, QBO, Arctic region, Stratospheric sudden warming

Japan Geoscience Union Meeting 2014
(28 April - 02 May 2014 at Pacifico YOKOHAMA, Kanagawa, Japan)

PEM36-05 Room:312 Time:April 28 10:00-10:15

Temporal variations of O3 and NO in the middle atmosphere above Syowa Station observed by a millimeter-wave radiometer

OHYAMA, Hirofumi[1*] ; ISONO, Yasuko[1] ; UEMURA, Miku[1] ; NAGAHAMA, Tomoo[1] ; MIZUNO, Akira[1] ; TSUTSUMI, Masaki[2] ; EJIRI, Mitsumu[2] ; NAKAMURA, Takuji[2]

[1]Solar-Terrestrial Environmental Laboratory, Nagoya University, [2]National Institute of Polar Research

Precipitation of energetic particle into the atmosphere impacts abundances of atmospheric constituents in the middle atmosphere. Highly energetic solar protons, which directly enter the middle atmosphere, cause increase of HOx and NOx species. Energetic electrons also increase NOx in the thermosphere, and the downward transport in the polar vortex moves the produced NOx to lower altitudes. These NOx species cause a decrease of O_3 in the middle atmosphere through catalytic reactions [Seppälä et al. 2006; Daae et al., 2012]. To investigate the effect of NOx on O_3 variation in the polar region, a ground-based millimeter-wave spectroscopic radiometer was installed at Syowa Station, Antarctica in March 2011. The instrument has recorded brightness temperature spectra of rotational emission from the atmospheric O_3 and NO molecules. From the NO spectra, both multiple short-term enhancements and seasonal variation of NO column are observed [Isono et al., 2014]. The short-term enhancements are correlated with the energetic particle precipitation. In the present study, O_3 profiles are retrieved from the brightness temperature spectra between 238.94-239.24 GHz, whose spectral range has sensitivity to the O_3 abundance between 20 and 70 km. The optimal estimation scheme is used for the O_3 profile retrieval, along with radiative transfer calculation through the use of the NCEP reanalysis data and spectroscopic parameters. Since the O_3 spectra are integrated over 1 hour every 6 hours, we usually derive four O_3 profiles in a day. We present the result of O_3 retrieval and discuss how the O_3 mixing ratios at given altitudes response to the short-term NO column enhancement.

Keywords: ozone, nitric oxide, remote sensing

Japan Geoscience Union Meeting 2014
(28 April - 02 May 2014 at Pacifico YOKOHAMA, Kanagawa, Japan)

PEM36-06 Room:312 Time:April 28 10:15-10:30

Current status of Syowa lidar project in the prioritized observation project for VIII-th term JARE

EJIRI, Mitsumu K.[1*] ; TSUDA, Takuo[1] ; NISHIYAMA, Takanori[1] ; ABO, Makoto[2] ; TOMIKAWA, Yoshihiro[1] ; SUZUKI, Hidehiko[3] ; KAWAHARA, Takuya[4] ; TSUTSUMI, Masaki[1] ; NAKAMURA, Takuji[1]

[1]National Institute of Polar Research, [2]Graduate School of System Design, Tokyo Metropolitan University, [3]College of Science, Rikkyo university, [4]Faculty of Engineering, Shinshu University

The National Institute of Polar Research (NIPR) is leading a six year prioritized project of the Antarctic research observations since 2010. One of the sub-project is entitled ”the global environmental change revealed through the Antarctic middle and upper atmosphere”. Profiling dynamical parameters such as temperature and wind, as well as minor constituents is the key component of observations in this project, together with a long term observations using existent various instruments in Syowa, Antarctica (69S, 39E). As a part of the sub-project, Rayleigh/Raman lidar was installed at Syowa Station in January, 2011 and has been operated at more than 350 nights (>3000 hours clear sky) by February, 2014. The Rayleigh/Raman lidar observes temperature and clouds in the mesosphere, the stratosphere and part of the troposphere, and providing seasonal and yearly variations of temperature profiles and data of gravity wave characteristics in the middle atmosphere, as well as high altitude clouds of PMC (polar mesospheric clouds) and PSC (polar stratospheric clouds). In order to extend the height coverage to include mesosphere and lower thermosphere region, and also to extend the parameters observed, a new resonance scattering lidar system with tunable wavelengths is developed at NIPR in Tachikawa (36N, 139E). The lidar transmitter is based on injection-seeded, pulsed alexandrite laser for 768-788 nm (fundamental wavelengths) and a second-harmonic generation (SHG) unit for 384-394 nm (second harmonic wavelengths). The laser wavelengths are tuned in to the resonance wavelengths by a wavemeter that is well calibrated using a wavelength-stabilized He-Ne laser. The new lidar has capabilities to measure density variations of minor constituents such as atomic iron (Fe, 386 nm), atomic potassium (K, 770 nm), calcium ion (Ca^+, 393 nm), and aurorally excited nitrogen ion ($N_2{}^+$, 390-391 nm) and temperature profiles in the mesosphere and lower thermosphere (MLT) region using resonance scatter of K. Currently, the fundamental laser pulses are transmitted with 120-160 mJ/pulse at approximately 25 Hz (i.e., $\sim$3-4 W) and the backscattered signal is received with a 35 cm diameter telescope. The new lidar system will be installed two years later at Syowa Station and provide information on the mesosphere and lower thermosphere as well as the ionosphere. This unique observation is expected to make important contribution to studies on the atmospheric vertical coupling process and the neutral and charged particle interaction. In this talk, current status of the research, observations, and system developments, as well as future plans will be presented.

Keywords: Lidar, Antarctic observation, middle and upper atmosphere, Resonance scattering, Rayleigh scattering, Raman scattering

Japan Geoscience Union Meeting 2014
(28 April - 02 May 2014 at Pacifico YOKOHAMA, Kanagawa, Japan)

PEM36-07 Room:312 Time:April 28 10:30-10:45

A daytime observation of polar mesospheric clouds with Syowa Rayleigh Raman lidar system equipped with a new etalon unit

SUZUKI, Hidehiko[1*] ; NAKAMURA, Takuji[2] ; EJIRI, Mitsumu[2] ; ABO, Makoto[3] ; YAMAMOTO, Akihiro[4] ; KAWAHARA, Taku d[4] ; TOMIKAWA, Yoshihiro[2] ; TSUTSUMI, Masaki[2] ; TSUDA, Takuo[2] ; NISHIYAMA, Takanori[2]

[1]Rikkyo University, [2]National Institute of Polar Research, [3]Tokyo Metropolitan University, [4]Shinshu University

A Rayleigh/Raman lidar system has been operated by the Japanese Antarctic Research Expedition (JARE) since February, 2011 (JARE 52nd) in Syowa Station Antarctica (69.0S, 39.5E). Polar Mesospheric Cloud (PMC) was detected by the lidar at 22:30UT (+3hr for LT) on Feb 4th, 2011, the first day of a routine operation. This event is the first time to detect PMC over Syowa Station by a lidar [Suzuki et al., 2013]. However, signal to noise ratio (SNR) of the PMC event was not so good due to a large shot noise from a daytime background signal. Moreover, a receiver system was mainly designed for nighttime observations. Therefore, observation of PMC during the midnight Sun, which also corresponds to PMC most active period, was difficult. Thus, to improve SNR of the PMC observation with Syowa Rayleigh/Raman lidar during daytime, a narrow bandpass Fabry-Perot etalon system has been developed and installed in the receiver system on Dec 2013 by JARE 55th. In this paper, Prompt report of a PMC observation with Syowa Rayleigh Raman lidar system equipped with the new etalon unit is presented.

Keywords: polar mesospheric cloud, noctilucent cloud, lidar, Antarctic

Japan Geoscience Union Meeting 2014
(28 April - 02 May 2014 at Pacifico YOKOHAMA, Kanagawa, Japan)

PEM36-08 Room:312 Time:April 28 11:00-11:15

Study on generation and sustaining mechanism for an SSL during a night of high auroral activity above Tromsoe

TAKAHASHI, Toru[1*] ; NOZAWA, Satonori[1] ; TSUDA, Takuo[2] ; OYAMA, Shin-ichiro[1] ; FUJIWARA, Hitoshi[3] ; TSUTSUMI, Masaki[2] ; KAWAHARA, Takuya[4] ; SAITO, Norihito[5] ; WADA, Satoshi[5] ; KAWABATA, Tetsuya[1] ; MATUURA, Nobuo[1] ; HALL, Chris[6]

[1]STEL, Nagoya Univ., [2]NIPR, [3]Faculty of Science and Technology, Seikei Univ., [4]Faculty of Engineering, Shinshu Univ., [5]RIKEN, [6]Univ. of Tromso

We will report observational results about an SSL (Sporadic Sodium Layer) that appeared on 22 January 2012 above Tromso, Norway (69.6deg N, 19.2deg E). An SSL is sudden formation (more precisely, from observer's viewpoint) of a dense thin sodium layer superposed on a normal sodium layer. Characteristic of an SSL is suitable for investigating, in particular, fine structures in the atmosphere such as small scale waves and turbulences. For example, Tsuda et al., GRL, 2011GL048685 [2011] found out a short-period wavelike structure on an SSL with sodium lidar operated Tromso, Norway.

Some generation mechanisms for SSLs have been proposed and discussed. A high correlation between an SSL and a sporadic E (Es) layer occurrences has been reported, and several authors proposed mechanisms how SSLs are generated by association of the Es layers [e.g., von Zahn and Hansen, JATP, 50, 93-104, 1988]. Kirkwood and von Zahn, JAP, 53, 389-407 [1991] have suggested that a strong electric field that generates an Es layer plays an important role for generation of an SSL as well in the auroral region. Recently, Matuura et al. JGR, 118, 1-12, jgra.50414 [2013] have proposed another mechanism that an electric current loop plays an important role for the convergence of positive ions including metallic ions.

Altitudinal temperature gradients have been also discussed as a candidate for an SSL generation. Clemesha et al., JASTP, j.jastp.2010.03.017 [2010] showed that an SSL tended to be located in the region where the temperature gradient is negative. A sodium lidar measurement exhibited a 40 K temperature increase on the topside of the SSL [Gardner et al., JGR, 98, 16,865-16,873, 1993].

We like to point out two concerns to be improved for the previous studies. First, although an SSL is complex phenomenon resulting from the confluence of various mechanisms, most studies focused on one mechanism alone. Second is a temporal resolution to calculate the neural temperature and sodium density. Since the sodium density inside an SSL varies largely and quickly in an order of seconds, data with insufficient resolution mislead our understanding. The temporal resolutions of five minutes used in previous studies are insufficient. In this study, we have derived neutral temperature and sodium density with a 15 second. Furthermore, we have used data obtained with the EISCAT UHF radar, meteor radar and photometer together with the sodium LIDAR at Tromso.

On 22 January 2012, an SSL was observed by the sodium lidar at about 94 km about 19 minutes after hard auroral precipitations. From 2118 UT to 2142 UT, the sodium density inside the SSL was from 2 and 6 times greater than the background sodium density. After 2142 UT the peak of the SSL went up to 96 km and the SSL became thinner than it was. The peak sodium density decreased, but it was still a few times higher than the background sodium density from 2142 UT to 2400 UT. We have calculated the temperature with a 15 second resolution, and have found that there are no remarkable enhancements in temperature profiles inside the SSL from 2118 to 2142 UT. It would be worth to point out that from 2200 to 2400 UT the SSL stayed in the local temperature minimum of the background atmosphere. Gardner et al. JGR. 2004JD005670 [2005] argued that the sodium density has a negative correlation with temperature at topside of the sodium layer. Therefore, our result is likely to indicate that the temperature profile contributes sustention of the SSL in this event. To investigate other candidate mechanisms for the SSL generation, we have analyzed the EISCAT radar data. The EISCAT radar detected an Es layer simultaneously with the SSL. The Es layer was located on about 94 km altitude where the SSL was located from 2118 UT to 2200 UT. However, after 2200 UT the Es layer was located on 2 km below the SSL. This result is likely to indicate that the Es layer contributes the SSL generation.

Keywords: Sporadic sodium layer, sodium lidar, aurora, EISCAT radar, meteor radar

Japan Geoscience Union Meeting 2014
(28 April - 02 May 2014 at Pacifico YOKOHAMA, Kanagawa, Japan)

PEM36-09 Room:312 Time:April 28 11:15-11:30

Seasonal variation of Polar Mesosphere Winter Echo (PMWE) observed by PANSY radar

NISHIYAMA, Takanori[1*] ; SATO, Kaoru[2] ; TSUTSUMI, Masaki[1] ; SATO, Toru[3] ; NAKAMURA, Takuji[1] ; NISHIMURA, Koji[1] ; KOHMA, Masashi[2] ; TOMIKAWA, Yoshihiro[1] ; EJIRI, Mitsumu[1] ; TSUDA, Takuo[1]

[1]National Institute of Polar Research, [2]Department of Earth and Planet Science, Graduate School of Science, The University of Tokyo, [3]Graduate School of Informatics, Kyoto University

In the lower thermosphere at the altitude of around 100 km, both neutral turbulence and ionization of atmosphere due to solar radiations cause irregularities of reflective index, and as a result back scatter echoes from that altitude are frequently observed by radars on the ground. In the mesosphere, Polar Mesosphere Summer Echo (PMSE) is reported to be a strong echo associated with ice particles, which are produced around the coldest mesopause region in the polar summer, by a number of past radar observations [*Cho and Rottger*, 1997; *Rapp and Lūbken*, 2004]. It should be also noted that occurrence rate of PMSE is very high (80-90%) [*Bremer et al*., 2003]. On the other hand, Polar Mesosphere Winter Echo (PMWE) is also known as back scatter echo from 55 to 85 km in the mesosphere, and it has been observed by MST and IS radar in polar region during winter [e.g., *Ecklund and Balsley*, 1981; *Czechowsky et al*., 1989; *Lūbken et al*., 2006; *Strelnikova and Rapp*, 2013]. Due to the lack of of free electrons and ice particles in the dark and warm mesosphere during winter, it is suggested that PMWE requires strong ionization of neutral atmosphere associated with precipitations of Solar Energetic Particles (SEPs) during geomagnetically disturbed periods [*Kirkwood et al*., 2002; *Zeller et al*., 2006]. However, the detailed generation process of PMWE has not been identified yet, partly because the reported PMWE occurrence rate was quite low (2.9%) [*Zeller et al*., 2006].

In the Ⅷ-th six-year project of the Japanese Antarctic Research Expedition (JARE) from 2010, the middle and upper atmosphere research is one of the sub-projects of the prioritized research project entitled 'Global warming revealed from the Antarctic', and comprehensive ground based observations with various remote sensing instruments for the middle and upper atmosphere have been operating continuously in Syowa station. We analyzed data obtained by PANSY (Program of the Antarctic Syowa MST/IS) radar, which is the core instrument of the project, focusing on PMWE in the context of neutral-plasma atmospheric coupling process between the middle and upper atmosphere. PANSY radar is a 47 MHz VHF radar with 125 kW (full system 500 kW) output power, and it is the largest MST radar composed 5,000 m^2 (full system 20,000 m^2) antenna array in Antarctica at the moment. PANSY has already identified a number of PMWE near local noon since operation of mesosphere observation mode was started in June 2012.

We would like to show seasonal variations of occurrence characteristics of PMWE between June 2012 and July 2013. Taking full advantage of PANSY radar's detectability, we calculated monthly-averaged height-time section of backscatter echo power in austral winter between 2012 and 2013. The result demonstrated that durations of PMWE strongly depended on hours of sunlight, although occurrence heights of PMWE, which range from 60 to 80 km, were fixed on every month and year. These statistical characteristics of PMWE were consistent with previous studies suggesting ionization at the PMWE height due to solar radiation play a dominant role in generation of PMWE [*Zeller et al*., 2006; *Lūbken et al*., 2006]. However, the mean occurrence rate of PMWE estimated by our study was 20-30%, which was considerably higher than that of previous studies. It implies that atmospheric turbulence in the mesosphere would be driven by breakings of atmospheric gravity waves more frequently than past observations, especially in Antarctica, and the role of atmospheric gravity waves cannot be ignored when considering the long-termed climate changes.

Keywords: Polar Mesosphere Winter Echo, PANSY radar, Atmospheric gravity wave, Neutral-plasma interaction

Japan Geoscience Union Meeting 2014
(28 April - 02 May 2014 at Pacifico YOKOHAMA, Kanagawa, Japan)

PEM36-10 Room:312 Time:April 28 11:30-11:45

Analysis of atmospheric gravity waves observed by airglow imaging at Syowa Station (69S,39E), Antarctica

MATSUDA, Takashi S.[1*] ; NAKAMURA, Takuji[2] ; EJIRI, Mitsumu K.[2] ; TSUTSUMI, Masaki[2] ; SHIOKAWA, Kazuo[3] ; TAGUCHI, Makoto[4] ; SUZUKI, Hidehiko[4]

[1]Graduate University for Advanced Studies, [2]National Institute of Polar Research, [3]Solar-Terrestrial Environment Laboratory, Nagoya University, [4]Rikkyo University

Atmospheric gravity waves (AGWs), which are generated in the lower atmosphere, transport significant amount of energy and momentum into the mesosphere and lower thermosphere and cause the mean wind accelerations in the mesosphere. This momentum deposit drives the general circulation and affects the temperature structure. Among many parameters to characterize AGWs, horizontal phase velocity is very important to discuss the vertical propagation. Airglow imaging is a useful technique for investigating the horizontal structures of AGWs at around 90 km altitude. Recently, there are many reports about statistical characteristics of AGWs observed by airglow imaging. However, it is difficult to compare these results obtained at various locations because each research group uses its own method for extracting and analyzing AGW events. In order to deal with huge amounts of imaging data obtained on different years and at various observation sites, without bias caused by different event extraction criteria for the observer, we have developed a new statistical analysis method for obtaining the power spectrum in the horizontal phase velocity domain from airglow image data. This method was applied to the data obtained at Syowa Station, Antarctica, in 2011 and compared with a conventional event analysis in which the phase fronts were traced manually in order to estimate horizontal characteristics. This comparison shows that our new method is suitable for deriving the horizontal phase velocity characteristics of AGWs observed by airglow imaging technique.

We plan to apply this method to airglow imaging data observed at Syowa Station in 2002 and between 2008 and 2013, and also to the data observed at other stations in Antarctica (e.g. Rothera Station (67S, 68W) and Halley Station (75S, 26W)), in order to investigate the behavior of AGWs propagation direction and source distribution in the MLT region over Antarctica. In this presentation, we will report interim analysis result of the data at Syowa Station.

Keywords: atmospheric gravity wave, airglow imaging

Japan Geoscience Union Meeting 2014
(28 April - 02 May 2014 at Pacifico YOKOHAMA, Kanagawa, Japan)

PEM36-11 Room:312 Time:April 28 11:45-12:00

First detection of daytime tweek atmospherics observed at Moshiri and Kagoshima, Japan

OHYA, Hiroyo[1*] ; SHIOKAWA, Kazuo[2] ; MIYOSHI, Yoshizumi[2]

[1]Graduate School of Engineering, Chiba University, [2]Solar-Terrestrial Environment Laboratory, Nagoya University

It is well known that tweek atmospherics can be observed only at night except for solar eclipse days, because daytime attenuation rate of the tweeks is much larger (˜70 dB/1000 km) than that in nighttime (˜3 dB/1000 km). In this presentation, we firstly report detection of daytime tweeks at Moshiri (Geographic coordinate: 44.37^{o}N, 142.27^{o}E) and Kagoshima (31.48^{o}N, 130.72^{o}E), Japan, on non-solar eclipse days in December, 1980. The daytime tweeks were observed both before and during a large magnetic storm during 16-20 December, 1980. The minimum Dst value was -240 nT at 04:00 UT on 20 December. The average occurrence numbers of the daytime tweeks at Moshiri and Kagoshima were 2.7 and 0.3 tweeks per minute, respectively. The local times (LT) when the daytime tweeks occurred were through 07:00 - 17:00 LT at Moshiri, while they were 07:00 - 09:00 LT and 15:00 - 17:00 LT at Kagoshima. All the daytime tweeks show clear frequency dispersion. The average duration was 18.94 ms, while that of nighttime tweeks is ˜50 ms. The average reflection heights of daytime tweeks at Moshiri and Kagoshima were 86.2 km and 94.7 km, respectively. The average reflection heights of nighttime tweeks at Moshiri and Kagoshima in same period were 87.1 km and 92.1 km, respectively. The variation of the daytime tweek reflection height was higher than that of nighttime tweeks. The horizontal propagation distance in daytime cannot be estimated from the dispersion, because the duration was too short to estimate the distance.

We found through a theoretical consideration that the VLF/ELF attenuation on the D-region ionosphere depends not only on the ionospheric height, but also the sharpness of electron density profiles, β. The β is a conventional parameter proposed by Wait and Spies [1964]. When the β increases, the attenuation decreases. Even daytime, when the β is occasionally large, the attenuation would become less down to be able to observe the tweeks. In this talk, we will show the results of the daytime tweeks and discuss their occurrence mechanism.

Japan Geoscience Union Meeting 2014
(28 April - 02 May 2014 at Pacifico YOKOHAMA, Kanagawa, Japan)

PEM36-12 Room:312 Time:April 28 12:00-12:15

Long term variation of geomagnetic Sq field over 100 years

TAKEDA, Masahiko[1*]

[1]Data Analysis Center for Geomag. and Space Magnetism, Kyoto Univ

The long-term variation of the geomagnetic Sq field over 100 years at several observatories was studied in the Y-component as well as the ionospheric conductivity estimated by the IRI model. The amplitude of the geomagnetic Y-component (Sq(Y)) depended strongly on solar activity, and showed features similar to those in the solar activity even when 11-years running averages were employed. The solar activity dependence of Sq(Y) can be fully explained by that of the ionospheric electrical conductivity, and wind velocity tends to be large for low solar activity; and slower in the middle of the 1900s in response to higher long-term solar activity. On the other hand, other long-term variations were not clear in the wind velocity. Although the dynamo theory predicts that the Sq current is enhanced when geomagnetic main field intensity decreases, the result of the present analysis does not necessarily support this prediction.

Keywords: geomagnetic daily variation, long-term variation, solar activity, main field strength, elecric conductivity, wind velocity

Japan Geoscience Union Meeting 2014
(28 April - 02 May 2014 at Pacifico YOKOHAMA, Kanagawa, Japan)

PEM36-13 Room:312 Time:April 28 12:15-12:30

Long-term variation in the upper atmosphere as seen in the geomagnetic solar quiet (Sq) daily variation

SHINBORI, Atsuki[1*] ; KOYAMA, Yukinobu[2] ; NOSE, Masahito[2] ; HORI, Tomoaki[3] ; OTSUKA, Yuichi[4] ; YATAGAI, Akiyo[4]

[1]Research Institute for Sustainable Humanosphere (RISH), Kyoto University, [2]Data Analysis Center for Geomagnetism and Space Magnetism Graduate School of Science, Kyoto Universi, [3]Nagoya University Solar Terrestrial Environment Laboratory Geospace Research Center, [4]Solar-Terrestrial Environment Laboratory, Nagoya University

It has been well-known that the geomagnetic field on the ground shows a regular variation with a fundamental period of 24 hours during a solar quiet day. This daily variation depends on local time, latitude, season and solar cycle and has been called solar quiet (Sq) geomagnetic field daily variation. The Sq variation is mainly produced by magnetic effects due to ionospheric currents flowing in the E region of the ionosphere around 105 km. The global pattern of the Sq variation of the H-component shows positive and negative changes in the equatorial and middle-latitude regions around noon, respectively. The Sq current system expected from the geomagnetic field perturbations consists of two large current vortices: one is an anticlockwise current in the northern hemisphere and the other is a clockwise current in the southern hemisphere. The Sq current is dominant in the daytime ionosphere where ionospheric conductivity is relatively large, and is driven by electric fields originating from the ionospheric dynamo via the interaction between ionized and neutral particles. According to the Ohm's law, the main variables in the Sq amplitude are the ionospheric conductivity, the polarization electric field, the solar diurnal tide, and the intensity of the ambient magnetic field at the E-region height. Then, to investigate the long-term variation in the Sq amplitude is important for understanding the physical mechanism of long-term variation in the upper atmosphere related to solar activity and lower atmospheric change such as global warming. In this study, we investigated long-term variation in the Sq amplitude using 1-hour geomagnetic field data obtained from 184 geomagnetic observation stations within a period of 1947-2012 in order to clarify the physical mechanism of long-term variation in the upper atmosphere. For the analysis of long-term observation data obtained from a lot of geomagnetic stations, we took advantage of the IUGONET data analysis system (metadata database search system and data analysis software). The Sq amplitude is defined as a difference of the H-component of geomagnetic field between the maximum and minimum values each solar quiet day. We identified the solar quiet day as the day when the maximum Kp value is less than 4 for each day. As a result, the Sq amplitude observed at all the geomagnetic stations showed a clear dependence on the 11-year solar activity and it tended to be enhanced significantly during solar maximum. The Sq amplitude became the smallest around the minimum of 23/24 solar cycle in 2008-2009. The relationship between the Sq amplitude and F10.7 solar activity index was not linear but nonlinear. This nonlinearity could be interpreted as the decrease of production rate of electrons and ions in the ionosphere for the strong extreme ultraviolet (EUV) and ultraviolet (UV) fluxes. In order to minimize an effect of solar activity including the long-term variation in the Sq amplitude, we calculated second orders of fitting curve between the F10.7 solar index and Sq amplitude during 1947-2012, and examined the residual Sq amplitude defined as the deviation from the fitting curve. As a result, majority of the residual Sq trends passed through the trend test showed a negative value without dependence on geographical latitude and longitude. The tendency was strong in India, the southern part of Africa, and the northern part of America and Europe. In a region of northern part of America and Europe, the secular variation of magnetic inclination becomes relatively large, compared with other regions. Therefore, the long-term trend in the residual Sq amplitude could be linked to a change in the ionospheric conductivities associated with the secular variation of the ambient magnetic field and the upper atmosphere and electro motive force (UxB) via the interaction between ionized and neutral particles.

Keywords: Geomagnetic solar quiet daily variation, Solar activity, Long-term variation, Geomagnetic secular variation, Ionospheric conductivity, Global warming

Japan Geoscience Union Meeting 2014
(28 April - 02 May 2014 at Pacifico YOKOHAMA, Kanagawa, Japan)

PEM36-14 Room:312 Time:April 28 12:30-12:45

Temporal increases of horizontal speed of frontal Es observed by HFD

TOMIZAWA, Ichiro[1*] ; MIYAWAKI, Masami[1]

[1]Center for Space Science and Radio Engineering, The University of Electro-Commnunications

In the yearly analysis of the horizontal speed of frontal Es by using the HFD observation data of the year 2012, we found some events which showed temporal increase and then decrease within the time scale from 40 to 270 minutes. The rate of the temporal speed enhancements were only 2.4 % in all frontal Es events in 2012, and the enhances were mainly observed aroun 21h JST in summer. The rate of the speed enhancement were less than 30 %, but some peak speeds increased up to more than 200 m/s. The duration times varied from 40 to 300 min, but most of the events terminated within 150 min. The average leading and trailing times were 35 and 50 min, respectively, so the trailing part took long time. The cause of temporal speed variation can be related to time variation of horizontal electric field or of horizontal wind speed of neutral atmosphere in the E layer. The former should show coincidence over the wide area but the latter would show some time difference. Analyzing pair data over 100 km separation, we obtained time delay less than 20 min. It is therefore interpreted that the temporal speed increase is caused by the change of the horizontal wind speed. Because the distance between successive Es front shows the minimum of less than 50 km around the speed peak, and increases upto 200 km both to the start and to the end, it can be attributed to the inequally spaced Es front. Combining all separation distances for each event, we get the outer size of the temporal variation as 400 km for 65 %, and as the maximum of 1400 km. On the otherhand, it can be related to a non-isotropic structure because the peak speed did show different values for the separate stations. Based on those observational results, it is concluded that the temporal speed increase may be introdued by a spiral-like, instead of linear, structure.

Keywords: frontal Es, horizontal speed, temporal increase, HF Doppler observation

Japan Geoscience Union Meeting 2014
(28 April - 02 May 2014 at Pacifico YOKOHAMA, Kanagawa, Japan)

PEM36-15 Room:312 Time:April 28 14:15-14:30

Study of medium-scale traveling ionospheric disturbances (MSTID) with sounding rockets and ground observations

YAMAMOTO, Mamoru[1*] ; KATO, Tomohiro[1] ; ISHISAKA, Keigo[2] ; YOKOYAMA, Tatsuhiro[3] ; IWAGAMI, Naomoto[3] ; TAKAHASHI, Takao[5] ; TANAKA, Makoto[5] ; ENDO, Ken[6] ; KUMAMOTO, Atsushi[6] ; WATANABE, Shigeto[7] ; YAMAMOTO, Masa-yuki[8] ; ABE, Takumi[9] ; SAITO, Susumu[10] ; TSUGAWA, Takuya[3] ; NISHIOKA, Michi[3] ; BERNHARDT, Paul[11] ; LARSEN, Miguel[12]

[1]RISH, Kyoto University, [2]Toyama Prefectural University, [3]NICT, [4]School of Science, University of Tokyo, [5]ICT Education Center, Tokai University, [6]School of Science, Tohoku University, [7]School of Science, Hokkaido University, [8]Kochi University of Technology, [9]JAXA/ISAS, [10]ENRI, [11]NRL, [12]Clemson University

Medium-scale traveling ionospheric disturbance (MSTID) is an interesting phenomenon in the F-region. The MSTID is frequent in summer nighttime over Japan, showing wave structures with wavelengths of 100-200 km, periodicity of about 1 hour, and propagation toward the southwest. The phenomena are observed by the total electron content (TEC) from GEONET, Japanese dense network of GPS receivers, and 630 nm airglow imagers as horizontal pattern. It was also measured as Spread-F events of ionograms or as field-aligned echoes of the MU radar. MSTID was, in the past, explained by Perkins instability (Perkins, 1973) while its low growth rate was a problem. Recently 3D simulation study by Yokoyama et al (2009) hypothesized a generation mechanism of the MSTID, which stands on electromagnetic E/F-region coupling of the ionosphere. The hypothesis is that the MSTID first grows with polarization electric fields from sporadic-E, then show spatial structures resembling to the Perkins instability. We recently conducted a observation campaign to check this hypothesis. We launched JASA ISAS sounding rockets S-310-42 and S-520-27 at 23:00 JST and 23:57JST on July 20, 2013 while an MSTID event was monitored in real-time by the GPS-TEC from GEONET. We found 1-5mV/m northeastward/eastward electric fields during the flight. Variation of electric fileds were associated with horizontal distribution of plasma density. Wind velocity was measured by the TME and Lithium releases from S-310-42 and S-520-27 rockets, respectively, showing southward wind near the sporadic-E layer heights. These results are consistent to the expected generation mechanism shown above. In the presentation we will discuss electric-field results and its relationship with plasma density variability together with preliminary results from the neutral-wind observations.

Keywords: MSTID, Sounding rocket, Electric field, GPS-TEC, Observation campaign

Japan Geoscience Union Meeting 2014
(28 April - 02 May 2014 at Pacifico YOKOHAMA, Kanagawa, Japan)

PEM36-16 Room:312 Time:April 28 14:30-14:45

Characteristics of O630nm emission associated with equatorial ionization anomaly obtained with IMAP/VISI

SAKAMOTO, Daiki[1] ; SAKANOI, Takeshi[1*] ; PERWITASARI, Septi[1] ; OTSUKA, Yuichi[2] ; SAITO, Akinori[3] ; AKIYA, Yusuke[3] ; HOZUMI, Yuta[3] ; YAMAZAKI, Atsushi[4]

[1]Grad. School of Science, Tohoku University, [2]STEL, Nagoya University, [3]Grad. School of Science, Kyoto University, [4]ISAS / JAXA

The Equatorial Ionization Anomaly (EIA) is occurred by plasma upwelling due to eastward electric field in the dayside magnetic equator, and descends to both northern and southern hemispheres along the field line. Density maximum appears around geomagnetic latitudes of +/-15 degree at both hemispheres. Since most of the past studies carried out with ground experiments, it is difficult to observe a wide area and study the variability of the northern and southern O630nm emission associated with EIA.

IMAP/VISI on the International Space Station(ISS) measures O630 nm airglow emission in the nightside hemisphere at an altitude of 400km. It covers the latitudinal range between +/-52 degrees with a typical spatial resolution of 1x14 km. Because of the wide observation coverage, it is possible to observe the variability of O630nm airglow associated with the EIA.

In this study, we carried out a statistical analysis using IMAP/VISI data from September 2012 to December 2013 to understand the variability of O630nm airglow associated with the EIA, particularly on its local time dependence, seasonal variation and geomagnetic activity. We derived the integrated intensity of O630nm emission along latitude with the four criteria as follows: (1) The O630nm emission in the EIA is greater than the background airglow that was determined by emission intensity in the middle latitude. (2) Latitudinal distribution of O630nm emission in the EIA is fully measured. (3) The northern and southern O630nm emission in the EIA is clearly separated. (4) The moon phase is smaller than 0.5. In case that the moon phase is bigger than 0.5 then we used the data when the moon did not appear.

We find that the time dependence of O630nm emission which is decreased from the evening toward the post mid-night. But there is a large variance in the intensity at the same local time. This fact suggests that other process, such as the longitude and/or seasonal variation, may affect the O630nm emission associated with the EIA in addition to the local time dependence.

On the seasonal dependence, we find that O630nm emission in the EIA in the winter hemisphere is greater than that in the summer hemisphere. This is consistent with the model that the thermospheric tidal wind affects the 630 nm intensity, namely, the tidal wind decreases the altitude of O630 nm emission layer and finally gain the O630 nm intensity.

To examine the longitudinal dependence, we used the data in equinox (September and October, 2013) and find that O630nm emission in the EIA in the northern hemisphere is greater than that in the southern hemisphere where the dip equator is the south of geographic equator (longitude is between 200 degree ? 310 degree). This is also consistent with the model that the thermospheric tidal wind controls the O630 nm intensity by making a vertical motion of emission layer.

Finally, we investigate the magnetic storm dependence on O630 nm intensity and find that significant decrease of O630nm intensity in the EIA happens during the period when the Dst index is larger than 90. From this fact, it is plausible that westward electric field in Region 2 current system penetrates to the low latitude region during the main phase of magnetic storm and reduce the formation of EIA.

Keywords: ISS, airglow, thermosphere, ionosphere, equatorial ionization anomarly, IMAP

Japan Geoscience Union Meeting 2014
(28 April - 02 May 2014 at Pacifico YOKOHAMA, Kanagawa, Japan)

PEM36-17 Room:312 Time:April 28 14:45-15:00

Analysis of the airglow structures using the simultaneous observations by ISS-IMAP and all-sky imagers

YUKINO, Hideko[1*] ; SAITO, Akinori[1] ; OTSUKA, Yuichi[2] ; SAKANOI, Takeshi[3]

[1]Dept. of Geophysics, Kyoto Univ., [2]STEL, Nagoya Univ., [3]Grad. School of Science, Tohoku Univ.

The spatial structure of the atmospheric gravity waves in the mesosphere was analyzed using the simultaneous observational data of ISS-IMAP and the all-sky imager at Hawaii. There are a plenty of ground-based observations of the atmospheric gravity waves in the mesosphere and the thermosphere. The problem of the ground-based observation is that it cannot distinguish spatial variations from temporal variations for the structures whose scale size is larger than its field-of-view. ISS-IMAP was launched on July 21, 2012 to observe the atmospheric gravity waves whose scale size is larger than 100 km. The altitude of the International Space Station (ISS) flies around 400 km altitude, and its orbital inclination angle is 51.6 degrees. ISS-IMAP/VISI (Visible-light and infrared Spectrum Imager) observes the airglow in the mesosphere and the ionosphere. The spatial resolution of the VISI imaging observation is from 10 km to 25 km. The airglow wavelengths observed by VISI are 630 nm, 730 nm, and 762 nm and by the ground-based all-sky image of Hawaii (20.48 N, 156.2 W) are 630 nm and 557.7-nm with 5.5 minutes interval. The observational data of ISS-IMAP/VISI and an all-sky imager in Hawaii were investigated for the nights when VISI made the observation over Hawaii, and the sky over the imager was clear. The night when the plasma bubble was detected by the ground-based all-sky imager, the plasma bubble was detected by the 630nm airglow observation of ISS-IMAP/VISI. The spatial and vertical structures of the airglow that were observed by the ground-based imager and the ISS-IMAP/VISI were analyzed. The sensitivity of the observation of ISS-IMAP/VISI will also be discussed in the comparison of the ground-based observation.

Keywords: airglow, plasma bubble, ISS-IMAP

Japan Geoscience Union Meeting 2014
(28 April - 02 May 2014 at Pacifico YOKOHAMA, Kanagawa, Japan)

PEM36-18 Room:312 Time:April 28 15:00-15:15

Horizontal structures of ionized Helium in the topside ionosphere of dusk side observed by ISS-IMAP/EUVI

HOZUMI, Yuta[1*] ; SAITO, Akinori[1] ; YAMAZAKI, Atsushi[2] ; MURAKAMI, Go[2] ; YOSHIKAWA, Ichiro[3]

[1]Department of Geophysics, Graduate School of Science, Kyoto University, [2]Institute of Space and Astronautical Science / Japan Aerospace Exploration Agency, [3]The University of Tokyo

Horizontal structures of ionized Helium in the topside ionosphere of dusk side were obtained with the Extreme Ultra Violet Imager (EUVI) of the ISS-IMAP (Ionosphere, Mesosphere, upper Atmosphere and Plasmasphere mapping) mission. EUVI has taken image of He He II radiation (30.4 nm) from the International Space Station (ISS) since October 2012. In this work, images taken in 2013 were analyzed. North-south asymmetry and longitudinal structure of ionized Helium were found. Seasonal dependence of these horizontal structures will be discussed.

Keywords: Topside ionosphere, ISS-IMAP, Ionoized Helium

Japan Geoscience Union Meeting 2014
(28 April - 02 May 2014 at Pacifico YOKOHAMA, Kanagawa, Japan)

PEM36-19 Room:312 Time:April 28 15:15-15:30

Study of ionospheric disturbance characteristics during solar flare events using the SuperDARN Hokkaido radar

WATANABE, Daiki[1] ; NISHITANI, Nozomu[1*]

[1]Solar-Terrestrial Environment Laboratory, Nagoya University

Ionospheric disturbances during solar flare events have been studied by various kinds of observation instrument in the last few decades. Kikuchi et al. (1985) reported on the positive Doppler shift in the HF Doppler system data during solar flare events, and indicated that there are two possible factors of Doppler shift, i.e., (1) apparent ray path decrease by changing refraction index due to increasing electron densities in the D-region ionosphere, and (2) ray path decrease due to descending reflection point associated with increasing electron density in the F-region ionosphere.

In this study, we use the SuperDARN Hokkaido Radar to investigate the detailed characteristics of solar flare effects on ionospheric disturbances. We focus on the positive Doppler shift of ground / sea scatter echoes just before sudden fade-out of echoes. Davies et al. (1962) showed that if the factor (1) is dominant, the Doppler shift should have positive correlation with slant range and negative correlation with elevation angle and frequency. On the other hand, if the factor (2) is dominant, the Doppler shift should have negative correlation with slant range and positive correlation with elevation angle and frequency. While Kikuchi et al. (1985) studied solar flare events and mainly discussed frequency dependence of Doppler shift, we study mainly slant range and elevation angle dependence, for the first time to the best of our knowledge. We found that the factor (1), in other words, increase of electron densities at D-region ionosphere, is dominant during solar flare events. This result is consistent with that of Kikuchi et al. (1985). In order to study characteristics of ionospheric disturbance in more detail, we are studying relationship between timing / amplitude of ionospheric disturbance and that of the solar irradiation changes, by comparing the HF radar data with high wavelength resolution irradiation data for X-ray and EUV from RHESSI and SDO satellites. Generally, X-ray radiation becomes more important for the changes in the D-region during solar flare events. Therefore we investigate relationship between X-ray flux changes and electron density variation in the D-region ionosphere intensively. Furthermore, we estimated electron density changes in the ionsosphere by analyzing elevation angle dependence of Doppler shift in radar echoes quantitatively. We are estimating electron density by considering chemical reaction and photoreaction caused by solar radiation. We will compare the two electron density changes deduced from different two ways and evaluate the amplitude of ionospheric disturbance observed by the HF radar. More detailed analysis result will be reported.

Keywords: SuperDARN, Hokkaido radar, solar flares, ionospheric disturbances, photochemical reaction, range dependence

Japan Geoscience Union Meeting 2014
(28 April - 02 May 2014 at Pacifico YOKOHAMA, Kanagawa, Japan)

PEM36-20 Room:312 Time:April 28 15:30-15:45

Thermospheric tidal effects on the ionospheric midlatitude summer nighttime anomaly

CHEN, Chia-hung[1*] ; LIN, Charles[1] ; CHANG, Loren[2] ; HUBA, J. D.[3] ; SAITO, Akinori[4] ; LIU, Jann-yenq[2]

[1]Department of Earth Science, National Cheng Kung University, Tainan, Taiwan, [2]Institute of Space Science, National Central University, Chung-Li, Taiwan, [3]Plasma Physics Division, Naval Research Laboratory, Washington, D. C., USA, [4]Department of Geophysics, Kyoto University, Kyoto, Japan

This study use a 3D physics-based ionospheric model, SAMI3, coupled with the National Center for Atmospheric Research Thermosphere Ionosphere Electrodynamics General Circulation Model (TIEGCM) and Global Scale Wave Model (GSWM) to simulate the mesospheric and lower thermosphreic tidal effects on the development of midlatitude summer nighttime anomaly (MSNA). Using this coupled model, the diurnal variation of MSNA electron densities at 300 km altitude is simulated on both June solstice (day of year (DOY) 167) and December solstice (DOY 350) in 2007. Simulation results show successful reproduction of the southern hemisphere MSNA structure including the eastward drift feature of the southern MSNA, which is not reproduced by the default SAMI3 runs using the neutral winds provided by the empirical Horizontal Wind Model 93 (HWM93) neutral wind model. A linear least squares algorithm for extracting tidal components is utilized to examine the major tidal component affecting the variation of southern MSNA. Results show that the standing diurnal oscillation component dominates the vertical neutral wind manifesting as a diurnal eastward wave-1 drift of the southern MSNA in the local time frame. We also find that the stationary planetary wave-1 component of vertical neutral wind can cause diurnal variation of the summer nighttime electron density enhancement around the midlatitude ionosphere.

Keywords: Midlatitude Summer Nighttime Anomaly, thermospheric tidal effect

Japan Geoscience Union Meeting 2014
(28 April - 02 May 2014 at Pacifico YOKOHAMA, Kanagawa, Japan)

PEM36-21 Room:312 Time:April 28 15:45-16:00

Horizontal ion drag effect on the thermospheric mass density anomaly in the cusp

MATSUMURA, Mitsuru[1*] ; TAGUCHI, Satoshi[2]

[1]Center for Space Science and Radio Engineering, University of Electro-Communications, [2]Graduate School of Informatics and Engineering, University of Electro-Communications

CHAMP satellite observations have revealed that the thermospheric mass density in the cusp region is statistically larger by a factor of about 1.3 than that in its adjacent region. Many studies have pointed out that the upward mass transport due to heating is important for the generation of the mass density anomaly, but what confines the heating rate to the cusp is controversial. We have paid attention to the effect of the horizontal mass transport. Our reasoning on this point is as follows. Ionospheric convection gives momentum to the neutral air through ion drag, and the ion drag can modify the distribution of the neutral mass density. Our recent results from numerical simulations have indicated that the ion drag enhances the neutral mass density in the cusp that the terminator overlaps. In this paper, we report on the result about more general situations including cases when the terminator is located away from the cusp. Our results show that the mass density anomaly is confined to the cusp by ion drag, irrespective of the location of the terminator. We show detailed relations between the ion drag distribution and the mass density enhancement or depletion.

Keywords: thermosphere, mass density, cusp, CHAMP satellite

Japan Geoscience Union Meeting 2014
(28 April - 02 May 2014 at Pacifico YOKOHAMA, Kanagawa, Japan)

PEM36-22 Room:312 Time:April 28 16:15-16:30

Edge of polar cap patches

HOSOKAWA, Keisuke[1*] ; TAGUCHI, Satoshi[1] ; OGAWA, Yasunobu[2]

[1]University of Electro-Communications, [2]National Institute of Polar Research

A highly sensitive all-sky EMCCD airglow imager (ASI) has been operative in Longyearbyen, Norway (78.1N, 15.5E) since October 2011. One of the primary targets of this optical observation is a polar cap patch which is defined as an island of enhanced plasma density in the F region drifting anti-sunward across the central polar cap. Since the electron density within patches is often increased by a factor of 2?10 above that in the surrounding region, all-sky airglow measurements at 630.0 nm wavelength are capable of visualizing their spatial distribution in 2D fashion.

During a 4-h interval on the night of December 4, 2013, a series of polar cap patches was observed by the ASI in Longyearbyen. By using the high-quality ASI images, we estimated the gradients in the leading/trailing edges of the patches and found that the gradient in the leading edge is 2-3 times steeper than that in the trailing edge. We also identified finger-like undulating structures growing along the trailing edge of the patches. Generation of these fingers is probably governed by a structuring through the gradient-drift instability which is known to occur only along one side of patches.

From these observations, we suggest that such a structuring process can transport and mix the patch plasma across their trailing edges so that the scale size of the edges get extended. This means that the structuring through the plasma instability can strongly influence the large-scale shape of patches. Such a knowledge is of particular importance for better understanding the space weather effects of patches on the trans-ionospheric satellite communications in the polar cap region.

Keywords: Polar cap ionosphere, Airglow, Polar patches, Plasma instability

Japan Geoscience Union Meeting 2014
(28 April - 02 May 2014 at Pacifico YOKOHAMA, Kanagawa, Japan)

PEM36-23 Room:312 Time:April 28 16:30-16:45

Correlation analysis between equatorial electrojet,pre-reversal enhancement and equatorial spread F in Southeast Asia

KUNITAKE, Manabu[1*] ; TSUGAWA, Takuya[1] ; YOKOYAMA, Tatsuhiro[1] ; NISHIOKA, Michi[1] ; YAMAMOTO, Kazunori[1] ; ISHIBASHI, Hiromitsu[1] ; NAGATSUMA, Tsutomu[1] ; MARUYAMA, Takashi[1] ; ISHII, Mamoru[1] ; SHIOKAWA, Kazuo[2]

[1]NICT, [2]STE Lab., Nagoya Univ.

At the equatorial latitudes, the reversal of dayside eastward electric field to westward around sunset is often accompanied by a strengthened eastward electric field. The strengthened eastward electric field is called as the pre-reversal enhancement (PRE). PRE is considered to be the primary process acting on the equatorial spread F (ESF) onsets. Relationships between PRE strength, ESF onsets, and equatorial electrojet (EEJ) strength have been investigated by using ionosonde observation and magnetometer observation. Uemoto et al. (2010) found that PRE strength and ESF onsets are suppressed when pre-sunset integrated EEJ from 2 hours to 1 hour prior to sunset is negative owing to the evening counter electrojet, by statistical analysis of observations in the Southeast Asia low-latitude ionospheric network (SEALION). Their analyzing period is from November 2007 to October 2008. The period is in solar minimum phase.

We use SEALION data from 2007 to 2013. Therefore, our analyzing period covers not only solar minimum phase but also solar maximum phase. Statistical analyses for each year are conducted. Further, detailed case study is conducted. Significant day-to-day variations of EEJ strength, PRE strength, and ESF onsets are picked up from these seven years data. Then, we investigate how and to what extent day-to-day variations of EEJ strength relate to the day-to-day variations of PRE strength and ESF onsets. The magnetometer data in our study were obtained at Phuket (geographic lat. 8.09N, geographic long. 98.32E, dip lat. -0.2) and Kototabang (0.20S, 100.32E, dip lat. -10.1). The ionosonde data in our study were obtained at Chumphon (10.72N, 99.37E, dip lat. 3.0), Chiang Mai (18.76N, 98.93E, dip lat. 12.7), and Kototabang (0.20S, 100.32E, dip lat. -10.1).

Reference

Uemoto J., T. Maruyama, S. Saito, M. Ishii, and R. Yoshimura, Relationships between pre-sunset electrojet strength, pre-reversal enhancement and equatorial spread-F onset, Ann. Geophys., vol. 28, pp. 449-454, 2010.

Acknowledgements

The ionosonde at Chiang Mai is operated under agreements between NICT, Japan and Chiang Mai University (CMU), Thailand. The ionosonde at Chumphon and the magnetometer at Phuket are operated under agreements between NICT and King Mongkut ′ s Institute of Technology Ladkrabang (KMITL), Thailand. The magnetometer at Kototabang has been operated in collaboration among the Solar-Terrestrial Environment Laboratory (STEL), Nagoya University, Japan, the Research Institute for Sustainable Humanosphere (RISH), Kyoto University, Japan, and the National Institute of Aeronautics and Space (LAPAN), Indonesia. The ionosonde at Kototabang has been operated in collaboration among NICT, RISH and LAPAN. We thank Mr. Yamazaki for manual scaling of ionosonde data.

Keywords: electrojet, equatorial spread F, day-to-day variation, SEALION

Japan Geoscience Union Meeting 2014
(28 April - 02 May 2014 at Pacifico YOKOHAMA, Kanagawa, Japan)

PEM36-24 Room:312 Time:April 28 16:45-17:00

Low-latitude ionosphere dynamics as deduced from meridional ionosonde chain: Ionospheric ceiling

MARUYAMA, Takashi[1*] ; UEMOTO, Jyunpei[1] ; ISHII, Mamoru[1] ; TSUGAWA, Takuya[1] ; SUPNITHI, Pornchai[2] ; KOMOLMIS, Tharadol[3]

[1]National Institute of Information and Communications Technology, [2]King Mongkut's Institute of Technology Ladkrabang, [3]Chiang Mai University

Peculiar ionospheric features at low latitudes originate in the earth's magnetic field configuration that has a shape of arch. Near the magnetic equator, the daytime eastward electric field raises the ionosphere to high altitudes where the ion-neutral collision frequency reduces. The ionospheric plasma slips down over off-equatorial latitudes along the arch-shaped magnetic field line by the earth's gravity acceleration and the reduced ion-neutral drag, which is called the fountain effect. As a consequence, the latitudinal distribution of ionospheric critical frequency (foF2) forms two crests at low latitudes and a trough above the magnetic equator, which is well-known equatorial anomaly in foF2 distribution. As for the diurnal variation of the ionosphere above the magnetic equator, foF2 once increases in the morning and decreases before noon along with the development of the equatorial anomaly, which is called noon bite-out. Another feature at the magnetic equator, associated with the fountain effect, is the relatively steady ionospheric peak height (hmF2) around noon, even though the EXB drift is upward throughout the daytime. However, not much attention has been paid to hmF2 except for the time rate of change of it in connection with the vertical plasma drift velocity.

Interest in the equatorial anomaly has been focused mostly on foF2 (or NmF2), and there have been a few studies on hmF2 variations associated with equatorial anomaly development. In this paper, we revisit the equatorial anomaly in terms of height variations. For this purpose, we analyzed scaled ionogram parameters from three stations located along the magnetic meridian that is a primary component of Southeast Asia low-latitude ionospheric network (SEALION); one at the magnetic equator and the others at conjugate off-equatorial latitudes near 10 degrees magnetic latitude.

The daytime hmF2 was investigated for each season during the solar minimum period, 2006-2007 and 2009. The peak height increased for approximately 3 hr after sunrise at all locations, as expected from the daytime upward EXB drift. The apparent upward drift ceased before noon at the magnetic equator, while the layer continued to increase at the off-equatorial latitudes, reaching altitudes higher than the equatorial height around noon. The noon time restricted layer height at the magnetic equator did not depend on the season, while the maximum peak height at the off-equatorial latitudes largely varied with season. The daytime specific limiting height of the equatorial ionosphere was termed ionospheric ceiling. Numerical modeling using the SAMI2 code reproduced the features of the ionospheric ceiling quite well. Dynamic parameters provided by the SAMI2 modeling were investigated and it was shown that the ionospheric ceiling is another aspect of the fountain effect, in which increased diffusion of plasma at higher altitudes has a leading role.

Keywords: equatorial anomaly, fountain effect, ionospheric ceiling, EXB drift, SEALION

Japan Geoscience Union Meeting 2014
(28 April - 02 May 2014 at Pacifico YOKOHAMA, Kanagawa, Japan)

PEM36-25 Room:312 Time:April 28 17:00-17:15

Three-dimensional high-resolution plasma bubble modeling

YOKOYAMA, Tatsuhiro[1*] ; SHINAGAWA, Hiroyuki[1] ; JIN, Hidekatsu[1]

[1]National Institute of Information and Communications Technology

Equatorial plasma bubble (EPB) is a well-known phenomenon in the equatorial ionospheric F region. As it causes severe scintillation in the amplitude and phase of radio signals, it is important to understand and forecast the occurrence of EPB from a space weather point of view. The development of EPB is known as a evolution of the generalized Rayleigh-Taylor instability. Numerical modelings of the instability on the equatorial two-dimensional plane have been conducted since the late 1970's, and the nonlinear evolution of the instability has been clearly presented. Recently, three-dimensional (3D) modelings became popular tools for further understanding of the development of EPB such as 3D structure of EPB, meridional wind effects and gravity wave seeding. One of the biggest advantages of the 3D model is that the off-equatorial E region which is coupled with the equatorial F region can be included in the model. It is known from observations that the conductance of the off-equatorial E region controls the growth rate of the Rayleigh-Taylor instability, that is, sudden decrease of the E-region conductance around the sunset accelerates the evolution of the instability. We have developed a new 3D high-resolution model for EPB, and studied internal structure of EPB and the contribution of the off-equatorial E region. As it is necessary to use high-order numerical schemes to capture sharp plasma density gradient of EPB, we adopted the CIP scheme which can keep the third-order accuracy in time and space. The simulated EPB has asymmetrical density gradients at east and west walls, and the growth rate changes significantly depending on the condition of the off-equatorial E region. In the future, we will integrate the high-resolution model into whole atmosphere-ionosphere coupled model (GAIA) to study the growth of EPB under the realistic background conditions.

Keywords: plasma bubble, equatorial spread F, equatorial ionosphere, numerical simulation

Japan Geoscience Union Meeting 2014
(28 April - 02 May 2014 at Pacifico YOKOHAMA, Kanagawa, Japan)

PEM36-P01 Room:Poster Time:April 28 18:15-19:30

Basic development of a small balloon-mounted telemetry with its operation system

KONO, Hiroki[1*] ; KAKINAMI, Yoshihiro[1] ; YAMAMOTO, Masa-yuki[1]

[1]Kochi Univ. of Tech

1. Introduction

In Japan, the high altitude balloon for scientific observation has been continuously launched by JAXA. The balloon has a possibility to reach 50 km altitude without severe environmental condition for onboard equipments, being operated with lower cost than sounding rockets, however, development of such large-scale scientific observating balloons by university laboratories is still difficult. Being coupled with rapid improvement of tiny semiconductor sensors recently, laboratory-basis balloon experiments using small weather balloons have been becoming easily in these years (e.g. Near Space Ventures, Inc., 2013).

Although the balloon is very small as its diameter of 6 feets, excluding its extra buoyancy and the weight of the balloon itself, it is expected that loading mass capacity of about 2 kg is remained for payloads to send it up to about 35 km. However, operation of such small balloons in Japan is not in general because precise prediction of a landing area of the payload is difficult, thus high-risk situation for balloon releases is still remained. In this study, we aim to achieve practical engineering experiments of weather balloons in Japan in order to operate laboratory level scientific observation within a university. Here we report an approach of developing many devices currently in progress.

2. Equipments development

We have been developing devices onboard a small tethered balloon for the future weather balloon release experiments. That is, one is a small-size and light-weight telemeter system of about 250 g that can be mounted on a commercially available balloon, while another is a ground station device that receives data from the telemeter. A combination of a wireless module, a GPS receiver, a barometer, a temperature and humidity meter, a camera, an accelerometer, an electronic compass, a power monitor sensor is mounted on the telemeter, and the measured values by each sensors can be transmitted in real time to the ground station device. Newly developed software for balloon operation can be run on a PC connected with the ground station device, it is possible to provide the operator the sensor information visualized in real time based on the position coordinates set on the ground station device using the software before the launch.

Real-time mapping of the balloon coordinates can be realized to rewrite a KML file to be input into the Google Earth continuously. In addition, azimuth and elevation of the balloon can be calculated by spherical trigonometry from obtained the GPS position. Providing these angles to a newly developed rotater to be mounted on a camera tripod, it is possible to track a small antenna automatically to the balloon direction continuously.

3. Result of the experiment

A tethered balloon experiment was performed for evaluating the developed telemeter system, however, there occurred unexpected issue in the communication distance. As a result, in the telemeter line, operating limit of the distance between the ground station and the telemeter is significantly shortened to approximately 110 m. It was almost different from our pre-experiment confirmation of a packet loss rate of 0% at 270 m distance in a preliminary experiment on ground.

Therefore, evaluation of the antenna rotator was carried out only at close range, i.e., in severe condition. It is because maximum elevation of the rotator was limited physically at 50 degrees or less, and there exists about 5 to 10 m error in the GPS positioning operated in the single receiver mode.

Nevertheless, it was possible to track the balloon continuously in a stable situation even in the shortened communication distance. In addition, the software and telemeter system worked as expected, the problem was not found in particular.

In this presentation, the data obtained by the tethered balloon experiment and detail of the developed equipments will be shown.

Keywords: Weather balloon, Tethered balloon, Stratosphere, Upper atmosphere, Telemeter, Embedded system

Japan Geoscience Union Meeting 2014
(28 April - 02 May 2014 at Pacifico YOKOHAMA, Kanagawa, Japan)

PEM36-P02 Room:Poster Time:April 28 18:15-19:30

Impacts of stratospheric sudden warming events in the mesosphere and lower thermosphere

WATANABE, Kumiko[1*] ; TANAKA, Takashi[1] ; MIYOSHI, Yasunobu[2]

[1]Department of Earth and Planetary Sciences, Graduate School of Sciences, Kyushu University, [2]Department of Earth and Planetary Sciences, Faculty of Sciences, Kyushu University

Impacts of stratospheric sudden warming (SSW) events on the middle and upper atmosphere have been widely recognized. However, due to an insufficient number of global observations, SSW's effects on the general circulation in the mesosphere and lower thermosphere (MLT) are not well known. In this study, we investigate the short term variation of the temperature, zonal wind and meridional wind in the MLT region during SSW events using a general circulation model that contains the region from the troposphere to the thermosphere. We conducted GCM simulation with meteorological reanalysis data during the period from November 1, 2008 to March 31, 2010. Our results show that the temperature drop occurs in the Southern hemisphere, during SSW events. This means that SSW influences the general circulation in the summer hemisphere. Furthermore, it is found that the temperature in winter polar region in the lower thermosphere increases during SSW events. This is related to upward propagation of the planetary wave excited in the mesosphere.

Keywords: stratospheric sudden warming, mesosphere, lower thermosphere

Japan Geoscience Union Meeting 2014
(28 April - 02 May 2014 at Pacifico YOKOHAMA, Kanagawa, Japan)

PEM36-P03 Room:Poster Time:April 28 18:15-19:30

Vertical profiles of atmospheric temperature between upper troposphere and mesosphere obtained from Rayleigh/Raman lidar

NISHIYAMA, Takanori[1*] ; NAKAMURA, Takuji[1] ; EJIRI, Mitsumu[1] ; ABO, Makoto[2] ; KAWAHARA, Taku d[3] ; TSUDA, Takuo[1] ; SUZUKI, Hidehiko[4] ; TSUTSUMI, Masaki[1] ; TOMIKAWA, Yoshihiro[1]

[1]National Institute of Polar Research, [2]Graduate School of System Design, Tokyo Metropolitan University, [3]Faculty of Engineering, Shinshu University, [4]Faculty of Science, Rikkyo University

Atmospheric gravity waves (AGWs) propagating upward from lower atmospheric sources play a dominant role in transportating and depositing energy and momentum from upper troposphere (UT) to lower mesosphere (LM). Particularly, in polar region, these effects of AGWs are well-known to strongly decelerate the polar night jet and drive large scale meridional circulation from the summer pole towards the winter pole. In addtion, it is suggested that considerations of the realistic propagation property of AGWs may largely improve a significant bias of climate model. Therefore, investigation of the activity of AGWs between UT and LM based on continuous observational studies can be regarded as one of important isuues.

The National Institute of Polar Research (NIPR) is leading a six year prioritized project of the Antarctic research observations since 2010. One of the sub-projects is entitled 'the global environmental change revealed through the Antarctic middle and upper atmosphere'. As a part of the sub-project, a Rayleigh/Raman lidar (RR lidar) was installed at Syowa, Antarctica (69S, 39E) in January, 2011. The operation has been conducted since February 2011 and the RR lidar has kept measuring temperature profiles continuously between approximately 10 and 80 km for almost 3 years.

The RR lidar system in Syowa can obtain photon count data for 4 channels simultaneously, and each data is recorded separately in binnary format. The data from 3 channeles, i.e., Raman (10-30km), Rayleigh-Low (20-65km), Rayleigh-High (30-80km), corresponding to differenet height ranges are used for estimations of temperature profiles from UT to LM. In oreder to estimate height continuous profiles of atmospheric temperature based on the 3 different channeles, we are examing the following analysis methods. (1) The temperature for Rayleigh-High and Rayleigh-Low channels estimated by solving the lidar equation can be assigned to temperature at an initial height for the lidar equation in Rayleigh-Low and Raman channels, respectively. (2) The initial heights for the lidar equation can be determined automatically taking into account time and height dependent shot noises due to background luminosity. (3) The error propagations from the initial height to lower heights are evaluated by assigning artificial temperature offset ranging from -50 to 50 K.

The height continuous temperature profiles between UT and LM obtained from improved analysis methods would allows us to investigate important scientific issues such as temporal and height variabilities of potential energy per unit mass of AGWs and the relationship between occurrence of Polar Stratospheric Clouds and background atmospheric temperature. In this presentation, we will report the detail of the analysis methods and future perspectives including open data base of temperature profiles.

Keywords: Rayleigh/Raman lidar, Atmospheric temperature, Mesosphere, Stratosphere, Atmospheric Gravity Waves, Polar Stratospheric Clouds

Japan Geoscience Union Meeting 2014
(28 April - 02 May 2014 at Pacifico YOKOHAMA, Kanagawa, Japan)

PEM36-P04 Room:Poster Time:April 28 18:15-19:30

Tunable resonance scattering lidar system for Antarctic observation: Current status

TSUDA, Takuo[1*] ; EJIRI, Mitsumu[1] ; NISHIYAMA, Takanori[1] ; ABO, Makoto[2] ; MATSUDA, Takashi[1] ; KAWAHARA, Takuya[3] ; NAKAMURA, Takuji[1]

[1]National Institute of Polar Research, [2]Graduate School of System Design, Tokyo Metropolitan University, [3]Faculty of Engineering, Shinshu University

We are developing a new resonance scattering lidar system to be installed at Syowa Station (69S, 39E) in Antarctica. For the new lidar system, we have employed a tunable alexandrite laser covering the resonance scattering wavelengths of two neutral species, which are atomic potassium (K, 770.11 nm) and atomic iron (Fe, 386.10 nm), and two ion species, which are calcium ion (Ca^+, 393.48 nm) and aurorally excited nitrogen ion ($N_2{}^+$, 390.30 nm, 391.08 nm). Thus the tunable resonance scattering lidar system will provide information on the mesosphere and lower thermosphere as well as the ionosphere. Using the tunable lidar and co-located other instruments, we will conduct a comprehensive ground-based observation of the low, middle, and upper atmosphere above Syowa Station. This unique observation is expected to make important contribution to studies on the atmospheric vertical coupling process and the neutral and charged particle interaction. In this presentation, we report current status of the tunable lidar system in development and test observations at National Institute of Polar Research in Tachikawa, Japan.

Keywords: Resonance scattering lidar, Antarctica, Syowa Station, K layer, Fe layer

Japan Geoscience Union Meeting 2014
(28 April - 02 May 2014 at Pacifico YOKOHAMA, Kanagawa, Japan)

PEM36-P05 Room:Poster Time:April 28 18:15-19:30

Doppler-free spectroscopy experiments for the Antarctic Potassium resonant lidar

KAWAHARA, Takuya[1] ; TSUDA, Takuo[2*] ; NISHIYAMA, Takanori[2] ; EJIRI, Mitsumu[2] ; ABO, Makoto[3] ; NAKAMURA, Takuji[2]

[1]Faculty of Engineering, Shinshu University, [2]National Institute Polar Research, [3]System Design, Tokyo Metropolitan University

The National Institute of Polar Research (NIPR) is leading a six year prioritized project of the Antarctic research observations since 2010. One of the sub-projects is entitled ”the global environmental change revealed through the Antarctic middle and upper atmosphere”. Profiling dynamical parameters such as temperature and wind, as well as minor constituents is the key component of observations in this project, together with long-term observations using existent various instruments in Syowa, the Antarctic (39E, 69S). As one of the instruments in this project, a new resonance scattering lidar system with tunable wavelengths is developed to be installed and operated at the Syowa Station. The lidar transmitter is based on injection-seeded, pulsed alexandrite laser for 768-788 nm (fundamental wavelengths) and a second-harmonic generation (SHG) unit for 384-394 nm (second harmonic wavelengths). In order to tune the seeder laser to absolute Potassium resonance line, Doppler-free spectroscopy with a Potassium cell is crucial. The measurement was done at NIPR and the Doppler-free spectrum was recorded with 0.005 pm wavelength resolution. Three absorptions spaced with 0.05pm at the cross-over wavelength were clearly measured. In this talk, details of the experiment will be shown.

Keywords: Antarctica, lidar, Potassium, resonant scattering, Doppler Free

Japan Geoscience Union Meeting 2014
(28 April - 02 May 2014 at Pacifico YOKOHAMA, Kanagawa, Japan)

PEM36-P06 Room:Poster Time:April 28 18:15-19:30

Development of a 3D sodium lidar: synchronous experimentation and validation

MURANAKA, Wataru[1*] ; KAWAHARA, Taku d[2] ; NOZAWA, Satonori[3]

[1]GSI, Shinshu University, [2]Faculty of Engineering, Shinshu University, [3]STE Lab., Nagoya University

Shinshu University, Nagoya University and RIKEN developed an all solid-state, high-power Na lidar for the temperature/wind measurements in the MLT region over EISCAT radar site in Tromso (69 N), Norway. Current observation is five-direction mode applied to the fixed direction such as vertical and 30 degree tilted to the north, south, east and west from the vertical.

We are now updating the lidar to multi-direction system which has never been done with resonant lidars. The transmission system uses two mirrors with electric rotary stages to emit laser light to any direction of the sky. Receiver system uses a telescope controlled by a PC. The coordination of the telescope is done with direction of so me blight stars. This repeatability pointing to the same direction is 5.3 mrad.

In this talk, we will discuss the experimental results of the synchronized experiments with the laser direction and telescope field-of-view.

Keywords: sodium, lidar, three diminutional

Japan Geoscience Union Meeting 2014
(28 April - 02 May 2014 at Pacifico YOKOHAMA, Kanagawa, Japan)

PEM36-P07 Room:Poster Time:April 28 18:15-19:30

Analysis of the factors of seasonal variation of the thermosphere-mesosphere NO observed at Syowa Station

UEMURA, Miku[1] ; ISONO, Yasuko[1] ; MIZUNO, Akira[1] ; NAGAHAMA, Tomoo[1] ; EJIRI, Mitsumu K.[2] ; TSUTSUMI, Masaki[2] ; NAKAMURA, Takuji[2*]

[1]Solar-Terrestrial Environment Laboratory, Nagoya University, [2]National Institute of Polar Research

When high-energy particles such as solar protons and energetic electrons fall down to the earth's atmosphere, the nitrogen oxides (NO, NO2) are increased in the mesosphere and the upper stratosphere in the polar regions (e.g. Lopez-Puertas et al. 2005). In collaboration with the National Institute of Polar Research, Nagoya University Solar-Terrestrial Environment Laboratory installed a millimeter-wave spectroscopic radiometer at Syowa Station in Antarctica. We have conducted continuous observation of the NO spectrum since January 2012. The NO column density derived from this observation shows a seasonal variation that the NO column density increases up to about 1.7×10^{15} cm^{-2} in winter and decreases down to about 0.5×10^{15} cm^{-2} in summer. In order to understand the mechanism of the seasonal variation, we compared it with seasonal variation of CO vertical distribution in thermosphere-mesosphere and the length of sunshine hours at Syowa Station. Since CO photochemical lifetime is longer than or equal to the horizontal and vertical transport in the thermosphere and the stratosphere, CO can be considered as a good tracer of atmospheric transport. We used CO data obtained by AULA / MLS (Version3.3).

The CO volume mixing ratio in a latitude range of 65 S-75 S and an altitude range of 0.1-0.01 hPa shows a tendency that the mixing ratio increased in winter and decreased in summer. The peak altitude of the mixing ratio changed from upper altitude to lower altitude during winter, suggesting downward transport of the atmosphere. The commencements of the increment of the NO column density and the CO mixing ratio were almost coincident, but the temporal variation patterns of NO and CO did not agree well with each other especially in the decrement phase. On the other hand, the temporal variation pattern of the NO column density and the length of night time showed good correlation throughout the period during which the NO enhancement was significant. Thus the variation of the NO column density in the lower thermosphere-mesosphere is considered to be caused by both the descending of the air mass and the photochemical process.

In this poster, we will present more detailed discussion on the relationship among the NO column density, CO mixing ratio, and length of the night time based on the dataset including the new data acquired this year.

Keywords: microwave spectroscopy, Nitric Oxide

Japan Geoscience Union Meeting 2014
(28 April - 02 May 2014 at Pacifico YOKOHAMA, Kanagawa, Japan)

PEM36-P08 Room:Poster Time:April 28 18:15-19:30

Small spatial scale field aligned currents in middle and low latitudes as observed by the CHAMP satellite

NAKANISHI, Kunihito[1*] ; IYEMORI, Toshihiko[1] ; AOYAMA, Tadashi[1] ; LUHR, Hermann[2]

[1]Department of Geophysics, Graduate School of Science, Kyoto University, [2]GeoForschungsZentrum, GFZ, Potsdam, Germany

The magnetic field observation by the CHAMP satellite shows the ubiquitous existence of small scale (1-5 nT) magnetic fluctuations with period around a few tens seconds along the satellites. From characteristics of the amplitude and period, they can be interpreted as the spatial structure of small scale field-aligned currents generated by the ionospheric dynamo driven by atmospheric gravity waves propagating from the lower atmosphere. The mechanism is the following; first, the gravity waves generated by the lower atmospheric disturbance propagate to the ionosphere; the neutral winds oscillate, cause ionospheric dynamo and Pedersen and Hall currents flow; because the dynamo region is finite, the currents cause polarized electric fields; and the polarized electric fields propagate along the geomagnetic filed as Alfven waves accompanied by field-aligned currents, at the same time, the ionospheric currents divert to the filed aligned currents; finally the CHAMP satellite observes the spatial structure of the filed aligned currents generated in this way as a temporal change along the path, because the temporal variation of the gravity waves are slow enough, i.e., more than a few minutes, that is, that of field aligned current can be ignored and nearly constant for the satellite crossing the currents.

This time we analyze correlation relation of the two components perpendicular to the geomagnetic field to find the following tendencies. About the magnetic data at the observed point, 1) if inclination and declination are plus and plus respectively, a correlation coefficient tends to be minus; 2) if inclination and declination are plus and minus respectively, it tends to be plus; 3) if inclination and declination are minus and plus respectively, it tends to be plus; 4) if inclination and declination are minus and minus respectively, it tends to be minus.

We report the model of the current system consistent to the characteristics of the magnetic fluctuations including the tendency of the correlation relation.

Keywords: spatial structure of field aligned currents, middle and low latitudes, the CHAMP satellite, atmospheric gravity wave, the lower atmospheric origin, correlation relation

Japan Geoscience Union Meeting 2014
(28 April - 02 May 2014 at Pacifico YOKOHAMA, Kanagawa, Japan)

PEM36-P09 Room:Poster Time:April 28 18:15-19:30

Atmospheric origin of small-scale magnetic fluctuations as observed by CHAMP above the ionosphere

AOYAMA, Tadashi[1*] ; IYEMORI, Toshihiko[2] ; NAKANISHI, Kunihito[1]

[1]Graduate School of Science, Kyoto University, [2]Graduate School of Science, Kyoto University

We analyzed magnetic field data obtained by a LEO(Low Earth Orbit) satellite, CHAMP(altitude 300˜450 km), and found out the global distribution of the short-period(10˜40 s) and small-amplitude(0.1˜5 nT) magnetic fluctuations in middle and low latitudes. We have reported that these fluctuations are small-scale structure(˜100 km) of the field-aligned currents generated by dynamo action in the ionospheric E-layer and the dynamos are caused by the atmospheric gravity waves (horizontal scale is ˜100 km) because of the characteristics of geographical and seasonal dependence of their amplitude.

In this paper, we focus on the mesoscale meteorological events to clarify the atmospheric origin such as typhoon which is possible to generate atmospheric gravity waves, and compare with magnetic fluctuations as observed by the CHAMP satellite above the ionosphere. We trace from the location of CHAMP to each footpoint in the E-layer along geomagnetic field line, and then compared with meteorological phenomena beneath the footpoint.

As a result, we detected large amplitudes of geomagnetic fluctuation above typhoons.

Keywords: field-aligned current, ionospheric dynamo, atmospheric gravity wave, acoustic resonance, CHAMP satellite, typhoon

Japan Geoscience Union Meeting 2014
(28 April - 02 May 2014 at Pacifico YOKOHAMA, Kanagawa, Japan)

PEM36-P10 Room:Poster Time:April 28 18:15-19:30

Optimization of notification system for bright meteor signals by using wide angle images at multiple sites

IYONO, Atsushi[1*] ; WADA, Naoki[2]

[1]Dept. of Fundamental Science, Okayama university of Science, [2]Graduate School of Science, Okayama university of Science

1. Purpose and Background

The sky monitoring system by using wide angle images have been maintained until Nov. 2011 at Okayama University of Science. The CCD camera system provides the slow shutter images every 3 second, and they have been transferred simultaneously to data storage server via the Internet connection. This system enables to monitor the real time condition of the sky. In the obtained images, bright meteors and sometimes fire balls were registered. We have been developing our new system which can provide quick analysis results for meteor and fire ball at the moment of observations. In this report, we describe the new sensor systems of thermography and low frequency sounds to increase the detection efficiency of brighter meteors and fire balls.

2. System

In the sky monitor system, CCD camera with wide angle lens and image server system have been operated in 24 hours/day. The exposure of CCD cameras has been set to be 4 second. The acquired image data have been stored in PC system via the internet ftp command. 28,800 images(500MB data

size) are stored in each day. In offline mode, images are processed with contrast enhancement module, image differentiating and object detection module. To detect meteors and fire balls effectively, we activated the IR image seosors and low frequency sound sensors as well as imaging devices.

3. Development

Our purposes are that new analysis system for online processing of images, IR sensors and low frequency seonsors have been developed in order to provied the information of the arrival of meteor and fireballs, arrival directions and brightness profiles. We are going to present new system and analysis result in this reports

Keywords: meteor, fireball, simultaneous? observation, meteor shower

Japan Geoscience Union Meeting 2014
(28 April - 02 May 2014 at Pacifico YOKOHAMA, Kanagawa, Japan)

PEM36-P11 Room:Poster Time:April 28 18:15-19:30

Measurement of propagation characteristics of MF band radio waves in lower ionosphere by S-310-40 sounding rocket

ISHISAKA, Keigo[1*] ; ITAYA, Keita[1] ; ASHIHARA, Yuki[2] ; ABE, Takumi[3] ; ENDO, Ken[4] ; KUMAMOTO, Atsushi[4]

[1]Toyama Prefectural University, [2]NARA National College of Technology, [3]ISAS/JAXA, [4]Tohoku University

The ionospheric D region is important in radio wave propagation because it absorbs energy from waves at MF, HF and VHF, and it reflects LF and VLF signals. Then D region is present only during daylight hours. Therefore, in the night-time, the MF band radio waves are propagated as far as an area where its radio waves cannot be propagated in the daytime. This reason why the radio waves cannot receive is that the D region is disappeared at night. However, the MF band radio waves that transmit from distant place have not been often received at the mid latitude in the night-time. In this time the sporadic E region cannot be observed by the ionogram. We guess that the D region appear in the lowest ionosphere like a daytime. To farther study the structure of the lowest ionosphere, we propose a method to measure the very low electron densities that occur at altitudes from 50 km to 90 km using the partial and perfect reflection characteristics of electromagnetic waves.

S-310-40 sounding rocket experiment was carried out at Uchinoura Space Center (USC) at 23:48 JST on 19 December, 2011. The purpose of this experiment is the investigation of characteristics of radio wave propagation in the ionosphere and the estimation of electron density structure in the lower ionosphere, when the intensity of radio wave measured on the ground will be attenuate at night-time. In order to measure the radio waves, a LF/MF band radio receiver (LMR) is installed on the sounding rocket. The LMR has measured the propagation characteristics of four radio waves at frequencies of 60 kHz (JJY signal from Haganeyama radio station), 405 kHz (NDB station from Minami-Daito), 666 kHz (NHK Osaka broadcasting station) and 873 kHz (NHK Kumamoto broadcasting station) in the region from the ground to the lower ionosphere. The LMR consists of a loop antenna, a pre-amplifier and a detector circuit. The loop antenna is set up in the nose cone, which is transparent to the LF/MF band radio waves, and is not deployed during the flight. Therefore, the LMR can measure the relative attenuation of radio waves from the ground up to the ionosphere. Furthermore the loop antenna consists of three loop antennas in order to measure three components of four radio waves. Then we can obtain the propagation directions of radio waves in the ionosphere directly.

A propagation vector can be obtained from the propagation characteristic of radio wave. It is possible to estimate electron density profile from a propagation vector, because the propagation vector is dependent on the electron density profile in the radio wave propagation region. We have estimated the electron density profile by the propagation vector. When the electron density profile estimated by the propagation vector was compared with the electron density profile measured with the Langmuir probe and the impedance probe onboard the S-310-40 sounding rocket, it was found that electron density becomes the maximum at an altitude of 104 km.

We show the results of propagation characteristics of radio waves in the ionosphere and explain the propagation vector of radio wave in the ionosphere. And the electron density profile in the ionosphere can be estimated by the propagation vector. We will show the result that it is investigated the influence the lowest ionosphere region has on a MF band radio wave in this study.

Keywords: ionosphere, propagation characteristic of radio wave, rocket experiment

Japan Geoscience Union Meeting 2014
(28 April - 02 May 2014 at Pacifico YOKOHAMA, Kanagawa, Japan)

PEM36-P12 Room:Poster Time:April 28 18:15-19:30

Measurement of LF Standard-Frequency Waves JJY along the track of Shirase during JARE55: Preliminary Report

KITAUCHI, Hideaki[1*] ; NOZAKI, Kenro[1] ; ITO, Hiroyuki[1] ; KONDO, Takumi[1] ; TSUCHIYA, Shigeru[1] ; IMAMURA, Kuniyasu[1] ; NAGATSUMA, Tsutomu[1]

[1]NICT

We developed a highly sensitive, reliable receiving system for the purpose of reception of low frequency (LF) radio waves. The system consists of digital lock-in amplifiers and crossed-loop antennas. Digital lock-in amplifier (DLA) employs phase-sensitive detection (PSD) of periodic signal multiplied by the input reference source of the known signal frequency. This makes it possible to realize very narrow bandpass filter around the reference frequency, detecting/measuring that of very weak signal even in noisy environment. The antenna, on the other hand, consists of orthogonally crossed, larger double loops (receivers R_X, R_Y) and smaller doubles (transmitters T_X, T_Y): the former receivers R_X, R_Y receive LF radio signals of x-, y-components, the latter transmitters T_X, T_Y transmit an instant, weak signal from each x-, y-component for self calibration purpose. The self calibration test is performed by transmitting a weak LF signal for an instant every an hour from the transmitter T_X, T_Y respectively, and receiving this signal from the receivers R_X, R_Y to obtain preassigned field strength. This test indicates if the receivers of the system are working properly and allows us to obtain reliable measurements.

We apply the receiving system to measure the field intensity and phase of the standard frequency and time signals (SFTS) JJY of LF 40 kHz and 60 kHz during the summer expedition of the 55th Japanese Antarctic Research Expedition (JARE), from November 2013 to April 2014. Figure 1 shows temporal evolution of the field intensities JJY 40 kHz (light blue dots) and 60 kHz (brown dots) as well as the self-calibrating radio signals. Our receiving system detects both the LF JJY radio signals even offshore Syowa Station, Antarctic, about 14,000 km away from those transmitting stations. Also the field intensities of the self calibration test show about a consistent preassigned value, assuring the measurements.

Keywords: low frequency (LF) radio waves, call sign JJY of 40 kHz and 60 kHz, standard frequency and time signals (SFTS), self calibration, Japanese Antarctic Research Expedition (JARE), Japanese Antarctic Research Icebreaker Shirase

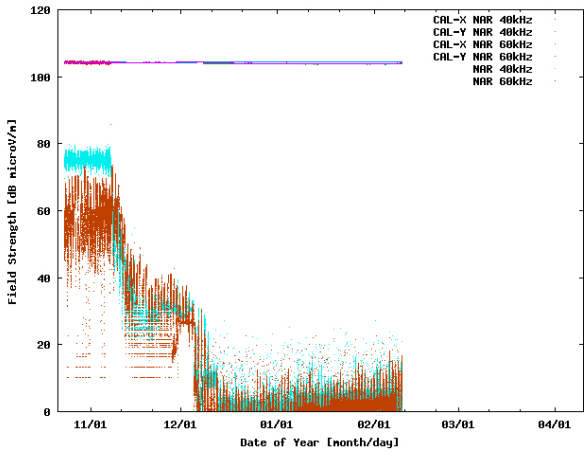

Japan Geoscience Union Meeting 2014
(28 April - 02 May 2014 at Pacifico YOKOHAMA, Kanagawa, Japan)

PEM36-P13 Room:Poster Time:April 28 18:15-19:30

Velocity distribution of electrons generating plasma waves around the wake of an ionospheric sounding rocket

ENDO, Ken[1*] ; KUMAMOTO, Atsushi[1] ; KATOH, Yuto[1]

[1]Department of Geophysics, Graduate School of Science, Tohoku University

When a body moves in plasma at supersonic velocity, a rarefied plasma region called 'plasma wake' is formed behind the body. Wakes can develop behind a solar system body immersed in solar-wind plasma as well as behind spacecraft such as satellites and ionospheric sounding rockets. There are several studies which report plasma waves around the wakes of a satellite and of the moon. Although there are not so many studies which report plasma waves generated in association with the rocket wake, observational results from two rocket experiments performed in 1998 and 2012 have shown generation of plasma waves around the wake of a rocket. It is very important to reveal the generation process of plasma waves near the rocket wake for understanding the universal physics related to the interaction between streaming plasma and a non-magnetized body as well as for interpreting wave data obtained in rocket experiments more accurately.

Our analysis has revealed three kinds of plasma waves observed in the S-520-26 rocket experiment in 2012. They are likely to be electrostatic electron cyclotron harmonic (ESCH) waves, upper hybrid resonance (UHR) mode waves, and whistler mode waves. They have spin-phase dependence in characteristic manners. These results indicate that the plasma waves should be generated inhomogeneously around the rocket. We have performed numerical calculations of plasma dispersion relations by assuming anisotropic velocity distribution functions such as electron beam and temperature anisotropy. As a result, positive linear growth rates have been obtained in the wave number and frequency ranges of UHR mode waves and ESCH waves in addition to electrostatic whistler mode waves. Accordingly, there have to be electrons with some anisotropic velocity distribution functions which are equivalent to those we assumed in the calculations. However, we have to clarify what kind of velocity distribution can be generated around the actual wake through the interaction between a sounding rocket and ionopsheric plasma.

Singh et al. (1987) has performed a one-dimensional simulation of plasma entering a void region from the two sides using a Vlasov-Poisson code. They have found counterstreaming electron beams in the very near wake. However, their study concentrates on electrons on the wake axis and does not indicate distribution functions in other areas. Besides, temperature anisotropy could not be treated in their simulation because it is performed in one dimension in velocity space.

In order to investigate inhomogeneity of electron distribution functions around the rocket wake, we are developing a Vlasov-Poisson code with one-dimensional space and two-dimensional velocity space, which is redesigned from the simulation code used in Singh et al. (1987). In this simulation, we deal with cases that electrons and ions are filling in a void space. The time evolution can be understood as spatial distribution along the wake axis. The direction of one-dimensional space is along the geomagnetic fields, along which electrons and ions can move easily. The size of space is 10 m, which is divided into 1024 grids in the calculation.

In this presentation, we clarify the frequency range and spatial distribution of the plasma waves around the wake based on the analyses of S-520-26 rocket experiment data. We also discuss the velocity distribution of the electrons which can generate the plasma waves as observed. In addition, we report initial results of our simulation for investigating the velocity distribution of electrons around the wake.

Keywords: ionosphere, sounding rocket, wake, plasma wave, Vlasov simulation

Japan Geoscience Union Meeting 2014
(28 April - 02 May 2014 at Pacifico YOKOHAMA, Kanagawa, Japan)

PEM36-P14 Room:Poster Time:April 28 18:15-19:30

Atmospheric Neutral Analyzer for mass-resolved velocity distribution measurements: Verification of mass analyzer

SHIMOYAMA, Manabu[1*] ; HAYASHI, Ayuko[1] ; ITO, Fumihiro[1] ; HIRAHARA, Masafumi[1]

[1]STEL, Nagoya University

In order to understand the temporal and spatial variability of the ionosphere-thermosphere system, simultaneous measurements of the composition and density of the neutral atmosphere and the velocity distribution of individual species are essential. However, most conventional types of instruments for neutral atmosphere lack the simultaneous capability of measuring neutral atmospheric velocity and resolving neutral mass.

We have designed the Atmospheric Neutral Analyzer (ANA) instrument to measure the detailed, mass-resolved 2-dimensional velocity distribution of neutral species, from which the corresponding density, mass composition, bulk velocity and temperature were derived. In this presentation, we will report the results from laboratory experiments for the performance verification on the prototype of mass analyzer along with the detailed and overall design determined by numerical simulation.

Keywords: neutral upper atomosphere, velocity distribution function, mass analysis

Japan Geoscience Union Meeting 2014
(28 April - 02 May 2014 at Pacifico YOKOHAMA, Kanagawa, Japan)

PEM36-P15 Room:Poster Time:April 28 18:15-19:30

Observation of resonance scattering light of Lithium vapor under daytime and moonlight condition and neutral wind analys

KIHARA, Daiki[1*] ; KAKINAMI, Yoshihiro[1] ; YAMAMOTO, Masa-yuki[1] ; WATANABE, Shigeto[2] ; HARD, Lucas[3] ; LARSEN, Miguel[3] ; YAMAMOTO, Mamoru[4] ; HABU, Hiroto[5] ; ABE, Takumi[5]

[1]Kochi Univ. of Tech., [2]Hokkaido Univ., [3]Clemson Univ., [4]Kyoto Univ., [5]ISAS/JAXA

1.Introduction

For the purpose of measurement of neutral atmospheric wind in lower thermosphere, we observed resonance scattering light of sunlit Lithium vapor released from a sounding rocket in the evening thermosphere in 2007 (e.g. Yamamoto et al., 2008). At that time, we successfully measured thermospheric neutral wind profile between 110 km and 400 km. In 2012, we observed resonance scattering light of sunlit Lithium at dawn, and estimated lower thermospheric neutral wind between 76 km and 127 km.

On July 4, 2013, a U.S.-Japan collaborative rocket experiment to observe neutral wind profile in daytime lower thermosphere with Lithium release was carried out at WFF (Wallops Flight Facility), NASA. A rocket to operate chemical release of Lithium was launched at 10:31:40 EDT (14:31:40 UTC). The rocket launched to southeastern direction released Lithium vapor three times between at about 90 km and 130 km altitude during the upleg, at about 40 km horizontally away from a ground-based observation site in WFF. Here we tried to observe of Lithium clouds from the ground-based and airborne observations with collaboration of Kochi University of Technology (KUT) and Clemson University.

On July 20, 2013, a rocket experiment to observe neutral wind profile in moonlit lower thermosphere with Lithium release was carried out at USC (Uchinoura Space Center), Japan. The S-520-27 rocket to operate chemical release of Lithium was launched at 23:57:00 JST and released Lithium vapor three times between at about 80 km and 120 km altitude during the downleg under the almost full moon condition (Moon age was 12). Here we tried to observe of Lithium clouds from 3 ground-based sites and an airplane.

2.Observations

Airborne observation of Lithium cloud was carried out under a condition with the sun at the backward direction while it flew to north-northeast at about 10 km (33,000 feet) altitude and at about 300 km away from the ground site at the southeastern direction. An observation site was set in WFF on ground. In order to detect the Lithium clouds in daytime skies with good S/N ratio, digital cameras (Canon EOS Kiss X4, Nikon D90) with 2 nm band pass filters (BPF) at 671 nm wavelength were used for all digital cameras. We installed three digital cameras in the aircraft NASA-8 and set two digital cameras on the ground site. A video camera (Watec, WAT-120N) with a 12 nm BPF was also used in the aircraft and on ground, respectively.

The Lithium clouds under moonlight condition was observed by using digital cameras, Watec, and cooled EM-CCD (BITRAN BQ-87EM) with 2 nm and 12 nm BPF from the JAXA airplane Hisyo as well as three ground-based observation sites (USC, Tanegashima and Muroto).

3.Results

A Lithium cloud under daytime sky condition was observed for about 25 minutes from the aircraft. The released Lithium vapor formed red clouds along the rocket trajectory just after the release. Afterwards, the Lithium trails were spread into complex shapes by strong wind shear in the altitude. We successfully observed Lithium clouds by the airborne observation.

A Lithium cloud under moonlight sky condition was observed for about 90 seconds from the aircraft and two ground sites.

4.Summary

We successfully observed 2 chemical releases of Lithium from the aircrafts and ground sites on July, 2013, in daytime and midnight. We succeeded the detection of resonance scattering light of Lithium vapor under daytime and moonlight sky condition in lower thermosphere. Owing to this experiment, we confirmed that we can measure altitude profile of the neutral atmospheric wind in lower thermosphere at almost all local time by using the chemical release of Lithium.

In this paper, we will discuss that the observed emission intensity of the resonance scattering light of Lithium vapor under daytime and moonlight sky condition in lower thermosphere, obtained results of the S/N ratio, preliminary results and problems of the neutral atmospheric wind measurement in daytime lower thermosphere.

Keywords: sounding rocket, thermosphere, neutral wind, Lithium Ejection Systems, airborne observation

Japan Geoscience Union Meeting 2014
(28 April - 02 May 2014 at Pacifico YOKOHAMA, Kanagawa, Japan)

PEM36-P16 Room:Poster Time:April 28 18:15-19:30

Improvement of the method for estimating thermospheric temperature using small FPIs and evaluation of their temperatures

NAKAMURA, Yoshihiro[1*] ; SHIOKAWA, Kazuo[1] ; OTSUKA, Yuichi[1] ; OYAMA, Shin-ichiro[1] ; NOZAWA, Satonori[1]

[1]Solar-Terrestrial Environment Laboratory, Nagoya University

Fabry-Perot interferometer (FPI) is an instrument that can measure the temperature and wind velocity of the thermosphere from the ground through observation of airglow emission at a wavelength of 630.0nm. The Solar-Terrestrial Environment Laboratory (STEL), Nagoya University, has five FPIs as parts of the Optical Mesosphere Thermosphere Imagers. Two of those FPIs, possessing a large aperture etalon (diameter: 116mm), were installed at Shigaraki, Japan in 2000 and in Tromso, Norway, in 2009. The other three small FPIs, using 70-mm diameter etalons, were installed in Thailand, Indonesia, and Australia in 2010-2011. They use highly-sensitive cooled-CCD cameras with 1024-1024 pixels to obtain interference fringes. However, appropriate temperature has not been obtained from the interference fringes using these new small-aperture FPIs. In the present study we aimed to improve the procedure of temperature derivation using these small etalon FPIs, to evaluate the accuracy for obtained temperatures and to perform statistical analysis of the temperature data obtained for 2-3 years.

The FPIs scan the sky in north, south, east, and west directions repeatedly by rotating a light receiving mirror. We determined each center of the laser fringe and sky fringes for north, south, east, and west directions. Then we found that they are slightly a few pixels different depending on the mirror directions. This difference of fringe centers seems to be due to distortion of the optics body, which is caused by the motion of the heavy scanning mirror on top of the optics. Thus, we decided to determine the fringe center for each direction. After this revision, we could make a reliable temperature determination. In this presentation, we show these procedures of temperature derivation and relation between airglow intensity and standard deviations of obtained temperatures as accuracy of temperature derivation. We also discuss effects of the etalon gap drift due to changes in etalon temperature for accuracy of measured thermospheric temperatures and winds.

Keywords: Fabry Perot Interferometers, thermospheric temperature

Japan Geoscience Union Meeting 2014
(28 April - 02 May 2014 at Pacifico YOKOHAMA, Kanagawa, Japan)

PEM36-P17 Room:Poster Time:April 28 18:15-19:30

Statistical characteristics of MSTIDs observed by 630-nm airglow imager and HF-radar echoes at Paratunka, Russia

MINOURA, Takeshi[1*] ; SUZUKI, Shin[1] ; SHIOKAWA, Kazuo[1] ; OTSUKA, Yuichi[1] ; NISHITANI, Nozomu[1] ; HOSOKAWA, Keisuke[2]

[1]Solar-Terrestrial Environment Laboratory, Nagoya University, [2]Department of Communication Engineering and Informatics, University of Electro-Communications

Medium-scale traveling ionospheric disturbances (MSTIDs), which typically have a horizontal scale of 100-500 km and a period of ˜1 h, are frequently observed in the F region ionosphere at middle latitudes. To date, quite a few observations of MSTIDs have been carried out especially in the middle latitudes; they predominantly had a northwest-southeast, (northeast-southwest) frontal structure and propagated southwestward (northeastward) in the northern (southern) hemisphere, however their generation and propagation mechanisms are not clear yet. Suzuki et al. [2009] investigated two dimensional characteristics of a nighttime MSTID using the SuperDARN Hokkaido HF radar at Rikubetsu, (43.5 N, 143.6 E), Japan, and an OI 630-nm airglow imager located at Paratunka (53.0 N, 158.2 E), Russia, within the radar field of view (FOV). The Doppler velocities of MSTID echoes observed by the SuperDARN radar showed systematic polarity changes which were consistent with airglow intensity variations. The electric field estimated from the airglow and SuperDARN observations, however, seems to be improbable and the E-F coupling processes would be important to explain the inconsistency. We investigated statistical characteristics of nighttime MSTIDs. Based on the coordinated airglow and SuperDARN measurements from 2011 to 2013, we investigated the relation between the MSTID amplitudes in the 630-nm airglow intensity and the Doppler velocities of the FAI echoes associated with the MSTID pattern. This study may give an observational insight into the E-F coupling quantitatively.

In this presentation, we will report the statistics of the relation of the FAI echoes and airglow signatures of the observed MSTIDs (5 events), which showed spatially conjugation in the radar FOV.

Keywords: airglow imager, Hokkaido SuperDARN radar, MSTID

Japan Geoscience Union Meeting 2014
(28 April - 02 May 2014 at Pacifico YOKOHAMA, Kanagawa, Japan)

PEM36-P18 Room:Poster Time:April 28 18:15-19:30

Detection of ionospheric disturbances caused by the earthquake using HFD

TAKABOSHI, Kazuto[1*] ; NAKATA, Hiroyuki[1] ; TAKANO, Toshiaki[1] ; TOMIZAWA, Ichiro[2]

[1]Graduate shool of Engineering, Chiba University, [2]Center for Space Science and Radio Engineering,Univ. Electro-Comm

Many studies have reported that ionospheric disturbances occur after giant earthquakes. This is because the acoustic wave and/or atmospheric gravity wave are excited by the ground perturbations or tsunami. The HF Doppler observation is suitable for detection of ionospheric disturbances since this can observe ionospheric vertical drift from Doppler shift of radiowaves (5006 and 8006 kHz) transmitted from the Chofu campus of UEC. In this study, usng Doppler shift data of 5006 kHz, ionospheric disturbances associated with earthquakes are ditected. When Doppler shift is fluctuated intensely after propagation time of Rayleigh wave from the seismic center to the observation points, the fluctuation is determined as a disturbance associated with the earthquakes.

In 55 events of earthquakes (M≥6.0) occurred around Japan since 2003, fluctuations by earthquakes are detected in 14 events and the smallest magnitude is 6.4. No fluctuation is detected in some larger earthquakes than M6.4. Since the ionosphere is unstable at night, received frequency is disturbed and it is hard to determine the fluctuations caused by earthquake. In addition, the observation points are not always located near the seismic centers. When earthquakes occur near observation points at the daytime, it is expected that the fluctuations caused by earthquakes are observed even if the magnitudes of the earthquakes is smaller than M6.4.

We also examined the relationship between direction of fault and fluctuations of HFD data. Most of the earthquakes in Japan are reverse fault type. Because a hanging wall slides up in this type of an earthquake, it is expected that initial perturbation of a sound wave excided by the hanging wall is upward. Actually, in most of the events Doppler shifts are negative, which means that the ionosphere moves upward. Next we examined a normal-fault-type earthquake (Fukushima hama-dori earthquake, 2011/4/11), in which a hanging wall slips down. In this event, the epicenter is located at the east of Fukushima prefecture. Doppler data of three observation points (Iitate, Sugadaira, Kiso) are examined. In Iitate observatory, which is the closest to the epicenter, Doppler data shows that ionosphere moved only upward. On the contrary, in the other two points, Doppler data shows that ionosphere moved downward first and then upward, or upward first and then downward. Therefore, fluctuations of ionosphere can not be determined only by a type of fault. More detailed analysis using the seismometer is necessary.

Keywords: ionosphere, HFD, earthquake, acoustic wave, atmospheric gravity wave, fault

Japan Geoscience Union Meeting 2014
(28 April - 02 May 2014 at Pacifico YOKOHAMA, Kanagawa, Japan)

PEM36-P19 Room:Poster Time:April 28 18:15-19:30

Observations of seismo-traveling ionospheric disturbance during the 2011 Tohoku earthquake using HF Doppler

CHOU, Min-yang[1*] ; TSAI, Ho-fang[1] ; LIU, Jann-yenq[2]

[1]Department of Earth Science,National Cheng-Kung University,Taiwan, [2]Institute of Space Science, National Central University, Taiwan

This paper reports seismo-traveling ionospheric disturbances (STIDs) induced by the 11 March 2011 M9.0 Tohoku-oki earthquake and following pan-Pacific tsunami by two networks of HF (high-frequency) Doppler sounding systems in Japan and Taiwan. The Hilbert-Huang Transform (HHT) is applied to analyze Doppler frequency shifts (DFSs) detecting STIDs, while the time delay, circle, ray-tracing, and beam-forming methods are used to compute the propagation of the detected STIDs. Both STIDs induced by the Rayleigh waves and tsunami of the Tohoku-oki earthquake are detected and discussed.

Keywords: STIDs, Ionosphere, earthquake, tsunami

Japan Geoscience Union Meeting 2014
(28 April - 02 May 2014 at Pacifico YOKOHAMA, Kanagawa, Japan)

PEM36-P20 Room:Poster Time:April 28 18:15-19:30

Spectrum of the neutral atmospheric waces derived from a numerical simulation of an earthquake

SHIMIZU, Yuki[1*] ; NAKATA, Hiroyuki[1] ; TAKANO, Toshiaki[1] ; MATSUMURA, Mitsuru[2]

[1]Grad. School of Eng. , Chiba Univ., [2]Center for Space Science and Radio Engineering, University of Electro-Communications

It is important to examine the ionospheric disturbances excited by earthquakes, since this contributes to monitoring tsunamis from satellites. There are many reports of ionospheric disturbances occurred by giant earthquakes, such as the 2011 off the Pacific coast of Tohoku Earthquake. But characteristics of atmospheric disturbances, connecting the ionospheric disturbances with the ground and the sea surface, is not clarified because broad observation of the atmosphere in high resolution is difficult. In this study, calculating the spectra from the temporal variations of neutral atmospheric waves determined by a numerical simulation, we derived the features of the propagation of the atmospheric waves.

In this simulation, two dimensional model is used. The atmospheric perturbation is created by a vertical velocity assuming an upward motion of the sea surface or ground surface. Calculating the temporal variations of neutral density, we derived their spectra.

As a result, it is shown that behavior of atmospheric waves is different for the frequency. For a notable example, variations around 1 mHz propagate to high altitudes 450 km ˜500 km and long distance 800 km. On the other hand, variations around 10 mHz propagate almost the same distance in lower altitude of 300 km or less. In addition, variation at 4 mHz are located above the epicenter at 350 km. This causes the variation of GPS-TEC at 4 mHz associated with earthquakes that have ever been reported.

Keywords: ionosphere, earthquake, acoustic wave, gravity wave

Japan Geoscience Union Meeting 2014
(28 April - 02 May 2014 at Pacifico YOKOHAMA, Kanagawa, Japan)

PEM36-P21 Room:Poster Time:April 28 18:15-19:30

Ionospheric effects on the F region during the Sunrise for the annular solar eclipse over Taiwan on 21 May 2012

CHUO, Yu-jung[1*]

[1]Department of Information Technology, Ling Tung University

On 21 May (20:56, Universal Time; UT, on 20 May), 2012, an annular solar eclipse occurred, beginning at sunrise over southeast China and moving through Japan, sweeping across the northern Pacific Ocean, and completing its passage over the western United States at sunset on 20 May (02:49 UT, 21 May), 2012. We investigated the eclipse area in Taiwan, using an ionosonde and global positioning system (GPS) satellites measurements. The measurements of foF2, hmF2, bottomside scale height around the peak height (Hm), and slab thickness (B0) were collected at the ionosonde station at Chung-Li Observatory. In addition, we calculated the total electron content (TEC) to study the differences inside and outside the eclipse area, using 3 receivers located at Marzhu (denoted as MATZ), Hsinchu (TNML), and Henchun (HENC). The results showed that the foF2 values gradually decreased when the annularity began and reached a minimum level of approximately 2.0 MHz at 06:30 LT. The hmF2 immediately decreased and then increased during the annular eclipse period. The TEC variations also appeared to deplete in the path of the eclipse and opposite to the outside passing area. Further, the rate of change of the TEC values (dTEC/dt measured for 15 min) was examined to study the wave-like fluctuations. The scale height near the F2 layer peak height (Hm) also decreased and then increased during the eclipse period. To address the effects of the annular eclipse in the topside and bottomside ionosphere, this study provides a discussion of the variations between the topside and bottomside ionospheric parameters during the eclipse period.

Keywords: ionospheric physics, ionospheric disturbances, solar radiation effects

Japan Geoscience Union Meeting 2014
(28 April - 02 May 2014 at Pacifico YOKOHAMA, Kanagawa, Japan)

PEM36-P22 Room:Poster Time:April 28 18:15-19:30

Horizontal shapes of mid-latitude sporadic-E observed with GPS-TEC

MAEDA, Jun[1*] ; HEKI, Kosuke[1]

[1]Graduate school of Science, Hokkaido University.

The horizontal shapes of sporadic-E (Es) have remained uncovered due to the lack of effective observation methods. We use a dense array of Global Positioning System (GPS) receivers in Japan to map horizontal shapes of mid-latitude sporadic-E layers and explore their diversity. The spatial and temporal resolutions of the GPS array are ˜25 km (in horizontal) and 30 s, respectively, which is ideal for studying the horizontal shape and movement of sporadic-E. Sporadic-E can be identified as positive anomalies of total electron content (TEC) along the line of sight between a satellite and a ground-based GPS station.

The results of GPS-TEC observation, i.e., mapping of positive TEC anomaly caused by mid-latitude sporadic E are presented in this presentation with a special emphasis on latitudinal and temporal variations of horizontal shapes of Es-layers. We analyzed ˜100 Es events in 2010-2013 to examine the latitudinal dependence of Es frontal structures with three study areas at different latitudes near ionosondes, namely Sarobetsu (geographical latitude: 45.16 N), Kokubunji (35.71 N) and Yamagwa (31.20 N).

As a result, strong Es shares the large-scale frontal structure as a common shape regardless of the occurrence latitude and time (e.g., morning, afternoon, and the evening). The horizontal structures of large-scale fronts are typically elongated in east-west (E-W) with the length and width of ˜300 km and ˜30 km, respectively. However, lengths vary from 30 to 300 km by occasion. The alignment of frontal structures prefers E-W, ENE-WSW and NE-SW alignment with some exception of NW-SE and NNW-SSE aligned structures.

We will also discuss the possible mechanisms for formation, development, and movement of mid-latitude sporadic-E based on the results of our observations and proposed theories.

Keywords: Sporadic-E, GPS, TEC

Japan Geoscience Union Meeting 2014
(28 April - 02 May 2014 at Pacifico YOKOHAMA, Kanagawa, Japan)

PEM36-P23 Room:Poster Time:April 28 18:15-19:30

GPS-TEC observation using two-frequency software receiver

ASHIHARA, Yuki[1*] ; KOMATSU, Kazuki[1]

[1]Dept. of Electrical Engineering, Nara National College of Technology

Global Positioning System (GPS) is a high accuracy positioning system that uses radio waves transmitted from several GPS satellites. The carrier signals of GPS satellites, there are two frequencies of L1 (1575.42MHz) and L2 (1227.60MHz). In the ionospheric plasma, the refractive index depends on the electron density. In addition, since the plasma is dispersive medium, each of L1 and L2 waves has different refractive indexes. Therefore, it is occurred propagation delay time (phase difference) in between these signals.

GPS-TEC (GPS Total Electron Contents) is a method to obtain the total electron contents along the line of satellite (LOS) from the phase difference between these signals. GPS-TEC is very useful technique to observe ionospheric electron density, but two-frequency GPS receiver is very expensive. Therefore, GPS-TEC has calculated by using GEONET data in most cases in Japan.

In the informatics and communication field, software receiver is being widely for demodulating the baseband signal, as a background of higher performance of computers. In this study, we build a software GPS receiver system, and receive the two-frequency signals. And we will evaluate the GPS-TEC data obtained by this observation.

Keywords: ionosphere, GPS-TEC, software receiver

Japan Geoscience Union Meeting 2014
(28 April - 02 May 2014 at Pacifico YOKOHAMA, Kanagawa, Japan)

PEM36-P24 Room:Poster Time:April 28 18:15-19:30

Total electron content observation by using GPS, QZSS and BeiDou

KINUGASA, Natsuki[1*] ; TAKAHASHI, Fujinobu[1]

[1]Yokohama National University

There are several methods for observation of total electron content (TEC). TEC can be obtained from the measurement of global navigation satellite system (GNSS) such as GPS. Recently, RNSS (regional navigation satellite system) has been developed in China and Japan. We are trying to use RNSS for TEC observation.

RNSS makes TEC observation stable since a satellite is tracked continuously for long time. It is of benefit to study of plasmasphere because the altitude is higher than GNSS. There is also drawback. Since the direction of vector from grand receiver to satellite is not so variable, it is hard to observe the horizontal electron density distribution of ionosphere. This problem can be solved by combining with measurements of RNSS and GNSS. That is called multi-GNSS.

TEC can be caluculated from the difference of delay between dual-frequency. The inter-frequency bias which remain in TEC measurement are required to estimated and removed. We will present model of ionospheric electron density distributionfor the bias estimation procedure. We have constructed the observation system for GPS, Japanese QZSS, and Chinese BeiDou in Yokohama National University. Various observational results will be shown and discussed.

Keywords: TEC, QZSS, BeiDou, GPS, ionosphere, plasmasphere

Japan Geoscience Union Meeting 2014
(28 April - 02 May 2014 at Pacifico YOKOHAMA, Kanagawa, Japan)

PEM36-P25 Room:Poster Time:April 28 18:15-19:30

Total Electron Content prediction model over Japan using an artificial neural network

NISHIOKA, Michi[1*] ; TSUGAWA, Takuya[1] ; MARUYAMA, Takashi[1] ; ISHII, Mamoru[1]

[1]National Institute of Information and Communications Technology

Forecasting Total Electron Content (TEC) is important for Space Weather; for predicting propagation delay of the radio waves in the ionosphere. Although several empirical and theoretical models have been developed, no model is available for forecasting TEC over Japan. Our purpose is to accomplish an operational TEC model over Japan using an artificial neutral network (ANN) technique which is developed by Maruyama [2007]. In our model, absolute TEC values for each day from 27^{o}N to 45^{o}N in latitude and 127^{o}E to 145^{o}E in longitude were projected on a two-dimension TEC map, that is, a local-time and latitudinal map. Then the time-latitudinal variation was fitted by using the surface harmonic function. The coefficients of the expansions were modeled by using a neural network technique. For the learning process, we used absolute TEC value from 1997 to 2013. The input parameters are proxies of the season, the solar activity, and the geomagnetic activity. Thus, daily two-dimensional TEC maps can be obtained for any day when the input parameters are provided. We used input parameters which are available in real-time by some institutes and achieved one-day TEC prediction over Japan.

Keywords: Ionosphere, Total Electron Content, Operational model, artificial neural network

Japan Geoscience Union Meeting 2014
(28 April - 02 May 2014 at Pacifico YOKOHAMA, Kanagawa, Japan)

PEM36-P26 Room:Poster Time:April 28 18:15-19:30

Statistical Analyses of Ionospheric Storms Over 50 Years In Japan

NAKAMURA, Maho[1*] ; KAMOGAWA, Masashi[1]

[1]Dpt. of Phys., Tokyo Gakugei Univ.

Statistical analyses of the ionospheric storms over Japan are carried out based on the long-term observations over 50 years in Japan. While there are many types of ionospheric variations such as ionospheric storms, plasma bubbles, TIDs and so on, ionospheric storms are most large fluctuations of electron density in the ionosphere. In general, the increase of the electron density is termed positive storm and the decrease of it is termed negative storm [1]. The positive storms cause satellite-positioning errors due to the delay of radio propagation and negative storms cause HF radio communication outages due to lowering the maximum usable frequency. Because these two types of ionospheric storms shows different characteristics on the duration, scale, and the seasonal dependences, we analyzed ionospheric storm occurrences using critical frequency of the F2 layer; foF2 obtained from ionograms over 4 observation sites (Wakkanai, Kokubunji, Yamagawa, and Okinawa) operated by National Institute of Information and Communications Technology, Japan (NICT) [2]. We extracted ionospheric storms based on the differences between the daily observation values and the one-month median in Japan for more than 50 years. Extracted storms of each station will be analyzed by the occurrences, duration, seasonal dependence and geomagnetic variations.

References
[1] G. W. Prolss, Ionospheric F-region storms, Vol. 2 of Hand book of Atmospheric Electro- dynamics, CRC Press, 1995.
[2] World Data Center for Ionosphere, http://wdc.nict.go.jp/.

Keywords: ionospheric storms, eritical frequency F2 layer, satelite navigation

Japan Geoscience Union Meeting 2014
(28 April - 02 May 2014 at Pacifico YOKOHAMA, Kanagawa, Japan)

PEM36-P27 Room:Poster Time:April 28 18:15-19:30

Statistical analysis of the Speckle applying the ”Hinode” / XRT

YAMADA, Masanori[1*] ; NOZAWA, Satoshi[1] ; SHIMIZU, Toshifumi[2]

[1]Graduate School of Science and Engineering, Ibaraki University, [2]Institute of Space and Astronautical Science, Japan Aerospace Exploration Agency (ISAS/JAXA)

“ When a charge-coupled device (CCD) image is taken, white noise will appear identically main CCD image. For examlpe, the trajectory of noise is watched like scar, small spot and snowstorm, which is call as spike, unwanted signal, and so on. In this study, noise is called “ Speckle ” . The speclke is due to the particle nature of photon when CCD is hitted by Solar Energitc Particle(SEP) or cosmic ray.
SEPs have high energy of 10 keV - 10 GeV, which are generated by solar flare, coronal mass ejection(CME). This reason is that SEP plays an important role in space weather. When SEPs with hige energy of GeV order will come to earth magnetosphere, low earth orbit (LEO) stellite would be damaged the potential of single events like SEPs effect.

For this reason, this study analyzed Hinode / X-Ray Telescope (XRT) images and detected speckles. Analysis period is from January 2011 to July 2013. As a result speckles were periodic fluctuations and significant increased, when on 00:04 UT March 7 2012, X5.4 Flare occurred.
Number of detected speckles had a time zone is 3 or 4 times as high as before the occurrence of the Flare. In addition periodic fluctuations are synchronized with orbital period. Moreover information of the satellite orbit indicates speckles increases over the High Latitude Zone (HLZ). Although this is suggested SEPs flow in HLZ, there is a region with high geomagnetic latitude, so speckles are caused by charged particles of non-SEPs.

This study reports on detailed consequence. Besides it looks at the correlations between decrease or increase in speckles and information of the satellite orbit or solar activity.

Keywords: Space Weather, SEP, Flare, CME, Hinode/X-Ray Telescope(XRT)

Japan Geoscience Union Meeting 2014
(28 April - 02 May 2014 at Pacifico YOKOHAMA, Kanagawa, Japan)

PEM36-P28 Room:Poster Time:April 28 18:15-19:30

Seasonal-longitudinal dependence of the occurrence of equatorial plasma bubbles obserbed by ISS-IMAP

TAKAHASHI, Akira[1*] ; NAKATA, Hiroyuki[1] ; TAKANO, Toshiaki[1] ; SAITO, Akinori[2]

[1]Chiba University, [2]Kyoto University

Equatorial plasma bubbles (EPBs) are local depletions of the electron density in the ionosphere. Ionospheric irregularities are included in EPBs and cause radio signal scintillation. Recently, reseach on applying GNSS to Air Navigation System has progressed, therefore, it becomes more necessary to investigate the generation mechanism and the morphology of EPBs.

In this study, we analyzed seasonal-longitudinal dependence of the occurrence of EPBs using airglow-images obtained by ISS-IMAP (Ionosphere, Mesosphere, upper Atmosphere, and Plasmasphere mapping).In 630-nm airglow images, EPBs are visualized as black lines. 181 events are selected during 2012/09 - 2013/08. To calculate the longitudinal denpendence of occurence rate, we divide the ionosphere into 36 longitude bins, each 10 degrees wide. Since EPBs are observed at low and middle latitude, the total obserbation time is accumlated when |latitude| $<$30. We calculate the occurrence rate as the number of EPBs detected over the total observation time.

The occurrence rate is high at the African-Atlantic-American regeions in the equinoctial seasons. On the other hand, the occurance rate is also high at American-Pacific resions in summmer, which is not obtained in the previous study, Burke et al. [2004], in which EPBs are detected using plasma density data on DMSP satellite. The altitude of DMSP is 840 km, which is higher than the observation altitude of ISS-IMAP, that is about 250 km. Therefore, it is conceivable that the difference of occurrence rate of EPB is due to the altitude of the observations. This imply that ISS-IMAP observation could detect EPBs not developed to higher altitude.

Based on above, we will present seasonal-longitudinal variability of the Rayleigh-Taylor instability growth rate, contributing the development of EPBs using ionosphere model and other observational data.

Keywords: Equatorial ionosphere, Plasma bubble, airglow, ISS-IMAP

Japan Geoscience Union Meeting 2014
(28 April - 02 May 2014 at Pacifico YOKOHAMA, Kanagawa, Japan)

PEM37-01 Room:414 Time:April 30 11:00-11:15

A coherent modulation of pulsating aurora at Pc5 frequency

SAKA, Osuke[1*] ; HAYASHI, Kanji[2] ; KLIMUSHKIN, Dmitri[3] ; MAGER, Pavel[3]

[1]Office Geophysik, [2]U. Tokyo, [3]Russian Academy of Sciences

Ground and satellite magnetometer observations and all-sky video images revealed that the Pc5 pulsations that occurred in 17 January 1994 showed a wide distribution in longitude from Alaska, USA (0 MLT) to the Hudson bay, Canada (11 MLT) and in latitudes from 62N (L=4.5) to 70N (L=8.5).

Auroras in all-sky image were composed of field line resonance (FLR) in higher latitudes in 67-70N and pulsating aurora (PsA) in lower latitudes in 62-67N.
It is found that the PsA, FLR, and field magnitude at the geosynchronous altitudes were all oscillated coherently at Pc5 periodicities.

We conclude that the coherent modulation of FLR and PsA are attributable to toroidally and poloidally polarized Pc5 pulsations, respectively, generated by the polarization splitting of the Alfven spectrum by the finite plasma pressures.(1), (2).

References
1. Klimushkin, D.Yu., Mager, P.N., Glassmeier, K.-H., 2004. Ann.Geophys.
2. Saka, O., Hayashi, K., Klimushkin, D.Yu, Mager, P.N., 2014. JASTP.

Keywords: Pc5 pulsations, pulsating aurora, poloidal mode

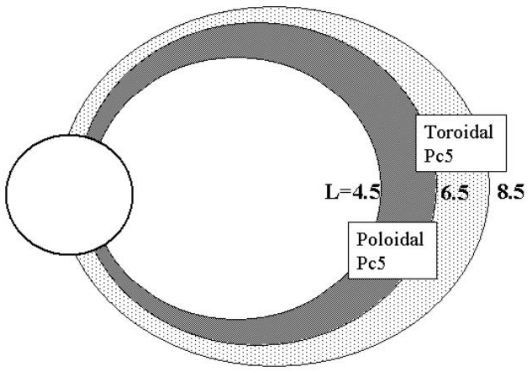

Japan Geoscience Union Meeting 2014
(28 April - 02 May 2014 at Pacifico YOKOHAMA, Kanagawa, Japan)

PEM37-02 Room:414 Time:April 30 11:15-11:30

Generation of pulsating aurora: Role of cold electron and electric field

SATO, Natsuo[1*] ; KADOKURA, Akira[1] ; TANAKA, Yoshimasa[1] ; NISHIYAMA, Takanori[1]

[1]National Institute of Polar Research

Pulsating auroras are common phenomena, which are observed universally during the recovery phase of substorm in the auroral and subauroral zones. But, even today, generation mechanism of fundamental characteristics of pulsating aurora, such as, their periodicity, their shapes, and their motion are not understood. Simultaneous observations onboard satellites and on the ground are important method to examine such fundamental characteristics of pulsating aurora. We examined some selected pulsating auroral events, which obtained onboard THEMIS spacecraft and the THEMIS ground-based all-sky camera network. THEMIS satellites were located in the post midnight sector near the equatorial plane in the magnetosphere. We found following signatures of particle, field and wave in the magnetosphere at the onset and during pulsating aurora; 1) All pulsating aurora associate with high-energy (>5 keV) electron flux enhancement, 2) Cold electron flux (<20 eV) and electric field intensity show QP (quasi-periodic) modulation in association with pulsating aurora, 3) and their QP modulation sometimes show one-to-one correspondence to QP modulation of ELF wave intensity, for both type of electromagnetic lower-band chorus wave and electrostatic ECH (electron cyclotron harmonic) wave, 4) But, not all pulsating aurora associate with ELF wave enhancement.

In this talk we focus on the event which THEMIS-A, D, E spacecraft crossed a clear boundary between strong pulsating auroral region and non-pulsating auroral region. In this strong pulsating auroral region, electric field, ULF-ELF (<300Hz) electric field waves, and cold electron flux are modulated in association with pulsating aurora, but the activity of lower-band chorus wave is very low or nothing. When the spacecraft entered into non-pulsating auroral region all of QP activity became quiet/stop. It is interesting to note that high-energy electron (>10 keV) flux was almost the same for both of the regions, but cold electron flux suddenly decreased and temperature suddenly increased when the spacecraft entered into non-pulsating auroral region. We will discuss the role of cold electron, electric field and ELF waves for the generation of pulsating aurora.

Keywords: aurora, pulsating aurora, chorus wave, magnetosphere, ionosphere, polar region

Japan Geoscience Union Meeting 2014
(28 April - 02 May 2014 at Pacifico YOKOHAMA, Kanagawa, Japan)

PEM37-03 Room:414 Time:April 30 11:30-11:45

High-resolution correlation analysis between VLF/ELF chorus waves and pulsating aurora observed at Athabasca, Canada

SUNAGAWA, Naoki[1*] ; SHIOKAWA, Kazuo[1] ; MIYOSHI, Yoshizumi[1] ; KATAOKA, Ryuho[2] ; OZAKI, Mitsunori[3] ; SAWAI, Kaoru[3] ; IAN, Schofield[4] ; MARTIN, Connors[4]

[1]Solar-Terrestrial Environment, [2]National Institute of Polar Research, [3]Kanazawa University, [4]Athabasca University

We investigate dynamic switching of arrival time difference between pulsating aurora intensity and chorus waves which were observed on 7 February 2013 at Athabasca in Canada (L=4.4), using a crossed-loop antenna and a narrow field-of-view EMCCD camera. Power spectra of pulsating auroral intensity and chorus wave intensity at 1.5-2.5 kHz show a same pulsation period at 0.1-0.15 Hz. Arrival time difference between pulsating aurora intensity and chorus waves are evaluated by using cross-correlation analysis. We found that two patterns of arrival time difference switches with a time scale of a few tens seconds. One pattern shows that electrons reached ionosphere later than the associated chorus waves with a delay time of 2 s, consistent with the theoretical value for south-going electrons reflected at the ionosphere in the southern hemisphere. The other pattern shows that electrons reached ionosphere earlier by 4.5 s than the associated chorus waves, consistent with the theoretical value for south-going chorus waves reflected at the ionosphere in the southern hemisphere. These results firstly show that interaction process of high-energy electrons and chorus waves are changing with a time scale of a few tens seconds.

Keywords: pulsating aurora, chorus waves, Wave-particle interactions, ground-based observation

Japan Geoscience Union Meeting 2014
(28 April - 02 May 2014 at Pacifico YOKOHAMA, Kanagawa, Japan)

PEM37-04 Room:414 Time:April 30 11:45-12:00

Relativistic electron precipitations in association with diffuse aurora

KURITA, Satoshi[1*] ; KADOKURA, Akira[2] ; MIYOSHI, Yoshizumi[3] ; SATO, Yuka[2] ; MISAWA, Hiroaki[1] ; MORIOKA, Akira[3]

[1]Tohoku Univ., [2]National Institute for Polar Research, [3]STEL, Nagoya Univ.

It has been widely thought that diffuse auroras are generated by electron precipitations in the energy range from a few keV to tens keV. Recent simulation results based on the quasi-linear theory showed that the scattering by whistler-mode waves plays an important role in the production of precipitating electrons responsible for diffuse auroras. A test particle simulation on electron-whistler interactions shows that relativistic electrons can be scattered into the loss cone simultaneously with the electrons in the energy range from a few keV to tens keV. Thus, it is expected that relativistic electrons precipitate into the atmosphere in association with diffuse auroras if whistler-mode waves contribute to generation of diffuse auroras. To examine this hypothesis, we investigated conjugate observations of SAMPEX and the all sky camera at Syowa Station on the dawn side, where diffuse auroras are frequently observed. In this study, we show a case study that relativistic electron ($>$1 MeV) precipitations observed by SAMPEX are associated with the diffuse aurora observed at Syowa Station. The SAMPEX observation shows that the enhancement of precipitating relativistic electrons are well correlated with that of precipitating $>$150 keV electrons, indicating that electrons in the energy range from a few keV to 1 MeV precipitate into the atmosphere simultaneously. It is observational evidence that whistler mode waves contribute to generation of diffuse auroras.

Keywords: diffuse aurora, whistler mode wave, relativistic electron, radiation belts, wave-particle interaction

Japan Geoscience Union Meeting 2014
(28 April - 02 May 2014 at Pacifico YOKOHAMA, Kanagawa, Japan)

PEM37-05 Room:414 Time:April 30 12:00-12:15

Refilling of Plasmasphere

WATANABE, Shigeto[1*]

[1]Hokkaido University

Satellite observations have revealed that ions are heated in the ionospheric polar region and are flowing to the magnetosphere. The fluxes of H+, He+, and O+ are ˜1011 ions m-2 s-1, ˜1011 ions m-2 s-1, ˜1010 ions m-2 s-1, ˜1010 ions m-2 s-1 during the solar maximum and ˜1010 ions m-2 s-1, ˜109 ions m-2 s-1, ˜109 ions m-2 s-1 near the solar minimum condition, respectively. The large amount of ions, including heavy ions such as O+, contributes the refilling of plasmasphere and inner magnetosphere. The ions are formed often as conics / transversely accelerated ion in the topside polar ionosphere. To understand the refilling process, the refilling time scale and the effects to the structure and dynamics of plasmasphere and inner magnetosphere, we have developed a three dimensional model of Atmosphere ? Plasmasphere including Electrodynamics (APE model). The model calculates densities, velocities and temperatures for electron, O2+, N2+, NO+, O+, He+ and H+ at altitudes from 90 km to 10 Re and for N2, O2, O, He and H in the thermosphere, and electric fields in the ionosphere, plasmasphere and inner magnetosphere. We calculate also parallel and perpendicular components of ion and electron temperatures to include the effect of perpendicular heating of ion in the polar ionosphere. The results show clearly the importance of ion heating in the polar region for the structure of plasmasphere, the refilling and the response to the magnetic disturbance.

Japan Geoscience Union Meeting 2014
(28 April - 02 May 2014 at Pacifico YOKOHAMA, Kanagawa, Japan)

PEM37-06 Room:414 Time:April 30 12:15-12:30

M/Q=2 Ion Cyclotron Whistlers Observed by Akebono

MATSUDA, Shoya[1*] ; KASAHARA, Yoshiya[1] ; GOTO, Yoshitaka[1]

[1]Kanazawa University

It is well known that lightning whistler wave is caused by lightning discharge, and propagates along geomagnetic field lines as R-mode plasma wave below several tens kHz. Ion cyclotron whistler wave, which is one of Electromagnetic Ion Cyclotron (EMIC) mode waves, has close relation to lightning whistler [1]. One of most important features is the lowest frequency of ion cyclotron whistler which denotes the local crossover frequency of the EMIC mode wave. R-mode lightning electron whistler is converted into L-mode ion cyclotron wave at local crossover frequency between electron whistler and ion cyclotron branches along the propagation path. Propagation characteristics of ion cyclotron whistler strongly depend on ion concentrations in plasma as well as nature of general EMIC waves. These facts suggest that we can estimate ion species and concentrations at observation point and/or along the propagation paths of the ion cyclotron whistlers.

Watanabe at al. [2] reported first observation of M/Q=2 ion cyclotron whistler measured by the ISIS-2 satellite. According to their analysis, M/Q=2 ion cyclotron whistlers were observed at an altitude region around 1,360 km. They suggested that these M/Q=2 ion cyclotron whistlers are caused by deuterons (D^+) from ionosphere of the Earth, and they named them ”deuteron whistlers”.

In the current study, we report M/Q=2 ion cyclotron whistlers observed by the Akebono satellite at an altitude region around 4,500 km, which is the highest altitude where M/Q=2 ion cyclotron whistlers were observed so far. We found that these events had obvious frequency gap near the cyclotron frequency at half of cyclotron frequency of H^+. Hence, these events are precious evidence that some amount of M/Q=2 ion exists in the inner magnetosphere.

In this paper, we study ion concentration in the inner magnetosphere estimated from crossover frequencies of ion cyclotron whistlers observed by Akebono. Recently, it is pointed out that wave-particle interaction is important process to control innermagnetospheric physics. Our results become prior information of future satellite mission such as ERG [3] in the inner magnetosphere and/or simulations such as ray tracing method.

[1]Gurnett, D. A., S. D. Shawhan, N. M. Brice, and R. L. Smith (1965), Ion cyclotron whistlers, *J. Geophys. Res.*, 70(7), 1665-1688, doi:10.1029/JZ070i007p01665.

[2]Watanabe, S., T. Ondoh (1975), Deuteron whistler and trans-equatorial propagation of the ion cyclotron whistler, *Planet. Space Sci.*, vol. 24, 359-364.

[3]Miyoshi, Y., Ono, T., Takashima, T., Asamura, K., Hirahara, M., Kasaba, Y., Matsuoka, A., Kojima, H., Shiokawa, K., Seki, K., Fujimoto, M., Nagatsuma, T., Cheng, C.Z., Kazama, Y., Kasahara, S., Mitani, T., Matsumoto, H., Higashio, N., Kumamoto, A., Yagitani, S., Kasahara, Y., Ishisaka, K., Blomberg, L., Fujimoto, A., Katoh, Y., Ebihara, Y., Omura, Y., Nose, M., Hori, T., Miyashita, Y., Tanaka, Y.-M. and Segawa, T. (2013) The Energization and Radiation in Geospace (ERG) Project, in *Dynamics of the Earth's Radiation Belts and Inner Magnetosphere* (eds D. Summers, I. R. Mann, D. N. Baker and M. Schulz), American Geophysical Union, Washington, D. C.. doi: 10.1029/2012GM001304

Keywords: ion cyclotron whistler, M/Q=2 ion, EMIC wave, Akebono satellite

Japan Geoscience Union Meeting 2014
(28 April - 02 May 2014 at Pacifico YOKOHAMA, Kanagawa, Japan)

PEM37-07 Room:414 Time:April 30 12:30-12:45

Sub-packet structures in the EMIC triggered emission observed by the THEMIS probes

NAKAMURA, Satoko[1*] ; OMURA, Yoshiharu[2] ; SHOJI, Masafumi[3] ; NOSE, Masahito[4]

[1]Department of Geophysics, Graduate School of Science, Kyoto University, [2]Reserach Institute for Sustainable Humanosphere, Kyoto University, [3]Solar-Terrestrial Environment Laboratory, Nagoya University, [4]Graduate School of Science, Kyoto University

We analyse Electromagnetic Ion Cyclotron (EMIC) triggered emission by the data from the THEMIS probes. These phenomena have recently received much attention because of the possibility of their strong interaction with energetic particles in the inner magnetosphere in spite of their scarceness in observations[1,2,3]. For 1400-1445 UT on 9 September 2010, THEMIS A, D and E observed strong EMIC waves with rising tone emissions. The probes were located near the dayside magnetopause at 8 R_E of the radial distance from the Earth, 13 MLT, and a few degrees of the geomagnetic latitude. During this time interval, the geomagnetic field was very distorted by the variation in the solar wind. We assume these emissions were excited around minimum-B pockets in accordance with the magnetospheric compression. It is found the rising tone emissions comprise of some smaller rising tones, which are called ”sub-packet structures”[4]. We compare these observed sub-packet structures with the nonlinear wave growth theory developed by Omura et al. [5]. The observed relationship between the amplitudes and frequencies of the emissions are well explained by the theory, and it is also found that the threshold and optimum amplitudes for the nonlinear growth agree well with the observed dynamic spectra.

[1]Pickett, J. S., et al. (2010), Cluster observations of EMIC triggered emissions in association with Pc1 waves near Earth’s plasmapause, Geophys. Res. Lett., 37 (9), doi: 10.1029/2010GL042648.

[2]Shoji, M., and Y. Omura (2012), Precipitation of highly energetic protons by helium branch electromagnetic ion cyclotron triggered emissions, J. Geophys. Res., 117 (A12), doi:10.1029/2012JA017933

[3]Omura, Y., and Q. Zhao (2012), Nonlinear pitch angle scattering of relativistic electrons by EMIC waves in the inner magnetosphere, J. Geophys. Res., 117 (A8), doi:10.1029/2012JA017943.

[4]Shoji, M., and Y. Omura (2013), Triggering process of electromagnetic ion cyclotron rising tone emissions in the inner magnetosphere, J. Geophys. Res. Space Physics, 118, 5553?5561, doi:10.1002/jgra.50523.

[5]Omura, Y., J. Pickett, B. Grison, O. Santolik, I. Dandouras, M. Engebretson, P. M. E. Decreau, and A. Masson (2010), Theory and observation of electromagnetic ion cyclotron triggered emissions in the magnetosphere, J. Geophys. Res., 115 (A7), doi:10.1029/2010JA015300.

Japan Geoscience Union Meeting 2014
(28 April - 02 May 2014 at Pacifico YOKOHAMA, Kanagawa, Japan)

PEM37-08 Room:414 Time:April 30 14:15-14:30

Statistical analysis of ionospheric Pi2 pulsations observed at mid and low latitude by the SuperDARN Hokkaido radar

TERAMOTO, Mariko[1*] ; NISHITANI, Nozomu[2]

[1]JAXA, ISAS, [2]Solar-Terrestrial Environment Laboratory, Nagoya University

Ultra-low-frequency waves with the periods of 40-150 s are categorized as Pi2 pulsations, which occur over a wide rage of latitude in the night side at substorm onsets. To identify the generation mechanism of Pi2 pulsations, a number of studies using different devices such as ground-based magnetometers and satellites have been carried out. These study provide spatial properties of Pi2 pulsations on the ground and in the inner magnetosphere and suggested that high- and mid-latitude Pi2 pulsations are associated with Alfven waves in the auroral region, while the cavity mode resonance established in the plasmasphere by the fast mode waves has been proposed as a possible Pi2 source at mid and low latitudes.

The interaction of Pi2 pulsations with the ionosphere creates current systems that modify the amplitude and spatial scale size of the waves. In order to construct a coherent view of Pi2 signals measured by ground-based magnetometers, radars and satellites, the effect of the ionosphere needs to be understood.

In present study, statistical studies of Pi2 pulsations in the ionosphere were performed with the SuperDARN Hokkaido radar at Rikubetsu (AACGM magnetic coordinates: 36.5○, 214.7○). The radar can observe the Doppler velocity of ionospheric plasma due to the electric field of Pi2 pulsations in the mid- and low-latitude ionosphere. We investigated the spatial characteristics of the similarity, amplitude ratio, and cross phase between Pi2 pulsations observed by the radar and a ground magnetometer Memanbetsu (MMB) which is located close to the radar site. We will present the results and discuss the interaction of Pi2 pulsations with the ionosphere.

Japan Geoscience Union Meeting 2014
(28 April - 02 May 2014 at Pacifico YOKOHAMA, Kanagawa, Japan)

PEM37-09 Room:414 Time:April 30 14:30-14:45

Pi pulsations in the near-earth magnetotail at substorm onset

SAKURAI, Tohru[1*] ; KADOKURA, Akira[2] ; TANAKA, Yoshimasa[2] ; SATO, Natsuo[2]

[1]Tokai University, [2]National Institute of Polar Research

The THEMIS satellite observations showed that Pi 1 and Pi 2 period range oscillations of the magnetic and electric fields play an important role at a substorm onset in the near-Earth magnetotail. They associated energetic particle accelerations toward the inner magnetosphere. The energetic particle accelerations were observed with very similar oscillation signatures to the Pi 1 and Pi 2 period range oscillations observed in the magnetic and electric fields.. This observation suggests that the Pi 1 and Pi 2 period range oscillations might play an important role for contribution to the auroral particle accelerations at substorm onset in the near-Earth magnetotail . The examination has been done on a substorm event observed on 28 February, 2009 at a THEMIS GBO station, Kuujjuaq (KUUJ) (Mag. Lat.=66.89 N, Mag. Lon.=13.23 E, Mag. Midnight =4.15 UT, L-value = 6.4) in the west coast at the high latitude of the North America Continent. This substorm event was simultaneously observed in the near-Earth magnetotail by the three THEMIS satellites, THEMIS-A, -E, and ?D located in the midnight region at ˜8 Re, ˜8 Re and ˜11 Re, respectively. The data examined in this study are the magnetic field, all-sky images (ASI) and keograms (ASK) obtained at KUUJ and the satellite observations of the magnetic field, electric field, and the electron and ion energy spectra in the ESA peir, and peer data. The results show very interesting facts of the Pi 1 and Pi 2 period range oscillations in the magnetic field and auroral activities observed on the ground and their conjunctions of the magnetic, electric fields, and the associated accelerated particles in the near-Earth magnetotail. The implication of this work provides the importance of the Pi 1 and Pi 2 period range oscillations for controlling the substorm onset plasma processes in the near-Earth magnetotail.

Keywords: Magnetospheric Physics, Substorm, Pi pulsations

Japan Geoscience Union Meeting 2014
(28 April - 02 May 2014 at Pacifico YOKOHAMA, Kanagawa, Japan)

PEM37-10 Room:414 Time:April 30 14:45-15:00

Substorm onset process: Ignition of auroral acceleration and related substorm phases

MORIOKA, Akira[1*] ; MIYOSHI, Yoshizumi[2] ; KASABA, Yasumasa[3] ; SATO, Natsuo[4] ; KADOKURA, Akira[4] ; MISAWA, Hiroaki[1] ; MIYASHITA, Yukinaga[2]

[1]PPARC, Tohoku University, [2]STEL, Nagoya University, [3]Dep. of Gephys. Tohoku University, [4]NIPR

The substorm onset process was studied on the basis of the vertical evolution of auroral acceleration regions derived from auroral kilometric radiation (AKR) spectra and Pi pulsations on the ground. The field-aligned auroral acceleration at substorm onset demonstrated two distinct phases. Low-altitude acceleration (h˜3000-5000 km), which accompanied auroral initial brightening, pre-breakup Pi2, and direct current of ultra-low frequency (DC-ULF) pulsation, was first activated and played an important role (pre-condition) in the subsequent substorm expansion-phase onset. Pre-breakup Pi 2 is suggestive of the ballooning-mode wave generation, and negative decrease in DC-ULF suggests increasing field-aligned current (FAC). We called this stage the substorm initial phase. A few minutes after this initial phase onset, high-altitude acceleration, which accompanied auroral breakup and poleward expansion with breakup Pi 1 and Pi 2 pulsations, suddenly broke out in an altitude range from 8000-16000 km. Thus, substorm expansion onset originated in the magnetosphere-ionosphere (M-I) coupling region, i.e., substorm ignition in the M-I coupling region. It is suggested that current disruption and subsequent violent energy release from the tail region take place after this ignition. Statistical investigations revealed that about 65% of earthward flow bursts observed in the plasma sheet were accompanied by enhanced low-altitude AKR, suggesting that flow braking of bursts causes FAC and resulting low-altitude field-aligned acceleration in the M-I coupling region. On the basis of these observations, we propose a substorm onset scenario in which FAC that originated from the braking of plasma flow bursts first enhances low-altitude acceleration (substorm initial phase onset), and then the increasing FAC induces current-driven instability in the M-I coupling region, which leads to high-altitude acceleration and resulting substorm expansion-phase onset.

Keywords: substorm, aurora, acceleration region, substorm onset

Japan Geoscience Union Meeting 2014
(28 April - 02 May 2014 at Pacifico YOKOHAMA, Kanagawa, Japan)

PEM37-11 Room:414 Time:April 30 15:00-15:15

drivers of the magnetospheric convection

FUJITA, Shigeru[1*] ; TANAKA, Takashi[2]

[1]Meteorological College, [2]Kyushu University

We present here the role of the plasma bulk flow in generation of the magnetosphere-ionosphere convection. Traditionally, the magnetospheric convection is studied with the perpendicular flow because this flow is equivalent with the speed of migration of the magnetic field. For example, the perpendicular force balance equations are utilized in discussion of the dynamo generation ($E*J<0$) in the cusp-mantle region [Tanaka, 1995]. However, since the plasma kinetic energy flux and the internal energy flux are transported along the plasma bulk flow, it is evident that the plasma bulk flow should be considered in generation of the magnetospheric convection. In
addition, the global MHD simulation reveals that the plasmas are accelerated into the cusp from the magnetosheath along the magnetic field. Thus, the plasma bulk flow transports energy into the magnetosphere.

At first, we discuss the dynamo in the cusp-mantle region based on the full set of physical principles (mass conservation, momentum conservation, and energy conservation). As a result, the load in the lower-latitude side of the cusp is invoked by plasma compression due to sudden deceleration of the field-aligned flow from the magnetosheath. The adiabatic assumption invokes pressure enhancement associated with plasma compression. Thus, energy should be supplied to compensate increase in the plasma pressure. As the kinetic energy is much smaller than the electromagnetic energy in the magnetosphere, the electromagnetic energy is converted to the thermal energy. Therefore, the load appears in the lower-latitude side of the cusp. On the other hand, in the cusp-mantle region, plasmas are squeezed with the field-aligned flow toward the lobe region. This yields plasma rarefaction, which eventually invokes energy conversion from the thermal energy to the electromagnetic energy. Thus, the dynamo appears. This process is also explained in terms of the slow mode expansion fan in the cusp-mantle region.

Next, we define an unique magnetospheric energy convection in the dayside magnetosphere. It is noted that the Poynting flux activated in the cusp-mantle region is transported across the dayside magnetosphere to the dayside magnetopause. The electromagnetic energy is totally deposited here. The deposited electromagnetic energy is converted into the thermal energy in the magnetopause. Then we need a mechanism of transporting this thermal energy elsewhere. The MHD simulation shows the thermal energy and the high-speed solar-wind kinetic energy are transported into the cusp from the magnetosheath. This flow goes to the mantle region. Then, the thermal energy transported from the magnetosheath via the cusp is partially converted into the electromagnetic energy in the cusp-mantle region. Finally, the loop of energy convection is completed.

The magnetospheric energy convection is unique because the energy convection and the mass convection show quite different behavior. On the other hand, in the normal fluid like the atmosphere, the energy convection is related to the mass convection in the atmospheric global circulation (convection).

Keywords: magnetospheric convection, MHD simulation, bulk flow, energy conversion, magnetospheric energy convection, cusp dynamo

Japan Geoscience Union Meeting 2014
(28 April - 02 May 2014 at Pacifico YOKOHAMA, Kanagawa, Japan)

PEM37-12 Room:414 Time:April 30 15:15-15:30

Sudden pressure enhancement and tailward retreat in the near-Earth plasma sheet: THEMIS observation and MHD simulation

YAO, Yao[1*] ; EBIHARA, Yusuke[1] ; TANAKA, Takashi[2]

[1]Research Institute for Sustainable Humanosphere, Kyoto University, [2]SERC, Kyushu University

Plasma pressure enhancement is one of the drastic substorm-associated phenomena in the inner magnetosphere. In a substorm occurred on 1 March 2008, four of THEMIS (Time History of Events and Macroscale Interactions during Substorms) probes were almost aligned along the sun-Earth line, which was suitable for investigating spatial-temporal evolution of the near-Earth plasma sheet in a substorm. They observed a sudden increase in the plasma pressure at the inner probe (at ∼7.2 Re), followed by the outer probes (at ∼7.5, ∼8.3, and ∼10.4 Re), that is the high pressure region propagates tailward. Hereinafter, we call this sudden pressure enhancement (SPE). We compared the observations with simulation results of a global magnetohydrodynamics (MHD) simulation, and found a fairly good agreement between them in terms of the followings. (1) Tailward propagation of the SPE can be seen only at off-equator after the substorm onset. In the equatorial plane, an earthward propagation of the SPE precedes the tailward propagation. (2) Observations from the three inner probes show that the SPE consists of two enhancements. The first one is attributed to the convergence of bulk flow energy flux, namely flow braking. The latter one is due to the convergence of the thermal energy flux and subsequent inflation of the plasma sheet. (3) Plasma flow turned from the tailward-and-toward-the-equatorial-plane to earthward-and-away-from-the-equatorial plane near the onset from the simulation results. We discuss the spatial-temporal evolution of the plasma flow and the magnetic field during the substorm.

Keywords: substorm, THEMIS observation, Global MHD simulation, Sudden pressure enhancement

Japan Geoscience Union Meeting 2014
(28 April - 02 May 2014 at Pacifico YOKOHAMA, Kanagawa, Japan)

PEM37-13 Room:414 Time:April 30 15:30-15:45

Evolution of theta aurora during strong positive IMF Bz and varying IMF By condition

OBARA, Takahiro[1*]

[1]PPARC, Tohoku University

Formation of the theta aurora, which appears under the condition of northward IMF and greater IMF magnitude, is investigated from the analysis of the numerical MHD simulation. The theta aurora is caused by the transient convection after a sign change of IMF By. This transient convection must include a replacement of lobe field lines from old IMF orienting fields, a rotation of plasma sheet to opposite inclination, and a reformation of ionospheric convection cells. In the midst of these reconfigurations, old and new convection system must coexist in the magnetosphere-ionosphere system. In this stage, the polar cap and tail lobes are continuously encroached by the new open field lines connected to the new IMF. Whereas magnetic field lines accumulated in new lobes tend to rotate the outer plasma sheet in the opposite direction, the old merging cell convection still continues to generate closed field lines that must return to dayside against the new lobe formation. As time progresses, the growth of new lobes results in the blocking of the return path toward dayside of closed field lines generated in the old merging cell to form the kink structure in the plasma sheet. Losing their return path, these closed field lines generated from old lobes accumulated on the night side. The theta aurora appears at the foot point of these accumulated closed field lines. In the presentation, we will demonstrate some observational results brought by satellites and ground based instruments, which support above mentioned hypothesis for theta aurora foramation.

Keywords: IMF, Strong northward IMF, Varying IMF By, Theta aurora, Simulation, Observation

Japan Geoscience Union Meeting 2014
(28 April - 02 May 2014 at Pacifico YOKOHAMA, Kanagawa, Japan)

PEM37-14 Room:414 Time:April 30 15:45-16:00

Substorm Onset: Correlation between Ground and Space Observations

CHENG, Chio[1*] ; CHANG, T. F.[2]

[1]Plasma and Space Science Center, National Cheng Kung University, [2]Institute of Space and Plasma Sciences, National Cheng Kung University

The observations of substorm onset phenomena in the magnetosphere and ionosphere are examined to study their correlation and to understand the substorm onset mechanism. In particular, we examine the Pi2 wave structure, propagation, frequency and growth rate in the magnetosphere observed by the THEMIS satellites in the near-Earth plasma sheet and the structure and propagation of the substorm auroral onset arcs. We show the correlation between the substorm onset wave-like arcs and the Pi2 pulsations in terms of wave structure, propagation, and the exponential growth of arc intensity and Pi2 wave amplitude. In particular, the azimuthal mode numbers of the Pi2 waves and the wave-like arc structure are estimated to be ˜100-200. The correlation between the ground and space phenomena strongly supports the kinetic ballooning instability (KBI) as the cause of substorms. KBI is the most natural mechanism for explaining the unstable Pi2 waves in the strong cross-tail current region and the KBI parallel electric field can accelerate electrons along the magnetic field lines into the ionosphere to produce the substorm onset wave-like arcs.

Keywords: substorm, magnetospheric dynamics, THEMIS observation

Japan Geoscience Union Meeting 2014
(28 April - 02 May 2014 at Pacifico YOKOHAMA, Kanagawa, Japan)

PEM37-15 Room:414 Time:April 30 16:15-16:30

Investigation of substorm triggering mechanism based on THEMIS data

MACHIDA, Shinobu[1*] ; MIYASHITA, Yukinaga[1] ; IEDA, Akimasa[1] ; ANGELOPOULOS, Vassilis[2] ; MCFADDEN, James P.[3]

[1]Solar-Terrestrial Environment Laboratory, Nagoya University, [2]IGPP/EPSS, UCLA, [3]SSL, UC Berkeley

In this study, we show the result of superposed epoch analysis on the THEMIS probe data during the period from November, 2007 to April, 2009 by setting the origin of time axis to the substorm onset determined by Dr. Toshi Nishimura based on the THEMIS all sky imager (THEMS/ASI) data. We have restricted the time interval from t = -100 sec to t = 100 sec and the region to -7.5 >X(Re) >-23, and investigated various variations associated with substorm onset.

It was confirmed that earthward flows start at t = -60 sec in the region around X = -14 Re, and then they move toward the Earth. At t = 0, the dipolarization of the magnetic field starts at X ˜-10 Re, and simultaneously the magnetic reconnection starts at X ˜-20 Re. These variations support the validity of our Catapult Current Sheet Relaxation model for substorm onset.

Interestingly, the absolute value of dawnward plasma flow velocity |Vy|decreases in the plasma sheet and the plasma sheet boundary layer during the interval -20 <t(sec) <20. By analyzing individual event of |Vy|decrease, it was confirmed that the plasma flows turn from the duskward convective flows (Vy >0) to the dawnward flows (Vy <0) on average, associated with substorm onset, so that the value of Vy once becomes to zero around t = 0. This variation was found to be related to the deflection of the flows when they encounter with the Earth's dipole magnetic field as they approach to the Earth, which is the same reason already known to cause the tailward flows around X = -10 Re when the earthward flows reach that region.

Keywords: substorm, magnetotail, magnetic reconnection, dipolarization, THEMIS probes

Japan Geoscience Union Meeting 2014
(28 April - 02 May 2014 at Pacifico YOKOHAMA, Kanagawa, Japan)

PEM37-16 Room:414 Time:April 30 16:30-16:45

Global MHD simulations of magnetosphere and 3-dimensional visualization

OGINO, Tatsuki[1*]

[1]Solar-Terrestrial Environment Laboratory, Nagoya University

A study on perpendicular and parallel current generation mechanism in the magnetosphere is important problems in interaction between the solar wind and earth's magnetosphere-ionosphere. Moreover, classification to fundamental MHD quantities and MHD modes is also essential for understandings of the mechanism. Thus we have executed a high resolution global 3D MHD simulation and a 3D graphic diagnostics.

As the solar wind and IMF becomes abnormal conditions, plasma turbulence are strongly excited near boundary layers in the magnetosphere. In the plasma sheet magnetic reconnection occurs in patchy and intermittent manner to produce streamer-like structure. At the magnetopause, more regular vortex train in association with current generation is formed for northward IMF.

Dayside reconnection occurs in patchy and intermittent manner to give seeds of plasma turbulence. As the results, complicated and strong vortex turbulence appears in flank magnetopause. We will demonstrate those phenomena from 3-dimensional visualization method of simulation results to discuss relationship between the currents and vortices in boundary layers. In particularly we will stress relationship among parallel and perpendicular components of vorticity and current, and also compressibility in order to understand the fundamental picture of magnetospheric dynamics. Moreover we will separate the fundamental MHD quantities to various MHD modes in the whole volume, which can make clear their roles on the vorticity and current generation mechanisms.

Keywords: global MHD simulation, current generation mechanism, vorticity and compressibility, roles of MHD modes, magnetic reconnection, magnetospheric dynamics

Japan Geoscience Union Meeting 2014
(28 April - 02 May 2014 at Pacifico YOKOHAMA, Kanagawa, Japan)

PEM37-17 Room:414 Time:April 30 16:45-17:00

Two-spacecraft reconstruction of a three-dimensional magnetic flux rope at the Earth's magnetopause

HASEGAWA, Hiroshi[1*] ; SONNERUP, Bengt[2] ; ERIKSSON, Stefan[3] ; NAKAMURA, Takuma[4]

[1]Institute of Space and Astronautical Science, JAXA, [2]Dartmouth College, [3]University of Colorado, [4]Los Alamos National Laboratory

We present first results of a data analysis method, developed by Sonnerup and Hasegawa [2011], for reconstructing three-dimensional (3-D), magnetohydrostatic structures from data taken as two closely spaced satellites traverse the structures. The method is applied to a flux transfer event (FTE), which was encountered on 27 June 2007 by at least three (TH-C, TH-D, and TH-E) of the five THEMIS probes and was situated between two oppositely directed reconnection jets near the subsolar magnetopause under a southward interplanetary magnetic field condition. The recovered 3-D field indicates that a magnetic flux rope with a diameter of about 3000 km was embedded in the magnetopause. The FTE flux rope obviously had a significantly 3-D structure, because the 3-D field reconstructed from the data from TH-C and TH-D (separated by 390 km) better predicts magnetic field variations actually measured along the TH-E path than does the 2-D Grad-Shafranov reconstruction [Hau and Sonnerup, 1999] using the data from TH-C (which was closer to TH-E than TH-D and was at about 1000 km from TH-E). Such a 3-D nature suggests that reconnected field lines from the two reconnection sites may have been entangled in a complicated way through their interaction with each other. The generation process of the observed 3-D flux rope is discussed on the basis of the reconstruction results and anisotropy of observed electron pitch-angle distributions.

Reference:
Hau, L.-N., and B. U. O. Sonnerup (1999), Two-dimensional coherent structures in the magnetopause: Recovery of static equilibria from single-spacecraft data, J. Geophys. Res. Space Physics, 104, 6899-6917.
Sonnerup, B. U. O., and H. Hasegawa (2011), Reconstruction of steady, three-dimensional, magnetohydrostatic field and plasma structures in space: Theory and benchmarking, J. Geophys. Res. Space Physics, 116, A09230, doi:10.1029/2011JA016675.

Keywords: magnetopause, magnetic flux rope, magnetic reconnection, magnetohydrostatic equilibrium, formation-flying observations

Japan Geoscience Union Meeting 2014
(28 April - 02 May 2014 at Pacifico YOKOHAMA, Kanagawa, Japan)

PEM37-P01 Room:Poster Time:April 30 18:15-19:30

Auroral vortex, auroral surge, and vortical current in the ionosphere associated with the Pi2 pulsations

SAKA, Osuke[1*] ; HAYASHI, Kanji[2]

[1]Office Geophysik, [2]U. Tokyo

The auroral breakup event occurred at 0500UT 27 January 1986 in central Canada is studied using all-sky video image from two optical stations (GWR and SHM) and magnetometer data from three ground stations including the optical stations.

The spatiotemporal motion of the ionospheric vortical current explained the ground magnetometer data in the auroral zone. During the activation of the current vortex, auroras composed of the shear layers rotating clockwise and the auroral surge propagating westward were observed.

It is found that the auroral surge first appeared at the onset latitudes propagated poleward passing through the auroral vortex and became the poleward boundary aurora-surge (PBAS)(1).

References
1. Saka, O., K. Hayashi, D. Koga (2012), JASTP.

Keywords: Aurora dynamics, Pi2 pulsation, Ionospheric current vortex

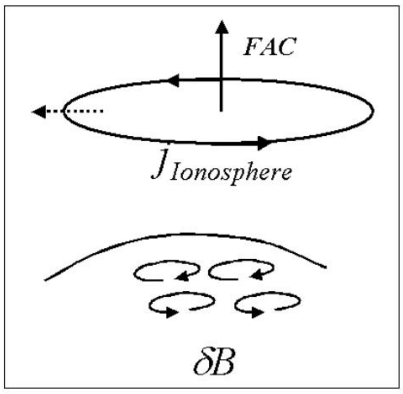

Japan Geoscience Union Meeting 2014
(28 April - 02 May 2014 at Pacifico YOKOHAMA, Kanagawa, Japan)

PEM37-P02 Room:Poster Time:April 30 18:15-19:30

Generation mechanism of steady-state field-aligned currents: A general theory in terms of plasma convection

WATANABE, Masakazu[1*]

[1]International Center for Space Weather Science and Education, Kyushu University, [2]Department of Earth and Planetary Sciences, Faculty of Sciences, Kyushu University

It is well known that field-aligned currents (FACs) play an important role in that they transfer electromagnetic energy and momentum from the magnetosphere to the ionosphere. Recent global magnetohydrodynamic (MHD) simulations indicate that in almost all cases the pressure gradient force is the major driver of FACs [Tanaka, 2003, 2007]. The inertia force becomes appreciable only in very special cases such as the preliminary impulse (PI) in sudden commencements (SCs) [Fujita et al., 2003]. Thus the pressure gradient mechanism is working universally and represents the essence of the dynamical nature of the magnetosphere. What is less or not at all understood, however, is the role of plasma convection in FAC generation. One misconception is that plasma convection is irrelevant to pressure gradient-driven FACs. In fact, convection plays a vital role in energy conversion. This paper describes a general theory of steady-state FACs, with an emphasis on the importance of plasma convection. FACs are created and maintained through the following two processes that occur spatially contiguously with each other. (1) A ”dynamo” process in which plasma thermal energy is converted to electromagnetic energy. A magnetospheric dynamo is necessary in order to sustain a steady-state FAC system. This dynamo is generated by expanding plasma flow (div($\mathbf{v}$) $>$0) that is characterized by the slow mode in MHD waves. The wave normal is directed to the $-$ grad(B) direction, and the flow speed in the wave normal direction (the ”normal” component) becomes the phase speed of the slow mode wave. Slow mode disturbances do not associate FACs. (2) A process in which field-perpendicular currents transform into field-aligned currents. This process occurs by a mode conversion of the waves from slow to Alfvenic. If the pressure gradient has a component perpendicular to both the wave normal and the magnetic field (the ”tangential” component), it produces a magnetic tension and consequently excites Alfven mode disturbances. The flow speed in the wave normal direction becomes the phase speed of the Alfven mode wave. The Alfven mode is associated with tangential plasma flow, and consequently the plasma motion becomes rotational.

References

Fujita et al. (2003), J. Geophys. Res., 108(A12), 1416, doi:10.1029/2002JA009407.
Tanaka (2003), J. Geophys. Res., 108(A8), 1315, doi:10.1029/2002JA009668.
Tanaka (2007), Space Sci. Rev., 133, 1, doi:10.1007/s11214-007-9168-4.

Keywords: field-aligned current, dynamo, convection

Japan Geoscience Union Meeting 2014
(28 April - 02 May 2014 at Pacifico YOKOHAMA, Kanagawa, Japan)

PEM37-P03 Room:Poster Time:April 30 18:15-19:30

Multi-spacecraft analysis of tailward plasma flows in the near-Earth plasma sheet : THEMIS observations

OKAMOTO, Shunichi[1*] ; TAKADA, Taku[2]

[1]Kochi National of College of Technology Department of Electrical Engineering and Information Science, [2]Kochi National of College of Technology

In the near-Earth's plasma sheet, the magnetic field is abruptly dipolarized, associated with an aurora activity. In this region, most of plasma flows are earthward, while some are tailward. Although the candidate mechanism for such tailward flow is considered as rebound flows and/or a part of vortex flows, the quantitative occurrence rate is not fully understood. In this work, we selected events that THEMIS spacecraft observed tailward flows near the magnetic dipolarization region, and then categorized in flow patterns before the tailward flows. Based on the results, we statistically analyzed the categolized events, and estimated the space structure of tailward flows by multi-spacecraft analysis. Consequently, we show the occurrence rate of such rebound flows and the vortex flows.

Keywords: Dipolarization, Tailward flow

Japan Geoscience Union Meeting 2014
(28 April - 02 May 2014 at Pacifico YOKOHAMA, Kanagawa, Japan)

PEM37-P04 Room:Poster Time:April 30 18:15-19:30

Simultaneous observation of a field-aligned current by the JAXA QZS satellite and a MAGDAS ground observatory

TAKEUCHI, Yuuto[1] ; KAWANO, Hideaki[2*] ; HIGASHIO, Nana[3] ; MATSUMOTO, Haruhisa[3] ; BAISHEV, Dmitry G.[4] ; UOZUMI, Teiji[2] ; ABE, Shuji[2] ; YUMOTO, Kiyohumi[2] ; YOSHIKAWA, Akimasa[2] ; MAGDAS/CPMN, Group[2]

[1]Department of Earth and Planetary Sciences, Kyushu University, [2]International Center for Space Weather Science and Education, Kyushu University, [3]Japan Aerospace Exploration Agency, [4]Yu.G.Shafer Inst. of Cosmophysical Research and Aeronomy, Siberian Branch, Russian Academy of Sci.

In this paper we conduct a QZS-MAGDAS conjunction study of a field-aligned current (FAC). QZS (Quasi-Zenith Satellite) is operated by JAXA, and MAGDAS is the ground magnetometer network mainly operated by ICSWSE (International Center for Space Weather Science and Education), Kyushu Univ.

There have been only limited number of papers on satellite-ground conjunction studies of FACs, because satellites usually passes overhead at a ground observatory in a short time.
On the other hand, the footpoint of QZS stays near one ground point in Siberia, Russia, because the orbit of QZS is close to that of geosynchronous satellites on the Japanese meridian. Moreover, a few Siberian MAGDAS observatories exist near the QZS footpoint.

Another advantage of QZS is that, unlike geosynchronous satellites, QZS has 41deg inclination and 0.1deg eccentricity which enable QZS to stay for a long time at northern high latitudes in the magnetosphere; this high-latitude feature increases the detectability of FACs, because the FAC magnitude is in general smaller near the equator, i.e., the FAC source region in the magnetosphere. Thus, the pair of QZS and Siberian MAGDAS is expected to have more chances of simultaneously observing the same FAC than past satellite-ground pairs.

We have been searching for events in which, when QZS and a Siberian MAGDAS observatory were located near the same field line (calculated by the Tsyganenko 96 model), QZS and MAGDAS simultaneously observed transient magnetic field perturbations.

In this paper we present such an event observed by QZS and a Siberian MAGDAS observatory CHD (Chokurdakh). We have found that the transient magnetic perturbations of this event can be interpreted to have been generated by the motion of a local current circuit consisting of line FACs and an ionospheric current. More details will be presented at the meeting.

Japan Geoscience Union Meeting 2014
(28 April - 02 May 2014 at Pacifico YOKOHAMA, Kanagawa, Japan)

PEM37-P05 Room:Poster Time:April 30 18:15-19:30

Comparison between particle environment around GEO from global MHD simulation and that from LANL satellite

NAGATSUMA, Tsutomu[1*] ; YAMAMOTO, Kazunori[1] ; KUBOTA, Yasubumi[1] ; TANAKA, Takashi[1]

[1]National Institute of Information and Communications Technology

Substorm injection is one of the important element of magnetospheric substorm, like auroral break up. Studying substorm injection is important to understand the physics of substorms. Also, substorm injection temporaly changes the particle environment around satellites at GEO. And dynamical variations of particle environment around GEO is one of the causes of satellite anomaly due to surface charging. We try to evaluate our magnetospheric global MHD simulation code by comparing output from global MHD code and LANL satellite particle data. Previous work has be done by Nakamura [2009]. We will examine the possibility of substorm injection prediction using global MHD simulation. Detailed comparison between simulation and observation will be shown in our presentation.

Keywords: Space Weather Forecast, Magnetosphere, Substorm, Modeling, Global MHD simulation, Geosynchronous orbit

Japan Geoscience Union Meeting 2014
(28 April - 02 May 2014 at Pacifico YOKOHAMA, Kanagawa, Japan)

PEM37-P06 Room:Poster Time:April 30 18:15-19:30

Energy dispersion and trajectory of particles injected from the magnetotail in magnetospheric quiet conditions

YAMAUCHI, Satoko[1*] ; NAGAI, Tsugunobu[2]

[1]Tokyo Institute of Technology, [2]Tokyo Insutitute of Technology

Particle injection is sudden enhancement in flux of energetic charged particles, commonly observed at geosynchronous orbit ($6.6R_E$), and associated with magnetospheric substorms. Since 2007, dispersive particle injections have been observed in the further dawnside of the magnetosphere ($>10R_E$) than geosynchronous orbit in quiet conditions with the spacecraft Geotail and THEMIS. Although only electron injections are observed in most cases, both electron and ion injections are observed in some cases. The injected population displays energy dispersion in which more energetic particles arrive at a given location earlier than less energetic particles. This dispersion occurs because of energy dependence of particle drift in the magnetospheric magnetic field. In order to investigate the time delay, we have calculated electron trajectories in the inner magnetosphere. We assume that the magnetospheric magnetic field is a simple dipole and the magnetospheric electric field is sum of a convection electric field and a corotation electric field, and obtain the particle trajectories in the equatorial plane using particle drift velocity. We find that the time delay is related to the intensity of the convection electric field. The simulations and observations show that electrons drift from the nightside through the dawnside to the dayside while ions drift from the nightside through the duskside to dayside. However, in the range given by the dipole field, it is not possible to explain the energy dispersion as observed. The shape of the magnetic field is different from the magnetic dipole in the magnetic tail region because the magnetosphere is stretched by the solar wind. In order to provide a more realistic magnetic field model in the magnetosphere, we use the Tsyganenko model that is an empirical magnetic field model of the magnetosphere. In this study, multi-satellite observations and test particle simulations are carried out to explore mechanisms in energization and transport of electrons in the quiet magnetosphere.

Keywords: magnetosphere, perticle injection, energy dispersive, Tsyganenko, quiet condition, trajectory

Japan Geoscience Union Meeting 2014
(28 April - 02 May 2014 at Pacifico YOKOHAMA, Kanagawa, Japan)

PEM37-P07 Room:Poster Time:April 30 18:15-19:30

Time development of the Dipolarization Front and its interactions with the dipole-field region obtained by 2-1/2 dimensi

UCHINO, Hirotoshi[1*] ; MACHIDA, Shinobu[2]

[1]Earth and Planetary Sciences Graduate School of Schience, Kyoto University, [2]Solar-Terrestrial Environment Laboratory, Nagoya University

Bursty bulk flows with increasing B_z (northward component of the magnetic field), which are caused by magnetic reconnections in the magnetotail, are called Dipolarization Front (DF). Under the picture of the Near Earth Neutral Line model, which is one of the models explaining the triggering of substorms, the compression of the dipole region by DF and the pileup of DF itself around the near-Earth plasma sheet boundary cause a wide increase of B_z in the night magnetosphere. Although there are many observational studies of DFs by spacecraft, there are no full-particle simulations that examine the case in which the DF approaches to the dipole region.

In this context, we have performed two-dimensional full-particle simulations for the initial magnetic configuration which is akin to Earth's dipole magnetic field together with a stretched magnetic field by the thin current sheet. We have generated the magnetic reconnection and earthward plasma flows accompanied by B_z, and examined the time development of the flows and the interactions with Earth's dipole-field.

In our simulations, a minimal region of the northward magnetic field where B_z does not increase have been formed between the dipole region and flux pileup region, different from the common picture of Dipolarization. The reason of this can be considered as follows; (1) the earthward flows transport and accumulate the plasmas of the current sheet around the near-Earth plasma sheet boundary, (2) the pressure of the accumulated plasmas decelerate the flow, (3) B_z piles up in the tailward of the boundary. This result is different from the common effect of the DF that it broadly increases B_z in the night side of the magnetosphere. Because of the two-dimensionality in our simulations, the accumulated plasmas cannot leave in the Y-direction (eastward), producing such characteristic region. We also discuss on the structure of the particle flow velocity and particle density distributions near the DF by comparing with observational results.

Keywords: Substorm, Dipolarization Front, Dipolarization

Japan Geoscience Union Meeting 2014
(28 April - 02 May 2014 at Pacifico YOKOHAMA, Kanagawa, Japan)

PEM37-P08 Room:Poster Time:April 30 18:15-19:30

3D Full kinetic simulations of plasma flow interaction with meso- and micro-scale magnetic dipoles

USUI, Hideyuki[1*] ; ASHIDA, Yasumasa[2] ; SHINOHARA, Iku[3] ; NAKAMURA, Masao[4] ; YAMAKAWA, Hiroshi[2] ; MIYAKE, Yohei[1]

[1]Graduate school of system engineering, Kobe University, [2]Research Institute for Sustainable Humanosphere, [3]Japan Aerospace Exploration Agency/Institute of Space and Astronautical Science, [4]Osaka Prefecture University

Plasma flow response to a magnetic dipole and the resulting formation of a magnetosphere depends on the intensity of the magnetic moment of the dipole. In this study, we examined plasma flow interactions with a magnetic dipole which is much smaller than the Earth's intrinsic magnetic dipole by performing three-dimensional full Particle-In-Cell simulations. The size of a magnetic dipole immersed in a plasma flow is characterized by distance L from its center at which the equilibrium is satisfied between the pressure of the magnetic field of the dipole and that of the plasma flow. In the Earth's magnetosphere, L implies the magnetopause location. We particularly focused on meso- and micro-scale magnetic dipoles in which L is comparable to and smaller than the gyroradius of ions in the flow. In the meso-scale case, ions kinetics should be dominantly considered while electrons whose gyroradius is sufficiently small can be treated as fluid. In the micro-scale, however, electrons as well as ions should be treated particles because L becomes small and the electron kinetics cannot be ignored either. Our interest is in the formation of current layer at the magnetosphere boundary in the both scales. Corresponding to the formation of a magnetosphere, the boundary current also depends on the size of the magnetosphere.

In the meso-scale case, the boundary current is dominated by the electron diamagnetic current at the large density gradient found at the distance of L. This signature is similar to the case of the Earth's magnetosphere. In the micro-scale case, however, the trajectories of ions and electrons gyration play an important role to determine the boundary current. Since the ion's gyroradius is larger than L, charge separation between ions and electrons occurs in the upstream region. As particles approach to the inner dipole, the electron gyroradius becomes small and electron drift motion becomes dominant. It is also confirmed that static electric field caused by the charge separation affect the plasma dynamics and the resulting current flow.

Keywords: Magnetic dipole, Meso-scale, Plasma response, Boundary current layer, Plasma particle simulation

Japan Geoscience Union Meeting 2014
(28 April - 02 May 2014 at Pacifico YOKOHAMA, Kanagawa, Japan)

PEM37-P09 Room:Poster Time:April 30 18:15-19:30

Estimation of the plasma sheet thickness in the Mercury's magnetosphere from the MESSENGER observations: IMF dependence

MORIMOTO, Yuya[1*] ; TAKADA, Taku[2]

[1]Kochi National College of Technology Department of Electrical Engineering and Information Science, [2]Kochi National College of Technology

Only two of spacecraft arrived at the Mercury until now: NASA's MESSENGER which went into orbit around Mercury in 2011 and Mariner 10 which investigated Mercury for two years from 1974. Although the Mercury's magnetosphere was first found by the Mariner 10, the magnetosphere has not been quantitatively understood. With the observations of magnetic field, we deduced the thickness of the plasma sheet and examined its dependence on the IMF (Interplanetary Magnetic Field) As a result, the plasma sheet thickness is estimated as 0.12-0.19 R_M during the northward IMF, and 0.02-0.08 R_M during the southward IMF. Bi-polar magnetic field signatures, which can be associated with the plasma flow in the plasma sheet, are observed both during northward and southward IMF. We then discuss the substorm-related phenomena in the Mercury's plasma sheet.

Keywords: MESSENGER, Mercury's Magnetsphere, plasma sheet, plasma flow, substorm

Japan Geoscience Union Meeting 2014
(28 April - 02 May 2014 at Pacifico YOKOHAMA, Kanagawa, Japan)

PCG11-01 Room:421 Time:April 28 10:00-10:15

Problems of DC Probe Measurement onBoard Mini/Microsatellite

OYAMA, Koichiro[1*]

[1]Plasma and Space Science Center, National Cheng Kung Universoty,Taiwan, [2]International Center for Space Weather Study and Education

DC Langmuir probe is one of the key instruments to study ionosphere by satellite. It needs a counter electrode whose conductive surface are is at least 1000 times larger than that of surface area of the electrode. This requirement is usually fulfilled for large satellites which have been launched so far for ionosphere study. Now we are jumping into an era to use tiny satellites. Then we will encounter serious problems for DC Langmuir probe measurements. Conductive surface area of the satellite becomes much less than 1000 times, or even equal to the surface area of electrode. As a result, measurement of electron density becomes unreliable, because potential of the electrode with respect to the satellite (counter electrode) cannot reach ambient plasma potential where electron density is calculated. For the worst case, DC Langmuir probe is in double probe region, where the maximum current is controlled by ion current. An electronics needs to measure low current. although to measure the low current is not impossible with low frequency response. Another more serious problem is contamination of electrode as well satellite surface. To avoid the effect of contamination, probe bias of DC Langmuir probe need to be swept with about 10 Hz. These two factors make it possible to use DC Langmuir probe, because to measure low current with high frequency is not possible. We review problems which raises for the ionosphere measurement by small satellite, and propose one solution to avoid these problems to accomplish accurate measurements. The data which have been used here are the contribution of three students, G. S. Jiang, W. H. Chen, and Y. W. Hsu, Plasma and Space Science Center, National Cheng Kung University,Taiwan.

Keywords: microsatellite, Dc Langmuir probe, surface area, contamination

Japan Geoscience Union Meeting 2014
(28 April - 02 May 2014 at Pacifico YOKOHAMA, Kanagawa, Japan)

PCG11-02 Room:421 Time:April 28 10:15-10:30

Canadian Instrument Participation in Japanese Space Science Mission: A Retrospective Look

YAU, Andrew[1*]

[1]University of Calgary

Canada has participated in a number of Japanese space science satellite and sounding rocket missions by contributing scientific instruments and participating in related science investigations since the 1980s, including the Akebono (EXOS-D) and Nozomi (Planet-B) satellite and the SS520-2, S520-23, and S520-26 sounding rocket missions. We review the experience of this participation, including the resulting scientific benefits and the lessons learned.

Keywords: space instrument, space plasma, satellite

Japan Geoscience Union Meeting 2014
(28 April - 02 May 2014 at Pacifico YOKOHAMA, Kanagawa, Japan)

PCG11-03 Room:421 Time:April 28 11:00-11:15

Development of Miniaturized Plasma Wave Receiver using ASIC

ZUSHI, Takahiro[1*] ; HANGYO, Kensuke[1] ; ONISHI, Keisuke[1] ; KOJIMA, Hirotsugu[1] ; YAMAKAWA, Hiroshi[1]

[1]Research Institute for Sustainable for Humanosphere

Plasma waves are an important physical phenomenon for understanding the electromagnetic environments in space. The plasma wave receiver is roughly divided into two types: a waveform receiver and a spectrum analyzer. Spectrum analyzer provides the frequency spectrums with low noises and high frequency resolution. On the other hand, waveform receiver provides the waveform. Though the waveform has more noise than the spectrum provided by the spectrum analyzer, only the waveform has phase information of a plasma wave. Thus it play a complementary role. However, these plasma wave receivers occupy a large amount of space because of its analog circuits, so a late scientific satellite has only a kind of plasma wave receiver. We have developed miniaturized waveform capture (WFC), a kind of waveform receiver, and sweep frequency analyzer (SFA), a kind of spectrum analyzer, using ASIC (Application Specific Integrated Circuit). We realized 6ch WFC in a chip of 5 mm x 5 mm. We execute experiment expose this chip to radiation. We find that though radiation influence WFC component, especially switched capacitor filter, our WFC fit for the space radiation environment. The SFA has fine frequency resolution, but its time resolution is poor. We propose a new kind of SFA combined with FFT. It has an improved time resolution without losing time resolution. We have developed analog circuits in the new SFA using ASIC technology. Furthermore, we propose the multipoint plasma wave observation system that consisted of some sensor probes using these miniaturized plasma wave receiver. We plan the sounding rocket experiment for performance test of this sensor probe.

Japan Geoscience Union Meeting 2014
(28 April - 02 May 2014 at Pacifico YOKOHAMA, Kanagawa, Japan)

PCG11-04 Room:421 Time:April 28 11:15-11:30

Development of a wide-field X-ray imaging spectrometer for solar system exploration

EZOE, Yuichiro[1*]

[1]Tokyo Metropolitan University

We present our development of a wide-field X-ray imaging spectrometer for solar system exploration. In the past decade or so, various types of X-ray emission have been discovered in the solar system (Bhardwaj et al., 2007, Planet. Space, Sci., Ezoe et al., 2011, Adv. Space, Res.). These X-rays are often associated with energetic particles in planetary magnetosphere and neutrals in planetary atmosphere and cometary coma. Therefore, X-ray observations of solar system objects will lead to better understanding of solar system environments and astrophysical phenomena.

For this purpose, we are developing a wide-field X-ray imaging spectrometer for future exploration missions such as GEO-X (Ezoe et al. 2014, Space Sci. Symposium) and JMO (Sasaki et al. 2011, EPSC-DPS). This instrument is composed of an ultra light-weight X-ray telescope and a low-power radiation-hard semiconductor pixel sensor. The telescope covers a wide field of view of ~4 deg in diameter in 0.3–2 keV with the angular resolution of <5 arcmin. It uses sidewalls of etched holes through thin 4-inch silicon wafers for X-ray mirrors (Ezoe et al., 2010, Mircosys. Tehc.). The detector covers a wide area of ~20 x 20 mm^2 with a ~300 x 300 um^2 pixel. It is an active pixel sensor developed by MPE and PNsensor (Strueder et al., 2010, SPIE). Compared to X-ray CCDs, this type is more radiation hard and allows higher frame time less than 1 ms. This instrument can satisfy stringent resource constraints in the exploration missions. The mass, size, and power are estimated to be ~10 kg, ~30 cm cubic, and ~10 W, respectively. Multiple units of this instrument are considered for GEO-X to achieve a wider field of view, while one unit will meet science requirements of JMO. In this presentation, we will describe design, fabrication, and performance of the instrument components and future prospects.

Keywords: X-ray, imaging spectroscopy, Earth’s magnetosphere, Jupiter, Mars

Japan Geoscience Union Meeting 2014
(28 April - 02 May 2014 at Pacifico YOKOHAMA, Kanagawa, Japan)

PCG11-05 Room:421 Time:April 28 11:30-11:45

ENA Imaging On board the DESTINY Mission

BRANDT, Pontus[1*] ; MITCHELL, Donald[1] ; WESTLAKE, Joseph[1] ; KEIKA, Kunihiro[2]

[1]The Johns Hopkins University Applied Physics Laboratory, [2]Solar-Terrestrial Environment Laboratory, Nagoya University

Energetic Neutral Atom (ENA) imaging is a technique that enables remote imaging of space plasma and neutral clouds. Several current space-borne missions including Cassini, IMAGE, TWINS, Chandrayaan-1, IBEX, and several future missions such as JUICE make use of ENA imaging to investigate magnetospheric plasma acceleration and evolution; structure and acceleration mechanisms in the boundary between the heliosphere and the interstellar medium; and surface and atmosphere interactions (terrestrial upper atmosphere, terrestrial moon, the Galilean moons, and Titan).

Demonstration and Experiment for Space Technology and INterplanetary voYage (DESTINY; See Kawakatsu et al., this conference) is an innovative technology demonstration mission that is being proposed to JAXA with a low-thrust increase of the apogee of an equatorial orbit, followed by a lunar swing-by, and finally an insertion in to a halo orbit around the Sun-Earth L2 point. This trajectory provides a historical opportunity to perform ENA imaging of the two following compelling targets.

- **The terrestrial magnetosphere:** the equatorial vantage point will offer the first compound view of how ions flow out from the polar ionospheres, , plasma stagnation at the sub-solar magnetopause, ion energization in the plasmasheet out to about 20 R_E and the subsequent heating and earthward transport that forms the terrestrial ring current.

- **The boundary between the heliosphere and the interstellar medium:** the NASA/IBEX and Cassini missions have revealed a global pattern and possibly dynamics that are believed to originate from ions charge exchanging in the heliosheath. A multitude of compelling science questions have arisen from the combined analysis of these two data sets that have demonstrated that ENA imaging is perhaps the only tool capable of remotely probing the global structure and acceleration processes in this important region.

The key to observing these targets in a new light that goes beyond previous missions is the ability to image with high angular and energy resolution, with a wide field of view (FOV) that can image large portions of the regions simultaneously. In this presentation we discuss a concept of an ENA camera to perform imaging from DESTINY. The ENA camera design is capable of imaging ENAs in the $\leq$1keV - 100 keV range with an angular resolution down to 2 degrees and an energy resolution down to 20%. The current design has a FOV of 120x90 degrees, which dramatically increases the duty cycle over single-telescope detectors on spinning platforms.

Japan Geoscience Union Meeting 2014
(28 April - 02 May 2014 at Pacifico YOKOHAMA, Kanagawa, Japan)

PCG11-06 Room:421 Time:April 28 11:45-12:00

A compact, broad-beam, low-energy, LED-based, UV photoelectron source for the calibration of plasma analysers.

BEDINGTON, Robert[1*] ; SAITO, Yoshifumi[1]

[1]Solar System Science Division, Institute of Space and Astronautical Science, JAXA

Electrostatic electron analyser instruments are used to make in-situ measurements of space plasmas and are typically designed to detect electrons with energies from a few eV to a few tens of keV. To make optimal use of such instruments, a complete calibration is performed in a laboratory vacuum chamber before flight. An electron source and a moveable stage are used so that the instrument response can be characterised at every relevant electron energy and beam direction. For an ideal calibration, the source should be a uniform, collimated electron beam of controllable energy and flux, which is sufficiently broad in diameter to cover the entrance aperture of the electron analyser instrument being tested.

Various sources are used for such purposes, including radioactive beta-emitters and thermionic emission guns — although the former have fixed flux and are broad-band in energy, and the latter are expensive and produce only a narrow beam with limited energy ranges and limited dynamical control. To produce a broad, uniform, highly-controllable, long-lifetime, monoenergetic beam, UV photoelectron sources are generally preferable. These consist of a UV light source which illuminates a photocathode causing it to release photoelectrons. These electrons, which are released with negligible kinetic energy, are accelerated toward a high transmission grid by an electric field. The source can thus be as wide as the grid and the photocathode, as spatially uniform as the light that falls on the photocathode, and as collimated and monoenergetic as the photocathode and grid are flat and parallel (and thus the E field uniform). The electron flux can be adjusted by adjusting the UV lamp intensity, and the electron energy can be varied by adjusting the strength of the grid-photocathode E-field.

Traditionally the UV photons are created using gas discharge lamps (e.g. mercury, xenon, deuterium), however these typically have poor dynamical control, can create large amounts of background light and are bulky and inefficient. In recent years however, advances in solid-state technologies have enabled increasingly powerful, efficient and affordable LEDs of various UV wavelengths. Accordingly this has enabled compact, low-power, UV-stimulated electron sources that can have intensities that vary between 10 to 10^{-9} electrons cm^{-2} s^{-1}.

To meet the requirements for calibrating the electron analysers for the SCOPE (cross Scale COupling in Plasma universE) mission, a 9cm beam diameter, UV photoelectron source of this nature has been built and is being tested. Weighing approximately 1.5kg (excluding power supplies) and consisting of rugged, low cost components it can be mounted inside the vacuum chamber with great flexibility, including on a motorised translation stage.

The SCOPE mission requires several FESA (Fast Electron energy Spectrum Analyser) instruments for 10eV to 30keV electrons and several EISA (Electron Ion Spectrum Analyser) instruments for 10eV to 20keV electrons and ions. The first duty of the new electron source is the testing of prototype developments for the EISA instrument: namely measuring the electron transmission properties of carbon foil and assessing the secondary electron emission performance of candidate dynode materials

Keywords: Electron energy analyzer, Plasma spectrometer, Particle source, Ultra-violet photoelectron, Calibration, UV LED

Japan Geoscience Union Meeting 2014
(28 April - 02 May 2014 at Pacifico YOKOHAMA, Kanagawa, Japan)

PCG11-07 Room:421 Time:April 28 12:00-12:15

Characterization of Exoplanets with High Contrast Instruments

KAWAHARA, Hajime[1*]

[1]Department of Earth and Planetary Science, The University of Tokyo

Small exoplanets in the habitable zone (HZ) have been recently discovered by Kepler spacecraft and by ground-based radial velocity surveys. Now one of most interesting issues in this field is how to characterize them. In this presentation, I review our approaches to develop the instruments of direct imaging for the Thirty Meter Telescope (TMT) and other ground-based telescopes. These instruments aim to detect exoplanets in the HZ around late-type stars. I show that the search for the oxygen 1.27 micron bands as a biomarker is promising with the ground-based direct imaging (Kawahara+12 ApJ). I also show that the combination of extreme adaptive optics and coronaraphs for the direct imaging is also valuable for other characterization of exoplanets, for instance, for detection of exoplanetary molecules in close-in planets.

Keywords: exoplanets, terrestrial planets, direct imaging, biomarker

Japan Geoscience Union Meeting 2014
(28 April - 02 May 2014 at Pacifico YOKOHAMA, Kanagawa, Japan)

PCG11-08 Room:421 Time:April 28 12:15-12:30

Development of geocoronal Hydrogen Lyman Alpha Imaging CAmera (LAICA)

SATO, Masaki[1*] ; KAMEDA, Shingo[1] ; YOSHIKAWA, Ichiro[2] ; TAGUCHI, Makoto[1] ; FUNASE, Ryu[2] ; KAWAKATSU, Yasuhiro[3]

[1]Rikkyo University, [2]University of Tokyo, [3]JAXA

Hydrogen and helium atoms are the main constituents of the outermost region of the earth's atmosphere. These atoms resonantly scatter solar ultraviolet radiation causing an ultraviolet glow in this region, called geocorona. Hydrogen Lyman alpha radiation (121.567 nm) is the brightest. To date, various observations of the geocorona have been made. The geocorona comprises three main particle populations: ballistic, escaping, and satellite. Escaping particles are present at all altitudes, and they become particularly dominant at higher altitudes. In previous observations, the geocorona was identified to extend to an altitude of about 20R_E. The geocoronal distribution reveals asymmetries from day to night, dawn to dusk, and north to south. Recently, abrupt temporary increases (from 6% to 17%) in the total number of hydrogen atoms in the spherical shell from a geocentric distance of 3R_E to 8R_E have been recorded during several observed geomagnetic storms.

Past exploration of the geocorona has mainly been obtained from earth orbiters. Therefore, several low altitude (˜8R_E) observations have been made. On the other hand, in order to obtain the geocoronal distribution at high altitude, it is necessary to observe the geocorona from the outside in. However, there have been very few such observations (only Mariner 5, Apollo 16, and Nozomi). Among them, only Apollo 16 obtained an image. However, the observational FOV was about 10R_E.

In this study, we are developing a LAICA (geocoronal hydrogen Lyman Alpha Imaging CAmera) which will go onboard the very small deep space explorer PROCYON that will escape the earth and navigate interplanetary space. From such an explorer, our equipment can perform wide FOV (more than 25R_E) imaging of the geocoronal distribution. The first observation will be conducted one week after the launch for a period of one or two weeks. Subsequently, observations will continue for about three months. These observations will be conducted in higher temporal resolutions than that obtained from earth orbiters. The prototype of the LAICA has now been manufactured for testing and verification. And the flight model will have been completed by May. This presentation will show the development status.

Keywords: geocorona, Lyman alpha line, exosphere, earth's atmosphere

Japan Geoscience Union Meeting 2014
(28 April - 02 May 2014 at Pacifico YOKOHAMA, Kanagawa, Japan)

PCG11-P01 Room:Poster Time:April 28 18:15-19:30

Effects of finite electrode area ratio on Langmuir probe measurement

CHEN, Wen-hao[1*] ; JIANG, Guo-hsiang[1] ; HSU, Yu-wei[1] ; FANG, Hui-kuan[3] ; OYAMA, Koichiro[2] ; CHENG, Chio[2]

[1]Institute of Space and Plasma Sciences, National Cheng Kung University, [2]Plasma and Space Science Center, National Cheng Kung University, [3]Department of Physics, National Cheng Kung University

Langmuir probe(LP) is a widely used instrument for measuring electron density and temperature on satellites and rockets. Recently pico- and nano- satellites have become more popular, when the surface area of satellite is similar to the probe, the effects on LP measurement due to limited satellite surface area need to be considered, and these effects may cause LP measurement inaccurate. We have investigated the effect of satellite surface area, satellite and probe contamination and LP sweeping frequency in laboratory. Also we have found that the satellite and probe voltage will decrease when a large quantity of electrons are attracted by probe voltage and the contamination effect of satellite surface becomes major.

In summary, a solution to these problems is suggested.

Keywords: Langmuir probe, finite electrode area ratio, electrode surface contamination, pico/nano-satellite, electron temperature, electron density

Japan Geoscience Union Meeting 2014
(28 April - 02 May 2014 at Pacifico YOKOHAMA, Kanagawa, Japan)

PCG11-P02 Room:Poster Time:April 28 18:15-19:30

Development of Electron Temperature and Density Probe (TeNeP) for Nano- and Micro-satellites -II

JIANG, Guo-siang[1*] ; CHEN, Wen-hao[1] ; HSU, Yu-wei[1] ; OYAMA, Koichiro[2] ; CHENG, Chio[2]

[1]Institute of Space and Plasma Sciences, National Cheng Kung University, [2]Plasma and Space Science Center, National Cheng Kung University

The nano/micro-satellite becomes popular for the study of near earth environment. To measure the electron temperature (T_e) and electron density (N_e) in the ionosphere, we have developed the Electron Temperature and Density Probe (TeNeP). The TeNeP measures T_e and N_e based on principles of electron temperature probe (ETP) and planar impedance probe (IP). By combining systems of ETP and IP, T_e and N_e can be measured by one single probe. The TeNeP system has advantages not only as being small, light weighted and low power consumption that fulfills the needs of instruments onboard nano/micro-satellites. It also overcomes problems associated with electrode surface contamination and satellite/probe surface area ratio for DC Langmuir probes.

Keywords: Electron Temperature and Density Probe, nano/micro-satellite, Electron Temperature, Electron Density, electrode surface contamination, satellite/probe area ratio

Japan Geoscience Union Meeting 2014
(28 April - 02 May 2014 at Pacifico YOKOHAMA, Kanagawa, Japan)

PCG11-P03 Room:Poster Time:April 28 18:15-19:30

Development of the small probe system to measure plasma wave for the sounding rocket experiment

ONISHI, Keisuke[1*] ; ZUSHI, Takahiro[1] ; KOJIMA, Hirotsugu[1] ; YAMAKAWA, Hiroshi[1]

[1]Research Institute for Sustainable Humanosphere, Kyoto University

Plasma filling the space is very rarefied. Ions and electrons in space plasma don’t exchange their kinetic energy through their collision but through plasma waves. Hence observing plasma wave is essential for measuring space electromagnetic environment. We propose the multipoint plasma wave observation system that consisted of some sensor probes.

The present paper shows the achievements in designing the small sensor probe system which is dedicated to the sounding rocket experiment. The experiment is performance test of the small sensor probe which measures the standard wave in outer space. The necessary components for the small sensor probe are Li-Ion battery, wireless LAN device, plasma wave receiver, A/D converter, and CPU. All of them should be installed in the cubic body with an edge of 10 cm. Therefore, we chose one-chip microcomputers as wireless LAN device, A/D converter, and CPU. The wave receiver is miniaturized by designing the analog ASIC (Application Specific Integrated Circuit).

The wave receiver has the function of observing electromagnetic waves in the frequency up to 100 kHz and we want to take three-axis data at the same time. So, we should design A/D converter which has three simultaneous sampling and sampling frequency over 200 kHz to fulfill the sampling theorem.

We also designed other necessary systems, such as attitude sensor and wireless communication system with the sounding rocket.

Keywords: Space plasma, Plasama wave, Small sensor probe, Sounding rocket

Japan Geoscience Union Meeting 2014
(28 April - 02 May 2014 at Pacifico YOKOHAMA, Kanagawa, Japan)

PCG11-P04 Room:Poster Time:April 28 18:15-19:30

Plasma properties of the space plasma operation chamber at NCKU in Taiwan

FANG, Hui-kuan[1*] ; HSU, Yu-wei[2] ; CHEN, Wen-hao[2] ; JIANG, Guo-hsiang[2] ; OYAMA, Koichiro[3] ; CHENG, Chio[3]

[1]Department of Physics, National Cheng Kung University, [2]Institute of Space and Plasma Sciences, National Cheng Kung University, [3]Plasma and Space Science Center, National Cheng Kung University

The space plasma operation chamber (SPOC), a research facility designed to calibrate and test satellite/rocket-borne instruments and study space plasma processes, is constructed at NCKU in 2009. It is a cylindrical chamber of 2m in diameter and 3m in length. Plasma is produced by two back-diffusion type sources installed at the center of both chamber sides. The sources produce ions of controllable drifting energy from a few ten to several hundred eV and density up to 10^6 cm^{-3}. These ions are neutralized by thermal electrons emitted from Nickel cathodes, and collide with neutral molecules in the chamber of pressure ~2.2×10^{-4} Torr, and a plasma environment with ion temperature ~300K and electron temperature ~1000-3000K is formed in the chamber. This paper presents measurement results of a retarding potential analyzer (RPA), an electron temperature and density probe (TeNeP) and a Langmuir probe installed on the 2-axis moving system in SPOC. The thermal and beam component ion energy distributions at different distances from the ion source and the electron temperature/density spatial distributions in the SPOC will be presented. The collision process of ions with neutral molecules will also be discussed.

Keywords: Plasma properties, space plasma operation chamber, back-diffusion plasma source, retarding potential analyzer, electron temperature and density probe, Langmuir probe

Japan Geoscience Union Meeting 2014
(28 April - 02 May 2014 at Pacifico YOKOHAMA, Kanagawa, Japan)

PCG11-P05 Room:Poster Time:April 28 18:15-19:30

Construction of a calibration system for developing space-borne particle analyzers

ITO, Fumihiro[1*] ; HIRAHARA, Masafumi[1] ; SHIMOYAMA, Manabu[1] ; HAYASHI, Ayuko[1] ; ISHIGURO, Keisuke[1] ; KOGISO, Shun[1]

[1]Solar-Terrestrial Environment Laboratory, Nagoya University

To study physical phenomena in the terrestrial/planetary ionosphere and magnetosphere, it is essential to consider effects of ionized particles and neutral particles which influence each other. For detailed investigations, in-situ observations by spacecraft are required. So we have been developing space-borne particle analyzers for planetary atmospheres with new technologies. As developing these analyzers, it is necessary to construct an appropriate calibration system for them.

For the calibration, we set the analyzer in a vacuum chamber, and irradiate an ion beam towards it, and investigate its response. We have already been constructing a calibration system (ion beam line) which can irradiate an ion beam of which energy per charge range is from 10keV/charge to 150keV/charge. It is necessary, however, for the system to irradiate a suprathermal ion beam of several tens eV/charge. Particularly the system provides the other species of atomic ion beams: H^+, He^+, O^+, N^+, Ar^+, over the energy per charge range from 10eV/charge to 10keV/charge in addition to the other species of molecular ions like $N_2{}^+$, $O_2{}^+$, $CO_2{}^+$. We have been constructed a new beam line which can irradiate an ion beam of which energy per charge range is from 10eV/charge to 10keV/charge. Eventually, we will construct a calibration system which can control each beam line integratedly. In this paper, we report the development of the suprathermal ion beam line.

The suprathermal ion beam line is mainly composed of six parts: (a) ion source, (b) electromagnetic ion mass spectrometer, (c) beam expander, (d) main acceleration, (e) vacuum chamber, (f) multi-axial turntable. In the ion source, introduced gases form a gas cylinder are ionized by thermal electrons emitted from filaments. The ionized particles are initially accelerated and discriminated by the electromagnetic ion mass spectrometer. The discriminated ion beam is expanded by electrostatic 2D raster scanning, and is parallelized through the deceleration and acceleration in the beam expander. The ion beam is accelerated or decelerated for the specific energy in the main acceleration. The analyzer is set on the turntable in the chamber. Incident angles of the beam are controlled by changing the elevation and azimuth of the turntable system. We can control the beam property to change parameters: (1) thermal electrons flux and its acceleration voltage, (2) pre-acceleration voltage for ionized particles, (3) strength of the magnetic field of the electromagnet, (4) raster scanning and parallelized electric field for enlarging the beam cross-section uniformly, (5) main acceleration/deceleration voltage, (6) elevation and azimuth of the turntable system. We have also been developing a system which can control them centrally and remotely by using a computer. As interfaces, we use wireless LAN, RS-232, and USB and make programs with LabVIEW. We have added a monitoring and alert system for multipoint vacuum components.

So far, we have constructed the system expect for the turntable system and can irradiate a specific energy beam which is expanded and parallelized sufficiently. We set up a MCP measurement system to measure the beam intensity and cross-section profile. We will present the updated status of calibration system and the beam properties in this paper.

Keywords: calibration system, ion beam line, suprathermal ion beam, particles analyzer, magnetic ion mass spectrometer, remote control

Japan Geoscience Union Meeting 2014
(28 April - 02 May 2014 at Pacifico YOKOHAMA, Kanagawa, Japan)

PCG11-P06 Room:Poster Time:April 28 18:15-19:30

Verification of engineering models of medium energy particle analysers for ERG

KASAHARA, Satoshi[1*] ; ASAMURA, Kazushi[1] ; MITANI, Takefumi[1] ; TAKASHIMA, Takeshi[1] ; HIRAHARA, Masafumi[2] ; SHIMOYAMA, Manabu[2] ; YOKOTA, Shoichiro[1]

[1]ISAS, [2]Nagoya University

ERG (Exploration of energization and Radiation in Geospace) is a geospace exploration spacecraft, which is planned to be launched in FY2015. The mission goal is to understand the radiation belt dynamics especially during space storms. The key of this mission is the observations of electrons and ions in medium-energy range (10-200 keV), since these particles excite various electromagnetic waves (e.g., EMIC waves, magnetosonic waves, and whistler waves), which are believed to play significant roles in the relativistic electron acceleration and loss. Engineering models (EMs) of medium energy electron analyser and ion mass spectrometer have been developed and their performances and tolerances are tested. We report the results of these verification tests on EMs.

Keywords: Geospace exploration spacecraft ERG, medium energy ion, medium energy electron

Japan Geoscience Union Meeting 2014
(28 April - 02 May 2014 at Pacifico YOKOHAMA, Kanagawa, Japan)

PCG11-P07 Room:Poster Time:April 28 18:15-19:30

The results in the initial operation of the Neutral Mass and Velocity Spectrometer (NMS) onboard the CASSIOPE satellite

KURIHARA, Junichi[1*] ; HAYAKAWA, Hajime[2] ; KOIZUMI-KURIHARA, Yoshiko[2]

[1]Graduate School of Science, Hokkaido Univeristy, [2]The Institute of Space and Astronautical Science/Japan Aerospace Exploration Agency

We report on the results in the initial operation of the Neutral Mass and Velocity Spectrometer (NMS) instrument that is one of the Enhanced Polar Outflow Probe (e-POP) mission payloads onboard the CASSIOPE satellite. The scientific objective of the e-POP mission is to explore the escape of plasma from the polar ionosphere and the escape of neutral particles from the upper atmosphere and their interactions. The NMS instrument is expected to contribute toward a quantitative understanding of occurrence morphology of neutral particles with non-thermal velocity distributions. Therefore, NMS was developed based on a new principle, which is different from previous satellite-borne neutral mass spectrometers. The NMS instrument has an entrance aperture for incoming neutral particles is perpendicular to the ram direction of the satellite in order to take in neutral particles using the satellite velocity of 7-8 km/s. The NMS instrument consists of three parts: an ionization part, a detection part, and data processing part. The ionization part has an electrostatic thermionic electron gun to ionize the neutral particles by the electron beam. In the detection part, the ionized neutral particles are perpendicularly accelerated by the electric field for the Time of Flight (TOF) mass spectrometry, and the two-dimensional positions are detected with a Microchannel Plate (MCP) and a resistive anode. The two-dimensional position detection provides the relative velocities of neutral particles with a certain mass and the original velocity distribution is derived by subtracting the satellite velocity from the relative velocities.

In the initial operation of the satellite, though the NMS instrument had nothing wrong in the status, it was found that charged particles a few orders of magnitude more than expected were detected if the electron gun was off. At present, we suppose this can be caused by the incident neutral particles ionized by collisions with internal surfaces of the instrument. The influence of the collision in the velocity distribution measurement and the results of the analysis in the routine operation are discussed in this paper.

Keywords: neutral mass spectrometer, atmospheric escape, non-thermal velocity distribution

Japan Geoscience Union Meeting 2014
(28 April - 02 May 2014 at Pacifico YOKOHAMA, Kanagawa, Japan)

PCG11-P08 Room:Poster Time:April 28 18:15-19:30

Development and evaluation of the drive system of InSb imager mounted on infrared cameras for Jovian aurora

NOGUCHI, Eriko[1*] ; KOTANI, Koji[2] ; SAKANOI, Takeshi[1] ; KAGITANI, Masato[1] ; ICHIKAWA, Takashi[3]

[1]Geophys., Graduate School of Science, Tohoku Univ., [2]Electronics, Graduate School of Engineering, Tohoku Univ., [3]Astronomy, Graduate School of Science, Tohoku Univ.

In Tohoku University, infrared observation system is being developed for self-owned 60cm telescope. The purpose of this research is to develop a driving system of a Focal Plane Array (FPA) mounted on both an infrared camera and Echelle spectrometer and to evaluate observation possibility for various specific objects by establishing a method to determine adequate operating conditions based on detailed evaluation and analysis of a FPA.

First, from the previous researches, we estimated the required S/N to reveal the variation of some specific Jovian objects. In the case of H3+ aurora, the required S/N and the limit imaging time are 15 and 15s, respectively. For H2 aurora, they are 5 and 1200s. For equatorial temperature field, they are 5 and 7200s. Based on these, we showed the noise indicator, is composed of an upper limit of read noise and leakage current of FPA to realize the required S/N, considering the emission from a telescope and terrestrial atmosphere, and object.

Next, based on the driving mechanism of the FPA: CRC463(Raytheon) used in this research, we revealed that adequate bias is under -3.0V:Vdet, and over -4.0V :Vdduc. In this condition, Full Well(FW) is increased from 0.02V to 0.4V when bias(Vdet-Vdduc) is set at 0.6V, and we succeeded in the imaging of halogen lamp. And, we made improvements as follows.1. Increasing of conductivity of thermal path in the IR camera. This successfully decreased the temperature near FPA from 45K to 20K, resulting in the decrease of both the leakage current from 17,145e/s to 200e/s and the read noise from 453e$_{rms}$ to 320e$_{rms}$.2. Verifying the specific problem on CRC463, and we suggested new driving sequence based on frame to frame control. This resulted in the decrease in the read noise (to 200e$_{rms}$). This made it possible to precisely evaluate the performance of this system.3. Improving bias circuit in FPA driving system. The noise in output was reduced, resulting in the decrease of read noise (to 90e$_{rms}$).

Thanks to the above, it became possible to evaluate the performance parameters of FPA by Photon Transfer Curve method. As the result, in the case of 0.6V bias, DSNU and PRNU were evaluated as 38 ‰ and 16 ‰, respectively. In addition, leakage current, FW and system gain were 200e/s, 133,000e, and 10.9e/DN. We confirmed that the quantum efficiency is 0.85. We also evaluated the NEDT. With a 2.3μm filter and incident flux of 400K of blackbody, the NEDT reaches 45mK, is the equivalent performance compared to the third generation FPAs. As well, the performance parameters of our system other than the leakage current are equivalent to those of the NASA's IRTF system using the same FPA.

And, we evaluated the bias dependences on FW, leakage current and system gain. Using the results, we established the method to determine the adequate bias setting to realize the maximum S/N for specific object. As a result, following estimations were obtained. Using this FPA driving system, H3+ aurora can be observed at the maximum S/N=30 when the bias and exposure time are set at 0.5V and 15s. In the case of H2 aurora, the maximum S/N is 3.14 after binning, when the bias and imaging time are 0.4V and 1200s, respectively. Obtained S/N is below the requirement. It is needed to decrease leakage current under 81e/s. The case of temperature field, the maximum S/N is 52.7 with accumulating 28times, when total imaging time is 7200s, and the bias is set at 0.4V. To decrease accumulating times, bias should be set at 0.9V. If the leakage current will be under 100e/s, the S/N will be over 40 with an accumulation.

In summary, we developed FPA driving system for IR observation instrument mounted on telescope of Tohoku University for planetary observation. We evaluated the performance in detail, and developed the method to determine the adequate bias conditions for each observational object. Decreasing the leakage current is the remaining issue since it is two orders of magnitude larger than the FPA ' s specification.

Keywords: Focal plane array drive system, IR telescope of Tohoku Univ., long-term observation for planet, NASA IRTF

Japan Geoscience Union Meeting 2014
(28 April - 02 May 2014 at Pacifico YOKOHAMA, Kanagawa, Japan)

PCG11-P09 Room:Poster Time:April 28 18:15-19:30

A study for candidate scientific instruments for DESTINY

IWATA, Takahiro[1*] ; KAWAKATSU, Yasuhiro[1]

[1]Institute of Space and Astronautical Science, JAXA

DESTINY (Demonstration and Experiment of Space Technology for Interplanetary Voyage) aims to demonstrate new technologies of high energy orbit insertion, large scale ion engine, ultra light-mass solar panel, etc., which will be useful for deep-space mission by Epsilon launch vehicles. DESTINY has possibility to equip scientific mission instruments when system design makes the margin of the resource. DESTINY can conduct scientific observations for a half to one year on the Halo orbit of solar-terrestrial Lagrange 2 (L2) point. If conditions permit, DESTINY will leave L2 Halo orbit, and transfer to the next destination. Potential scientific topics include in-situ observation and remote sensing from L2 for, such as, plasma, energetic particles, and the magnetosphere in the plasma sheet of terrestrial magnetosphere. It is considered to be useful for the pilot observations for future infrared, gamma-ray, and cosmic-ray space astronomical telescope. It is probable to observe and monitor Near Earth Objects (NEO), inter-planetary and inter-stellar dust. It is also valuable to observe ultra-violet and X-ray emission from planetary phenomena. The mass allocated for the instruments is, however, currently estimated as in the range of between a few and ten kilograms. DESTINY will play roles as pilot experiments for these full-scale observations.

Keywords: Epsilon Rocket, DESTINY, Lagrange point

Japan Geoscience Union Meeting 2014
(28 April - 02 May 2014 at Pacifico YOKOHAMA, Kanagawa, Japan)

PCG11-P10 Room:Poster Time:April 28 18:15-19:30

BepiColombo Euro-Japan Joint mission to Mercury: MMO Project Status update

HAYAKAWA, Hajime[1*] ; MAEJIMA, Hironori[1] ; BEPICOLOMBO, Project team[1]

[1]ISAS/JAXA

BepiColombo is a ESA-JAXA joint mission to Mercury with the aim to understand the process of planetary formation and evolution in the hottest part of the proto-planetary nebula as well as to understand similarities and differences between the magnetospheres of Mercury and Earth.

The baseline mission consists of two spacecraft, i.e. the Mercury Planetary Orbiter (MPO) and the Mercury Magnetospheric Orbiter (MMO). JAXA is responsible for the development and operation of MMO, while ESA is responsible for the development and operation of MPO as well as the launch, transport, and the insertion of two spacecraft into their dedicated orbits.

MMO is designed as a spin-stabilized spacecraft to be placed in a 400 km x 12000 km polar orbit. The spacecraft will accommodate instruments mostly dedicated to the study of the magnetic field, waves, and particles near Mercury. While MPO is designed as a 3-axis stabilized spacecraft to be placed in a 400km x 1500 km polar orbit. Both spacecraft will be in same orbital plane.

Critical Design Review(CDR) for MMO project is completed in November 2011 while ESA Spacecraft CDR is completed in Novemver 2013. MMO stand alone FM AIV is started from September 2012 and expected to be finished on this autumn. MMO FM will be transported to ESA/ESTEC to attend stack level (MCS) final AIV. BepiColombo is expected to be launched in 2016 summer.

10th BepiColombo science working team (SWT) meeting, which discusses science related matters, was held on September 2013 at Lapland. In this paper, we will report the latest information of BepiColommbo MMO project status.

Keywords: Mercury, Planetary Exploration, International Collaboration

Japan Geoscience Union Meeting 2014
(28 April - 02 May 2014 at Pacifico YOKOHAMA, Kanagawa, Japan)

PCG11-P11 Room:Poster Time:April 28 18:15-19:30

Magnetic Cleanliness of BepiColombo MMO

MATSUOKA, Ayako[1*] ; NAKAZAWA, Satoru[2]

[1]ISAS/JAXA, [2]JSPEC/JAXA

In the terrestrial planets, Earth and Mercury has the intrinsic dipole magnetic field. The Mercury magnetic moment is relatively smaller than that of Earth; the magnetic field intensity on the Mercury surface is about 1 percent of that on the earth surface. Therefore the Mercury magnetospheric condition is significantly affected by the variation in the solar wind, and varies with the short period. The magnetic field around Mercury and its nature has been studied by MESSENGER which was launched by NASA and arrived at Mercury in 2011. However, because the magnetic field around Mercury is summation of the intrinsic and external origin, and MESSENGER always has the perigee in the north hemisphere, the Mercury intrinsic magnetic moment has not been determined accurately. BepiColombo is planed to be launched in 2016 and arrive at Mercury in January 2024. It consists of two satellites, MMO built by JAXA, and MPO by ESA, which will observe together the magnetic field around Mercury. BepiColombo has advantages to determine the accurate magnetic moment, which is one of the major scientific target of the BepiColombo project. The orbit shape is not biased, and the measurement at two locations enables to separate the intrinsic field and the external contribution. For the accurate measurement of the magnetic field, it is very important to suppress the magnetic noise generated by the components installed on the satellite. In the phase of the development of the satellite, the design of the every component was examined not to cause the magnetic noise which would degrade the magnetic field measurement. During the manufacturing period, components were controlled not to be magnetized. The means of the magnetic cleanliness of MMO and the result of the system EMC test, where the magnetic moment of MMO was measured, are reported.

Keywords: Mercury, magnetic field

Japan Geoscience Union Meeting 2014
(28 April - 02 May 2014 at Pacifico YOKOHAMA, Kanagawa, Japan)

PCG38-01 Room:423 Time:May 1 09:00-09:15

Surface zonal flows induced by thermal convection in rapidly rotating thin spherical shells

SASAKI, Youhei[1*] ; TAKEHIRO, Shin-ichi[2] ; ISHIOKA, Keiichi[3] ; NAKAJIMA, Kensuke[4] ; HAYASHI, Yoshi-yuki[5]

[1]Department of Mathematics, Kyoto University, [2]Research Institute for Mathematical Sciences, Kyoto University, [3]Department of Earth and Planetary Sciences, Kyoto University, [4]Department of Earth and Planetary Sciences, Kyushu University, [5]Department of Earth and Planetary Sciences, Kobe University

Surface flows of Jupiter and Saturn are characterized by the broad prograde zonal jets around the equator and the narrow alternating zonal jets in mid- and high-latitudes. It is not yet clear whether those surface jets are the result of fluid motions in the ”shallow” weather layer, or they are produced by convective motions in the ”deep” region. ”Shallow” models consider atmospheric motions driven by the solar differential heating and the intrinsic heat flow from the deeper region under the assumption of hydrostatic balance in the vertical direction as a result of the thin atmospheric layer compared with the radius of the planet. These models can produce narrow alternating jets in mid- and high-latitudes, while the equatorial jets are not necessarily prograde. On the other hand, ”deep” models, which describe thermal convection in rapidly rotating spherical shells whose thickness is comparable to the radius of the planet, can produce equatorial prograde flows easily, while it seems to be difficult to generate alternating jets in mid- and high-latitudes.

Recently, Heimpel and Aurnou (2007) proposed thin spherical shell models and show that the equatorial prograde zonal jets and alternating zonal jets in mid- and high-latitudes can be produced simultaneously when the Rayleigh number is sufficiently large and convection becomes active even inside the tangent cylinder. However, they assume eight-fold symmetry in the longitudinal direction and calculate fluid motion only in the one-eighth sector of the whole spherical shell. Such artificial limitation of the computational domain may influence on the structure of the global flow field. For example, zonal flows may not develop efficiently due to the insufficient upward cascade of two-dimensional turbulence, or stability of mean zonal flows may change with the domain size in the longitudinal direction. In the present study, we perform numerical simulations of thermal convection in the whole thin spherical shell domain while coarse spatial resolution and slow rotation rate compared to Heimpel and Aurnou (2007) are used due to the limit of computational resources.

We consider Boussinesq fluid in a spherical shell rotating with constant angular velocity. The non-dimensionalized governing equations consist of equations of continuity, motion, and temperature. The non-dimensional parameters appearing in the governing equations, the Prandtl number, the Ekman number, the modified Rayleigh number, and the radius ratio, are fixed to 0.1, 10^{-4}, 0.05, and 0.75, respectively. The initial condition of the velocity field is state of rest and that of the temperature field is conductive state with random temperature perturbations. After time integration for 35000 rotation period, kinetic energy is saturated and statistically steady state seems to establish. Obtained velocity field satisfies Taylor-Proudman theorem; it is almost uniform in the direction of the rotation axis. An equatorial prograde surface zonal jet emerges in the region outside the tangent cylinder. In the inside of the tangent cylinder, the surface zonal flows are retrograde, but eastward spike features appear near the tangent cylinder in low latitudes. Correspondingly, coherent small scale convective motions exist in these latitudinal zones. It is expected that these convective motions excite topographic Rossby waves which remove westward angular momentum from these zones, producing eastward spike features. This mechanism may explain the origin of the strong thin jet at about 25 degrees north observed on the surface of Jupiter.

Acknowledgement : Numerical computations were carried out on the Earth Simulator (ES2) at the Japan Agency for Marine Earth Science and Technology.

Reference : Heimpel, M., Aurnou, J. (2007) Icarus, 187, 540–557.

Keywords: atmospheres of the gas giant planets, banded structure, equatorial prograde jet, Rossby waves, Jupiter, Saturn

Japan Geoscience Union Meeting 2014
(28 April - 02 May 2014 at Pacifico YOKOHAMA, Kanagawa, Japan)

PCG38-02 Room:423 Time:May 1 09:15-09:30

Numerical modeling of Cloud-level Convection in Venus Atmosphere

SUGIYAMA, Ko-ichiro[1*] ; KAWABATA, Takuya[2] ; ODAKA, Masatsugu[2] ; NAKAJIMA, Kensuke[2] ; ISHIWATARI, Masaki[3]

[1]ISAS/JAXA, [2]Department of Cosmosciences, Graduate School of Science, Hokkaido University, [3]Graduate school of Science, Kobe University

Cellular convection has long been thought to occur in the cloud layer of Venus, because some evidences for convection are obtained from radio occultation and spacecrafts data. However, the convective structure in the cloud layer is still unclear. Some numerical studies are performed to examine convective structure of the cloud layer (Baker et al., 1998, 2000, Imamura et al., 2014), but the domain of the model atmosphere in their numerical experiment is two-dimensional. In this presentation, we perform three-dimensional numerical calculation of convection using the same settings of Baker et al. (1998) in order to investigate a possible three-dimensional structure of convection in the cloud layer in statistically steady state.

The numerical model used in this paper is a cloud resolving model that is mainly used to simulate moist convection in Jupiter's atmosphere (Sugiyama et al., 2009, 2011, 2014), but condensation and chemical reaction are not considered in this experiment. The same sub-grid turbulence and radiation processes of Baker et al. (1998) are included in our model. The settings of the experiment are also based on those of Baker et al. (1998). In these settings, the altitudes of the lower and upper boundaries are 40 km and 60 km levels, respectively, and the layer between 48 km level and 55 km level is almost neutral.

The vertical motion obtained in our numerical experiment is characterized by wide, weak, warm updrafts and narrow, strong, cold downdrafts. This qualitative characteristic of convective motion is consistent with that obtained in Baker et al. (1998). The maximum velocity of downdrafts is about 10 m/s, while the mean vertical velocity is about 3 m/s. The downdrafts are driven by the cooling caused by the turbulent diffusion above the neutral layer and thermal flux at the upper boundary. The horizontal cell size is about 20 km, which is somewhat smaller than that of observed typical cloud-top cells in ultraviolet images; the sizes of the observed cells are typically 100-200 km and in some cases a few tens of kilometers across.

Keywords: Venus atmosphere, convection, numerical modeling

Japan Geoscience Union Meeting 2014
(28 April - 02 May 2014 at Pacifico YOKOHAMA, Kanagawa, Japan)

PCG38-03 Room:423 Time:May 1 09:30-09:45

Convectively-generated gravity waves on Mars and their influence on the upper atmosphere

WATANABE, Ayuka[1] ; IMAMURA, Takeshi[2*] ; MAEJIMA, Yasumitsu[3]

[1]Department of Earth and Planetary Science, The University of Tokyo, [2]Institute of Space and Astronautical Science, Japan Aerospace Exploration Agency, [3]Meteorological Research Institute, Japan Meteorological Agency

Gravity waves in the Martian atmosphere have been identified through various observations. The sources of the waves are still unclear, although topographically-generated gravity waves have been studied using regional models and incorporated into Mars GCMs with parameterizations. Here we investigate convective generation of gravity waves on Mars using a two-dimensional regional model based on the non-hydrostatic meteorological model CReSS. The heating source of the convection model is considered a horizontally-uniform heating of the atmosphere near the surface by sunlight and a localized heating caused by absorption of sunlight by dust clouds. The results show that tntense convection is generated as a result of a thin atmosphere, leading to generation of short-period, large-phase velocity (both in horizontal and vertical) waves. Such waves can reach high altitudes without serious dissipation; the horizontal wavelengths and the amplitudes of the gravity waves reproduced in the lower thermosphere are consistent with the density fluctuations measured during aerobraking experiments. The waves attain saturation amplitudes above ˜80 km altitude.

We further investigated the properties of vertical propagation and dissipation in the thermosphere using linear wave solutions based on the wave parameters observed in the convection experiment. Gravity waves reaching the thermosphere are damped by molecular diffusion and heat the atmosphere. The vertical profile of the heating rate shows two maxima: the lower one is located near the altitude where the amplitude peaks, and is generated by the sensible heat flux divergence, and the upper one is generated by the viscous dissipation of kinetic energy. These heating rates are comparable to other dominant processes such as EUV heating.

Keywords: Mars, gravity wave, convection

Japan Geoscience Union Meeting 2014
(28 April - 02 May 2014 at Pacifico YOKOHAMA, Kanagawa, Japan)

PCG38-04 Room:423 Time:May 1 09:45-10:00

A proposal of Martian dust devil observation by combination with eletromagnetic and acoustic wave measurements

YAMAMOTO, Masa-yuki[1*] ; TAKAHASHI, Yukihiro[2] ; ISHISAKA, Keigo[3] ; SATO, Mitsuteru[2] ; OGOHARA, Kazunori[4] ; KAMOGAWA, Masashi[5] ; MIYAMOTO, Hideaki[6] ; ABE, Takumi[7]

[1]Kochi University of Technology, [2]Hokkaido University, [3]Toyama Prefectural University, [4]University of Shiga Prefecture, [5]Tokyo Gakugei University, [6]The University Museum, The University of Tokyo, [7]Institute of Space and Astronautical Science, Japan Aerospace Exploration Agency

Mars 2020 rover is planned to launch by NASA in 2020, as the almost same package of the Mars Science Laboratory (named Curiosity after its successful landing in August 2012). The announcement of opportunity (AO) for scientific/technology payloads to be onboard the NASA Mars 2020 rover was called for to the scientists community in world wide in September 2013. Here, we introduce our proposed instrument designed for electromagnetic (EM) and acoustic wave (AW) measurements that have never been operated on Mars.

Low-frequency EM and AW are important for monitoring atmospheric events because of their long-distant propagating characteristics more than 1000 km. Electrical discharges could be a hazard for instruments and future human activities on Mars, hence it should be treated as one of the strategic knowledge gaps (SKGs) for future missions. Our concept is that combining EM and AW measurements, precise distance information of dust storms and/or dust devils can be obtained by using two independent velocities of light (c) and sound (Cs) because discharges could be generated by electro-static processes in low-pressure dusty atmosphere and the process also generates shock waves in acoustic/infrasonic pressure wave range. Moreover, wind roaring sound, shock waves by meteors entries, and operational sounds by rover itself will be recorded as the world first ”Martian sound.”

Our EM and AW detection system consists of antennae, microphones, and common receiver circuits with on-board software. For E-field detection, a legacy monopole of 10 cm will be used as a vertical antenna. Two orthogonal loop antennae should be applied for B-field with direction-finding system. However, instead of pop-up devices, these 3 antennae will be compressed into a fixed 10 cm cubic antenna to be equipped on rover surface. Although a legacy receiver circuit can be used, we can minimize it into a postcard size by applying a newly-developed chip device. Analyses of EM and AW for monitoring discharges can be operated by on-board software to reduce data volume. Similar software is used in GLIMS operated on JEM-Kibo/ISS, where only the most significant events will be sent to the Earth in priority basis.

EM sensing in the Martian atmosphere is significant for the future human exploration on Mars. Although the environment on Martian surface is too severe to survive even in fair climate condition, human activities on Mars is obviously dangerous especially when it is under the storm-like condition. Thus, dust devils on Martian surface are significant for the future human exploration, especially, electrostatic discharge events could be serious hazards for astronauts as well as for Martian base facilities. However, the EM condition on the Martian surface has never been measured in detail. Hence, we consider the remote-sensing of the dust devils and discharge events from a single site on Mars with simple sensors could be a potential instrumentation.

Here, as a proposal to the NASA 2020 AO, we introduce one of the most promising remote-sensing methods for dust devils and discharge events by using a combination of EM and AW. According to its rarefied atmospheric pressure condition on Martian surface, about 1/100 of the Earth’s surface, dust particles can easily be flown up by surface wind then could effectively produce charged particles by convection. Based on previous studies on the Earth, such charged particles possibly produce discharge events. Drastic changes in EM fields can be observed even at far-distant observatory, more than 1000 km away from the exact coordinates of discharges. AW also could be a remote-sensing method when there exists the atmosphere. Especially, low frequency AW less than 1 Hz can propagate for long distance more than 100 km even in the rarefied atmosphere. If we use two independent velocities of light (for EM) and sound (for AW), we can identify source coordinates of every discharge events within a few tenth km.

Keywords: Mars, electromagnetic wave, acoustic wave, discharge, dust devil, lander

Japan Geoscience Union Meeting 2014
(28 April - 02 May 2014 at Pacifico YOKOHAMA, Kanagawa, Japan)

PCG38-05 Room:423 Time:May 1 10:00-10:15

Observation of a few months temporal variability of UV brightness in Venus with Pirka telescope

IMAI, Masataka[1*] ; TAKAHASHI, Yukihiro[1] ; WATANABE, Shigeto[1] ; WATANABE, Makoto[1]

[1]Department of Cosmosciences, Graduate School of Science, Hokkaido University

The superrotation, which is a phenomenon that Venusian atmosphere moves westward at a velocity 60 times faster than the planetary rotation, is a unique atmospheric system of Venus. There are several theories to explain what drive the superrotation, but it is still unknown. Yamamoto and Tanaka (1997) suggested that the Kelvin wave in equator and the Rossby wave in mid-latitude, which propagating at an altitude of 70 km or higher, play an important role in the driving of the superrotation. They also suggested that the Kelvin and Rossby wave forms the Y-feature when they balanced. The Y-feature is the bright and dark pattern in UV range, and it has a planetary scale. From the Pioneer Venus spacecraft observation, it was revealed that the propagation and the distribution of UV features cause variation in several time scales [Del Genio and Rossow, 1982, 1990], but it has not been understood which dynamical processes determine these time scales. In our study, we focused on about 2-month brightness variation. That variation seems to be strongly associated with the Rossby wave because there is inverse correlation between low-latitude and mid-latitude, suggesting the existence of quasi-barotropic eddy. After the Pioneer Venus mission, there were no further observations to reveal the mechanism of the 2-month variation.

In this study, we observed the Venusian UV brightness variation as a function of latitude and time. We carried out the ground-based observations with Multi-Spectral Imager (MSI) onboard the Pirka telescope. The Pirka 1.6 m telescope, owned and operated by the graduate school of science in Hokkaido University, is primarily dedicated to the observations of solar planets. Using this system, we can monitor the planetary scale UV-features ($\sim$ 5,000 km) in Venus atmosphere over 8 hours in a day at 365 nm wavelength. In 2013, we carried out about 2 months total observations from mid-Aug. to mid-Nov.

There was a problem to estimate the absolute brightness variation because we observed Venus in the daytime and the correction of the extinction of the Earth's atmosphere had some difficulty. To investigate the brightness variation, we perform additional procedure for each image that we normalize the brightness in each latitudinal band with the mean brightness in 70^{o}N-70^{o}S area. Our results showed two types of UV feature. One showed the strong periodicity in both of equatorial region and mid-latitude and it also had the symmetric structure between northern and southern hemisphere. The other one did not show the strong periodicity and had the symmetric structure. We suppose that the Y-feature does not always exist and the balance of the Kelvin and Rossby wave might be lost when the periodicity and the symmetry disappear. From our observations, it seems to take more than 2 months to return from the asymmetric phase to symmetric phase. Additionally, we found that 2-month variation of brightness in each latitudinal band showed weak inverse correlation between both hemispheres like a seesaw. Such inverse correlation was not seen in the past Pioneer Venus observation. In this paper, we discuss the dynamical state of Venus during our observations and show further observation plans.

Keywords: Venus, Pirka telescope, superrotation, Y-feature

Japan Geoscience Union Meeting 2014
(28 April - 02 May 2014 at Pacifico YOKOHAMA, Kanagawa, Japan)

PCG38-06 Room:423 Time:May 1 10:15-10:30

Spatiotemporal variations of brightness temperatures in the middle atmosphere of Venus revealed by Subaru/COMICS

SATO, Takao M.[1*] ; SAGAWA, Hideo[2] ; KOUYAMA, Toru[3] ; IMAMURA, Takeshi[1] ; SATOH, Takehiko[1]

[1]Institute of Space and Astronautical Science, Japan Aerospace Exploration Agency, [2]National Institute of Information and Communications Technology, [3]National Institute of Advanced Industrial Science and Technology

The middle atmosphere (60-100 km altitudes) of Venus plays an important role in determining its own environment. Venus is completely shrouded by a curtain of dense clouds (50-70 km) with total optical thickness of 20-40 at visible wavelengths. The upper sulfuric acid (H_2SO_4) clouds reflect ˜76% of the incident solar radiation back to space (Crisp and Titov, 1997). More than 70% of the solar energy absorbed by Venus is deposited at altitudes higher than 64 km mainly due to absorption of unknown UV absorbers mixed in the upper cloud (Tomasko et al., 1980, 1985). This horizontally and vertically unusual heating in the cloud layer excites the thermal tides, which are the key process to understand the atmospheric super-rotation. In order to elucidate this mysterious atmospheric phenomenon, it is fundamental to investigate horizontal and vertical thermal structure in the middle atmosphere.

We conducted Venus observations at three mid-infrared wavelengths (8.66, 11.34, and 12.84 micron) with the Cooled Mid-Infrared Camera and Spectrometer (COMICS), mounted on the 8.2-m Subaru Telescope, during the period of October 25-29, 2007 (UT). Thermal radiations at these wavelengths (brightness temperature: 230-240 K) are most sensitive to altitudes of ˜70 km. The angular diameter of Venus and the solar phase angle (Earth-Venus-Sun angle) at the observation period were ˜25 arcsec and ˜90 deg (i.e., both the dayside and nightside hemispheres were observed), respectively. The spatial resolution of the observed images, which was determined by astronomical seeing, was ˜200 km for the sub-observer point. This was the first time that such high spatially-resolved images had been obtained at mid-infrared wavelengths (Mitsuyama et al., 2008).

From images at 8.66 micron, we obtained three important findings. First, the brightness temperatures at cloud top altitudes (˜70 km) in north high-latitudes seemed to be synchronized with those in south ones during the period, which implies that the rotational speeds of them were nearly identical in both high-latitudes. Such atmospheric synchronization has not been reported by any previous mid-infrared ground-based (Diner et al., 1982; Orton et al., 1991) and spacecraft (Taylor et al., 1980; Zasova et al., 2007) observations mainly because of low spatial resolution and tilt of Venus' north pole toward the Earth, and of restricted distribution of sounding, respectively. Second, the center-to-limb curves (dayside and nightside) showed a day-night asymmetry across the morning terminator except that those on October 25 were nearly symmetric. The magnitude of this asymmetry was variable from one day to the next. Such day-night asymmetric features would result from the differences of temperature and/or cloud optical thickness. Finally, there were some streaky and patchy patterns in the whole disk after high-pass filtering. These patterns, typical amplitude of which was ˜0.5 K, varied from day to day. It is worth noting that streaky patterns obtained on October 28 were similar to a well-known horizontal Y-shape structure seen in UV. The above three findings were commonly seen at the other wavelengths.

In this talk, we show the observational results and discuss what kind of atmospheric parameters are responsible for the anomalous features of planetary scale center-to-limb curves through radiative transfer calculations.

Keywords: Venus, middle atmosphere, ground-based observation, atmospheric synchronization, center-to-limb curve, small-scale streaky and patchy patterns

Japan Geoscience Union Meeting 2014
(28 April - 02 May 2014 at Pacifico YOKOHAMA, Kanagawa, Japan)

PCG38-07 Room:423 Time:May 1 10:30-10:45

Energy spectra of atmospheric motions simulated by a high-resolution general circulation model of Venus

KASHIMURA, Hiroki[1*] ; SUGIMOTO, Norihiko[2] ; TAKAGI, Masahiro[3] ; OHFUCHI, Wataru[4] ; ENOMOTO, Takeshi[5] ; TAKAHASHI, Yoshiyuki O.[6] ; HAYASHI, Yoshi-yuki[6]

[1]ISAS, [2]Keio Univ., [3]Kyoto Sangyo Univ., [4]JAMSTEC, [5]DPRI, Kyoto Univ., [6]CPS/Kobe Univ.

The dynamics of the Venus atmosphere is unclear because of the lack of observational data. Many researchers have developed General Circulation models (GCM) for the Venus atmosphere and have attempted to simulate atmospheric motions of Venus. Because the planetary rotation period of Venus is much longer than the Earth, long-term integrations are needed for the solution to achieve a statistically steady state. Therefore, the simulations have been performed by low-resolution ($\sim$ T21; i.e., about 5.6 deg x 5.6 deg grids) models. We have developed a simplified Venus version of the AFES (Atmospheric GCM for the Earth Simulator) (Sugimoto et al. 2012) and performed a very high-resolution simulation. In this paper, we report and discuss kinetic energy spectra obtained from the high-resolution simulation.

The dynamical core of AFES is descretized by the spectral method in horizontal. The model resolution is T159 (i.e., about 0.75 deg x 0.75 deg grids) and L120 (Δz is about 1 km). In the model, the atmosphere is dry and forced by the solar heating with the diurnal change and Newtonian cooling that relaxes the temperature to the zonally uniform basic temperature which has a virtual static stability of Venus with almost neutral layers. To prevent numerical instability, the biharmonic hyper-diffusion is included with 0.01 days of e-folding time for the truncation wavenumber. The coefficient of the vertical eddy diffusion is 0.15 m^2 s^{-1}. A sponge layer is set above 80 km to prevent the reflection of waves. The dry convective adjustment scheme is used to avoid statically unstable state. A fast zonal wind in a solid-body rotation and the temperature field that balances (gradient wind balance) with the zonal wind are given as the initial state. Time-integrations are performed until the solution achieves a statistically steady state.

We calculate the horizontal kinetic energy per unit mass per unit wavenumber from the spectral coefficients of the vertical vorticity and horizontal diffusion (Koshyk & Hamilton 2001). The energy decreases by –5/3 power law in a range from wavenumber 4 to 45. Both in lower and higher wavenumber sides, the energy shows higher decreasing rate.

A feature of the energy spectral of aircraft observations (Nastrom & Gage 1985) and high-resolution GCM calculation of the Earth (Takahashi et al. 2006) is that the energy decreases by –3 power law in low-wavenumber range (n $<$80) and by –5/3 power law in higher range. Terasaki et al. (2011) have reported that the –3 power law in synoptic scale is due to Rossby waves and the –5/3 power law in the mesoscales is due to gravity waves. The energy spectrum that we have obtained shows –5/3 power law in the wavenumber range lower than the Earth cases. This implies that the gravity waves may dominant even in scales of several thousand kilometers in the Venus atmosphere. A reason for the Rossby wave not being dominant in these scales may be the slow planetary rotation. The effect of the hyper-diffusion may appear in the range near the truncation wavenumber.

[Acknowledgement] This study was conducted under the joint research project of the Earth Simulator Center with title “Simulations of Atmospheric General Circulations of Earth-like Planets by AFES.”

Keywords: Venus atmosphere, general circulation model, high-resolution, kinetic energy spectra

Japan Geoscience Union Meeting 2014
(28 April - 02 May 2014 at Pacifico YOKOHAMA, Kanagawa, Japan)

PCG38-08 Room:423 Time:May 1 11:00-11:15

Microphysical properties of Venusian upper hazes observed with an Imaging-Polarimetry system " HOPS "

ENOMOTO, Takayuki[1*] ; SATOH, Takehiko[2] ; NAKATANI, Yoshikazu[3] ; SATO, Takao M.[1] ; HOSOUCHI, Mayu[4] ; NAKAKUSHI, Takashi[5]

[1]SOKENDAI, [2]ISAS/JAXA, [3]Kyoto University, [4]University of Tokyo, [5]Wakayama University

The high albedo of Venus is due to optically very thick main cloud deck which covers the whole planet. The small particles (hazes) which were distributed above the main cloud deck were discovered by the observations from Pioneer Venus Orbiter (PVO) which arrived at Venus in December 1978. Kawabata et al. [1980] found, from the data of Orbiter Cloud Photopolarimeter (OCPP) onboard PVO, that abundant sub-micrometer sized particles " hazes " were distributed above the main cloud deck mostly in polar regions. The optical thickness of the haze layer was reported to reduce during the PVO mission period [Sato et al., 1996]. Coincidently, decrease of the SO_2 abundance was also reported [Esposito, 1985]. After the PVO mission, however, the variation of the optical depth of the hazes has not been studied, so it is not clear what this correlation means for the generation and maintenance of hazes and whether a similar correlation between them exist today. Our study provides the latest information about the microphysical properties of hazes by ground-based monitoring observations which have not been done since PVO.

To monitor the distribution of the Venusian upper hazes, we developed an imaging-polarimetry system " HOPS " (Hida Optical Polarimetry System) and performed observations by attaching it to the 65cm refracting telescope at Hida Observatory of Kyoto University. As HOPS provides spatially resolved polarization map, polarization in an arbitrary area can later be obtained just by summing up the corresponding pixels for comparison with previous measurements. This is the biggest advantage of imaging polarimetry against the aperture measurements. HOPS is a " two beam type " polarimetry instrument which enables high accurate measurements against variable atmospheric conditions. The effect of variable atmospheric transparency, non-uniformity of sensitivities over the CCD pixels and different throughputs of two beams can be corrected through arithmetic operations in image processing.

The observations were carried out at solar phase angles around 39deg. (Jul., 2013), 56deg. (Aug., 2013), 58deg. (Oct., 2012), 85deg. (Aug., 2012) and 129 deg. (May, 2012) at 4 selective wave lengths 438nm (B), 546nm (G), 650nm (R) and 930nm (IR); G and IR data can be compared with similar wavelength data of PVO/OCPP. We averaged observed degree of linear polarization over the polar regions (latitudes higher than 60 deg.) and compared with the report of PVO. A clear difference is seen in IR data. The neutral point of our data is found to be at around 75 deg. while the point of PVO/OCPP is around 40 deg. This difference may indicate the different situation of the distribution and size parameters of hazes.

To analyze the obtained polarization data, we developed a radiative transfer calculation code using Adding?Doubling method with the Stokes parameters fully treated [de Haan et al., 1987, Hovenier et al., 2004]. It is possible to analyze three wavelengths IR, R, and G neglecting the Rayleigh scattering effect because Rayleigh scattering cross-sections for IR, R G and B are about 0.21, 0.083, 0.041, 0.0096μm^2 while Mie scattering cross-sections for a main cloud particle are the order of 7μm^2. We treated haze particle effective radius r_{eff} and optical depth τ_h as free parameters, respectively. The effective variance of hazes was fixed to 0.18 and parameters for main cloud layer were taken from Hansen and Hovenier [1974]. Single scattering albedos were assumed to be 1 for both haze and cloud layers. The resultant parameters for northern and southern polar region are r_{eff} = 0.22, 0.20μm, τ_h = 0.09, 0.05 at IR, respectively. The optical depth is smaller compared with the initial observations of PVO τ_h = 0.25 but comparable with those observed during the declining phase. Such declination of the abundance of SO_2 is also observed by Venus Express orbiter [Marcq et al., 2012], so our results are consistent with the report of the correlation with it.

Keywords: Venus, Hazes, Imaging-Polarimetry, Radiative transfer analysis

Japan Geoscience Union Meeting 2014
(28 April - 02 May 2014 at Pacifico YOKOHAMA, Kanagawa, Japan)

PCG38-09 Room:423 Time:May 1 11:15-11:30

Estimation of wind at the cloud top of Venus

IKEGAWA, Shinichi[1*] ; TAKESHI, Horinouchi[2]

[1]Graduate School of Environmental Science, Hokkaido University, [2]Faculty of Environmental Earth Science, Hokkaido University

A number of theories have been proposed to explain the formation of the super-rotation in the Venus atmosphere. Among them, we focused on the Gierasch mechanism. To validate the mechanism, it is required to investigate the horizontal momentum transport by eddies with an accuracy sufficient to resolve the eddies with scales smaller than several thousand kilometers. In this study, we used the ultraviolet images from Venus Monitoring Camera (VMC) onboard ESA's Venus Express. The VMC data have some random and coherent noises, so the simple cross-correlation methods used in previous studies do not necessarily provide an high accuracy. Here, we suggest a new and robust method to estimate wind velocity vectors accurately by using multiple images, thereby reducing the effect of noises. The accuracy of its results is estimated statistically. The results are also examined from the dynamical point of views. Contrary to conventional expectation, the magnitude of horizontal wind divergence has similar magnitude to its rotation on the horizontal scale of several thousand kilometers. It is discussed how the results are explained.

Keywords: Venus, super-rotation, estimation of wind

Japan Geoscience Union Meeting 2014
(28 April - 02 May 2014 at Pacifico YOKOHAMA, Kanagawa, Japan)

PCG38-10 Room:423 Time:May 1 11:30-11:45

Studying the Venusian atmosphere on the 2012 transit of Venus

KANAO, Miho[1*] ; NAKAMURA, Masato[1] ; SHIMIZU, Toshifumi[1] ; IMAMURA, Takeshi[1]

[1]ISAS/JAXA

The solar satellite Hinode observed the transit of Venus on June 5-6th 2012. The solar optical telescope (SOT) observed the dark Venus disk against the bright solar surface. The images were acquired continuously for the wavelength of 396.8, 430.5 450.4, 555.0, 668.4 nm with unprecedented spatial scale (∼0.3 arcsec).

The purpose is the derivation of the latitudinal and vertical distribution of the cloud particle, SO2 and SO from the transmittance for considering the global dynamics. We calculated the transmittance normalized by the unattenuated solar intensity after the data correction processes including the removal of the solar limn darkening and the calibration for the plate scale.

The altitude as the transmittance of 0.5 (∼90 km) in the Venus atmosphere has the slant toward the equator. The difference is 9.1 km in the evening and 6.1 km in the morning. In the equatorial region (latitude $\leq$ 40 degree), the fluctuation of the altitude is observed. The amplitude for the wavelength shorter than 400 nm is a few times larger than that of 430.5 nm. We would show the consideration to explain the longitudinal distribution of the altitude of the Venus disk.

Keywords: planetary atmosphere, the transit of Venus

Japan Geoscience Union Meeting 2014
(28 April - 02 May 2014 at Pacifico YOKOHAMA, Kanagawa, Japan)

PCG38-11 Room:423 Time:May 1 11:45-12:00

Millimeter Wave Band Monitoring of Venusian and Martian Middle Atmosphere with SPART Telescope

MAEZAWA, Hiroyuki[1*] ; IKEDA, Yoshinori[1] ; OSAKI, Shigeki[1] ; HORIUCHI, Kouske[1] ; KIRIDOSHI, Ryosuke[1] ; TANEKURA, Naruaki[1] ; SAGAWA, Hideo[3] ; NISHIMURA, Atsushi[1] ; OHNISHI, Toshikazu[1] ; TOKUMARU, Munetoshi[2] ; KONDOU, Syusaki[2] ; MIZUNO, Akira[2] ; KANZAWA, Tomio[4] ; HANDA, Kazuyuki[4] ; IWASHITA, Hiroyuki[4] ; MAEKAWA, Jun[4] ; OYA, Masaaki[4] ; KUNO, Nario[4]

[1]Osaka Prefecture University, [2]STEL Nagoya University, [3]NiCT, [4]Nobeyama Radio Observatory

To understand the influences of the activities of the central star on the middle atmospheres of the surrounding terrestrial planets, we have performed millimeter-wave-band monitoring of the atmospheres of Venus and Mars by using a 10-m radio telescope called SPART (solar planetary atmosphere research telescope). The telescope employs highly sensitive superconducting SIS mixer receivers in the 100- and 200-GHz bands for the front-end and a commercially available FFT spectrometer (1-GHz bandwidth and 67-kHz resolution) for the back-end. Millimeter-wave-band heterodyne sensing is a powerful technique that can be utilized to trace the abundance and vertical distribution of minor constituents in a planetary middle atmosphere.

In 2011, we began observations of the middle atmospheres of Venus and Mars in the 100-GHz band. In 2012, the telescope had problems with the azimuth gear, motor, and synchro-to-digital converter unit, which resulted in a pause in telescope operation. In 2013, we repaired these problems and resumed the substantive operation test. We are currently restarting double-band full remote monitoring of the spectral lines of minor constituents such as ^{12}CO J=2-1 at 230 GHz, ^{13}CO J=2-1 at 220 GHz, and ^{12}CO J=1-0 at 115 GHz toward Venus and Mars. This season, the apparent diameter of Venus is greater than the beam size at the 200-GHz band (35 arcsec.). We adopted position switching and on-the-fly modes for 100- and 200-GHz-band observations, respectively. The latter two-dimensional mapping allows us to cover the entire disk of Venus. The retrieved CO abundance variation is compared with the data of high-energy particles, X-rays, solar wind velocity/density, and other measured parameters. The data are associated with flare, coronal mass ejection, and solar proton events.

In this conference, the current status of the SPART project and the millimeter-wave-band monitoring will be presented.

Keywords: planet, solar activity, radio telescope, heterodyne spectroscopy, middle atmosphere, remote sensing

Japan Geoscience Union Meeting 2014
(28 April - 02 May 2014 at Pacifico YOKOHAMA, Kanagawa, Japan)

PCG38-12 Room:423 Time:May 1 12:00-12:15

Observation of a wave structure of stratospheric haze in Jupiter's polar regions by the ground based telescope

GOUDA, Yuya[1*] ; TAKAHASHI, Yukihiro[1] ; WATANABE, Makoto[1]

[1]Department of Cosmosciences, Graduate School of Science, Hokkaido University

Stratospheric haze formed by aerosol particles covers both polar regions in Jupiter. It has been reported based on the imaging using a methane band filter at 889 nm that the stratospheric haze can be measured. They show bright cap structures covering polar regions and the edge of the cap shows a wave structure spreading in longitudinal direction. This structure can be seen more clearly in the Jupiter's south pole than the north pole, and wave is clear at a latitude of about 67 S [Sanchez-Lavega, 2008].

Jupiter's polar areas have been investigated by the Hubble Space Telescope (HST) from 1994 to 1999 and the Cassini ISS in 2000. This wave structure is known to exist for several years in Jupiter's both polar regions. These observations suggested that this wave structure is caused by planetary Rossby waves because this wave structure presents for a longer period and moves westward relative to the background flow. However, the origin and mechanism keeping to this wave structure, the vertical structure of the wave, change of the propagation velocity of the wave in the short time scale, and north-south asymmetry of the wave structure are unclear so far, because of lack of the observations in short time scale (monthly scale). We have carried out the monthly monitoring of Jupiter from 2011 to 2014 with the 1.6 m Pirka telescope of Hokkaido University.

In this paper, we show results of our observations of the wave structure in Jupiter's polar region. We found a north-south asymmetry of the wave structure in the polar areas. The wave structure at 67 N spread to 42 N in the northern hemisphere, however it does not so in the southern one. In addition, we found that the wave structure has varied in the vertical direction a bit between altitude of 361 mbar and 750 mbar.

Keywords: Jupiter, haze, ground-based observation, Rossby wave

Japan Geoscience Union Meeting 2014
(28 April - 02 May 2014 at Pacifico YOKOHAMA, Kanagawa, Japan)

PCG38-13 Room:423 Time:May 1 12:15-12:30

Observing Jupiter with an infrared camera NIIHAMA

SATOH, Takehiko[1*] ; YONEDA, Mizuki[2] ; KAGITANI, Masato[2] ; KUHN, Jeff[3]

[1]Japan Aerospace Exploration Agency, [2]Tohoku University, [3]University of Hawaii

An infrared camera, NIIHAMA (1024x1024 pixels, PtSi array sensor), is attached to the SOLAR-C telescope (45-cm diameter off-axis Gregorian reflector) atop Haleakara in December 2013 and is now observing Jupiter.

NIIHAMA's 6-position wheel houses Dark, J, H, K, 3.4-micron (for Jupiter's H_3^+ aurora) and 2.26-micron (for Venus night-side IR emission) filters. The primary target of this project is to monitor the brightness of Jupiter's aurora simultaneously with SPRINT-A/HISAKI and other telescopes. However, due to smaller aperture of telescope, rather low quantum efficiency of PtSi sensor, etc., Jupiter's aurora has not yet been imaged so far. On the other hand, the satellite Io while in Jupiter's shadow was observed in K band, and the night-side IR emission of Venus was successfully imaged in 2.26-micron filter. We report the result of first-light observations and also discuss improvement and observing plans in near future.

Keywords: Infrared camera, Jupiter, aurora, Io, Venus, Haleakala

Japan Geoscience Union Meeting 2014
(28 April - 02 May 2014 at Pacifico YOKOHAMA, Kanagawa, Japan)

PCG38-14 Room:423 Time:May 1 12:30-12:45

Self-driven auroral acceleration process at Jupiter captured by continuous monitoring of Hisaki satellite with HST

KIMURA, Tomoki[1*] ; TAO, Chihiro[3] ; BADMAN, Sarah[2] ; YOSHIOKA, Kazuo[1] ; MURAKAMI, Go[1] ; YAMAZAKI, Atsushi[1] ; TSUCHIYA, Fuminori[4] ; FUJIMOTO, Masaki[1]

[1]JAXA/ISAS, [2]Lancaster University, [3]IRAP, Fance, [4]Tohoku University

Two possible drivers have been proposed for planetary auroral acceleration processes: magnetosphere-solar wind interaction referred to as an 'external driver' and shear flow of magnetospheric plasma around a planet referred to as an 'internal driver'. Recent observations of Jupiter's aurora indicated significant responses of auroral intensity and morphology to the solar wind. These results are suggestive of the 'external driver' for Jupiter. On the other hand, there have not been reported dynamics of the 'internal driver' for Jupiter yet which should be essential because of Jupiter's fast rotation and internal plasma source Io. Here we firstly report dynamics of the 'internal driver' based on long-term continuous observation of extreme ultraviolet (EUV) aurora by Hisaki satellite. The long-term variations in EUV aurora are compared with solar wind extrapolated from Earth's orbit by numerical simulation. We found dramatical brightening and decay of EUV aurora during the solar wind quiet period. The brightening occurs once every a few days followed by sudden decay with a timescale less than a half of rotation (˜5 hours), which is significantly faster than the solar wind daily variations. Highly-resolved auroral imaging by Hubble Space Telescope captured expansion of diffuse aurora down to latitudes of Io's footprint aurora during the brightening. These observations are indicative of hot plasma deeply injected into the inner magnetosphere around Io's orbit independently from the solar wind, followed by rapid energy dissipation through auroral emissions and possibly other radiation and/or chemical processes.

Keywords: Hisaki satellite, Hubble Space Telescope, Jupiter, aurora

Japan Geoscience Union Meeting 2014
(28 April - 02 May 2014 at Pacifico YOKOHAMA, Kanagawa, Japan)

PCG38-15 Room:423 Time:May 1 14:15-14:30

Characteristics of O+ velocity distributions at Venus and ion acceleration mechanisms: ASPERA-4 observations

MASUNAGA, Kei[1*] ; FUTAANA, Yoshifumi[2] ; TERADA, Naoki[3]

[1]STEL, Nagoya Univ., [2]Swedish Institute of Space Physics, [3]Grad. Sch. of Sci., Tohoku Univ.

O^+ ion velocity distributions for high energy O^+ beams ($>$100 eV) around Venus are statistically studied. The study shows that O^+ acceleration is controlled by the local convection electric field produced by the local proton and local magnetic field. In the magnetosheath, velocity distributions show a trend that perpendicular velocity component shifts from initial phase of the ring distribution to the local proton velocity. This indicates that gyro motions of the pickup ion immediately collapse after pickup and the ions are incorporated into the local proton flow. The pickup ions only escape through the $+E_L$ hemisphere. In the dayside induced magnetosphere in the $+E_L$ hemisphere, measurements show a scattered velocity distribution of O^+. This velocity distribution has two ion components depending on whether their gyro radius is larger or not than the scale of the induced magnetosphere. For O^+ ions with small gyro radius ($<$500 km), the O^+ velocity distribution appears on the middle phase of the ring distribution. On the other hand for the O^+ ions with a large gyro radius ($>$500 km), the O^+ velocity distribution is similar to the one in the magnetosheath. This means that in the induced magnetosphere two types of ions are mixed up: pickup ions subject to the E x B drift and ions moving with the local proton bulk velocity. Since both ion components flow tailward, they are convected toward the nightside. In the nightside of the induced magneto- sphere, velocity distribution shows initial and last phase of the ring distributions and parallel beam (3D ring distribution). This suggests that ion pickup occurs at the center of the plasma sheet. There is no evidence of an electric potential in the plasma sheet because the O^+ parallel beam velocity is larger than the parallel velocity component of the local proton. Our result suggests that the local convection condition is rather important to discuss ion acceleration mechanisms at Venus than the solar wind condition.

Keywords: Venus, ion escape, ion acceleration, Venus Express, ASPERA

Japan Geoscience Union Meeting 2014
(28 April - 02 May 2014 at Pacifico YOKOHAMA, Kanagawa, Japan)

PCG38-16 Room:423 Time:May 1 14:30-14:45

Characteristics of boundary layer between the magnetosheath and Martian ionosphere during solar wind penetration events

MATSUNAGA, Kazunari[1*] ; SEKI, Kanako[1] ; HARA, Takuya[1] ; BRAIN, David A.[2] ; LUNDIN, Rickard[3] ; FUTAANA, Yoshifumi[4] ; BARABASH, Stas[4]

[1]Solar-Terrestrial Environment Laboratory, Nagoya University, [2]Laboratory for Atmospheric and Space Physics (LASP), University of Colorado at Boulder, [3]Space Physics Swedish Institute of Space Physics (IRF), Umea, Sweden, [4]Space Physics Swedish Institute of Space Physics (IRF), Kiruna, Sweden

Deceleration of the solar wind due to the mass loading by planetary heavy ions forms the magnetic pile-up region around unmagnetized planets such as Mars and Venus. The Martian magnetic pile-up region diverts shocked solar wind plasma around the planet at altitudes typically in excess of 800 km [e.g., Vignes et al., 2000]. Mars Global Surveyor (MGS) measurements have shown, on one hand, that shocked solar wind (magnetosheath) plasma occasionally penetrates into much lower altitudes ($\sim$400km) [e.g., Brain et al., 2005; Crider et al., 2005]. Our previous statistical study of these solar wind penetration events using MGS magnetic field and electron observations revealed that both solar wind dynamic pressure (Psw) and the orientation of the interplanetary magnetic field (IMF) control the occurrence of the events. However, MGS cannot observe the solar wind regions due to its orbital design.

In this study, we focused on the simultaneous observation of the penetration events by MGS and Mars Express (MEX). MEX possess the ion mass analyzer (IMA) and electron spectrometer (ELS), which are parts of plasma packages of ASPERA-3. MEX partly observed the solar wind region, since the orbit of MEX is elliptical orbit. We can thus obtain the solar wind density and velocity from MEX data. Among the simultaneous observation data by MEX and MGS, we identified 46 simultaneous observation events of the solar wind penetration. We divided the 46 events into the low Psw ($\leq\sim$4nPa) and high Psw ($\geq\sim$4nPa) events. The solar wind penetration event on January 20, 2005 is observed during the high Psw periods, while the event on February 20, 2005 is during the low Psw periods. We investigated characteristics of the boundary layers between the magnetosheath and the ionosphere. We found that the electron flux shows a gradual decrease in the boundary in the high Psw event. On the one hand, intermittent appearance of both the magnetosheath plasma and the ionosphere plasma in the boundary is during the low Psw event. The signature of the boundary layer resembles with the K-H instability signature seen in LLBL (low-latitude boundary layer) in the Earth's magnetotail [e.g., Hasegawa et al., 2006]. We also report the results of statistical analysis of 46 simultaneous observation events.

Keywords: Mars, Ionospheres, Induced magnetosphere, Solar wind, Unmagnetized planet

Japan Geoscience Union Meeting 2014
(28 April - 02 May 2014 at Pacifico YOKOHAMA, Kanagawa, Japan)

PCG38-17 Room:423 Time:May 1 14:45-15:00

Effects of ion-ion collisions on vertical distribution of CO2+ in Martian ionosphere based on multi-fluid MHD simulation

KOYAMA, Kyohei[1*] ; SEKI, Kanako[1] ; TERADA, Naoki[2] ; TERADA, Kaori[2]

[1]Solar-Terrestrial Environment Laboratory, NAGOYA University, [2]Graduate School of Science, Tohoku University

Comparison of the mass fraction of CO2 and N2 with regard to the total mass of each terrestrial planet suggests importance of the atmospheric escape to space in Martian atmospheric evolution [Chassefiere et al., 2006]. It has been considered that heavy CO_2^+ ions are difficult to escape based on known atmospheric escape processes. Observations of a large amount of CO_2^+ ion escape by the Mars Express thus challenged the existing escape processes. Vertical distribution of CO_2^+ density in the ionosphere is one of important factors that determine the rate of CO_2^+ escape. Chemical reactions in ionosphere have been implemented in previous studies using multi-species MHD simulations [e.g., Ma et al., 2004; Terada et al., 2009]. The velocity difference between ion fluid cannot be reproduced by the multi-species MHD approximation. On one hand, the importance of vertical transport in the upper ionosphere (>300km altitude) was pointed out by some ionospheric models [Fox and Hac, 2009]. Multi-fluid MHD code [e.g., Najib et al., 2011] can solve such ion-species dependent velocity.

In this study, we developed a multi-fluid MHD simulation code. Our code includes ion-ion collisions in order to investigate their effects on the vertical distribution of CO_2^+ density in the Martian ionosphere. Three cases of the simulation runs are carried out: Multi-fluid MHD with ion-ion collision (Case1), multi-fluid MHD without ion-ion collision (Case2), and all ion species have the same vertical velocity corresponding to multi-species approximation (Case3). We compared the results after each simulation run reached to a quasi-steady state. The CO_2^+ density at altitude 460 km were turned out to be 82, 190, and 11 cm^{-3}, respectively for the Cases 1-3. The results suggest that inclusion of ion-ion collision is important to reproduce the realistic CO_2^+ transport from lower to upper ionosphere.

Keywords: Mars, ionosphere, Atmospheric escape, Multi-fluid MHD

Japan Geoscience Union Meeting 2014
(28 April - 02 May 2014 at Pacifico YOKOHAMA, Kanagawa, Japan)

PCG38-18 Room:423 Time:May 1 15:00-15:15

Temporal variability of exospheric sodium density

KAMEDA, Shingo[1*] ; FUSEGAWA, Ayaka[1] ; KAGITANI, Masato[2] ; YONEDA, Mizuki[2]

[1]Rikkyo University, [2]Tohoku University

Mercury's atmosphere is very thin and it is also called "surface-bounded exosphere". In the detected species, e.g., H, He, O, Na, Mg, K, and Ca, Na emission (NaD) is the brightest and has been most frequently observed. Solar-photon-stimulated desorption, sputtering by impacting solar particles, and meteoroid vaporization are considered to be the source processes of Mercury's sodium. However, the primary process among these three processes is unclear as yet. The resonance scattering constitutes exospheric emission. The NaD emission is well suited for study by ground-based observations because of its high intensity. Past observations have shown that the temporal variation and north-south asymmetry of intensity of sodium emission.

We have observed Mercury sodium exosphere at the Haleakala Observatory in Hawaii since April 2011. The observations were performed using a 40 cm Schmidt-Cassegrain telescope, a high-dispersion spectrograph, and a CCD camera. We determined the temporal variation of the sodium density using the observational data. It is possible that the temporal variation of the sodium density is caused by variation of solar wind magnetic field if solar wind ion sputtering is the primary source process of Mercury exosphere. To verify this assumption, we checked the temporal variation of solar wind magnetic field observed by MESSENGER, and then we compared these variations with our observational result.

In this presentation, we show our observational results and discuss the dominant source process.

Japan Geoscience Union Meeting 2014
(28 April - 02 May 2014 at Pacifico YOKOHAMA, Kanagawa, Japan)

PCG38-19 Room:423 Time:May 1 15:15-15:30

Study of heavy ion dynamics in the Mercury's magnetosphere with offset dipole

YAGI, Manabu[1*] ; SEKI, Kanako[2] ; MATSUMOTO, Yosuke[3] ; DELCOURT, Dominique[4] ; LEBLANC, Francois[4]

[1]Tohoku Univ., [2]Nagoya Univ., [3]Chiba Univ., [4]CNRS

From Mariner 10 and MESSENGER observations, Mercury's magnetosphere is thought to be a miniature of the Earth's magnetosphere. While these two magnetospheres have several characteristics in common, some critical differences are also evident. First, there is no atmospheric layer, but only tenuous exosphere. Second, the kinetic effects of heavy ions might not be negligible because Mercury's magnetosphere is relatively small compared to the large Larmor radii. Trajectory tracings is one of the dominant methods to estimate the kinetic effect of heavy ions which originate the exosphere, though the results of the simulation are quite sensitive to the electric and magnetic field. Hence, it is important to provide a realistic field model in the trajectory tracings. In order to construct a large scale structure, we developed a MHD simulation code, and adopted to the global simulation of Mercury's magnetosphere. We performed four solar wind conditions of the northward IMF, and the results showed that the global configurations such as the location of magnetopause depend heavily on the dynamic pressure, while the solar wind electric field contributes little to the magnetospheric configuration. On the other hand, the results of statistical trajectory tracings of exospheric sodium ions depend not only on the dynamic pressure but also on the solar wind electric field. In the results, we identified two efficient acceleration processes and formation of the 'sodium ring' which is formed by the accelerated ions drifting around the planet by magnetic gradient of the dipole field. When the solar wind dynamic pressure is low, acceleration by magnetospheric convection is efficient in the vicinity of Mercury. When the dynamic pressure is high, entry of the accelerated ions picked-up in the magnetosheath into the magnetosphere becomes dominant. The entry point of sodium ions changes due to the variation of the solar wind electric field, which causes a difference in the sodium ring's shape for the same solar wind dynamic pressure cases. Recent observation by MESSENGER revealed the weaker dipole field of Mercury than the past estimation based on Mariner 10 as well as large offset of dipole which could change the global configuration of Mercury's magnetosphere and behavior of sodium ions. In the presentation, we will also discuss the ongoing simulation including the above configuration of intrinsic magnetic field of Mercury especially focus on how will this affect the acceleration mechanisms.

Keywords: Mercury's magnetosphere, test particle simulation, MHD simulation

Japan Geoscience Union Meeting 2014
(28 April - 02 May 2014 at Pacifico YOKOHAMA, Kanagawa, Japan)

PCG38-20 Room:423 Time:May 1 15:30-15:45

Structure and time variability of Io plasma torus observed by EXCEED onboard the HISAKI satellite

TSUCHIYA, Fuminori[1*] ; YOSHIKAWA, Ichiro[2] ; YOSHIOKA, Kazuo[3] ; KIMURA, Tomoki[3] ; YAMAZAKI, Atsushi[3] ; MURAKAMI, Go[3] ; KAGITANI, Masato[1] ; TERADA, Naoki[1] ; KASABA, Yasumasa[1] ; SAKANOI, Takeshi[1]

[1]Tohoku University, [2]The University of Tokyo, [3]ISAS/JAXA

Spatial distribution and time variability of emission lines of sulfur ions in Io plasma torus (IPT) measured by EUV spectrograph (EXCEED) onboard the HISAKI satellite are presented. The satellite has been launched on 14 Sep. 2013 and begun regular observation of IPT and Jupiter's UV aurora since middle of Dec. and it will continue until the end of Feb. A wide slit whose designed field of view (FOV) is 400 x 140 arcsec was chosen to measure both radial and latitudinal distributions of IPT. Jupiter's north aurora was guided at the center of FOV and its spectrum was simultaneously observed. Averaged spatial distribution of sulfur emission lines is consistent with previous observations. Looking at the time variability of IPT, new features were found from the EXCEED observation. The most surprising one is periodic variation synchronized with Io's orbital period. The variations in dawn and dusk sides were out-of-phase, suggesting the bright region is co-rotating with Io. The amplitude of the periodic variation is larger than those of well-known Jupiter's rotation periodicities in shorter wavelength and becomes smaller as increasing wavelength. The wavelength dependence suggests significant electron heating and/or hot electron production processes associated with Io. Another noticeable feature is long-term change in dawn-dusk asymmetry of the emission intensity which had not been reported so far. The asymmetry has been assumed to be a proxy of large scale dawn-to-dusk electric field generated in Jovian magnetotail and the origin of the variation observed will be discussed in detail. Sporadic change in the emission intensity of IPT associated with the aurora brightening event is expected to investigate in detail with the EXCEED observation to reveal energy transport process between inner and middle/outer magnetospheres. The expected event has not been detected so far and further continuous observation will be expected to resolve this issue.

Japan Geoscience Union Meeting 2014
(28 April - 02 May 2014 at Pacifico YOKOHAMA, Kanagawa, Japan)

PCG38-21 Room:423 Time:May 1 15:45-16:00

Plasma dynamics of Io plasma torus seen from the EXCEED

YOSHIOKA, Kazuo[1*] ; MURAKAMI, Go[1] ; KIMURA, Tomoki[1] ; YAMAZAKI, Atsushi[1] ; TSUCHIYA, Fuminori[2] ; KAGITANI, Masato[2] ; YOSHIKAWA, Ichiro[3]

[1]Institute of Space and Astronautical Science, Japan Aerospace Exploration Agency, [2]Planetary Plasma and Atmospheric Research Center, Graduate School of Science, Tohoku University, [3]The University of Tokyo

Major ions in Io plasma torus have many allowed transition lines in the EUV and their radiation easily escapes to become observable from outside the region. In other words, Jovian inner magnetosphere is able to be monitored by the EUV spectral observation remotely. Moreover, with the atomic database which provides the cross sections to the ambient electron, transition probabilities, and these temperature dependence, EUV observations can be a very important diagnostic of ion densities, electron density, and its temperature.

The EUV spectroscope EXCEED on the Hisaki spacecraft has started to observe the Jovian magnetosphere from the Earth orbit since the end of 2013. The spacecraft is dedicated for the solar system planets so that all the observation window is spared for planetary science. The spectral range is from 52 to 148 nm and its resolution is 0.3 nm with one of the narrowest slit. The field of view is 400 arc-seconds which corresponds to around 18 RJ. Therefore, it can observe whole region of Io plasma torus at one time. Moreover, it can achieve better spatial resolution than 1 RJ. It is the first time to get a whole spectral images of Io plasma torus in the EUV with such a high performance instrument. In this presentation, we will show the first results of EXCEED observation with its high spectral resolution slit for Io plasma torus.

Keywords: EUV, Io plasma torus, Jovian magnetosphere, Hisaki, EXCEED

Japan Geoscience Union Meeting 2014
(28 April - 02 May 2014 at Pacifico YOKOHAMA, Kanagawa, Japan)

PCG38-22 Room:423 Time:May 1 16:15-16:30

Dust-plasma interaction in Saturn's inner magnetosphere and its magnetosphere-ionosphere coupling

SAKAI, Shotaro[1*] ; WATANABE, Shigeto[1]

[1]Dep. Cosmosciences, Hokkaido University

We investigated the magnetosphere-ionosphere coupling with a dust-plasma interaction in Saturn's inner magnetosphere by using a modeling of ionosphere and inner magnetosphere. From our previous model, it was revealed that the magnetospheric ion velocity was significantly reduced by the electric fields generated by the ion-dust collisions when the dust density is high and the thickness of dust distribution is large. It was consistent with observations when the dust density is larger than ~10^5 m^{-3} for ionospheric conductivity of 1 S. An average electron density of Saturn's ionosphere obtained from radio occultations by Cassini spacecraft was ~10^{10} m^{-3} at 2000 km where density had a peak and gradually decreased with the increasing altitude. The density was ~10^8 m^{-3} at 10000 km. Plasma densities calculated by models also were similar to the observations and the topside temperature is ~650 K. However, electron densities from those models were calculated at the altitudes below 4000 km.

We estimated the ionospheric Pedersen conductivity from the plasma densities, and the plasma temperatures and velocities by using a magnetohydrodynamics model. We used the magnetospheric plasma temperature, which was 2 eV, as a boundary condition to investigate the magnetospheric influences. The plasma density was about 10^9 m^{-3} at the altitude of 1200 km, and it decreased to about 10^7 m^{-3} at the altitude of 10000 km. Below 10000 km altitudes the light ion has the upward velocity, while heavy ions have zero or downward velocity at low altitudes. This might be due to the difference of mass. The electron temperature increased to 20000 K at the altitude of 10000 km due to the heat flow from the inner magnetosphere. The electron temperature was about 2000 K at the altitude of 1000 km, and the collision and joule heating were contributing to the temperature below 2000 km. The peak density changed between about 10^8 and 10^{10} m^{-3} during one Saturn's day, and the electron density decreased with increasing the altitude. On the other hand, the electron temperature didn't depend on the local time. The Pedersen conductivity was the maximum 0.77 S on day time and the minimum 0.30 S on dawn time. The Pedersen conductivity strongly depends on the ionospheric plasma density.

We estimated the magnetospheric ion velocity by using the calculated conductivity. The Pedersen conductivity was the largest value at L = 3 and it decreased with the increase of the distance from Saturn. The conductivity changed in local time. The maximum was on the day time and the minimum was on the dawn time. The calculated ion velocity decreases from the co-rotation speed outside 3.5 R_S. The ion velocity was 60-80% of the co-rotation speed in the inner magnetosphere. The ion velocity was smaller than the co-rotation speed since the magnetospheric electric field is smaller than the co-rotational electric field when the current due to the ion-dust collision flows in the inner magnetosphere. The ion velocity strongly depended on the local time since the conductivity also depended on the local time. It is suggested that the dispersion of the observed speeds could show the dependence of local time. The ion velocity is fast during the solar irradiation since the Pedersen conductivity is large, while it becomes slow after the sunset because of the small conductivity.

The magnetosphere-ionosphere coupling is significantly important for the dust-plasma interaction. It is impossible to understand the dust-plasma interaction in Saturn's inner magnetosphere without understanding of the Saturn's ionosphere, since the magnetosphere and ionosphere is intimately-connected.

Keywords: Saturn, Dust-plasma interaction, Magnetosphere-ionosphere coupling, Dusty plasma

Japan Geoscience Union Meeting 2014
(28 April - 02 May 2014 at Pacifico YOKOHAMA, Kanagawa, Japan)

PCG38-23 Room:423 Time:May 1 16:30-16:45

Relation between Kronian magnetospheric convection and auroral emission from MHD simulation with solar wind data observe

FUKAZAWA, Keiichiro[1*] ; WALKER, Raymond J.[2] ; ERIKSSON, Stefan[3]

[1]Research Institute for Information Technology, Kyushu University, [2]UCLA, IGPP, [3]Laboratory for Atmospheric and Space Physics, University of Colorado at Boulder

In a series of our simulation studies we have reported that vortices formed at Saturn's dawn magnetopause in simulations when IMF was northward. We interpreted these vortices as resulting from the Kelvin Helmholtz (K-H) instability. In addition, thanks to the recent developments of computer performance, we have been able to perform the high resolution global MHD simulations of the Kronian magnetosphere. In these simulations we obtained the signature of the field-aligned currents from the K-H vortices in Saturn's auroral ionosphere and found small patchy regions of upward field-aligned current which may be related to auroral emissions. These patchy aurorae resembling our results have been reported from Cassini observations.

In our previous simulations we used the constant and simple solar wind conditions to understand the basic behavior of Kronian magnetosphere. In this study we have used Cassini observations of the solar wind upstream of Saturn to drive a simulation. Using these solar wind data we simulated the Kronian magnetosphere from 2008-02-12/14:00:31 to 2008-02-13/01:59:31 when the Hubble Space Telescope (HST) observed the Kronian UV auroral emissions. In these solar wind conditions there are several enhancement of the solar wind dynamic pressure (shock) and polarity reversal in the IMF components.

From these simulation the shape and convection of Kronian magnetosphere dynamically changed according to the variation of dynamic pressure and IMF directions. As the results, layered convection formed between the corotation region and magnetopause. Furthermore these convection interacted each other, then the large vortex configurations appeared. The calculated configuration of field aligned currents from the simulation also showed the layered and patchy distributions. In addition the upward field aligned current appeared in the dawn side mainly which resembles the configuration of auroral emission by HST.

Japan Geoscience Union Meeting 2014
(28 April - 02 May 2014 at Pacifico YOKOHAMA, Kanagawa, Japan)

PCG38-24 Room:423 Time:May 1 16:45-17:00

Study of dynamics of the Jovian magnetosphere-II: energy transportation process to the inner magnetosphere

MIZUGUCHI, Takahiro[1*] ; MISAWA, Hiroaki[1] ; TSUCHIYA, Fuminori[1] ; OBARA, Takahiro[1] ; KASAHARA, Satoshi[2]

[1]Planetary Plasma and Atmospheric Research Center, Graduate School of Science, Tohoku University, [2]Institute of Space and Astronautical Science/ Japan Aerospace Exploration Agency

We have researched response of the Jovian inner magnetosphere to the substorm-like event which occurred in the night side of the middle/outer magnetosphere. The transport of magnetic flux tube is one of important issues in the global dynamics of the Jovian magnetosphere [Kivelson et al., 2005]. The magnetic flux tubes are carried outward from the Io plasma torus with the slowly outflowing plasma. As they move outward, alternative flux tubes should be returned to the torus through rapid inflow of lower-dense flux tubes. Goal of this study is to reveal the role of the substorm-like event in the transport of magnetic flux tube in the Jovian magnetosphere.

In this study, substorm-like events were identified by using the in-situ observation data obtained by the Plasma Wave Subsystems (PWS), Energetic Particle Detector (EPD) and Magnetometer (MAG) onboard the Galileo orbiter. X-lines where the substorm-like events are thought to start were located at around 60-80 RJ [Woch et al., 2002]. Narrowband KilOMetric radiation (nKOM) which was remotely observed by PWS was used to find response of the inner magnetosphere to the substorm-like event. The source of nKOM is suggested to be located at the outer edge of the Io torus (8-10 RJ) (Reiner et al., 1993).

In the preceding studies, Louarn et al. (2001) reported nKOM correlated with inward flow burst during Jovian substorm-like event reported by Woch et al.(1998) and Krupp et al.(1998). The report implies that the generation mechanism of nKOM relate with the return of magnetic flux tube to inner magnetosphere. However, it has not been revealed well yet how inner and outer magnetospheres couple each other during substorm-like event.

On the other hand, Dubyagin et al.(2011) reported about deeply penetrating flow burst at the terrestrial magnetosphere. They reported that an inward flow burst penetrated into the inner magnetosphere when its entropy was less than that of the inner magnetosphere, while flow burst did not penetrated when its entropy was larger than that of the inner magnetosphere.

We have analyzed Jupiter's several inward flow events which are expected to relate with tail reconnection and nKOM radiation by using the data obtained by Galileo. We also have applied Dubyagin's entropy analysis method to Jupiter's cases in order to reveal that how reconnection event at the outer magnetosphere couple with the inner magnetosphere.

In this presentation, we will show preliminary results on relations of Jovian substorm-like event and phenomena of inner magnetosphere.

Keywords: Jovian magnetosphere, magnetospheric dynamics, substorm, plasma density, Galileo, nKOM

Japan Geoscience Union Meeting 2014
(28 April - 02 May 2014 at Pacifico YOKOHAMA, Kanagawa, Japan)

PCG38-25 Room:423 Time:May 1 17:00-17:15

Jupiter's decametric Io-C modulation lanes observed by LWA1 (2)

IMAI, Kazumasa[1*] ; SHIMANOUCHI, Yoshiaki[1] ; CLARKE, Tracy[2] ; HIGGINS, Charles A.[3] ; IMAI, Masafumi[4]

[1]Kochi National College of Technology, [2]Naval Research Laboratory, [3]Middle Tennessee State University, [4]Kyoto University

The Long Wavelength Array (LWA) is a low-frequency radio telescope designed to produce high-sensitivity, high-resolution images in the frequency range of 10-88 MHz. The Long Wavelength Array Station 1 (LWA1) is the first LWA station completed in April 2011, and is located near the VLA site in New Mexico, USA. LWA1 consists of a 256 element array, operating as a single-station telescope. Each LWA1 beam provides dual orthogonal linear polarizations such that it is possible to reconstruct the full Stokes parameters for each tuning. The first Jupiter radio observation using LWA1 was made by Tracy Clarke (PI) from December, 2011. The initial analyses of Io-A/C, Io-B, and Io-D event, show many spectral features such as S-bursts, narrow-band events (N-bursts), as well as modulation lanes and Faraday lanes.

The modulation lanes in Jupiter's decametric radiation, which were discovered by Riihimaa [1968], are groups of sloping parallel strips of alternately increased and decreased intensity in the dynamic spectral plots. We present LWA1 observations of modulations lanes detected across a Jovian decametric Io-C burst that contains both right hand circular and left hand circular emission. The modulation lanes cross both handedness of polarization, suggesting that the emissions may be coming from the same hemisphere. These results add important information regarding the emission mechanism of Jupiter's decametric emissions.

Keywords: Jupiter radio, decametric wave, modulation lane, radio source, radio emission mechanism, LWA1

Japan Geoscience Union Meeting 2014
(28 April - 02 May 2014 at Pacifico YOKOHAMA, Kanagawa, Japan)

PCG38-26 Room:423 Time:May 1 17:15-17:30

Observations of Polarization of Auroral Kilometric Radiation by KAGUYA and its Lunar Occultations

HASHIMOTO, Kozo[1*] ; GOTO, Yoshitaka[2] ; UDA, Kazuaki[2] ; KASAHARA, Yoshiya[2] ; ONO, Takayuki[3]

[1]Professor Emeritus, Kyoto University, [2]Kanazawa University, [3]Tohoku University

In KAGUYA (SELENE) LRS[1], WFC-H[2] observes wave spectra in 1kHz-1,000kHz and various plasma waves like Auroral Kilometric Radiation (AKR), electron plasma waves, and broadband electrostatic waves have been observed. This system can observe wave polarizations by two pairs of dipole antennas. We have analyzed the AKR polarizations.

Kaguya moves behind the Moon every rotation. The occultations of AKR radiated from the Earth occur. Such occultation observation by the 32 channel burst receiver of lunar orbiter RAE2 was reported in [3,4]. The polarizations were not measured then. The polarization of AKR is defined with respect to the magnetic field from a view point of plasma waves. On the other hand, the polarization is observed with respect to the propagation direction. Both polarizations depend on the source hemisphere. When only one hemisphere can be seen due to the occultation, the source hemisphere is identified and the polarization can be measured correctly. This result is also useful when both hemispheres are seen after the occultation. We show the results and their interpretations.

References

[1] T. Ono, A. Kumamoto, Y. Kasahara, Y. Yamaguchi, A. Yamaji, T. Kobayashi, S. Oshigami, H. Nakagawa, Y. Goto, K. Hashimoto, Y. Omura, T. Imacahi, H. Matsumoto, and H. Oya, The Lunar Radar Sounder (LRS) Onboard the KAGUYA (SELENE) Spacecraft, The Kaguya Mission to the Moon (Guest Editors: A. Matsuoka, C.T. Russell), Space Science Reviews, 154, Nos. 1-4, 145-192, DOI:10.1007/s11214-010-9673-8, 2010

[2] Y. Kasahara, Y. Goto, K. Hashimoto, T. Imachi, A. Kumamoto, T. Ono, and H. Matsumoto, Plasma Wave Observation Using Waveform Capture in the Lunar Radar Sounder on board the SELENE Spacecraft, Earth, Planets and Space, 60, 341-351, 2008.

[3] J.K. Alexander and M.L. Kaiser, Terrestrial Kilometric Radiation 1. Spatical Structure Studies, J. Geophys. Res., 81, 5948-5956, 1976

[4] J.K. Alexander and M.L. Kaiser, Terrestrial Kilometric Radiation 2. Emission From the Magnetospheric Cusp and Dayside Magnetosheath. J. Geophys. Res., 82, 98-104, 1977

Keywords: AKR, Polarization, Occultation, KAGUYA, Moon

Japan Geoscience Union Meeting 2014
(28 April - 02 May 2014 at Pacifico YOKOHAMA, Kanagawa, Japan)

PCG38-P01 Room:Poster Time:May 1 18:15-19:30

Study of the Venus' upper haze

TAKAGI, Seiko[1*] ; ARNAUD, Mahieux[2] ; VALERIE, Wilquet[2] ; ANNCARINE, Vandaele[2] ; IWAGAMI, Naomoto[1]

[1]Graduate School of Science,the Univ. of Tokyo, [2]Belgian Institute for Space Aeronomy

Venus is completely shrouded by a thick cloud deck floating at 45 – 70 km. The major material of the cloud deck is thought to be H_2SO_4 – H_2O droplets. The upper haze on Venus lies above the cloud layer surrounding the planet, ranging from the top of the cloud ($\sim$70 km) up to as high as 90 km. The upper haze particles with an effective radius of $\sim$0.25 μm was suggested from Pioneer Venus Orbiter (PV) measurements. The particles were most likely composed of sulfuric acid in terms of refractive index $\sim$1.45. The haze vertical optical thickness in the polar region at 365 nm was found to be 0.8 above the main cloud of 1 μm particles by PV measurements. By comparison, the optical thickness of the haze above the main cloud at low latitudes was found to be 0.06 [Kawabata et al., 1980]. Knibbe et al. (1998) and Braak et al. (2002) observed a gradual decrease of the haze particle column density during the PV mission. Braak et al. (2002) reported a correlation between the decrease of SO_2 abundance [Esposito et al., 1988; Na et al., 1990] and that of the polar haze optical thickness. However, it is unclear how haze are produced and composition of haze.

The upper layer detected (above the clouds) is characterized by a SO_2 mixing ratio increase with altitude from 85 to 105 km [Belyaev et al., 2012]. It shows a new source of SO_2 at high altitude. One possible source of SO_2 in the upper haze layer could be photo-dissociation of H_2SO_4 vapor resulting from evaporation of acid aerosol droplets. However, recent upper limit of H_2SO_4 from sub-mm ground-based observation makes this theory less likely [Sandor et al., 2012]. The cause of the phenomena given above is still controversial.

The Solar Occultation at InfraRed (SOIR) on board Venus Express (ESA) is designed to measure the atmospheric transmission at high altitudes (70 – 220 km) in the IR (2.2 – 4.3 μm) with high resolution by solar occultation. The SOIR data obtained in 2006 – 2009 are analyzed to examine the upper haze at altitude above 90 km. Vertical and latitudinal distribution of haze extinction, optical thickness and mixing ratio are calculated in using SOIR data statistically. Extinctions and optical thickness at low latitude are two times thicker than those of high latitude. One of the notable results is that mixing ratios increase at altitude above 90 km at both high and low latitudes. It is speculated that sources of haze are transported upward from under altitude 90 km and haze is produced at high altitude. From comparison with the vertical distributions of SO and SO_2 mixing ratios reported by Belyaev et al. (2012), it is speculated about the correlation between sulfuric compound and haze.

Keywords: Venus, upper haze, Venus Express, SOIR, cloud

Japan Geoscience Union Meeting 2014
(28 April - 02 May 2014 at Pacifico YOKOHAMA, Kanagawa, Japan)

PCG38-P02 Room:Poster Time:May 1 18:15-19:30

Observation of CO2-ice cloud in the Martian mesosphere by using PFS onboard Mars Express

SATO, Yuki[1*] ; KASABA, Yasumasa[1] ; MARCO, Giuranna[2] ; AOKI, Shohei[1] ; NAKAGAWA, Hiromu[1] ; KURODA, Takeshi[3]

[1]Planetary Atmosphere , TOHOKU University, [2]IAPS,INAF,Italy, [3]Planetary Plasma and Atmospheric Research Center , TOHOKU University

Almost all of constituent of martian atmosphere is CO2 (95%). It condenses at very high altitude (60˜100km) and become cloud. CO2-ice cloud have been observed by many instrument , but it was difficult to clearly judge whether observed cloud is made of CO2 or not. However OMEGA, visible and near-infrared imaging spectrometer onboard Mars Express, have provided the first spectroscopic identification of a cloud as being composed of CO2 (Montmessin et al, 2007) CO2-ice cloud has characteristic spectral feature emission peak at 4.26μm. Recent study reported that CO2-ice cloud distributes around equator in spring equinox to early summer and mid latitude in local autumn. (Maattanen et al,2010 , Montmessin et al,2007 2006, Clancy et al 2007) However, it is not clear about cloud feature (particle size or opacity).

We try to observe CO2-ice cloud using high spectral resolution instrument PFS, infrared fourier spectrometer onboard Mars Express. Strong point of PFS is that spectral resolution is ten times greater than that of OMEGA and We can see spectral feature of CO2-ice cloud (spike at 4.26μm) more clearly. Another point is that PFS and OMEGA observe almost the same point , so two instruments can observe CO2-ice cloud at the same time. For the first step, we check the data where OMEGA observed CO2-ice cloud (10 orbits) and found CO2-ice cloud like feature all of the 10 orbits. However emission peak appears at shorter wavelength (at 4.25 μm) . In order to judge whether this signal is real or not, we compared PFS spectra and OMEGA spectra observed at the same point. When PFS observe signal at 4.25μm , OMEGA also show strong signal at 4.26μm ,so we can say PFS signal is real. In some orbit, PFS observed different signal from that of OMEGA. It is double spike feature at 4.25μm and 4.28μm which OMEGA can not resolve. It is possible that double peak feature shows different cloud feature, for example, particle size.Now we are trying radiative transfer model and discuss how cloud spectral feature changes when we changes cloud parameter (size distribution, altitude, cloud opacity).

Keywords: Mars, CO2-ice cloud

Japan Geoscience Union Meeting 2014
(28 April - 02 May 2014 at Pacifico YOKOHAMA, Kanagawa, Japan)

PCG38-P03 Room:Poster Time:May 1 18:15-19:30

Numerical Modeling of Moist Convection in Giant planets

SUGIYAMA, Ko-ichiro[1*] ; NAKAJIMA, Kensuke[3] ; ODAKA, Masatsugu[2] ; KURAMOTO, Kiyoshi[2] ; HAYASHI, Yoshi-yuki[4]

[1]ISAS/JAXA, [2]Graduate school of Science, Kobe University, [3]Department of Cosmosciences, Graduate School of Science, Hokkaido University, [4]Graduate school of Science, Kobe University

It is now widely accepted that moist convection is a common phenomenon in giant planets atmosphere. The moist convection is thought to play an important role in determining the mean vertical structure of the atmosphere; the mean vertical profiles of temperature, condensed components, and condensible gases in the moist convection layer is thought to be maintained by the statistical contribution of a large number of clouds driven by internal and radiative heating/cooling over multiple cloud life cycles. However, the averaged structure of the giant planets atmosphere and its relationship to moist convection remain unclear. For the purpose of investigating the above problem, we developed a cloud resolving model and investigated a possible structure of moist convection layer in Jupiter ′ s atmosphere with using the model (Sugiyama et al., 2009, 2011, 2014). In this presentation, we perform two-dimensional calculations of moist convection and demonstrate a possible structure in the atmospheres of Saturn, Uranus, and Neptune.

The basic equation of the model is based on quasi-compressible system (Klemp and Wilhelmson, 1978). The cloud microphysics is implemented by using the terrestrial warm rain bulk parameterization that is used in Nakajima et al. (2000). We simplify the radiative process, instead of calculating it by the use of a radiative transfer model. The model atmosphere is subject to an externally given body cooling that is a substitute for radiative cooling. Because the vertical profile of net radiative heating is not observed in giant planets except Jupiter, the layer between 2 bar level and the tropopause, which corresponds to the observed cooling layer in Jupiter, is cooled. The body cooling rate is set to be 100 times larger than that observed in Jupiter ′ s atmosphere in order to save the CPU time required to achieve statistically steady states of the model atmosphere.

The domain extends 960 km in the horizontal direction. The vertical domains are 400 km for Saturn case and 600 km for Uranus case and Neptune case, which are based on the one-dimensional thermodynamical calculation (Sugiyama et al., 2006). The spatial resolution is 2 km in both the horizontal and the vertical directions. The temperature and pressure at the lower boundary is also based on the thermodynamical calculation. The initial temperature profile follows adiabatic from lower boundary to tropopause and is constant above the tropopause. The abundances of condensable gases used in the each calculation are taken at 0.1, 1, 3, and 10 times solar.

The results obtained in Saturn case with 1 times solar abundance of condensible gases are discussed below; the results of other planets and the dependency on the abundances of condensable gases will be demonstrated at the meeting. The major characteristic of vertical motion in the moist convection layer obtained in Saturn case is that downdrafts are stronger than updrafts; this characteristic is obviously different from that obtained in Jupiter case (Sugiyama et al., 2009). Sugiyama et al. (2009) demonstrates that the vertical motion in the moist convection layer of Jupiter is characterized by narrow, strong, cloudy updrafts and wide, weak, dry downdrafts. On the other hand, the characteristics of mean vertical structure are consistent with those obtained in Jupiter case. Due to the active transport associated with convection, considerable amounts of H_2O and NH_4SH cloud particles exist above the NH_3 condensation level, while the mixing ratios of all condensible gases decrease with height from the H_2O condensation level. The stable layer associated with the H_2O condensation level acts as a fairly strong barrier for vertical convective motion; the vertical profile of root mean square of vertical velocity has local minimum at this level.

Keywords: atmosphere of giant planets, moist convection, numerical modeling, cloud resolution model

Japan Geoscience Union Meeting 2014
(28 April - 02 May 2014 at Pacifico YOKOHAMA, Kanagawa, Japan)

PCG38-P04 Room:Poster Time:May 1 18:15-19:30

Two dimensional numerical study on Venusian gravity waves by using mesoscale model

ANDO, Hiroki[1*] ; SUGIYAMA, Ko-ichiro[1] ; IMAMURA, Takeshi[1] ; ODAKA, Masatsugu[2] ; NAKAJIMA, Kensuke[3]

[1]ISAS/JAXA, [2]Hokkaido University, [3]Kyusyu University

Recently Venusian gravity waves are often observed. For example, Airglow measurements of O_2 found the gravity waves with horizontal wavelength of ∼100 km at 110 km altitude. UV images also detect gravity waves with the horizontal wavelength of 60-150 km at the cloud top level (70 km altitude). However, only a specific altitudes can be observed in these measurements, thus it is difficult to examine the propagation characteristics and momentum flux of waves. Radio occultation measurements also detect upward propagating waves from the vertical temperature profiles within the altitude range of 65-90 km and suggests that waves with the vertical wavelength of 5-10 km are dominant by the spectral analysis. However, horizontal resolution in this measurement is ∼200 km, then small scale gravity waves cannot be observed. Therefore, it is difficult to understand how these gravity waves have their influence on the Venusian atmosphere.

In this study we developed a new Venusian mesoscale model and examined the propagation characteristic of the waves. In the model, we simulated the generation and propagation of the waves including the convective motion in the Venusian cloud layer. We will make a presentation about the initial analysis results.

Keywords: Venus atmosphere, Gravity waves, Numerical study

Japan Geoscience Union Meeting 2014
(28 April - 02 May 2014 at Pacifico YOKOHAMA, Kanagawa, Japan)

PCG38-P05 Room:Poster Time:May 1 18:15-19:30

Temporal variations of Venus O2 night airglow using IRTF/CSHELL

OHTSUKI, Shoko[1*] ; IWAGAMI, Naomoto[2] ; ROBERT, Severine[3] ; SAGAWA, Hideo[4] ; KOUYAMA, Toru[5] ; SATO, Takao M.[6]

[1]Senshu University, [2]University of Tokyo, [3]Belgian Institute for Space Aeronomy, [4]National Institute of Information and Communications Technology, [5]Information Technology Research Institute, [6]Institute of Space and Astronautical Science, Japan Aerospace Exploration Agency

Venus 1.27-micron O_2 night airglow is the indicator of the general circulation at about 95 km in Venus. Recent observations reported that the airglow emission showed the temporal variations with a period of a few hours and days [e.g. Ohtsuki et al., 2008; Gerard et al., 2008]. Such variations may be caused by the upward momentum transport and fluctuations by atmospheric waves. In recent years, the importance of planetary-scale waves on the general circulation of the Venus atmosphere has been recognized. Forbes and Konopliv [2007] suggested the propagation of planetary-scale waves originated in the cloud deck into the upper atmosphere. However, effects of planetary-scale waves on the Venus upper atmosphere have not been investigated yet.

We conducted 5-days monitoring observation of the airglow to detect the planetary-scale waves with IRTF/CSHELL from 11-15 July 2012, 3 and 5 February 2014. The 1.27-micron O_2 night airglow in the Venus atmosphere can pass through the Earth's atmosphere with a help of the Doppler shift. We obtained spectral image cubes at the wavelength of R-branch of the airglow band, which includes several rotational lines. In order to cover spectral information continuously, a slit drifted across Venus' nightside disk. The spatial resolution of the image is governed by seeing. The typical seeing was 0.6" to 1.5" in our observing run and corresponds to 200-450km at the center of Venus' disk. Under such conduction, we may detect airglow structures of small scales due to atmospheric waves; this is smaller than the region of enhanced airglow having a horizontal scale of ˜3000km. We can also derive the hemispherical distribution of the rotational temperature. To coincide with our observations, SOIR/Venus Express stellar occultations were conducted. We can try to compare our horizontal temperature map and vertical temperature profile from SOIR data.

In this presentation, we will show temporal variation of the airglow distributions in July 2012 and report a preliminary result of our new observations in February 2014.

Japan Geoscience Union Meeting 2014
(28 April - 02 May 2014 at Pacifico YOKOHAMA, Kanagawa, Japan)

PCG38-P06 Room:Poster Time:May 1 18:15-19:30

Observing plan for planetary atmosphere using IR heterodyne spectroscopy in 2014

NAKAGAWA, Hiromu[1*] ; AOKI, Shohei[1] ; KASABA, Yasumasa[1] ; MURATA, Isao[1] ; SAGAWA, Hideo[2]

[1]Tohoku University, [2]National Institute of Information and Communications Technology

We propose a new developed infrared heterodyne instrument, called Mid-Infrared LAser Heterodyne Instrument (MILAHI), for our dedicated telescope at the top of Mt. Haleakala, Hawaii. It addresses the key physical/meteorological parameters, such as the atmospheric temperature profiles, abundance profiles of the atmospheric compositions and their isotopes, and wind velocity. The observational sensitivity of MILAHI is discussed in this paper. The scientific target of MILAHI is to understand highly variable phenomena in the planetary atmospheres. The nature of atmospheric activity in various time-scale will be investigated by continuous monitoring with our dedicated telescope, in order to increase our understanding of planetary atmospheric dynamics, photochemistry, and meteorology. New measurements with high spatial/spectral resolutions constrain the three-dimensional distributions of temperature and compositions. The D/H and other isotopic ratios, diagnostic of the terrestrial atmosphere evolution, will be accurately measured in H_2O and CO_2. The atmospheric chemistry will be studied by monitoring O_3, H_2O_2, H_2O, and HDO. Mapping of the H_2O isotopes reveal the mechanism of complex interaction between regolith-aerosols-atmosphere-polar caps on Mars. Direct measurements of wind velocity and temperature allow the first monitoring of the middle atmosphere oscillations to investigate the effects of the gravity waves from the lower atmosphere on the upper atmosphere for various seasons and dust loadings. A number of organics molecule bands in the mid-infrared regime will be accurately measured in planetary/cometary/stellar atmospheres. In addition to these interconnected objectives, serendipitous searches with our advantage of dedicated use for astronomical/atmospheric transient events which occur at frequent and unpredictable intervals (e.g. dust storm) will enhance our knowledge of the composition and dynamics of the astronomical sources.

Keywords: infrared spectroscopy, heterodyne, laser, observation, planetary atmosphere, isotopes

Japan Geoscience Union Meeting 2014
(28 April - 02 May 2014 at Pacifico YOKOHAMA, Kanagawa, Japan)

PCG38-P07 Room:Poster Time:May 1 18:15-19:30

Visual Orbit Design for the Next Mars Exploration Mission

OGURA, Satoshi[1] ; KAWAKATSU, Yasuhiro[1] ; MATSUOKA, Ayako[1] ; TAGUCHI, Makoto[2*]

[1]ISAS/JAXA, [2]Rikkyo University

In December, 2011, the working group concerned with the Japanese next Mars exploration mission began to study the use of orbiters to investigate the mechanisms of carbon dioxide and water escape from the Martian atmosphere, and the role played by the solar wind. This will be the successor to the first Japanese mission to Mars involving the NOZOMI spacecraft, and two different orbiters will be deployed around the planet. Orbiter-A will carry out in-situ observations of electric and magnetic fields, particles, plasma and the atmosphere at an altitude of about 100 km above the Martian surface. Orbiter-B will capture images of the escaping atmosphere and monitor solar-wind conditions. The mission life will be a Mars year. This paper describes a visual method for determining the orbits of both spacecraft, and presents examples of possible orbits.

The orbital constraints proposed by the working group are as follows.

Orbital constraints for Orbiter-A

A1. The periapsis altitude is around 150 km.

A2. The apoapsis altitude is between 5000 and 7000 km.

A3. The period during which periapsis occurs on the dayside of the planet is more than two thirds of the mission life.

Orbital constraints for Orbiter-B

B1. The apoapsis altitude is about 4-6 R_M.

B2. The period during which the orbiter is exposed to the solar wind is more than three quarters of the mission life.

B3. The period during which the orbiter can image the local time zone of 12-15 h at the planetary limb is more than three quarters of the mission life.

Orbital constraints for combined observations by both orbiters

C1. The number of times during which Orbiter-B is exposed to the solar wind and can also image Orbiter-A, whose solar zenith angle and altitude are less than 60 deg and about 300-800 km, respectively, is more than one hundred during the mission life.

C2. When C1 is satisfied, the angle between the line-of-sight of the imager onboard Orbiter-B and the velocity vector of Orbiter-A is within 90 ± 20 deg.

The orbital elements are obtained by solving the Lagrange planetary equations for a two-body boundary-value problem, taking only the J2 perturbation into account. Constraint A3 is chosen as an example for explaining the visual method of orbital design. The orbiter's longitude of ascending node and argument of periapsis in a Mars-Sun fixed coordinate system are taken as design variables, and the orbital constraint is used as an evaluation function. A contour map for a period in which periapsis occurs on the dayside is plotted in a coordinate system in which the longitude of ascending node and argument of periapsis are the X and Y axes, respectively. A mission profile is placed on the map, along which the changes in the longitude of ascending node and argument of periapsis during the mission period are plotted. The mission profile can be placed at anywhere on the map, since its shape can be kept almost constant by selecting an initial position determined by the position and direction of the spacecraft during Mars orbit insertion. By looking at the map, it then becomes easy to identify an appropriate initial point for the mission profile that maximizes the period during which periapsis occurs on the dayside.

By the method described above, it is possible to visually determine rough values for the longitude of ascending node and argument of periapsis that are suitable for the mission. This technique is also applicable to the general design of orbits around a planet by choosing a coordinate system appropriate for the given orbital constraints.

Keywords: atmospheric escape of Mars, Mars orbiter

Japan Geoscience Union Meeting 2014
(28 April - 02 May 2014 at Pacifico YOKOHAMA, Kanagawa, Japan)

PCG38-P08 Room:Poster Time:May 1 18:15-19:30

A Circumpolar Stratospheric Telescope for Observations of Planets ? FUJIN

MAEDA, Atsunori[1*] ; TAGUTI, Makoto[1] ; YOSIDA, Kazuya[2] ; SAKAMOTO, Yuji[2] ; NAKANO, Toshihiko[2] ; SHOJI, Yasuhiro[3] ; TAKAHASHI, Yukihiro[4] ; NAKAMOTO, Jumpei[4] ; IMAI, Masataka[4] ; WATANABE, Makoto[4] ; GODA, Yuki[5]

[1]College of Science, Rikkyo University, [2]Graduate School of engineering, Tohoku University, [3]JAXA/ISAS, [4]Graduate School of Science, Hokkaido University, [5]School of Science, Hokkaido University

It is important to conduct long-term continuous observations of time-dependent events in planetary atmospheres and plasmaspheres. The aim of the FUJIN project is to carry out continuous observations of planets using a telescope that is lifted by a balloon to the polar stratosphere. The FUJIN-1 experiment was organized at Taiki Aerospace Research Field in Taiki-cho, Hokkaido, Japan, from May to June 2013, but the experiment was canceled due to a failure found in the balloon operation system provided by JAXA. However, the results of various prelaunch ground tests clearly established the feasibility of the experiment.

We have recently begun organizing the FUJIN-2 experiment, in which scientific observations of planets will be conducted in the Arctic. Wind speed in the stratosphere is very low during April and May. The FUJIN-2 experiment will be conducted during this period in 2015 at ESRANGE in Kiruna, Sweden, since this is when Venus will be in the most favorable position for observations. The gondola will be recovered somewhere in the Scandinavian peninsula after one or two days of continuous observations.

In summer, an eastern circumpolar wind is dominant in the stratosphere. If a balloon is flown under these conditions, it will take a week to fly from Kiruna to Alaska and more than two weeks for it to fly back to Scandinavia along a constant-latitude path around the Earth. We are currently organizing another experiment (FUJIN-3) involving such a circumpolar flight that will be conducted in 2017 or later. The system used in FUJIN-2 will also be used for FUJIN-3, but with the inclusion of a high-sensitivity CCD camera and a liquid-crystal tunable filter. Venus, Jupiter, and Mercury will be the planets of interest for FUJIN-3. Moreover, a next-generation stratospheric telescope with a meter-class aperture, a mobile gondola to approach the center of the polar vortex, and a super-pressure balloon for year-round observations are being studied to upgrade the FUJIN system for future use.

Keywords: Circumpolar, Stratospheric, Telescope, Venus, FUJIN-project

Japan Geoscience Union Meeting 2014
(28 April - 02 May 2014 at Pacifico YOKOHAMA, Kanagawa, Japan)

PCG38-P09 Room:Poster Time:May 1 18:15-19:30

Study of fast resistive magnetic reconnection in the upper atmosphere of Venus

SAKAMOTO, Hitoshi[1*] ; TERADA, Naoki[1]

[1]Graduate School of Science, Tohoku University

Although Venus has no intrinsic magnetic field, magnetic field exists in the upper atmosphere through the interaction of the solar wind. In the dayside ionosphere of Venus, small magnetic rope-like structures called 'flux ropes'were often observed when solar wind dynamic pressure was low. Pioneer Venus Orbiter (PVO) observed flux ropes on more than 40% of the orbits passing through the dayside lower ionosphere, and founds its occurrence rate maximizes at altitude170km [Elphic et al., 1983].

So far some models to generate flux ropes have been proposed (K-H instability [Wolff et al., 1980], nonlinearity associated with the Hall effect [Kleeorin et al., 1994]), but the generation mechanism is not yet understood. In this study, we propose a new model to generate flux ropes based on recently proposed fast resistive magnetic reconnection [Loureiro et al., 2007]. This fast resistive reconnection occurs in a very long Sweet-Parker (SP) current sheet. The growth rate in the linear stage is proportional to the one-quarter power of the Lundquist number, and the current sheet is unstable under the condition that the Lundquist number is more than 10 to the power of 4. According to MHD simulation results [Samtaney et al., 2009], a chain of plasmoids is formed after reconnection at many points in the current sheet. Such a chain structure is similar to flux ropes. In the dayside ionosphere of Venus, a very long current sheet can form, where the fast resistive magnetic reconnection occur. Therefore, we considered a model to generate flux ropes through the formation of a very long current sheet and subsequent fast resistive reconnection in the dayside ionosphere of Venus, and then examined its applicability. The outline of the generation model we propose in this study is as follows: First, the interplanetary magnetic field (IMF) carried by the solar wind penetrates into the dayside lower ionosphere when solar wind dynamic pressure is high. Then, the field reversal structure resulting from an IMF turning penetrates there, and a very long SP current sheet is created. Finally, flux ropes are generated through the fast resistive reconnection in the current sheet.

In order to examine the applicability of our model, we estimated the altitude profiles of the Lundquist number, the growth rate of the fast resistive reconnection, and the SP current sheets thickness by using the result of a hybrid simulation in the upper atmosphere of Venus [Terada et al., 2002]. From the profiles, we chose the altitudes corresponding to specific Lundquist numbers, and we consider that the fast resistive reconnection can occur if the following conditions are satisfied at the chosen altitudes. First one is that the fast resistive reconnection can grow sufficiently. Second one is that the SP current sheet thickness is larger than the observed flux rope radius [Elphic et al., 1983]. Consequently, we found that our model is applicable between near 170 km altitude (Lundquist number is 10 to the power of 5 at this altitude) and near 230 km altitude (Lundquist number is 10 to the power of 6 at this altitude). We will show the result of MHD simulation performed with the parameters at these applicable altitudes.

Keywords: reconnection, ionosphere, Venus

Japan Geoscience Union Meeting 2014
(28 April - 02 May 2014 at Pacifico YOKOHAMA, Kanagawa, Japan)

PCG38-P10 Room:Poster Time:May 1 18:15-19:30

Estimation of the ion acceleration in the Ganymede polar magnetosphere by the Galileo spacecraft observation

WATANABE, Shinya[1*] ; KATOH, Yuto[1] ; KUMAMOTO, Atsushi[1] ; ONO, Takayuki[1] ; KURTH, William S.[2] ; HOSPODARSKY, George[2]

[1]Department of Geophysics, Graduate School of Science, Tohoku University, [2]Department of Physics and Astronomy, University of Iowa Iowa City, Iowa, USA.

Ganymede is one of the Jovian moons and is known as the only satellite that has an intrinsic magnetic field [Gurnett et al., 1996]. Since Ganymede is located in the Jovian magnetosphere, corotating magnetospheric plasma always blows toward Ganymede's magnetosphere [e.g. Kivelson et al., 1998]. Since the spatial scale of Ganymede's magnetosphere is comparable to the Larmor radius of magnetospheric ions, the characteristic plasma environment around Ganymede is formed due to the interaction between Ganymede's magnetosphere and Jovian magnetospheric plasma. Although previous studies discussed the morphology of Ganymede's magnetosphere and its plasma environment, most of them are still unknown and understanding of the interaction is necessary to reveal processes occurring in Ganymede's magnetosphere.

In the present study, we discuss the plasma environment observed in Ganymede's polar region by the Galileo spacecraft. First, we have identified Upper-Hybrid Resonance (UHR) frequency by the Plasma Wave Subsystem (PWS) and have analyzed the electron density at the point of observation. We have analyzed four Ganymede encounters including those on orbits G01 and G02 which have been analyzed in the previous study. Since the most dominant ion in Ganymede's magnetosphere is O+ [Vasyliunas and Eviatar, 2000], we assumed that the O+ density equals the electron density. Based on the results of this analysis, we have plotted the distribution of O+ density in the altitude range from 264 km to 5262 km and have revealed that the number density decreases rapidly with distance from Ganymede. Next, we have discussed the ion outflow from Ganymede's polar region. Based on the obtained distribution, we have found that the density distribution can be expressed by r^-5.98, where r is the distance from Ganymede. Assuming that the flux is conserved along the path of the ion outflow and that the cross section of the flux tube of outflow is proportional to r^2 and r^3, we have estimated that the ion velocity reaches 17.3 km/s and 14.5 km/s, respectively, at the distance of 500 km from Ganymede. This result is consistent with the previous study which suggested the outflow O+ velocity is 18 km/s from observations of the Galileo PLS instrument [Vasyliunas and Eviatar, 2000]. We also discuss candidate mechanisms for the ion outflow from Ganymede's polar region and report the current status of a simulation code which we are developing so as to discuss the outflow process quantitatively.

Keywords: Ganymede, magnetosphere, outflow, acceleration

Japan Geoscience Union Meeting 2014
(28 April - 02 May 2014 at Pacifico YOKOHAMA, Kanagawa, Japan)

PCG38-P11 Room:Poster Time:May 1 18:15-19:30

In-flight calibration of HISAKI/EXCEED by stellar observations

MURAKAMI, Go[1*] ; YOSHIOKA, Kazuo[1] ; YAMAZAKI, Atsushi[1] ; KIMURA, Tomoki[1] ; TSUCHIYA, Fuminori[2] ; KAGITANI, Masato[2] ; YOSHIKAWA, Ichiro[3]

[1]ISAS/JAXA, [2]Tohoku University, [3]The University of Tokyo

The extreme ultraviolet (EUV) telescope EXCEED (Extreme Ultraviolet Spectroscope for Exospheric Dynamics) onboard the Japan's small satellite HISAKI (SPRINT-A) will be launched in August 2013. The EXCEED instrument will observe tenuous gases and plasmas around the planets in the solar system (e.g., Mercury, Venus, Mars, Jupiter, and Saturn). One of the primary observation targets is Jupiter, whose magnetospheric plasma dynamics is dominated by planetary rotation. In the EUV range, a number of emission lines originate from plasmas distributed in Jupiter's inner magnetosphere. The EXCEED instrument is designed to have a wavelength range of 52-148 nm with a spectral resolution of 0.3-1.0 nm. The spectrograph slits have a field of view of 400 x 140 arc-seconds (maximum), and the attitude fluctuations are stabilized within 5 arc-seconds. The optics of the instrument consists of a primary mirror with a diameter of 20cm, a laminar type grating, and an EUV detector using microchannel plates (MCPs). The surfaces of the primary mirror and the grating are coated with CVD-SiC.

After the launch of the HISAKI satellite and the initial check out of the instrument for 2 months, we performed in-orbit calibrations of the EXCEED instrument by stellar observations. We observed the standard stars GD71, HZ2, and FEIGE110, and measured the absolute sensitivity and the spatial resolution of the EXCEED instrument. As a result, the absolute sensitivity was ˜1-2 cm^2 and the spatial resolution was ˜16 arc-seconds. In this presentation, we report the overview and initial results of the in-orbit calibration of EXCEED.

Keywords: HISAKI, EXCEED, EUV

Japan Geoscience Union Meeting 2014
(28 April - 02 May 2014 at Pacifico YOKOHAMA, Kanagawa, Japan)

PCG38-P12 Room:Poster Time:May 1 18:15-19:30

Coordinated observation of Io plasma torus using Hisaki/EXCEED and gourd-based telescopes

KAGITANI, Masato[1*] ; ANDREW, Steffl[2] ; BADMAN, Sarah[3]

[1]Tohoku university, [2]Southwest Research Institute, [3]University of Leicester

EXCEED is an EUV spectrograph onboard an earth-orbiting space telescope, Hisaki(SPRINT-A). One of the primal mission goal of Hisaki/EXCEED is to reveal radial transport of mass and energy in the Jovian magnetosphere. At the begging of January 2014, intense campaign observations of Jovian aurora and Io plasma torus were made using Hisaki/EXCEED, Hubble Space Telescope and other ground-based telescopes covering wavelength range from EUV through IR. We will present results of spectroscopic observation of Io plasma torus using the R.C. spectrograph attached to Kitt-Peak 4-meter telescope and an Echelle spectrograph attached to Haleakala 40-cm telescope.

The 4-meter R.C. Spectrograph was set up covering 550nm through 800nm which could successfully detect NaD (589nm), SIII 631.2nm, SII 671.6/673.1nm, and OII 731.9/733.0nm as well. A field-of-view was 98 arcseconds along the slit and the slit center was pointed at the dawn or dusk edge of the centrifugal equator. We could get 54 spectra from the observation during January 4th through 10th, 2014.

The Haleakala spectrograph is a high-resolution echelle spectrograh with an integrated field unit (IFU) which enables to capture 2-d distribution of [SII] 671.6/673.1nm emission with spectral resolution of 67000 over a field-of-view of 41” by 61”. The 40-cm telescope was observing Io plasma torus all over the night during the observing campaign period.

Based on preliminary analysis of the EUV spectrum from EXCEED/Hisaki, visible spectrum from Kitt-Peak 4-meter and Haleakala 40-cm, emission peaks of SIII and OII was located outward compared to the SII emission peak which is consistent with results from previous studies. More accurate analysis including pointing calibration and flux calibration are ongoing, the result will be presented at the meeting.

Keywords: Hisaki/EXCEED, Io plasma torus

Japan Geoscience Union Meeting 2014
(28 April - 02 May 2014 at Pacifico YOKOHAMA, Kanagawa, Japan)

PCG38-P13 Room:Poster Time:May 1 18:15-19:30

Coordinated observation of Jupiter thermosphere and radiation belt in January 2014

KITA, Hajime[1*] ; MISAWA, Hiroaki[1] ; TSUCHIYA, Fuminori[1] ; FUJISAWA, Shota[1] ; SAKANOI, Takeshi[1] ; KASABA, Yasumasa[1]

[1]Tohoku Univ.

In order to evaluate the solar UV/EUV heating effect on the Jovian radiation belt, we made coordinated observations for both temperature of the Jovian thermosphere using an infrared telescope and synchrotron radiation from the radiation belt (JSR) using a radio interferometer. JSR is the most effective probe for the dynamics of the Jovian radiation belt through remote sensing from the Earth. Recent intensive observations for JSR reveal short term variations of JSR with the time scale of days to weeks, but their causalities are not understood well. It is theoretically expected that the Jovian thermosphere is heated by solar UV/EUV radiation, and planetary atmospheric neutral wind is driven by solar UV/EUV heating. Then, induced dynamo electric field is mapped into the radiation belt and induces radial diffusion. From this scenario, the total flux density of JSR is expected to correlate with the solar UV/EUV flux.

Previous studies confirmed that the total flux density of JSR varied corresponding to the solar UV/EUV variations though it is unclear whether the temperature of the Jovian thermosphere actually varied during this event. The purpose of this study is to confirm whether sufficient solar UV/EUV heating occurs on the Jovian thermosphere and it actually causes variations of JSR total flux density. We made coordinated observations of the NASA Infra-Red Telescope Facility (IRTF) and the Giant Metrewave Radio Telescope (GMRT). From the infrared spectroscopic observations, we measured thermospheric temperature of H_3^+ ion. From the radio interferometer, we measured the total flux density and brightness distribution of JSR.

The IRTF is a 3 m infrared telescope located in Mauna Kea, Hawaii. The IRTF observations were made on Jan 3, 8, and 13 in 2014. We used the high spectral resolution spectrometer, CSHELL, and observed H_3^+ 3.9530 microns emission (Q(1,0)) and 3.4547 microns doublet emission (R(4,3) and R(4,4)). We assumed local thermodynamic equilibrium at the equatorial region and calculated thermospheric temperature from the two emission line ratio. The GMRT is a large radio interferometer located in India. The GMRT observations were made from Dec 31 to Jan 16 with a few days interval. The typical duration of observation time was 2 hours per day, and the observation frequency was 235 and 610 MHz. During this period, the SOHO satellite showed that the solar EUV flux increased from Dec 26, reached at the maximum flux on Jan 8, and then decreased to Jan 16. A preliminary analysis of the IRTF data showed that the temperature increased from Jan 3 to Jan 8, and decreased from Jan 8 to Jan 13. This is the first result that shows the temperature response of Jovian upper atmosphere to the solar UV/EUV heating. We will also introduce analyzed results of the GMRT data and discuss the relationship between Jovian thermosphere and radiation belt.

Keywords: Jupiter, thermosphere, radiation belt, infrared observation, radio interferometer

Japan Geoscience Union Meeting 2014
(28 April - 02 May 2014 at Pacifico YOKOHAMA, Kanagawa, Japan)

PCG38-P14 Room:Poster Time:May 1 18:15-19:30

Data analysis of Jupiter's decametric radio emission observed by LWA1

SHIMANOUCHI, Yoshiaki[1*] ; IMAI, Kazumasa[1] ; CLARKE, Tracy[2] ; HIGGINS, Charles A.[3] ; IMAI, Masafumi[4]

[1]Kochi National College of Technology, [2]Naval Research Laboratory, [3]Middle Tennessee State University, [4]Kyoto University

We present new results in the study of Jupiter's decametric emission obtained using the newly commissioned Long Wavelength Array Station 1 (LWA1). The LWA1 is a low frequency radio array operating in the frequency band between 10 and 88 MHz. The array consists of 256 dual polarization dipole stands, and observations are possible with up to four simultaneous beams, each of which has two independent tuning frequencies. The LWA1 is well suited to studying details of Jovian phenomena due to its high sensitivity as well as high time and frequency resolution over a wide bandwidth. We present LWA1 observations and the developed data analysis software by using IDL. The observed Io-C dynamic spectrum on March 10, 2012 shows the modulation lanes of both left and right hand polarization components share the same lane structure. It indicates that the both left and right hand Io-C radiations are emitted from the southern hemisphere. And the locations of the radio sources along the Jupiter's magnetic field should be very close.

Keywords: Jupiter radio, decametric wave, data analysis, radio source, radio emission mechanism, LWA1

Japan Geoscience Union Meeting 2014
(28 April - 02 May 2014 at Pacifico YOKOHAMA, Kanagawa, Japan)

PCG38-P15 Room:Poster Time:May 1 18:15-19:30

Long Term Variations of Jupiter's Auroral Radio Emissions - II

MISAWA, Hiroaki[1*] ; YONEDA, Mizuki[2] ; MORIOKA, Akira[1] ; TSUCHIYA, Fuminori[1] ; MIZUGUCHI, Takahiro[1]

[1]PPARC, Tohoku Univ., [2]PPARC, Tohoku Univ. / IFA, Univ. Hawaii

It is known that Jupiter's auroral radio emission (hereafter JAR) shows long term variations with the time scale of about a decade. The variations were first considered to be initiated by the solar activities in 1960's, however, longer term analyses in 1970's showed the variations relate with the Jovicentric declination of the earth (De). So far, their plausible causalities are considered to be brought by 1) De relating to amount of reachable rays to the earth, and 2) the geocentric declination of Jupiter relating to incidence angle of the radio wave to the terrestrial ionosphere. However, considering solar cycle dependence on the terrestrial auroral radio activity (e.g. Kumamoto et al., 2003), the solar activity control may not be negligible for the long term variations. Furthermore, we have not known well long term relationship between JAR and Jupiter's substorm-like process which may be controlled by Io's volcanic activity.

In order to assess the previously proposed causalities and the other effects, we have investigated occurrence features of JAR using the radio wave data observed outside the terrestrial ionosphere; i.e., by the WIND satellite after 1995. We have derived year-scale occurrence probabilities for 0.7 - 14 MHz around Jupiter's occultation periods, where the frequency range includes both Jupiter's decameter and hectometer radio emissions (so-called DAM and HOM, respectively). As the result, the yearly-scale occurrence probabilities show almost monotonous decrease from 1995 to 2005, then gradual increase after 2005, but change to somewhat complex nature with increase and decrease after 2009. The tendency is roughly similar for DAM and HOM, and also quite roughly similar for Io-related and non-Io-related DAMs. On the other hand, the JAR variation features do not seem to correspond to individual variation of De, solar activity and solar wind, but seem to somewhat correlate with those of Iogenic gas luminosity. These results imply that multiple causalities and/or Jupiter's internal process(es) control the long term variations.

Acknowledgements: We would greatly appreciate M. Kaiser and the WIND/WAVES team for providing the radio wave data.

Keywords: Jupiter, auroral radio emission, long term variation, Io's volcanic activity, Iogenic gas